10 January 2008 | www.nature.com/nature | $10

THE INTERNATIONAL WEEKLY JOURNAL OF SCIENCE

nature

THE GENETICS OF SEX

A basal fungus as a model for sex determination

GALACTIC ANTIMATTER
The positron source identified

NANOTECHNOLOGY
Silicon goes thermoelectric

TOXOPLASMOSIS
'Plant' hormone found in protozoon

NATUREJOBS
Museum life

$10.00US $12.99CAN
02>
0 71486 03070 6

nature 451, 107-222 10 January 2008

www.nature.com/nature

no.7175 npg

MILLIPORE™

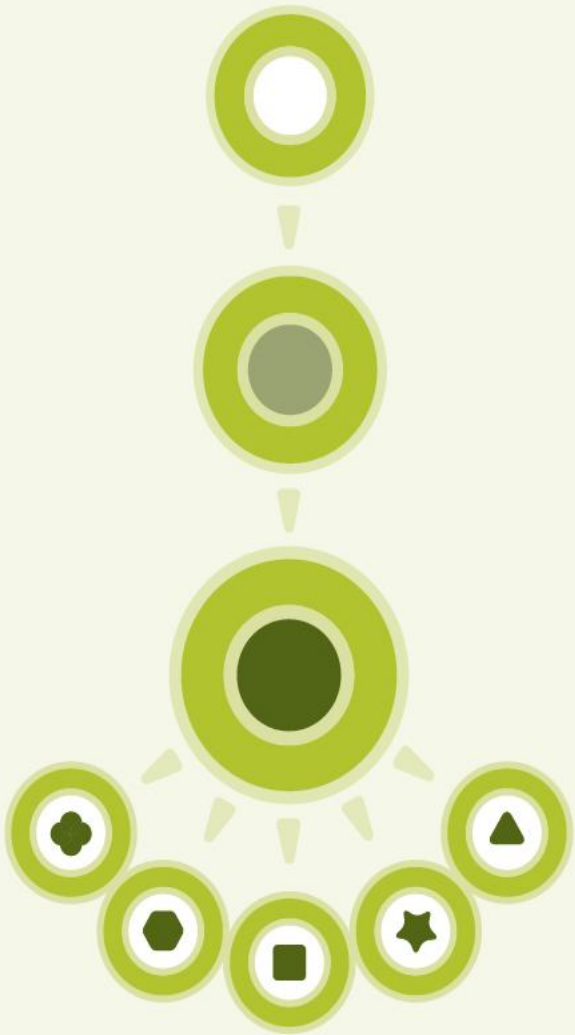

CELL BIOLOGY
CELL SIGNALING
DRUG DISCOVERY
IMMUNODETECTION
LAB WATER
PROTEIN BIOMARKERS
STEM CELL RESEARCH

NEXT GENERATION?

Give rise to controlled differentiation.

We stand with you in our investment in and commitment to stem cell research. By combining Upstate® and Chemicon® products and services with our years of experience supporting Life Science research, we successfully partner with the world's leading scientists to develop proven solutions for human and murine, adult and embryonic stem cell research.

ADVANCING LIFE SCIENCE TOGETHER™

Visit www.millipore.com/stem_cells for more information on this and other ways Millipore supports Life Science research.

THE EXPERTISE OF
CHEMICON® & UPSTATE®
IS NOW A PART OF MILLIPORE

My Tetra Is . . . Leakproof

The Mini-Protean® Tetra cell winged locking mechanism locks out leaks.

The Mini-PROTEAN Tetra systems for mini vertical gel electrophoresis feature an innovative locking mechanism that eliminates leakage issues commonly associated with gel electrophoresis. The patented* design makes it easy to lock handcast or precast gels into the electrophoresis module, ensuring leakproof operation and accurate experimental data. Designed to run as many as four SDS-PAGE gels simultaneously, the Mini-PROTEAN Tetra systems offer high throughput and a unique design to meet all your electrophoresis needs.

Key Features

- Patented locking system to eliminate leaks
- Capacity to run up to 4 mini SDS-PAGE gels
- Easy conversion from electrophoresis cell to blotting apparatus
- Error-proof design to ensure correct polarity and orientation

* U.S. patent 6,436,262.

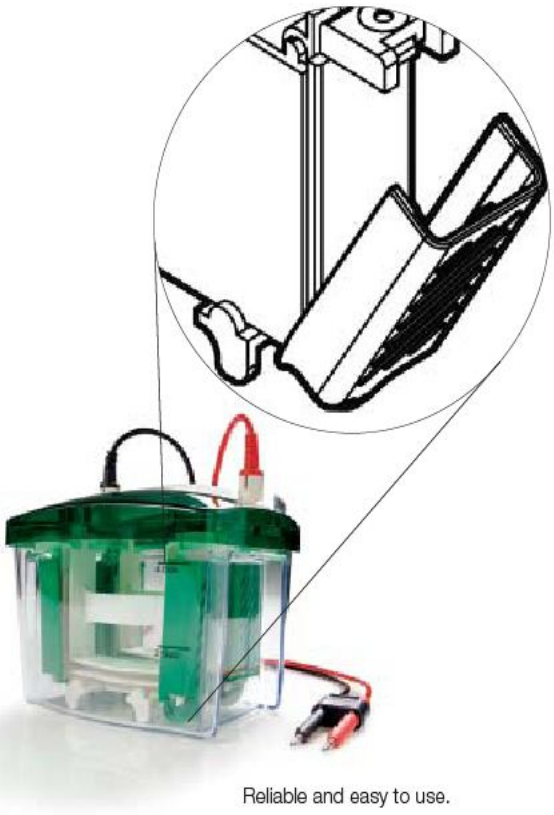

Reliable and easy to use.

Gene Knockdown guaranteed.

HuSH-29™ shRNA Expression Plasmids

- All shRNA vectors delivered as 5 ug of highly purified, transfection-ready plasmid DNA. No plasmid preparation required.
- The successful use of OriGene shRNA vectors have been recently cited
- OriGene shRNAs can be rapidly validated in HEK293T cells together with OriGene TrueClone cDNAs

Downregulation of HIF1A Expression by HuSH Contructs

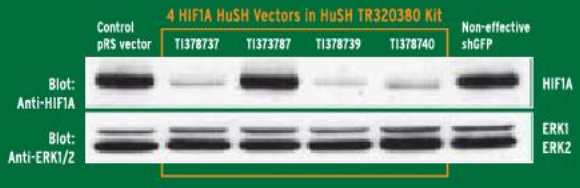

HEK239T cells were contransfected with pCMV-HIF1A cDNA together with four shRNA contructs against HIF1A. Western blot data demonstrates that three out of the four constructs significantly downregulates the cotransfected HIF1A expression.
More details can be found at www.origene.com/rna

ORIGENE
Your Gene Company

1-888-267-4436 • origene.com

Nature Publishing Group
The Macmillan Building,
4 Crinan St, London N1 9XW, UK
e-mail: nature@nature.com

NATURE'S MISSION, 1869:
'The objective which it is proposed to attain by this periodical may be broadly stated as follows. It is intended, first, to place before the general public the grand results of scientific work and scientific discovery; and to urge the claims of science to move to a more general recognition in education and in daily life…Secondly, to aid scientific men [sic] themselves, by giving early information of all advances made in any branch of natural knowledge throughout the world, and by affording them an opportunity of discussing the various scientific questions which arise from time to time.'

Nature's mission statement was updated in 2000:
www.nature.com/nature/about

Submissions and Guide to Authors:
www.nature.com/nature/authors

Author and referee policies and services:
www.nature.com/authors

Nature® (ISSN 0028-0836) is published weekly on Thursday, except the last week in December, by Nature Publishing Group, a division of Macmillan Publishers Ltd (The Macmillan Building, 4 Crinan Street, London N1 9XW). Registered as a newspaper at the British Post Office.
US Periodicals postage paid at New York, NY, and additional mailing post offices.
North and South American orders to: *Nature*, Subscription Dept, 342 Broadway PMB 301, New York NY 10013-3910, USA. Other orders to *Nature*, Brunel Road, Basingstoke, Hants RG21 2XS, UK.

Identification code for *Nature*: 0028-0836/03.
US POSTMASTER: send address changes to *Nature*, Subscription Dept, 342 Broadway PMB 301, New York, NY 10013-3910, USA; CPC PUB AGREEMENT #40032744.
Published in Japan by NPG Nature Asia-Pacific, Chiyoda Building, 2-37 Ichigayatamachi, Shinjuku-ku, Tokyo 162-0843, Japan.

nature publishing group

nature

J. CAMPBELL, AERO-NEWS NETWORK/NASA

Putting theory into practice: the physics of gravity, p. **130**.

GETTY

A blast from the past — but the threat remains, pp. **107**, **114**.

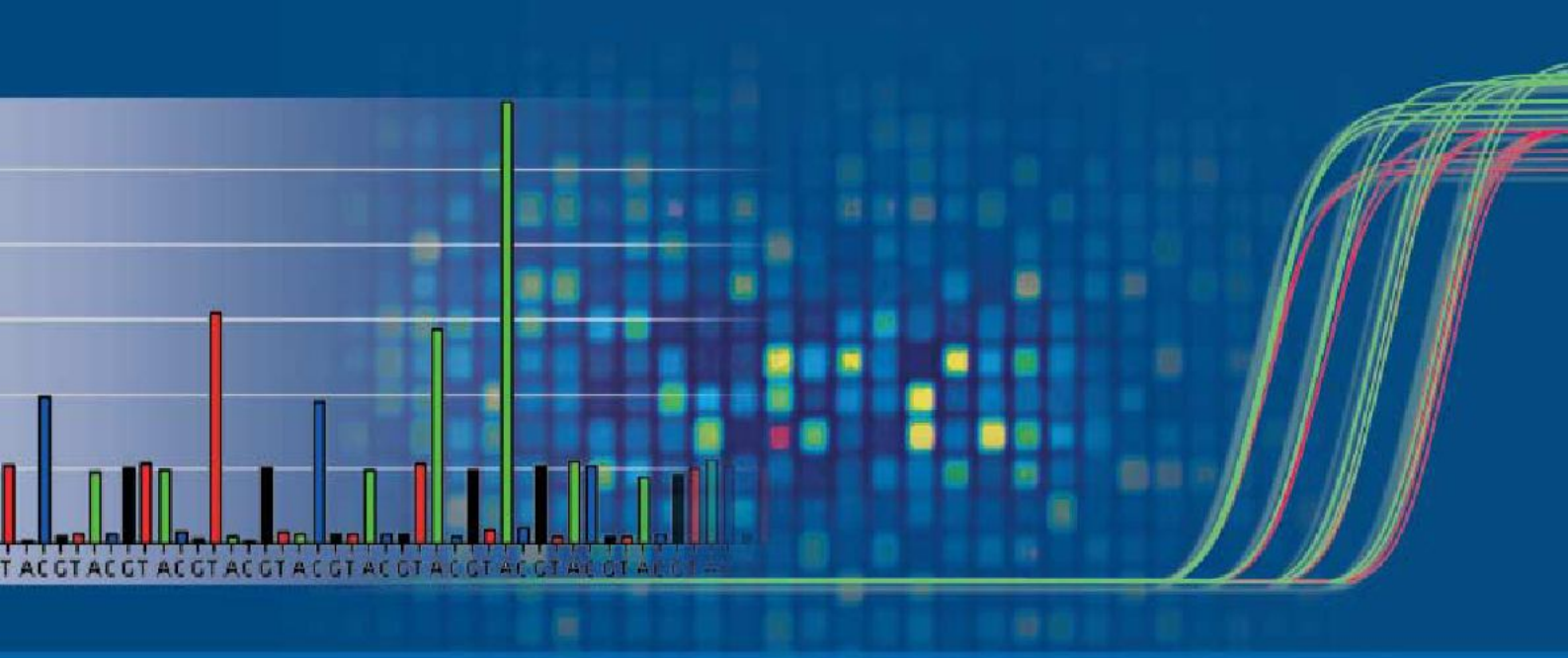

www.roche-applied-science.com

Enabling Technologies for Genomics Discovery

From Genome to Gene Function

Stay on the forefront of genomics research with Roche Applied Science's precision-engineered instruments, new applications, and innovative technologies. We combine world-class technologies for sequencing, microarrays, and real-time PCR with our extensive high-quality reagents portfolio and well-known reputation for committed product support, providing you with the most comprehensive toolkit available:

454 SEQUENCING

Genome Sequencer FLX System
Sequence DNA with an unparalleled combination of data completeness and speed.

NimbleGen®

NimbleGen™ DNA Microarrays
Target and evaluate whole genomes or specific regions of interest with long oligos at high resolution (2.1 million probes).

LightCycler®

LightCycler® 480 Real-Time PCR System
Use real-time PCR to quantify genes and to detect genetic variation.

Discover... Analyze... Validate.
Visit ***www.roche-applied-science.com*** for more information or to find a local representative.

Roche Diagnostics GmbH
Roche Applied Science
68298 Mannheim, Germany

Roche

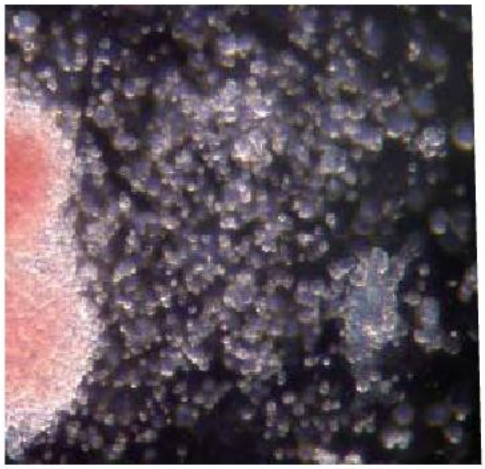

The production of cells with developmental potential on a par with embryonic stem cells from adult human tissue marks the start of a new era in stem cell research, pp. **141**, **135**.

ARTICLES

LETTERS

An RNA template guides genome-wide DNA rearrangements in the protozoan *Oxytricha trifallax*, p. **153**.

NATURE ONLINE

ADVANCE ONLINE PUBLICATION

PUBLISHED ON 9 JANUARY 2008

Histone H2AX-dependent $GABA_A$ receptor regulation of stem cell proliferation
M Andäng, J Hjerling-Leffler, A Moliner, T K Lundgren, G Castelo-Branco, E Nanou, E Pozas, V Bryja, S Halliez, H Nishimaru, J Wilbertz, E Arenas, M Koltzenburg, P Charnay, A El Manira, C F Ibañez & P Ernfors
doi:10.1038/nature06488

Lethargus is a *Caenorhabditis elegans* sleep-like state
D M Raizen, J E Zimmerman, M H Maycock, U D Ta, Y-j You, M V Sundaram & A I Pack
doi:10.1038/nature06535

THIS WEEK'S PODCAST

This week's podcast features the discovery that a well known human pathogen contains 'the wrong kind of hormone'. *Toxoplasma gondii* uses an apparently hijacked plant hormone in a metabolic pathway involved in the switch between dormancy and active growth. As we don't seem to have borrowed this hormone, it may be a good point of attack for antitoxoplasmosis drugs.
www.nature.com/podcast

THIS ISSUE

STEM CELLS GET PERSONAL Another important step in the rapidly developing world of human stem cells is reported in this issue. Human cells taken from adult donors have been reprogrammed to produce iPS (induced pluripotent stem) cells, resembling embryonic stem cells in their main characteristics. It may soon be possible to use such procedures routinely to isolate patient-specific cells in culture. [Article p. **141**; News & Views p. **135**]

V. GOOD? Is the world ready for a *Bridget Jones' Diary* for scientists? Publishers Delacorte Press seem to think so: the cover of *A Version of the Truth*, by Jennifer Kaufman and Karen Mack, has the authentic 'chick lit' feel of the best-selling journal. It's reviewed in Books & Arts this week, together with two more fact-oriented examples of the emerging 'science-as-fiction' genre. [Books & Arts p. **128**]

SHAPING UP Bacteria were once regarded as little more than variously shaped vessels in which the basic chemistry of life can proceed in a protected environment. But in the past decade it has become clear

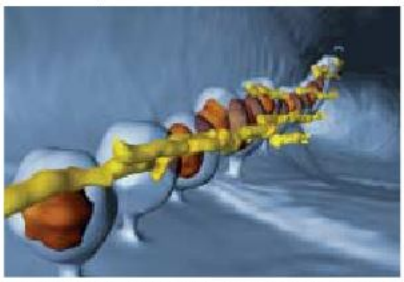

Z. LI/G. JENSEN, CALTECH

Hidden depths: there's structure aplenty in bacteria.

that there is much more to it than that, and the era of bacterial cell biology is now upon us. Bacterial cells have an organized and dynamic subcellular architecture, complete with cytoskeletal proteins and molecular organization very like that of eukaryotes. In fact, for many fundamental aspects of cellular organization, bacteria may be the best place to start asking the questions. [News Feature p. **124**]

RNA IN CHARGE The ciliate *Oxytricha trifallax* cuts up and removes most of its nuclear DNA during one developmental stage, stitching 5% of its chromosomes back together at specific points. Nowacki *et al.* have made the extraordinary discovery that maternal RNA remaining in the new cell can act as a template for the chromosomal rearrangements, as shown by the disruption caused when several RNAs are removed from the cell. This points to a new role for RNA in genome rearrangement *in vivo*. [Article p. **153**; News & Views p. **131**]

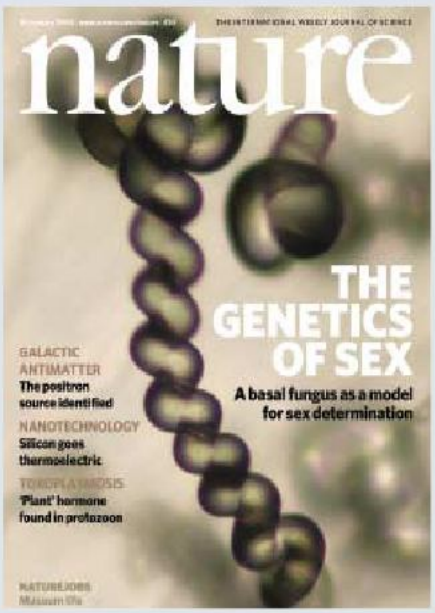

The fungus *Phycomyces blakesleeanus* is perhaps best known as the light-sensing model pioneered by Nobel laureate Max Delbrück. Work reported in this issue may raise its profile as a model in a different area, the development of sex determination. In this, as in other fungi, sex determination is not controlled by a whole chromosome, but by a small region of the genome. A combined genomic, genetic, molecular and bioinformatic approach has been used to identify this sex locus. Two genes are involved, encoding transcription factors that, like the SRY protein involved in sexual differentiation in humans, contain a high mobility group domain. In addition, a set of repetitive elements is found only on the chromosome containing the sex locus, suggesting a general mechanism for the early steps in the evolution of sex determination and sex chromosome structure in eukaryotes. On the cover, a spiralled hypha of a *Phycomyces* strain in which both *sexM* and *sexP* genes are co-expressed to induce the formation of this pseudo-sexual structure. [Letter p. **193**]

Local antimatter unveiled

Antimatter is not an exotic rarity found only in the depths of the Universe: there are large quantities in our own Galaxy. We know this because we see the 511-keV γ-ray emission line, a signature of electron–positron annihilation, coming from the general direction of the Galactic Centre. The origin of the positrons has remained a mystery, but the distribution of the annihilation line radiation provides a clue. Astronomers now have the tools that can work out that distribution, and analysis of more than four years of spectroscopic data from the INTEGRAL satellite reveals an unexpected distribution of the 511-keV γ-ray emission from the inner Galactic disk, suggesting that the positrons originate in binary stars containing black holes or neutron stars. [Letter p. **159**]

Silicon goes thermoelectric

Thermoelectric materials, capable of converting a thermal gradient to an electric field and vice versa, could be useful in power generation and refrigeration. But the fabrication of the available high-performance thermoelectric materials is not easily scaled up to the volumes needed for large-scale heat energy scavenging applications. Nanostructuring improves thermoelectric capabilities of some materials, but good thermoelectric materials tend not to take readily to nanostructuring. How about silicon? It can be processed on a large scale but has poor thermoelectric properties. Two groups now show that silicon's thermoelectric properties can be vastly improved by structuring it into arrays of nanowires and carefully controlling nanowire morphology and doping. So with more development, silicon may have potential as a thermoelectric material. [Letters pp. **163**, **168**; News & Views p. **137**]

The wrong kind of hormone?

Calcium signalling plays an important role in determining the virulence of the human pathogen *Toxoplasma gondii*, an apicomplexan protozoon. A study of the mechanisms involved has uncovered a surprising agent for this signalling: the plant hormone abscisic acid. Comparative genomics reveals that the pathway for synthesis of the plant hormone

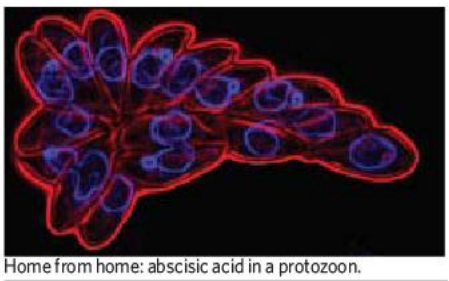

Home from home: abscisic acid in a protozoon.

was acquired by endosymbiosis. This pathway controls a crucial developmental switch between lytic growth and dormancy, which is a key component of pathogenesis. The plant-like nature of this pathway may be exploited to develop new therapeutics as shown by the ability of a specific inhibitor of abscisic acid biosynthesis to protect mice from lethal infection. [Letter p. **207**; www.nature.com/podcast]

Anticancer microRNAs

Recent studies have highlighted global downregulation of microRNAs in cancers,

and have shown that artificial downregulation of all microRNAs can enhance tumour growth. Array-based microRNA profiling of human breast cancer cells that are metastatic to bone and lung now implicates two microRNAs, miR-126 and miR-335, in breast cancer tumorigenesis and metastasis. Loss of miR-335 expression promotes breast cancer cell invasion by targeting the transcription factor *SOX4* and tenascin C, a protein involved in cell adhesion. In breast cancer patients, loss of miR-126 and miR-335 expression is indicative of a poor prognosis. [Article p. **147**]

'Difficult' oil could be a gas

More than half of the world's oil inventory consists of biodegraded heavy oil and tar sand deposits. Recovery of oil from these sources is complicated and expensive. Recent findings suggest that anaerobic bacteria may cause this hydrocarbon degradation, but the actual degradation pathway occurring in oil reservoirs remains obscure. Using a combination of laboratory oil degradation experiments and analysis of oilfield samples, it is now shown that the dominant process of subsurface biodegradation is methanogenesis, involving anaerobic degradation of oil hydrocarbons to produce methane. This suggests an alternative way of exploiting these 'difficult' oilfields: by accelerating the natural hydrocarbon degradation process, it may be possible to recover energy as methane, rather than conventionally as oil. [Letter p. **176**]

Against the flow

Hydrothermal circulation at the axis of mid-ocean ridges occurs when water seeps through fissures on the seafloor and travels down towards molten rock where it warms, finally emerging as super-heated fluid at hydrothermal vents. These vent systems account for much of the heat and mass transfer from the crust to the ocean. It is commonly thought that the direction of circulation in these systems is *across* the ridge axis, with recharge occurring along faults away from the axis. This view is based mainly on modelling. Now, after seven months of monitoring of microearthquake locations beneath a hydrothermal vent field on the East Pacific Rise, Tolstoy *et al.* report that here at least, the hydrothermal down-flow zone is probably located on the ridge axis, with hydrothermal circulation oriented *along* the ridge axis. [Letter p. **181**]

Like shelling worms

Machaeridians are small shell-like fossils, abundant in marine seafloor settings from the early Ordovician to the Carboniferous. Since the fossils were first reported 150 years ago, they have been variously assigned to arthropods, echinoderms, annelids and molluscs. A new find in Morocco resolves these problematic affinities, because the animal's soft parts are well preserved. The 'shells' are in fact calcareous plates, carried as armour on the back of a hitherto unknown form of segmented annelid worm. [Letter p. **185**; News & Views p. **133**]

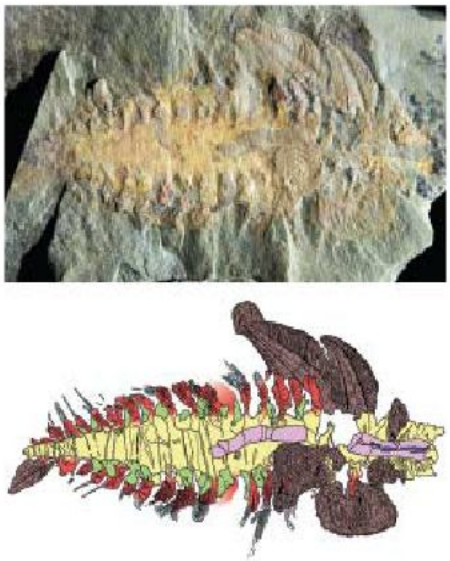

Soft evidence: preserved tissues reveal a worm-like shape.

Choosy about cooperating

If natural selection favours selfish behaviour, how is it that cooperation is so common in many species, including humans? Working with evolutionary simulations, McNamara *et al.* propose a novel evolutionary mechanism based on a positive coevolutionary feedback between cooperativeness and choosiness. If individuals vary in their degree of cooperativeness, and if they can decide whether or not to continue interacting with each other on the basis of their respective levels of cooperativeness, then cooperation can gradually evolve from an uncooperative state. On this model, individual behavioural differences are the key to the evolution of cooperation. [Letter p. **189**]

Key role for superoxides

In chronic granulomatous disease (CGD), phagocytes lack NADPH oxidase activity and are unable to generate superoxide, making sufferers susceptible to recurrent microbial infections. The precise mechanism involved — and the reasons for exaggerated inflammation in CGD — are unclear. Experiments in genetically engineered CGD mice infected with *Aspergillus fumigatus*, a frequent infection in CGD patients, supports the theory that superoxide-dependent conversion of tryptophan to kynurenine is defective in CGD, compromising antimicrobial resistance, inflammation, and T-cell homeostasis through a single, as yet unknown mechanism. The finding raises the possibility that replacement therapy with natural kynurenines might help control pathologic inflammation and susceptibility to infection in CGD patients. [Letter p. **211**]

Abstractions

BOOK REVIEW AUTHOR

Fictional portrayals of scientists conducting cutting-edge research are rarely found on book shop shelves. On page 128, Jennifer Rohn, a cell biologist at University College London and editor of an online forum called LabLit.com dedicated to the genre, reviews three recent novels that feature scientists as protagonists. She spoke to *Nature* about her efforts to improve scientists' fictional standing.

What is LabLit.com and why did you start it?

While doing my PhD, I read a novel about laboratory scientists and was bothered that I couldn't easily find other books like it. You can read fiction about everything else, but scientific research as a topic is rare. Yet science is rife with discovery, competition, jealousy, passion and life-threatening diseases — all makings of a good story. In 2005, I started LabLit.com to generate interest in fictionalized science by shedding light on scientists in their natural habitat.

What does a good work of lab lit need to offer?

Any work of fiction must be a great story with great characters. But I do love it when an author is also able to go into detail about science in an unobtrusive way.

Was it a challenge to review three books?

The challenge was finding a common theme. Two of the books focus on nature — often the subject in instances where science does feature in literature. *A Version of the Truth* by Jennifer Kaufman and Karen Mack is a chick-lit book set in a university animal behaviour department; *The Expeditions* by Karl Iagnemma follows a naturalist expedition of the American west in the nineteenth century.

Do you think publishers are prejudiced against publishing fiction about science?

Yes. Most publishers balk at the idea of publishing a fictional book about science. For example, the book I reviewed with the most scientific detail — *The Gift* by Jon Kalb, which delves into the ruthless world of hominid fossil hunting — was not traditionally published. It is available print-on-demand by the author. I think for this genre there is considerable opportunity for print-on-demand.

What are some lab lit classics?

Cantor's Dilemma by Carl Djerassi, inventor of the contraceptive pill, which is about a Nobel winner falsifying data. And *As She Climbed Across the Table* by Jonathan Lethem, which I think could entertain even the biggest sciencephobe. It's about a physicist who discovers a black hole and falls in love with it, and offers a good sense of how scientists can obsess about their topics. ■

MAKING THE PAPER

Steve Larter

Microbes could provide cleaner energy from Earth's oil reserves.

Geochemist Steve Larter and his colleagues may have found a way to drive energy production from the world's diminishing oil supplies that minimizes damage to the environment. And the process might even be agreeable to the oil industry.

Humans are not the only organisms reliant on Earth's oil supplies. Bacteria found in oil reservoirs both at Earth's surface and below it degrade oil, turning it into a viscous substance that makes recovery and refining more costly and difficult.

Geologists have long known about these oil-degrading microorganisms, but how they go about their business in subsurface oil reservoirs has been a matter of debate. Several studies suggested that oil in these reservoirs is degraded by oxygen-dependent 'aerobic' bacteria using oxygen in meteoric groundwater. But degraded oil has also been found in places with no direct access to oxygen-rich surface water.

Under an oil-industry-funded project called 'Bacchus' (http://tinyurl.com/2ebq7y), Larter, of the University of Calgary in Canada, and his colleagues discovered that anaerobic microorganisms can degrade oil hydrocarbons by fermentation, producing methane as a byproduct.

These organisms react water with hydrocarbons in the oil to produce acetic acid, hydrogen and carbon dioxide; they then combine the H_2 and CO_2 to form methane. "It's literally oil plus water equals life and a little gas," says Larter.

Larter says the work was inspired by a 1999 *Nature* paper (K. Zengler *et al. Nature* **401**, 266–269; 1999). On the basis of results from lab experiments, Zengler and his colleagues had proposed a mechanism for near-surface hydrocarbon degradation by anaerobic microbes.

"Their basic mechanism was broadly correct, but was subtly wrong for subsurface oil reservoirs," says Larter. His team used a combination of microbiological studies, laboratory oil-degradation experiments and case studies from the oilfields of the North Sea, South America, China and western Canada. The western Canadian fields are home to one of the world's largest accumulations of biodegraded oil (see page 176).

At present, the oil industry could use this knowledge of how biodegradation works to predict and target where the less-biodegraded oil is located within reserves. Taking oil from these areas would decrease the use of energy-costly recovery processes, such as steam-assisted gravity drainage, which uses steam to melt oil from reservoir rocks.

But in future, the work of Larter's team could dramatically change the energy-recovery process. The methane produced by the oil-degrading microorganisms provides the same amount of energy as oil, but emits less CO_2 when burned. And the intermediate H_2 — described by Larter as "the holy grail" of alternative energy because it is hard to produce cheaply, but carries no carbon signature — could also be used as fuel.

"If the process could be accelerated and methane or H_2 recovered from oilfields at economic rates, this could be a way for the oil industry to keep doing what it's doing, but move easily and quickly to lower carbon emission energy-recovery routes," he says. Although he admits that at the moment this "seems like a very long shot".

With these prospects still far off, Larter is doing his best to reduce his own carbon footprint. He walks to work and uses public transport. "I wear out lots of boots," he says. ■

FROM THE BLOGOSPHERE

One of the new blogs on the block at Nature Network is 'Stripped Science' (http://network.nature.com/blogs/user/strippedscience), in which Viktor Poór posts short comic strips about lab life. Viktor is a PhD student working on a peptide called hepcidin that is important in iron metabolism.

Working in the lab can be quite boring — repeating the same steps of pipetting or centrifugation all day long — and Viktor wonders what lab life might be like from a bacteria's point of view. He also has some amusing fantasies about fighting boredom in the microscope room. In another strip, he shows how cell-culture contamination can be turned from a frustration into a pastime, and in another, he offers biologists some tips about the best way to spend their time at conferences — and it isn't listening to the presentations, networking or sightseeing.

Stripped Science brings smiles of recognition to Nature Network users, including, no doubt, any bacteria among them. Viktor welcomes comments and suggestions, which you can make online at the blog, now posting at a regular frequency of twice a week. ■

Visit Nautilus for regular news relevant to *Nature* authors ▸ http://blogs.nature.com/nautilus and see Peer-to-Peer for news for peer-reviewers and about peer review ▸ http://blogs.nature.com/peer-to-peer.

nature

Vol 451 | Issue no. 7175 | 10 January 2008 **www.nature.com/nature**

EDITORIAL

LONDON **nature@nature.com**
The Macmillan Building, 4 Crinan Street, London N1 9XW
Tel: +44 (0)20 7833 4000 Fax: +44 (0)20 7843 4596/7
EDITOR-IN-CHIEF: Philip Campbell
PUBLISHING EXECUTIVE EDITOR: Maxine Clarke
EDITORIALS: Philip Campbell, Colin Macilwain
NEWS/FEATURES/ONLINE NEWS: Oliver Morton, Geoff Brumfiel, Daniel Cressey, Michael Hopkin, Nicola Jones, Anna Petherick, Katharine Sanderson, Sarah Tomlin, Gaia Vince
BUSINESS NEWS: Colin Macilwain
BOOKS & ARTS/CORRESPONDENCE & ESSAYS/COMMENTARIES: Sara Abdulla, Joanne Baker, Lucy Odling-Smee, Sarah Tomlin
NEWS AND VIEWS: Tim Lincoln, Andrew Mitchinson, Sadaf Shadan, Richard Webb
PHYSICAL, CHEMICAL AND EARTH SCIENCES: Karl Ziemelis, Rosamund Daw, Joshua Finkelstein, Magdalena Helmer, Juliane Mössinger, Karen Southwell, Joanna Thorpe, John VanDecar, Liesbeth Venema
BIOLOGICAL SCIENCES: Ritu Dhand, Lesley Anson, Tanguy Chouard, Henry Gee, Marie-Thérèse Heemels, Rory Howlett, Claudia Lupp, Barbara Marte, Deepa Nath, Ursula Weiss **INSIGHTS/REVIEWS/PROGRESS:** Lesley Anson
SUBEDITORS: Colin Sullivan, Sarah Archibald, Catherine Cassidy, Davina Dadley-Moore, Isobel Flanagan, Paul Fletcher, Jenny Gillion, Dinah Loon, David Price, Chris Simms, Anna York
EDITORIAL PRODUCTION: James McQuat, Alison Hopkins, Marta Rusin, Charles Wenz, Lauren Wethmar **MANUFACTURING PRODUCTION:** Jenny Henderson, Stewart Fraser, Susan Gray, Jocelyn Hilton, Yvonne Strong
ART AND DESIGN: Martin Harrison, Wesley Fernandes, Madeline Hutchinson, Barbara Izdebska, Paul Jackman, Fern McNulty, Nik Spencer
ADMINISTRATION: Pauline Haslam, Karen Jones, Helen Anthony, Lisa Griffin, Jayne Henderson, Aimee Knight, Alison McGill, Jenny Meyer, Alison Muskett, Nichola O'Brien
PRESS OFFICE: Ruth Francis, Katherine Anderson, Rachel Twinn

WASHINGTON DC **nature@natureDC.com**
968 National Press Building, 529 14th St NW, Washington DC 20045-1938
Tel: +1 202 737 2355 Fax: +1 202 628 1609
EDITORIAL: Eric Hand, Gene Russo, Leslie Sage, Jeff Tollefson, Alexandra Witze
ADMINISTRATION: Katie McGoldrick, Kenneth Simpson

NEW YORK **nature@natureny.com**
75 Varick St, 9th Floor, New York, NY 10013-1917
Tel: +1 212 726 9200 Fax: +1 212 696 9006
EXECUTIVE EDITOR: Linda Miller
EDITORIAL: I-han Chou, Chris Gunter, Kalyani Narasimhan, Helen Pearson

BOSTON **nature@boston.nature.com**
25 First Street, Suite 104, Cambridge, MA 02141
Tel: +1 617 475 9275 Fax: +1 617 494 4960
EDITORIAL: Angela Eggleston, Joshua Finkelstein, Heidi Ledford **ADMINISTRATION:** Eric Schwartz

SAN FRANCISCO **nature@naturesf.com**
225 Bush Street, Suite 1453, San Francisco, CA 94104
Tel: +1 415 403 9027 Fax: +1 415 781 3805
EDITORIAL: Erika Check Hayden, Natalie DeWitt, Alex Eccleston
ADMINISTRATION: Jessica Kolman

SAN DIEGO **r.dalton@naturesf.com**
3525 Del Mar Heights Road, PMB No. 462, San Diego, CA 92130
Tel: +1 858 755 6670 Fax: +1 858 755 8779
EDITORIAL: Rex Dalton

MUNICH **a.abbott@nature.com**
Josephspitalstrasse 15, D-80331 München
Tel: +49 89 549057-13 Fax: +49 89 549057-20
EDITORIAL: Alison Abbott, Quirin Schiermeier

PARIS **d.butler@nature.com**
2 rue Moreau Vincent, 37270 Véretz Tel: +33 2 47 35 72 15
EDITORIAL: Declan Butler

TOKYO **editnature@natureasia.com**
Chiyoda Building 5-6th Floor, 2-37 Ichigaya Tamachi, Shinjuku-ku, Tokyo 162-0843
Tel: +81 3 3267 8751 Fax: +81 3 3267 8754
EDITORIAL: David Cyranoski, Mika Nakano, Akemi Tanaka

CONTRIBUTING CORRESPONDENTS
AUSTRALASIA: Carina Dennis Tel: +61 2 9404 8255
INDIA: K. S. Jayaraman Tel: +91 80 2696 6579
ISRAEL: Haim Watzman Tel: +972 2 671 4077
SOUTH AFRICA: Michael Cherry Tel: +27 21 886 4194
WASHINGTON DC: Meredith Wadman Tel: +1 202 626 2514
MISSOURI: Emma Marris Tel: +1 573 256 0611

NATURE ONLINE

www.nature.com/nature

CHIEF TECHNOLOGY OFFICER: Howard Ratner **PUBLISHING DIRECTOR, NATURE.COM:** Timo Hannay
WEB PRODUCTION/DESIGN: Jeremy Macdonald, Glennis McGregor, Alexander Thurrell
WEB PRODUCTION TECHNOLOGIES: Heather Rankin **APPLICATION DEVELOPMENT:** Peter Hausel
NATURE PODCAST: Adam Rutherford, Kerri Smith, Sara Abdulla

PUBLISHING

LONDON **feedback@nature.com**
The Macmillan Building, 4 Crinan Street, London N1 9XW
Tel: +44 (0)20 7833 4000 Fax: +44 (0)20 7843 4596/7
MANAGING DIRECTOR: Steven Inchcoombe
PUBLISHER: Sarah Greaves
ASSISTANT PUBLISHER: Samia Mantoura **PUBLISHING ASSISTANT:** Claudia Banks

TOKYO **feedback@natureasia.com**
Chiyoda Building 5-6th Floor, 2-37 Ichigaya Tamachi, Shinjuku-ku, Tokyo, 162-0843
Tel: +81 3 3267 8751 Fax: +81 3 3267 8754
PUBLISHING DIRECTOR — ASIA-PACIFIC: David Swinbanks
ASSOCIATE DIRECTOR — ASIA-PACIFIC: Antoine E Bocquet

DISPLAY ADVERTISING

MANAGEMENT: John Michael

NORTH AMERICA **display@natureny.com**
NEW ENGLAND: Sheila Reardon
Tel: +1 617 494 4900 Fax: +1 617 494 4960
NEW YORK/MID-ATLANTIC/SOUTHEAST: Jim Breault
Tel: +1 212 726 9334 Fax: +1 212 696 9481
MIDWEST: Mike Rossi
Tel: +1 212 726 9255 Fax: +1 212 696 9481
WEST: George Lui
Tel: +1 415 781 3804 Fax: +1 415 781 3805

EUROPE/REST OF WORLD **display@nature.com**
GERMANY/SWITZERLAND/AUSTRIA: Sabine Hugi-Fürst
Tel: +41 52 761 3386 Fax: +41 52 761 3419
UK/IRELAND/DENMARK/FRANCE/BELGIUM/EASTERN EUROPE: Jeremy Betts
Tel: +44 (0)20 7843 4959 Fax: +44 (0)20 7843 4749
SCANDINAVIA (EXCL. DK)/THE NETHERLANDS/ITALY/SPAIN/PORTUGAL/ISRAEL/ICELAND:
Graham Combe Tel: +44 (0)20 7843 4969 Fax: +44 (0)20 7843 4749

JAPAN **display@natureasia.com**
Kate Yoneyama, Ken Mikami
Tel: +81 3 3267 8765 Fax: +81 3 3267 8746

SPONSORSHIP

EUROPE/NORTH AMERICA **e.green@nature.com**
NATURE BUSINESS DEVELOPMENT EXECUTIVE: Emma Green
Tel: +44 (0)20 7833 4000 Fax: +44 (0)20 7843 4749

NATUREJOBS

naturejobs@nature.com

Please refer to panel at the start of the *NatureJobs* section at the back of the issue.

MARKETING & SUBSCRIPTIONS

USA/CANADA/LATIN AMERICA **subscriptions@natureny.com**
Nature Publishing Group, 75 Varick St, 9th Floor, New York, NY 10013-1917
Tel: (USA/Canada)+1 866 363 7860; (outside USA/Canada) +1 212 726 9365
MARKETING: Sara Girard **FULFILMENT:** Karen Marshall

JAPAN/CHINA/KOREA **subscriptions@natureasia.com**
Chiyoda Building 5-6th Floor, 2-37 Ichigaya Tamachi, Shinjuku-ku, Tokyo, 162-0843
Tel: +81 3 3267 8751 Fax: +81 3 3267 8746
MARKETING/PRODUCTION: Keiko Ikeda, Takesh Murakami

EUROPE/REST OF WORLD **subscriptions@nature.com**
Nature Publishing Group, Subscriptions, Brunel Road, Basingstoke, Hants RG21 6XS, UK
Tel: +44 (0)1256 329242 Fax +44 (0)1256 812358
MARKETING: Katy Dunningham, Elena Woodstock

INDIA **npgindia@nature.com**
Nature Publishing Group, 3A, 4th Floor, DLF Corporate Park, Gurgaon 122002
Tel: +91 124 2881053/54 Fax: +91 124 2881052
HEAD OF BUSINESS DEVELOPMENT, INDIA: Jaishree Srinivasan **MARKETING:** Harpal Singh Gill

Annual subscriptions (including post and packing)

INSTITUTIONAL/CORPORATE RATE:	$2,730
PERSONAL RATE:	$199
STUDENT RATE:	$99
POSTDOC RATE:	$119

Printed in USA. Individual rates available only to subscribers paying by personal check or credit card. Orders for student/postdoc subscriptions must be accompanied by a copy of student ID. Rates apply to USA, Canada, Mexico/Central & South America.
Add 7% GST tax in Canada (Canadian GST number 140911595).
BACK ISSUES: US$20.00.

SITE LICENSES, FULFILMENT & CUSTOMER SERVICES

feedback@nature.com

SITE LICENSES: npg.nature.com/libraries
FULFILMENT: Dominic Pettit
CUSTOMER SERVICE: Gerald Coppin

Fill up on the latest research.

Sign up for monthly Table of Contents e-alerts from *Obesity* and receive the latest research and news delivered directly to your desktop at no charge.

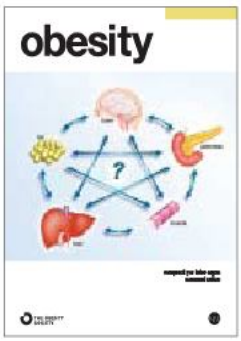

It's as easy as 1, 2, 3

1. Log on to www.nature.com/obesity

2. Register by clicking on the E-alert sign up tab at the top of the screen

3. Watch as the latest news and research is delivered directly to your inbox

www.nature.com/obesity

nature publishing group npg

nature REPORTS climate change
the news behind the science, the science behind the news

The Climate Change Podcast

Tune in over the next three months for interviews with the people behind the science, insights from journalists covering the research, and opinions from climate experts.

Each of the three monthly shows will report on issues before, during, and after the UN Climate Conference in Bali.

In the first instalment, discover elements that could tip us over into dangerous climate change, look at the future for the IPCC, and learn how the ´escalator effect' is killing off species.

Free to download from the *Nature Reports Climate Change* website
www.nature.com/climate

Produced with support from NERC

NATURAL ENVIRONMENT RESEARCH COUNCIL

nature publishing group npg

nature

www.nature.com/nature

Vol 451 | Issue no. 7175 | 10 January 2008

Resurgent nuclear threats

The world faces great risks from nuclear weapons that need to be urgently addressed by political leaders and scientists worldwide. There is now a window of opportunity to do so.

If any reminder was needed of today's nuclear threat, one need look no further than Pakistan, a country that possesses nuclear warheads, is riddled with Islamic extremism and stands on the brink of chaos. The world needs to ask itself the question posed in 2005 by Sam Nunn, former chairman of the Senate Armed Services Committee: on the day after a nuclear weapon goes off in one of our cities, what would we wish we had done to prevent it? That question challenges not only politicians but also those scientists who have the expertise and influence to help.

An analysis on page 114 explores the current status of the international framework to combat the new threats. It will be followed in weeks to come by articles that analyse aspects of the issue, and address what can be done.

Non-proliferation is a broad and complex issue, but the main imperatives for progress are all too starkly clear: no new nuclear weapons or weapons material; no new nuclear-weapons states; no role for nuclear weapons in foreign policy; and no 'loose nukes' — in other words, lock down and secure all existing weapons and stockpiles of weapons-grade material.

Political will is desperately needed, in particular for multilateral and international action. The 1992 US–Russian Cooperative Threat Reduction programme to secure and dismantle weapons and materials of mass destruction was a major step in the right direction, but its internationalization has so far extended to cleaning up a chemical-weapons dump in Albania. In 2004, the United Nations security council adopted a resolution requiring all states to implement national legislation making illegal all non-state activities to develop weapons of mass destruction. This April, states must report to the United Nations on their compliance, but it is expected that only a handful of countries have even begun to implement such legislation, not least because of a lack of hardware, expertise and surveillance.

Manifesto for the future

The cause of nuclear disarmament and non-proliferation was last year taken up by Nunn and three other prominent US statesmen: George Shultz and Henry Kissinger, former secretaries of state, and William Perry, a former secretary of defence. These unlikely political bedfellows, some of whom have previously been staunch advocates of nuclear might, have created a manifesto supporting the above four measures and more (see http://tinyurl.com/23o4ao). They want to take US and Russian missiles off alert, increase warhead cuts, quickly secure weapons material worldwide, ratify the Comprehensive Nuclear-Test-Ban Treaty, ban any further production of nuclear-weapons material worldwide, stop rogue states acquiring military capacities under the guise of nuclear energy, and reinforce considerably the powers of the International Atomic Energy Agency.

All four statesmen are now convinced that, in the context of current threats, the nuclear arsenals of the five official nuclear-weapons states have become more of a liability than an asset. They embrace the position that those states must now, after a decade of fruitless vacillation, take the lead in substantially reducing their own nuclear postures and arsenals. This is not to appease aspiring nuclear powers such as Iran and North Korea, but is a considered strategy to win multilateral support for broader, tougher and faster measures on the major current threats of nuclear terrorism and nuclear proliferation.

The manifesto is both welcome and significant, not least because it represents an America that the world has not seen for too long, and one that could potentially transform international non-proliferation efforts. The proposals have had significant domestic influence, being cited regularly in the current US presidential campaign and broadly adopted as policy by all the leading Democratic candidates. But they have been largely unheard of outside the United States. One urgent need in support of the manifesto is to internationalize it.

"The nuclear arsenals of the five official nuclear-weapons states have become more of a liability than an asset."

Vocal support

Scientists have several critical roles to play. One is simply to be heard, both within government and the forums, but also more publicly, as independent voices — a role whose value was well demonstrated during the cold war between the United States and the Soviet Union. In contrast, for example, scientists and scientific organizations in southeast Asia and in India and Pakistan have not been prominent in issues of disarmament and non-proliferation. This, combined with the lack of non-governmental arms-control organizations in the region, has given the nuclear establishments in India and Pakistan a monopoly over expertise and advice, and inhibited open public debate.

Technological improvements are important too, in particular the enhancement of remote sensing to constantly monitor nuclear facilities. Technology could also help avoid political tensions by removing doubts one way or another about the motivations of a country's nuclear programme.

Scientists also need to work together internationally to develop new ideas. It is depressing that to find such collaboration in this context one has to look to Princeton University in New Jersey to find a programme bringing together Indian and Pakistani researchers to work on the nuclear threat. Here a handful are studying, for example, overly trigger-happy warning systems that could result in accidental firings within a three-minute decision window. They are also seeking to inform national policy-makers on the impact of a limited regional nuclear war, and to look at ways to limit a south Asian arms race.

With US elections this year, and negotiations getting under way for the 2010 review of the nuclear non-proliferation treaty, now is the time for scientists to make themselves heard. ■

Don't panic

Whether to build the International Linear Collider is an open question, but R&D on it should be supported.

Big science has taken a hit in recent budget cuts both in the United States, where significant lay-offs at Fermilab in Batavia, Illinois, are now threatened, and in the United Kingdom, which is to chop tens of millions of pounds over the next few years from astronomy and high-energy physics (HEP) budgets. In both cases, one significant casualty has been participation in the development of the International Linear Collider (ILC; see page 112), the envisaged successor to CERN's Large Hadron Collider (LHC). The latter has suffered delays; and is not likely to see its first useful collisions until 2009. Time to take stock.

The ILC as currently proposed will collide electrons with positrons at energies up to 500 GeV. This is only half of the collision energy originally espoused for such a machine, a reduction necessitated by technological and financial realism. But that reduction has an impact on the machine's potential. The ILC could provide observations that are critical in understanding what the LHC might uncover, but it will not greatly expand the frontiers of the unknown that can be explored.

The HEP community is well experienced at managing costs within budgets and coordinating activities internationally. Based near Geneva, CERN, for example, is the most expensive of the world's three major HEP accelerator centres, and has an annual budget of about US$1 billion. This journal believes that such sums constitute money well spent in principle. That's because these efforts provide the only means to explore in depth ultimate questions about the fundamental matter and forces that make the Universe behave as it does, because such questions inspire many citizens and also because they give rise to technological skills and spin-offs that contribute to nations' economies.

Now imagine three alternative requests for funds in 2011.

- The dream scenario: "The LHC has seen signs of the Higgs sector predicted by well-established models and has also detected a plethora of new particles that indicate that our ideas about deeper symmetries were only partly right, and point the way to understanding the mysterious dark matter and energy that make up most of our Universe. Please give us $X billion over ten years for a machine to explore further."
- The sleepless-nights scenario: "The LHC has seen signs of the Higgs sector but hasn't found the predicted signatures of deeper symmetries. Please give us…"
- The nightmare scenario: "The LHC has seen nothing new. Please give us…"

"These efforts provide the only means to explore in depth ultimate questions about the fundamental matter and forces that make the Universe behave as it does."

Each is likely to stimulate very different responses from physicists' paymasters and from citizens at large.

The HEP community has perhaps rashly developed a substantial sub-community of physicists actively developing the ILC concept. But the community as a whole has weathered strong turbulence from the ups and downs of national budgets over past decades. It is robust enough to do what it now should: cut back but not abandon its futuristic efforts and bide its time for a few years, in the hope and faith that imminent experiments will make a powerful case for long-term investment in whatever machine is appropriate. And countries rightly motivated to support continued R&D on future colliders should seize the unexpected opportunity to take the lead. ■

Spread the word

Evolution is a scientific fact, and every organization whose research depends on it should explain why.

Three cheers for the US National Academy of Sciences for publishing an updated version of its booklet *Science, Evolution, and Creationism* (see www.nap.edu/sec). The document succinctly summarizes what is and isn't science, provides an overview of evidence for evolution by natural selection, and highlights how, time and again, leading religious figures have upheld evolution as consistent with their view of the world.

For a more specific and also entertaining account of evolutionary knowledge, see palaeontologist Kevin Padian's evidence given at the *Kitzmiller* v. *Dover* trial (see http://tinyurl.com/2nlgar). Padian destroys the false assertions by creationists that there are critical gaps in the fossil record. He illustrates the fossil-rich paths from fish to land-based tetrapod, from crocodile to dinosaur to feathered dinosaur to bird, from terrestrial quadruped to the whale, and more besides.

Creationism is strong in the United States and, according to the Parliamentary Assembly of the Council of Europe, worryingly on the rise in Europe (see http://tinyurl.com/2knrqy). But die-hard creationists aren't a sensible target for raising awareness. What matters are those citizens who aren't sure about evolution — as much as 55% of the US population according to some surveys.

As the National Academy of Sciences and Padian have shown, it is possible to summarize the reasons why evolution is in effect as much a scientific fact as the existence of atoms or the orbiting of Earth round the Sun, even though there are plenty of refinements to be explored. Yet some actual and potential heads of state refuse to recognize this fact as such. And creationists have a tendency to play on the uncertainties displayed by some citizens. Evolution is of profound importance to modern biology and medicine. Accordingly, anyone who has the ability to explain the evidence behind this fact to their students, their friends and relatives should be given the ammunition to do so. Between now and the 200th anniversary of Charles Darwin's birth on 12 February 2009, every science academy and society with a stake in the credibility of evolution should summarize evidence for it on their website and take every opportunity to promote it. ■

Unlock the Power of Gene Expression Analysis with the Right Combination

TaqMan® Arrays and the 7900HT Fast Real-Time PCR System. The Superior, Single-Solution for High-Throughput Gene Expression Analysis.

Achieve optimal performance and flexibility in high-throughput gene expression analysis when you combine TaqMan® Arrays with the 7900HT Fast Real-Time PCR System. Choose from pre-designed TaqMan® Gene Signature Arrays, configurable TaqMan® Gene Sets, or TaqMan® Custom Arrays. Each format offers the accuracy, reproducibility, and specificity you expect from an industry leader. Experience high-throughput and performance synergy in a winning combination.

TaqMan® Arrays:

- Convenient for disease target classes and pathways
- Proven quality, speed, and ease-of-use
- Pre-loaded with TaqMan® Gene Expression Assays
- Increased sensitivity and precision
- Ideal for small and archival tissue samples
- Low sample consumption
- 384-well loading without liquid-handling robotics

7900HT Fast Real-Time PCR System

- Proven gold standard, industry-leading performance
- Interchangeable block formats offer easy application adaptability and flexibility
- Seamless integration with TaqMan Arrays
- Automation Accessory provides hands-free plate-loading and unloading for 24-hour operation
- Powerful software tools enable high quality data analysis

Access more information at www.7900HT.com

Applied Biosystems

For Research Use Only. Not for use in diagnostic procedures.

Practice of the patented 5′ Nuclease Process requires a license from Applied Biosystems. The purchase of the TaqMan® Array includes an immunity from suit under patents specified in the product insert to use only the amount purchased for the purchaser's own internal research when used with the separate purchase of an Authorized 5′ Nuclease Core Kit. No other patent rights are conveyed expressly, by implication, or by estoppel. For further information on purchasing licenses contact the Director of Licensing, Applied Biosystems, 850 Lincoln Centre Drive, Foster City, California 94404, USA. The TaqMan® Array is covered by U.S. Patents Nos. 6,514,750, 6,942,837, 7,211,443, and 7,235,406. Microfluidic Card developed in collaboration with 3M Company. The Applied Biosystems 7900HT Fast Real-Time PCR System is a real-time thermal cycler covered by one or more of US Patents Nos. 6,814,934, 5,038,852, 5,333,675, 5,656,493, 5,475,610, 5,602,756, 6,703,236, 6,818,437, 7,008,789, 6,563,581, 6,965,105 and 6,719,949 and corresponding claims in their non-US counterparts, owned by Applera Corporation. No right is conveyed expressly, by implication or by estoppel under any other patent claim, such as claims to apparatus, reagents, kits, or methods such as 5′ nuclease methods. Further information on purchasing licenses may be obtained by contacting the Director of Licensing, Applied Biosystems, 850 Lincoln Centre Drive, Foster City, California 94404, USA.

RESEARCH HIGHLIGHTS

NEUROBIOLOGY

Sleep stimulation

Nature Med. doi:10.1038/nm1693 (2007)

Drugs that target the neurotransmitter adenosine could one day replace or enhance brain implants to calm the tremors that are symptomatic of Parkinson's disease.

Deep brain stimulation is a technique that uses electrodes to deliver electrical impulses to specific regions far inside the brain. Lane Bekar and Maiken Nedergaard of the University of Rochester in New York and their colleagues have found that adenosine, which is associated with sleepiness, is crucial to the technique's beneficial effects.

The researchers used a drug to induce symptoms of Parkinson's disease in mice, then showed that the tremors could be dampened by treating the animals with adenosine. They also found that dosing the mice with a compound that blocks adenosine receptors exacerbated the tremors.

NANOTECHNOLOGY

Memory sticks

Nature Nanotech. doi:10.1038/nnano.2007.417 (2008)

Carbon nanotubes have often been tipped as contenders in the race to replace silicon computing with something faster and smaller. Gehan Amaratunga at the University of Cambridge, UK, and his colleagues have now produced a memory device that works by bending one nanotube towards another.

They developed a tiny capacitor in which one carbon nanotube can store electric charge. A second nanotube generates 'on' and 'off' states when a voltage is applied by bending enough to touch the first nanotube, charging the first nanotube up.

Although they have put information onto the device, the authors have not yet tried to read it back. But because their system works similarly to computer memory in widespread use today, they propose that conventional circuits linked to the device might be able to read the data.

D. NASH

J. HATLEBERG/SMITHSONIAN INST.

The red in the blue

Geology 36, 83–86 (2008)

The Hope Diamond (pictured), the largest known deep blue diamond in the world, glimmers red for several minutes after exposure to ultraviolet light.

Contrary to expectation, almost all natural blue diamonds phosphoresce red as well as blue or green light, and the colour and duration of their glow creates a fingerprint unique to every gem. The phosphorescence patterns arise from defects in the diamonds' chemical structures, which affect how radiation — in this case ultraviolet light — bumps electrons into higher energy states and how that energy is released as photons.

Sally Eaton-Magaña at the Naval Research Laboratory in Washington DC and her team arrived at this conclusion after measuring the phosphorescence of the Hope and 66 other natural blue diamonds. No man-made or treated diamonds phosphoresced red in the experiment. The researchers propose that spectrometers could be used to authenticate stolen blue diamonds and tell natural gems from synthetic ones.

EVOLUTION

Chemical arms-race

Science 319, 88–90 (2008)

Caterpillars of the Alcon blue butterfly (*Maculinea alcon*; pictured below (left) with *Myrmica rubra*) trick ants into caring for them by mimicking the surface chemistry of ant larvae. Researchers have found that the bluff locks Alcon blues and the ants they parasitize into localized evolutionary arms races.

David Nash at the University of Copenhagen in Denmark and his co-workers discovered that the more caterpillars 'taste' like their potential hosts, the quicker they fool ants into 'adopting' them. The team studied several ant colonies of either *Myrmica ruginodis* or *Myrmica rubra*. The chemical signatures of the first species' larvae were similar across its populations, because of regular gene flow between them, so colonies in the Alcon blues' range were more or less equally susceptible to the free-riding caterpillars.

But there was more variation among the colonies of the second type of ant that share habitat with the Alcon blue than in those that did not. This species rarely exchanges genetic information between colonies, and this finding suggests that the parasitized ants are under pressure to evolve against the butterfly, which responds by countering the ants' evolutionary innovations.

MATERIALS SCIENCE

Forbidden zone

Phys. Rev. Lett. 99, 235503 (2007)

Why do some solids grow with 'forbidden' fivefold and twelvefold symmetries, which cannot be produced by any regular stacking of atoms, when rearranging their atoms into perfect crystals would be thermodynamically more stable?

Aaron Keys and Sharon Glotzer of the University of Michigan, Ann Arbor, have performed computer simulations to explain how these 'quasicrystals' form.

Like crystals, quasicrystals expand from a tiny nucleus of solid that forms

spontaneously in a supercooled liquid. Keys and Glotzer report that a quasicrystal nucleus grows by incorporating ready-formed clusters of atoms with icosahedral shapes, which have five- and twelvefold symmetries and cannot themselves grow indefinitely. This creates packing mismatches. Reorganizing the atoms in the enlarging nucleus to correct for the mismatches is a slow process, and quasicrystal growth outpaces it, preventing the formation of a regularly ordered crystal.

CHEMICAL BIOLOGY

Platinum result

Nature Chem. Biol. doi:10.1038/nchembio.2007.58 (2007)

Common chemotherapy drugs based on platinum, such as cisplatin and oxaliplatin, target different combinations of DNA sequences when that DNA is bound to structures called nucleosomes compared with when it is not, according to Curt Davey and his colleagues at Nanyang Technological University in Singapore.

Nucleosomes comprise bundles of proteins and DNA, and package DNA into chromosomes. Although scientists knew where these drugs act on nucleosome-free DNA, they understood little about how the drugs work in living cells.

The additional details, elucidated with X-ray crystallography, may make the process of screening potential anticancer medicines with fewer side effects than cisplatin and oxaliplatin more efficient. The findings could also help in the design of more specific compounds — if drugs could home in on nucleosomes in certain positions, they could better target relevant genes.

FLUID DYNAMICS

What goes around

Phys. Rev. Lett. **99**, 234302 (2007)

Large-scale ocean flows are often mapped using buoys that broadcast signals to satellites. Yoann Gasteuil and his colleagues at the École Normale Supérieure in Lyon, France, have developed a miniature instrument that freely follows smaller-scale currents.

Their wireless sensor, which measures just over 2 centimetres in diameter, can record the temperature and velocity of its surrounding medium and transmit that information via radio waves. The sensor's density is matched to that of the fluid, so it neither sinks nor floats and is carried along by convection flows.

So far Gasteuil and his team have recorded the size and speed of rising hot plumes and cool sinking ones in a desktop water tank, and have taken measurements of heat transport, which varies considerably between circulation cycles.

ZOOLOGY

Face space

Brain Behav. Evol. doi:10.1159/000108607 (2008)

Certain types of paper wasp are the only insects known to be able to recognize individuals of their own species by the pattern of markings on their faces. A study comparing brain size and structure in wasps with and without this ability might aid zoologists trying to understand the evolution of facial processing in the brain.

E. A. TIBBETTS & J. DALE

Wulfila Gronenberg at the University of Arizona, Tucson, and his co-workers looked at the neural structures of four species of paper wasp, two of which can recognize the faces of wasps of their own species.

The face-recognizing wasps had neither bigger brains nor larger primary visual centres than the others. So telling contrasting facial markings apart may be no more taxing for these insects (such as *Polistes dominulus*, pictured above) than discriminating between different foods or predators, the researchers suggest. If this is the case, it may distinguish the wasps from other creatures capable of facial recognition, and could provide clues to how finely tuned facial processing evolved from primitive brains in 'higher' organisms.

JOURNAL CLUB

Dirk Brockmann
Max-Planck Institute for Dynamics and Self-Organization, Göttingen, Germany

A physicist enthuses about criticality in biological development.

Physicists often overestimate the impact of their work on biological research. A biologist recently joked to me that physicists are rather like consultants: they appear without being asked and don't tell you anything new. As a physicist studying the spread of infectious diseases, I reckon there is some truth in this.

But biologists can underestimate our insights, too. The joke turned my mind to a paper by three physicists who applied the theory around spontaneous symmetry breaking to the development of body axes (J. Soriano *et al. Phys. Rev. Lett.* **97**, 258102; 2006).

Spontaneous symmetry breaking occurs in, for example, a cooling magnetic material. At high temperatures, magnetic spins are randomly arranged, but as the material cools patches form in which the spins are aligned. At a critical temperature, the spins align throughout the material. A small, external magnetic field can then determine the system's fate, setting all the spins in a particular direction.

Soriano and his team studied symmetry breaking in developing hydra — multicellular organisms with clearly defined head and foot ends. Hydra can establish their body axis from a jumbled ball of cells, reminiscent of the way a magnetic material orders its spins as it cools. Patches of cells develop similar gene-expression profiles. This creates a system that is critically sensitive to tiny temperature gradients, which determine the direction of the body axis.

Impressively, Soriano and his team worked out the exponent in the size distribution of cell patches expressing a particular gene as a function of the age of the developing hydra. Through this, they related axis development to other self-organized critical systems physicists study, such as forest fires.

Discuss this paper at **http://blogs.nature.com/nature/journalclub**

NEWS

Accelerator plans stalled after US and UK cuts

The machine on which the world's particle physicists have staked the future of their discipline hangs in the balance owing to budget cuts.

On 18 December, the US Congress passed a spending bill slashing funding for the International Linear Collider (ILC), a 31-kilometre machine to collide electrons with positrons, by three-quarters to just $15 million in 2008, money that has already been spent. The United States pays for around a third of the collider's roughly $100-million–120-million annual global research and development effort. And a week earlier, the United Kingdom announced that it was withdrawing from the project, describing plans for it as "not credible". The decision will help make up an £80-million ($160-million) shortfall at the funding body responsible for UK high-energy physics.

"This makes things look pretty grim for a real international machine."

The situation is "dire", says Barry Barish at the California Institute of Technology in Pasadena, who heads the global design effort. The linear collider's design was scheduled to be finished in 2010 but will now be delayed until at least 2012. "We have to defer, delay and stretch out," he says.

Burton Richter, a Nobel laureate and former director of the Stanford Linear Accelerator in California, says the project is fragmented politically, with international collaboration at a low: "This now makes things look pretty grim for a real international machine."

The linear collider is the planned successor to the Large Hadron Collider (LHC), a proton accelerator scheduled to begin operation at CERN, the European particle-physics laboratory near Geneva, in the next few months. By smashing beams of electrons and positrons at energies of up to 500 GeV, the linear collider will provide a cleaner signal than its LHC counterpart. Barish's team says it will cost around $7 billion.

Given that the LHC has not begun work, it might seem surprising that physicists are planning a next-generation machine. But years of design, environmental assessments and lobbying are required to build such a large and expensive device, says Brian Foster, a physicist at the University of Oxford, UK, who is the project's European director. "These things don't just pop out of the air," he says. "A very large amount of preparatory work is required."

The collider's proponents are organized into three regions — Asia, Europe and the United States. America's main contribution has come from physicists at Fermilab, the high-energy physics laboratory in Batavia, Illinois. But following deep budget cuts, the 170 employees working on the linear collider have been diverted to other projects, says Stephen Holmes, Fermilab's associate director for

FERMILAB

India aims for 'quantum jump' in science

BANGALORE

India's prime minister Manmohan Singh has announced unprecedented funding for science education and research, saying it is a top priority for his government. He has announced a range of schemes to attract students and replenish government agencies' shrinking pool of scientific personnel.

India plans to pay science students.

IISER

"We are planning to fund 30 new Central Universities, five new Indian Institutes of Science Education and Research, eight new Indian Institutes of Technology, and 20 new Indian Institutes of Information Technology," Singh said. In the next five years, he added, India will also be launching 1,600 polytechnics, 10,000 vocational schools and 50,000 skill-development centres. One million schoolchildren will receive science innovation scholarships of 5,000 rupees (US$130) each over the next five years, and 10,000 scholarships of 100,000 rupees per year will go to those enrolling on science degree courses.

Discipline-specific education programmes will be launched in strategic sectors such as nuclear and space sciences "to capture talent at the school leaving stage itself".

Singh unveiled the schemes while opening the week-long 95th Indian science congress, the largest annual meeting of Indian scientists, at Visakhapatnam on 3 January. "We need a quantum jump in science education and research," Singh said. "This agenda can no longer wait. The time has come for action, and I assure you of my highest personal commitment." Singh said a plan for implementing the proposals will be devised in the next six months. Funding the schemes has required a fivefold increase in the education budget for 2007–12.

The science community has largely welcomed the initiatives, although some express caution. "The money must be spent in a short period of time," says Dipankar Chatterji, a molecular biophysicist at the Indian Institute of Science in Bangalore. "This poses a tremendous challenge to the heads of these institutions." ■

K. S. Jayaraman

Budget hole: the International Linear Collider would be built from superconducting cavities.

accelerators. Holmes is unsure why Congress slashed the project's funding, but the US government announced a tighter budget for the rest of science too, in part due to the cost of the Iraq war (see *Nature* **451**, 2; 2008).

Physicists in other partner nations do not expect the withdrawals to undermine their own governments' commitments to the collider. In Japan, this year's budget for high-energy physics is already assured — although the government has not yet decided whether it will support the collider — says Mitsuaki Nozaki, a physicist at KEK, the high-energy accelerator research organizarion in Tsukuba and Asian regional director for the collider's design effort. In Germany, work on the superconducting cavities that make up the core of the accelerator will continue, says Rolf-Dieter Heuer, who heads research at the German electron synchrotron, DESY, in Hamburg.

But the prospects for building the machine are murkier now than at any previous point during its planning. Many had hoped that the United States might offer to host the project at Fermilab, but even before the cuts Raymond Orbach, who heads the US Department of Energy's Office of Science, called for the collider to be delayed until results come from the LHC in a few years' time.

"You need the results from the LHC to say if the ILC energies are high enough," Richter says. "Nobody wants to build a machine that isn't going to do anything."

Keith Mason, who heads the UK Science and Technology Facilities Council, has gone further, saying the plan for the accelerator "is not credible financially, politically or in any other way".

Nevertheless, the project's supporters plan to soldier on. Barish says the group will divert research from the United States in an effort to salvage the design phase, and Foster says UK physicists are campaigning to bring the nation back into the project.

Richter says all eyes are on the US budget for 2009 to see if 2008 was a one-year dip. "If something isn't done in the president's budget submission in February or in some kind of supplemental bill, I think the ILC as we now see it is in very big trouble." ■

Eric Hand and Geoff Brumfiel

See Editorial, page 108.

HAVE YOUR SAY
Comment on any of our news stories, online.
www.nature.com/news

Could global gardening fix climate change?

Using biomass fuel on a massive scale in combination with carbon sequestration could return atmospheric carbon dioxide to pre-industrial levels within decades, according to a new analysis.

Peter Read calls his proposal global gardening. To make it work, an area the size of France and Germany would have to be enlisted for growing biomass fuels for a quarter of a century.

"This is the first time it's been demonstrated that you can manage carbon levels in the atmosphere" using biomass, says Read, an economist at Massey University's Centre for Energy Research in Palmerston North, New Zealand. Such a move may be necessary to avoid abrupt climate change, he says.

Referees at the journal *Climatic Change* rejected Read's paper, but editor Stephen Schneider elected to publish it as an editorial commentary.

"Peter has some very clever and controversial ideas," says Schneider, a climatologist at Stanford University in California. "*Climatic Change* has long been a venue where clever and controversial ideas can get aired — as long as they are in perspective."

"You can manage carbon dioxide using biomass."

Read envisions an array of plantations supplying commodities such as energy and timber, as well as a livelihood for countless communities. A second phase could combine biomass energy with carbon sequestration, moving society to the point where it sequestered more carbon than it emitted.

Gregg Marland, a climate researcher currently working at the International Institute for Applied Systems Analysis in Laxenburg, Austria, has numerous doubts about the proposal, including crop productivity, implementation and land use. He co-authored a commentary suggesting that it's unclear whether Read's vision is "a dream or a nightmare".

But it's still a useful thought experiment, he says. "I think what Peter has done is paint a picture: if we really get into trouble with carbon dioxide, how can we back off?" ■

Jeff Tollefson

SPECIAL REPORT

Nuclear war: the threat that never went away

In the first of a series of articles covering nuclear issues, **Declan Butler** looks at the nuclear non-proliferation treaty and finds that there has never been a better climate for negotiation.

"What gets my juices flowing is my conviction that a terrorist will explode a nuclear bomb in one of our US cities by 2014. And the truth is that this is a preventable catastrophe. It will be despite a wealth of things that we could have done. Afterwards, we will say that we should have done these things — some of which we didn't do at all, or didn't do expeditiously enough."

Graham Allison, director of the Belfer Center for Science and International Affairs at Harvard University in Cambridge, Massachusetts, is one of many in the field of nuclear security acutely aware of how much the world has changed — and of the need to change international approaches to the issue accordingly.

In the 1960s, when the international nuclear non-proliferation treaty (NPT) was negotiated, there were five nations with nuclear weapons and the risk was of full-scale nuclear war.

The new nuclear threats involve smaller numbers of weapons, and come in three flavours: that terrorists will obtain and use a nuclear bomb; that nuclear weapons will be acquired and used by states in regional conflict; and that established nuclear weapons states will blur the line between nuclear and conventional weapons and use nuclear tactical battlefield weapons.

"The nuclear non-proliferation treaty is at a dangerous tipping point."

The NPT is now at a dangerous tipping point, say experts such as Allison, who warn that unless rapid progress is made on non-proliferation issues, there is a real risk of nuclear weapons being used for the first time since the bombing of Hiroshima and Nagasaki. The issues will come to a head at an intergovernmental meeting in 2010 in Vienna, Austria, of the NPT's 189 members. On the table are likely to be controversial proposals to end flouting of the NPT by withdrawing the right that countries have enjoyed to develop civil uranium-enrichment technology — which can be diverted to military ends. Low-enriched uranium fuel would instead be supplied via multilaterally controlled fuel banks and enrichment facilities, under the authority of the International Atomic Energy Agency (IAEA). But the NPT review conference, which is held every five years, will above all be a measure of the international community's resolve to generate much-needed impetus for a suite of wide-ranging related steps designed to reinforce the NPT to deal with current threats.

Consensus on tightening-up the non-proliferation regime will be impossible unless the five official nuclear-weapons states — the United States, Russia, China, France and Britain — agree to take concrete steps to remove nuclear weapons from their security doctrines, to not build new weapons, and to accelerate dismantlement of existing arsenals.

The grand bargain

The original aim of the NPT, which came into force in 1970, was to restrict the weapons to the five countries that already openly possessed them, all of which agreed to take steps to disarm. As part of the 'grand bargain', other states agreed not to develop nuclear weapons, but were guaranteed an 'inalienable right' to use nuclear energy for peaceful purposes, dubbed atoms for peace.

Over the past decade, the nuclear-weapons states' reluctance to embrace their side of the NPT bargain has stalled non-proliferation efforts and countries such as India and Pakistan have tested weapons. Huge progress was made at review conferences in 1995 and 2000, including a package deal of 13 steps to further the NPT's twin goals of non-proliferation and disarmament by the existing nuclear-weapons states, such as a commitment to a Comprehensive Nuclear-Test-Ban Treaty (CTBT) and a Fissile Material Cut-Off Treaty to outlaw the production of new weapons material.

The reaction to the 11 September terrorist attacks in 2001 stopped progress, and the 2005 review conference ended with almost no agreement. "The 13 steps have been rolled back or forgotten about," says Jean du Preez, an arms expert at the Monterey Institute of International Studies in California. Indeed, non-proliferation efforts have if anything gone backwards.

TIME LIFE/DOE/GETTY IMAGES

The United States and China, signatories to the CTBT, have failed to ratify it, and so prevented the treaty entering into force. And the US 2002 Nuclear Posture Review, while making cuts to the country's weapons infrastructure, flew in the face of its NPT commitments by increasing the role of nuclear weapons in its security doctrine and expanding the scenarios in which they might be used to include attacks on countries with biological or chemical weapons.

Nuclear arms-races

North Korea's testing of a nuclear device in 2006, and Iran's possible pursuit of nuclear weapons also pose significant challenges to the NPT. There is risk of a domino effect — if Iran acquires nuclear weapons, so will Saudi Arabia in response, launching a nuclear arms-race in the increasingly volatile Middle East.

Many experts are cautiously optimistic, however, that the current crises in nuclear non-proliferation are concentrating minds in capitals worldwide, and may actually generate a renewed political commitment to disarmament, which could be a springboard to a stronger regime. Momentum for disarmament is growing, particularly in the United States, whose leadership is critical to kick-starting non-proliferation efforts. "The United States

now realizes that if it is to make progress on its own agenda it needs to re-embrace multilateral non-proliferation efforts," says du Preez. Gordon Brown's UK government has also adopted a much more proactive line on disarmament than his predecessor's.

This year's US presidential elections will be critical to the NPT review, and the Democrat candidates have broadly backed a re-engagement with multilateral efforts. "But whoever gets elected, non-proliferation issues will get a much more sympathetic hearing," says Bates Gill, director of the Stockholm International Peace Research Institute in Sweden.

There are two main negotiation tracks emerging in the run-up to 2010. The nuclear-weapons states want to reinterpret the treaty to bring in much tighter restrictions on civil nuclear use, in what may amount to a rethinking of the 'atoms for peace' philosophy that has been the core of the NPT. But such moves are not going to fly with the countries lacking nuclear weapons unless the nuclear-weapons states themselves agree to measures to hold up their part of the NPT bargain.

The predicted expansion of nuclear power for energy generation, entailing an increase in facilities and nuclear material, and the repeated flouting of IAEA safeguards on civil nuclear power, have led to calls for a ban in 2010 on the spread of technologies for uranium enrichment and reprocessing of spent fuel. Such technologies are inherently dual-use, and countries that possess such facilities are, in reality, virtual weapons states, as it takes little to redirect the technology to a weapons programme should they so wish.

Although tougher safeguards could make it more difficult for covert programmes to escape detection, as long as facilities are under national control, a determined state can abuse the system or withdraw from the NPT completely. "The Iran crisis has put the question of national enrichment facilities in the spotlight," says Frank von Hippel, a nuclear-weapons expert at Princeton University in New Jersey.

Hence the NPT agenda is likely to contain a proposal to resuscitate plans from the 1940s to bring enrichment facilities and reprocessing plants under multilateral control, with a restricted number of tightly guarded and controlled facilities acting as fuel banks for other countries. But it is clear from preparatory meetings for the NPT conference that many countries will only support further restrictions if the weapons states make concessions on several key issues. Although 'rogue states' have been the main public focus of non-proliferation, they are only one part the picture. The arms and stockpiles of the weapons states are also a big problem.

NASA/ESA/HUBBLE HERITAGE TEAM

AAS CONFERENCE WATCH
Get blog reports from the American Astronomical Society meeting.
http://blogs.nature.com/news/blog

NPT cheats are nothing new for the treaty, and are at least amenable in theory to containment by diplomacy and sanctions, says Roland Timerbaev, a retired Russian ambassador, and one of the founding fathers of the NPT. In reality, cheats remain outliers and the majority of NPT members stick to the rules. The NPT's success is often overlooked, he adds, saying that without it, some 30–40 states would have acquired weapons. For Timerbaev, the greater risks to the non-proliferation regime are to be found in the continued existence of large nuclear arsenals, in the expansion of nuclear power, and in the huge and inadequately secured stockpiles of weapons-grade fissile material worldwide.

The way forward

There are many steps that could be taken quickly. One is early US ratification of the CTBT to provide impetus for planning the next review of the NPT. Wide ratification of the Fissile Material Cut-Off Treaty, which has lain dormant since its creation in 1995, would commit states to halting any new production of fissile materials. It is seen as the means to bring the unofficial weapons states, India, Pakistan, North Korea and Israel under a verifiable regime.

New reductions in arms remain important, but more crucial in the short term is 'outlawing' not the nuclear weapons themselves but any active role for them in policy. The goal is to reach a norm where it is as unacceptable for a country to have any active role for nuclear weapons as it is now to invoke the use of chemical or biological weapons. This issue of de-emphasis is key for non-weapons states such as South Africa, says du Preez. "If you only have a dozen weapons, but you say you are willing to use them and are making threatening postures, it is the opposite of the modus operandi of the cold war where nukes were a weapon of last resort. There is now a crossing of the line between conventional and nuclear weapons," he says.

The steps to getting rid of nuclear weapons from national security policies are well-trodden, and include the 13 steps to disarmament agreed by the weapons states at the 2000 review conference. What has been missing is political will. With new administrations in the United States, Britain and France, that may be forthcoming at the 2010 NPT review conference. There's a possible perfect storm gathering, says du Preez, and "all it needs is a spark" to re-ignite non-proliferation efforts. ■

See Editorial, page 107.

Imperial College Healthcare NHS Trust

Director of Nursing, London

Attractive Salary

Imperial College Healthcare NHS Trust is the first Academic Health Science Centre in the UK and brings together world class research, teaching and clinical services. This exciting and ground breaking new Trust, created from the merger of Hammersmith Hospitals, St. Mary's NHS Trust and integration with Imperial College London, has in excess of 9,700 staff and a budget of £760 million. The Trust is changing the way the NHS works and improving health outcomes by delivering the highest quality of integrated healthcare research and service provision. With the recent appointment of Professor Stephen Smith as the new Chief Executive, the Trust is now seeking to appoint a Director of Nursing of the highest calibre to help deliver this truly pioneering initiative.

This is a post that will realise your best ambitions, as you bring your experience at, or near, board level to the Trust. The Trust is setting out to be different, so your track record of implementing change and improving performance will be a huge asset. However, successfully improving the care of our patients is the over-riding criterion for the future. You will be a member of the Trust Board and will:

- Ensure that Nursing and Midwifery contributes to the delivery of world class care within the context of integrated research and education.
- Provide professional leadership for Nursing and Midwifery within the Trust.
- Advise the Trust on the implementation and development of nursing and clinical strategies in line with the vision and priorities.
- Act as the Trust lead for Patient Experience, and Patient and Public Involvement across the Trust.

If you have the aspiration, drive and an unquenchable desire to take on such a challenge, then please come and talk to us.

For an informal discussion and a candidate pack, please contact Ian Young, HR Director, on 020 8846 7484, or email him at ian.young@imperial.nhs.uk
To apply, please send your CV to Ian Young, HR Department, 2nd Floor Education Centre, Charing Cross Hospital, Fulham Palace Road, London W6 8RF
Closing date for applications is Friday 25th January.

U121934R

Imperial College Healthcare NHS
NHS Trust

CRG

Head of CRG-PRBB Core Facilities ref. HCF 1207

The Center for Genomic Regulation (CRG, (http://www.crg.es/) is a leading genomics research institute, associated with the University Pompeu Fabra (UPF) and located at the Parc de Recerca Biomèdica de Barcelona (PRBB, http://www.prbb.org/). The CRG contains six research programmes: Gene Regulation, Differentiation and Cancer, Cell Biology and Development, Systems Biology, Genes and Disease and Genomic Bioinformatics, and has a partnership with the EMBL through the Systems Biology programme. The PRBB includes three other institutions devoted to biomedical research: the Department of Life and Health Sciences of the UPF (CEXS/UPF, http://www.upf.edu/cexs/), the Municipal Institute of Medical Research (IMIM, http://www.imim.es/) and the Centre for Regenerative Medicine of Barcelona (CMRB, http://www.cmrbarcelona.org/). To give support to this scientific community the CRG has built state of the art Genomics and Light microscopy facilities, as well as Screening and FACS facilities. New developments contemplate a top of the art proteomics facility.

The CRG is looking for a **Head of Core Facilities** presently located at the CRG and new ones that will be developed to provide services for all scientists of the PRBB and external customers. The candidate should be responsible for the administration and organization of all core facilities, the satisfaction of the customers, continue updating of the facilities to keep them at the forefront of technology, and decisions about new facilities. The Head of Core Facilities will report to the Executive Committee of the CRG, as well as to the PRBB Core Facility Board. The candidate should have a science degree and experience in administration. Previous experience in coordinating and running core facilities will be considered a plus. The candidate should be fluent in English, and knowledge of Spanish and/or Catalan would be desirable.

The CRG offers an open ended contract, submitted to periodic evaluations by the Scientific Advisory Board and ad hoc reviewers, and a competitive salary depending on qualification and experience. The successful candidate will participate in the leading structures of the CRG/PRBB. Applications with a CV, list of publications, a proposal for the structure and management of core facilities, and the addresses of at least three potential referees, should be sent to:

Miguel Beato, Director
Centre de Regulacio Genomica
Dr. Aiguader 88, 08003-Barcelona, Spain
rrhh@crg.es

Applications Deadline: 6 weeks after the publication of this ad.

W121006R

cnio
Centro Nacional de Investigaciones Oncológicas

DIRECTOR - CANCER CELL BIOLOGY PROGRAMME (REF: DCCB)

Spanish National Cancer Research Centre (CNIO)

The Spanish National Cancer Research Centre (CNIO) is establishing a new Cancer Cell Biology Programme committed to advancing discovery into the molecular bases of cancer, with particular emphasis on cellular aspects of cancer development.
We seek an experienced Senior Scientist with a superior record of accomplishment in cancer research to coordinate and lead our new Cancer Cell Biology Programme. Qualifications include a PhD and/or MD degree, an extensive publication record, proven ability to obtain substantial funding and strong leadership qualities. The successful candidate is expected to run his/her own active research group. In addition, he/she will be responsible for identifying and recruiting Senior and Junior group leaders to set up independent research groups within the Programme.

We seek a highly motivated Senior Scientist with:

- A minimum of 15 years of research experience as Head of a competitive research laboratory within the field of cancer cell biology.
- An excellent track record of publications, grant support and experience in coordinating and directing national and international projects.
- Excellent leadership and communication skills to attract other senior and junior investigators to create a cohesive and highly competitive research programme in the general field of Cancer Cell biology.

The CNIO offers:

- The opportunity to be part of one of the few European Cancer Research Centres of excellence that effectively combines basic and applied research.
- An energetic, dynamic working environment with a multidisciplinary approach to cancer research, equipped with state-of-the-art technology and facilities.
- The opportunity to establish, direct and expand a new research programme.
- An attractive benefits package.

Applications must include a detailed CV and synopsis of research experience. To apply contact our Personnel Department directly by Email: Personal@cnio.es quoting the reference DCCB on all correspondence. All enquiries and applications will be treated confidentially.

Centro Nacional de Investigaciones Oncológicas (CNIO)
Melchor Fernández, Almagro, 3, 28029 Madrid, Spain.
Tel: +34 91 2246900, Fax: +34 91 2246980
http://www.cnio.es

W120962R

China bows to public over chemical plant

BEIJING

In an unusual capitulation to public pressure, Beijing is to relocate a controversial billion-dollar chemical plant away from the picturesque seaport of Xiamen in southeast China.

The decision, hailed as a milestone for China's environmental and democratic movements, follows the release of an environmental-impact assessment of the project at a public hearing in December. The relocation is even more surprising given that sources close to central government reveal the plant had been given the go-ahead because of the special relationship between Chen Youhao — the plant's Taiwanese investor and a fugitive of Taiwan — and some of China's top party leaders.

"This is the first time public opinion was properly expressed through official channels and had an impact on government policies," says Liu Jianqiang, a Beijing-based environment writer who is a visiting scholar at the University of California, Berkeley. Some commentators regard the orchestrated incident as the most significant public event in China since the 1989 Tiananmen Square student demonstration that was so brutally suppressed.

Construction of the plant, owned by Dragon Aromatics, part of Chen's Xianglu and Dragon Group, began in November 2006 in Xiamen's Haicang district, which has a population of 100,000. It is set to produce 800,000 tonnes of paraxylene annually, used to make plastics and polyester.

The plant's health and environmental dangers were made public last March when Zhao Yufen, a researcher at the College of Chemistry and Chemical Engineering at Xiamen University, led a petition to the Beijing parliament calling for the plant to be relocated away from residential areas. "Paraxylene is highly toxic and could cause cancer and birth defects," said Zhao in an interview with the Chinese newspaper *China Business*.

Lian Yue, a prominent writer living near Xiamen, posted the article on his blog, prompting fervent national debate. On 1 June, tens of thousands Xiamenese protested peacefully against the 'Xiamen PX Project' and the company's pollution records in the region.

This development alarmed officials in Beijing. A few days later, deputy environment minister Pan Yue called for an independent environmental-impact assessment of the plant as well as of Xiamen's urban development plans. Pan also suggested that the relevant parties should comply with recently announced regulations on environmental-impact assessments that require a public-consultation process and the release of relevant information to the public.

AP/COLOR CHINA PHOTO

Marchers on the streets of Xiamen protest against plans for a chemical plant in the region.

On 5 December, a 14-page version of the strategic environmental-impact assessment report, conducted by the Chinese Research Academy of Environmental Sciences, was released on Xiamen Net, the government's official website. The report criticized the Xianglu and Dragon Group's repeated emissions breaches and their disregard of requests since 2003 from the local environmental protection bureau to tackle the problems. Although it was less concerned about the environmental effects of the plant, the report pointed out serious flaws in a development scheme for Haicang that was pursuing the conflicting goals of industrialization and urbanization in such a small region. The plant may now be moved to Zhangzhou.

The relocation is the latest incident in which China's environmental problems have catalysed a democratic movement where the public has challenged the collusion between big business and local governments in their pursuit of economic growth at any cost. ■

Jane Qiu

SCORECARD

Phoning home
Mars explorers should be able to avoid feelings of despair and isolation, thanks to a virtual world similar to Second Life that NASA is planning for participants on 800-day missions to the red planet.

Seasonal goodwill
A Christmas punch-up at a South Pole research station resulted in one staff member being sacked and another being evacuated to hospital. Speculation over the cause ranges from over-imbibing to a woman to sheer isolation.

ZOO NEWS

It's raining reptiles
A cold snap in Florida has prompted a shower of iguanas. The cold-blooded creatures have been raining out of the trees they call home as evening temperatures drop and render them immobile. Locals report that many of the lizards "come back to life" if they are placed in the sun. Wildlife managers say they are pleased the invasive pests are being knocked out of action.

NUMBER CRUNCH

173 metres is the height of SOLAÉ, Mitsubishi Electric's record-breaking elevator testing tower (pictured), which opens later this month in Japan.

1,000 metres is the height contestants in the 2008 space elevator games will have to reach to claim the US$2-million prize money.

0 is the number of contestants in the 2007 games who managed that year's target height of 100 metres in the allotted time limit.

Sources: Wired, Daily Telegraph, Mitsubishi Electric, The Spaceward Foundation, Miami Herald

MITSUBISHI ELECTRIC

SIDELINES

Fears for oldest human footprints

Threats to the world's oldest hominid footprints in Tanzania are again stirring debate over how to best protect the 3.7-million-year-old tracks.

Discovered by Mary Leakey's team in 1978, the 23-metre-long track of footprints at an isolated site called Laetoli were in 1995 covered with an elaborate protective layer after they began to deteriorate with exposure. Now weathering has begun to undermine those protections, raising concerns that the prints preserved in a volcanic ash bed could be harmed by erosion, livestock or humans.

It has prompted Tanzanian anthropologist, Charles Musiba, now at the University of Colorado in Denver, to call for the creation of a new museum to reveal and display the historic prints. But other anthropologists question this idea — as they did when the tracks were covered — because Laetoli is several hours' drive into Ngorongoro National Park, making guarding and maintaining any facility extremely difficult. Musiba presented his proposal for the museum last month at the International Symposium on the Conservation and Application of Hominid Footprints, in South Korea. He says that Tanzania now has the scientific capacity and the funds to construct and monitor a museum.

J. READER/SPL

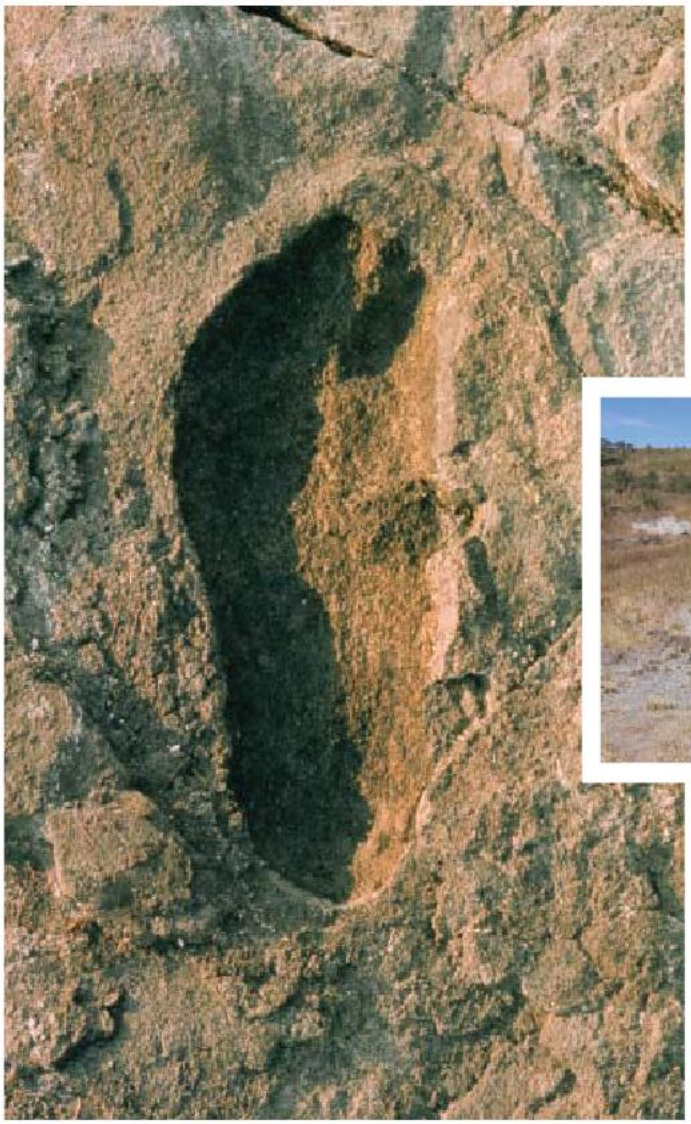

One of the hominid footprints, preserved in 3.7-million-year-old volcanic ash, that suggested the upright, bipedal, free-striding gait of modern man.

Vegetation threatens to erode the trail of fossilized footprints at Laetoli in the Ngorongoro National Park, Tanzania.

"I feel compelled to bring this issue out," says Musiba. "The current conditions show the protections are temporary. A fully fledged museum could be part of a walking safari trail for tourists."

But this concept worries other researchers such as anthropologists Tim White of the University of California, Berkeley, and Terry Harrison at New York University. They are among a group that favours cutting the entire track out of the hillside, then installing it in a museum in a Tanzanian city, either Dar es Salaam or Arusha. "If they are uncovered, they will be a magnet for trouble," says White. "Then the prints will be worn away."

Donatius Kamamba, who is head of the National Museum in Dar es Salaam and also director of the Tanzanian Department of Antiquities — the agency responsible for the Laetoli footprint site — expressed surprise over the erosion report and the museum proposal. He says that his agency will investigate the site, but he questions the feasibility of moving an ash bed that could potentially crumble apart.

The protective layer now in place was constructed by specialists from the Getty Conservation Institute in Los Angeles. A layer of dirt had been placed over the footprints by researchers such as Leakey and White. But acacia seeds weren't sifted out of the soil, so trees started growing, threatening to tear apart the layer of hardened volcanic ash. Getty conservationists Neville Agnew and Martha Demas removed the old layer and growth, covered the prints with a special fabric mat designed to limit water intrusion, then covered this with cleaned soil and rocks. This worked well until the past couple of years, when increased rains filled the surrounding run-off ditches with silt, leading to erosion exposing the mat's edges. All agree that the mat needs to be covered swiftly, in case, for example, local tribespeople attempt to remove it for other uses. But a long-term solution is still up for debate.

The National Museum is currently undergoing an expansion. Harrison thinks Tanzania would be wise to consider putting the footprints there. But archaeologist Audax Mabulla, of the University of Dar es Salaam, favours Musiba's suggestion. "We should open a small section of the footprints in an environmentally friendly building," says Mabulla. "Then people can have access and appreciate them."

Whatever happens, concerns are mounting about immediate improvements because the rainy season is already under way. ■

Rex Dalton

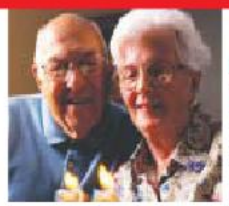

AGEING MAKES THE IMAGINATION WITHER
Memory decline in old age may also mean a less vivid imagination.
www.nature.com/news

SNAPSHOT

Making light work of indoor gardening

This strange crop has never seen the light of day — strong light destroys the carefully contrived balance of nitrogen and phosphate inside their closed glass containers, which would prevent the plants from flowering. Instead, these designer blooms use light-emitting diodes (LEDs) as their only source of light energy.

Tokyo-based Stanley Electric, a manufacturer of lighting devices for cars, developed the cultivation technique in collaboration with Yasuhiro Mori, a researcher at Tokai University in Kanagawa, Japan. They have so far produced roses and torenias. It took the research group five years to arrive at the successful exposure levels of blue, red and green LEDs. Stanley Electric plans to put the plants, which require little space and care, on the market this spring. ■

David Cyranoski

STANLEY ELECTRIC

SciBX

Science–Business eXchange

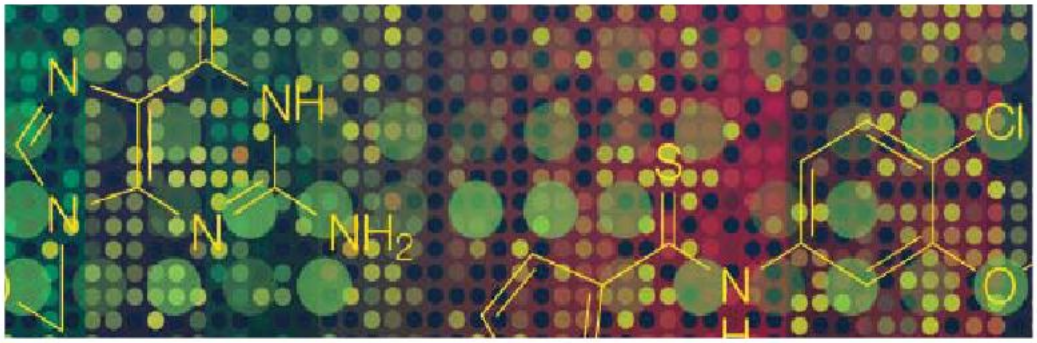

Introducing SciBX

Science-Business eXchange

Available January 31, 2008

From the Makers of BioCentury and Nature

New weekly publication designed to improve the efficiency and speed with which innovative life science research is translated into commercial value.

SciBX will provide the scientific context, commercial impact and critical next steps required to more effectively manage biopharma business.

Reserve Your Copy Today | www.scibx.com

BioCentury®

nature publishing group npg

Software magnates give $30 million to telescope

Two Microsoft billionaires gave $30 million on 3 January to build the Large Synoptic Survey Telescope (LSST), a proposed $389-million instrument that would make time-lapse movies of the sky, which astronomers could scour for brief celestial events.

Bill Gates gave $10 million to the project, which has 23 partners. The foundation set up by ex-Microsoft executive and space tourist Charles Simonyi gave $20 million.

When complete in 2014, the 8.4-metre mirror will focus light onto a 3.2-billion-pixel digital camera, taking 15-second exposures of huge swaths of the sky, scanning the entire sky every three or four nights. Planned for the mountains of northern Chile, scientists could use the LSST to watch supernovae, active galactic centres and near-Earth asteroids.

A colourful discovery in Costa Rica

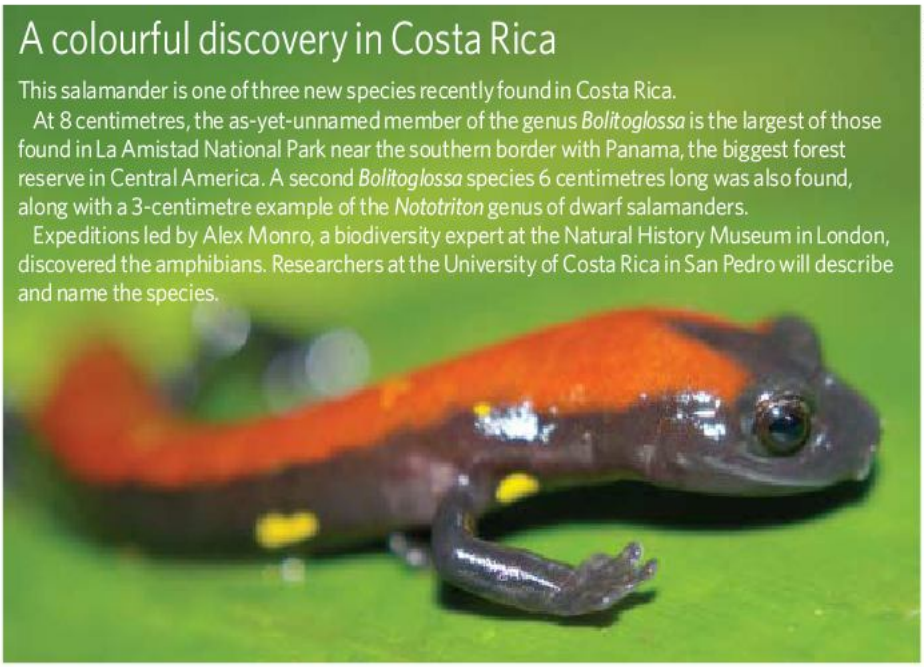

A. MONRO/NHM

This salamander is one of three new species recently found in Costa Rica.

At 8 centimetres, the as-yet-unnamed member of the genus *Bolitoglossa* is the largest of those found in La Amistad National Park near the southern border with Panama, the biggest forest reserve in Central America. A second *Bolitoglossa* species 6 centimetres long was also found, along with a 3-centimetre example of the *Nototriton* genus of dwarf salamanders.

Expeditions led by Alex Monro, a biodiversity expert at the Natural History Museum in London, discovered the amphibians. Researchers at the University of Costa Rica in San Pedro will describe and name the species.

Creator and first chair of climate-change panel dies

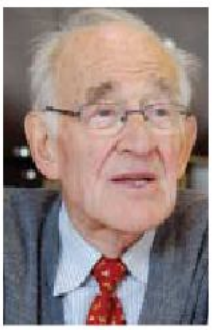

STOCKHOLM UNIV.

Bert Bolin.

Bert Bolin, who helped to create the Nobel-prizewinning Intergovernmental Panel on Climate Change (IPCC) and served as its first chairman from 1988 to 1997, died on 30 December in Stockholm, aged 82.

A meteorologist by training, Bolin performed early work on the global carbon cycle. He later served in several science advisory roles to the Swedish government and as scientific director of the European Space Agency. Bolin helped to create the IPCC's structure of three independent working groups, and guided the publication of its first two reports in 1990 and 1995.

"He was not only an excellent scientist, he was a man of impeccable integrity," says climate researcher Robert Watson, who succeeded Bolin as IPCC chair. "It was his ability to chair in an objective fashion that gave the IPCC real credibility not only with the scientific community, but with the political community as well."

China amends patent-rights law to boost innovation

Academics in China will now be able to own the patent rights for intellectual property resulting from publicly funded work. An amended version of the Chinese science and technology constitution aims to encourage innovation by allowing scientists to own their intellectual property and to spin off companies using their inventions. Tax regulations will also be changed to encourage innovation in high-tech enterprises.

The amendment to the Law on Science and Technology Progress was passed on 29 December and will come into force on 1 July. The new law also allows researchers doing high-risk experiments to report them as incomplete or failed without damaging their chances of future funding.

Zoo's abandoned polar bear cubs 'will be left to die'

Polar bear cubs born at Nuremberg Zoo in southern Germany will not be hand-reared, but will instead be left to die if their mothers reject them. Zoo officials said last week that they wanted "at all costs" to avoid the media and public attention surrounding Knut, the 13-month-old polar bear cub that was originally hand-reared at Berlin Zoo.

Nuremberg Zoo's two bears, Vera and Wilma, each gave birth to an estimated two cubs a few weeks ago in a cave in their enclosure. The cubs can be heard crying loudly, but Wilma has been observed occasionally strolling out of the cave, sparking fears that she might be about to reject her cubs, like Knut's mother Tosca. It is believed that Vera's two cubs have already died and been eaten by their mother, although zookeepers have not been in the cave to check, for fear of disturbing the inexperienced mothers.

NUREMBERG ZOO

A newborn cub — now thought to be dead — sits by the paws of its mother at Nuremberg Zoo.

Breeding polar bears in captivity is extremely difficult. The zoo hopes that, if their babies were to die this time, having had this experience, the young females will be more likely to bring up healthy cubs the next time they give birth.

National Academies updates book on evolution

On the same day that Mike Huckabee won the Republican presidential caucus in Iowa — having revealed during a candidates' debate that he does not believe in the theory of evolution — the US National Academy of Sciences released its latest version of a book to explain to the American public why evolution works.

It is the third time that the academy has weighed in with such educational material. "We're trying to give the public coherent explanations and concrete examples of the impact of evolution," says academy president Ralph Cicerone. The book, *Science, Evolution, and Creationism*, is available at www.nap.edu/sec. It includes descriptions of fossils such as the Canadian *Tiktaalik*, a creature that had features somewhere between those of fish and four-legged walking animals.

The Institute of Medicine also weighed in as a co-sponsor of the book, citing the importance of evolution for understanding infectious and emerging diseases today.

See Editorial, page 108.

Providential outcome

A winning combination of isolation, local involvement and a broad ecological remit are making the management of the seas around Colombia's San Andrés islands a model for other conservationists, reports **Mark Schrope**.

F. VIOLA

The locals claim that the waters around the picture-postcard Caribbean island of Old Providence come in seven shades of blue; the surrounding corals come in a far greater range of hues and colours. Just a couple of kilometres offshore and 35 metres down, for instance, you can dive to Turtle Rock, a 12-metre megalith covered in red, yellow and neon green sponges with a 1.5-metre growth of bushy black coral at its peak. The seas of the San Andrés archipelago, a part of Colombia about 800 kilometres north west of the country's coast (and in fact much closer to Nicaragua) boast many fine reefs, impressive for both their quantity — Old Providence has the second largest barrier reef in the Americas — and their quality. The archipelago's reefs, although not pristine, are some of the healthiest in the Caribbean. And the intriguing mixture of autonomy and local representation that forms the basis of their management may be able to keep them that way.

Valuable lessons

In 2000 the San Andrés archipelago — Old Providence (also known by its Spanish name, Providencia), the more heavily populated San Andrés and an assortment of other islands, rocks and reefs — became the centrepiece of Colombia's Seaflower Biosphere Reserve, named after the ship that a group of Puritans used to reach the islands and settle there in 1631. The reserve covers 300,000 square kilometres — a whopping 10% of the Caribbean Sea. In 2005, a core region of 65,000 square kilometres was designated a Marine Protected Area (MPA), with associated restrictions on fishing, tourism and the like.

> "So many Marine Protected Areas in the developing world have been put in place and end up being paper parks."
> — Jack Sobel

Marine ecologists widely agree that a global system of such MPAs is the last hope for many reef systems and their associated fisheries, but the step between designating MPAs and making them truly effective, both ecologically and bureaucratically, has been notoriously challenging. Lessons learned in Colombia could eventually affect marine resources elsewhere in the Caribbean and beyond. "It seems like really exciting things are going on there," says John Parks of the US National Ocean Service, who has worked on establishing MPAs with groups around the globe. "The creative thinking that has gone into making this possible is something that other nations would very obviously benefit from tapping into, including the United States."

Two key factors in the MPA's apparent success are a historical lack of strong marine regulations in the area and a significant amount of local autonomy. Following the adoption of its new constitution in 1991, in 1993 Colombia's legislature transferred most of the control of, and responsibility for, environmental resources to 33 so-called regional autonomous corporations. The Corporation for the Sustainable Development of the Archipelago of San Andrés, Old Providence and Santa Catalina, known as CORALINA, is responsible for environmental planning, management and research, with a hand in everything from training scuba divers in best practices for protecting the region's reefs to teaching school children the value of the region's resources.

Like many remote areas of Colombia, the archipelago suffers from endemic unemployment, so CORALINA is working to develop vocational programmes. Some, but not

all these, are tailored to fishermen affected by conservation efforts. One focus is to promote the islands' reefs and underwater cliffs such as Turtle Rock as attractions for scuba divers and other ecotourists. Because development is restricted, the islands have no five-star resorts, and nor will they — the visitors CORALINA has in mind are interested in a purer remote-island experience, especially on Providence.

Local involvement

Unlike most environmental agencies, CORALINA can single-handedly develop and implement management plans that cover both the land and the surrounding seas, and the law gives it the muscle it needs to enforce its regulations. Between 1995 and 1997, the agency issued multiple warnings to two hotels on San Andrés, which with 60,000 inhabitants is by far the most populous island in the archipelago. The hotels were failing to comply with new sewage-treatment regulations CORALINA had imposed. When its warnings were ignored, CORALINA shut the hotels for two months. Not surprisingly, the hotels backed down. More surprisingly, perhaps, they were subsequently converted from beaten opponents to willing fellow travellers. "Today one of these hotels is part of our environmental stars programme," says Elizabeth Taylor, CORALINA's executive director. "People have been really changing."

Observers say that one of the most essential elements of the CORALINA model is the mandated involvement of local people. This provides the sort of accountability that avoids regulations and restraints being easily dismissed as the impositions of outsiders. Taylor's position is elected locally, and the agency is overseen not by a government official, but by a board of directors that has to include elected members from local businesses as well as representatives from the national and local governments. At least 3 of the 14 board members have to be from the islands' native population — descendants of planters and slaves from other Caribbean islands — which makes up a significant minority on San Andrés and an overwhelming majority on the much less populated Old Providence. Each board member's vote has the same weight.

As well as playing a specific role in governing CORALINA, locals have been heavily involved in the process of tailoring regulations to specific places. Whereas some environmental measures — such as a ban on fishing with nets — apply to the whole of the biosphere reserve, others, such as measures needed to protect an important conch habitat, need to be more specific. These more restricted areas are parts of the MPA set up in 2005, which includes extensive no-fishing zones and even a no-access zone accessible only for research and monitoring. "They have managed to designate a fairly significant portion of that large archipelago a no-take status, which we think is very important," says Jack Sobel, with the Washington DC-based Ocean Conservancy and a member of CORALINA's international advisory committee.

To delineate the reserve's various restricted zones, CORALINA sponsored hundreds of workshops, with various stakeholders mapping out what they knew about the best and most critical resources, and saying which areas they wanted to see protected. Later work included scientific surveys. Using a geographical information system to manage the various inputs, CORALINA proposed a variety of potential zoning schemes, which were further altered in consultation with locals. Hundreds of stakeholders signed on to the scheme before official enactment by CORALINA, and many locals have embraced the results. According to a survey commissioned by CORALINA, 96% of fishermen say they believe that the MPA will benefit them. Dairo Casanova, owner of a snorkelling and ecotourism centre on San Andrés, talks enthusiastically about regulations that blocked spearfishing on some reefs that he depends on for snorkeling tours, turning the activity into an offense that can get its perpetrators a weekend in jail.

The support is not universal. Some native islanders have charged that the national government is manipulating CORALINA to prevent proper native representation on the board. But overall, says Taylor, "I think today we can say we have a lot of support from the local community, especially in San Andrés. The people in Old Providence still have some resistance, but not the majority."

Giovanna Peñaloza, who manages CORALINA's Old Providence office, says the fishermen there are not concerned so much about closed areas per se, but rather with enforcement. Foreign fishermen, they say, either don't know which areas are closed or don't care. CORALINA recognizes that the ultimate long-term success of the reserve and the MPA will require a number of changes — especially stepping up enforcement, which is currently managed by Colombia's agricultural ministry. To that end, the group is now finishing a proposal for funds from the Inter-American Development Bank that would enable major improvements to the system.

If the funds come through, the group would be able to purchase new boats for enforcement and monitoring work, set up buoy lines around protected zones and establish dedicated MPA offices on the islands instead of handling management out of CORALINA's limited existing facilities.

"So many MPAs in the Caribbean and elsewhere in the developing world have been put in place and end up being paper parks," says Sobel, "I think CORALINA is not likely to repeat those mistakes. It's a very talented group of people, and with the amount of planning and outreach they've done, I think they will be effective." Parks says that as CORALINA expands its efforts, he hopes recognition of their work will also expand. "We need these stories to be told. We need people to understand that we can do this, and that if we do it the right way, our children will have that future." ■

Mark Schrope is a Florida-based freelance writer.

F. VIOLA

Elizabeth Taylor (left), Giovanna Peñaloza and Felipe Cabeza at CORALINA's Old Providence office.

BACTERIA'S NEW BONES

Long dismissed as featureless, disorganized sacks, bacteria are now revealing a multitude of elegant internal structures. **Ewen Callaway** investigates a new field in cell biology.

Nearly a decade ago Jeff Errington, a microbiologist at Newcastle University in England, was toying with a strange bacterial protein known as MreB. Take it away from microbes, and they lose their characteristic cylindrical shape. The protein's obvious role in structure and even its sequence suggested a shared ancestry with actin, a protein that produces vast, fibrous networks in complex cells, forming the framework of their internal structure, or cytoskeleton. But no one had ever seen MreB in action under the microscope until Errington found just the right combination of fluorescent labels and fixatives.

In a 2001 paper, he presented MreB (orange in the illustration below) fluorescing brilliantly and painting barbershop-pole stripes around the rod-shaped bacterium *Bacillus subtilis*[1]. "We got these amazing pictures. It was one of those few times in a scientific career when you do an experiment that completely changes your way of thinking," says Errington.

For more than a century, cell biology had been practised on 'proper' cells — those of the eukaryotes (a category that includes animals, plants, protists and fungi). The defining characteristic of eukaryotic cells is their galaxy of internal structures: from the pore-studded nucleus that contains the genome, to the fatty sacs of the Golgi, to the myriad mitochondria, and of course the networks of protein highways that ferry things around the cell and give it shape and the capacity for movement. These elements form a catalogue of cell biology's greatest discoveries, and all of them are absent in bacteria. Hundreds to thousands of times smaller than their eukaryotic cousins, and seemingly featureless, bacteria were rarely invited to the cell biology party. But Errington's discovery has been part of a movement that is changing that.

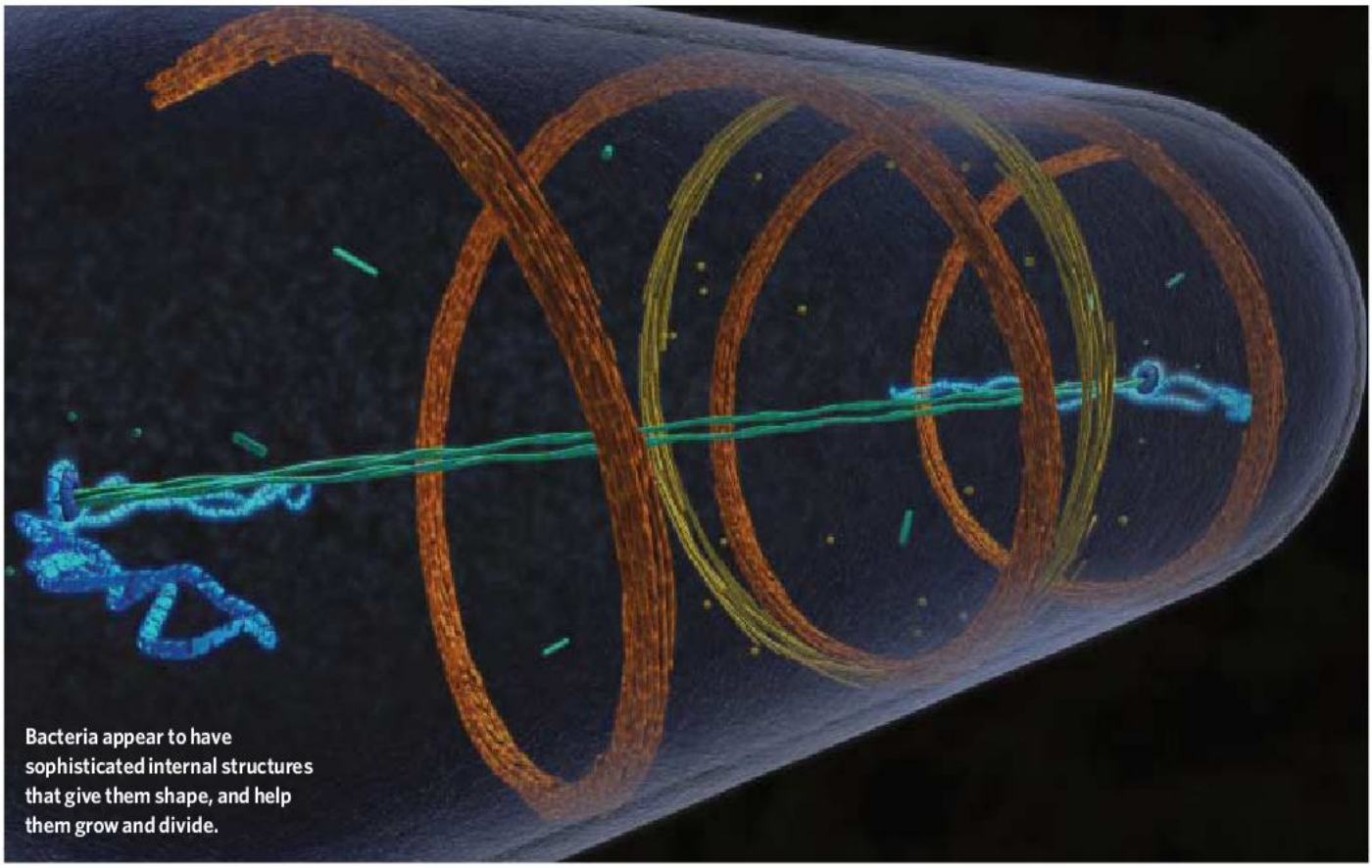

J. IWASA

Bacteria appear to have sophisticated internal structures that give them shape, and help them grow and divide.

Dyche Mullins, a cell biologist at the University of California, San Francisco had spent most of his career untangling the network of molecular cables and scaffolding that enforces order in the eukaryotic cell. With Errington's paper, Mullins saw the lowly bacterium anew. "There was a lot of organization in bacterial cells we were just missing," he says. He has since devoted much of his time to studying them. Last month, Mullins chaired the annual meeting of the American Society for Cell Biology in Washington DC. That he was chosen for the job is a clear indication that bacteria have made it on to the guest list.

Lucy Shapiro, a microbiologist at Stanford University in California gave bacteria an hour-long tribute at the meeting. "People more or less thought the bacterial cell was a swimming pool and the chromosome was this ball of spaghetti," says Shapiro, whom many credit for launching the field of bacterial cell biology.

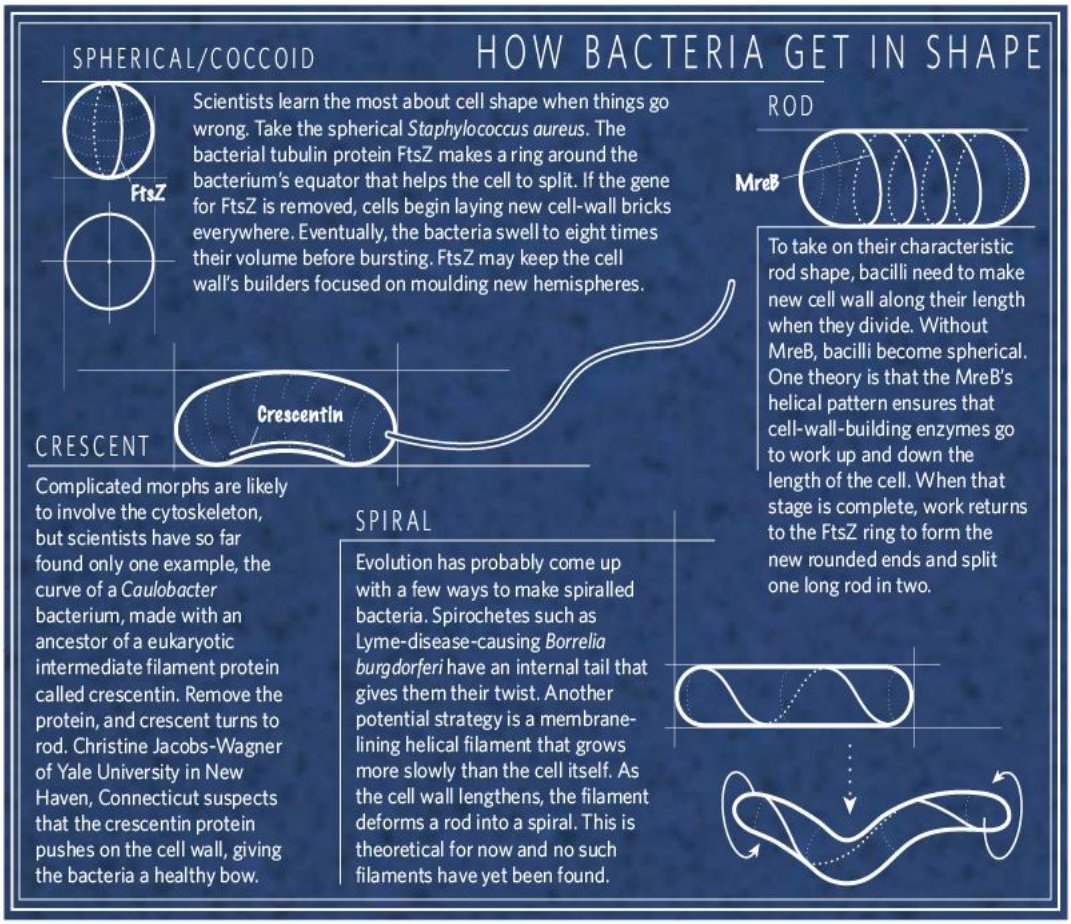

External contractors

Busied by growth, propagation and little else, a bacterium's life can seem an endless cycle of fecundity. Well-fed bacteria in rich, sterile culture can divide every half hour or so. The cytoskeleton is the linchpin of efficient cell growth and division, but researchers are only starting to explain how.

Take FtsZ (illustrated in yellow opposite), a protein that ties a belt around the belly of nearly every species of bacterium. Without FtsZ — a barely recognizable cousin of the eukaryotic protein tubulin — rod-shaped bacteria called bacilli grow longer and longer without splitting in two. Somehow FtsZ cinches the dividing cell closed, says Harold Erickson, a cell biologist at Duke University Medical Center in Durham, North Carolina. Tubulin is involved in eukaryote cell division, but its role is completely different. Microtubules, formed from tubulin, pull chromosomes apart during cell division through a process that has been studied extensively.

Erickson started out studying tubulin. But intrigued by the pictures of internal FtsZ structures coming out of other labs in the 1990s, he began reading up on FtsZ. When the time came to reapply for a grant, he devoted half of his proposal to the bacterial protein. "I decided, 'I don't have any great ideas about what to do with tubulin,'" he recalls. It took a couple of applications to get funding, but Erickson hasn't looked back.

Squeezing two cells out of one is just one of the cytoskeleton's duties. When bacteria divide they need to resculpt a rigid cell wall built out of peptidoglycan, a polymer consisting of sugar and amino-acid bricks. Without the MreB protein wound around the shell of a bacillus, it grows spherical (see 'How bacteria get in shape'). The protein directs the construction and destruction of the cell wall, says Zemer Gitai, a microbiologist at Princeton University in New Jersey. One theory is that MreB and its relatives build a protein scaffold inside the cytoplasm that tells the cell wall's enzyme contractors outside the cytoplasm where to lay new bricks. Because two layers of membrane separate the MreB helix from the cell wall, other proteins must forge the connection, says Gitai.

Also, when a bacterium divides, each new cell must have its own DNA. Most of a bacterium's thousand or so genes sit on a long chromosome, but smaller rings of DNA called plasmids also help a cell by supplying antibiotic resistance and other perks.

Mullins's lab studies a bacterial version of actin, called ParM, which ensures that as a cell splits in two, each receives a copy of a specific plasmid. Without the protein, many cells will invariably lose the plasmid and the drug resistance it provides.

To avoid this fate, a strand of ParM molecules (shown in green, opposite) latches onto two freshly replicated plasmids (purple), like the chain to a pair of handcuffs. The two circles start close to one another, but as more ParM molecules leap onto the chain, the plasmids spread to opposite ends of the cell. Mullins's group found that the ParM chain grows pretty much on its own — a startling contrast to our own actin, which requires other players to speed extension. Although related to actin, ParM works more like tubulin, constantly reinventing itself by adding and shedding units. "That blows my mind," Mullins says.

His team is now looking at how other plasmids ensure their legacy, to say nothing of the bacterial chromosome, a DNA loop thousands of times longer than any individual plasmid. "We know very little. For me, the most important unanswered question in cell biology is how bacteria segregate their chromosomes," says Mullins.

The wealth of questions and dearth of answers makes the field very attractive. Every time a new bacterium is sequenced, research-

ers have the opportunity to find new structural elements, often with surprising roles. One of the latest additions is an actin protein, MamK, found in bacteria endowed with iron-containing structures called magnetosomes. By sensing Earth's magnetic tug, the bacteria can position themselves in the environment best suited to their needs. For the compass to work, a cell's dozen or so magnetosomes need to line up in a row, and MamK forms their track[2]. Arash Komeili, a microbiologist at the University of California, Berkeley who first identified the protein's role says that by scouring genome databases he has found genes similar to MamK in bacteria with no magnetosomes.

K. LOUNATMAA/SPL

Electron microscopy suggests that *Echerichia coli* and other bacteria have no organized internal structure.

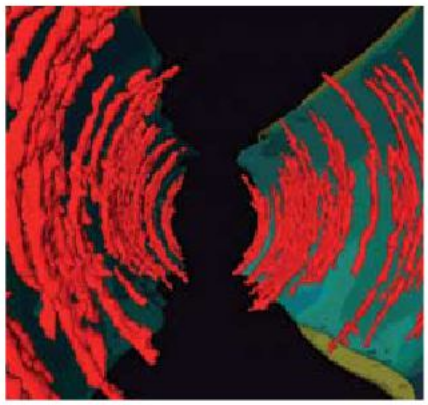

Z. LI & G. JENSEN, CALTECH

Cryo-electron tomography of a mutant *Caulobacter* shows gobs of FtsZ filaments (red) lining the constriction site as the cell tries to divide.

Seeing is believing

Although bacterial cell biologists such as Komeili can use genomics to hunt for new features of the cytoskeleton, pictures make a stronger case, he says. Advances in optics and microscopy are one reason the bacterial cell is only now getting its dues. At a few micrometres, bacteria are often not much longer than the limits of a light microscope, so even the best lens in the world won't bring any detail to a molecular cable a few nanometres thick.

Peering deeper into a bacterial cell requires abandoning the light waves that obscure detail. Electrons, which have a far shorter wavelength than visible light, provide staggering insights into eukaryotic cell structure, such as the ribosome-studded endoplasmic reticulum or the perfectly arranged bundle of microtubules that build a cilium tail. In bacteria, the same electrons paint a blurry mush. Even the most recent edition of the hallowed text *Molecular Biology of the Cell* sees bacteria under the magnification of an electron microscope as chaotic vessels: "This cell interior appears as a matrix of varying texture without any obvious organized internal structure," the authors write.

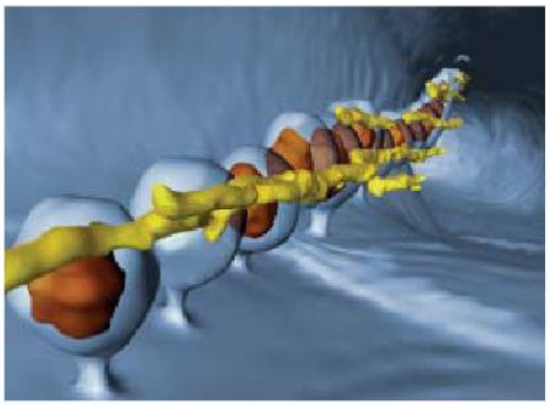

Z. LI & G. JENSEN, CALTECH

An actin-like filament called MamK (yellow) organizes a chain of magnetosomes (iron-containing structures) in the magnetic bacterium *Magnetospirillum magnetotacticum*.

A more promising technology — cryo-electron tomography — might be the answer. Instead of coating cells with gold or dousing them in harsh fixatives, cryo-EM, as it is often called, takes pictures of flash-frozen samples. "We're looking at cells in a nearly native state," says Grant Jensen, a biologist at California Institute of Technology in Pasadena. The gentle treatment keeps the bacterial cytoskeleton intact. "If you thawed them out, most of them would probably swim away."

Cryo-EM has the added benefit of allowing researchers to combine numerous angles of a cell into a three-dimensional picture, just like a computed tomography scan does. Recently, Jensen's lab collected images of rings of FtsZ lining the insides of a bacterium called *Caulobacter* and pinching its membrane — a model predicted by others but never seen before.

When early searches for bacterial genes resembling eukaryote scaffold-protein genes found nothing, scientists assumed that these proteins evolved after bacteria split from eukaryotes, some 1.5 billion to 2 billion years ago. The discovery of the bacterial cytoskeleton has turned that conclusion on its head.

FtsZ may be the great-grandfather of cell division, says Erickson, whose lab recently showed that the protein makes rings inside microscopic droplets of oil, a stand-in for early life. Although cell division now is an elaborate choreography between dozens of players, the earliest cells may have needed just FtsZ to split in two. Erickson points out that the protein contains none of the amino acids, such as tryptophan and arginine, that some believe only to have shown up later in evolution.

As cytoskeletons evolved, they took on new chores and snowballed in complexity. At some stage after eukaryotes branched off from bacteria, the eukaryote cytoskeleton seems to have frozen in time. From yeast through to people, its proteins do many of the same jobs, such as towing sister chromosomes to opposite ends of a dividing cell or making sure the endoplasmic reticulum nestles up against the nucleus. More complex eukaryotes might use actin to flex muscles and keratin to make hair, but those tasks are variations on a theme.

Not so with bacteria, says Mullins. Actins that determine cell shape work differently across the bacterial world, and some rod-shaped bacteria, such as tuberculosis, don't even have them. Due to their vast numbers and unicellular lifestyle, "bacteria can play around with fundamental mechanisms for doing things in a way that eukaryotes can't", he says.

But the shared trait of bacterial and eukaryotic cytoskeleton proteins — self assembly — means that bacteria can shed light on the workings of more complex species. For example, the molecular structure of MreB explained how actin molecules stick together. And in most cases, bacterial proteins yield to laboratory tinkering with less resistance than the eukaryotic kind. Turning up the expression of actin, for instance, kills many eukaryotic cells, but bacteria don't seem to mind.

And bacteria, because they have few genes, are ideal for addressing fundamental questions about all cellular life. Although cytoskeletons seem to act as organizing centres in bacteria and eukaryotes, no one yet understands how these proteins travel to precise spots in a cell, to one end or the other or to the site where one cell splits in two.

As well as being intellectually stimulating, probing the insides of bacteria has practical applications, and bacterial cell biologists recognize the need to remind funding agencies such as the National Institutes of Health of that. For example, a chemical named A22 slows bacterial growth by stopping MreB from forming into long cables, and without FtsZ many bacteria will die. No antibiotics yet target the bacterial cytoskeleton, but with drug resistance on the rise, structures such as the MreB helix and the FtsZ ring could prove to be chinks in the bacterial armour.

But as researchers struggle to piece together the bacterial cell, cures for disease are far from the minds of most. For Mullins, the field's progress has vindicated his dive into the bacterial swimming pool, although he and others still haven't come close to its deep end. "There's a lot of unexplored biology," he says. ■

Ewen Callaway recently completed an internship at *Nature*'s Washington DC office.

1. Jones, L. J. F., Carballido-López, R. & Errington, J. *Cell* **104,** 913–922 (2001).
2. Komeili, A., Li, Z., Newman, D. K. & Jensen, G. J. *Science* **311,** 242–245 (2006).

Conservation: in a rut, we need rut-inspired solutions

SIR — Your Editorial 'The great divide' (*Nature* **450**, 135–136; 2007) pointed to a persistent and problematic issue plaguing conservation: the gap between research and practice. You suggest that conservation biologists should spend more time working with local practitioners and get out of their ruts.

It's true that conservation biology is in a rut. So we need rut-inspired solutions.

The ruts are the cultures and institutions that impede engagement by conservation scientists. A descendant of population biology, conservation science inherited cultures and institutions that may have been suitable for other sciences but are not suitable for conservation science. We are blocked on several fronts.

First, conservation science traditionally focused narrowly on biology, largely omitting the social sciences and humanities. Because conservation is fundamentally the management of human behaviour, this omission has impeded effective application of research. Thankfully, efforts are under way to broaden and integrate conservation research.

Second, engaging society in conservation science is still controversial. And until we sort out what constitutes appropriate engagement, it will rightly remain so.

Third, engagement is generally not valued highly as a professional activity.

The Society for Conservation Biology should publicly declare that engagement is a crucial responsibility of academic conservation scientists. Candidates and reviewers for promotion and tenure could cite this to justify their choices. Such a statement could have intangible and knock-on effects for other scientists too.

To promote effective engagement — and escape this rut — we conservation scientists must first engage our own cultures and institutions.

Kai M. A. Chan
Institute for Resources, Environment and Sustainability, AERL Rm 438, 2202 Main Mall, University of British Columbia, Vancouver, British Columbia V6T 1Z4, Canada

Conservation: academics should 'conserve or perish'

SIR — Your Editorial 'The great divide' (*Nature* **450**, 135–136; 2007) underlines the immense gap between academia and practice in conservation biology. This is simply an evolutionary consequence of selective forces at play for academics.

Turning one's research findings into actions is good for conservation but not necessarily for an academic career. It reduces the time available for preparing manuscripts — and academics in conservation biology are evaluated on their publications, rather than on their involvement in saving species from extinction.

We suggest that an 'impact factor' should be created, inspired by the conventional metric of scientific publications, to assess tenureship applications for academic positions in the field.

This impact factor would be based on an estimation of how much worse the conservation status of an endangered species or ecosystem might be in the absence of the candidate's research. It would select for targeted investigation that should help to fill in 'the great divide', and would exclude opportunistic ecology papers claiming to be of conservation significance.

Such a dual evaluation process would not mean that all conservation academics should become green activists. The role of academics in society is, and should remain, to understand and explain the complexity of the world. It includes supporting evidence-based policy-making in biodiversity conservation.

Guillaume Chapron*, Raphaël Arlettaz†
*Grimsö Wildlife Research Station, Swedish University of Agricultural Sciences, 73091 Riddarhyttan, Sweden
†Conservation Biology Division, Institute of Zoology, University of Bern, Baltzerstrasse 6, 3012 Bern, Switzerland

Frog transparency led to discovery of melatonin

SIR — Your News in Brief story 'See-through frog offers inside information' (*Nature* **449**, 521; 2007) describes the production of a transparent frog by genetic manipulation. But translucent amphibians were first artificially created 90 years ago.

C. P. McCord and F. P. Allen (*J. Exp. Zool.* **23**, 207–224; 1917) reported that a crude acetone extract of bovine pineal glands fed to *Rana pipiens* tadpoles caused such a pronounced lightening of their skins that the larger viscera were visible through the dorsal body wall. The tadpoles' transparency varied according to the concentration of pineal extract in the water in which they were swimming.

Some 40 years later, the dermatologist A. B. Lerner followed up these observations and discovered that a pineal indole caused the melanin granules in frog melanocytes to aggregate and the skin to lighten — he named this factor melatonin (A. B. Lerner *et al.* *J. Am. Chem. Soc.* **80**, 2587; 1958).

So the suggestion made by S. Castroviejo-Fisher and colleagues in Correspondence, of using naturally transparent arboreal glass frogs of the family Centrolenidae for biomedical research, is not without precedent ('Transparent frogs show potential of natural world' *Nature* **449**, 972; 2007).

Thomas C. Erren*, Russel J. Reiter†, V. Benno Meyer-Rochow‡
*Institute and Policlinic for Occupational and Social Medicine, University of Cologne, Kerpener-strasse 62, 50937 Köln, Lindenthal, Germany
†Department of Cellular and Structural Biology, University of Texas Health Science Center at San Antonio, San Antonio, Texas 78229-3900, USA
‡School of Engineering and Science, Jacobs University Bremen, 28759 Bremen, Germany

Schizophrenia is a disease, so electrons aren't at risk

SIR — In your News & Views article 'Schizophrenic electrons' (*Nature* **450**, 492–493; 2007), electrons are called 'schizophrenic' because they display split personalities. This inappropriate use of metaphor perpetuates a misunderstanding of a serious illness. Multiple personalities are not a feature of schizophrenia. Rather, schizophrenia is characterized by a combination of 'positive' and 'negative' symptoms. The positive symptoms include delusions, hallucinations and thought disorders, whereas the negative symptoms include social withdrawal, flattened affect and lack of motivation.

I am willing to concede that electrons may have personalities; even that some electrons have split personalities. But to claim that electrons are 'schizophrenic' would require evidence beyond that described in the article.

Ronald Chase
Department of Biology, McGill University, Montreal, Quebec H3A 1B1, Canada

Schizophrenia does not mean split personality

SIR — I was astonished to see the terms 'schizophrenic' and 'split personality' being used interchangeably in a News & Views article on high-temperature superconductivity (*Nature* **450**, 492–493; 2007).

Although the usefulness of the concept of 'schizophrenia' in mental health is contested, the consensus is that it does not have anything to do with a 'split personality' (whatever that is). Why, then, is *Nature* perpetuating this inaccurate and potentially offensive usage of 'schizophrenic'?

Alex C. W. May
Northwest Institute for Bio-Health Informatics, ISBE, University of Manchester, Oxford Road, Manchester M13 9PT, UK

Contributions to this page may be sent to correspondence@nature.com.

BOOKS & ARTS

From bench to book

Web publishing and marketing might put more science into fiction and attract new readers.

A Version of the Truth
by Jennifer Kaufman & Karen Mack
Delacorte Press: 2008. 336 pp. $24

The Expeditions
by Karl Iagnemma
Dial Press: 2008. 336 pp. $24

The Gift: Discovery, Treachery & Revenge
by Jon Kalb
Special Delivery Books: 2007. 140 pp. £7

Jennifer Rohn

In a darwinian scrum for the attention of an increasingly distracted audience, authors who want to write fiction about science, but not straight science fiction, have their work cut out. The gates of publication are typically guarded by humanities graduates who may have no scientific affinity.

To slip through the net, stories about scientists are often sugar-coated. Fictionalized accounts of historical scientific figures are on the rise, with speculative novels about Charles Darwin, Carl Friedrich Gauss, Alexander von Humbold, Alan Turing, Kurt Gödel and Alfred Wegener having appeared over the past few years. Forensic science-based police procedurals are also flourishing. In contrast, novels about modern scientists doing experiments in labs or field stations, such as Allegra Goodman's *Intuition*, are rare.

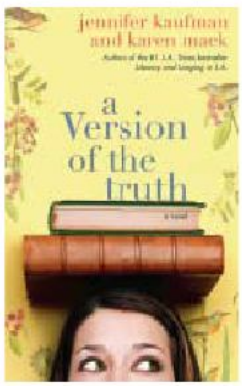

Inspecting what does make the cut is therefore a lesson in the market constraints of the publishing industry. The cover of *A Version of the Truth*, with its gentle pastels, nature drawings and beautiful young woman, betrays it as a *Bridget Jones' Diary* for boffins. Cassie Shaw, an impoverished and unglamorous young widow with only a secondary-school education, lies about her academic credentials to land an administrative job at the local university's science department. Soon she's upgrading her wardrobe and capturing the eye of the dishy professor. Where it deviates from the formula is that Cassie is a nature enthusiast, far preferring a ramble in the woods to the party scene — it's *The Devil Wears Prada* meets *Walden Pond*.

Details about scientific life in this novel are thin enough to avoid spooking even the most squeamish scienceophobe. Although the professor is said to be an animal behaviouralist, we only ever see him delivering show-stopping undergraduate lectures, chaperoning drunken field trips and quoting Emerson. Happily the characters are multidimensional, and it is refreshing to deal with a romantic female lead who gets excited by reading naturalist John Muir. Authors Jennifer Kaufman and Karen Mack even slip in a few gentle riffs about the scientific process without shattering the 'chick lit' spell.

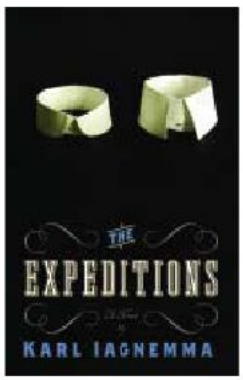

The Expeditions, penned by a mechanical engineer, also looks at science through the less threatening lens of nature. Set in the United States in the 1840s, it is a coming-of-age tale about 16-year-old Elisha Stone who, having developed a passion for mucking about with beetles and frogs in the local creek, runs away and signs up to a 'scientific' expedition into Canada's largely uncharted Northwest Territories.

Elisha is caught between the disparate philosophies of the two men of science on the trip: Professor Tiffin, a dreamy, buffoonish academic in search of native artefacts; and Silas Brush, a hard-nosed practicalist who is surveying the land for valuable resources such as timber and iron. In the end, both men are revealed to have less than pure motivations and Elisha decides that his love for science is only a romantic notion, best abandoned. Author Karl Iagnemma's division of science into theory and practice seems clichéd, and Elisha's change of heart, somewhat forced. *The Expeditions* may please fans of Wild West adventures, but it says little about science or a person's reasons for loving it — or leaving it.

The only work of serious 'lab lit' in this trio is *The Gift*. Billed as a tell-all from the cut-throat world of hominid fossil-hunting, the plot centres around a classic fraud scenario loosely based on that of Piltdown Man. Bert Wilde, a ruthless field researcher, will stop at nothing to get ahead, including murder, rape, a gold-digging marriage and grant bribery. Ron Slater, Wilde's graduate student, seeks revenge on Wilde with a devious plot that plays on the older researcher's egotism and lust for glory.

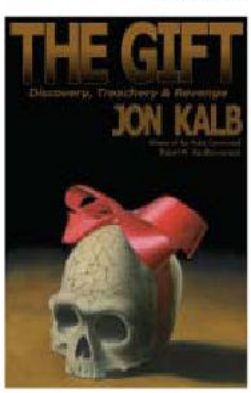

Author Jon Kalb — a geologist who has led many hominid surveys in Ethiopia — follows the minutiae of field study in the Rio Grande valley. Characters unearth and scan bone fragments, consult academic journals and discuss palaeontological theories as seriously as they might in a departmental seminar. Yet the facts serve the plot, which is tempered by humour, the atmospheric Tex-Mex setting and snappy dialogue.

Given *The Gift*'s uncompromising approach to technical detail, it is probably no coincidence that the book is self-published. Although excessive detail might be tolerated in general fiction (think of the exhaustive whale trivia in *Moby-Dick* and painstaking descriptions of linotype in John Updike's *Rabbit Redux*), the nuts and bolts of the scientific method seem less palatable.

In the past, 'vanity publishing' carried stigma and a significant price-tag. But the web's spirit of rampant self-promotion has rendered it more socially acceptable. And the technology behind digital print-on-demand (POD) publishing has now become cost-effective enough to make it available free to authors. Website LuLu.com paved the way, and in 2006 Amazon stepped into the arena with CreateSpace.com, which offers higher quality and more production options, with the obvious advantage of being more directly linked to the company's powerful distribution channels.

All that's missing is marketing. Maybe the authors' own websites and blogs, and popular review sites such as Goodreads.com, will bring these books to the attention of readers who are hungry for more science in their fiction. Just as social networking sites such as MySpace have allowed artists to promote their music without a record label intermediary, such venues, coupled with the freedom of POD publishing, might offer new opportunities for undiluted novels about the lives and activities of scientists. ■

Jennifer Rohn is a research fellow at the MRC Laboratory for Molecular Cell Biology at University College London, Gower Street, WC1E 6BT, UK, and the editor of LabLit.com.

EXHIBITION

Dreamscapes

Henry Nicholls

Sleep can be uncertain and dreams so surprising. This very unpredictability makes *Sleeping and Dreaming* perfect curatorial territory for the Wellcome Collection, London's brave venue where science, art and culture converge.

This exhibition lets you ponder an early electroencephalogram machine, peer at a nightmarish vision by Francisco de Goya, survey alarm clocks made in four different centuries, watch a cataplectic fit unfold, find the Salvador Dali and Luis Buñuel film *Un Chien Andalou* on continuous loop and wish you owned a Hizamakura clip-on pillow, to make your desk more comfortable for a nap.

From a central corridor the visitor steps off into the intimacy of dark, spotlit antechambers, each addressing the show's central themes. As a narcoleptic visited by inspiring hallucinations while slipping into sleep, I particularly enjoyed the recess exploring the creativity that may flow from dreams. Here one can listen to 'Yesterday', which Paul McCartney apparently woke up humming, view a cast of *Cyclopoma spinosum* (a fossil fish that Swiss-born zoologist Louis Agassiz claimed to have reconstructed in his sleep) and admire Otto Loewi's Nobel certificate, awarded in 1936 for his dream-inspired discovery of neurotransmitters.

Aristotle and Freud make understated appearances, allowing room for other scientific responses to sleeping and dreaming. Most of these are anecdotal. The rich artistic and cultural interpretations, by contrast, have greater impact.

N. KLINGER

Restless reveries: a long-exposure photograph captures a subject's movements during sleep.

There is a lively presence of contemporary art, with the central space occupied by two intriguing pieces. At one end, German photographer Nils Klinger captures sleep in a single still by leaving the shutter open on his slumbering subject for the time it takes a candle, the sole light source, to burn down ('Die Schlafenden', pictured). At the other, London-based sculptor Laura Ford has installed two kneeling child-like figures with donkeys' heads "to recall the fantastical slumbers of *A Midsummer Night's Dream*". The combination makes a disturbing piece.

Sleeping and Dreaming is a result of a collaboration between the Wellcome Collection and its German analogue, the Deutsches Hygiene-Museum in Dresden, from which the exhibition has just transferred. Both are a result of visionary philanthropy — pharmaceutical entrepreneur Sir Henry Wellcome in Britain and industrialist and oral-hygiene pioneer Karl August Lingner in Germany.

The Wellcome Collection offers a place to "consider what it means to be human" and the Deutsches Hygiene-Museum aspires to reveal mankind's "multilayered cultural, physical, and psychological nature". I await their next joint venture, *War and Medicine*, with interest. ■

Henry Nicholls is a London-based science writer and author of *Lonesome George: The Life and Loves of the World's Most Famous Tortoise*.

Sleeping and Dreaming **runs at the Wellcome Collection, London until 9 March. See www.wellcomecollection.org.**

Rex appeal

Victorian Popularizers of Science: Designing Nature for New Audiences
by Bernard Lightman
University of Chicago Press: 2007.
528 pp. $45

The Earth on Show: Fossils and the Poetics of Popular Science, 1802–1856
by Ralph O'Connor
University of Chicago Press: 2008.
448 pp. $45

Frank A. J. L. James

The popularization of science has become a growth area for historical study. It is a natural continuation of the historian's quest to understand the social and cultural context and impact of science, and a consequence of scientists' admonitions over the past 20 years that the public should be better informed.

Implied is that the efforts of earlier generations of scientists fell short of making their work accessible to the public. But Lightman's and O'Connor's books paint a very different picture, at least with respect to the nineteenth century. Their insights come soon after Aileen Fyfe's *Science and Salvation* (2004) and David Knight's *Public Understanding of Science* (2006).

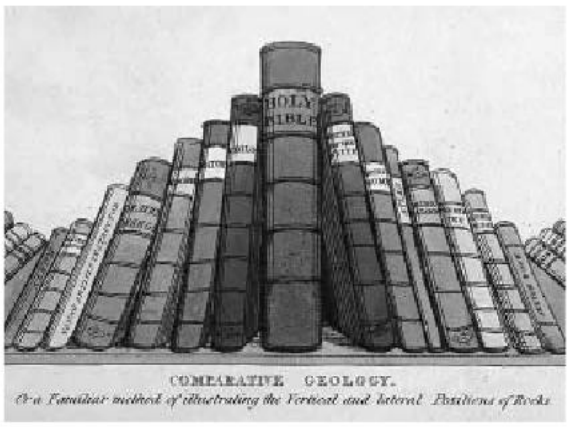

At the start of the nineteenth century, science was not an independent profession. Practitioners were often closely linked to medicine and the Church, at least in Britain, the country studied in *Victorian Popularizers of Science* and *The Earth on Show*. In France, there were more opportunities to pursue a scientific career. By 1900, science was widely practised independently in Europe and the United States, and the term 'scientist', coined by William Whewell in 1833, settled into the vocabulary. Science as a body of knowledge had become largely separated from theology.

This trajectory is tracked by Canadian historian of science Bernard Lightman in his survey of popular science in Victorian Britain. He begins with the Anglican ascendancy, in which most scientific work was undertaken by members of the Church of England, frequently those in holy orders. He moves on through showmen such as John Pepper (of Pepper's ghost fame), to biologist Thomas Huxley and evolution, and the astronomer Robert Stawell Ball.

Lightman maps the careers of some 30 popularizers, many sparsely covered before, who derived their income from writing science books, including Rosina Zornlin and John George Wood. Strikingly, many of these were professional writers or journalists and not scientific practitioners. Lightman reveals that the print runs of these now obscure figures were roughly the same as those for books published by well known scientific practitioners such as Ball, Huxley and natural philosopher John Tyndall. This suggests that the contemporary reading public could not easily distinguish between material written by a practising

scientific figure and a professional writer.

Because the history of popular science has been studied only recently and has concentrated largely on Victorian Britain, there is little to compare it with in terms of other periods or countries. But the large number of editions of Jane Marcet's various *Conversation* books from the early nineteenth century — and not discussed by Lightman, being pre-Victorian — indicates that there could have been a steady growth in science books before the Victorian boom.

Lightman has only one chapter on how scientific information was displayed, and uses images simply to enliven his text. By contrast, every image Ralph O'Connor uses advances his argument on the popularization of just one science, palaeontology. What Lightman gains in breadth, O'Connor makes up in depth.

O'Connor integrates the many genres that made fossils popular in the nineteenth century, using images from newspapers, books, magazines and pamphlets — including a striking one from 1828, where books were arranged to look like geological strata (pictured) — as well as John Martin's paintings, lecture illustrations, displays, dioramas and panoramas (for advertisements and handbills). O'Connor shows that promoting knowledge about geology was then similar to the marketing of other types of literature and art — science was an integral part of culture.

Books such as these, and Peter Bowler's eagerly anticipated history of popular science literature during the first half of the twentieth century, have much to offer today's debate about science education and engagement. Many of the 'public understanding of science' initiatives launched in the 1980s came to grief when the 'real' rather than the 'evaluative' world intervened. Looking back at the Royal Society's 1985 report on the subject, one wonders whether some historical perspective might have helped. History, full of contingency as it is, will not, of course, repeat itself. But the present boom in scholarship on the history of popular science should ensure that we come to appreciate our predecessors' efforts. ■

Frank A. J. L. James is president of the British Society for the History of Science and professor of the History of Science at the Royal Institution, 21 Albemarle Street, London W1S 4BS, UK. He is author of *Christmas at the Royal Institution*.

Pulling power

The Universal Force: Gravity, Creator of Worlds
by Louis A. Girifalco
Oxford University Press: 2007. 288 pp. £19.99

Sean Carroll

Gravity, the weakest known force, is the most obvious in our everyday life. The urge to understand it has challenged generations of great physicists, from Galileo and Newton to Einstein and Hawking. Yet gravity remains aloof and mysterious. The attempt to reconcile it with quantum mechanics is one of the most ambitious and urgent programmes of modern physics. Small wonder popular books on the topic — such as Louis Girifalco's addition — have an enduring appeal.

Our understanding of gravitation is encapsulated in Einstein's general theory of relativity. This supposes that space and time together form a dynamical four-dimensional manifold whose curvature influences the motion of matter. Girifalco tackles this well-trodden ground in the time-honoured way: by focusing on the historical development of the concepts and the colourful scientists involved.

Scientists today typically share a distorted and oversimplified view of the development of their subject, passed down through shared anecdotes of a series of brilliant insights and heroic discoveries. The reality is understandably messier and Girifalco weaves an interesting narrative from the complex history of this field. He opens with an extended discussion of Newton before introducing the ancient Greeks and the Copernican revolution.

Girifalco's historical focus allows him to include material rarely covered in other books on gravity. For example, he digresses to contrast the personalities and skills of Michael Faraday and James Clerk Maxwell and the development of modern electromagnetism — the first true field theory that builds a crucial bridge between newtonian gravity and relativity.

J. CAMPBELL, AERO-NEWS NETWORK/NASA

Even to Stephen Hawking — here enjoying zero gravity in a jet — the force remains mysterious.

The Universal Force fills a niche. Many people who might be interested in physics can be turned off by its abstraction, and physicists have an unfortunate predilection for explaining their subject to non-experts by simply watering down the explanations they would give to their students. For anyone interested in the more human side of science, this work is a valuable contribution.

The emphasis on storytelling over concepts, however, creates pedagogical challenges. For instance, the book is free of pictures and diagrams: a puzzling omission. A picture of the patterns made by iron filings in the presence of a magnet would have helped explain Faraday's lines of magnetic force. Referring to the bending of light by curved space-time, the author writes: "There is a picturesque two-dimensional model that can help our understanding." Shame we don't get to see it.

Modern gravitational physics is not the author's specialty — he is a solid-state theorist — and it shows in the sections on general relativity and curved space-time. Girifalco is correct to emphasize that general relativity is essentially a very simple theory, its intimidating reputation notwithstanding. But it is harder than he makes it out to be in saying, "the laws of physics are the same for everybody, everywhere". Properly interpreted, this motto could equally well apply to newtonian gravity.

Similarly, many of the most exciting aspects of general relativity get short shrift. Black holes and the Big Bang each get a brief chapter, and there is almost nothing about the thrilling prospects for gravitational waves. Hawking's epochal (if theoretical) discovery that black holes emit radiation is a mere footnote, and no mention of string theory sullies the pages. Yes, these subjects have been thoroughly picked over in other books, but a reader expecting an introduction to some of Einstein's more recent progeny will feel cheated.

Caveats aside, Girifalco is a fluid writer, and his stories are compelling. This book about the force of gravity has its feet firmly on the ground. ■

Sean Carroll is a senior research associate in physics at the California Institute of Technology, 1200 E. California Blvd, Pasadena, California, USA. He is author of *Spacetime and Geometry*.

NEWS & VIEWS

MOLECULAR BIOLOGY

RNA rules

Meng-Chao Yao

Studies of an old genetic puzzle in a little-known protozoan reveal a new frontier in the expanding world of RNAs: an RNA template guides genome-wide DNA rearrangements during sexual reproduction.

Ciliated protozoa are unicellular organisms the analysis of which — largely because of the unusual organization of their genome — has led to fascinating fundamental discoveries, such as those of telomeres and catalytic RNAs. These protozoa contain both a germline nucleus and a somatic (non-germline) nucleus. The somatic genome is functional in the maternal protozoan, but degrades after fertilization. The germline genome, by contrast, is transcriptionally inert in the mother cell, but is transmitted to progeny, where it gives rise to both the germline and the somatic nuclei. The differentiation of the somatic nucleus from the inherited germline nucleus involves extensive genome rearrangements, including DNA deletion, fragmentation and amplification, to produce a greatly altered genome. On page 153 of this issue, Nowacki *et al.*[1] show that a part of this process is orchestrated by RNA templates of maternal origin.

A highly unusual form of genomic rearrangement was discovered in the ciliated protozoan *Oxytricha nova* almost two decades ago by Prescott and colleagues[2]. They found that the gene encoding the actin protein seemed normal in the somatic genome, but in the germline genome it was fragmented into nine pieces, all of which were scrambled in their position and orientation. This observation suggested that, in order to function, the actin-encoding gene must be unscrambled after every sexual reproduction — a stunning possibility that raised fundamental questions about why genes become scrambled and how they are put back together accurately. In the ensuing years, other scrambled genes were discovered and were found to be quite common in *O. nova* and closely related species. But the mysteries of 'why' and 'how' remained.

By following a trail of RNA, researchers have subsequently succeeded in demystifying nature's ingenious workings. RNA is emerging as an essential regulator of the activity of various genes, particularly through a process known as RNA interference (RNAi). In ciliated organisms RNA even directs DNA deletion, a common process that removes and eliminates small, internal DNA segments without altering the order of the remaining segments. For example, in *Tetrahymena* and *Paramecium* DNA segments originating from the germline genome are apparently transcribed into double-stranded RNA, which is processed into small RNA sequences just like those that mediate RNAi. These short sequences then seek out and help modify chromatin (the complex of DNA and histone proteins in the chromosomes) containing the same DNA sequence, marking it for deletion[3,4]. This intriguing process of RNA-guided DNA deletion hinted at new possibilities and put the focus on RNA.

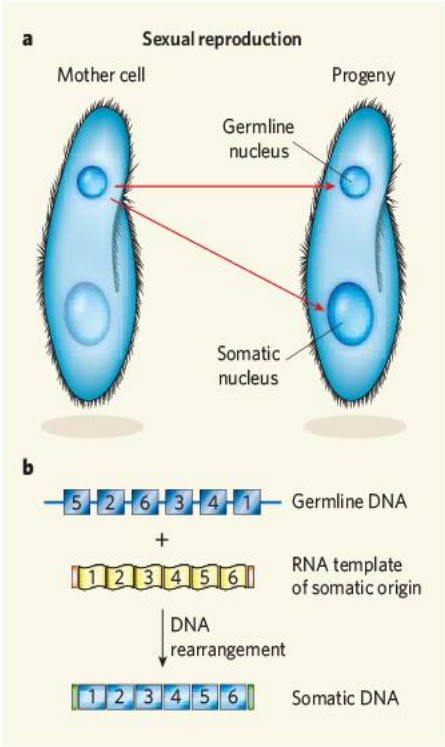

Figure 1 | RNA-guided genome rearrangement. Nowacki *et al.*[1] studied the unscrambling of germline DNA in the ciliated protozoan *Oxytricha trifallax*. **a**, During sexual reproduction, the germline genome is transferred to the progeny to give rise to both germline and somatic genomes. **b**, The authors find that, although the somatic genome is not directly transferred to the progeny, an RNA copy of it serves as a template for the unscrambling of the rearranged germline DNA to give rise to the new somatic genome.

Perhaps the biggest challenge for cells in unscrambling a gene is knowing which gene segments to put together. The only source of this information is probably the unscrambled parental somatic genome. Could an RNA copy of this be made and used as a template for the rearrangement process?

Nowacki *et al.*[1] tested this bold idea in *Oxytricha trifallax*. They detected likely RNA-template candidates for two genes that are scrambled during sexual reproduction, and selectively destroyed them using RNAi. They found that the rearrangement process was affected, leading to progeny with incorrectly or only partially unscrambled genes.

Another approach the authors took was to inject these unicellular organisms with RNA (or DNA) that had been designed to contain sequences altered in a specific way. Remarkably, the progeny of these cells contained the gene targets of these RNA sequences in the correct (altered) order. (Nowacki *et al.* suggest that the unscrambling associated with DNA injection is also mediated by RNA.) These striking results leave little doubt that RNA is the template for DNA rearrangement in *O. trifallax*.

The implications of Nowacki and colleagues' findings are far-reaching. To unscramble all the rearranged genes, a large fraction of the somatic genome must be transcribed into RNA. In fact, the entire genome might be transcribed equally, because the one gene in the authors' study that did not require unscrambling was also transcribed, and could even be coerced into reordering when the cells were injected with an altered RNA template.

The RNA copy of the genome must then be transported to the nascent somatic nucleus of the progeny to guide rearrangement. Thus, a new system of inheritance is established whereby the somatic genomic information is inherited independently of the germline genome through a transient 'RNA genome'. A proof of this non-mendelian form of inheritance came from the demonstration that the new gene order induced by the injection was passed on to subsequent generations as predicted. Similar heritable changes have also been reported to occur in mice after RNA injection[5].

The form of inheritance observed by Nowacki *et al.* (Fig. 1) is remarkable. Were it to

occur in humans, it would mean that we would be able to inherit adaptive immunity to infectious diseases such as polio, which requires rearrangement of DNA in somatic immune cells — the lymphocytes. Although adaptive immunity is not known to be heritable, the inheritance of somatic genetic information in ciliates has long been known to occur[6]. Further support for this form of inheritance comes from studies of DNA deletion in ciliates.

In *Tetrahymena* and *Paramecium*, if a germline sequence is also present in the somatic genome, its deletion is blocked, and the situation is perpetuated in subsequent generations[7,8]. It is thought that the maternal somatic genome may produce RNA to interfere with the small RNAs (produced from the germline genome) that guide somatic DNA deletion. Some researchers have even postulated that the whole germline genome is transcribed to produce small RNAs to guide DNA deletion, and that the entire somatic genome is transcribed to produce RNA that blocks the deletion of genes destined for the somatic nucleus, thereby establishing sequence specificity for DNA deletion[3,9].

Nowacki and colleagues' study[1] gives credence to these ideas. Thus, somatic genomic RNA may occur widely in ciliates to direct DNA rearrangements and affect inheritance; gene unscrambling could be a specific effect of transcription of the somatic genome into RNA. Once the mechanism for gene scrambling has evolved, mutational gene rearrangements in the germ line are tolerated and accumulate, resulting in an altered genome through evolution.

The study of Nowacki *et al.* ventures into *terra incognita*, as little is known about DNA rearrangement that is guided by a template. The process must be precise enough to recreate functional coding sequences on a genomic scale, and seems to involve local RNA-directed DNA synthesis — the authors found that sequences near rearrangement sites, but not those farther away, were copied from the RNA at high frequencies. There is no reason why similar processes should not occur in other organisms. Altering gene structure can be an effective mechanism for stable differentiation, and RNA is probably the most informative molecule to guide such alterations. The challenge is knowing where to look for it — as the odd and beautiful ciliates have once again reminded us, this is a rich and diverse world. ■

Meng-Chao Yao is at the Institute of Molecular Biology, Academia Sinica, Taipei 11529, Taiwan.
e-mail: mcyao@imb.sinica.edu.tw

1. Nowacki, M. *et al. Nature* **451,** 153–158 (2008).
2. Greslin, A. F., Prescott, D. M., Oka, Y., Loukin, S. H. & Chappell, J. C. *Proc. Natl Acad. Sci. USA* **86,** 6264–6268 (1989).
3. Mochizuki, K. *et al. Cell* **110,** 689–699 (2002).
4. Yao, M.-C., Fuller, P. & Xi, X. *Science* **300,** 1581–1584 (2003).
5. Rassoulzadegan, M. *et al. Nature* **441,** 469–474 (2006).
6. Sonneborn, T. M. *Annu. Rev. Genet.* **11,** 349–367 (1977).
7. Duharcourt, S. *et al. Genes Dev.* **9,** 2065–2077 (1995).
8. Chalker, D. L. & Yao, M.-C. *Mol. Cell. Biol.* **16,** 3658–3667 (1996).
9. Garnier, O., Serrano, V., Duharcourt, S. & Meyer, E. *Mol. Cell. Biol.* **24,** 7370–7379 (2004).

MATERIALS SCIENCE

Desperately seeking silicon

Cronin B. Vining

Using silicon as a 'thermoelectric' material to convert heat into electricity would be a technological leap forward. But silicon conducts heat so well that nobody thought that could work — until now.

Thermoelectric materials convert heat into electric current, and vice versa. If they could be made more efficient at that conversion, they might be used to suck up waste heat from fossil-fuel combustion processes to make electric current, or as an alternative to photovoltaic cells for converting solar warmth into electricity[1]. Silicon, the basic material of semiconductor electronics, is readily available, cheap and has a huge infrastructure and know-how for its production and manipulation. Those are reasons enough to seek a marriage between silicon and thermoelectric properties.

And indeed, silicon is a kind of thermoelectric material — the inefficient kind. In her classic 1947 paper on the efficiency of thermoelectric generators[2], the Hungarian–American physicist Mária Telkes concluded that "high efficiency could not be expected" for silicon, because it has such a high thermal conductivity. Silicon conducts heat too well to put it to any use: it is difficult to produce a temperature difference across it that is big enough to generate a useful voltage. Sixty years on, however, two papers in this issue[3,4] challenge Telkes's assessment. Boukai *et al.* (page 168)[3] use silicon nanowires with a rectangular cross-section and Hochbaum *et al.* (page 163)[4] use round silicon nanowires to achieve thermoelectric efficiencies comparable to those of the best commercial thermoelectric materials.

Thermoelectric efficiency is described in terms of the thermoelectric 'figure of merit', ZT, defined as $S^2T/\rho k$. Here, T is the material's temperature, ρ its electrical resistivity, k its thermal conductivity and S is the Seebeck coefficient, defined as the increase in potential difference per unit temperature rise. Bulk silicon has a ZT of about 0.01 at 300 kelvin (27 °C). For metal wires, the best value at 300 K is about 0.03. Values of 0.7–1.0 are now found in commercially available thermoelectric materials based on bismuth-telluride semiconductors. The first really solid report of much higher figures of merit, up to 2.4, came in 2001, in thin films of a complex semiconductor[5]. But high electrical and thermal losses in these thin films have so far kept them from the commercial big time.

Hochbaum *et al.*[4] now quote a ZT value of 0.6 for their silicon nanowires. Boukai *et al.*[3] cite about 0.4 at 300 K, and around 1 at 200 K — not earth-shattering in comparison with existing materials. But in this context it's worth remembering the old adage about dogs walking on their hind legs: it is not done well, but you are surprised to find it done at all. How exactly does it work?

The answer would seem to be, because size matters. The nanoscale geometries of the silicon wires reduce the thermal conductivity by about 100 times, to a value that is not just low for silicon, but low for any solid. Qualitatively, why this happens is not hard to see. Heat is carried by various particles: phonons, representing lattice vibrations, and charged particles such as electrons and holes (a hole is the absence of an electron, and can be thought of as a kind of positive charge). Introducing obstacles — in the case of the nanowires, edges — reduces that heat flow.

But there remains a modest quantitative problem. Hochbaum *et al.*[4] point out that no available theory can adequately explain why their values for the thermal conductivity are so very low. Boukai *et al.*[3] report even lower values, less than that of silica, whose amorphous structure presents a formidable barrier to heat flow. Admittedly, this won't be the first time that some downward revision to our norms has been required: the concept of 'minimum thermal conductivity' has always had a degree of Slack[6] in it.

Boukai and colleagues' rectangular nanowires were in general smaller than the circular nanowires of Hochbaum and colleagues, with cross-sections of 10 nm by 20 nm and 20 nm by 20 nm, compared with diameters of 20–300 nm for the circular nanowires. This smaller size seems to have led to additional effects. First, it reduces the electrical conductivity of the rectangular nanowires, partly negating the benefit of their decreased thermal conductivity. Second, and more importantly (as this quantity is squared in the expression for the figure of merit), it greatly increases their Seebeck coefficient.

The authors attribute this increase to a phenomenon called phonon drag. Phonons carry heat by thermal diffusion from hot regions to cold. Along the way, they may collide with electrons and holes, losing some of their energy, and in some cases dragging the charge carriers along. The result is a larger Seebeck coefficient, larger thermal voltages and a higher efficiency. For all previously known 'good' thermoelectric materials, phonon drag has been a small, even

negligible, effect. Now, engineering phonon drag would seem poised to become a new tool for improving thermoelectric materials.

Although size seems to be the decisive difference between the two sets of results[3,4], there are other possibly crucial differences between them: surface roughness, nanowire length and substrate material (in Boukai and colleagues' study[3], the nanowire array was suspended above a silicon wafer; in Hochbaum and colleagues' study[4], it was bedded on silicon dioxide). Sorting out all the science behind these results might take time. We need to develop predictive models, understand the optimum size and doping levels, extend the data to high temperatures, and find out what other materials might show the effects of low thermal conductivity and large phonon drag. And does one really need nanowires at all, or would some other nanoscale configuration do?

In one stroke (albeit from two directions), the thermoelectric capability of silicon has been improved by a factor of nearly 100. It thus leaps up the scale of thermoelectric materials from 'terrible' to 'not bad'. What happens next is anyone's guess; but I for one am no longer taking bets against silicon's thermoelectric future. ■

Cronin B. Vining is at ZT Services, 2203 Johns Circle, Auburn, Alabama 36830-7113, USA.
e-mail: nature@zts.com

1. Crabtree, G. W. & Lewis, N. S. *Phys. Today* **60** (3), 37–42 (2007).
2. Telkes, M. *J. Appl. Phys.* **18,** 1116–1127 (1947).
3. Boukai, A. I. *et al. Nature* **451,** 168–171 (2008).
4. Hochbaum, A. I. *et al. Nature* **451,** 163–167 (2008).
5. Venkatasubramanian, R., Siivola, E., Colpitts, T. & O'Quinn, B. *Nature* **413,** 597–602 (2001).
6. Slack, G. A. in *Solid State Physics* Ser. 34 (eds Ehrenreich, H., Seitz, F. & Turnbull, D.) 1–71 (Academic, New York, 1979).

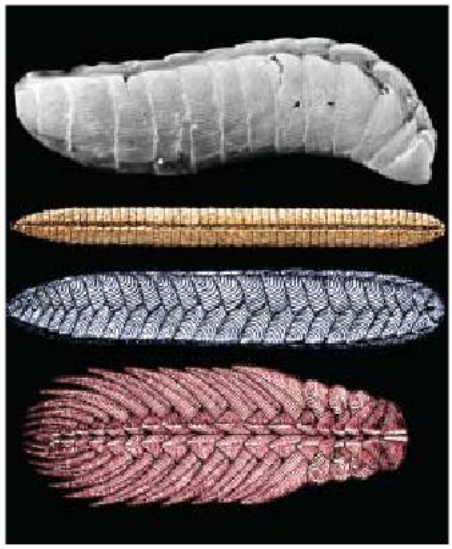

Figure 1 | The machaeridians. Top, a complete machaeridian scleritome from 425-million-year-old deposits in New York state[3]. Length, 5.4 mm. Bottom, dorsal reconstructions of presumed complete scleritomes (not to scale) showing the diversity of scleritomes within the three families of machaeridians[9] — running upper to lower, the Lepidocoleidae, Turrilepadidae and Plumulitidae. The fossil specimen (top) is a lepidocoleid; that described by Vinther *et al.*[1] is a plumulitid. All scleritomes are shown with the presumed head to the right. (Top image courtesy of A. Högström; bottom images courtesy of J. Dzik.)

PALAEONTOLOGY

Ancient worms in armour

Jean-Bernard Caron

It requires a quirk of fossilization for the soft parts of an animal to be preserved. Study of such a specimen of the mysterious machaeridians provides these organisms with a well defined evolutionary home.

A 480-million-year-old fossil from Morocco, described by Vinther *et al.* on page 185 of this issue[1], ends a long controversy over a group of enigmatic fossils called the machaeridians. Now convincingly interpreted as primitive segmented (annelid) worms, the extinct machaeridians had a scaly 'armour' of mineralized shell plates over or around a soft body of previously unknown form. This armour represents an adaptation not seen in modern segmented worms, and raises a host of questions about the group's evolution and origins.

Efforts to unravel the machaeridian mystery have faced great challenges. The fossils are common in ancient marine deposits, but are tiny. A complete armour (known as the scleritome) is often smaller than a fingernail. Moreover, the finding of articulated shell plates is extremely rare. No wonder, then, that these animals have been studied by only a handful of scholars since they were first described in 1857 — one of the most comprehensive accounts of the group is a venerable 1926 monograph[2]. Discoveries of rare articulated specimens have added more knowledge on the morphology, mode of growth and function of the scleritome[3]. But, apart from the recognition of three distinct families of machaeridian (Fig. 1), such studies have not really helped to clarify the wider taxonomic position of the group.

Previous speculations have allied machaeridians to the molluscs, the arthropods or, particularly, the echinoderms. Stefan Bengtson first convincingly suggested a possible relationship to the annelids[4]. On the basis of microstructural studies of shell plates[5], he soundly refuted the echinoderm hypothesis, but unfortunately subsequent indications of a link to the annelids[6] remained untested. Palaeontologists are sceptics by nature, and most were waiting to see a specimen with the body attached to the plates to be convinced.

Vinther and colleagues' study[1] is based on the oldest known machaeridian scleritome. This remarkable specimen has defied the usual odds of fossil preservation by retaining traces of the elusive soft body. After death, soft body parts typically decompose quickly. Exactly what conditions caused this specimen to be preserved is unknown, but low oxygen levels might have had a role. Admittedly, the specimen will not seem as spectacular to the novice as other, more famous 'soft-bodied' fossils[7]. There is some evidence of disarticulation, and the head is missing, which is a pity because the head section might have provided important morphological information for taxonomy. But the limited disarticulation has allowed some plates to become detached, revealing the body outline of the enigmatic animal underneath (see Fig. 1 of the paper[1] on page 186).

The crucial information lies in the numerous protrusions bearing prominent filaments in bundles along both sides of the animal. The authors interpret these to be parapodia, bearing chaetae, features that are typical of marine bristle worms or polychaetes (literally meaning 'very hairy'). Thus, the fossil machaeridians seem to have found a home at last within this larger group. But why some ancient annelids should develop a complex mineralized scleritome, endure for hundreds of millions of years, and then disappear entirely, remain questions for the future.

What are the other implications of this study? Annelids today are thought to be composed of two major groups[8], the Clitellata (including earthworms and leeches) and the Polychaeta. It is not well understood which of these two groups is the more primitive (basal), and the interrelationships of the polychaetes are still poorly resolved. Whether the machaeridians can help answer these questions is doubtful. Possession of a mineralized scleritome, the presumed ability to roll up, and a fixed number of plates growing by increments are all features of Vinther and colleagues' fossil and of members of the other machaeridian families, but are not present in the modern groups of polychaete[3]. So perhaps current evidence favours positioning the machaeridians as 'stem-group annelids', that is, not belonging to any modern group of annelids (Fig. 2). On the other hand, identifying machaeridians as primitive polychaetes removes problems arising from their putative assignment to other groups of animals (such as molluscs), and helps constrain broader evolutionary models.

Meanwhile, the deeper origins of the machaeridians have yet to be elucidated. It has been speculated that the roots of this group may lie in the Cambrian explosion, a time of rampant morphological innovation starting about 540 million years ago when mineralized skeletal parts appear suddenly in different groups of animals. Some isolated shells from the Lower

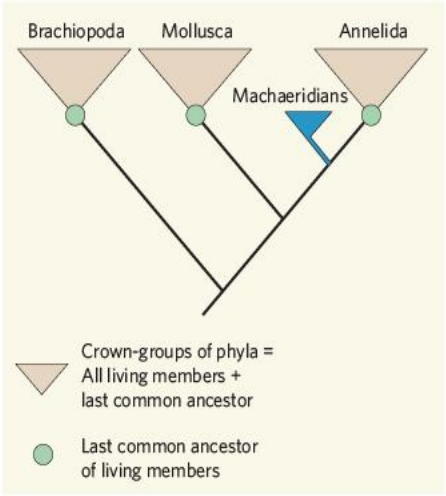

Figure 2 | Machaeridians in evolutionary context. The Annelida, Mollusca and Brachiopoda are all constituent phyla of a bigger group called the Lophotrochozoa. The machaeridians had a long run in the evolutionary record, occurring from at least 480 million years ago to around 275 million years ago. These worms had a cosmopolitan distribution, and were members of benthic communities dominated by shelly organisms. On the evidence of the new species described by Vinther *et al.*[1], the machaeridians are probable stem-group annelids: that is, they diverged from the annelid lineage before the advent of modern members of the group.

Cambrian, around 530 million years ago, look surprisingly similar in morphology to machaeridian plates, and are thought to belong to a similar type of scleritome[4]. But without finding articulated, soft-bodied specimens, their relationships will remain unclear. By the Middle Cambrian, some 25 million years later, primitive groups of polychaetes were already firmly established, as the fossils of the Burgess Shale in the Canadian Rockies demonstrate[7], but none of these forms bears shell plates.

Other than machaeridians, older or contemporaneous fossils with scleritomes (mineralized or not) are very rare, and are equally difficult to classify[9]. Animals such as the Cambrian *Halkieria* and *Wiwaxia*[10] are quite unlike machaeridians, although they provide parallels in their body-plan construction. New discoveries of fossils with preserved soft tissues, particularly from the Cambrian, and new technologies for exploring potential soft tissues beneath the shell plates, will help us to refine our models of early animal evolution.

In this context, it will be essential to find other examples of machaeridian soft-tissue anatomy to confirm that the different families of machaeridian are indeed related to each other. Perhaps different types of organisms will be discovered beneath what seem to be similar types of shell plates. Let's hope that we don't have to wait another 150 years for the next significant fossil to surface. ■

Jean-Bernard Caron is in the Department of Natural History, Royal Ontario Museum, 100 Queen's Park, Toronto, Ontario, M5S 2C6, Canada.
e-mail: jcaron@rom.on.ca

1. Vinther, J., Van Roy, P. & Briggs, D. E. G. *Nature* **451,** 185–188 (2008).
2. Withers, T. H. *Catalogue of the Machaeridia (Turrilepas and its Allies) in the Department of Geology* (British Museum (Natural History), London, 1926).
3. Högström, A. E. S. & Taylor, W. L. *Palaeontology* **44,** 113–130 (2001).
4. Bengtson, S. *Lethaia* **3,** 363–392 (1970).
5. Bengtson, S. *Jugoslavica* **12,** 1–10 (1978).
6. Jell, P. A. *Alcheringa* **3,** 253–259 (1979).
7. Conway Morris, S. *Phil. Trans. R. Soc. Lond. B* **285,** 227–274 (1979).
8. Rouse, G. W. & Fauchald, K. *Zoologica Scripta* **26,** 139–204 (1997).
9. Dzik, J. in *Problematic Fossil Taxa* (eds Hoffman, A. & Nitecki, M. H.) 116–134 (Oxford Univ. Press, 1986).
10. Conway Morris, S. & Peel, J. S. *Nature* **345,** 802–805 (1990).

CONSERVATION BIOLOGY

Cats, rats and seabirds

Matthieu Le Corre

Cats kill birds, and therefore eradicating cats from an island would seem to be a good strategy for protecting the native population of seabirds. But that thinking does not take account of ecological complications.

When alien species colonize islands, some of the native inhabitants usually suffer. Seabirds are commonly the victims in these sad cases, because they or their chicks or eggs are especially prone to becoming the prey of introduced mammals. Over the past 20 years, conservation workers in different parts of the world have expended much time and effort to eradicate predators such as cats and rats from selected islands[1]. The upshot has often been an improvement in the status of the species under threat.

But matters are not always straightforward in conservation biology, as Rayner *et al.* demonstrate in a paper in *Proceedings of the National Academy of Sciences*[2]. Using a 35-year data set, they show empirically that the eradication of cats from Little Barrier Island, an oceanic island off the coast of New Zealand's North Island, led to a severe decrease in the breeding success of the resident seabird, a burrowing species called Cook's petrel (Fig. 1). The reason, it seems, was an explosion in the number of rats, which tend to prey on the petrel chicks and eggs, and which resulted from the absence of cats. The impact of the rats on the petrels depended on habitat altitude, with birds nesting at lower elevations suffering less severely. Rayner *et al.* are not sure why this should be; they speculate, however, that the difference is because of the greater availability of other food sources for the rats at lower altitudes.

The authors' principal results seem to support theoretical models showing that, when cats and rats both kill an endangered bird species, the eradication of cats may accelerate the decline of the bird as a consequence of an increase in rat numbers. This possible outcome, termed the 'mesopredator release effect'[3], must clearly be taken into account when planning conservation projects.

Relationships of communities invaded by several species can be complex[1]. Adding to that complexity is variation in the life-histories of threatened species. For example, most seabird species have long lifespans, low reproductive rates and delayed maturity, making them very sensitive to changes in adult survival but less sensitive to changes in reproduction rates[4]. This is the reason seabirds are so vulnerable as 'by-catches' in fishing operations. Each year, techniques such as longline fishing cause the death of thousands of adult birds, albatrosses being prominent examples; the result has been collapses in certain seabird populations in the southern oceans[5].

For mammal invasions, seabird life-history traits are likewise an important factor. Cats (average weight 2.5 kilograms) are efficient predators that can kill both adults and chicks of most small or medium-sized species of seabird (weighing up to 1 kg). Furthermore, by killing the breeding adults, cats indirectly affect the breeding success of the birds because both parents are indispensable for rearing a chick. Rats (average weight 70–400 g, depending on the species) are also efficient predators, but their size makes them less dangerous to adults. Instead, they tend to eat eggs or small chicks, and most studies have shown that, for seabirds, breeding success is indeed the main

P. REESE/NATUREPL.COM

Figure 1 | Cook's petrel, *Pterodroma cookii*. This seabird is pelagic, coming to land only to breed; breeding locations include Rayner and colleagues' study site of Little Barrier Island[2]. The bird is classified as "endangered" by the World Conservation Union[11].

Common name	Latin name	Breeding location	Main causes of decline
Fiji petrel	*Pseudobulweria macgillivrayi*	Fiji	Predation by cats and rats
Mascarene black petrel	*Pseudobulweria aterrima*	Réunion	Predation by cats and rats, urban light-induced mortality
Beck's petrel	*Pseudobulweria becki*	Melanesia	Predation by cats and rats
Chatham petrel	*Pterodroma axillaris*	Chatham Island	Predation by introduced predators; competition with another seabird for breeding burrows
Jamaica petrel (possibly extinct)	*Pterodroma caribbaea*	Jamaica	Predation by rats and mongooses
Magenta petrel	*Pterodroma magentae*	Chatham Island	Predation by cats and rats
Galapagos petrel	*Pterodroma phaeopygia*	Galapagos Islands	Predation by introduced predators
Balearic shearwater	*Puffinus mauretanicus*	Balearics	Predation by cats; bycatch in longline fisheries

Figure 2 | Petrels in peril. The eight species of petrel (family Procellariidae) classified as "critically endangered" by the IUCN[11]. For all species, predation by introduced mammals is the main cause of decline. The Mascarene black petrel of Réunion suffers particularly from being attracted to the bright lights of urban areas. Should it fall to the ground in the city, it is unable to take off as it can from its usual clifftop home, and falls prey to urban mammals and motor vehicles.

demographic trait influenced by rats[6].

The lethal combination of cats and rats on islands is all too common, and threatens endemic petrels (Fig. 2) and other seabirds and animals all over the world. Conservation managers require guidelines for eradication programmes[7], and in some cases simultaneous eradication of both cats and rats may not be possible[8]. In such cases, which species should be tackled first? Mathematical models simplify reality, and in the original model[3] of the relationships between cats, rats and birds, the different impacts of cats and rats on the different age classes of the native prey were not considered.

Rayner *et al.*[2] confirm the model prediction that, as a likely consequence of mesopredator (rat) release, the breeding success of Cook's petrels would decrease substantially following cat eradication. However, the increase in survival of adult seabirds, free from cat predation and immune to rat predation, could have offset the corresponding decrease in reproduction; adult survival was something Rayner *et al.* did not measure. Given the occurrence of a mesopredator release effect, it might seem that cats should not always be the first to be eradicated, especially if a population explosion of rats (or a similar species such as mice[9]) might follow. But this must be contrasted with the different impacts of cats and rats on the different age classes of seabird species — even if the eradication of cats leads to an increase in rat density, this might not necessarily mean a decline in a seabird population.

In providing the first evidence of a mesopredator release effect on an island, Rayner *et al.* show, yet again, that in the real world of conservation a solution may not always be as simple as it at first seems. They also show once more the value of long-term ecological monitoring. As is only to be expected, however, the interface between theoretical models of the different impacts of cats and rats on seabird populations[6,10] and long-term field data requires more detailed scrutiny. Only by continual testing of models with data in different circumstances, including such factors as habitat altitude or the age-structured population of the native prey, will we be able to find out what is really best for the birds. ■

Matthieu Le Corre is in the Laboratoire Ecomar, Université de La Réunion, F-97715 Saint Denis de La Réunion, France.
e-mail: lecorre@univ-reunion.fr

1. Courchamp, F., Chappuis, J.-L. & Pascal, M. *Biol. Rev.* **78,** 347–383 (2003).
2. Rayner, M. J., Hauber, M. E., Imber, M. J., Stamp, R. K. & Clout, M. N. *Proc. Natl Acad. Sci. USA* **104,** 20862–20865 (2007).
3. Courchamp, F., Langlais, M. & Sugihara, G. *J. Anim. Ecol.* **68,** 282–292 (1999).
4. Weimerskirch, H. *Biology of Marine Birds* (CRC Press, Cleveland, Ohio, 2002).
5. Lewison, R. L., Crowder, L. B., Read, A. J. & Freeman, S. A. *Trends Ecol. Evol.* **19,** 598–604 (2004).
6. Jones, H. P. *et al. Conserv. Biol.* **22** (in the press).
7. Brooke, M., Hilton, G. M. & Martin, T. L. F. *Anim. Conserv.* **10,** 380–390 (2007).
8. Rodríguez, C., Torres, R. & Drummond, H. *Biol. Conserv.* **130,** 98–105 (2006).
9. Huyser, O., Ryan, P. & Cooper, J. *Biol. Conserv.* **92,** 299–310 (2000).
10. Peck, D., Faulquier, L., Pinet, P., Jaquemet, S. & Le Corre, M. *Anim. Conserv.* (in the press).
11. IUCN Species Survival Committee *2007 IUCN Red List of Threatened Species* (IUCN, Gland, Switzerland, 2007).

STEM CELLS

A new year and a new era

Martin F. Pera

Manipulating cells from adult human tissue, scientists have generated cells with the same developmental potential as embryonic stem cells. The research opportunities these exciting observations offer are limitless.

In 2006, a groundbreaking study[1] showed that when adult mouse skin cells are manipulated to transiently express four transcription factors (Oct4, Sox2, Kfl4 and Myc), they can become reprogrammed — that is, transformed back to the equivalent of an early embryonic state, as occurs during the cloning of animals from adult cells. Four studies, including one on page 141 of this issue by Park *et al.*[2], now show that the introduction and expression of the same transcription factors[2–3] or a slightly modified combination of them[4–5] can also trigger the reprogramming of differentiated human cells.

Park and colleagues reprogrammed differentiated human cells from various sources (fetal and neonatal, as well as cells isolated from a skin biopsy of an adult volunteer) into what are known as induced pluripotent stem (iPS) cells, which have all the properties of stem cells derived from human embryos. Starting with the human counterparts of the genes encoding the same four transcription factors used for reprogramming mouse cells, the authors managed to reprogramme differentiated fibroblast cells derived from human embryonic stem cells into iPS cells at a relatively high frequency (0.1%). With fibroblasts from fetal tissues, the yield of iPS-cell colonies was also good. But, using this combination of genes, the authors did not obtain any iPS-cell colonies from neonatal fibroblasts, adult mesenchymal stem cells or adult fibroblasts.

To optimize their protocol for primary neonatal or adult human cells, Park *et al.* introduced two additional genes: *hTERT* (which encodes the catalytic subunit of human telomerase enzyme) and the gene for SV40 large T antigen. Although this modified protocol gave only a small percentage of reprogrammed cells, the introduction of these powerful immortalizing and transforming factors enabled iPS-cell colonies to develop in culture from the adult human cells.

The mechanisms by which SV40 large T antigen and hTERT improve the recovery of iPS-cell colonies are not known. Fibroblasts and other cultured diploid cells derived from postnatal human tissues often contain a significant, but highly variable, proportion of cells that are not actively dividing, or cells that are senescent or terminally differentiated and can no longer proliferate. By inhibiting the activities of the tumour-suppressor genes *RB1* (retinoblastoma) and *TP53* (p53 tumour suppressor), SV40 large T antigen can profoundly influence a range of cellular processes,

including cell-cycle regulation, and, along with hTERT, can immortalize human cells[6]. So it is possible that a central effect of these two proteins is to activate the cell-division machinery and enable the four transcription factors to access chromatin (the complex of DNA and histone proteins in chromosomes), thereby facilitating reprogramming.

Are the iPS cells that Park *et al.* generated, or indeed those obtained in the related studies[3–5], truly pluripotent — that is, do they have the potential to develop into various cell types? The best available assay for the developmental potential of human iPS cells is to test whether they can form teratomas (benign tumours containing cells from various differentiated tissues). Park and colleagues[2] do not report on teratoma formation by iPS-cell lines derived from neonatal or adult tissue, and their characterization of the differentiation of these cells *in vitro* is not extensive.

Similarly, the *in vitro* and *in vivo* data reported in the *Science* paper[4] raise some questions about the developmental potential of the reprogrammed cells derived from neonatal fibroblasts. The authors of the study[3] published in *Cell* used the teratoma test to establish pluripotency of the iPS-cell lines they derived from adult tissues, although, compared with embryonic stem cells, these lines showed some differences in their global patterns of gene expression. Finally, the related study[5] in *Nature Biotechnology* did not include extensive data on the developmental potential of the generated iPS cells. Further comparison of the iPS-cell lines generated in these studies with those derived from embryos is clearly warranted.

Several questions about the mechanism of the reprogramming process arise from these exciting observations[2–5]. So far, all successful direct reprogramming of differentiated mouse and human cells has relied for gene delivery on viral vectors that integrate into the cell's genome. It is therefore possible that the reprogramming in part depends on the effects of integration, or worse still, on other undetected genetic changes.

A crucial point that remains to be established is which genes are sufficient and necessary for reprogramming per se, and which are required for the induction of proliferation in the target cells. So far, the data implicate *OCT4* and *SOX2*, which lie at the heart of the transcriptional network that regulates pluripotency[7], in the reprogramming. Other factors studied seem to facilitate the reprogramming process, and so there might be many different combinations of these genes capable of achieving the same end.

Other questions remain. How do the differentiated state of the target cell, its cell-cycle status and its genetic background influence the efficiency of its reprogramming? And are human iPS cells truly equivalent to embryonic stem cells? Many of the same questions initially arose in the context of cloning by the technique of somatic cell nuclear transfer, which involves replacing an egg-cell nucleus with that of a differentiated adult cell. But the technique of direct reprogramming used in these four studies[2–5] is clearly far more amenable to addressing these questions.

The work of Park and colleagues[2], together with the related studies[3–5], proves beyond doubt that direct reprogramming is an efficient way of generating human pluripotent stem cells from adult cells. The results raise the hope that, one day, iPS cells might fulfil much of the promise of human embryonic stem cells in research and medicine. The generation of iPS cells through direct reprogramming avoids the difficult ethical controversies surrounding the use of embryos for deriving stem cells. The added advantage of direct reprogramming is that it enables patient-specific stem cells to be obtained for studying human disease and for tissue matching in transplantation. What is more, virtually any laboratory capable of carrying out the required cell-culture techniques can now perform direct reprogramming of adult cells. So the year 2008 promises to be very exciting for researchers interested in pluripotent stem-cell biology. ■

Martin F. Pera is at the Eli and Edythe Broad Center for Regenerative Medicine and Stem Cell Research, Keck School of Medicine, University of Southern California, Los Angeles, California 90033, USA.
e-mail: pera@usc.edu

1. Takahashi, K. & Yamanaka, S. *Cell* **126,** 663–676 (2006).
2. Park, I. H. *et al. Nature* **451,** 141–146 (2008).
3. Takahashi, K. *et al. Cell* **131,** 861–872 (2007).
4. Yu, J. *et al. Science* **318,** 1917–1920 (2007).
5. Nakagawa, M. *et al. Nature Biotechnol.* doi:10.1038/nbt1374 (2007).
6. Ahuja, D., Saenz-Robles, M. T. & Pipas, J. M. *Oncogene* **24,** 7729–7745 (2005).
7. Boyer, L. A., Mathur, D. & Jaenisch, R. *Curr. Opin. Genet. Dev.* **16,** 455–462 (2006).

PHYSICS

The force of fluctuations

Sébastien Balibar

Strange forces and effects dominate the world at the microscopic level. One such force, rooted in the random fluctuations of matter, has only now been accurately measured — 30 years after it was first predicted.

On page 172 of this issue, Hertlein *et al.*[1] present the first direct evidence for a force, known as the 'critical Casimir force', that is caused by the continual fluctuations of matter. The discovery is not a surprise: Michael Fisher and Pierre-Gilles de Gennes had predicted[2] the existence of the force in 1978, and indirect evidence for it had already been found[3–5]. Yet this new, strong evidence is extremely impressive — not least because of the weakness of the force that the authors have uncovered.

Forces are not just what you feel when, say, you push a door to open it. Many forces act without contact: gravitational or electrostatic forces are examples. Physicists have been studying these kinds of forces for more than a century to try to understand why things move, or sometimes don't. Mysteries remain not only at the largest of scales — the nature of the 'dark energy' that seems to be speeding up the expansion of the Universe is still unclear — but also at very small scales. It is this minute realm, inhabited by objects a micrometre or less across, that Hertlein and colleagues set out to explore.

Why bother? To answer that, and to explain how remarkable the tiny forces under investigation are, let us start with the ancestor of the authors' critical Casimir force, the plain old Casimir force. Imagine two metal plates placed a few micrometres apart. Sixty years ago, Hendrik Casimir proposed that two such plates should attract each other, even in a vacuum and in the absence of an electric charge[6]. Casimir forces are the best illustration of something both paradoxical and fundamental: the vacuum is not empty. Electromagnetic waves, such as light or radio waves, propagate in a vacuum, and bodies radiate electromagnetic waves with a temperature-dependent wavelength. Quantum physics predicts that, even at zero temperature, there are electromagnetic waves fluctuating in any vacuum.

Between Casimir's two plates, the only waves that can exist are those with a node (a zero of amplitude) at each plate. For the periodic waves that make up electromagnetic radiation, the distance between the plates must be a multiple of half the wavelength for this condition to be fulfilled. (A violin string works according to the same principle: it resonates when there is an integer number of half-wavelengths in the length of the string between its end and where it is held down.) The presence of the two plates eliminates many modes of electromagnetic fluctuation, and the energy of the system depends on the plate separation. If the energy depends on the separation, there must be a force that moves the plates to minimize that energy. These are Casimir forces, a consequence of quantum fluctuations of electromagnetic fields in confined geometries that is still under study[7].

Fisher and de Gennes's contribution[2] was to realize that Casimir forces can pop up in some situations where the fluctuations are of a classical rather than a quantum nature.

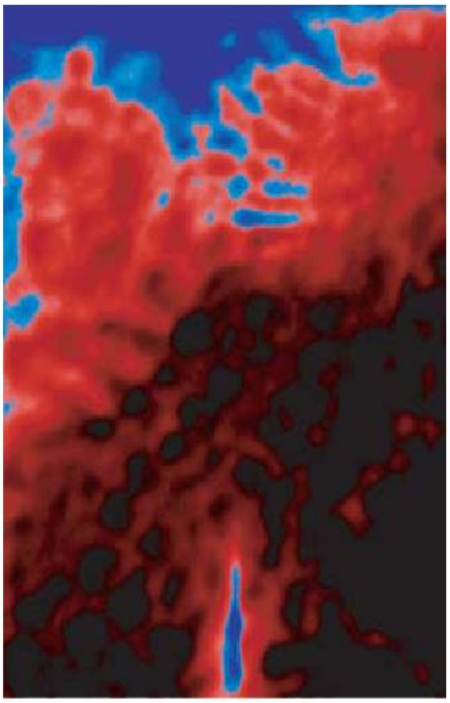
C. HERTLEIN *ET AL.*

Figure 1 | Critical fluctuations. The demixing of water and the solvent 2,6-lutidine (seen here in false colours), is Hertlein and colleagues' laboratory[1] for measuring the critical Casimir force.

Specifically, they occur when a physical system changes state continuously, for example in a liquid–gas transition, or during the phase separation of a liquid mixture near its 'critical' temperature. Above this critical temperature, the liquid–gas transition does not exist. Close to it, there are large density fluctuations, as if the system were hesitating between two very similar states. Fisher and de Gennes predicted that these fluctuations should also be affected by a confining geometry, just as in the original Casimir effect. If two plates are immersed in a fluid system close to its critical point, a critical Casimir force should arise.

This new force should differ significantly from the original Casimir force in two respects. First, it should depend strongly on temperature, because it is highly sensitive to the distance from the critical temperature. Second, it should be either attractive or repulsive, according to the nature of the two surfaces: if they attract the same component of the liquid mixture, the force should be attractive; if each attracts a different component, the force should be repulsive.

Several groups have tried either to obtain experimental evidence for these astonishing forces or to calculate their effects. Both proved extremely difficult. The first indirect evidence came in 1999, with studies of films of liquid helium on copper plates[3]. Liquid helium has a critical point at very low temperature, where it becomes a superfluid (it starts to flow without friction). Close to this point, the liquid film became thinner, and this phenomenon was successfully analysed by assuming the existence of critical Casimir forces.

Hertlein and colleagues' direct proof[1] comes from measuring the force between two solid objects: a silica plate and, about 0.1 micrometres away, a polystyrene sphere about 3 μm in diameter. Both plate and sphere could be treated such that the expected forces would be either attractive or repulsive. The authors immersed everything in a mixture of water and the organic compound 2,6-lutidine near the mixture's critical point at 307 kelvin (34 °C) (Fig. 1). Their extremely sensitive apparatus used the technique of total internal reflection microscopy to measure the force between the plate and the sphere to an accuracy of 1 femtonewton (10^{-15} N). The size of the Casimir force they found was less than 600 femtonewtons, and its sign could be changed by treating the surfaces differently. A neighbouring group of theorists at the University of Stuttgart in Germany calculated[8] the variation of the effect with temperature and distance; their result is almost exactly the same as that from the experiments.

Is this discovery of any practical importance? As is so often the case, it's too early to tell. But the authors suggest that, as their force can easily be tuned by changing the temperature or by a surface chemical treatment, it could be used to control the aggregation of colloids, a central problem in many areas of materials science. They also note that the original Casimir force turns out to be a problem for attempts to actuate microscale devices: for instance, it makes microcantilevers stick to neighbouring walls. By plunging such devices in a tailored liquid mixture, this mechanical problem could be suppressed by creating repulsive forces. They might well be right in their predictions. Even better, these new forces might find applications that no one has even thought of yet. ■

Sébastien Balibar is at the Laboratoire de Physique Statistique de l'Ecole Normale Supérieure, 24 rue Lhomond, 75231 Paris, France.
e-mail: balibar@lps.ens.fr

1. Hertlein, C., Helden, L., Gambassi, A., Dietrich, S. & Bechinger, C. *Nature* **451,** 172–175 (2008).
2. Fisher, M. E. & de Gennes, P.-G. *C. R. Acad. Sci. Paris B* **287,** 207–209 (1978).
3. Garcia, R. & Chan, M. H. W. *Phys. Rev. Lett.* **83,** 1187–1190 (1999).
4. Fukuto, M. *et al. Phys. Rev. Lett.* **94,** 135702 (2005).
5. Beysens, D. & Estève, D. *Phys. Rev. Lett.* **54,** 2123–2126 (1985).
6. Casimir, H. B. G. *Proc. Kon. Nederl. Akad. Wet. B* **51,** 793–795 (1948).
7. Kardar, M. & Golestanian, R. *Rev. Mod. Phys.* **71,** 1233–1245 (1999).
8. Vasilyev, O., Gambassi, A., Maciolek, A. & Dietrich, S. *Europhys. Lett.* **80,** 60009–60014 (2007).

QUANTUM MECHANICS

Evolution stopped in its tracks

Lev Vaidman

How do you watch the evolution of something that doesn't evolve? In the classical world, even posing this question would provoke raised eyebrows. But where quantum physics is involved, no question is too silly.

"A watched pot never boils," the saying goes, although the laws of physics tell us that this can't be true. More precisely, the cosy intuitions of classical physics tell us this can't be true. But enter the topsy-turvy realm of quantum physics, and the saying and the science converge. Specifically, a phenomenon known as the quantum Zeno effect states that if we find a system in a particular quantum state, and repeatedly and frequently check whether it is still in that state, it will remain in that state. It does this even if, without constant checking, it would evolve to another state. The watched quantum pot never boils.

Bizarre and abstruse as the whole thing might sound, it could have practical applications, in particular to the field of quantum information[1]. Hence the interest in theoretical studies such as that of De Liberato[2], which appears in *Physical Review A*. De Liberato looks more closely at systems that are subject to the quantum Zeno effect, and finds a procedure that allows us to observe how such systems try to evolve, even though they do not do so. Although Zeno measurements are part of this procedure, they do not stop the evolution. De Liberato instead finds a new, and in this case more powerful, method to hold a quantum system in a given state so that its evolution can still be measured.

But first, some background. The Zeno of the quantum Zeno effect is Zeno of Elea, a Greek philosopher of the fifth century BC from the colonies of southern Italy. In his arrow paradox, he postulated that an instant is indivisible; an arrow, therefore, cannot be in different places at the beginning and the end of an instant. Because, within any instant, the arrow cannot change its place, it can't in fact move at all. Somewhat surprisingly, and despite the development of mathematical tools such as calculus to deal with continuous motion, philosophers are still not sure that classical physics can provide a good answer to Zeno's paradox. What is the nature of the impetus that provides an instantaneous velocity[3]?

Quantum mechanics, oddly enough, has an answer. Its impetus is quantum-mechanical momentum, which is a property of a quantum state at any instant. The velocity of a moving quantum arrow, as represented by its associated quantum wave, can be estimated at any

NATURE|Vol 451|10 January 2008

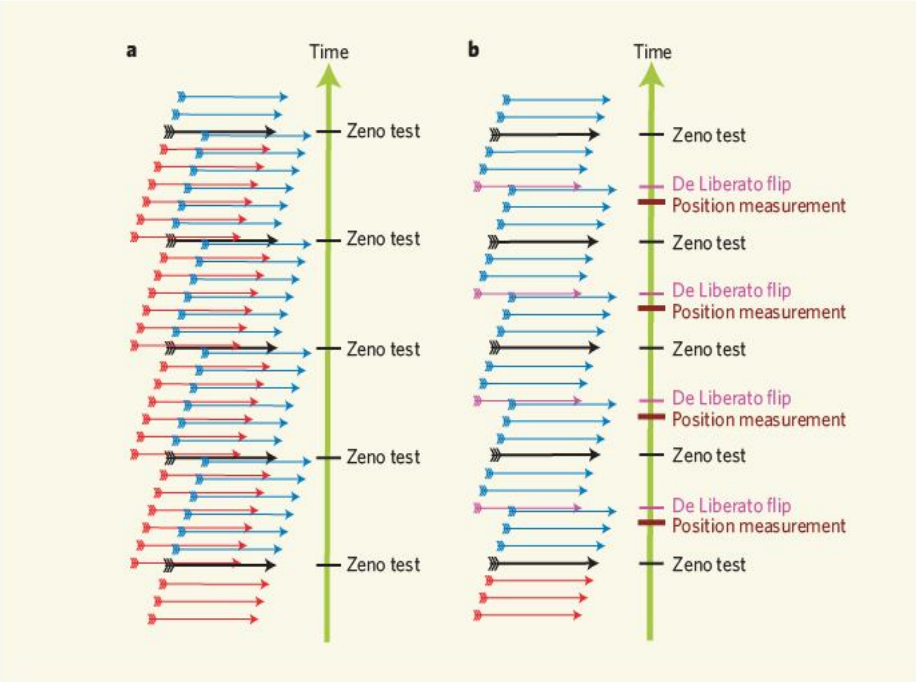

Figure 1 | A step forward, a step back. **a**, In accordance with the quantum Zeno effect, a quantum arrow with positive momentum (velocity to the right) is brought back to the same position by the frequent measurements made on it. Between these measurements, the arrow is described by two quantum states: one evolving to the future (blue arrows) and another to the past (red). The states are shifted in opposite directions and so a measurement of the arrow's average position will show it to be in the position of the Zeno test, making a measurement of its instantaneous velocity impossible. **b**, De Liberato[2] introduces a different scheme, in which the arrow steps back owing to a quick flip of the relative sign in the superposition of the original and the newly developed state. The future-evolving and past-evolving states are as a result always shifted by the same amount. Just before De Liberato flips, the shift is positive. It is very small relative to the uncertainty in the arrow's position, but (unlike in the scheme in **a**) we can now repeat the procedure many times to resolve the uncertainty and to measure the shift. The instantaneous velocity of the arrow can thus be measured, in spite of the Zeno tests holding the arrow at the origin.

time as its momentum divided by its mass. But although quantum mechanics gets rid of the original paradox, it supplies another unanswered question in the form of the quantum Zeno effect. Why does a quantum arrow stop when we frequently check a localized state of the arrow with non-zero momentum?

The answer is intimately bound up with the Heisenberg uncertainty relation, which states that a quantum system with a definite momentum cannot be exactly localized: its position is uncertain up to the width of its quantum wave. When our arrow moves a distance smaller than this width, its state becomes a superposition of the original quantum state and a new state. A measurement checking whether the arrow is still in the original state might find it there, or might not. The probability that the arrow has moved along is proportional to the square of the time that has elapsed since the last measurement, and becomes very small if the measurements are frequent. Increasing the number of measurements over a given time interval reduces the probability gradually to zero — the quantum Zeno effect kicks in.

Let's look more closely at the example of our arrow, which has a non-zero momentum and is initially localized at the origin. We perform very frequent Zeno measurements of the quantum state to check that the arrow is maintaining this momentum and that it returns to its localized state at each measurement. But between these Zeno measurements, one might think, the arrow can move a little to the right, in the direction of its momentum. Between these measurements, its average position will be shifted in proportion to its velocity, and this will allow its velocity to be measured.

This conclusion is in fact incorrect. Between two measurements, a quantum system is described by two quantum states: one evolving towards the future, defined by the first measurement, and one evolving towards the past, defined by the second measurement[4] (Fig. 1a). The first state is shifted to the right, and the second to the left; thus measuring the average position of the arrow between full Zeno measurements yields no shift.

The shift does not vanish, however, if the position measurements are made shortly before each Zeno measurement. Indeed, at this point, while the past-evolving state is near the origin, the future-evolving state is almost at its maximum shift. Thus, the arrow has a net shift to the right. For the Zeno effect to work, this shift has to be much smaller than the uncertainty in the arrow's position. Very many position measurements are needed to detect this tiny shift. If we continue the procedure long enough to get enough position measurements, then at some point a Zeno test is likely to fail. If the Zeno measurements are more frequent, they will take longer to fail, and more position measurements can be made; but in this case the shift to be measured becomes smaller, meaning that even more measurements are needed to detect it. The conclusion is that there is no way to measure the position shift, and thus the instantaneous velocity, of a system held by Zeno measurements.

But this is not so, as De Liberato[2] shows. His procedure (Fig. 1b) uses one device that performs two tasks: it holds the arrow, and it performs a position measurement on it. In each gap between Zeno tests, when the original state evolves into a superposition of the original state and a new state, De Liberato proposes a quick interaction to flip the relative signs of these states half-way between two tests. This change of sign shifts the arrow back to the left. At the time of the next Zeno test, the arrow is where it was originally, and the test succeeds with certainty. If the external conditions do not change, De Liberato's repeated sign flips will hold the arrow at the origin for ever — even if we do not perform Zeno tests between the flips.

De Liberato's position measurement comes just before the sign flip, at the time when the displacement is maximal. The state evolving into the past from the Zeno tests is just the time-reverse of the state evolving into the future, so at this point, both states are maximally displaced. The number of times we can repeat the procedure is not limited as before: the Zeno tests will not fail because of the motion of the arrow. The only possible reason for their failure is the disturbance of the state owing to position measurements. But this possibility is discounted by the so-called protective measurement regime[5], in which the coupling of the position measurement is weak and the state is protected from changes by the Zeno tests. We can measure the velocity of an arrow held at the origin.

Paradoxes have always been a driving force for understanding nature. Quantum mechanics, probably more than any other theory, is full of paradoxes[6]. Quantum mechanics helps to resolve Zeno's arrow paradox but leads to the quantum Zeno effect, which seems in itself inherently paradoxical. Work such as that of De Liberato[2] shows us that we have not yet uncovered all such secrets of quantum mechanics, which is now almost a century old. That is becoming increasingly relevant as technology transforms yesterday's quantum thought experiments into today's laboratory demonstrations, and even into practical devices. ■

Lev Vaidman is in the Physics Department, Tel Aviv University, Tel Aviv 69978, Israel.
e-mail: vaidman@post.tau.ac.il

1. Dowling, J. *Nature* **439,** 920–921 (2006).
2. De Liberato, S. *Phys. Rev. A* **76,** 042107 (2007).
3. Arntzenius, F. *Monist* **83,** 187–208 (2000).
4. Aharonov, Y. & Vaidman, L. *Phys. Rev. A* **41,** 11–20 (1990).
5. Aharonov, Y. & Vaidman, L. *Phys. Lett. A* **178,** 38–42 (1993).
6. Aharonov, Y. & Rohrlich, D. *Quantum Paradoxes: Quantum Theory for the Perplexed* (Wiley-VCH, Weinheim, 2005).

OBITUARY

Seymour Benzer (1921–2007)

Restless spirit, and pioneer in molecular genetics.

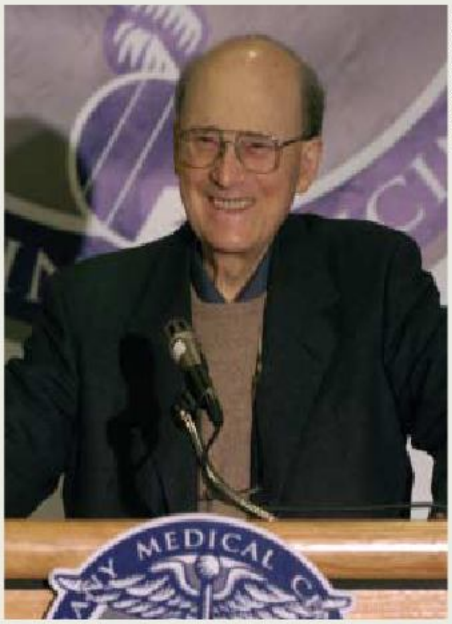

AP PHOTO/T. ROSKE

Seymour Benzer, one of the giants of twentieth-century biology, died on 30 November. Benzer, who maintained an active laboratory until the time of his death, was a unique figure who made seminal contributions to physics, molecular biology and behavioural genetics.

He was born in New York to immigrant Jewish parents from Poland, and grew up in Brooklyn. After graduating from Brooklyn College, he obtained his PhD in physics from Purdue University in 1947, where his discoveries in solid-state physics contributed to the development of the transistor. Relentlessly curious, Benzer possessed both a single-minded fascination with the mysteries of nature and the intellectual talent to unravel them. Purdue hired him as a physics professor, but almost immediately he began working in biology, taking the 'bacteriophage course' at Cold Spring Harbor Laboratory, followed by a two-year postdoc with Max Delbrück at the California Institute of Technology (Caltech). Benzer's style was to pioneer a new area, and then to move on to something new once the hordes had rushed in. As he said: "I like to take things that are fuzzy, and turn them into something tangible."

Benzer next took a series of sabbaticals, wandering the world of phage genetics to sojourn with François Jacob in Paris and Francis Crick in Cambridge, UK. It was during this period that he made some of his most important contributions to what is now viewed as the golden era of molecular genetics — the period following the publication of James Watson and Crick's double-helical structure of DNA that witnessed a feverish race to understand the mechanisms underlying the molecular basis of heredity.

Using bacteriophage T4, Benzer developed a technique to select for rare genetic-recombination events in organisms carrying different mutations in the *rII* locus, and showed that mutations can occur at many different sites in the same gene. By generating a fine-structure genetic map, he proved that genes are not indivisible units, but are composed of a linear array of chemical building-blocks, or bases, each of which can be subject to alteration. Moreover, by a simple argument, he deduced that the minimum unit of mutation is probably a single base pair of DNA. This idea was fundamental to connecting the structure of DNA to the reality of genetics. And, together with Fred Sanger's discovery that proteins are composed of precise sequences of amino acids, this work laid the foundations of the new science of molecular biology.

Most scientists would have been content to continue in this exciting field, but Benzer became characteristically restless. For him, once it became obvious how a problem could be solved, it was time to move on to another. This time, he was attracted to a far more formidable question: how genes influence behaviour. Traditional approaches to this problem had included studying how complex behavioural traits could be enhanced by selective breeding or altered by intercrossing. But Benzer had a different approach in mind: he would look for a model organism in which it would be possible to define single-gene mutations that altered specific behaviours. This strategy was clearly linked to his previous work on bacteriophage, and it established what he called genetic dissection as a valid method for analysing complex biological processes.

In search of such an organism, Benzer took a sabbatical with Roger Sperry at Caltech, where he tinkered with various animal models. Eventually, he chose the fruitfly *Drosophila*, and although his colleagues in the Sperry lab were not convinced, Benzer was undeterred. He once said: "If everyone you talk to says you shouldn't do something, you probably shouldn't do it, and if everyone says you should do something, you should also probably not do it; but if half the people you talk to tell you to do it and half say you're crazy, then you should definitely go ahead."

Benzer turned his sabbatical at Caltech into an indefinite stay and never touched a phage again. He founded the modern field of *Drosophila* neurogenetics and explored this area in his peripatetic style from 1967 until his death. His work showed not only that it is possible to dissect behaviour with single-gene mutations, but also that fruitflies are capable of far more sophisticated behaviour than had previously been thought possible. They could learn, they had a sense of time, and they showed complex, stereotyped courtship rituals.

To quantify these behaviours, Benzer built simple but ingenious devices, such as his counter-current apparatus for measuring phototaxis (an organism's movement in response to light). Using such tools, Benzer screened large numbers of flies to discover rare mutants with specific behavioural defects. This work, among his other achievements, laid the foundations for cloning genes controlling circadian rhythms and encoding potassium channels — crucial regulators of neuronal excitability — that had resisted all efforts at identification. Throughout, Benzer retained his arch and often ribald sense of humour, for example naming his learning and light-avoiding mutants dunce and photophobe, respectively. Almost 40 years later, hundreds of scientists continue in this experimental tradition, and entire meetings are devoted to neurogenetics.

In later years, Benzer turned his attention to the genetic control of ageing, discovering mutations that cause degeneration of the brain (Swiss cheese) or extended lifespan (Methuselah) in *Drosophila*, and opening the way to using the fruitfly as a model system in which to study neurodegenerative diseases such as Alzheimer's or Parkinson's.

Benzer remained active until his last days. A food-lover, he led expeditions to exotic ethnic restaurants, and into his eighties participated in matzoh-ball or potato-latke cook-offs with his friends. Watching him trundle tirelessly down the corridor of his laboratory draped in a smudged lab coat, pockets heavy with tools and packets of notes scrawled in his near-illegible, crabbed handwriting; holding court with his lab members around a small steel table in his cramped conference room, while sipping hot tea and munching Fig Newtons; and asking rare but razor-sharp questions well into his mid-eighties, it was difficult to escape the conclusion that Benzer had discovered some magical elixir of youth in *Drosophila* and was experimenting with it on himself — but not telling. Benzer was an original, a scientist's scientist, and his death in many ways marks the end of an era.

David Anderson (with additional contributions by Sydney Brenner)
David Anderson is in the Division of Biology, 216–276 Howard Hughes Medical Institute, California Institute of Technology, Pasadena, California 91125, USA.
e-mails: wuwei@caltech.edu; sbrenner@salk.edu

nature

Vol 451 | Issue no. 7175 | 10 January 2008 www.nature.com/nature

PUBLICATION POLICIES, AUTHOR GUIDELINES AND INFORMATION

This is a summary of *Nature*'s guide to authors, publication policies and other author information, available in full on the web via our main author information page at www.nature.com/nature/authors.

GETTING PUBLISHED IN *NATURE*

Please read www.nature.com/nature/authors/get_published before finalizing any original scientific research manuscripts you intend to submit to *Nature*. This section explains *Nature*'s editorial criteria, and how manuscripts are handled by the editors after submission and before acceptance for publication.

FORMATTING GUIDE

Please read www.nature.com/nature/authors/gta before finalizing and submitting your contribution. This section provides instructions for preparing, formatting and writing all types of contribution published by *Nature*.

PUBLICATION POLICIES

This section, at www.nature.com/authors, describes *Nature*'s conditions of publication, including policies on authorship; competing financial interests; duplicate publication; prepublicity and embargoes; materials and data availability; research on animal (including human) subjects; referees; corrections, retractions, errata and addenda to published papers; the complaints procedure and refutations; and copyright/licence to publish. All contributions, for whatever section of the journal, are considered for publication and published on the condition that authors agree to these policies.

SUBMISSIONS

These sections, at www.nature.com/nature/authors/submissions, contain our online service for presubmission enquiries and submission and tracking of Articles, Letters and Review-type manuscripts. Authors should read the formatting guide before using this service. Manuscripts should be prepared using our Word template (with style tags deleted before submission), which can be downloaded from the website. Authors who cannot submit online can submit by post, but *Nature* strongly recommends the online service. **Authors must not submit by both methods.** Authors experiencing operational difficulty in using the online submission service can send an enquiry to mtshelp@nature.com, with a brief explanation of the problem.

ONLINE SUBMISSIONS

For presubmission enquiries, submission of articles, and for return of revised submissions please see:
www.nature.com/nature/authors/submissions/subs

EDITORIAL CONTACTS AND AUTHOR SERVICES

This section at www.nature.com/nature/about/contact/editorial.html provides the addresses of *Nature*'s editorial offices; names of editorial staff; and contact details for advice, reprints, permissions, press office (press@nature.com), and other author-related contact information, including postal addresses for mailed submissions. Short biographies of editors are also available at www.nature.com/nature/about/editors.

FINAL SUBMISSIONS

This section at www.nature.com/nature/authors/submissions/final applies only if an Article or Letter has been accepted in principle for publication and the author has explicitly been asked by the editor for a final version. Authors will need to post (**by mail**, not e-mail or online) a package containing a disk or disks of the text, production-quality figures and supplementary information (if any). Authors must include in the package a hard-copy of all of these, a completed manuscript checklist and all relevant signed forms and declarations as requested by the editor.

SHORT VERSION OF GUIDE TO AUTHORS

See www.nature.com/nature/authors for full version. Contributors not used to *Nature*'s format requirements are strongly advised to read some papers in published issues before submission, to familiarize themselves with *Nature*'s style. *Nature*'s main formats for original research are Articles and Letters.

ARTICLES are original reports whose conclusions represent a substantial advance in understanding of an important problem and have immediate, far-reaching implications. They do not normally exceed **5 pages** of Nature and have **no more than 50** references. (One page of undiluted text is about 1,300 words.)

Articles have a summary for readers outside the discipline, separate from the main text and containing no references, of up to 150 words. The summary does not contain numbers, abbreviations, acronyms or measurements unless essential. It contains a brief account of the background and rationale of the work, followed by a statement of the main conclusions, introduced by the phrase 'Here we show' or its equivalent.

The Article itself typically has about 3,000 words of text, beginning with up to 500 words of referenced text expanding on the background to the work (some overlap with the summary is acceptable), followed by a concise, focused account of the findings, and ending with one or two short paragraphs of discussion. The text can contain a few short subheadings consisting of about 20 but no more than 40 characters (including spaces) each.

Figures are as small as possible: Articles typically have 5 or 6 figures. Legends and/or methods are additional to the main text. Methods Summaries are no longer than 300 words; Methods sections (which are published online) can be up to 1,000 words; legends should not exceed 100 words each and start with a one-sentence title for the figure, followed by a brief explanation of the parts and symbols.

LETTERS are short reports of original research focused on an outstanding finding whose importance means that it will be of interest to scientists in other fields. They do not normally exceed **4 pages** of Nature, and have **no more than 30** references. They begin with a **fully referenced paragraph** of not more than 300 words, aimed at readers in other disciplines. This paragraph contains a summary of the background and rationale for the work, followed by a one-sentence statement of the main conclusions introduced by the phrase 'Here we show' or its equivalent, and ending with two to three sentences describing the implications in context.

The main text which follows is typically up to 1,500 words long. This text can, if the author requires, start with a further brief paragraph of introductory material, not repeating information in the summary paragraph. A description of the research then follows. Any discussion at the end of the text should be as succinct as possible.

Figures are as small as possible: Letters typically have 3 or 4 figures. Legends and/or methods are additional to the main text. Methods Summaries are no longer than 300 words; Methods sections (which are published online) can be up to 1,000 words; legends should not exceed 100 words each and start with a one-sentence title for the figure, followed by a brief explanation of the parts and symbols.

OTHER TYPES OF CONTRIBUTION to *Nature* that are considered for publication via online submission are Communications Arising (which are scientific comments about peer-reviewed material previously published in *Nature*). See also www.nature.com/nature/authors/gta/others.html for: Reviews and Progress (presubmission enquiries to reviewsandinsights@nature.com); Commentary (synopses and enquiries to nature@nature.com); and Correspondence (submit to corres@nature.com).

See Authors and Referees @ NPG (www.nature.com/authors) for details of *Nature* journals' publication policies, author and referee services, author benefits, author magazine (*Nurture*) and for links to Nautilus and Peer to Peer blogs.

ARTICLES

Reprogramming of human somatic cells to pluripotency with defined factors

In-Hyun Park[1], Rui Zhao[1], Jason A. West[1], Akiko Yabuuchi[1], Hongguang Huo[1], Tan A. Ince[2], Paul H. Lerou[3], M. William Lensch[1] & George Q. Daley[1]

Pluripotency pertains to the cells of early embryos that can generate all of the tissues in the organism. Embryonic stem cells are embryo-derived cell lines that retain pluripotency and represent invaluable tools for research into the mechanisms of tissue formation. Recently, murine fibroblasts have been reprogrammed directly to pluripotency by ectopic expression of four transcription factors (*Oct4*, *Sox2*, *Klf4* and *Myc*) to yield induced pluripotent stem (iPS) cells. Using these same factors, we have derived iPS cells from fetal, neonatal and adult human primary cells, including dermal fibroblasts isolated from a skin biopsy of a healthy research subject. Human iPS cells resemble embryonic stem cells in morphology and gene expression and in the capacity to form teratomas in immune-deficient mice. These data demonstrate that defined factors can reprogramme human cells to pluripotency, and establish a method whereby patient-specific cells might be established in culture.

Pluripotency can be induced in somatic cells by nuclear transfer into oocytes[1] and fusion with embryonic stem cells[2], and for male germ cells by cell culture alone[3]. Ectopic expression of four transcription factors (*Oct4*, *Sox2*, *Klf4* and *Myc*) in murine fibroblasts is sufficient to yield iPS cells that resemble embryonic stem (ES) cells in their capacity to form chimaeric embryos and contribute to the germ lineage[4–7]. Direct, factor-based reprogramming might enable the generation of pluripotent cell lines from patients afflicted by disease or disability, which could then be exploited in fundamental studies of disease pathophysiology or drug screening, or in pre-clinical proof-of-principle experiments that couple gene repair and cell replacement strategies.

We attempted to use the original four reprogramming factors defined by ref. 4 (*OCT4*, *SOX2*, *KLF4* and *MYC*) to isolate iPS cells from human embryonic fibroblasts differentiated from H1-OGN cells, human ES cells that express the green fluorescence protein (GFP) reporter and neomycin (G418) resistance genes by virtue of their integration into the *OCT4* locus by homologous recombination (H1-OGN (ref. 8)). We differentiated H1-OGN cells *in vitro* for 4 weeks, and propagated a homogeneous population of fibroblast-like cells (dH1f, differentiated H1-OGN fibroblast; Fig. 1a). GFP expression was undetectable in dH1f cells, as assayed by flow cytometry (Supplementary Fig. 1). Expression of *OCT4*, *SOX2*, *NANOG* and *KLF4* was extinguished in dH1f cells, whereas *MYC* expression persisted at near-comparable levels to undifferentiated H1-OGN cells (Fig. 1b). The dH1f cells could be cultured readily for at least 14 passages, after which their proliferation slowed markedly. No dH1f cells survived selection in G418 (50 ng ml^{-1}), and no tumours formed after injection of dH1f cells into immune-deficient mice. Taken together, these data establish that dH1f cells represent differentiated human ES cell derivatives that have lost the essential features of pluripotency.

To ensure propagation of differentiated fibroblasts free of contamination by undifferentiated ES cells, we infected early passage dH1f cells with a lentiviral construct carrying the dTomato reporter gene, plated infected cells by serial dilution, and expanded individual

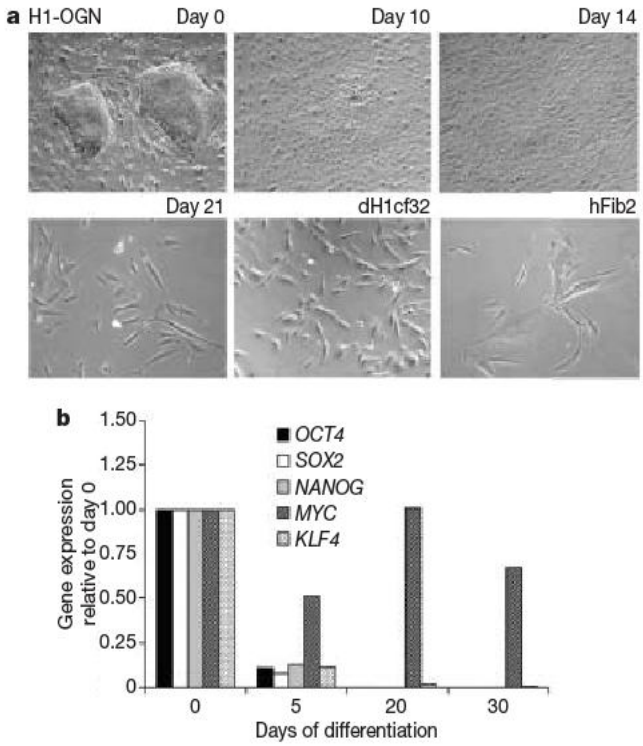

Figure 1 | Differentiation of human embryonic fibroblasts from human embryonic stem cells (H1-OGN). In the human ES cell line H1-OGN[8], the *OCT4* promoter drives expression of GFP-IRES-*neo*. **a**, Time course of differentiation of H1-OGN cells into a population of adherent fibroblasts, and subsequent expansion of a colony into a clonal fibroblast cell line (dH1cf32). The differentiated fibroblast derivatives of H1-OGN cells are morphologically indistinguishable from dermal fibroblasts cultured from an adult volunteer donor (hFib2). **b**, Quantitative real-time PCR demonstrates that the expression of a cohort of key pluripotency factors (*OCT4*, *SOX2*, *NANOG* and *KLF4*) is lost by the third week of differentiation, whereas expression of a fifth factor (*MYC*) persists.

[1]Division of Pediatric Hematology/Oncology, Children's Hospital Boston and Dana Farber Cancer Institute; Department of Biological Chemistry and Molecular Pharmacology, Harvard Medical School; Division of Hematology, Brigham & Women's Hospital, Boston, Massachusetts 02115, USA; and Harvard Stem Cell Institute, Cambridge, Massachusetts 02138, USA. [2]Department of Pathology, Brigham and Women's Hospital, and [3]Division of Newborn Medicine, Brigham & Women's Hospital and Children's Hospital Boston, Boston, Massachusetts 02115, USA.

colonies. Southern hybridization confirmed distinct single or double lentiviral integration sites in three cell lines, thereby confirming their clonal derivation from single cells (cloned dH1cf16, dH1cf32 and dH1cf34; Supplementary Fig. 2). Proliferation of the cloned dH1cf cells began to slow markedly after an additional 4–5 passages. The dH1cf clones were G418 sensitive, negative for expression of *GFP*, *OCT4* and *NANOG*, and failed to induce tumours in immune-deficient mice (Supplementary Fig. 3 and data not shown).

Reprogramming of human ES-cell-derived fetal fibroblasts

We infected cultures of dH1f and cloned dH1cf cells with a cocktail of retroviral supernatants carrying human *OCT4*, *SOX2*, *MYC* and *KLF4*. Seven days after infection, cells were plated in human ES cell culture medium supplemented with the ROCK inhibitor Y27632, previously shown to enhance survival and clonogenicity of single dissociated human ES cells[9]. By 14 days after infection, cultures of infected dH1f cells showed distinct small colonies that were picked and expanded. The resulting cultures harboured colonies for which morphology was indistinguishable from the parental H1-OGN cells (Fig. 2a). Selection with G418 was not required to identify cells with ES-cell-like colony morphology; rather, morphology itself sufficed, as reported for identification of murine iPS cells[10,11]. We performed ten independent infections of 1×10^5 dH1f cells with the four factors, and consistently observed approximately 100 human ES-cell-like colonies, for a reprogramming efficiency of ~0.1% (Table 1). Interestingly, we obtained human ES-cell-like colonies when we eliminated either MYC or KLF4 from the cocktails, although with markedly lower efficiency (Table 1). Infection of different clones of dH1cfs revealed a lower efficiency and delayed appearance of ES-cell-like colonies (between 6–47 colonies per 10^5 cells after 21 days). Expanded cultures of human ES-cell-like colonies from dH1cf clones carried the identical lentiviral integration site as the parental cell line, thereby confirming their derivation from the original dH1cf clone, and eliminating the possibility that a contaminating undifferentiated H1-OGN cell had been re-isolated (Supplementary Fig. 2).

Reprogramming of fetal, neonatal and adult fibroblasts

We next tested a diverse panel of human primary cells available from commercial sources, as well as primary dermal fibroblasts isolated from a skin biopsy from a healthy volunteer, which were obtained following informed consent for reprogramming studies under a protocol approved by the Institutional Review Board and Embryonic Stem Cell Research Oversight Committee of Children's Hospital Boston.

We isolated cells with human ES-cell-like morphology from cultures of MRC5 fetal lung fibroblasts around 21 days after infection with the four transcription factors. We were also able to identify human ES-cell-like colonies by introduction of the four factors into Detroit 551 cells, another human primary cell culture derived from fetal skin (data not shown). In contrast to our results with human ES-cell-derived fibroblasts (dH1f, dH1cf) and primary fetal cells (MRC5, Detroit 551), transduction of the four transcription factors into more developmentally mature somatic cells, for example, neonatal foreskin fibroblasts (BJ1), adult mesenchymal stem cells (MSC) and adult dermal fibroblasts (hFib2), resulted in slowed proliferation and cellular senescence, and we failed to identify colonies with obvious ES-cell-like morphology from any of these infected cell cultures. We reasoned that adult human somatic cells might require additional factors to grow in continuous cell culture and to be reprogrammed to pluripotency, and thus we supplemented the four factors (*OCT4*, *SOX2*, *MYC* and *KLF4*) with genes known to have a role in establishing human cells in culture: the catalytic subunit of human telomerase, *hTERT*[12], and SV40 large T, which has potent anti-apoptotic activity[13]. When *hTERT* and SV40 large T were introduced together with the four transcription factors into BJ1, MSC and hFib2 cells, the cultures grew more rapidly but still showed significant cellular loss and sloughing into the media. However, against the background of adherent cells, we were able to recognize colonies with human ES-cell-like morphology (Fig. 2a and Table 1). Individual colonies of human ES-cell-like cells were picked and expanded. All ES-cell-like colonies shared DNA fingerprints with the line from which they derived, thereby ruling out the possibility of contamination with

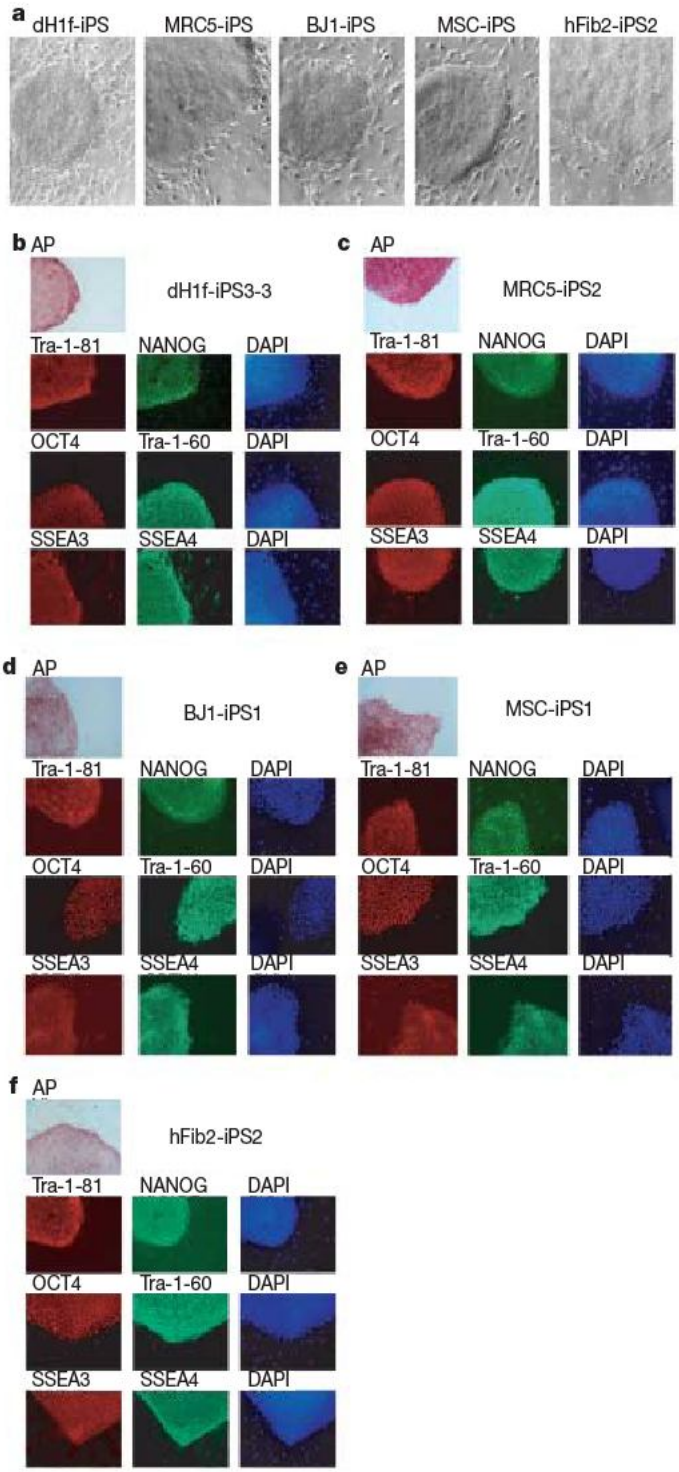

Figure 2 | Multiple cultured human primary somatic cells yield iPS cells. **a**, iPS cells produced from five independent human primary cell lines form colonies with a similarly compact, ES-cell-like morphology in co-culture with mouse embryonic feeder fibroblasts (MEFs). **b–f**, As shown via immunohistochemistry (IHC), human iPS cell colonies express markers common to pluripotent cells, including alkaline phosphatase (AP), Tra-1-81, NANOG, OCT4, Tra-1-60, SSEA3 and SSEA4. 4,6-Diamidino-2-phenylindole (DAPI) staining indicates the total cell content per field. Fibroblasts surrounding human iPS colonies serve as internal negative controls for IHC staining. dH1f-iPS3-3 (**b**, from H1-OGN differentiated fibroblasts), MRC5-iPS2 (**c**, from MRC5 human fetal lung fibroblasts), BJ1-iPS1 (**d**, from neonatal foreskin fibroblasts), MSC-iPS1 (**e**, from mesenchymal stem cells), hFib2-iPS2 (**f**, dermal fibroblast from healthy adult male).

existing human ES cells being carried in the laboratory (Supplementary Fig. 4).

Characterization of reprogrammed somatic cell lines

We analysed colonies selected for human ES-cell-like morphology from dH1f, MRC5, BJ1, MSC and hFib2 by immunohistochemistry, and detected expression of alkaline phosphatase, Tra-1-81, Tra-1-60, SSEA3, SSEA4, OCT4 and NANOG (Fig. 2b–f), all markers shared with human ES cells[14]. We also analysed gene expression by quantitative polymerase chain reaction (PCR) analysis, and noted that for derivatives of dH1f, dH1cf, MRC5, BJ1, MSC and hFib2, expression of *OCT4*, *SOX2*, *NANOG*, *KLF4*, *hTERT*, *REX1* and *GDF3* was markedly elevated over the respective fibroblast population, and comparable to the parental H1-OGN human ES cells (Fig. 3a–e). Expression of *MYC* did not vary markedly from the parental cell lines, suggesting that a consistent expression level was required to sustain cell proliferation in multiple cell types under our culture conditions (Fig. 3a–e). In murine iPS cells, retroviral expression of murine *Oct4*, *Sox2*, *Myc* and *Klf4* is silenced during iPS derivation and complemented by reactivation of expression from the endogenous gene loci[4–7]. We

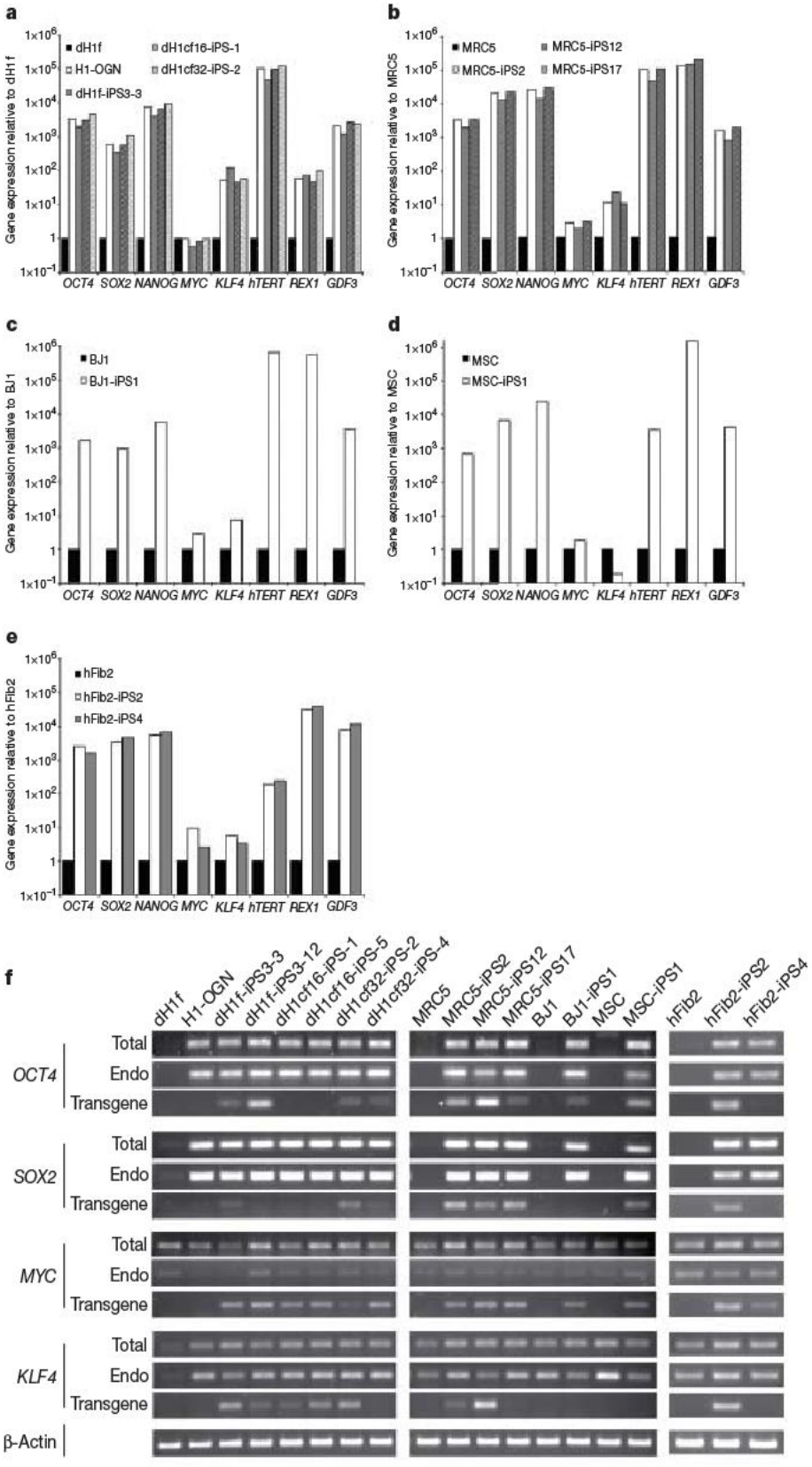

Figure 3 | Gene expression in human iPS cells is similar to human ES cells. **a**–**e**, Quantitative real-time PCR assay for expression of *OCT4*, *SOX2*, *NANOG*, *MYC*, *KLF4*, *hTERT*, *REX1* and *GDF3* in human iPS and parental cells. Individual PCR reactions were normalized against internal controls (β-actin) and plotted relative to the expression level in the parent fibroblast cell line. **a**, dH1f, dH1f-iPS3-3, dH1cf16-iPS-1 and dH1cf32-iPS-2 cells. **b**, MRC5-iPS2, MRC5-iPS12 and MRC5–iPS17. **c**, BJ1-iPS1. **d**, MSC-iPS1. **e**, hFib2-iPS2 and hFib2-iPS4. **f**, Transgene-specific PCR primers permit determination of the relative expression levels between total, endogenous (Endo) and retrovirally expressed (Transgene) genes (*OCT4*, *SOX2*, *MYC* and *KLF4*) via semi-quantitative PCR. β-Actin is shown as a positive amplification and loading control.

Table 1 | ES-cell-like colony formation with various donor cells and reprogramming factors

Cell line	OCT4 and SOX2	Three factors	Four factors	Six factors‡
ES-cell-derived fibroblasts dH1f	0	−OCT4*, 0; −SOX2†, 0; −KLF4, 63; −MYC, 11	118 ± 35	250
ES-cell-derived fibroblasts dH1cf (clones 16, 32, 34)	ND	ND	dH1cf16, 47; dH1cf32, 12; dH1cf34, 6	dH1cf16, 86; dH1cf32, 40; dH1cf34, 17
Fetal lung fibroblasts MRC5	ND	ND	39	ND
Neonatal foreskin fibroblasts BJ1	ND	ND	0	21
Mesenchymal stem cells	ND	ND	0	3
Adult dermal fibroblasts hFib2	ND	ND	0	7

The four factors were OCT4, SOX2, MYC and KLF4; the six factors were OCT4, SOX2, MYC, KLF4, hTERT and SV40 large T. Numbers are for colonies showing human ES-cell-like morphology per 10^5 infected cells. ND, not determined.
* No human ES-cell-like colonies but numerous (~10^2) colonies with flat morphology were observed.
† No colonies observed, not even the flat variety seen with the three-factor combination lacking OCT4.
‡ Only human ES-cell-like colonies scored, despite observation of frequent flat colonies.

analysed the expression of the endogenous loci and retroviral transgenes, and found that total expression of *OCT4*, *SOX2*, *MYC* and *KLF4* was comparable to human ES cells (Fig. 3f). Expression of the endogenous *OCT4* and *SOX2* loci was consistently upregulated relative to parental cells, and accompanied by variable levels of retroviral transgene expression, with silencing in some cells (Fig. 3f). These data suggest that expression of *OCT4* and *SOX2* is titrated to a specific range during selection in cell culture. There was variable but persistent expression of the retroviral *MYC* and *KLF4* transgenes (Fig. 3f). Single or multiple integrations (2–6 copies) of the *OCT4* and *SOX2* transgenes were detected by Southern blot analysis in different cell lines (Supplementary Fig. 5a, b).

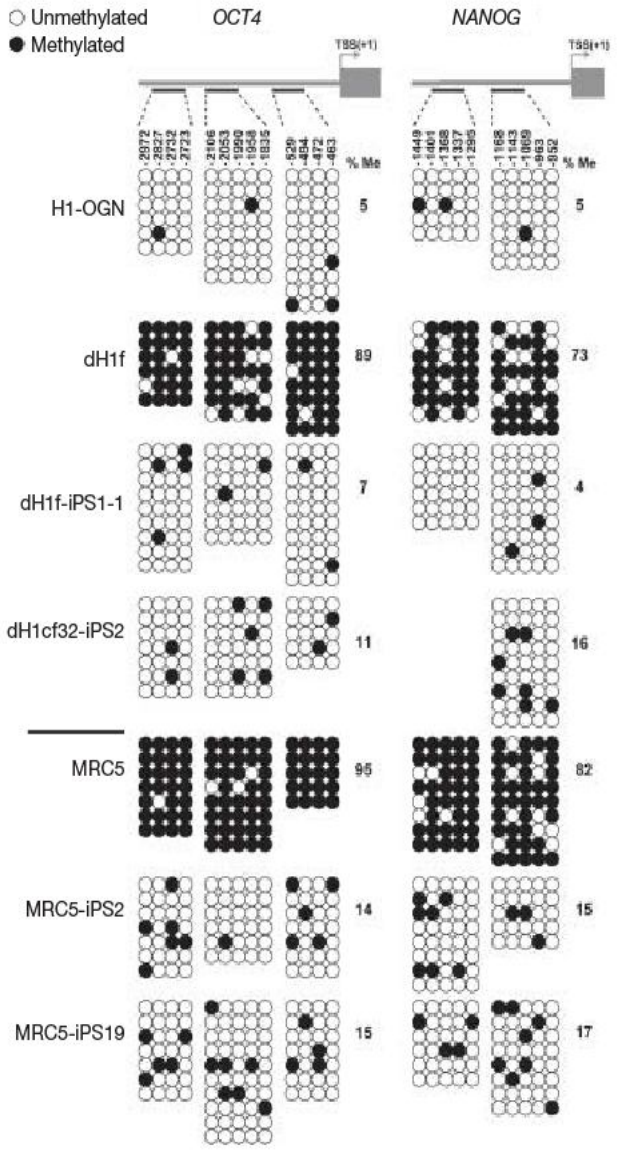

Figure 4 | iPS cells are demethylated at the *OCT4* and *NANOG* promoters relative to their fibroblast parent lines. Bisulphite sequencing analysis of the *OCT4* and *NANOG* promoters in H1-OGN human ES cells, dH1f differentiated fibroblasts, dH1f-iPS-1, dH1cf32-iPS2, as well as the MRC5 neonatal foreskin fibroblast line and its derivatives MRC5-iPS2 and MRC5-iPS19. Each horizontal row of circles represents an individual sequencing reaction for a given amplicon. White circles represent unmethylated CpG dinucleotides; black circles represent methylated CpG dinucleotides. The cell line is indicated to the left of each cluster. The values above each column indicate the CpG position analysed relative to the downstream transcriptional start site (TSS). The percentage of all CpGs methylated (% Me) for each promoter per cell line is noted to the right of each panel.

We were successful in recovering human ES-cell-like colonies from the postnatal BJ1, MSC and hFIB2 cells only when we used six factors in our retroviral cocktail (adding *hTERT* and SV40 large T to the original four factors). Although PCR analysis of genomic DNA from the bulk early post-infection cultures detected the respective retroviruses, the human ES-cell-like colonies that we ultimately isolated failed to show integration or expression of *hTERT* and SV40 large T (data not shown). We thus conclude that *hTERT* and SV40 large T are not essential to the intrinsic reprogramming of the recovered ES-cell-like cells. Because the six-factor cocktail showed a higher frequency of human ES-cell-like colony formation in all cell contexts tested (Table 1), we speculate that these factors may act indirectly on supportive cells in the culture to enhance the efficiency with which the reprogrammed colonies can be selected.

Reprogramming of somatic cells is accompanied by demethylation of promoters of critical pluripotency genes[2,15]. Therefore, we performed bisulphite sequencing to determine the extent of methylation at the *OCT4* and *NANOG* gene promoters for two parental cell lines and their reprogrammed ES-cell-like derivatives. As expected, H1-OGN human ES cells were predominantly demethylated at the *OCT4* and *NANOG* promoters. In contrast, the dH1f fibroblasts showed prominent methylation at these loci, consistent with transcriptional silencing in these differentiated cells. The ES-cell-like derivatives dH1f-iPS1-1 and dH1cf32-iPS2 revealed prominent demethylation, comparable to the state of these loci in H1-OGN human ES cells (Fig. 4, top). Similar data were obtained for MRC5 fetal lung fibroblasts, which showed prominent methylation of *OCT4* and *NANOG* loci, whereas analysis of the ES-cell-like derivatives MRC5-iPS2 and MRC5-iPS19 revealed prominent demethylation (Fig. 4, bottom). These data are consistent with epigenetic remodelling of the *OCT4* and *NANOG* promoters after retroviral infection, culture and selection for colonies with an ES-cell-like morphology.

Whereas expression analysis of a subset of genes by RT–PCR was consistent with reactivation of genes associated with pluripotency of human ES cells (Fig. 3), we performed global messenger RNA expression analysis on H1-OGN cells, parental fibroblast cells and their reprogrammed ES-cell-like derivatives. Clustering analysis revealed a high degree of similarity among the reprogrammed ES-cell-like derivatives (dH1f-iPS3-3, dH1cf16-iPS5, dH1cf32-iPS2, MRC5-iPS2 and BJ1-iPS1), which clustered together with the H1-OGN ES cells and were distant from the parental somatic cells, as determined by Pearson correlation (Fig. 5a). The differentiated dH1f and dH1cf derivatives of the H1-OGN human ES cells clustered tightly with the MRC5 fetal lung fibroblasts (Fig. 5a), suggesting their

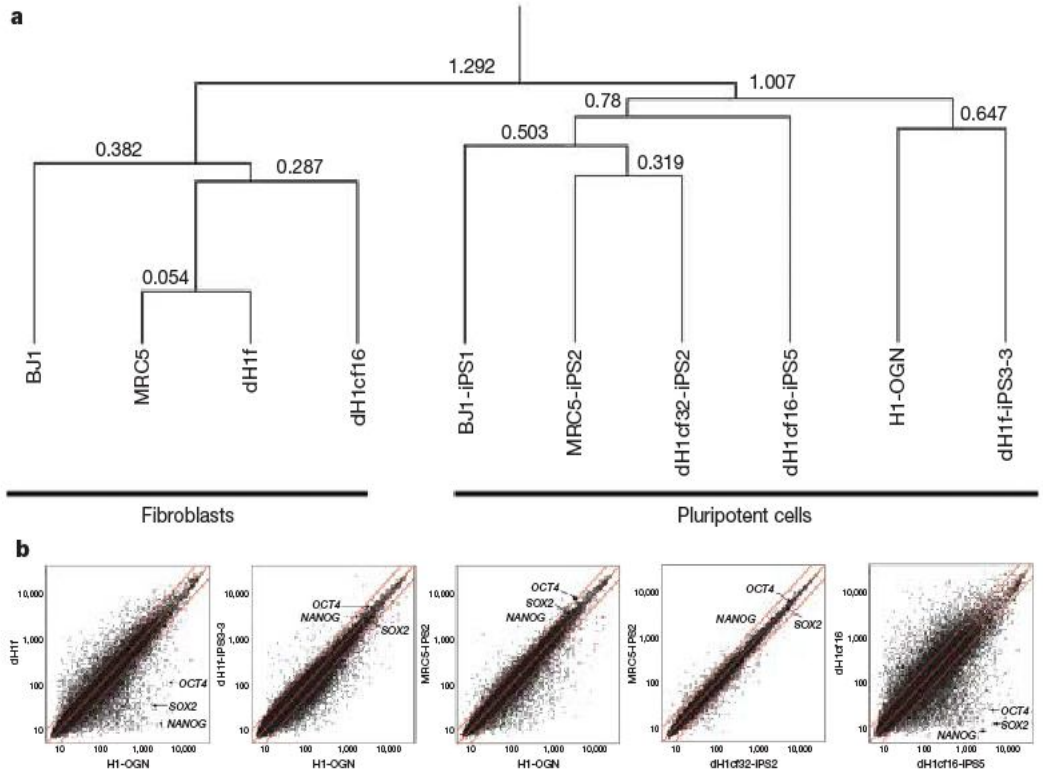

Figure 5 | Global gene expression analysis of iPS cells. **a**, A Pearson correlation was calculated and hierarchical clustering was performed with the average linkage method in H1-OGN, dH1f, dH1f-iPS3-3, dH1cf16, dH1cf-iPS cells (dH1cf16-iPS5 and dH1cf32-iPS2), MRC5, MRC5-iPS2, BJ1 and BJ1-iPS1 cells. The distance metric calculated by GeneSpring GX7.3.1 for comparisons between different cell lines is indicated above the tree lines. The fibroblast lines dH1f, dH1cf16, MRC5 and BJ1 cluster together, whereas iPS cells cluster together with the H1-OGN human ES cell line. **b**, Global gene expression patterns were compared between differentiated fibroblasts (dH1f, dH1cf16), reprogrammed somatic cells (dH1f-iPS3-3, MRC5-iPS2) and human ES cells (H1-OGN). Red lines indicate the linear equivalent and twofold changes in gene expression levels between the paired samples.

close resemblance to fetal fibroblasts. Analysis of scatter plots similarly shows a tighter correlation between reprogrammed somatic cells (dH1f-iPS3-3, MRC5-iPS2) and human ES cells (H1-OGN) than between differentiated fibroblasts (dH1f) and human ES cells (H1-OGN) or differentiated fibroblasts (dH1cf16) and their reprogrammed derivative (dH1cf16-iPS5) (Fig. 5b). Different lines of reprogrammed somatic cells are particularly well correlated (MRC5-iPS2 versus dH1cf32-iPS2) (Fig. 5b). Therefore, our data indicate that the cells reprogrammed from somatic sources are highly similar to embryo-derived human ES cells at the global transcriptional level.

Human ES cells will form teratoma-like masses after cell injection into immunodeficient mice, an assay that has become the accepted standard for demonstrating their developmental pluripotency[14,16,17]. We injected the human ES-cell-like cells derived from dH1f and dH1cf fibroblasts into $Rag2^{-/-}/\gamma c^{-/-}$ mice, and observed formation of well-encapsulated cystic tumours that harboured differentiated elements of all three primary embryonic germ layers (Fig. 6 and Supplementary Fig. 6). The human ES-cell-like cells derived from dH1f, dH1cf, MRC5 and MSCs differentiated *in vitro* into embryoid bodies, and RT–PCR of differentiated cells showed marker gene expression for all three embryonic germ layers: *GATA4* (endoderm), *NCAM* (ectoderm) and *Brachyury* and *RUNX1* (mesoderm; Supplementary Fig. 7). Some embryoid bodies manifest spontaneous beating, evidence of the formation of contractile cardiomyocytes with pacemaker activity[18] (data not shown). We dissociated embryoid bodies from human ES-cell-like cells derived from dH1f, dH1cf and

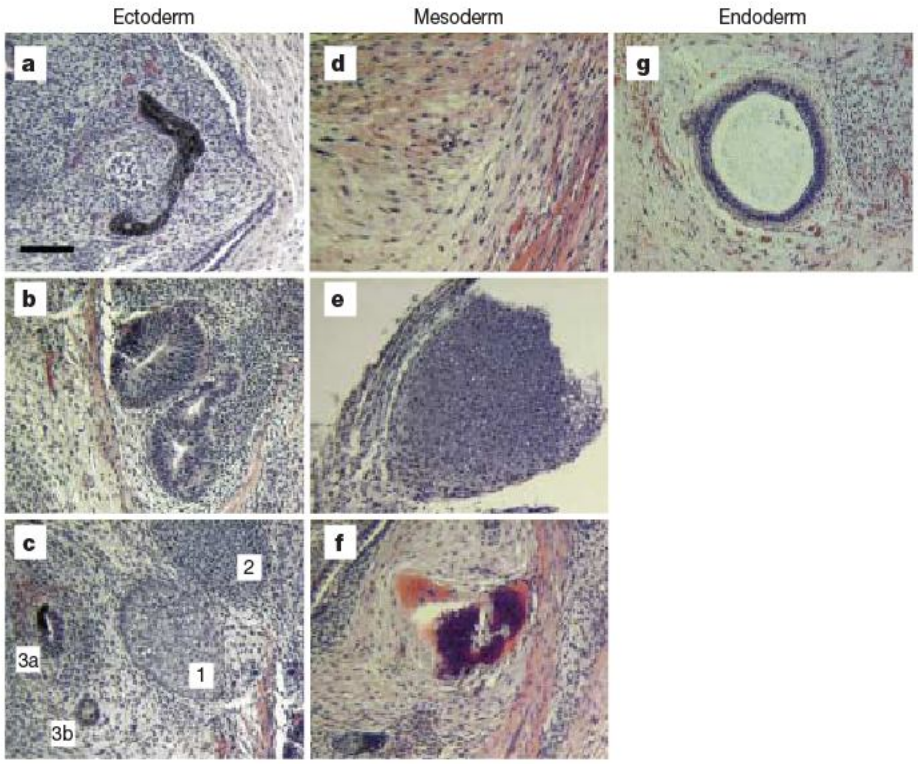

Figure 6 | Xenografts of human iPS cells generate well-differentiated teratoma-like masses containing all three embryonic germ layers. Immunodeficient mouse recipients were injected with human iPS cells (dH1f-iPS3-3) intramuscularly. Resulting teratomas demonstrate the following features in ectoderm, mesoderm and endoderm. Ectoderm: pigmented retinal epithelium (**a**), neural rosettes (**b**), glycogenated squamous epithelium (**c**); mesoderm: muscle (**d**), cartilage (**e**), bone (**f**); endoderm: respiratory epithelium (**g**). Of note, panel **c** contains all three germ layers: (1) glycogenated squamous epithelium, (2) immature cartilage, (3a) glandular tissue with surrounding stromal elements, and (3b) another small gland. All images were obtained from the same tumour. Tissue sections were stained with haematoxylin and eosin. Scale bar, 100 μm.

MSCs and plated cells in methylcellulose supplemented with haematopoietic cytokines, and detected robust formation of myeloid and erythroid colonies (Supplementary Fig. 8). Taken together, our analysis of the selected derivatives of the retrovirally infected cells suggests restoration of pluripotency. Hence, consistent with the precedent in the mouse, we labelled these cells human induced pluripotent stem (iPS) cells.

Conclusions

We observed that differentiated fibroblast derivatives of human ES cells, primary fetal tissues (lung, skin), neonatal fibroblasts and adult fibroblasts and MSCs can be reprogrammed to pluripotency using the same four genes (*OCT4*, *SOX2*, *KLF4* and *MYC*) that enable derivation of iPS cells from embryonic and adult fibroblasts in the mouse. When we eliminated single genes from the four-factor retroviral cocktail, we found that only *OCT4* and *SOX2* were essential, whereas *MYC* and *KLF4* enhanced the efficiency of colony formation (Table 1). As a significant percentage of mice carrying iPS cells develop tumours[6], eliminating these potentially oncogenic factors would be imperative before consideration of any clinical intervention with iPS cells. Taken together, our data demonstrate that OCT4, SOX2 and either MYC or KLF4 seem to be sufficient to induce reprogramming in human cells. Our data corroborate two recent reports published while this manuscript was under review[19,20]. Other combinations of factors, including novel factors, may also promote reprogramming, and indeed NANOG and LIN28 have been shown to complement OCT4 and SOX2 in reprogramming[20].

Our results establish the feasibility of reprogramming of human primary cells with defined factors, and furthermore we provide a method for obtaining, culturing and reprogramming dermal fibroblasts from adult research subjects, which should allow the establishment of human pluripotent cells in culture from patients with specific diseases for use in research. Clinical success with human iPS cells must await the development of methods that avoid potentially harmful genetic modification. Reprogramming with non-integrating virus or transient episomal gene expression, or more favourably, generation of iPS cells by biochemical means alone, is a worthy goal.

METHODS SUMMARY

Cell culture. The human ES cell line H1-OGN[8] was maintained in serum-free medium containing basic fibroblast growth factor (10 ng ml^{-1}). Differentiation medium was DMEM, 15% inactivated fetal calf serum (IFS), 1 mM Na-pyruvate, 4.5 mM monothioglycerol, 50 μg ml^{-1} ascorbic acid, 200 μg ml^{-1} iron-saturated transferrin and 50 units ml^{-1} penicillin/streptomycin. All fibroblasts were maintained in alpha-MEM, 10% IFS. Commercial fibroblast cell lines: MRC5 (from normal lung tissue of a 14-week-old male fetus; ATCC), BJ1 (neonatal foreskin; ATCC) and MSC (bone marrow mesenchymal stem cells, 33-yr-old male, Lonza).

Derivation of primary human fibroblast lines (hFib2). Primary skin fibroblasts were obtained via a 6-mm full-thickness skin punch biopsy from the volar surface of the forearm of a healthy volunteer male following informed consent (IRB and ESCRO, Children's Hospital Boston). Cultured outgrowths appeared after 7–14 days.

Retroviral production and human iPS cell induction. *OCT4*, *SOX2*, *KLF4* and *c-MYC* were introduced via the pMIG vector. SV40 large T was in pBABE-puro and *hTERT* was in pBABE-hygro (Addgene). dTomato was in lentivirus (provided by N. Geijsen). Viral infections were for 24 h and then seeded onto MEFs after 5 days. Human ES medium containing Y27632 (ref. 9) was substituted after 7 days. Chromosome counts (dH1f-iPS3-3, dH1cf32-iPS2, MRC5-iPS2, BJ-1-iPS1, BJ1-iPS3, MSC-iPS1 and hFib2-iPS1) were diploid. Karyotypes also indicated normal, diploid cells (Supplementary Fig. 9). The earliest cell line, dH1f-iPS3-3, has been in continuous culture for over 5 months (30 passages).

Bisulphite genomic sequencing. Bisulphite genomic DNA sample treatment and processing were performed simultaneously for all cell lines, with the exception of dH1f. Bisulphite conversion efficiency of non-CpG cytosines ranged from 80% to 99% for all individual clones for each sample.

Microarray analysis. RNA probes were prepared and hybridized to Affymetrix HG U133 plus 2 oligonucleotide microarrays according to the manufacturer's protocols (processed by the Biopolymer facility of Harvard Medical School). Microarrays were scanned and data was analysed using GeneSpring GX7.3.1.

Full Methods and any associated references are available in the online version of the paper at www.nature.com/nature.

Received 16 November; accepted 10 December 2007.
Published online 23 December 2007.

1. Wakayama, T. *et al.* Differentiation of embryonic stem cell lines generated from adult somatic cells by nuclear transfer. *Science* **292**, 740–743 (2001).
2. Cowan, C. A., Atienza, J., Melton, D. A. & Eggan, K. Nuclear reprogramming of somatic cells after fusion with human embryonic stem cells. *Science* **309**, 1369–1373 (2005).
3. Kanatsu-Shinohara, M. *et al.* Generation of pluripotent stem cells from neonatal mouse testis. *Cell* **119**, 1001–1012 (2004).
4. Takahashi, K. & Yamanaka, S. Induction of pluripotent stem cells from mouse embryonic and adult fibroblast cultures by defined factors. *Cell* **126**, 663–676 (2006).
5. Wernig, M. *et al. In vitro* reprogramming of fibroblasts into a pluripotent ES-cell-like state. *Nature* **448**, 318–324 (2007).
6. Okita, K., Ichisaka, T. & Yamanaka, S. Generation of germline-competent induced pluripotent stem cells. *Nature* **448**, 313–317 (2007).
7. Maherali, N. *et al.* Directly reprogrammed fibroblasts show global epigenetic remodeling and widespread tissue contribution. *Cell Stem Cell* **1**, 55–70 (2007).
8. Zwaka, T. P. & Thomson, J. A. Homologous recombination in human embryonic stem cells. *Nature Biotechnol.* **21**, 319–321 (2003).
9. Watanabe, K. *et al.* A ROCK inhibitor permits survival of dissociated human embryonic stem cells. *Nature Biotechnol.* **25**, 681–686 (2007).
10. Meissner, A., Wernig, M. & Jaenisch, R. Direct reprogramming of genetically unmodified fibroblasts into pluripotent stem cells. *Nature Biotechnol.* **25**, 1177–1181 (2007).
11. Blelloch, R., Venere, M., Yen, J. & Ramalho-Santos, M. Generation of induced pluripotent stem cells in the absence of drug selection. *Cell Stem Cell* **1**, 245–247 (2007).
12. Bodnar, A. G. *et al.* Extension of life-span by introduction of telomerase into normal human cells. *Science* **279**, 349–352 (1998).
13. Hahn, W. C. *et al.* Creation of human tumour cells with defined genetic elements. *Nature* **400**, 464–468 (1999).
14. Adewumi, O. *et al.* Characterization of human embryonic stem cell lines by the International Stem Cell Initiative. *Nature Biotechnol.* **25**, 803–816 (2007).
15. Tada, M., Takahama, Y., Abe, K., Nakatsuji, N. & Tada, T. Nuclear reprogramming of somatic cells by *in vitro* hybridization with ES cells. *Curr. Biol.* **11**, 1553–1558 (2001).
16. Lensch, M. W., Schlaeger, T. M., Zon, L. I. & Daley, G. Q. Teratoma formation assays with human embryonic stem cells: a rationale for one type of human-animal chimera. *Cell Stem Cell* **1**, 253–258 (2007).
17. Lensch, M. W. & Ince, T. A. The terminology of teratocarcinomas and teratomas. *Nature Biotechnol.* **25**, 1211 (2007).
18. Xu, C., Police, S., Rao, N. & Carpenter, M. K. Characterization and enrichment of cardiomyocytes derived from human embryonic stem cells. *Circ. Res.* **91**, 501–508 (2002).
19. Takahashi, K. *et al.* Induction of pluripotent stem cells from adult human fibroblasts by defined factors. *Cell* **131**, 861–872 (2007).
20. Yu, J. *et al.* Induced pluripotent stem cell lines derived from human somatic cells. *Science*. doi:10.1126/science.1151526 (20 November 2007).

Supplementary Information is linked to the online version of the paper at www.nature.com/nature.

Acknowledgements This research was funded by grants from the National Institutes of Health (NIH) and the NIH Director's Pioneer Award of the NIH Roadmap for Medical Research, and made possible through the generosity of Joshua and Anita Bekenstein. G.Q.D. is a recipient of the Burroughs Wellcome Fund Clinical Scientist Award in Translational Research.

Author Contributions I.-H.P. (project planning, experimental work, preparation of manuscript); R.Z., J.A.W., A.Y., H.H., P.H.L. (experimental work); T.A.I. (interpretation of teratoma pathology); M.W.L. (experimental work, preparation of manuscript); G.Q.D. (project planning, preparation of manuscript).

Author Information The microarray data have been deposited in GEO and given the series accession number GSE9832. Reprints and permissions information is available at www.nature.com/reprints. Correspondence and requests for materials should be addressed to G.Q.D. (george.daley@childrens.harvard.edu).

ARTICLES

Endogenous human microRNAs that suppress breast cancer metastasis

Sohail F. Tavazoie[1,2], Claudio Alarcón[1], Thordur Oskarsson[1], David Padua[1], Qiongqing Wang[1], Paula D. Bos[1], William L. Gerald[3] & Joan Massagué[1]

A search for general regulators of cancer metastasis has yielded a set of microRNAs for which expression is specifically lost as human breast cancer cells develop metastatic potential. Here we show that restoring the expression of these microRNAs in malignant cells suppresses lung and bone metastasis by human cancer cells *in vivo*. Of these microRNAs, miR-126 restoration reduces overall tumour growth and proliferation, whereas miR-335 inhibits metastatic cell invasion. miR-335 regulates a set of genes whose collective expression in a large cohort of human tumours is associated with risk of distal metastasis. miR-335 suppresses metastasis and migration through targeting of the progenitor cell transcription factor *SOX4* and extracellular matrix component tenascin C. Expression of miR-126 and miR-335 is lost in the majority of primary breast tumours from patients who relapse, and the loss of expression of either microRNA is associated with poor distal metastasis-free survival. miR-335 and miR-126 are thus identified as metastasis suppressor microRNAs in human breast cancer.

Although metastasis is the overwhelming cause of mortality in patients with solid tumours, our understanding of its molecular and cellular determinants is limited[1–3]. Transcriptional profiling has revealed sets of genes, or 'signatures', for which expression in primary tumours correlates with metastatic relapse or poor survival[4]. Some of these genes endow cancer cells with a more invasive phenotype, enhanced angiogenic and intravasation activity, the ability to exit from the circulation, or an ability to modify the metastasis microenvironment[5,6]. Such gene sets are thus providing numerous candidate mediators of metastasis to be validated through functional and clinical studies. Much less insight, however, has been gained into the regulatory networks that establish such altered gene expression states[7]. MicroRNAs (miRNAs) are attractive candidates as upstream regulators of metastatic progression because miRNAs can post-transcriptionally regulate entire sets of genes[8,9]. Recent work has revealed important roles for miRNAs and miRNA processing in tumorigenesis[10–12]. Large sets of miRNAs are underexpressed in human tumours compared to normal tissues[13], and interfering with miRNA processing enhances experimental tumorigenesis[11]. These findings suggest that this class of regulators contains suppressors of tumour progression and possibly metastasis. Therefore, we sought to identify human miRNAs that affect breast cancer metastasis to lung and bone—the two main sites of metastatic spread in this highly prevalent form of cancer.

Identification of miRNAs that suppress metastasis

We performed array-based miRNA profiling[14] of MDA-MB-231 human breast cancer cell derivatives that are highly metastatic to bone (1833 or 2287; denoted BoM1 lines) or lung (4175, 4173, 4180 and 4142; LM2 lines), as well as the parental, unselected MDA-MB-231 cell population. Out of 453 human miRNAs assayed, 179 miRNAs were expressed above background levels in one or more of the highly metastatic cells (data not shown). Notably, hierarchical clustering based on the expression of these miRNAs correctly classified the MDA-MB-231 derivatives into three groups comprising the BoM1 lines, the LM2 lines and the parental lines, respectively. Hierarchical clustering on the basis of the expression of the 20 miRNAs for which expression was most altered across various cell lines again correctly classified the MDA-MB-231 derivatives into these three groups (Fig. 1a). The most salient finding was a set of eight miRNAs for which expression was decreased across all metastatic sub-lines compared with their expression in the parental line (Fig. 1a). Through quantitative stem-loop polymerase chain reaction (qRT–PCR), we were able to validate the differential expression of seven of these miRNAs in MDA-MB-231 and representative LM2 and BoM1 sub-lines (Supplementary Fig. 1).

We focused on the six miRNAs (miR-335, miR-126, miR-206, miR-122a, miR-199a*, miR-489) whose expression was most decreased in metastatic cells on the basis of the combination weight of fold change in hybridization and PCR-based detection methods. Restoring the expression of miR-335, miR-126 or miR-206 in LM2 cells through retroviral transduction[10,15] (Supplementary Fig. 2) decreased the lung colonizing activity of these cells by more than fivefold (Fig. 1b). Restoration of miR-122a, miR-199a* or miR-489 expression decreased lung colonization at early time points but did not result in a significant decrease in lung colonization at the end point (Supplementary Fig. 3). Histological assessment of lungs revealed a marked decrease in the number of metastatic foci where bioluminescence imaging revealed a significant reduction (Fig. 1c and Supplementary Fig. 4). The decreased expression of these candidate miRNAs in both lung and bone metastatic cells suggested a role for these molecules in general metastatic activity of breast cancer cells. Indeed, expression of miR-335, miR-206 or miR-126 significantly decreased bone metastasis formation as assessed by bioluminescence imaging and histological analysis of hindlimbs subsequent to intracardiac injection of BoM1 cells into the arterial circulation (Fig. 1d, e).

Selective pressure for specific miRNA loss

Consistent with a selective pressure against these regulators during the metastatic process, quantitative PCR of rare metastatic foci revealed a reduction in expression of all three metastasis suppressor

[1]Cancer Biology and Genetics Program, [2]Department of Medicine, [3]Department of Pathology, Memorial Sloan-Kettering Cancer Center, New York, New York 10021, USA.

miRNAs in cells that had metastasized relative to the inoculated population (Supplementary Fig. 5a). Restoration of miR-335 or miR-206 expression in LM2 cells also significantly reduced their metastatic dissemination from the primary mammary tumour site (Supplementary Fig. 5b). miR-126 was not included in this assay because of its inhibitory effect on mammary tumour growth (see below).

To determine whether the expression of these miRNAs is lost in other human breast cancer cells with enhanced metastatic propensity, we inoculated mice with a purified population of malignant cells (CN34) obtained from the pleural fluid of a patient with metastatic breast cancer who was treated at our institution[6]. We then isolated human tumour cells from metastatic lesions that formed in the lungs (CN34-LM1 cells) and bones (CN34-BoM1 cells) of the mice. Both the CN34-LM1 and CN34-BoM1 derivatives displayed a loss of miR-335, miR-126 and miR-206 expression relative to the parental population from which they were isolated (Supplementary Fig. 5c). miR-335, miR-206 and miR-126 significantly reduced the ability of CN34-LM1 and CN34-BoM1 cells to metastasize to lung (Fig. 1f and Supplementary Fig. 5d) and bone (Fig. 1g), respectively. The expression of these miRNAs, therefore, is lost in multiple, independently derived, breast cancer samples and their restoration suppresses lung and bone metastasis in these distinct metastatic cell populations.

Distinct mechanisms of metastasis suppression

Cell proliferation, survival and migration are among the common functions required by tumour cells for metastatic progression in target microenvironments. Of the three miRNAs that suppressed metastasis, only miR-126 significantly suppressed overall tumour growth, as assessed by tumour volume (Fig. 2a and Supplementary Fig. 6). Immunohistochemistry on these mammary tumours revealed a decrease in proliferation (Supplementary Fig. 7a, b), but not apoptosis (Supplementary Fig. 7c). Consistent with this, restoration of miR-126 reduced the proliferation rate of LM2 cells as well as CN34-BoM1 cells *in vitro* (Fig. 2b). miR-126, therefore, suppresses tumorigenesis and metastasis, in part, through an inhibition of cancer cell proliferation.

In contrast to miR-126, restoring the expression of miR-335 or miR-206 did not alter the proliferation or apoptotic rates of LM2 cells

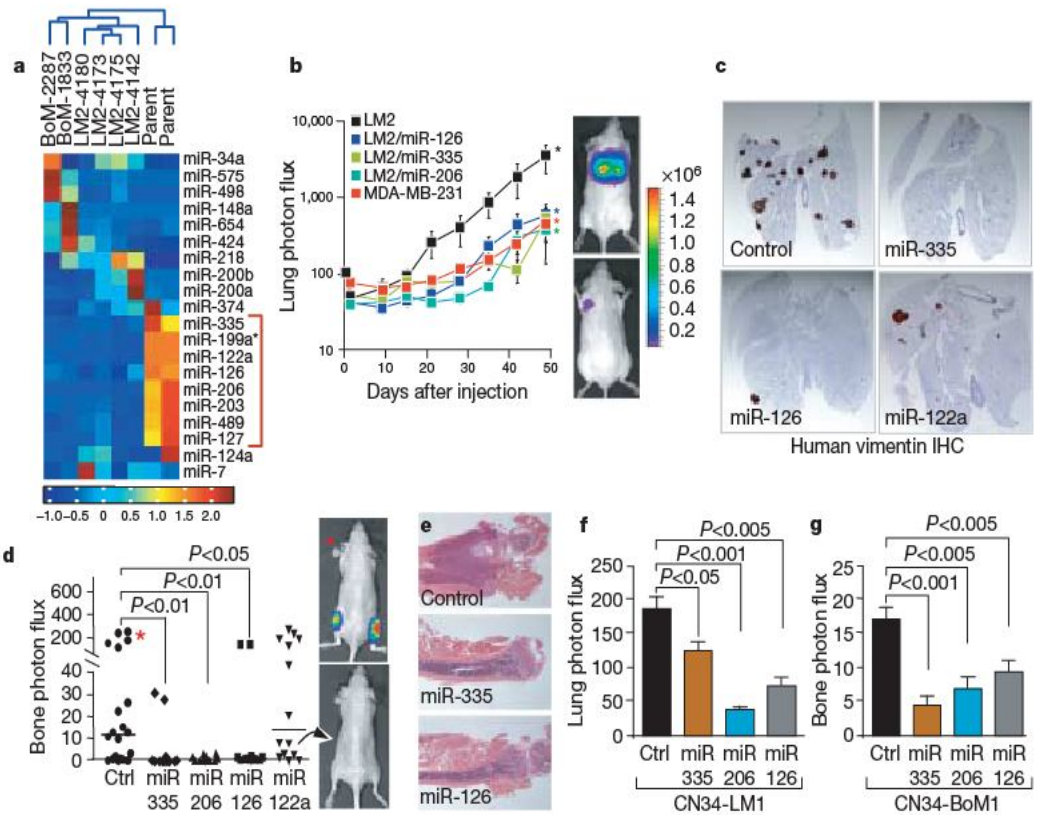

Figure 1 | Systematic identification of miRNAs that suppress lung and bone metastasis in multiple human breast cancer cell derivatives. a, Hierarchical clustering of normalized miRNA expression levels for the 20 miRNAs that displayed the highest coefficients of variation clusters the MDA-MB-231 derivatives into three groups comprised of the bone metastatic BM2 lines (2287 and 1833), the lung metastatic LM2 lines (4180, 4173, 4175, and 4142) and the parental MDA lines. The heatmap highlights a set of miRNAs whose expression decreases across all lung and bone metastatic derivatives (red bracket along the right). The scale bar across the bottom depicts standard deviation change from the mean. **b**, Bioluminescence imaging of lung metastasis by lung metastatic breast cancer cells with restored expression of specific miRNAs. 1×10^4 LM2 cells expressing individual miRNAs or the control hairpin, as well as the parental MDA-MB-231 cells, were inoculated intravenously into immunodeficient mice. Shown are representative mice corresponding to the LM2 set (top) and the MDA-MB-231 set (bottom) at day 50. Lung colonization was measured by bioluminescence and quantified. $n = 5$; error bars represent s.e.m.; asterisk, $P < 0.05$. **c**, Human-vimentin-stained images of representative lungs that emitted the median luciferase signal for each cohort. Lungs were extracted at 8 weeks after xenografting and representative images of sections were obtained at whole-field magnification. **d**, 2×10^4 BM2 cells expressing individual miRNAs or the control hairpin were inoculated into the arterial circulation via intracardiac injection of athymic mice. Bone metastasis was measured by bioluminescence and quantified as the normalized hindlimb photon flux. Shown are representative mice corresponding to marked data points. $n = 6$–10; horizontal line represents median signal for each cohort; *P*-values based on a one-tailed rank-sum test. **e**, Representative whole-field magnification images of haematoxylin- and eosin-stained femurs extracted from representative mice 7 weeks after intraventricular injection of indicated cancer cells. **f**, 2×10^5 primary human cancer derivative CN34-LM1 cells expressing individual miRNAs or the control vector were inoculated intravenously into immunodeficient mice. Lung colonization was measured by bioluminescence, quantified and normalized. $n = 8$; error bars represent s.e.m.; *P*-values based on a one-sided rank-sum test. **g**, 2×10^5 primary human cancer derivative CN34-BoM1 cells expressing individual miRNAs or the control vector were inoculated into the arterial circulation via intracardiac injection of immunodeficient mice. Bone metastasis was measured by bioluminescence, quantified and normalized. $n = 9$–10; error bars represent s.e.m.; *P*-values based on a one-tailed rank-sum test.

in vivo or *in vitro* but it induced an altered morphology. LM2 cells and CN34-BoM1 cells expressing miR-335 or miR-206 as a population contained a significantly lower fraction of elongated cells than did control cells (Fig. 2c and Supplementary Fig. 8). Despite these morphological changes, LM2 cells expressing these miRNAs continued to express the mesenchymal marker vimentin, *in vivo*, suggesting that the suppression of metastasis in these cells was not due to classical mesenchymal–epithelial transition (Supplementary Fig. 9). We postulated that such an alteration in shape may be associated with a decrease in cell motility, which would limit metastatic migration. Indeed, in trans-well migration assays, LM2 cells and CN34-BoM1 cells expressing miR-335 or miR-206 displayed a significant reduction in migration compared with controls (Fig. 2d). miR-335 and miR-206 also caused a significant reduction in invasive capacity, as assessed through matrigel invasion assays (Supplementary Fig. 10). These findings highlight cell-autonomous mechanisms of cell proliferation, migration and invasion through which specific miRNAs may suppress metastasis.

MicroRNA expression in clinical metastasis

To determine whether these miRNAs are associated with human metastasis, we determined by qRT–PCR the expression levels of miR-335 and miR-126 in 20 archived primary breast tumours. These tumours comprised large (>2.5 cm) and small (<2.5 cm) oestrogen receptor (ER)-positive and -negative subtypes that were surgically resected before administration of chemotherapy. This set consisted of primary tumours resected from 11 patients that ultimately relapsed to lung, bone, or brain as well as tumours resected from nine patients who did not suffer metastatic relapse (Supplementary Table 1). qRT–PCR (Supplementary Fig. 11) revealed that patients whose primary tumours displayed low expression of miR-335, miR-126 (Fig. 3a) or miR-206 (Supplementary Fig. 12) had a shorter median time to metastatic relapse. Notably, the low expression levels of miR-335 ($P = 0.0022$; median survival of 1.84 yr; hazard ratio (ratio of the predicted hazard (metastasis) for a member of the control group compared to that for a member of the test group) of 8.95) or miR-126 ($P = 0.0156$; median survival of 2.57 yr; hazard ratio of 5.08) were associated with very poor overall metastasis-free survival compared to the group whose tumours expressed a high level of these miRNAs. The median expression values of these miRNAs was more than eightfold lower in tumours from patients that ultimately relapsed compared to tumours from patients that did not relapse (Supplementary Fig. 11). The expression levels of these miRNAs were not significantly correlated with ER status or HER-2 (also called ERBB2) amplification status (Supplementary Table 1). The group of patients whose primary tumours had a low level of miR-122a or miR-199a expression, two miRNAs that do not suppress metastasis, showed no difference in metastasis-free survival compared to those with high expression (Fig. 3a and Supplementary Fig. 11). These findings uncover a significant association between the loss of metastasis suppressor miRNA expression in primary human breast tumours and the likelihood of future distal metastatic recurrence.

miR-335 regulates a set of metastasis genes

Given the strong association between the loss of miR-335 expression and clinical relapse, we wondered whether miR-335 loss could

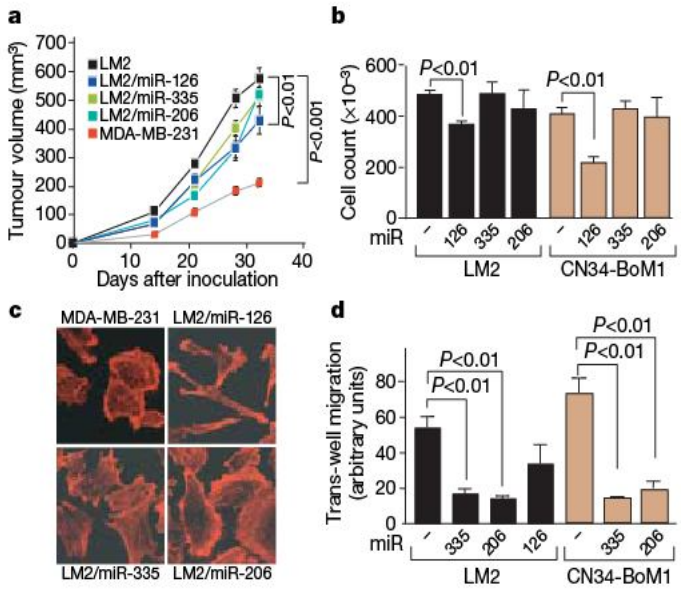

Figure 2 | miR-126 suppresses overall tumour growth and proliferation whereas miR-335 and miR-206 regulate migration and morphology. **a**, 5×10^5 LM2 cells expressing individual miRNAs or the control hairpin, as well as the parental MDA-MB-231 cells, were injected into the mammary fat pads of immunodeficient mice and tumour volumes were measured over time. $n = 5$ (MDA-MB-231, LM2/miR-126, LM2/miR-206) and $n = 10$ (LM2, LM2/miR-335); error bars indicate s.e.m.; *P*-values based on a one-sided Student's *t*-test at day 32. **b**, 5×10^4 LM2 or primary breast cancer line CN34-BoM1 expressing miR-126, miR-335 or miR-206 and control cells were seeded in triplicate and viable cells were counted at 5 days after seeding. $n = 3$; error bars represent s.e.m.; *P*-values obtained using a one-sided Student's *t*-test. **c**, Parental MDA-MB-231 cells and lung metastatic LM2 cells expressing miR-126, miR-335 or miR-206 were seeded onto glass slides. Cells were stained with the actin marker phalloidin and confocal images were obtained. **d**, 2.5×10^4 LM2 and CN34-BoM1 cells were transduced with the indicated miRNAs or a control hairpin, and trans-well migration was assessed. Images of cells that had migrated through trans-well inserts were obtained and analysed in automated fashion using Metamorph software. $n = 3$; error bars represent s.e.m.; *P*-values obtained using a one-sided Student's *t*-test.

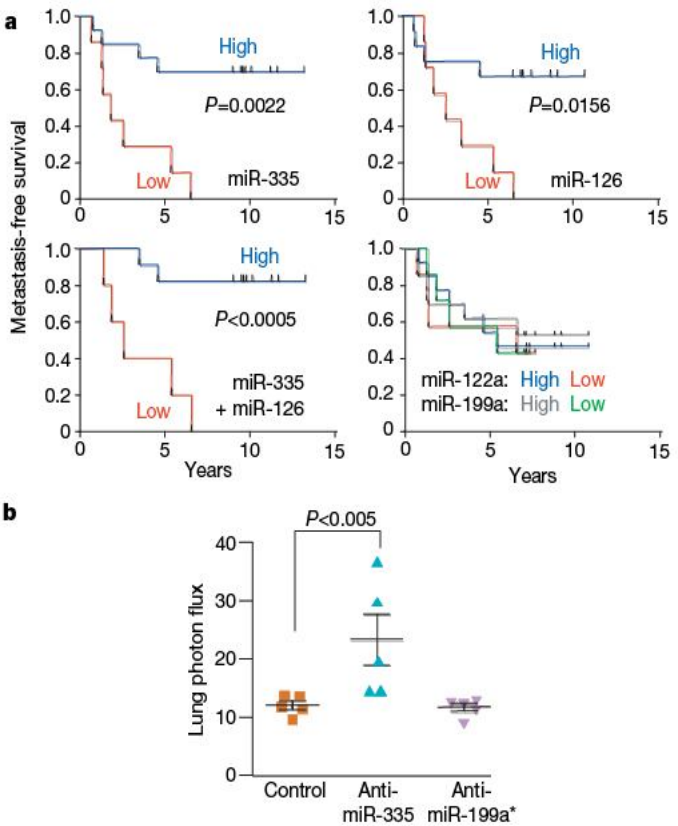

Figure 3 | Clinical association of miR-335 and miR-126 with metastasis-free survival. **a**, miR-335, miR-126, miR-122a and miR-199a expression was assessed in a set of 20 primary breast tumour samples through qRT–PCR. Kaplan–Meier curves depict metastasis-free survival of patients whose primary tumours contained low or high levels of the indicated miRNAs. *P*-values were obtained using a log-rank test. **b**, The parental MDA-MB-231 cells were transfected with antagomirs targeting endogenous miR-335, miR-199a* or a control antagomir. Four days after transfection, 1×10^4 LM2 cells from each cohort were inoculated intravenously into immunodeficient mice. Lung colonization was measured by bioluminescence at day 35 and quantified. $n = 5$; error bars represent s.e.m.; *P*-values based on a one-sided rank-sum test.

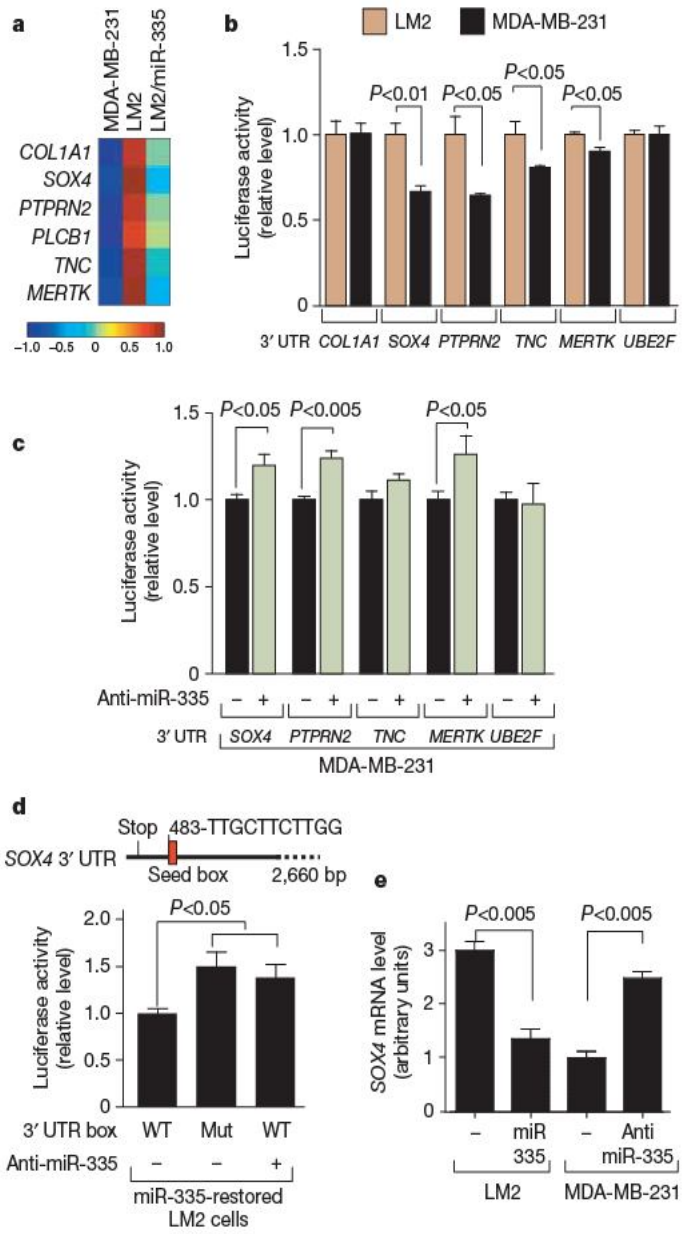

Figure 4 | A miR-335-regulated gene set includes *SOX4* as a miR-335 direct target. **a**, The miR-335 metastasis signature consists of genes downregulated by miR-335 and are also overexpressed in bone as well as lung metastatic MDA-MB-231 derivatives. The heatmap depicts the variance-normalized expression values for each gene averaged across two MDA-MB-231 samples, four LM2 samples and two LM2/miR-335 samples. The scale bar depicts standard deviation change from the mean for the expression value of each gene. **b**, UTR reporter assays of miR-335 metastasis genes in LM2 and MDA-MB-231 cells. Reporter constructs consisting of the luciferase sequence fused to the 3′ UTRs of the miR-335 metastasis genes as well as the control gene *UBE2F* were transfected into the LM2 and parental MDA-MB-231 cell lines. Luciferase activity of cells was assayed at 32 h after transfection and the values were normalized to the LM2 cell line. $n = 3$; error bars represent s.e.m.; *P*-values were obtained using a one-sided Student's *t*-test. **c**, Luciferase activity of MDA-MB-231 cells co-transfected with 3′ UTR reporter constructs with, or without, miR-335 antagomir was assayed at 32 h after transfection and normalized to control cells. $n = 3$; error bars represent s.e.m.; *P*-values obtained using a one-sided Student's *t*-test. **d**, Schematic diagram depicts seed sequence (red box) in *SOX4* UTR. The 60 bp containing this sequence or the miR-335 seed target site mutant were subjected to UTR reporter assays in LM2 cells with restored miR-335 expression. Luciferase activity of cells was also assayed in the presence or absence of the miR-335 antagomir. $n = 3$; error bars represent s.e.m.; *P*-values obtained using a one-sided Student's *t*-test. **e**, *SOX4* expression in LM2 and MDA-MB-231 cells was obtained through real time qRT–PCR in cells expressing miR-335 or transfected with the miR-335 antagomir. $n = 3$; error bars represent s.e.m.; *P*-values derived using a one-sided Student's *t*-test.

promote metastasis. To test this, we transfected the poorly metastatic MDA-MB-231 cells with an anti-miRNA antagomir[16] targeting either miR-335, miR-199a* or a control sequence. Indeed, inhibition of miR-335 enhanced the lung-colonizing ability of MDA-MB-231 cells compared with control cells (Fig. 3b). To identify putative metastasis genes that miR-335 suppresses, we transcriptionally profiled LM2 cells with restored miR-335 expression and arrived at the set of 756 genes for which expression is decreased (using a permissive threshold; see Methods) compared with control LM2 cells. We separately identified genes for which expression levels were increased across both bone and lung metastatic cells. On the basis of available gene expression data sets[17,18] we identified 116 genes for which expression was increased by at least twofold in both bone and lung metastatic MDA-MB-231 derivatives compared with the parental line (Supplementary Table 2). The overlap between these two lists yielded a set of six genes for which expression is high in metastatic cells and suppressed by miR-335 (Fig. 4a). This list of miR-335-regulated metastasis genes included genes previously implicated in extracellular matrix and cytoskeleton control, such as the type 1 collagen *COL1A1* (ref. 19); in signal transduction, such as the receptor-type tyrosine protein phosphatase *PTPRN2* (ref. 20), the c-Mer tyrosine kinase (*MERTK*)[21] and the phospholipase *PLCB1* (ref. 22); as well as in cell migration, such as tenascin C (*TNC*)[23] and the SRY-box containing transcription factor *SOX4* (refs 24, 25).

Bioinformatic analysis of the 3′ UTRs of these genes revealed them all to have at least six nucleotides of sequence complementarity to the miR-335 seed region (data not shown). To determine whether the altered expression of these genes in metastatic cells is, in part, mediated through their 3′ UTRs, we cloned the 3′ UTR of five of these genes downstream of a luciferase gene as a reporter, and assayed their expression in LM2 cells (low miR-335) and MDA-MB-231 cells (high miR-335). The expression from UTR reporters corresponding to *SOX4*, *PTPRN2*, *TNC* and *MERTK*, but not that of the control gene *UBE2F* lacking the miR-335 target sequence, was significantly lower in LM2 cells relative to MDA-MB-231 cells (Fig. 4b). Furthermore, inhibition of miR-335 in MDA-MB-231 cells by means of an antagomir was sufficient to enhance the expression of *SOX4*, *PTPRN2* and *MERTK*, but not the expression of a control *UBE2F* reporter (Fig. 4c). These results suggest that *SOX4*, *PTPRN2*, *MERTK* and possibly *TNC* are direct targets of endogenous miR-335.

SOX transcription factors are known to regulate progenitor cell development and migration[25]. In reporter assays, mutation of the miR-335 seed sequence in the *SOX4* UTR as well as miR-335 inhibition with an antagomir significantly increased reporter expression (Fig. 4d). Restoration of miR-335 expression in LM2 cells reduced endogenous *SOX4* messenger RNA expression, whereas miR-335 inhibition increased *SOX4* expression in MDA-MB-231 cells (Fig. 4e). The knockdown of *SOX4* in LM2 cells with either of two unique short hairpin RNAs (shRNAs) (Supplementary Fig. 13a) reduced the overall fraction of elongated cells, similar to the phenotype observed with miR-335 restoration in these cells (Supplementary Fig. 14a, b). The morphological change resulting from *SOX4* knockdown was also associated with a decrease in cell migration in a trans-well assay (Supplementary Fig. 14c). Another miR-335-regulated gene, *TNC*, also caught our attention, as its expression occurs in the invasive front of human carcinomas[26]. Knockdown of *TNC* in LM2 cells using either of two RNA interference molecules also reduced migration in a trans-well assay (Supplementary Fig. 14c). Notably, knockdown of *SOX4* or *TNC* significantly diminished the invasive ability of LM2 cells (Fig. 5a). Moreover, short-hairpin inhibition of *SOX4* or *TNC* significantly abolished metastasis by LM2 cells in lung colonization assays (Fig. 5b, c). Thus, miR-335 regulates metastasis through suppression of transcription factor SOX4 and extracellular matrix component tenascin C.

To determine whether the expression of the genes that miR-335 regulates is associated with human breast cancer metastasis, we examined primary breast tumour gene expression data sets with

corresponding disease outcome annotation[18,27]. Tumours in these cohorts for which aggregate six-gene expression scores exceeded one standard deviation from the mean were considered miR-335-signature-positive (equivalent to loss of miR-335 function). Patients whose primary breast tumours were positive for the miR-335 signature had a significantly worse metastasis-free survival both in the combined cohort of 368 patients (Fig. 5d) as well as in each cohort separately classified (Supplementary Fig. 15a). Consistent with the results of our functional studies, the miR-335 signature performed better as a predictor of overall metastasis rather than lung- or bone-specific metastasis (Supplementary Fig. 15b).

MicroRNAs as suppressors of metastasis

Multiple lines of evidence provided here argue for the involvement of specific miRNAs in suppressing breast cancer metastasis. miR-335, miR-206 and miR-126 are selectively downregulated across a number of highly metastatic human cell lines compared to the general tumour cell population and have demonstrated abilities to suppress metastasis of breast cancer cells to different organ sites. The expression of miR-335 and miR-126 in human mammary tumours is inversely associated with metastatic relapse of these tumours to distant organs, and the expression of miR-206 also shows a trend in the same direction. The expression of a set of genes regulated by one of these miRNAs, miR-335, is directly associated with relapse. We also establish two of these genes, *SOX4* and *TNC*, as *in vivo* mediators of metastasis. The role of *SOX4* in haematopoietic progenitor development[28] suggests that its transcriptional programme may be re-used not only for cancer cell invasion in cooperation with tenascin C but also for tumour initiation in the metastatic niche. miR-335 and miR-126 are expressed in normal human breast tissue[13]. Our findings on their roles in the pathogenesis of human breast cancer argue for an important function for these regulators in maintaining normal tissue integrity. Recently, miR-10b was identified as a miRNA whose overexpression in breast cancer cells promoted tumour growth and lung micrometastasis[12]. Our work expands on this by identifying miRNAs as clinically meaningful suppressors of metastasis. MicroRNAs are thus uncovered as another class of molecules, along with metastasis suppressor genes[29], that negatively regulate tumour progression.

The recent implication of miRNAs and miRNA processing in tumorigenesis[11,13] has raised interest in identifying the specific miRNAs for which loss of expression enhances tumorigenesis, the mechanisms by which they act, and the phenotypic advantages afforded to cells that lose miRNA expression. Our findings suggest that within a tumour, the loss of specific miRNAs provides a selective advantage for cells destined for metastatic colonization. A global downregulation of miRNAs in cancer may serve metastasis by reducing the threshold for loss of specific miRNAs in a subset of cells that will ultimately metastasize. That one such miRNA (miR-335) regulates a set of putative, and a subset of validated, metastasis genes argues that the multi-gene regulatory capacity of a miRNA can function as a barrier to tumour progression in humans. The strong association of the loss of miR-335 and miR-126 expression with metastatic relapse suggests the potential for the use of these molecules in prognostic stratification of breast cancer patients in addition to conventional clinical and pathological staging markers.

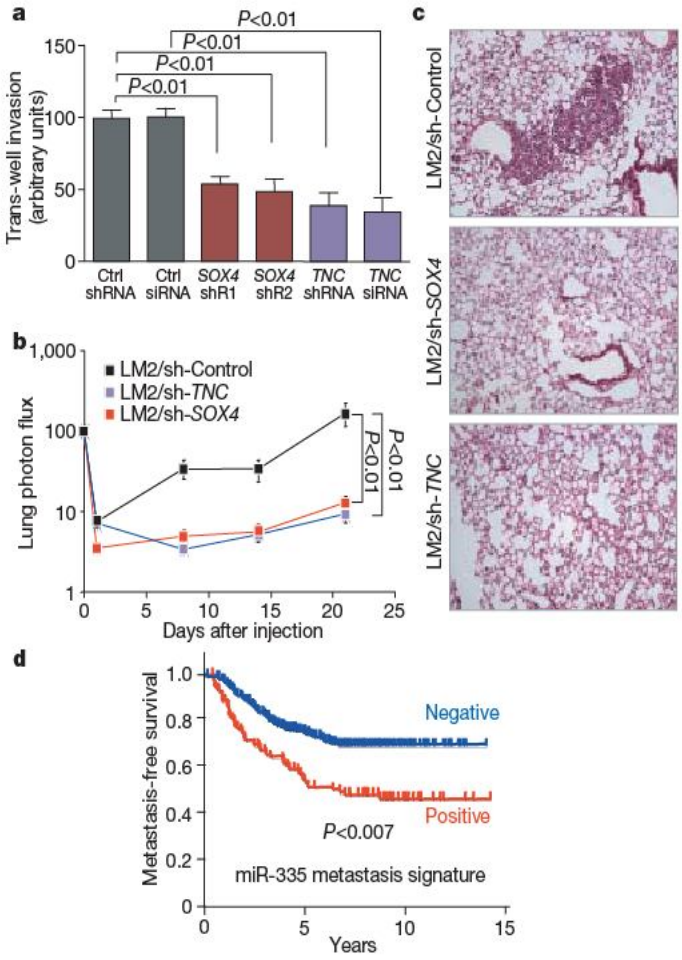

Figure 5 | miR-335 regulates metastasis and invasion through suppression of *SOX4* and *TNC*. **a**, 5.0×10^4 LM2 cells were transduced with short hairpin control vector, either of two shRNAs targeting *SOX4*, a hairpin targeting *TNC*, or an siRNA targeting *TNC*, and invasion of cells through a trans-well matrigel-coated membrane insert was quantified. $n = 6$; error bars represent s.e.m.; *P*-values based on a one-sided Student's *t*-test. **b**, 2×10^5 LM2 cells transduced with either a control short hairpin, a short hairpin targeting *SOX4* or one targeting *TNC* were inoculated intravenously into immunodeficient mice. Lung colonization was measured by bioluminescence and quantified. $n = 7$; error bars represent s.e.m.; *P*-values based on a one-tailed rank-sum test. **c**, Haematoxylin-and-eosin-stained images of representative lungs that were extracted at 4 weeks after cell inoculation. Representative images were obtained at 10× magnification. **d**, Kaplan–Meier curves for the combined Memorial Sloan Kettering and Erasmus Medical Center breast tumour cohorts (368 tumours) depicting metastasis-free survival of patients whose primary tumours expressed the miR-335 six-gene signature (positive) and those that did not (negative). $n = 368$; *P*-value based on the Mantel–Cox log-rank test.

METHODS SUMMARY

The MDA-MB-231 cell line and its metastatic derivatives[18,17,30] as well as the pleural effusion-derived CN34 cancer cells have been described previously[31]. All metastatic derivatives were obtained through *in vivo* selection in immunodeficient mice[17,18]. MicroRNA microarray profiling was performed using LC Sciences technology (LC Sciences, LLC). Mature miRNA expression was assayed using Taqman MicroRNA assays as previously described[32]. MicroRNA expression was achieved through retroviral transduction of metastatic cells using miR-Vec technology[15]. The miRNA vectors were provided by R. Agami[10]. In brief, they consist of approximately 500-bp fragments that span a given miRNA genomic region under the control of a CMV promoter[10,15]. All animal work was done in accordance with the MSKCC Institutional Animal Care and Use Committee. Statistical analyses were performed using the Graphpad Prism 5 software package. See Supplementary Methods for additional information regarding retroviral infections, transfections, shRNA and siRNA constructs, miRNA inhibition, analysis of miRNA and mRNA expression, miRNA expression profiling and hierarchical clustering, transcriptional profiling, tumour miRNA and gene expression analysis, survival analysis, trans-well migration and invasion assays, bioluminescence imaging, animal injections and inoculations, metastatic cell extraction, tumour and lung immunohistochemical and histological analyses, and image quantification.

Full Methods and any associated references are available in the online version of the paper at www.nature.com/nature.

Received 1 September; accepted 21 November 2007.

1. Fidler, I. J. The pathogenesis of cancer metastasis: the 'seed and soil' hypothesis revisited. *Nature Rev. Cancer* 3, 453–458 (2003).
2. Weigelt, B., Peterse, J. L. & van't Veer, L. J. Breast cancer metastasis: markers and models. *Nature Rev. Cancer* 5, 591–602 (2005).

3. Gupta, G. P. & Massague, J. Cancer metastasis: building a framework. *Cell* **127**, 679–695 (2006).
4. Nevins, J. R. & Potti, A. Mining gene expression profiles: expression signatures as cancer phenotypes. *Nature Rev. Genet.* **8**, 601–609 (2007).
5. Nguyen, D. X. & Massague, J. Genetic determinants of cancer metastasis. *Nature Rev. Genet.* **8**, 341–352 (2007).
6. Gupta, G. P. *et al.* Mediators of vascular remodelling co-opted for sequential steps in lung metastasis. *Nature* **446**, 765–770 (2007).
7. Seligson, D. B. *et al.* Global histone modification patterns predict risk of prostate cancer recurrence. *Nature* **435**, 1262–1266 (2005).
8. Lim, L. P. *et al.* Microarray analysis shows that some microRNAs downregulate large numbers of target mRNAs. *Nature* **433**, 769–773 (2005).
9. Chan, C. S., Elemento, O. & Tavazoie, S. Revealing posttranscriptional regulatory elements through network-level conservation. *PLoS Comput. Biol.* **1**, e69 (2005).
10. Voorhoeve, P. M. *et al.* A genetic screen implicates miRNA-372 and miRNA-373 as oncogenes in testicular germ cell tumors. *Cell* **124**, 1169–1181 (2006).
11. Kumar, M. S., Lu, J., Mercer, K. L., Golub, T. R. & Jacks, T. Impaired microRNA processing enhances cellular transformation and tumorigenesis. *Nature Genet.* **39**, 673–677 (2007).
12. Ma, L., Teruya-Feldstein, J. & Weinberg, R. A. Tumour invasion and metastasis initiated by microRNA-10b in breast cancer. *Nature* **449**, 682–688 (2007).
13. Lu, J. *et al.* MicroRNA expression profiles classify human cancers. *Nature* **435**, 834–838 (2005).
14. Calin, G. A. *et al.* MicroRNA profiling reveals distinct signatures in B cell chronic lymphocytic leukemias. *Proc. Natl Acad. Sci. USA* **101**, 11755–11760 (2004).
15. Chen, C. Z., Li, L., Lodish, H. F. & Bartel, D. P. MicroRNAs modulate hematopoietic lineage differentiation. *Science* **303**, 83–86 (2004).
16. Meister, G., Landthaler, M., Dorsett, Y. & Tuschl, T. Sequence-specific inhibition of microRNA- and siRNA-induced RNA silencing. *RNA* **10**, 544–550 (2004).
17. Kang, Y. *et al.* A multigenic program mediating breast cancer metastasis to bone. *Cancer Cell* **3**, 537–549 (2003).
18. Minn, A. J. *et al.* Genes that mediate breast cancer metastasis to lung. *Nature* **436**, 518–524 (2005).
19. Egeblad, M. *et al.* Type I collagen is a genetic modifier of matrix metalloproteinase 2 in murine skeletal development. *Dev. Dyn.* **236**, 1683–1693 (2007).
20. Varadi, A., Tsuboi, T. & Rutter, G. A. Myosin Va transports dense core secretory vesicles in pancreatic MIN6 beta-cells. *Mol. Biol. Cell* **16**, 2670–2680 (2005).
21. Graham, D. K. *et al.* Cloning and developmental expression analysis of the murine c-mer tyrosine kinase. *Oncogene* **10**, 2349–2359 (1995).
22. Lyu, M. S., Park, D. J., Rhee, S. G. & Kozak, C. A. Genetic mapping of the human and mouse phospholipase C genes. *Mamm. Genome* **7**, 501–504 (1996).
23. Ilunga, K. *et al.* Co-stimulation of human breast cancer cells with transforming growth factor-β and tenascin-C enhances matrix metalloproteinase-9 expression and cancer cell invasion. *Int. J. Exp. Pathol.* **85**, 373–379 (2004).
24. van de Wetering, M., Oosterwegel, M., van Norren, K. & Clevers, H. Sox-4, an Sry-like HMG box protein, is a transcriptional activator in lymphocytes. *EMBO J.* **12**, 3847–3854 (1993).
25. Hoser, M. *et al.* Prolonged glial expression of Sox4 in the CNS leads to architectural cerebellar defects and ataxia. *J. Neurosci.* **27**, 5495–5505 (2007).
26. Orend, G. & Chiquet-Ehrismann, R. Tenascin-C induced signaling in cancer. *Cancer Lett.* **244**, 143–163 (2006).
27. Wang, Y. *et al.* Gene-expression profiles to predict distant metastasis of lymph-node-negative primary breast cancer. *Lancet* **365**, 671–679 (2005).
28. Schilham, M. W., Moerer, P., Cumano, A. & Clevers, H. C. Sox-4 facilitates thymocyte differentiation. *Eur. J. Immunol.* **27**, 1292–1295 (1997).
29. Steeg, P. S. Metastasis suppressors alter the signal transduction of cancer cells. *Nature Rev. Cancer* **3**, 55–63 (2003).
30. Minn, A. J. *et al.* Distinct organ-specific metastatic potential of individual breast cancer cells and primary tumors. *J. Clin. Invest.* **115**, 44–55 (2005).
31. Gomis, R. R., Alarcon, C., Nadal, C., Van Poznak, C. & Massague, J. C/EBPβ at the core of the TGFβ cytostatic response and its evasion in metastatic breast cancer cells. *Cancer Cell* **10**, 203–214 (2006).
32. Chen, C. *et al.* Real-time quantification of microRNAs by stem-loop RT-PCR. *Nucleic Acids Res.* **33**, e179 (2005).
33. He, L. *et al.* A microRNA component of the p53 tumour suppressor network. *Nature* **447**, 1130–1134 (2007).

Supplementary Information is linked to the online version of the paper at www.nature.com/nature.

Acknowledgements We thank S. Tavazoie, M. Tavazoie, D. Nguyen, S. Kurdistani and X. Zhang for discussions and technical suggestions. We are grateful to R. Agami, C. Le Sage and R. Nagel for providing the miR-Vec constructs. We thank J. Baez, E. Montalvo, E. Suh, Z. Lazar, Y. Romin, A. Barlas, K. Manova-Todorova and members of the Molecular Cytology Core Facility. We thank X. Zhou of LC Sciences for miRNA profiling services as well as the MSKCC core facility for transcriptional profiling. J.M. was funded by a National Institutes of Health grant, and by grants of the Hearst Foundation and the Kleberg Foundation. S.F.T. is supported by the Olson Foundation grant and a Clinical Scholars Award. J.M. is an Investigator of the Howard Hughes Medical Institute.

Author Contributions S.F.T. and J.M. designed experiments. J.M. supervised research. S.F.T. and J.M. wrote the manuscript. S.F.T. performed experiments. C.A. helped with UTR cloning and reporter experiments and performed confocal microscopy. T.O. helped with TNC experiments. D.P. assisted with mammary fat pad experiments and lung extractions. Q.W. assisted with intracardiac injections. P.D.B. generated and validated *TNC* shRNA. W.L.G. obtained, classified and processed breast tumour samples. All authors discussed the results and commented on the manuscript.

Author Information The miR-335 microarray data is deposited at GEO under accession number GSE9586. Reprints and permissions information is available at www.nature.com/reprints. Correspondence and requests for materials should be addressed to J.M. (massaguj@mskcc.org).

ARTICLES

RNA-mediated epigenetic programming of a genome-rearrangement pathway

Mariusz Nowacki[1], Vikram Vijayan[2], Yi Zhou[1], Klaas Schotanus[1], Thomas G. Doak[1] & Laura F. Landweber[1]

Genome-wide DNA rearrangements occur in many eukaryotes but are most exaggerated in ciliates, making them ideal model systems for epigenetic phenomena. During development of the somatic macronucleus, *Oxytricha trifallax* destroys 95% of its germ line, severely fragmenting its chromosomes, and then unscrambles hundreds of thousands of remaining fragments by permutation or inversion. Here we demonstrate that DNA or RNA templates can orchestrate these genome rearrangements in *Oxytricha*, supporting an epigenetic model for sequence-dependent comparison between germline and somatic genomes. A complete RNA cache of the maternal somatic genome may be available at a specific stage during development to provide a template for correct and precise DNA rearrangement. We show the existence of maternal RNA templates that could guide DNA assembly, and that disruption of specific RNA molecules disables rearrangement of the corresponding gene. Injection of artificial templates reprogrammes the DNA rearrangement pathway, suggesting that RNA molecules guide genome rearrangement.

Parental RNA transcripts and microRNAs are critical for programming development in metazoa[1–4], raising the possibility that altered RNA molecules can reprogramme patterning on a developmental or evolutionary timescale[5]. Despite the suggestion of template-directed events involving "an ancestral RNA-sequence cache"[6] there has been limited evidence for a direct role of RNA as a template of information across generations[7,8]. Information transfer from RNA to DNA usually involves polymerization[9]. Here we show that RNA molecules can also organize DNA rearrangements, expanding the epigenetic influence of RNA beyond gene expression and priming or directing DNA and RNA synthesis, editing, modification or repair[9–11].

O. trifallax is a unicellular eukaryote harbouring two kinds of nuclei: germline micronuclei and somatic macronuclei. Diploid micronuclei are transcriptionally inert during vegetative growth but they transmit the germline genome through subsequent generations. Effectively polyploid macronuclei provide all vegetative gene expression, but degrade after fertilization, when new micronuclei and macronuclei develop. DNA differentiation in ciliates such as *Oxytricha* (also called *Sterkiella*) involves massive chromosome fragmentation and deletion of transposons and internally eliminated sequences (IESs), accomplishing 95% genome reduction, compressing a 1 Gb germline into one-twentieth of the space. Rearrangement of the remaining short segments (macronuclear destined segments; MDSs) by permutation or inversion, followed by telomere addition and amplification, produces mature macronuclear 'nanochromosomes', typically ~2 kb with just one gene[12].

Genome-wide rearrangements discard nearly all non-genic DNA in *Oxytricha*, packing a streamlined gene-rich (~30,000 genes) eukaryotic genome in only 50 Mb. Furthermore, hundreds of thousands of MDSs require unscrambling (reordering or inversion) to interpret the sequence information in their DNA. The remarkable degree of specificity and reproducibility suggests a highly accurate mechanism to programme rearrangements. The parental cell must provide sufficient information to assemble a fully functional macronucleus. The mechanisms that allow perfect recognition of hundreds of thousands of DNA sequences for elimination or reordering remain largely unknown. The discovery of homology-dependent maternal effects that modify DNA deletions may provide a clue[13,14].

Homology-dependent trans-nuclear comparison of germline and somatic genomes may regulate these DNA rearrangements. In *Tetrahymena*, germ-line-specific small RNAs called scan RNAs derive from the micronuclear-limited sequence and target DNA for elimination[15]. However, this model cannot explain fusion of unlinked or disordered DNA segments in *Oxytricha*, which can join segments smaller than the length of typical scan RNAs. DNA rearrangements in *Tetrahymena* are imprecise, involving no permutations.

In other species including *Paramecium*, DNA rearrangements occur at short direct repeats called pointers. Homologous recombination between identical repeats at MDS–IES boundaries can both remove the IESs between them and reorder MDSs, leaving one copy of the pointer in the final product. Pointers of 2–20 bp in *Oxytricha* (average length of 4 bp between nonscrambled junctions and 9 bp between scrambled junctions[16]) generally occur at the 3′ end of every MDS segment n and the 5′ end of segment $n + 1$, providing a simple linked list of final MDS order. Although necessary for DNA deletion in *Paramecium*[17], 2–20 bp pointers could not unambiguously guide rearrangement[18].

In refs 19 and 20, the authors proposed an epigenetic model in which an RNA or DNA template derived from the maternal macronucleus guides assembly of the new macronuclear chromosomes. Macronuclear templates could provide a scaffold to organize the layout of segment order and DNA deletion, using strand displacement and branch migration to align pointer pairs for recombination. Here we demonstrate that RNA templates can orchestrate this cascade of DNA rearrangements in *Oxytricha*. Injection of synthetic templates replaces the cellular programme, producing alternative epigenetically wired DNA rearrangements.

RNAi against putative templates disrupts rearrangement

To test the hypothesis that putative maternal RNA templates influence rearrangement, we induced RNA interference (RNAi) to target homologous RNA degradation. *Oxytricha* cells, before and during

[1]Department of Ecology and Evolutionary Biology, Princeton University, Princeton, New Jersey 08544, USA. [2]Department of Electrical Engineering, Princeton University, Princeton, New Jersey 08544, USA.

conjugation, were fed *Escherichia coli* producing double stranded RNA fragments of two macronuclear genes: either telomere-end-binding protein subunit α (*TEBPα* or *α-TBP*) or DNA polymerase α (*pol-α*). The germline versions in *O. trifallix* are broken into 17 and 48 scrambled segments, respectively[21,22].

RNA interference against putative RNA templates leads to aberrant (incorrect or completely blocked) gene unscrambling in the resulting progeny (Fig. 1). PCR screening of *TEBPα* segments 5–17, after treatment with the RNAi vector spanning segments 2–17 in order, reveals DNA molecules longer than the typical macronuclear product, but shorter than the micronuclear precursor (Fig. 1a, lane 1). Sequencing revealed these were partially and/or incorrectly rearranged. Some aberrant forms still contain IESs (Fig. 1b, examples 2–5 and 9), with a bias for retention between scrambled segments (black boxes in Fig. 1). IESs between non-scrambled segments (red in Fig. 1) are usually absent. This suggests different susceptibility between these two kinds of IESs to RNAi treatment, and possibly a mechanistic decoupling, consistent with observations that simple IES removal precedes unscrambling in the actin I gene in the related genus *Stylonychia*[23]. Some permutations (partial descrambling) occurred (Fig. 1b, examples 4–6; molecule 4 could be an unscrambling intermediate), and even large duplications (Fig. 1b, examples 7 and 8) or deletions (Fig. 1b, examples 8–9). All deletions occur between short direct repeats that provide alternative (cryptic) pointers for recombination—the type of error that occurs early during rearrangement[23].

RNAi against *pol-α* leads to almost complete abrogation of DNA elimination or rearrangement (Fig. 1c, lane 2) with no permutations at all, but with several examples of aberrant deletion at cryptic pointers (Fig. 1d, examples 3–7), including one large deletion between segments 4 and 31 (Fig. 1d, example 7). Approximately 85% of *pol-α* molecules surveyed between segments 3 and 31 (the RNAi vector spanned segments 16–29) 80 h post conjugation were identical in size to the germline precursor (Fig. 1c, lane 2, and Fig. 1d, example 2), indicating no rearrangement (which we confirmed by sequencing).

These results provide strong indirect support for an RNA-template model involving intracellular genome comparisons by means of RNA transcripts from the maternal macronucleus. In principle, RNAi would degrade or negatively influence any homologous RNAs (Supplementary Figs 3 and 4), including templates, yielding aberrant rearrangements of corresponding genes. In our experiments, all aberrant rearrangements are restricted to the targeted gene (that is, *pol-α* feeding does not influence *TEBPα* rearrangement and vice versa), suggesting that each macronuclear molecule may have its own RNA template, which acts in a homology-dependent manner.

Early presence of long, bidirectional RNA

The RNAi experiments are consistent with the presence during conjugation of double- or single-stranded maternal RNA transcripts from the parental macronucleus. Single-stranded RNA is a reasonable target for RNAi-induced post-transcriptional gene silencing in eukaryotes. If the maternal templates are RNA, then the question arises whether transcription is uni- or bi-directional, and what are the promoters? Normal gene promoters sometimes initiate transcription downstream of the first MDS; however, both 5′- and 3′-untranscribed regions may be scrambled or interrupted by several

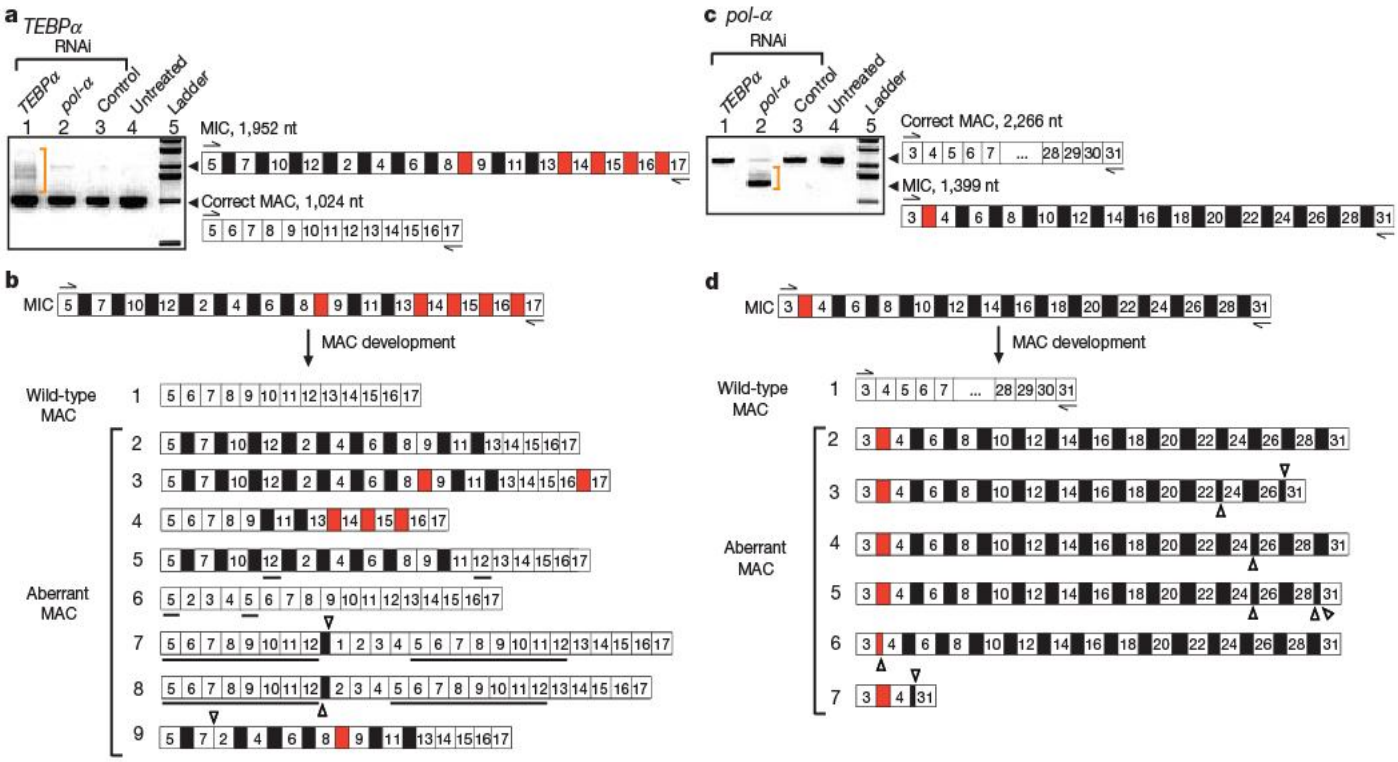

Figure 1 | RNAi against putative RNA templates leads to disruption of DNA rearrangement, with accumulation of aberrant products. MDS segments (white boxes) and IES regions (black boxes if located between nonconsecutive segments, red if consecutive) are drawn schematically, not to scale. The ladders are 1 kb (Invitrogen). **a**, PCR amplification of the *TEBPα* region between segments 5 and 17 from total DNA extracted from the sources treated with: *TEBPα* RNAi, *pol-α* RNAi and control double-stranded (ds)RNA (184 nucleotide (nt) dsRNA from feeding vector polylinker), as well as untreated cells. Only cells treated with *TEBPα* RNAi contain partial or incorrect rearrangements, on the basis of size (orange bracket). Cells treated with *TEBPα* RNAi were fed with dsRNA covering the region between segments 1 and 16. MAC, macronucleus; MIC, micronucleus. **b**, The sequence of several *TEBPα* PCR products between segments 5 and 17 in cells treated with *TEBPα* RNAi. IESs between both scrambled (black) and non-scrambled (red) MDSs are deleted from some molecules at both correct and incorrect (cryptic) repeats. Open triangles show the locations of cryptic junctions between neighbouring segments (if pointing up) and non-neighbouring segments (pointing down) on the basis of the precursor micronuclear order. Underlined segments are duplications. **c**, PCR amplification of *pol-α* between segments 3 and 31 from total DNA extracted from sources treated with: *TEBPα* RNAi, *pol-α* RNAi and control dsRNA (as above), as well as untreated cells. Only cells treated with *pol-α* RNAi show aberrantly rearranged products, on the basis of size (orange bracket). Cells treated with *pol-α* RNAi were fed with dsRNA covering the region between segments 16 and 29. **d**, Sequence of several *pol-α* PCR products between segments 3 and 31 in cells treated with *pol-α* RNAi.

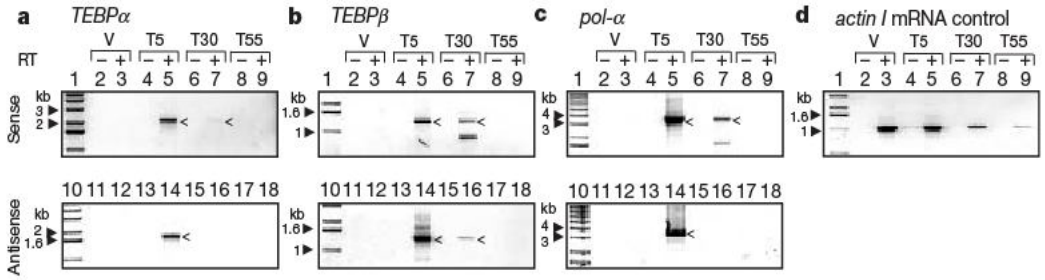

Figure 2 | Long sense and antisense transcripts are present during early development. RT–PCR of both strands from cells in a vegetative state (V) as well as 5 (T5), 30 (T30) and 55 (T55) hours post conjugation. Filled arrowheads indicate size of relevant markers (1 kb ladder, Invitrogen). Long, intron-containing maternal transcripts appear 5 h post conjugation and disappear 50 h later. The peak of polytene chromosome formation and DNA rearrangements is estimated to occur in this time window. Arrowheads indicate specific products. All non-specific amplification products were confirmed by sequencing to be unrelated. **a**, **b**, **c**, RT–PCR detection of both sense (+) and antisense (–) strands of *TEBPα*, *TEBPβ* and *pol-α* RNA templates, respectively. **d**, RT–PCR of *actin I* mRNA as a control for RNA in each sample.

IESs. Therefore, messenger RNA templates could not guide complete rearrangement. Another possibility is that telomeres themselves could promote transcription. This may allow unbiased transcription of all nanochromosomes, rather than gene-specific promoters. Complete transcription could also contribute to *Oxytricha*'s bias for tiny chromosomes with little extraneous DNA.

PCR with reverse transcription (RT–PCR) demonstrates the presence of antisense and sense transcripts of macronuclear chromosomes 5–30 h post conjugation (Fig. 2). These RNA transcripts are longer than messenger RNAs, contain telomeres (complementary DNA synthesis began at the telomere), are absent from vegetative cells, and disappear 55 h post conjugation. The presence of such RNA transcripts during early macronuclear development (estimated between meiosis and the peak of polytene chromosome formation) suggests they are available during DNA rearrangement and could therefore have a role. Figure 2 shows RT–PCR products for three different genes: two scrambled (*TEBPα*, *pol-α*) and one non-scrambled (*TEBPβ* or *β-TBP*); similar results were obtained for two other independent genes (not shown). *TEBPα* and *TEBPβ* transcripts both retain introns (*pol-α* has no introns in the surveyed region).

Injection of alternative DNA templates

Together, the detection of sense/antisense transcripts during development plus the RNAi experiments provide support for an RNA-template-based model. To test this model directly, we microinjected synthetic DNA or RNA versions of alternatively rearranged chromosomes into conjugating cells to ask whether this would specify the rearrangement pattern in the offspring.

We designed artificial macronuclear chromosomes to permute the natural order of two DNA segments in both *TEBPα* (Fig. 3a) and *TEBPβ* (Fig. 3c). *TEBPα* is scrambled in the germ line, requiring several DNA permutations to assemble a functional gene during development. *TEBPβ* normally requires only DNA deletion and no permutation (with identical MDS order in both nuclei). We chose these genes to test whether template-directed rearrangements act genome-wide or are specific to scrambled genes.

In two independent experiments, microinjecting the double-stranded, synthetic *TEBPα* chromosome (labelled '*TEBPα* sw78' template in Fig. 3, where SW indicates switched segment order) into the macronucleus of conjugating pairs of *Oxytricha* switches the order of segments 7 and 8, and injecting the synthetic *TEBPβ* molecule ('*TEBPβ* sw45' template) switches the order of segments 4 and 5. Each template slightly adjusts segment boundaries (Supplementary Fig. 1) to recruit existing sequence repeats as alternative pointers at new recombination junctions. Both templates contain single nucleotide substitutions (some creating restriction sites) to distinguish microinjected DNA from processed endogenous genes. Non-injected cells were used as controls. DNA was extracted from progeny one week after microinjection, permitting sufficient asexual growth. Injected cells grew slower than non-injected cells. In both cases, the F_1 progeny contained alternatively rearranged macronuclear chromosomes, following the reprogrammed order (*TEBPα* sw78 and *TEBPβ* sw45; Fig. 3b, d, e). In one case, the switched order was even the major product (Fig. 3d, lane 3).

Restriction mapping ruled out either the presence of microinjected DNA in the harvested cells or extended copying or incorporation of templates during rearrangement (Fig. 3b, lanes 5–8, and Fig. 3d, lanes 17–22). (Sequence analysis revealed a few exceptions; see section entitled 'Transfer of nucleotide substitutions'.) For *TEBPα*, the new junction formed between segments 6 and 8 creates a Tsp509I site, which distinguishes wild-type from switched chromosomes (Fig. 3b, lanes 1–4). For *TEBPβ*, the presence of two restriction sites (BbvCI and BsrGI) in MDS4 produces differently sized products in switched versus wild-type molecules (Fig. 3d, lanes 10–15). In addition, for *TEBPβ*, a simple PCR assay measuring the length from segment 4 to 6 yields a smaller product for switched versus wild-type chromosomes, because MDS5 is missing in the switched PCR product (Fig. 3d, lanes 2–8). PCR screening was not feasible for *TEBPα* because segments 7 and 8 are very small, encoding 6 and 10 amino acids, respectively, within the same α helix of the *TEBPα* protein[24].

We also examined DNA from *TEBPβ* sw45-injected cells two weeks post injection (Fig. 3d, lanes 4–5). These cells have an increase in the ratio of wild-type to switched chromosomes, possibly owing to a fitness decrease in cells burdened with the altered *TEBPβ* gene. Premature stop codons in the permuted version could produce a severely altered protein or possibly invoke nonsense-mediated mRNA decay (whereas the *TEBPα* permutation would cause a modest change in helix B of the encoded protein). Thus, we suggest that the use of synthetic templates to reprogramme DNA rearrangement provides a convenient epigenetic tool for reverse genetics in *Oxytricha*.

To test whether this epigenetic effect transferred to sexual offspring, we induced sexual conjugation by starving *TEBPβ* sw45-injected cells after two weeks of vegetative growth. Conjugating pairs were isolated and grown separately. Asexual progeny of individual pairs are denoted sw-A and sw-B. We detected the alternative rearrangement pattern in putative F_2 progeny (Fig. 3d, lanes 6–8, and Fig. 3e) and even in some putative F_3 (Supplementary Fig. 2), suggesting stable epigenetic inheritance of this alternative form. In one case (F_2 sw-B) the newly programmed pattern still predominates over wild type.

All PCR and restriction-based conclusions for *TEBPα* and *TEBPβ* (after one week) were confirmed by sequencing. Four out of 28 *TEBPα* clones and 18 out of 37 *TEBPβ* clones contained the expected alternative rearrangement. No sequenced *TEBPβ* products were wild type. One *TEBPα* molecule contains a 19 bp deletion, and one *TEBPβ* clone contains a 28 bp insertion (Supplementary Information). Nineteen *TEBPβ* clones contained aberrant deletions, some at cryptic pointers or imperfect repeats near deletion boundaries (Supplementary Information); 6 out of 19 still correctly adopted the programmed

junction between segments 4 and 6 (deleting segment 5), often observed on its own (Fig. 3d, arrowhead in lanes 19 and 20, clones 18 and 19). Aberrant rearrangements may derive from competition between synthetic and endogenous templates or from rogue microinjected molecules with polymerase errors—minor products of amplification. Cloning and re-sequencing the microinjected DNA revealed five correct as well as one aberrant product, which had segment 5 deleted (Supplementary Information). Therefore, such rearrangements could derive from a sub-population of injected templates.

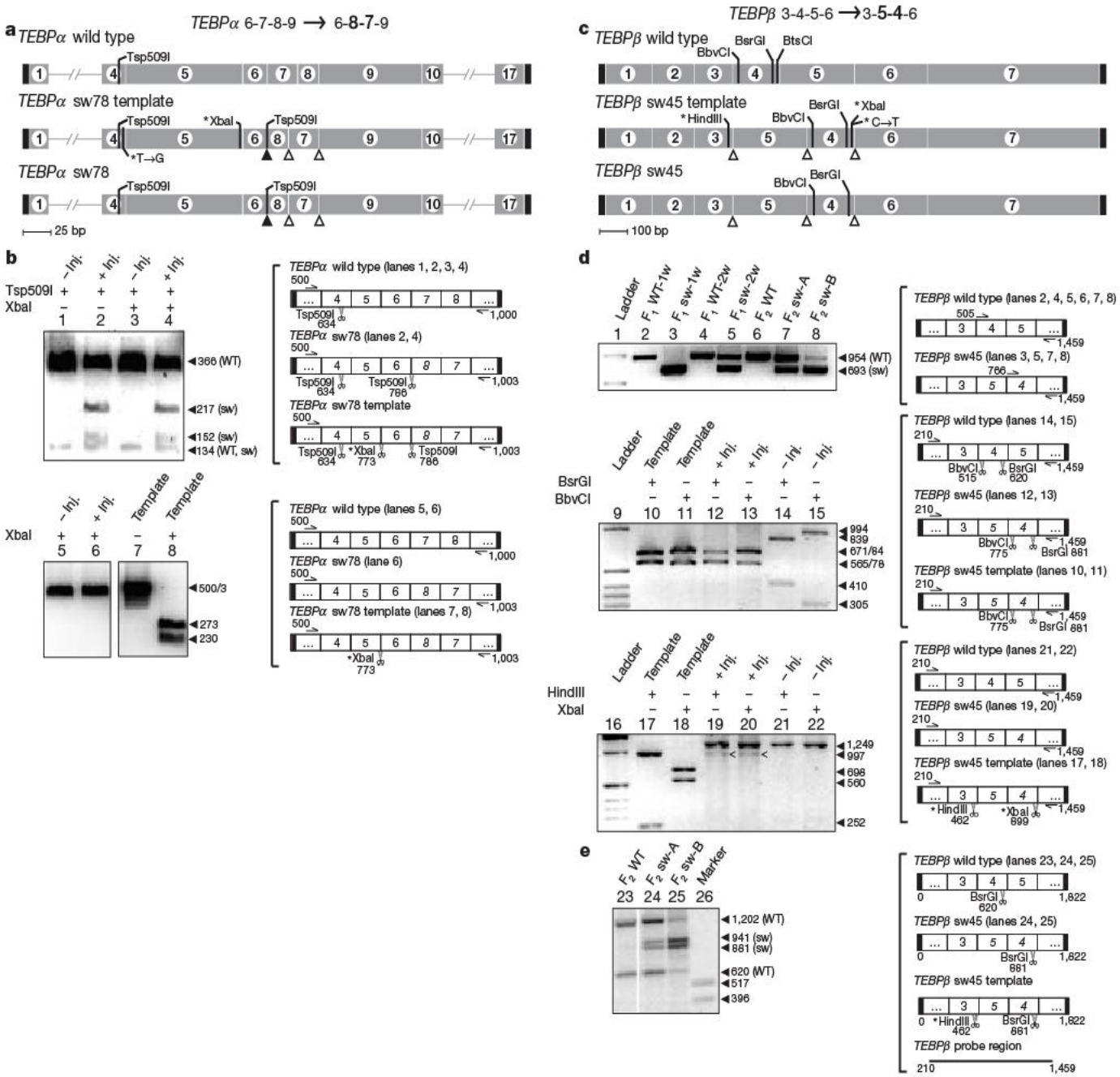

Figure 3 | Microinjection of alternative DNA templates produces alternatively rearranged chromosomes. **a**, Top, wild-type *TEBPα* macronuclear chromosome (labelled *TEBPα* wild type) with segments 1–17 colinear; middle, microinjected *TEBPα* template designed to switch (sw) the order of segments 7 and 8 (*TEBPα* sw78 template); bottom, map of resulting macronuclear product (*TEBPα* sw78), to scale. Asterisks, point mutations in synthetic templates; black rectangles, telomeres; open triangles, cryptic pointers to switch segment order; filled triangle, an unspliced 5 bp IES (see Supplementary Fig. 1). **b**, Left, PCR and restriction analysis of DNA microinjection products (ethidium bromide staining). Inj., injected. Right, single-sided arrows, PCR primers (in bp); scissors, restriction sites (in bp). Lanes 1–4 show presence of wild-type (WT) macronuclear product as well as a product from microinjected cells with segments 7 and 8 switched (*TEBPα* sw78; lanes 2, 4). Lanes 5–8 distinguish the microinjected template (lanes 7, 8) from the macronuclear product (lanes 5, 6). **c**, Top, wild-type *TEBPβ* macronuclear chromosome (*TEBPβ* wild type) with segments 1–7 colinear; middle, microinjected template designed to switch the order of segments 4 and 5 (*TEBPβ* sw45 template); and bottom, map of expected macronuclear product (*TEBPβ* sw45). **d**, PCR and restriction analysis of DNA microinjection products. Lanes 1–8 use a simple PCR length assay for the presence of a smaller product when the order of segments 4 and 5 has been reversed (lower band): one week (F_1 sw-1w) and two weeks (F_1 sw-2w) after microinjection, as well as the putative F_2 generation (epigenetic inheritance was also observed for putative F_3, see Supplementary Fig. 2; 1 kb DNA ladder (Invitrogen)). F_2 sw-A and F_2 sw-B are the asexual progeny of two independent conjugating pairs in the F_1; sw indicates injected cells or their progeny and WT indicates wild-type non-injected controls. Lanes 9–15 confirm the presence of the macronuclear product in which segments 4 and 5 are switched (*TEBPβ* sw45) in F_1 (one week post injection). Lanes 16–22 distinguish the microinjected template from the F_1 (one week) macronuclear product; arrowheads in lanes 19 and 20 point to aberrantly rearranged molecules lacking segment 5. **e**, Lanes 23–26, HindIII and BsrGI Southern analysis of total DNA extracted from the putative F_2 generation.

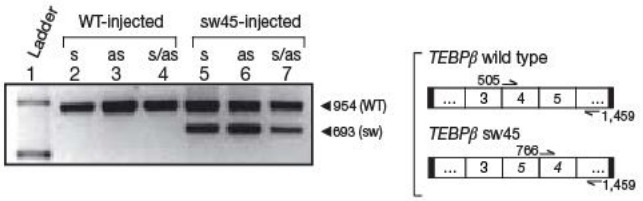

Figure 4 | Microinjection of alternative RNA templates leads to alternatively rearranged chromosomes. RNA microinjection of *TEBPβ* sw45 template. Sense (s), antisense (as), and combined sense and antisense (s/as) RNA templates were microinjected in both wild-type (control) and switched orientations. Lanes 5–7 display the expected macronuclear product if segments 4 and 5 have been switched (lower band). Primers are as in Fig. 3d. Lane 1, 1 kb ladder (Invitrogen).

Injection of alternative RNA templates

Because we expect that DNA injected in the previous experiments had the opportunity to be transcribed into RNA, we tested whether RNA injection could reprogramme genome rearrangement directly. We injected synthetic *TEBPβ* RNA templates in both sense and antisense directions in which segments 4 and 5 were permuted (*TEBPβ* sw45 template). Injecting wild-type *TEBPβ* RNA provided a control. In six independent experiments, we injected sense, antisense and a combination of sense and antisense RNA for both switched and control templates into the cytoplasm of cells during conjugation. The progeny of cells injected with any combination of RNA in the switched orientation produced macronuclear products in which segments 4 and 5 were permuted, in roughly similar proportion to the wild-type product (Fig. 4, lanes 5–7). All results were confirmed by sequencing (Supplementary Information).

Although RNA samples were DNase-treated after *in vitro* transcription and before injection, we tested whether any DNA may have been microinjected and concluded that this was unlikely (Supplementary Fig. 5).

Transfer of nucleotide substitutions

The influence of microinjected templates also extended to different germline alleles of the same gene (Supplementary Information), suggesting that a single sequence can programme the rearrangement pattern of multiple alleles, despite occasional template mismatches. Furthermore, a subset of mutations near pointers occasionally transferred from the synthetic template to rearranged molecules (Supplementary Information). Remarkably, a C-to-T substitution 4 bp from the end of MDS4 in the *TEBPβ* template transferred to all 40 sequenced molecules (DNA- or RNA-injected) that contained the programmed junction between MDS4 and MDS6 (Supplementary Information). We confirmed the absence of an allele or paralogue containing the 'T' nucleotide in *O. trifallax* strain JRB310 or JRB510 by screening hundreds of JRB310 reads from the *Oxytricha* genome project, as well as by studying expressed-sequence-tag clones from both strains, sequencing 24 JRB510 PCR clones, and performing BtsCI restriction mapping (not shown). Thus, the source of this T nucleotide is likely to be the template itself, implicating template-directed DNA repair.

Conclusions

We provide evidence for both the presence of long maternal RNA templates—RNA cached copies of DNA sequences from the previous generation—and the powerful influence of such molecules to guide genome rearrangements, even permuting the order of DNA sequences *in vivo* (Fig. 5). In particular, we have shown that microinjection of alternative DNA or RNA templates leads to stable epigenetic inheritance of alternative DNA rearrangement pathways, offering a key informational and regulatory role for RNA in transmitting a genome-rearrangement programme. The templating mechanism seems to be highly accurate, because most alternatively ordered molecules in this study contain precise recombination junctions, instructed by the synthetic template.

Our results are compatible with an earlier result showing that RNA injection in *Tetrahymena* leads to deletion of homologous sequences during development[25]. The injected RNA might trigger destruction of homologous RNA templates in *Tetrahymena*, for example, as in our RNAi experiments.

The transfer of some mutations from the template to the rearranged molecule (Supplementary Information) suggests that RNA could be a template for DNA synthesis or repair very close to the pointer, as in template-guided DNA repair[9]. A C-to-T mutation in the template that creates a TA dinucleotide close to a new pointer transferred efficiently to all rearranged molecules, whereas substitutions further away from a pointer transferred infrequently, consistent with local polymerase activity. The RNA-guided DNA rearrangements proposed here are distinct from previous indirect roles for RNA in mediating recombination[26–30].

The ability of RNA to programme DNA rearrangements suggests new approaches for genome manipulation *in vivo*, providing a tool for reverse genetics in *Oxytricha* and possibly in other systems; this also demonstrates an elegant mechanism for RNA-guided recombination that may be widespread, with somatic and evolutionary consequences for genome expression. For example, occasional templating of rearrangements by maternal mRNA could explain the paucity of introns in ciliates[12], converting them to IESs[31].

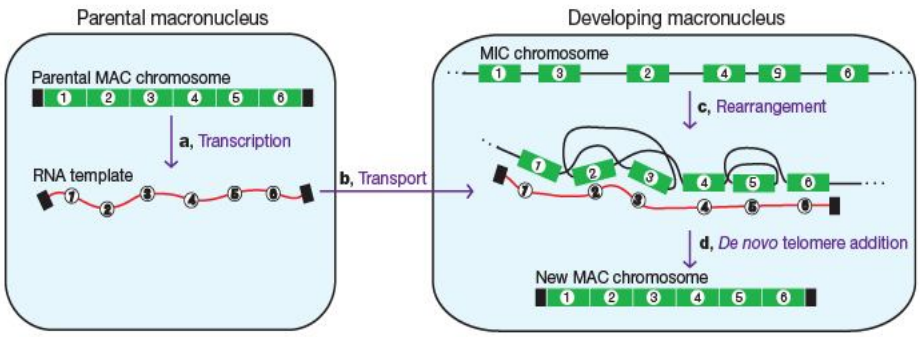

Figure 5 | Model for RNA guiding of genome rearrangements during macronuclear development in *Oxytricha*. **a**, Bidirectional RNA transcription of all DNA nanochromosomes (including injected DNA) in the old, maternal macronucleus (MAC) before its degradation. **b**, Transport of these RNA transcripts to the newly developing macronucleus, where they may act as scaffolds to guide rearrangements (deletion, permutation and inversion) of corresponding micronuclear (MIC) DNA sequences (**c**). This step would be notable and unprecedented, but perhaps possible if there were either local or extensive strand-separation of both the RNA template and the developing DNA (see ref. 20). In this illustration, segments 2 and 3 are switched and segment 5 is inverted (number upside down). **d**, *De novo* telomere addition (black rectangles) and amplification completes formation of new macronuclear nanochromosomes.

METHODS SUMMARY

RNAi. Double-stranded RNA feeding was performed using a *Paramecium* protocol[32], in which ciliates were fed with live bacteria, supplemented with algae. Silencing plasmids contained 1.5 kb of *TEBPα* or 1.8 kb of the *pol-α* macronuclear sequence (Supplementary Information).

RT–PCR. First-strand cDNA was synthesized using Superscript III RTS First-Strand cDNA Synthesis Kit (Invitrogen) with either a telomere-anchor primer (Supplementary Information) or oligo(dT)$_{20}$. Products were amplified for 28–37 cycles with Expand High Fidelity Plus or FastStart High Fidelity PCR Systems (Roche) using a linker primer in combination with gene-specific primers (Supplementary Information).

Template design. For *TEBPα*, we chose to switch the order of MDS7 and MDS8, which code for a region least likely to affect the telomere-binding domain[24]. We used MUMmer[33] to detect repeats within 14 bp of original pointer boundaries, and chose the longest cryptic repeats that would preserve the reading frame. For *TEBPβ*, we switched the order of MDS4 and MDS5, which permitted new pointers to be similar to wild-type pointers.

Microinjection of DNA and RNA. Synthetic templates were generated by means of PCR (with point mutations on the primers), followed by restriction digestion, ligating segments in the desired order, and cloning (see Supplementary Information). DNA versions were prepared by telomere-to-telomere PCR, and RNA versions of each strand were prepared by *in vitro* transcription of PCR products between the vector T7 promoter and the telomere on the opposite side. Approximately 5 pl (picoliters) DNA or 10 pl RNA was injected (Narishige IM 300) into the macronucleus or cytoplasm, respectively, of each cell in a mating pair visualized by phase-contrast inverted microscopy (Zeiss, Axiovert 200). Individual exconjugants were observed under the microscope and each cell displayed morphological features characteristic of sexual reproduction in *Oxytricha*, such as rounded cell shape or a large macronuclear anlagen. Thus, on the basis of cell morphology, the analysed F_2 cells were the progeny of F_1, and so on.

Full Methods and any associated references are available in the online version of the paper at www.nature.com/nature.

Received 3 August; accepted 5 November 2007.
Published online 28 November 2007.

1. King, M. L., Messitt, T. J. & Mowry, K. L. Putting RNAs in the right place at the right time: RNA localization in the frog oocyte. *Biol. Cell* **97**, 19–33 (2005).
2. Tadros, W. & Lipshitz, H. D. Setting the stage for development: mRNA translation and stability during oocyte maturation and egg activation in *Drosophila*. *Dev. Dyn.* **232**, 593–608 (2005).
3. Tang, F. *et al.* Maternal microRNAs are essential for mouse zygotic development. *Genes Dev.* **21**, 644–648 (2007).
4. Rassoulzadegan, M. *et al.* RNA-mediated non-mendelian inheritance of an epigenetic change in the mouse. *Nature* **441**, 469–474 (2006).
5. Herbert, A. & Rich, A. RNA processing and the evolution of eukaryotes. *Nature Genet.* **21**, 265–269 (1999).
6. Lolle, S. J., Victor, J. L., Young, J. M. & Pruitt, R. E. Genome-wide non-mendelian inheritance of extra-genomic information in *Arabidopsis*. *Nature* **434**, 505–509 (2005).
7. Peng, P., Chan, S. W., Shah, G. A. & Jacobsen, S. E. Plant genetics: increased outcrossing in hothead mutants. *Nature* **443**, E8 (2006).
8. Lolle, S. J., Pruitt, R. E., Victor, J. L. & Young, J. M. Lolle *et al.* reply. *Nature* **443**, E8–E9 (2006).
9. Storici, F., Bebenek, K., Kunkel, T. A., Gordenin, D. A. & Resnick, M. A. RNA-templated DNA repair. *Nature* **447**, 338–341 (2007).
10. Blum, B., Bakalara, N. & Simpson, L. A model for RNA editing in kinetoplastid mitochondria: "guide" RNA molecules transcribed from maxicircle DNA provide the edited information. *Cell* **60**, 189–198 (1990).
11. Maxwell, E. S. & Fournier, M. J. The small nucleolar RNAs. *Annu. Rev. Biochem.* **64**, 897–934 (1995).
12. Prescott, D. M. The DNA of ciliated protozoa. *Microbiol. Rev.* **58**, 233–267 (1994).
13. Chalker, D. L. & Yao, M. C. Non-mendelian, heritable blocks to DNA rearrangement are induced by loading the somatic nucleus of *Tetrahymena thermophila* with germ line-limited DNA. *Mol. Cell. Biol.* **16**, 3658–3667 (1996).
14. Duharcourt, S., Keller, A. M. & Meyer, E. Homology-dependent maternal inhibition of developmental excision of internal eliminated sequences in *Paramecium tetraurelia*. *Mol. Cell. Biol.* **18**, 7075–7085 (1998).
15. Mochizuki, K., Fine, N. A., Fujisawa, T. & Gorovsky, M. A. Analysis of a piwi-related gene implicates small RNAs in genome rearrangement in *Tetrahymena*. *Cell* **110**, 689–699 (2002).
16. Prescott, D. M. & DuBois, M. L. Internal eliminated segments (IESs) of Oxytrichidae. *J. Eukaryot. Microbiol.* **43**, 432–441 (1996).
17. Mayer, K. M. & Forney, J. D. A mutation in the flanking 5′-TA-3′ dinucleotide prevents excision of an internal eliminated sequence from the *Paramecium tetraurelia* genome. *Genetics* **151**, 597–604 (1999).
18. Landweber, L. F., Kuo, T. C. & Curtis, E. A. Evolution and assembly of an extremely scrambled gene. *Proc. Natl Acad. Sci. USA* **97**, 3298–3303 (2000).
19. Prescott, D. M., Ehrenfeucht, A. & Rozenberg, G. Template-guided recombination for IES elimination and unscrambling of genes in stichotrichous ciliates. *J. Theor. Biol.* **222**, 323–330 (2003).
20. Angeleska, A., Jonoska, N., Saito, M. & Landweber, L. F. RNA-guided DNA assembly. *J. Theor. Biol.* **248**, 706–720 (2007).
21. Prescott, J. D., DuBois, M. L. & Prescott, D. M. Evolution of the scrambled germline gene encoding α-telomere binding protein in three hypotrichous ciliates. *Chromosoma* **107**, 293–303 (1998).
22. Hoffman, D. C. & Prescott, D. M. Evolution of internal eliminated segments and scrambling in the micronucleargene encoding DNA polymerase α in two *Oxytricha* species *Oxytricha novo* is extremely scrambled. *Nucleic Acids Res.* **25**, 1883–1889 (1997).
23. Möllenbeck, M. *et al.* The pathway to detangle a scrambled gene. *PLoS Biol.* (submitted).
24. Horvath, M. P., Schweiker, V. L., Bevilacqua, J. M., Ruggles, J. A. & Schultz, S. C. Crystal structure of the *Oxytricha nova* telomere end binding protein complexed with single strand DNA. *Cell* **95**, 963–974 (1998).
25. Yao, M. C., Fuller, P. & Xi, X. Programmed DNA deletion as an RNA-guided system of genome defense. *Science* **300**, 1581–1584 (2003).
26. Paques, F. & Haber, J. E. Multiple pathways of recombination induced by double-strand breaks in *Saccharomyces cerevisiae*. *Microbiol. Mol. Biol. Rev.* **63**, 349–404 (1999).
27. Derr, L. K. & Strathern, J. N. A role for reverse transcripts in gene conversion. *Nature* **361**, 170–173 (1993).
28. Moore, J. K. & Haber, J. E. Capture of retrotransposon DNA at the sites of chromosomal double-strand breaks. *Nature* **383**, 644–646 (1996).
29. Nevo-Caspi, Y. & Kupiec, M. cDNA-mediated Ty recombination can take place in the absence of plus-strand cDNA synthesis, but not in the absence of the integrase protein. *Curr. Genet.* **32**, 32–40 (1997).
30. Teng, S. C., Kim, B. & Gabriel, A. Retrotransposon reverse-transcriptase-mediated repair of chromosomal breaks. *Nature* **383**, 641–644 (1996).
31. Chang, W.-J. *et al.* Intron evolution and information processing in the DNA polymerase alpha gene in spirotrichous ciliates: a hypothesis for interconversion between DNA and RNA deletion. *Biol. Direct* **2**, 6 (2007).
32. Galvani, A. & Sperling, L. RNA interference by feeding in *Paramecium*. *Trends Genet.* **18**, 11–12 (2002).
33. Kurtz, S. *et al.* Versatile and open software for comparing large genomes. *Genome Biol.* **5**, R12 (2004).

Supplementary Information is linked to the online version of the paper at www.nature.com/nature.

Acknowledgements This work was supported by awards from the NSF and NIH to L.F.L. and the SEAS senior thesis research fund to V.V. We thank J. Wang for technical assistance and all members of the laboratory for discussion.

Author Contributions M.N., V.V., Y.Z., T.G.D. and L.F.L. designed experiments; M.N., V.V., Y.Z. and K.S. performed the experiments; T.G.D. provided cells; M.N., V.V., Y.Z. and L.F.L. analysed the data; and M.N., V.V., Y.Z. and L.F.L. wrote the paper.

Author Information *TEBPα* and *TEBPβ* macronucleus and micronucleus sequences have been submitted to GenBank under accession numbers EU047938–EU047941. Reprints and permissions information is available at www.nature.com/reprints. Correspondence and requests for materials should be addressed to L.F.L. (lfl@princeton.edu).

LETTERS

An asymmetric distribution of positrons in the Galactic disk revealed by γ-rays

Georg Weidenspointner[1,2,3], Gerry Skinner[1,4,5], Pierre Jean[1], Jürgen Knödlseder[1], Peter von Ballmoos[1], Giovanni Bignami[1,8], Roland Diehl[2], Andrew W. Strong[2], Bertrand Cordier[6], Stéphane Schanne[6] & Christoph Winkler[7]

Gamma-ray line radiation at 511 keV is the signature of electron–positron annihilation. Such radiation has been known for 30 years to come from the general direction of the Galactic Centre[1], but the origin of the positrons has remained a mystery. Stellar nucleosynthesis[2–4], accreting compact objects[5–8], and even the annihilation of exotic dark-matter particles[9] have all been suggested. Here we report a distinct asymmetry in the 511-keV line emission coming from the inner Galactic disk (~10–50° from the Galactic Centre). This asymmetry resembles an asymmetry in the distribution of low mass X-ray binaries with strong emission at photon energies >20 keV ('hard' LMXBs), indicating that they may be the dominant origin of the positrons. Although it had long been suspected that electron–positron pair plasmas may exist in X-ray binaries, it was not evident that many of the positrons could escape to lose energy and ultimately annihilate with electrons in the interstellar medium and thus lead to the emission of a narrow 511-keV line. For these models, our result implies that up to a few times 10^{41} positrons escape per second from a typical hard LMXB. Positron production at this level from hard LMXBs in the Galactic bulge would reduce (and possibly eliminate) the need for more exotic explanations, such as those involving dark matter.

The main clue as to which of the sources of positrons are most important is expected to come from the distribution on the sky of the annihilation line radiation. With existing instrumentation, the emission appears to be diffuse; no point sources of annihilation radiation have yet been detected[10–13]. The 511-keV flux from the bright Galactic bulge region has been well measured to be about 1×10^{-3} photons $cm^{-2} s^{-1}$ (refs 1, 10, 14, 15), and its spatial distribution is well established to be symmetric about the Galactic Centre, with an extent of ~6° (full-width at half-maximum)[10,15,16]; these conclusions are unchanged by the present work. However, no firm conclusion as to the origin of the positrons has been possible because of the limited angular resolution and sensitivity of previous γ-ray instrumentation, and the complications arising from uncertainties in the distribution of potential positron sources and in the distribution and content of gas; uncertainties also exist in the structure and strength of magnetic fields in the Galaxy, and in the physics of positron diffusion and thermalization.

Annihilation radiation from the disk is more difficult to study because of its lower surface brightness[14,16], but it potentially provides complementary clues to the positron production processes involved. Only a few instruments have been capable of spatially resolving the (inner) disk emission from the brighter bulge emission. The sparse measurements that exist agree that the annihilation emission from the disk is strongest in the inner Galaxy, and simple models assuming symmetry suggest that it is brightest in the longitude range $|l| < 18$–$35°$ (refs 15–17). The latitude extent of the disk emission is still poorly constrained[14,16]. Using more than four years of data from the SPI imaging spectrometer on the INTEGRAL satellite (Supplementary Information), we have obtained new results on the disk component of the 511-keV emission that have important implications for the origin of positrons in the Galaxy. We not only clearly detect narrow 511-keV line emission from the inner Galactic disk[16], but we observe a distinct and surprising asymmetry in its distribution. This asymmetry is revealed in sky maps (Fig. 1a), in model fitting (Fig. 2), and in spectra of the inner disk emission (Fig. 3).

We have quantified the asymmetry using model fitting (Fig. 2). Our best estimate is that the flux from the inner disk at $-50° < l < 0°$ exceeds that from the inner disk at corresponding positive longitudes by a factor of about 1.8; a symmetric distribution (equal fluxes) can be excluded at the 3.8σ confidence level (Supplementary Information). The fluxes in these negative and positive longitude bands within 10° of the Galactic plane are $(4.3 \pm 0.5) \times 10^{-4}$ photons $cm^{-2} s^{-1}$ and $(2.4 \pm 0.5) \times 10^{-4}$ photons $cm^{-2} s^{-1}$, respectively. The uncertainties quoted here are 1σ statistical errors. No significant emission is yet detected from the outer disk ($|l| > 50°$). We have searched for systematic effects, such as background variations on orbital or other timescales, that might mimic the observed flux asymmetry, but after extensive efforts we have found none. It cannot be due to differences in exposure on the two sides of the Galactic Centre, which are rather similar—for example, the exposures in the Galactic plane around $l = -25°$ and $l = +25°$ differ by less than 10% (see Supplementary Information for details). Although this is the first time that such an asymmetry has been reported, we find that it is not inconsistent with measurements by previous, less-sensitive, instruments[15,17] (Supplementary Information).

Our results for the fluxes from the inner disk region and their asymmetry are not changed significantly if the bulge model is replaced by a halo component (comprising the emission peak at the Galactic Centre and fainter emission extending far beyond the bulge region), which provides an equally good description of the data[16]. Their robustness has been further demonstrated by using additional alternative models and subsets of observations to test in particular for the possibility that an asymmetry in the bright central emission influences conclusions about the disk emission further out. In all cases, the conclusion that the disk emission is asymmetric remains significant (Supplementary Information).

The distinct asymmetry in the annihilation flux from the inner disk is unexpected. It is in the opposite sense from, and much larger than, any difference that might be expected due to the Galactic stellar bar, whose closest limb is at positive longitudes[18]. A part of the inner disk flux must come from positrons associated with the ^{26}Al decay chain

[1]Centre d'Etude Spatiale des Rayonnements, CNRS/UPS, BP 44346, Toulouse Cedex 4, France. [2]Max-Planck-Institut für extraterrestrische Physik, Postfach 1312, 85741 Garching, Germany. [3]MPI Halbleiterlabor, Otto-Hahn-Ring 6, 81739 München, Germany. [4]CRESST and Code 661, NASA/GSFC, Greenbelt, Maryland 20771, USA. [5]Department of Astronomy, University of Maryland, College Park, Maryland 20742, USA. [6]DSM/DAPNIA/SAp, CEA Saclay, 91191 Gif-sur-Yvette, France. [7]ESA/ESTEC, SCI-SA, Keplerlaan 1, 2201 AZ Noordwijk, The Netherlands. [8]IUSS (Istituto Universitario di Studi Superiori), Lungo Ticino 56, 27100, Pavia, Italy.

that leads to a 1,809-keV γ-ray line. Using the 1,809-keV line flux, which has been relatively well established with COMPTEL[19,20] and SPI[21], and which is much more symmetric than the 511-keV emission seems to be, we predict a corresponding 511-keV emission that amounts to (28 ± 7)% of the emission that we see in the inner disk (Supplementary Information). Thus the dominant (non ^{26}Al) source of disk positrons must have an asymmetry of about 2.2, not 1.8. The asymmetry cannot be due to differences in the column densities of the interstellar medium (ISM) in which the positrons annihilate. Both 21-cm radio observations and measurements of high-energy γ-rays from cosmic-ray interactions indicate that typical ISM column densities on either side of the Galactic Centre are equal to within about 10%. Furthermore, spectroscopy of the 511-keV line emission from the two sides of the inner Galactic disk (see Fig. 3) suggests no differences in line shape that might indicate that the flux difference is associated with differing conditions in the ISM. We therefore propose that the annihilation asymmetry is in some way linked to the positron production.

As previously noted, X-ray binaries containing accreting stellar-mass black holes or neutron stars have been considered as possible candidates for sources of the positrons, partly because their concentration towards the Galactic bulge is similar to that seen in annihilation line radiation. If positrons escape with an energy of about 1 MeV, their lifetime in the ISM before they slow down and annihilate is thought to be ~ 10^5 years (ref. 22; for an ISM density of 1 cm^{-3}). The distance traversed in this time depends critically on the structure of the magnetic fields, but studies suggest that typically they do not diffuse more than about 100 pc from their sources[22,23], corresponding to ~1° at the distance of the Galactic Centre. Hence one would expect the annihilation radiation produced to be diffuse but to follow the large-scale distribution of the sources.

Our observed asymmetry in the 511-keV line emission from the Galactic disk suggests an association with X-ray binaries, specifically with LMXBs. Whereas LMXBs seen at lower (<20 keV) X-ray energies are approximately symmetrically distributed in the inner Galaxy, for reasons that are still not understood the distribution of LMXBs in the inner Galaxy seen in hard X-rays exhibits an asymmetry (Fig. 1b) that becomes more and more distinct with increasing energy. High-mass X-ray binaries do not, by contrast, show any significant imbalance. The number of LMXBs in the INTEGRAL/IBIS catalogue[24] at negative longitudes (45) is higher than that at positive longitudes (26) by a factor of 1.7. At higher energies[25], and particularly if one uses flux-weighted counts, the ratio becomes even larger (for example, for LMXBs detected above 100 keV we find a flux-weighted ratio of 2.8), but the statistical uncertainties become large. The differences cannot be attributed to differences in the IBIS survey sensitivity in the two regions, which are small (≲10%). A Kolmogorov–Smirnov test shows that the Galactic longitude distribution of hard LMXBs follows very well that of our asymmetric 511-keV flux model but not the best fit symmetric one (the maximum distance between the normalized integral distributions being such as to occur with chance probability of 41% in the former case, but only 2.1% in the latter—see Supplementary Information for

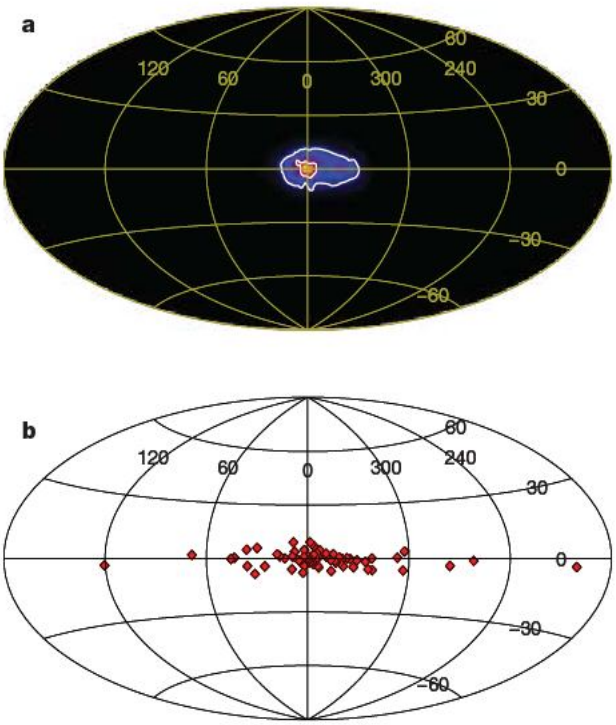

Figure 1 | A sky map in the 511-keV electron–positron annihilation line, and the sky distribution of hard LMXBs. In both maps, the Galactic Centre is at the origin, the Galactic plane is along the equator; Galactic longitude and latitude are shown in degrees. **a**, The 511-keV line map. The bright bulge region is prominent, as is the distinct asymmetry in the flux from the inner disk; contours correspond to intensity levels of 10^{-3} and 10^{-2} photons cm^{-2} s^{-1} sr^{-1}. The map is based on observations with the imaging spectrometer SPI on board the INTEGRAL satellite, and uses data obtained during 'guaranteed time' for the first 4.3 years of the mission and publicly available data from 'guest observer' observations for the first 3.3 years, supplemented by observing time awarded to the authors. The map was obtained using a MREM (Multi-Resolution Expectation Maximization) image deconvolution algorithm[28]. During the iterative image reconstruction, a filter is applied to the image correction to suppress artefacts due to statistics noise. Such filtering implies that low surface brightness emission which is still detectable by model fitting may not be present in the image, as is the case for some of the disk emission. **b**, The sky distribution of the hard LMXBs detected at energies above 20 keV with INTEGRAL/IBIS[24], showing the resemblance to that of the 511-keV annihilation line in **a**.

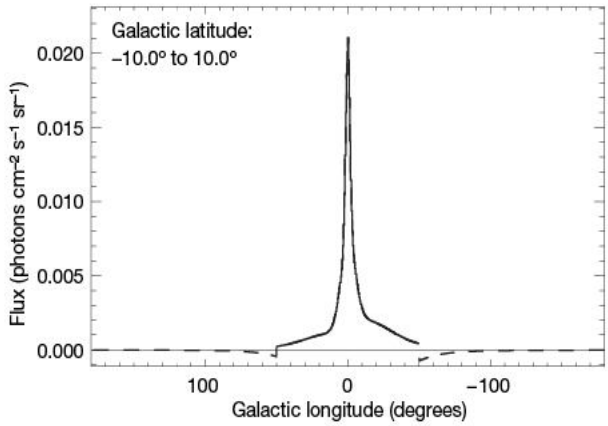

Figure 2 | The longitude profile of a model for the sky distribution of 511-keV electron–positron annihilation line radiation for Galactic latitudes $|b| < 10°$. The model was obtained by fitting to the same observations from which the map depicted in Fig. 1a was derived. The asymmetry in the annihilation flux from the inner disk is again evident. The depicted sky model consists of six components. The bright bulge was described by a superposition of two gaussian distributions located at the Galactic Centre. For the disk, a parameterized model of the Galactic distribution of the stellar population was used[29]. The parameters of the bulge and disk components were determined by fitting to our observations (see Supplementary Material for details). This disk model was then divided into four longitude intervals with boundaries at −180°, −50°, 0°, 50° and 180°. The two gaussians representing the bright bulge overlap with the two longitude intervals covering the inner disk region. This model was compared with the observations, finding the normalizations of the six components that best reproduce the data, using maximum likelihood as the test statistic. In this particular model, the normalizations of the two outer disk components are negative, but insignificant. Other models that provide equally acceptable fits to the data all lead to the same conclusions about the asymmetry in the inner disk region (and none of them attributes significant emission to the outer disk region). The solid lines show the model in the inner Galaxy; the dashed lines show the model in the outer Galaxy where formally the fit gives a negative, but not significant, flux.

details). We cannot, of course, exclude the possibility that the similarity of the distributions arises by chance. However, if the present asymmetric hard LMXB activity is typical of that over the 10^5 year expected lifetime of positrons in the ISM, these systems could explain the observed flux asymmetry in the 511-keV line. We note that it is possible that the IBIS sources considered here are not representative of the full source population of hard LMXBs, which may comprise at least a few hundred members (as inferred from lower energies) in all of the Galaxy[26]. A full evaluation will require a more complete inventory of hard LMXBs in the Galaxy and a detailed population-synthesis study beyond the scope of the present work.

The most natural explanation of an association between positron emission and hard X-ray binaries lies in the large numbers of positrons that are expected to be produced by γ-γ interactions in the hot innermost region of accretion disks. Some of these positrons may escape the inner dense regions in bipolar jets of electron–positron pair plasmas. Alternatively, the pair plasma could escape through wind outflow. The implied positron production rate per hard LMXB is of the order of 10^{41} s^{-1}. This is well within the wide range that has been suggested (see ref. 6 and references therein). In terms of energy, assuming that they have a kinetic energy of ~1 MeV, the escaping positrons would represent less than 1% of the hard X-ray luminosity of the LMXBs. The average 511-keV line flux per system is about 10^{-5} photons cm^{-2} s^{-1}, which is still well below upper limits that have been derived for selected objects[6,10,11].

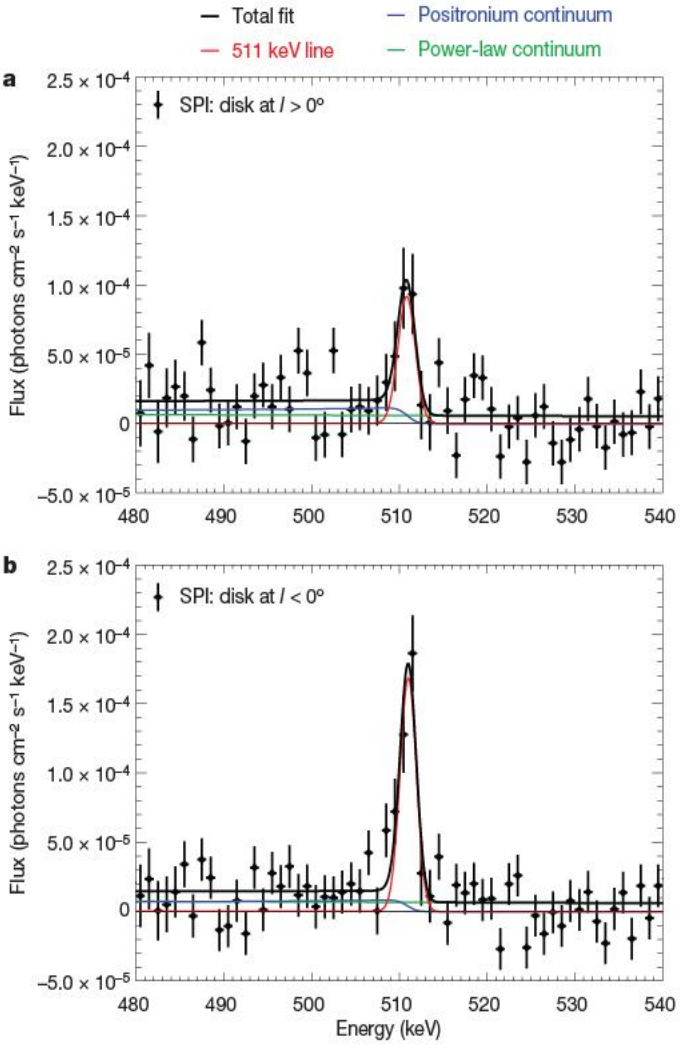

Figure 3 | Energy spectra of the γ-ray emission from the inner Galactic disk. The difference in the 511-keV electron–positron annihilation line flux from the inner Galactic disk in the longitude intervals $0° < l < 50°$ (**a**) and $-50° < l < 0°$ (**b**) is apparent; this difference is also seen in Figs 1a and 2. The spectra were determined by fitting to the data, in each energy bin, the 6 spatial components illustrated in Fig. 2. Error bars, 1 s.d. As the normalizations of each of the 6 model components are fitted individually, the spectra represent the disk emission despite the fact that the two gaussian bulge components spatially overlap with the two components representing the inner disk. The energy spectra were described by three emission components—the positron annihilation radiation, being the sum of a (narrow) 511-keV line (red) and the positronium continuum emission (blue), and a power law (green) representing the continuum emission from the Galactic disk due to cosmic-ray interactions in the ISM. The total spectrum is indicated in black. The similarity of the spectral distribution of the annihilation radiation from both sides of the inner disk suggests that the flux difference is not associated with differing conditions in the ISM.

If hard LMXBs are responsible for most of the positron production in the Galactic disk (that part not accounted for by ^{26}Al decay), then it is natural to ask whether the strong concentration of such systems around the Galactic Centre can explain the bulge component for the 511-keV emission. We estimate that they would account for about half of it. Although the expected contribution is uncertain (because of the limited number of objects involved) and we cannot exclude that it all arises in this way, our best fit models do suggest that there is additional bulge emission beyond that expected on a *pro rata* basis. This is consistent with our previous finding that it is difficult to explain all of the disk and bulge emission with positrons from LMXBs because their concentration towards the centre is insufficient[10]. Perhaps the hard LMXBs in the bulge contribute more positrons or a smaller fraction of them escape to large distances. Even if an additional bulge component is needed, there are many possible astrophysical positron sources that could contribute, such as type Ia supernovae[27] or the supermassive black hole Sgr A* (refs 7, 8). Hence there may be no necessity to invoke exotic explanations such as the annihilation of dark matter[9].

Received 30 March; accepted 16 November 2007.

1. Leventhal, M., MacCallum, C. J. & Stang, P. D. Detection of 511 keV positron annihilation radiation from the galactic center direction. *Astrophys. J.* **225**, L11–L14 (1978).
2. Clayton, D. D. Galaxy-Positronium origin of 476 keV galactic feature. *Nature Phys. Sci.* **244**, 137–138 (1973).
3. Clayton, D. D. & Hoyle, F. Gamma-ray lines from novae. *Astrophys. J.* **187**, L101–L103 (1974).
4. Prantzos, N. & Cassé, M. On the production of ^{26}Al by Wolf-Rayet stars—Galactic yield and gamma-ray line emissivity. *Astrophys. J.* **307**, 324–331 (1986).
5. Ramaty, R. & Lingenfelter, R. E. Gamma-ray line astronomy. *Nature* **278**, 127–132 (1979).
6. Guessoum, N., Jean, P. & Prantzos, N. Microquasars as sources of positron annihilation radiation. *Astron. Astrophys.* **457**, 753–762 (2006).
7. Cheng, K. S., Chernyshov, D. O. & Dogiel, V. A. Annihilation emission from the Galactic black hole. *Astrophys. J.* **645**, 1138–1151 (2006).
8. Totani, T. A RIAF interpretation for the past higher activity of the Galactic Center black hole and the 511 kev annihilation emission. *Publ. Astron. Soc. Jpn* **58**, 965–977 (2006).
9. Boehm, C., Hooper, D., Silk, J., Cassé, M. & Paul, J. MeV dark matter: Has it been detected? *Phys. Rev. Lett.* **92**, 101301 (2004).
10. Knödlseder, J. *et al.* The all-sky distribution of 511 keV electron-positron annihilation emission. *Astron. Astrophys.* **441**, 513–532 (2005).
11. Teegarden, B. J. & Watanabe, K. A comprehensive search for gamma-ray lines in the first year of data from the INTEGRAL spectrometer. *Astrophys. J.* **646**, 965–981 (2006).
12. De Cesare, G. *et al.* INTEGRAL/IBIS search for e^-e^+ annihilation radiation from the galactic center region. *Adv. Space Res.* **38**, 1457–1460 (2006).
13. Weidenspointner, G. *et al.* The sky distribution of positronium annihilation continuum emission measured with SPI/INTEGRAL. *Astron. Astrophys.* **450**, 1013–1021 (2006).
14. Milne, P. A., Kurfess, P. A., Kinzer, R. L., Leising, M. D. & Dixon, D. D. in *The Fifth Compton Symposium.* (eds McConnell, M. L. & Ryan, J. M.) 21–30 (AIP Conf. Proc. Vol. 510, American Institute of Physics, Melville, 2000).
15. Kinzer, R. L. *et al.* Positron annihilation radiation from the inner galaxy. *Astrophys. J.* **559**, 282–295 (2001).
16. Weidenspointner, G. *et al.* The sky distribution of 511 keV positron annihilation line emission as measured with INTEGRAL/SPI. In *Proceedings of 6th INTEGRAL Workshop* (ESA SP-622, ESA Publications Division, Noordwijk, in the press); preprint at ⟨http://arxiv.org/abs/astro-ph/0702621⟩ (2007).
17. Gehrels, N. *et al.* GRIS observations of positron annihilation radiation from the Galactic center. *Astrophys. J.* **375**, L13–L16 (1991).
18. Benjamin, R. A. *et al.* First GLIMPSE results on the stellar structure of the Galaxy. *Astrophys. J.* **630**, L149–L152 (2005).

19. Knödlseder, J. *et al.* A multiwavelength comparison of COMPTEL 1.8 MeV ^{26}Al data. *Astron. Astrophys.* **344**, 68–82 (1999).
20. Plüschke, S. *et al.* in *Proceedings of the Fourth INTEGRAL Workshop* (ed. Battrick, B.) 55–58 (ESA SP-459, European Space Agency, ESA Publications Division, Noordwijk, 2001).
21. Diehl, R. *et al.* ^{26}Al in the inner Galaxy. Large-scale spectral characteristics derived with SPI/INTEGRAL. *Astron. Astrophys.* **449**, 1025–1031 (2006).
22. Jean, P. *et al.* Spectral analysis of the Galactic e^+e^- annihilation emission. *Astron. Astrophys.* **445**, 579–589 (2006).
23. Gillard, W., Jean, P., Marcowith, A. & Ferrière, K. Transport of positrons in the interstellar medium. in *Proceedings of 6th INTEGRAL Workshop* (ESA SP-622, ESA Publications Division, Noordwijk, in the press); preprint at ⟨http://arxiv.org/abs/astro-ph/0702158⟩ (2007).
24. Bird, A. J. *et al.* The 3rd IBIS/ISGRI soft gamma-ray survey catalog. *Astrophys. J. Suppl. Ser.* **170**, 175–186 (2007).
25. Bazzano, A. *et al.* INTEGRAL IBIS census of the sky beyond 100keV. *Astrophys. J.* **649**, L9–L12 (2006).
26. Grimm, H.-J., Gilfanov, M. & Sunyaev, R. The Milky Way in X-rays for an outside observer. *Astron. Astrophys.* **391**, 923–944 (2002).
27. Schanne, S., Cassé, M., Sizun, P., Cordier, B. & Paul, J. Type Ia supernova rate in the Galactic Center region. In *Proceedings of 6th INTEGRAL Workshop* (ESA SP-622, ESA Publications Division, Noordwijk, in the press); preprint at ⟨http://arxiv.org/abs/astro-ph/0609566⟩ (2007).
28. Knödlseder, J. *et al.* Imaging the gamma-ray sky with SPI aboard INTEGRAL. in *Proceedings of 6th INTEGRAL Workshop* (ESA SP-622, ESA Publications Division, Noordwijk, in the press); preprint at ⟨http://arxiv.org/abs/astro-ph/0712.1668⟩ (2007).
29. Robin, A. C., Reylé, C., Derrière, S. & Picaud, S. A synthetic view on structure and evolution of the Milky Way. *Astron. Astrophys.* **409**, 523–540 (2003).

Supplementary Information is linked to the online version of the paper at www.nature.com/nature.

Acknowledgements This work is based on observations with INTEGRAL, an ESA project with instruments and science data centre funded by ESA member states (especially the PI countries: Denmark, France, Germany, Italy, Switzerland, Spain), Czech Republic and Poland, and with the participation of Russia and the USA. A.W.S. is supported by the German Bundesministerium für Bildung, Wissenschaft, Forschung und Technologie (BMBF/DLR).

Author Contributions G.W. led the work and performed the main analysis. G.S. was involved in editing and some of the statistical analysis and P.J. with the background modelling and spectral analysis. J.K. was responsible for the modelling and fitting software used. P.v.B., R.D., B.C., S.S. and C.W. critically discussed the analysis methods and the scientific interpretation. G.B. made general scientific contributions and shared his historical memory. A.W.S. provided critical evaluation of the manuscript and pointed out relevant literature. All the authors discussed the results and commented on the manuscript.

Author Information Reprints and permissions information is available at www.nature.com/reprints. Correspondence and requests for materials should be addressed to G.W. (Georg.Weidenspointner@hll.mpg.de).

LETTERS

Enhanced thermoelectric performance of rough silicon nanowires

Allon I. Hochbaum[1]*, Renkun Chen[2]*, Raul Diaz Delgado[1], Wenjie Liang[1], Erik C. Garnett[1], Mark Najarian[3], Arun Majumdar[2,3,4] & Peidong Yang[1,3,4]

Approximately 90 per cent of the world's power is generated by heat engines that use fossil fuel combustion as a heat source and typically operate at 30–40 per cent efficiency, such that roughly 15 terawatts of heat is lost to the environment. Thermoelectric modules could potentially convert part of this low-grade waste heat to electricity. Their efficiency depends on the thermoelectric figure of merit ZT of their material components, which is a function of the Seebeck coefficient, electrical resistivity, thermal conductivity and absolute temperature. Over the past five decades it has been challenging to increase $ZT>1$, since the parameters of ZT are generally interdependent[1]. While nanostructured thermoelectric materials can increase $ZT>1$ (refs 2–4), the materials (Bi, Te, Pb, Sb, and Ag) and processes used are not often easy to scale to practically useful dimensions. Here we report the electrochemical synthesis of large-area, wafer-scale arrays of rough Si nanowires that are 20–300 nm in diameter. These nanowires have Seebeck coefficient and electrical resistivity values that are the same as doped bulk Si, but those with diameters of about 50 nm exhibit 100-fold reduction in thermal conductivity, yielding $ZT=0.6$ at room temperature. For such nanowires, the lattice contribution to thermal conductivity approaches the amorphous limit for Si, which cannot be explained by current theories. Although bulk Si is a poor thermoelectric material, by greatly reducing thermal conductivity without much affecting the Seebeck coefficient and electrical resistivity, Si nanowire arrays show promise as high-performance, scalable thermoelectric materials.

The most widely used commercial thermoelectric material is bulk Bi_2Te_3 and its alloys with Sb, Se, and so on, which have $ZT=S^2T/\rho k\approx 1$, where S, ρ, k and T are the Seebeck coefficient, electrical resistivity, thermal conductivity and absolute temperature, respectively. It is difficult to scale bulk Bi_2Te_3 to large-scale energy conversion, but fabricating synthetic nanostructures for this purpose is even more difficult and expensive. Si, on the other hand, is the most abundant and widely used semiconductor, with a large industrial infrastructure for low-cost and high-yield processing. Bulk Si, however, has a high k ($\sim$150 W m^{-1} K^{-1} at room temperature)[5], giving $ZT\approx 0.01$ at 300 K (ref. 6). The spectral distribution of phonons contributing to the k of Si at room temperature is quite broad. Because the rate of phonon–phonon Umklapp scattering scales as ω^2, where ω is the phonon frequency, low-frequency (or long-wavelength) acoustic phonons have long mean free paths and contribute significantly to k at high temperatures[7–10]. Thus, by rational incorporation of phonon-scattering elements at several length scales, the k of Si is expected to decrease dramatically. The ideal thermoelectric material is believed to be a phonon glass and an electronic crystal. Here, we show that by using roughened nanowires, we can reduce the thermal conductivity to $\sim$1.6 W m^{-1} K^{-1}, with the phonon contribution close to the amorphous limit, without significantly modifying the power factor S^2/ρ, such that $ZT\approx 1$ at room temperature. Further reduction of nanowire diameter is likely to increase ZT to >1.

Wafer-scale arrays of Si nanowires were synthesized by an aqueous electroless etching (EE) method[11–13]. The technique is based on the galvanic displacement of Si by $Ag^+\rightarrow Ag^0$ reduction on the wafer surface. The reaction proceeds in an aqueous solution of $AgNO_3$ and HF acid. Briefly, Ag^+ reduces onto the Si wafer surface by injecting holes into the Si valence band and oxidizing the surrounding lattice, which is subsequently etched by HF. The initial reduction of Ag^+ forms Ag nanoparticles on the wafer surface, thus delimiting the spatial extent of the oxidation and etching process. Further reduction of Ag^+ occurs on the nanoparticles, not the Si wafer, which becomes the active cathode by electron transfer from the underlying wafer. Ag dentritic growth on the arrays can be washed off with deionized water after the synthesis. The arrays were washed in a concentrated nitric acid bath for at least one hour to remove all residual Ag from the nanowire surfaces. After the nitric acid bath, no Ag particles were observed during transmission electron microscopy (TEM) analysis and no Ag peaks appeared in the energy-dispersive X-ray spectra of the nanowires. Furthermore, the reaction proceeds at or near room temperature (295 K), so no diffusion of Ag atoms into a covalent solid lattice—such as Si—should be expected.

Nanowires synthesized by this approach were vertically aligned and consistent throughout batches, and across large areas up to wafer-scale. Figure 1a is a cross-sectional scanning electron microscope (SEM) image of one such array, and the inset shows a one-inch-square nanowire array. Key parameters of the reaction were identified using p-type $\langle 100\rangle$-oriented, nominally 10–20 Ω cm, Si as the etch wafer. Both etching time and $AgNO_3$ concentration controlled nanowire length, roughly linearly, down to 5 μm at short immersion times ($<$10 min). At longer etching times, nanowire lengths were controllable up to 150 μm, while longer wires were too fragile to preserve the array. Wafers cut to $\langle 100\rangle$, $\langle 110\rangle$ and $\langle 111\rangle$ orientations all yielded nanowire arrays etched normal to the wafer surface over most of the wafer area. Similar results were obtained for EE of both n- and p-type wafers with resistivities varying from 10 to 10^{-2} Ω cm ($\sim 10^{14}$ to 10^{18} cm^{-3} dopant concentrations). Because thermoelectric modules consist of complementary p- and n-type materials wired in series, the generality and scalability of this synthesis are promising for fabrication of Si-based devices.

After etching, the fill factor of the nanowires was approximately 30% over the entire wafer surface. The nanowires varied from 20 to 300 nm in diameter with an average diameter of approximately 100 nm, as measured from TEM micrographs (Fig. 1b). The

[1]Department of Chemistry, [2]Department of Mechanical Engineering, [3]Department of Materials Science and Engineering, University of California, Berkeley, California 94720, USA. [4]Materials Sciences Division, Lawrence Berkeley National Laboratory, Berkeley, California 94720, USA.
*These authors contributed equally to this work.

nanowires were single crystalline, as shown by the selected area electron diffraction pattern (top inset) and high-resolution TEM image of the Si lattice of an EE nanowire in Fig. 1c. In contrast to the smooth surfaces of typical vapour–liquid–solid (VLS)-grown, gold-catalysed Si nanowires (Fig. 1d)[14,15], those of the EE Si nanowires are much rougher. The mean roughness height of these nanowires varied from wire to wire, but was typically 1–5 nm with a roughness period of the order of several nanometres. This roughness may be attributed to randomness of the lateral oxidation and etching in the corrosive aqueous solution or slow HF etching and faceting of the lattice during synthesis.

The main advantage of using Si nanowires for thermoelectric applications lies in the large difference in mean free path lengths between electrons and phonons at room temperature: 110 nm for electrons in highly doped samples[16,17] and ~300 nm for phonons[10]. Consequently, incorporating structures with critical dimensions/spacings below 300 nm in Si should reduce the thermal conductivity without significantly affecting S^2/ρ. The thermal conductivity of these hierarchically structured Si nanowires was characterized using devices consisting of resistive coils supported on parallel, suspended SiN_X membranes[14,18]. This construction allows us to probe thermal transport in individual nanowires. The membranes are thermally connected through a bridging nanowire, with negligible leakage from heat transfer by means other than conduction through the wire. The thermal conductivity was extracted from the thermal conductance using the dimensions of the nanowire, as determined by SEM. To anchor the nanowire to the membranes and reduce thermal contact resistance, a Pt/C composite was deposited on both ends using a focused electron beam (Fig. 2a, also see Supplementary Information). The contact resistance at the interface between the nanowire and the pad is negligible relative to the nanowire thermal resistance. This condition was verified by measuring the thermal conductivity of a large nanowire (135 nm diameter) after two rounds of thermal anchoring with Pt/C pads. The second thermal anchoring doubled the contact area of the nanowire with the Pt/C pad and the SiN_X membrane, and the measured thermal conductivity of the wire remained unchanged. Hence, the nanowire thermal resistance dominates over that of the contacts (see Supplementary Fig. 2).

Figure 2b shows the measured thermal conductivity of both VLS and EE Si nanowires. It has been shown that the k of VLS Si nanowires is strongly diameter-dependent[14], which is attributed to boundary scattering of phonons. We found that EE Si nanowires exhibit a diameter dependence of k similar to that of VLS-grown wires. The magnitude of k, however, is five- to eightfold lower for EE nanowires of comparable diameters. Because the phonon spectrum is broad and Planck-like, k can be reduced by introducing scattering at additional length scales beyond the nanowire diameter[1–4,19]. In the case of the EE nanowires, the roughness at the nanowire surface behaves like secondary scattering phases. The roughness may contribute to higher rates of diffuse reflection or backscattering of phonons at

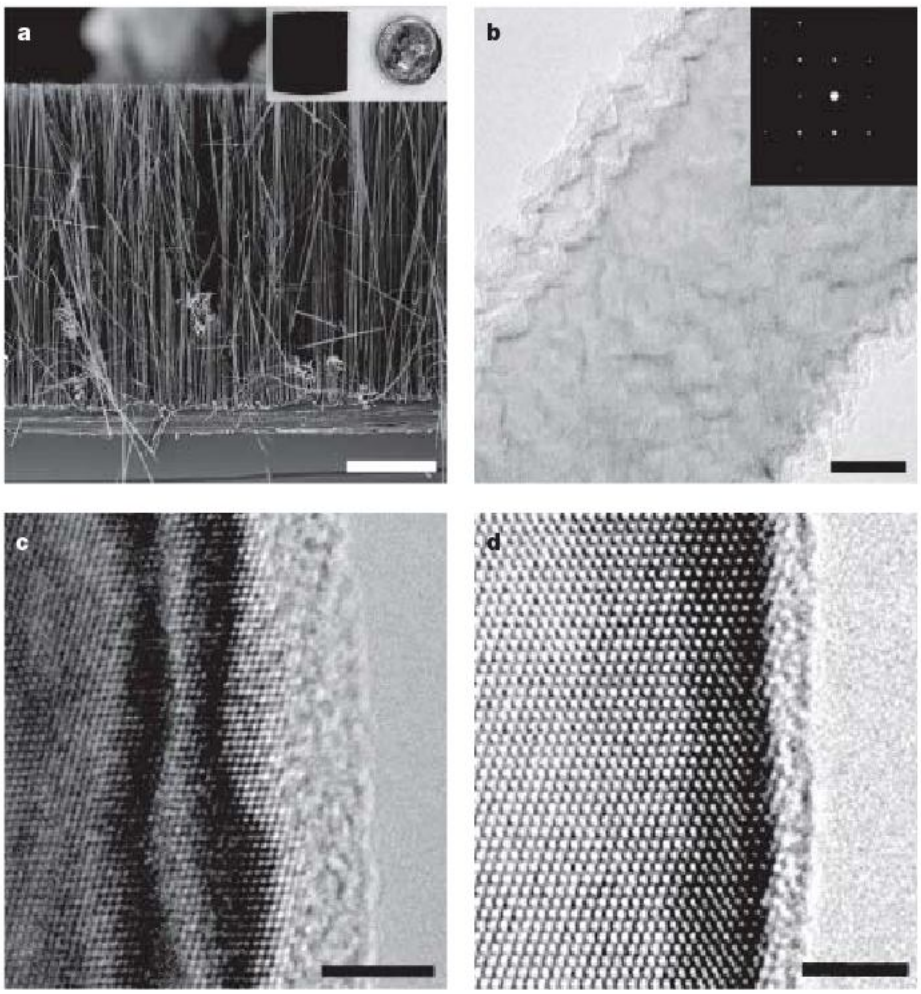

Figure 1 | Structural characterization of the rough silicon nanowires. **a**, Cross-sectional SEM of an EE Si nanowire array. Dendritic Ag growth can be seen within the array—a product of Ag^+ reduction onto the wafer during reaction. The Ag is etched in nitric acid after the synthesis, and elemental analysis confirms it is dissolved completely. Inset, an EE Si nanowire array Si wafer chip of the typical size used for the syntheses. Similar results are obtained on entire 4-inch wafers. The chip is dark and non-reflective owing to light scattering by, and absorbing into, the array. **b**, Bright-field TEM image of a segment of an EE Si nanowire. The roughness is clearly seen at the surface of the wire. The selected area electron diffraction pattern (inset) indicates that the wire is single crystalline all along its length. **c**, High-resolution TEM image of an EE Si nanowire. The roughness is evident at the interface between the crystalline Si core and the amorphous native oxide at the surface, and by undulations of the alternating light/dark thickness fringes near the edge. **d**, High-resolution TEM of a VLS-grown Si nanowire. Scale bars for **a**–**d** are 10 μm, 20 nm, 4 nm and 3 nm, respectively.

the interfaces. These processes have been predicted to affect the k values of Si nanowires, but not to the extent observed here[20,21]. The peak k of the EE nanowires is shifted to a much higher temperature than that of VLS nanowires, and both are significantly higher than that of bulk Si, which peaks at around 25 K (ref. 5). This shift suggests that the phonon mean free path is limited by boundary scattering as opposed to intrinsic Umklapp scattering.

While the above wires were etched from high-resistivity wafers, the peak ZT of semiconductor materials is predicted to occur at high dopant concentrations ($\sim 1 \times 10^{19}$ cm^{-3}; ref. 22). To optimize the ZT of EE nanowires, lower resistivity nanowires were synthesized from $10^{-1}\,\Omega$cm B-doped p-Si ⟨111⟩ and $10^{-2}\,\Omega$cm As-doped n-Si ⟨100⟩ wafers by the standard method outlined above. Nanowires etched from the $10^{-2}\,\Omega$cm and less resistive wafers, however, did not produce devices with reproducible electrical contacts, probably owing to greater surface roughness, as observed in TEM analysis. Consequently, more optimally doped nanowires were obtained by post-growth gas-phase B doping of wires etched from $10^{-1}\,\Omega$cm wafers (see Supplementary Information). The resulting nanowires have an average $\rho = 3 \pm 1.4\,\text{m}\Omega\text{cm}$ (as compared to $\sim 10\,\Omega$cm for wires from low-doped wafers).

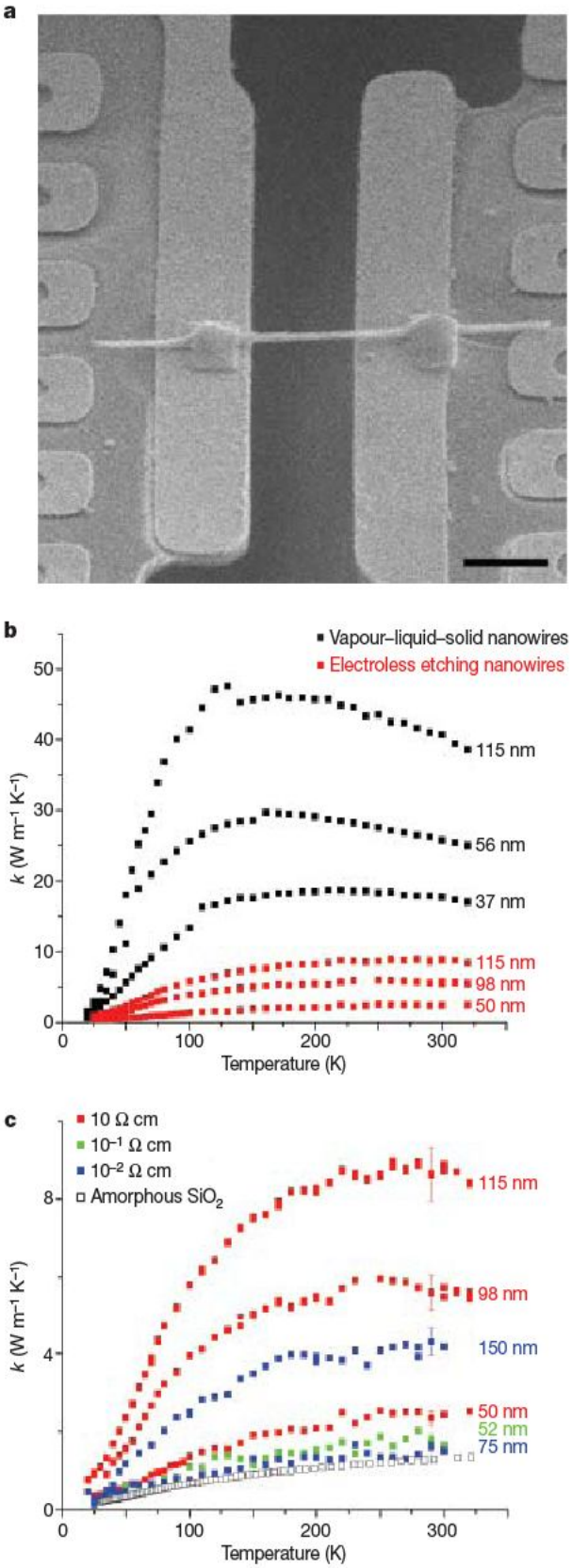

Figure 2 | Thermal conductivity of the rough silicon nanowires. **a**, An SEM image of a Pt-bonded EE Si nanowire (taken at 52° tilt angle). The Pt thin film loops near both ends of the bridging wire are part of the resistive heating and sensing coils on opposite suspended membranes. Scale bar, 2 μm. **b**, The temperature-dependent k of VLS (black squares; reproduced from ref. 14) and EE nanowires (red squares). The peak k of the VLS nanowires is 175–200 K, while that of the EE nanowires is above 250 K. The data in this graph are from EE nanowires synthesized from low-doped wafers. **c**, Temperature-dependent k of EE Si nanowires etched from wafers of different resistivities: $10\,\Omega$cm (red squares), $10^{-1}\,\Omega$cm (green squares; arrays doped post-synthesis to $10^{-3}\,\Omega$cm), and $10^{-2}\,\Omega$cm (blue squares). For the purpose of comparison, the k of bulk amorphous silica is plotted with open squares. The smaller highly doped EE Si nanowires have a k approaching that of insulating glass, suggesting an extremely short phonon mean free path. Error bars are shown near room temperature, and should decrease with temperature. See Supplementary Information for k measurement calibration and error determination.

Figure 2c shows the k of small-diameter nanowires etched from 10, 10^{-1}, and $10^{-2}\,\Omega$cm wafers. The post-growth doped nanowire (52 nm diameter) etched from a $10^{-1}\,\Omega$cm wafer has a slightly lower k than the lower-doped wire of the same diameter. This small decrease in k may be attributed to higher rates of phonon-impurity scattering. Studies of doped and isotopically purified bulk Si have revealed a reduction of k as a result of impurity scattering[6,23,24]. Owing to the atomic nature of such defects, they are expected to predominantly scatter short-wavelength phonons. On the other hand, nanowires etched from a $10^{-2}\,\Omega$cm wafer have a much lower k than the other nanowires, probably as a result of the greater surface roughness.

In the case of the 52 nm nanowire, k is reduced to $1.6 \pm 0.13\,\text{W m}^{-1}\,\text{K}^{-1}$ at room temperature. For comparison, the temperature-dependent k of amorphous bulk SiO_2 (data points used from http://users.mrl.uiuc.edu/cahill/tcdata/tcdata.html agree with measurement in ref. 25) is also plotted in Fig. 2c. As can be seen from the plot, k of these single-crystalline EE Si nanowires is comparable to that of insulating glass. Indeed, k of the 52 nm nanowire approaches the minimum k predicted and measured for Si: $\sim 1\,\text{W m}^{-1}\,\text{K}^{-1}$ (ref. 26). The resistivity of a single nanowire of comparable diameter (48 nm) was measured (see Supplementary Information) and the electronic contribution to thermal conductivity (k_e) can be estimated from the Wiedemann–Franz law[16]. For measured $\rho = 1.7\,\text{m}\Omega\,\text{cm}$, $k_e = 0.4\,\text{W m}^{-1}\,\text{K}^{-1}$, meaning that the lattice thermal conductivity ($k_l = k - k_e$) is $1.2\,\text{W m}^{-1}\,\text{K}^{-1}$.

By assuming the mean free path due to boundary scattering $\ell_b = Fd$, where $F > 1$ is a multiplier that accounts for the specularity of phonon scattering at the nanowire surface and d is the nanowire diameter, a model based on Boltzmann transport theory was able to explain[27] the diameter dependence of thermal conductivity in VLS nanowires, as observed in ref. 14. Because the thermal conductivity of EE nanowires is lower and the surface is rougher than that of VLS ones, it is natural to assume $\ell_b = d$ ($F = 1$), which is the smallest mean free path due to boundary scattering. However, this still cannot explain why the phonon thermal conductivity approaches the amorphous limit for nanowires with diameters ~50 nm. In fact, theories that consider phonon backscattering, as recently proposed by ref. 21, cannot explain our observations either. The thermal conductivity in amorphous non-metals[26] can be well explained by

assuming that the phonon mean free path $\ell = \lambda/2$, where λ is the phonon wavelength, which invokes a Debye-like short-range coherence in an atomically disordered lattice. However, there seems no justifiable reason to make this assumption for the single-crystal EE Si nanowires, because their diameters are about 100-fold larger than the lattice constant. To the best of our knowledge, there is currently no theory that can explain why a single-crystalline Si nanowire that is ~50 nm in diameter should behave like a phonon glass. On the basis of the difference between VLS and EE nanowires, we suspect that the roughness plays a strong role in screening a broad spectrum of phonons, fundamentally altering phonon transmission through these confined structures. The exact mechanism, however, remains unknown.

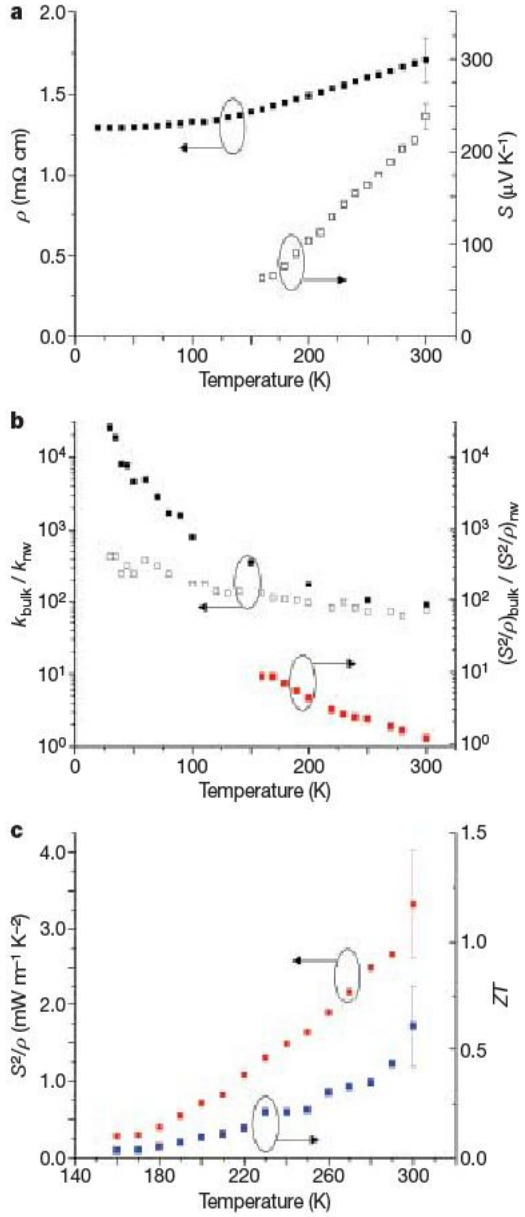

Figure 3 | Thermoelectric properties and *ZT* calculation for the rough silicon nanowire. **a**, S (open squares) and ρ (solid squares) of the highly doped EE 48 nm nanowire. See Supplementary Information for error analysis. **b**, Ratio of intrinsic bulk Si k (ref. 5) to that of a highly doped EE Si nanowire 50 nm in diameter. k_{bulk}:k_{nw} increases dramatically with decreasing temperature, from 100 at 300 K to 25,000 at 25 K (solid squares). As compared to highly doped bulk Si (1.7×10^{19} cm^{-3} As-doped, data adapted from ref. 6), k_{bulk}:k_{nw} increases from 75 at 300 K to 425 at 30 K (open squares). Red squares show the ratio of the power factor of optimally doped bulk Si relative to the nanowire power factor as a function of temperature. **c**, Single nanowire power factor (red squares) of the nanowire and calculated ZT (blue squares) using the measured k of the 52 nm nanowire in Fig. 2c. By propagation of uncertainty from the ρ and S measurements, the error bars are 21% for the power factor and 31% for ZT (assuming negligible temperature uncertainty, which seems valid given that the measurements are stable to better than ±100 mK).

To calculate the nanowire ZT, ρ and S measurements were carried out on individual highly doped nanowires. One such measurement on a 48 nm diameter wire is shown in Fig. 3a. Nanowires were measured in a horizontal geometry on 200 nm SiN_X films on Si substrates with a microfabricated heating element, and 2- and 4-point probe electrodes (see Supplementary Fig. 3). The power factor was calculated as $S^2/\rho = 3.3 \times 10^{-3}$ W m^{-1} K^{-2} for the nanowire at 300 K. The ratio of the power factor of optimally doped bulk Si to that of the EE Si nanowire as a function of temperature is plotted in Fig. 3b (with bulk values taken from ref. 6). The nanowire power factor decreases gradually relative to bulk with decreasing temperature, possibly due to a longer electron mean free path. On the other hand, as temperature decreases, the disparity between k of the nanowire and bulk grows. At low temperatures, long-wavelength phonon modes, which contribute strongly to thermal transport in bulk, are efficiently scattered in the roughened nanowires.

Figure 3b charts the ratio of k_{bulk}:k_{nw} for the 52 nm highly doped EE Si nanowire as a function of temperature. Whereas the k_{nw} is two orders of magnitude lower than k_{bulk} at room temperature, this ratio reaches more than four orders of magnitude at low temperature. Also shown is k_{bulk}:k_{nw} for highly doped bulk Si, for which k_{bulk}:k_{nw} is greatly reduced at low temperature. The large disparity persists unchanged, however, near room temperature. As a result, the degradation of the nanowire power factor with decreasing temperature is offset by the significant decrease in k, resulting in a relatively constant ZT enhancement factor for the EE Si nanowire.

ρ and S of the 48 nm nanowire were used for the ZT calculation because the diameter is close to that of the 52 nm wire for which k has been measured. The nanowire ZT is highest near room temperature at 0.6 (Fig. 3c). As compared to optimally doped bulk Si (~1×10^{19} cm^{-3}), the ZT of the EE nanowire is nearly two orders of magnitude greater throughout the temperature range measured[6]. The large increase in ZT is due to the significant decrease of k as compared to bulk while maintaining a high power factor. The hierarchical structuring of the EE Si nanowires allows selective scattering of phonons by dopants, nanoscale surface roughness, and dimensional confinement, while leaving electronic transport largely unaffected.

In conclusion, we have shown that it is possible to achieve $ZT = 0.6$ at room temperature in rough Si nanowires of ~50 nm diameter that were processed by a wafer-scale manufacturing technique. With optimized doping, diameter reduction, and roughness control, the ZT is likely to rise even higher. This ZT enhancement can be attributed to efficient scattering throughout the phonon spectrum by the introduction of nanostructures at different length scales (diameter, roughness and point defects). The significant reduction in thermal conductivity observed in this study may be a result of changes in the fundamental physics of heat transport in these quasi-one-dimensional materials. By achieving broadband impedance of phonon transport, we have demonstrated that the EE Si nanowire system is capable of approaching the limits of minimum lattice thermal conductivity in Si. Modules with the performance reported here, and manufactured from such a ubiquitous material as Si, may find wide-ranging applications in waste heat salvaging, power generation, and solid-state refrigeration. Moreover, the phonon scattering techniques developed in this study could significantly augment ZT even further in other materials to produce highly efficient solid-state thermoelectric devices.

METHODS SUMMARY

Nanowires were typically etched from B-doped Si wafers of different resistivities in aqueous solutions of 0.02 M $AgNO_3$ and 5 M HF for several hours. Excess Ag was removed in a nitric acid bath for at least one hour. Highly doped nanowires were achieved by annealing arrays at 850 °C for one hour in BCl_3 vapour. The

structure and microstructure of nanowire arrays and individual nanowires were characterized using SEM and TEM.

For thermal conductivity measurements, nanowires were either drop-cast onto the microfabricated devices from dispersions in isopropanol, or placed directly on the devices by micromanipulation with narrow tungsten probe tips (GGB Industries) mounted on a scanning stage (Marzhauser SM 3.25). The thermal conductivity of individual nanowires was measured by the previously described method[14,18].

The electrical conductivity and Seebeck coefficient of EE Si nanowires were measured by drop-casting isopropanol dispersions of nanowires onto Si wafer substrates coated with a 200-nm-thick silicon nitride film. Metal contact lines and a heating coil were fabricated on the same wafers using standard optical lithography (see Supplementary Fig. 3). 2- and 4-point I–V measurements, and dimensions from SEM images, were used to determine ρ for individual nanowires. S of single nanowires was measured by applying a current to the heating coil and measuring the temperature between the two inner 4-point probe contacts. 4-point measurements of both contact lines, and measured R versus T calibration curves were used to calculate the ΔT between them. S was calculated by $S = \Delta V/\Delta T$.

Full Methods and any associated references are available in the online version of the paper at www.nature.com/nature.

Received 7 June; accepted 9 October 2007.

1. Majumdar, A. Thermoelectricity in semiconductor nanostructures. *Science* **303**, 777–778 (2004).
2. Hsu, K. F. *et al.* Cubic $AgPb_mSbTe_{2+m}$: bulk thermoelectric materials with high figure of merit. *Science* **303**, 818–821 (2004).
3. Harman, T. C., Taylor, P. J., Walsh, M. P. & LaForge, B. E. Quantum dot superlattice thermoelectric materials and devices. *Science* **297**, 2229–2232 (2002).
4. Venkatasubramanian, R., Siivola, E., Colpitts, T. & O'Quinn, B. Thin-film thermoelectric devices with high room-temperature figures of merit. *Nature* **413**, 597–602 (2001).
5. Touloukian, Y. S., Powell, R. W., Ho, C. Y. & Klemens, P. G. (eds) *Thermal Conductivity: Metallic Elements and Alloys, Thermophysical Properties of Matter* Vol. 1, 339 (IFI/Plenum, New York, 1970).
6. Weber, L. & Gmelin, E. Transport properties of silicon. *Appl. Phys. A* **53**, 136–140 (1991).
7. Nolas, G. S., Sharp, J. & Goldsmid, H. J. in *Thermoelectrics: Basic Principles and New Materials Development* (eds Nolas, G. S., Sharp, J. & Goldsmid, H. J.) Ch. 3 (Springer, Berlin, 2001).
8. Asheghi, M., Leung, Y. K., Wong, S. S. & Goodson, K. E. Phonon-boundary scattering in thin silicon layers. *Appl. Phys. Lett.* **71**, 1798–1800 (1997).
9. Asheghi, M., Touzelbaev, M. N., Goodson, K. E., Leung, Y. K. & Wong, S. S. Temperature-dependent thermal conductivity of single-crystal silicon layers in SOI substrates. *J. Heat Transf.* **120**, 30–36 (1998).
10. Ju, Y. S. & Goodson, K. E. Phonon scattering in silicon films with thickness of order 100 nm. *Appl. Phys. Lett.* **74**, 3005–3007 (1999).
11. Peng, K. Q., Yan, Y. J., Gao, S. P. & Zhu, J. Synthesis of large-area silicon nanowire arrays via self-assembling nanochemistry. *Adv. Mater.* **14**, 1164–1167 (2002).
12. Peng, K., Yan, Y., Gao, S. & Zhu, J. Dendrite-assisted growth of silicon nanowires in electroless metal deposition. *Adv. Funct. Mater.* **13**, 127–132 (2003).
13. Peng, K. *et al.* Uniform, axial-orientation alignment of one-dimensional single-crystal silicon nanostructure arrays. *Angew. Chem. Intl Edn.* **44**, 2737–2742 (2005).
14. Li, D. *et al.* Thermal conductivity of individual silicon nanowires. *Appl. Phys. Lett.* **83**, 2934–2936 (2003).
15. Hochbaum, A. I., Fan, R., He, R. & Yang, P. Controlled growth of Si nanowire arrays for device integration. *Nano Lett.* **5**, 457–460 (2005).
16. Ashcroft, N. W. & Mermin, N. D. *Solid State Physics* Chs 1, 2 and 13 (Saunders College Publishing, Fort Worth, 1976).
17. Sze, S. M. *Physics of Semiconductor Devices* Ch. 1 (John Wiley & Sons, New York, 1981).
18. Shi, L. *et al.* Measuring thermal and thermoelectric properties of one-dimensional nanostructures using a microfabricated device. *J. Heat Transf.* **125**, 881–888 (2003).
19. Kim, W. *et al.* Thermal conductivity reduction and thermoelectric figure of merit increase by embedding nanoparticles in crystalline semiconductors. *Phys. Rev. Lett.* **96**, 045901 (2006).
20. Zou, J. & Balandin, A. Phonon heat conduction in a semiconductor nanowire. *J. Appl. Phys.* **89**, 2932–2938 (2001).
21. Saha, S., Shi, L. & Prasher, R. Monte Carlo simulation of phonon backscattering in a nanowire. *Proc. ASME Int. Mech. Eng. Congr. Exp. (5–10 November 2006)* art. no. 15668 1–5 (ASME, Chicago, 2006).
22. Rowe, D. M. (ed.) *CRC Handbook of Thermoelectrics* Ch. 5 (CRC Press, Boca Raton, 1995).
23. Brinson, M. E. & Dunstan, W. Thermal conductivity and thermoelectric power of heavily doped n-type silicon. *J. Phys. C* **3**, 483–491 (1970).
24. Ruf, T. *et al.* Thermal conductivity of isotopically enriched silicon. *Solid State Commun.* **115**, 243–247 (2000).
25. Cahill, D. G. & Pohl, R. O. Thermal conductivity of amorphous solids above the plateau. *Phys. Rev. B* **35**, 4067–4073 (1987).
26. Cahill, D. G., Watson, S. K. & Pohl, R. O. Lower limit to the thermal conductivity of disordered crystals. *Phys. Rev. B* **46**, 6131–6140 (1992).
27. Mingo, N., Yang, L., Li, D. & Majumdar, A. Predicting the thermal conductivity of Si and Ge nanowires. *Nano Lett.* **3**, 1713–1716 (2003).

Supplementary Information is linked to the online version of the paper at www.nature.com/nature.

Acknowledgements We thank T.-J. King-Liu and C. Hu for discussions and J. Goldberger for TEM analysis. We acknowledge the support of the Division of Materials Sciences and Engineering, Office of Basic Energy Sciences, DOE. A.I.H. and R.C. thank the NSF-IGERT and ITRI-Taiwan programs, respectively, for fellowship support. We also thank the National Center for Electron Microscopy and the UC Berkeley Microlab for the use of their facilities. R.D.D. thanks the GenCat/Fulbright programme for support.

Author Information Reprints and permissions information is available at www.nature.com/reprints. Correspondence and requests for materials should be addressed to A.M. (majumdar@me.berkeley.edu) and P.Y. (p_yang@berkeley.edu).

Vol 451|10 January 2008|doi:10.1038/nature06458

LETTERS

Silicon nanowires as efficient thermoelectric materials

Akram I. Boukai[1]†, Yuri Bunimovich[1]†, Jamil Tahir-Kheli[1], Jen-Kan Yu[1], William A. Goddard III[1] & James R. Heath[1]

Thermoelectric materials interconvert thermal gradients and electric fields for power generation or for refrigeration[1,2]. Thermoelectrics currently find only niche applications because of their limited efficiency, which is measured by the dimensionless parameter *ZT*—a function of the Seebeck coefficient or thermoelectric power, and of the electrical and thermal conductivities. Maximizing *ZT* is challenging because optimizing one physical parameter often adversely affects another[3]. Several groups have achieved significant improvements in *ZT* through multi-component nanostructured thermoelectrics[4–6], such as Bi_2Te_3/Sb_2Te_3 thin-film superlattices, or embedded PbSeTe quantum dot superlattices. Here we report efficient thermoelectric performance from the single-component system of silicon nanowires for cross-sectional areas of 10 nm × 20 nm and 20 nm × 20 nm. By varying the nanowire size and impurity doping levels, *ZT* values representing an approximately 100-fold improvement over bulk Si are achieved over a broad temperature range, including $ZT \approx 1$ at 200 K. Independent measurements of the Seebeck coefficient, the electrical conductivity and the thermal conductivity, combined with theory, indicate that the improved efficiency originates from phonon effects. These results are expected to apply to other classes of semiconductor nanomaterials.

The most efficient thermoelectrics have historically been heavily doped semiconductors because the Pauli principle restricts the heat-carrying electrons to be close to the Fermi energy[1] for metals. The Wiedemann–Franz law, $\kappa_e/\sigma T = \pi^2/3(k/e)^2 = (156\ \mu V\ K^{-1})^2$, where κ_e is the electronic contribution to κ, constrains $ZT = S^2\sigma T/\kappa$, where S is the Seebeck coefficient (or thermoelectric power, measured in $V\ K^{-1}$), and σ and κ are the electrical and thermal conductivities, respectively. Semiconductors have a lower density of carriers, leading to larger S values and a κ value that is dominated by phonons (κ_{ph}), implying that the electrical and thermal conductivities are somewhat decoupled[1]. κ can be reduced by using bulk semiconductors of high atomic weight, which decreases the speed of sound. However, this strategy has not yet produced materials with $ZT > 1$.

For a metal or highly doped semiconductor, S is proportional to the energy derivative of the density of electronic states. In low-dimensional (nanostructured) systems the density of electronic states has sharp peaks[7–9] and, theoretically, a high thermopower. Harnessing this electronic effect to produce high-*ZT* materials has had only limited success[10,11]. However, optimization of the phonon dynamics and heat transport physics in nanostructured systems has yielded results[4–6]. Nanostructures may be prepared with one or more dimensions smaller than the mean free path of the phonons and yet larger than that of electrons and holes. This potentially reduces κ without decreasing σ (ref. 12). Bulk silicon (Si) is a poor thermoelectric ($ZT_{300\ K} \approx 0.01$; ref. 13), and this phonon physics is important for our Si nanowires, in which the electronic structure remains bulk-like.

Figure 1 shows images of the devices and the Si nanowires we used for these experiments. Details related to the fabrication, calibration and experimental measurements are presented in the Supplementary

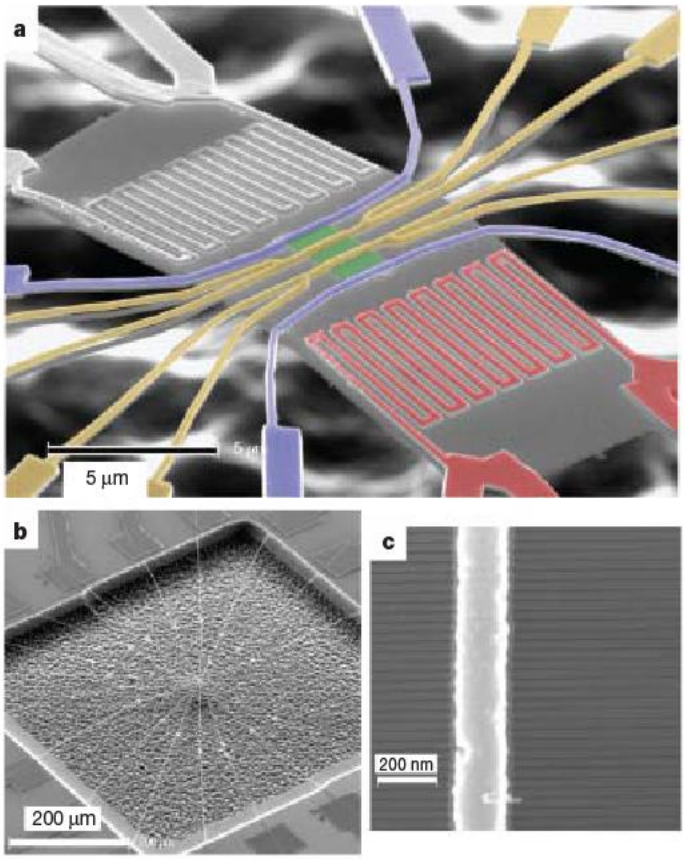

Figure 1 | Scanning electron micrographs of the device used to quantitate the thermopower and electrical and thermal conductivity of Si nanowire arrays. **a**, This false-colour image of a suspended platform shows all electrical connections. The central green area is the Si nanowire array, which is not resolved at this magnification. The four-lead yellow electrodes are used for thermometry to quantify the temperature difference across the nanowire array. The thermal gradient is established with either of the two Joule heaters (the right-hand heater is coloured red). The yellow and blue electrodes are combined to carry out four-point electrical conductivity measurements on the nanowires. The grey region underlying the nanowires and the electrodes is the 150-nm-thick SiO_2 insulator that is sandwiched between the top Si(100) single-crystal film from which the nanowires are fabricated, and the underlying Si wafer. The underlying Si wafer has been etched back to suspend the measurement platform, placing the background of this image out of focus. **b**, Low-resolution micrograph of the suspended platform. The electrical connections radiate outwards and support the device. **c**, High-resolution image of an array of 20-nm-wide Si nanowires with a Pt electrode.

[1]Division of Chemistry and Chemical Engineering, MC 127-72, 1200 East California Blvd, California Institute of Technology, Pasadena, California 91125, USA.
†These authors contributed equally to this work.

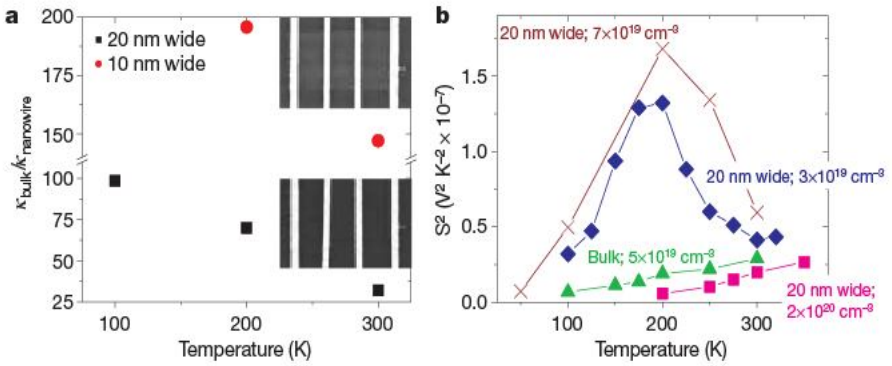

Figure 2 | Factors contributing to *ZT* for various Si nanowires. All nanowires are 20 nm in height. **a**, The temperature dependence of the thermal conductivity κ, presented as $\kappa_{bulk}/\kappa_{nanowire}$ to highlight the improvement that the reduction of κ in nanowires lends to *ZT*. κ_{bulk} values, which are slightly below the true bulk value for Si, are taken from an identically measured 520 nm × 35 nm-sized film. The inset scanning electron microscope micrographs show the region of the device containing the nanowires before (top) and after (bottom) the XeF_2 etch to remove the nanowires. **b**, The temperature dependence of S^2 for 20-nm-wide Si nanowires at various p-type doping concentrations (indicated on the graph). Note that the most highly doped nanowires (pink line) yield a thermopower similar to that of bulk Si doped at a lower level. For nanowires doped at slightly higher and slightly lower concentrations than the bulk, S peaks near 200 K. This is a consequence of the one-dimensional nature of the Si nanowires.

Information. The platform permits four-point measurements of the electrical conductivity of the nanowires, Joule heating to establish a thermal gradient across the nanowires, and four-point thermometry to quantify that gradient[10,14]. The resistance of the four-point thermometry electrodes is typically two orders of magnitude smaller than the resistance of the nanowires. The measurement platform is suspended in vacuum to allow measurement of nanowire thermal conductivity[15,16]. For all measurements, the Si nanowires could be selectively removed using a XeF_2 etch, thus allowing for measurements of the contributions to σ, S and κ from the platform and oxide substrate.

There are several ways to prepare Si nanowires, including materials methods for bulk production[17]. We wanted Si nanowires in which the dimensions, impurity doping levels, crystallographic nature, and so on, were all quantifiable and precisely controlled. We used the superlattice nanowire pattern transfer (SNAP) method[18], which translates the atomic control over the layer thickness of a superlattice into control over the width and spacing of nanowires. Si nanowires made via SNAP inherit their impurity dopant concentrations directly from the single-crystal Si epilayers of the silicon-on-insulator substrates from which they are fabricated[19]. These epilayers were 20- or 35-nm-thick Si(100) films on 150 nm of SiO_2, and were p-type impurity (boron) doped using diffusion-based doping[19]. Four-point probe conductivity measurements of the silicon-on-insulator films were used to extract dopant concentrations. We prepared nanowire arrays several micrometres long, with lateral width × thickness dimensions of 10 nm × 20 nm, 20 nm × 20 nm and 520 nm × 35 nm. The last approximates the bulk and, in fact, measurements on the sample obtained bulk values for S, σ and κ. Measurements of κ for our nanowires were consistent with literature values for materials grown (round) Si nanowires[16].

All values of S, σ and κ reported here are normalized to individual nanowires, although each experiment used a known number of nanowires ranging from 10 to 400. The Si microwires and nanowires were prepared using the same substrates, doping methods, and so on, but different patterning methods (electron-beam lithography versus SNAP).

Measurements of κ and S^2 for Si nanowires (and microwires) for different nanowire sizes and doping levels are presented in Fig. 2. More complete data sets, electrical conductivity data and a statistical analysis are presented in the Supplementary Information. The nanowire electrical conductivity is between 10 and 90% of the bulk, depending on nanowire dimensions. A reduced σ probably arises from surface scattering of charge carriers[19]. Nevertheless, all nanowires are highly doped and most exhibit metallic-like conductivity (increasing σ with decreasing T).

The temperature dependence of κ for a microwire and 10- and 20-nm-wide nanowires were recorded at modest statistical resolution to establish trends. This data indicated that κ drops sharply with shrinking nanowire cross-section (Fig. 2a) and that the 10-nm-wide nanowires exhibited a κ value ($0.76 \pm 0.15\ W\ m^{-1}\ K^{-1}$) that was below the theoretical limit of $0.99\ W\ m^{-1}\ K^{-1}$ for bulk Si (ref. 20). Thus, very large data sets were collected for 10- and 20-nm-wide nanowires to allow for a more precise determination of κ.

Our observed high *ZT* for Si nanowires (Fig. 3) occurs because κ is sharply reduced and the phonon drag component of the thermopower S_{ph} becomes large. Below, we show that S_{ph} increases because of a three-dimensional to one-dimensional crossover of the phonons participating in phonon drag and decreasing κ. However, we first discuss why our measured κ at 300 K for 10-nm-wide Si nanowires is less than κ_{min} (ref. 20).

The derivation of κ_{min} assumes that the minimum path length of wavelength λ phonons is $\lambda/2$ and that the phonons are described by the Debye model using bulk sound speeds with no optical modes. The $\lambda/2$ value is an order-of-magnitude estimate and is difficult to determine precisely, much like the minimum electron mean free path used to calculate the Mott–Ioffe–Regel σ_{min}. Also, κ_{min} is proportional to the transverse and longitudinal acoustic speeds of sound[20]. These are reduced in our nanowires at long wavelengths because the modes

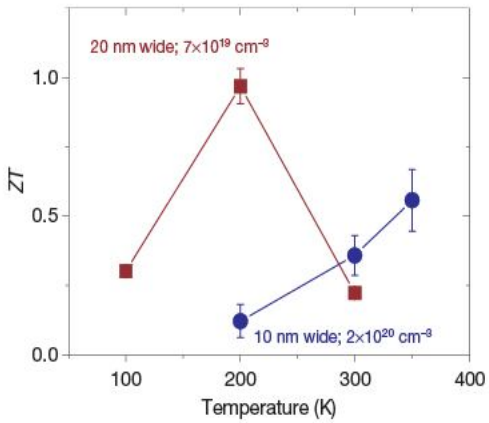

Figure 3 | Temperature dependence of *ZT* for two different groups of nanowires. The cross-sectional area of the nanowires, and the p-type doping level, are given. The 20-nm-wide nanowires have a thermopower that is dominated by phonon contributions, and a *ZT* value ~1 is achieved near 200 K. The smaller (10-nm-wide) nanowires have a thermopower that is dominated by electronic contributions. The *ZT* at 350 K is calculated using the thermal conductivity value for the 10-nm-wide nanowires at 300 K. The error bars represent 95% confidence limits.

become one-dimensional. The ratio of the one-dimensional to two-dimensional longitudinal speeds of sound is $[(1+\nu)(1-2\nu)/(1-\nu)]^{1/2} = 0.87$ where $\nu = 0.29$ is the Poisson ratio of Si. The transverse acoustic speed goes to zero at long wavelength because $\omega \propto k^2 d$ where d is the nanowire width[21]. Therefore, the bulk κ_{min} estimate above is invalid for our nanowires and values smaller than κ_{min} are attainable.

For all but the most highly doped nanowires, S peaks near 200 K (Fig. 2b). This peak is unexpected: similarly doped bulk Si exhibits a gradual decrease in S as T is reduced (green trace). For $T < 100$ K, a peaked $S(T)$ is observed for metals and lightly doped semiconductors and is due to phonon drag[13,22,23].

Phonon drag is generally assumed to vanish with decreasing sample dimensions because the phonon path length is limited by the sample size[24–26]. This seems to eliminate phonon drag as the reason for the peak in our nanowires. We show below that the phonon wavelengths participating in drag are of the order of or larger than the wire width. This leads to a three-dimensional to one-dimensional crossover of these modes and removes the cross-sectional wire dimensions from limiting the phonon mean path (see Fig. 4 inset). The nanowire boundaries are incorporated into the one-dimensional mode and are not an obstacle to phonon propagation. Therefore, the limiting size becomes the wire length (~1 μm) and phonon drag 'reappears' at very small dimensions.

In addition, classical elasticity theory[21] is valid for the phonon wavelengths considered here[27], leading to thermoelastic damping[21,28,29] of sound waves proportional to κ. Thus S_{ph} is further enhanced, owing to the observed reduced thermal conductivity κ. A detailed discussion is in the Supplementary Information.

It might seem that elasticity theory leads to a contradiction because κ is proportional to the mean phonon lifetime. If the phonon lifetimes increase as stated above, then κ should also increase. But because the elasticity expression is only valid for long-wavelength modes, and κ is the average of all modes, there is no contradiction.

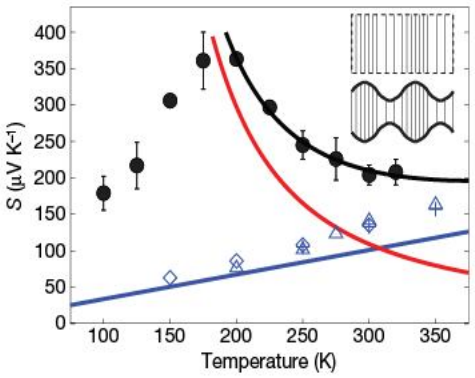

Figure 4 | Thermopower calculation plotted along with experimental data (black points) from a 20-nm-wide Si nanowire p-type doped at 3×10^{19} cm^{-3}. The black curve is the fitted expression for the total thermopower $S_e + S_{ph}$. The red curve is the phonon contribution S_{ph} and the blue line is the electronic term S_e arising from the fit. The fit has maximum error 6.1 μV K^{-1} and root-mean-square error 1.8 μV K^{-1}. The experimental error bars represent 95% confidence limits and at 150, 200 and 225 K are smaller than the data points. The blue data points are experimental values for bulk wires (doping 2×10^{20} cm^{-3}; crosses), 10-nm-wide nanowires (doping 7×10^{19} cm^{-3}; diamonds), and 20-nm-wide wires (doping 1.3×10^{20} cm^{-3}; triangles) where only a linear-T electronic contribution was found. This data are close to the extracted electronic contribution from the black data points (blue line) and shows that the fitted linear term is reasonable. The drop in S to 0 as $T \to 0$ occurs because the phonon mean free path reaches the sample size and the specific heat tends to 0 according to the third law of thermodynamics. The inset shows the character of a three-dimensional bulk longitudinal acoustic phonon mode (top) and a one-dimensional mode when the wavelength is larger or of the order of the width (bottom). The one-dimensional mode incorporates the existence of the boundary by transverse expansion (or compression) for longitudinal compression (or expansion). The ratio of the transverse strain to the longitudinal strain is the Poisson ratio (0.29 for Si).

We now consider separately the electronic and phonon contributions to the thermopower—$S = S_e + S_{ph}$—for the nanowire data at $T > 200$ K. Charge carriers dissipate heat to the lattice through a process that first involves momentum conserving (non-dissipative) electron–phonon collisions. The phonons that contribute to phonon drag cannot have a wavelength shorter than λ_{min}, which is determined by the size of the Fermi surface. Phonon drag is observed in metals only at low T because the Fermi surface is large and the heat carrying short-wavelength phonons have short lifetimes. At low T (<20 K), $S_{ph} \propto T^3$ from the phonon specific heat ($\propto T^3$). For $kT \gg \Theta_{Debye}$, the specific heat becomes constant and the number of phonons available for phonon–phonon scattering is $\propto T$, leading to $S_{ph} \propto 1/T$ (ref. 1).

For p-type Si, the holes are near the valence band maximum. The phonon drag modes are acoustic with the largest wavevector $k_{ph} = 2k_{Fermi} = 0.2$ Å^{-1} (for impurity doping of 3×10^{19} cm^{-3}). The shortest wavelength is $\lambda_{ph} = 2\pi/k = 31$ Å.

Umklapp (non-momentum-conserving) phonon–phonon scattering processes determine the rate of phonon heat dissipation. The Debye energy Θ_D sets the energy scale for Umklapp scattering. The number of Umklapp phonons available to dissipate the long-wavelength phonons is given by the Bose–Einstein function:

$$N_U = \frac{1}{e^{\Theta_D/T} - 1}$$

leading to a scattering rate $1/\tau_{ph} \propto N_U$. When $T \gg \Theta_D$, $1/\tau_{ph} \propto T$. Because $\Theta_D = 640$ K for Si, the full Bose–Einstein expression must be applied for $T \leq 350$ K. The electronic contribution S_e is estimated from the Mott formula[1]:

$$S_e(T) = \frac{\pi^2 k^2 T}{3e}\left(\frac{\partial \ln \sigma(\varepsilon)}{\partial \varepsilon}\right) \approx (283\mu\text{V K}^{-1})(kT/E_F)$$

where the conductivity derivative equals the reciprocal of the energy scale over which it varies (the Fermi energy E_F). Assuming hole doping occurs in the heavier Si valence band (mass 0.49), this leads to $E_F = 0.072$ eV = 833 K and $k_F = 0.1$ Å^{-1} for the number density of boron dopant atoms $n = 3 \times 10^{19}$ cm^{-3}. Thus $S_e(T) = aT$ where $a = 0.34$ μV K^{-2}.

The $T > 200$ K thermopower data of the 20-nm-wide wire (doping $n = 3 \times 10^{19}$ cm^{-3}) fits:

$$S = S_e + S_{ph} = aT + b[\exp(\Theta_D/T) - 1]$$

where a, b and Θ_D are varied to obtain the best fit (Fig. 4). The coefficients are $a = 0.337$ μV K^{-2}, $b = 22.1$ μV K^{-1}, and $\Theta_D = 534$ K. The coefficient a is almost identical to our estimate of 0.34 μV K^{-2}. Thus phonon drag explains the observed thermopower. Consistent with measurements[24] of phonon drag in bulk Si, S in our nanowires increases significantly at lighter doping. This data, plus a fit of the Fig. 4 data using the experimental $\Theta_D = 640$ K, is presented in the Supplementary Information. Rather than fitting by varying a, b and Θ_D, we fixed Θ_D to its known experimental value (640 K) and allowed only a and b to vary.

The phonon drag contribution to S is of the form[23,30]:

$$S_{ph} \propto \left(\frac{\tau_{ph}}{\mu T}\right)$$

τ_{ph}, the phonon lifetime, is $\propto 1/\kappa$ from elasticity theory. μ is the electron mobility. ZT scales as (neglecting S_e):

$$S_{ph} \propto \frac{1}{\mu T \kappa}$$

$$\sigma \propto n\mu$$

$$ZT \propto \frac{n}{\mu T \kappa^3}$$

leading to increased ZT with decreasing mobility. This is the opposite conclusion reached from when we consider only S_e (ref. 7).

We have combined experiment and theory to demonstrate that semiconductor nanowires can be designed to achieve extremely large enhancements in thermoelectric efficiency, and we have shown that the temperature of maximum efficiency may be tuned by changing the doping and the nanowire size. Theory indicates that similar improvements should be achievable for other semiconductor nanowire systems because of phonon effects. These nanowire thermoelectrics may find applications related to on-chip heat recovery, cooling and power generation. Additional improvements through further optimization of nanowire size, doping and composition should be possible.

METHODS SUMMARY

Single-crystalline Si nanowires were fabricated using the SNAP process[18]. The nanowires were doped p-type using a boron-containing spin-on dopant (see Supplementary Information for details)[19]. Electron-beam lithography was used to create Ti/Pt electrodes for the electrical and heat transport measurements. The entire device was suspended using a XeF_2 etch, leaving the nanowires anchored to a thin SiO island (see Supplementary Information for details). The nanowire electrical conductivity was measured by a Keithley 2400 using a four-point measurement to eliminate contact resistance. For measurement of S and κ, a temperature difference was created across the ends of the nanowires by sourcing a direct current through one of the resistive heaters. The resistance rise of each thermometer was recorded simultaneously using a lock-in measurement (Stanford Research Systems SRS-830) as the temperature was ramped upwards. The resistance of the thermometers was typically two orders of magnitude smaller than the nanowire array. For measurement of S, the thermoelectric voltage, as a response to the temperature difference, was recorded using a Keithley 2182A nanovoltmeter. A difference measurement was used to determine κ, whereby the κ value of the nanowires plus the oxide island was subtracted from the κ value of the oxide island. The thermal conductivity of the oxide island was determined by removing the nanowires with a highly selective XeF_2 etch (see Supplementary Information for details).

Received 15 June; accepted 2 November 2007.

1. MacDonald, D. K. C. *Thermoelectricity: An Introduction to the Principles* (Wiley, New York, 1962).
2. Mahan, G., Sales, B. & Sharp, J. Thermoelectric materials: New approaches to an old problem. *Phys. Today* **50**, 42–47 (1997).
3. Chen, G. *et al.* Recent developments in thermoelectric materials. *Int. Mater. Rev.* **48**, 45–66 (2003).
4. Venkatasubramanian, R. *et al.* Thin-film thermoelectric devices with high room-temperature figures of merit. *Nature* **413**, 597–602 (2001).
5. Harman, T. C. *et al.* Quantum dot superlattice thermoelectric materials and devices. *Science* **297**, 2229–2232 (2002).
6. Hsu, K. F. *et al.* Cubic $AgPb_mSbTe_{2+m}$: Bulk thermoelectric materials with high figure of merit. *Science* **303**, 818–821 (2004).
7. Hicks, L. D. & Dresselhaus, M. S. Thermoelectric figure of merit of a one-dimensional conductor. *Phys. Rev. B* **47**, 16631–16634 (1993).
8. Mahan, G. D. & Sofo, J. O. The best thermoelectric. *Proc. Natl Acad. Sci. USA* **93**, 7436–7439 (1996).
9. Humphrey, T. E. & Linke, H. Reversible thermoelectric nanomaterials. *Phys. Rev. Lett.* **94**, 096601 (2005).
10. Boukai, A., Xu, K. & Heath, J. R. Size-dependent transport and thermoelectric properties of individual polycrystalline bismuth nanowires. *Adv. Mater.* **18**, 864–869 (2006).
11. Yu-Ming, L. *et al.* Semimetal-semiconductor transition in $Bi_{1-x}Sb_x$ alloy nanowires and their thermoelectric properties. *Appl. Phys. Lett.* **81**, 2403–2405 (2002).
12. Majumdar, A. Enhanced thermoelectricity in semiconductor nanostructures. *Science* **303**, 777–778 (2004).
13. Weber, L. & Gmelin, E. Transport properties of silicon. *Appl. Phys. A* **53**, 136–140 (1991).
14. Small, J. P., Perez, K. M. & Kim, P. Modulation of thermoelectric power of individual carbon nanotubes. *Phys. Rev. Lett.* **91**, 256801 (2003).
15. Li, S. *et al.* Measuring thermal and thermoelectric properties of one-dimensional nanostructures using a microfabricated device. *J. Heat Transf.* **125**, 881–888 (2003).
16. Li, D. *et al.* Thermal conductivity of individual silicon nanowires. *Appl. Phys. Lett.* **83**, 2934–2936 (2003).
17. Morales, A. M. & Lieber, C. M. A laser ablation method for the synthesis of semiconductor crystalline nanowires. *Science* **279**, 208–211 (1998).
18. Melosh, N. A. *et al.* Ultra-high density nanowire lattices and circuits. *Science* **300**, 112–115 (2003).
19. Wang, D., Sheriff, B. A. & Heath, J. R. Complementary symmetry silicon nanowire logic: Power-efficient inverters with gain. *Small* **2**, 1153–1158 (2006).
20. Cahill, D. G., Watson, S. K. & Pohl, R. O. Lower limit to the thermal conductivity of disordered crystals. *Phys. Rev. B* **46**, 6131–6140 (1992).
21. Landau, L. D. & Lifshitz, E. M. in *Theory of Elasticity* 3rd edn, 138 (Butterworth Heinemann, Oxford, 1986).
22. Pearson, W. B. Survey of thermoelectric studies of the Group 1 metals at low temperatures carried out at the National Research Laboratories, Ottawa. *Sov. Phys. Solid State* **3**, 1024–1033 (1961).
23. Herring, C. Theory of the thermoelectric power of semiconductors. *Phys. Rev.* **96**, 1163–1187 (1954).
24. Geballe, T. H. & Hull, G. W. Seebeck effect in silicon. *Phys. Rev.* **98**, 940–947 (1955).
25. Behnen, E. Quantitative examination of the thermoelectric power of n-type Si in the phonon drag regime. *J. Appl. Phys.* **67**, 287–292 (1990).
26. Trzcinksi, R., Gmelin, E. & Queisser, H. J. Quenched phonon drag in silicon microcontacts. *Phys. Rev. Lett.* **56**, 1086–1089 (1986).
27. Maranganti, R. & Sharma, P. Length scales at which classical elasticity breaks down for various materials. *Phys. Rev. Lett.* **98**, 195504 (2007).
28. Lifshitz, R. & Roukes, M. L. Thermoelastic damping in micro- and nanomechanical systems. *Phys. Rev. B* **61**, 5600–5609 (2000).
29. Zener, C. Internal friction in solids. I. Theory of internal friction in reeds. *Phys. Rev.* **52**, 230–235 (1937).
30. Gurevich, L. The thermoelectric properties of conductors. *Zhumal Eksperimentalnoi I Teoreticheskoi Fiziki* **16**, 193–228 (1946).

Supplementary Information is linked to the online version of the paper at www.nature.com/nature.

Acknowledgements We thank D. Wang for discussions and J. Dionne, M. Roy, K. Kan and T. Lee for fabrication assistance. This work was supported by the Office of Naval Research, the Department of Energy, the National Science Foundation, the Defense Advanced Research Projects Agency, and a subcontract from the MITRE Corporation.

Author Contributions A.I.B., Y.B., J.-K.Y. and J.R.H. contributed primarily to the design and execution of the experiments. J.T.-K. and W.A.G. contributed primarily to the theory.

Author Information Reprints and permissions information is available at www.nature.com/reprints. Correspondence and requests for materials should be addressed to J.R.H. (heath@caltech.edu).

LETTERS

Direct measurement of critical Casimir forces

C. Hertlein[1], L. Helden[1], A. Gambassi[2,3], S. Dietrich[2,3] & C. Bechinger[1]

When fluctuating fields are confined between two surfaces, long-range forces arise. A famous example is the quantum-electrodynamical Casimir force that results from zero-point vacuum fluctuations confined between two conducting metal plates[1]. A thermodynamic analogue is the critical Casimir force: it acts between surfaces immersed in a binary liquid mixture close to its critical point and arises from the confinement of concentration fluctuations within the thin film of fluid separating the surfaces[2]. So far, all experimental evidence for the existence of this effect has been indirect[3–5]. Here we report the direct measurement of critical Casimir force between a single colloidal sphere and a flat silica surface immersed in a mixture of water and 2,6-lutidine near its critical point. We use total internal reflection microscopy to determine *in situ* the forces between the sphere and the surface, with femtonewton resolution[6]. Depending on whether the adsorption preferences of the sphere and the surface for water and 2,6-lutidine are identical or opposite, we measure attractive and repulsive forces, respectively, that agree quantitatively with theoretical predictions and exhibit exquisite dependence on the temperature of the system. We expect that these features of critical Casimir forces may result in novel uses of colloids as model systems.

The simple act of confining a fluid can give rise to new phenomena not observed in the bulk. An intriguing example is the critical Casimir force predicted to occur in binary fluid mixtures close to their critical point; like other critical phenomena, it is characterized by universal scaling functions that depend only on the internal symmetries of the system rather than on its specific material properties[7]. Colloidal particles suspended in binary liquids offer a particularly interesting setting for the experimental observations of such forces. At sufficiently small particle distances, concentration fluctuations of the solvent become confined between neighbouring colloidal surfaces and modify the pair interaction[8]. If the Casimir interaction strength is comparable to the thermal energy, drastic changes in the phase behaviour are expected. Reversible flocculation of silica colloids in water–2,6-lutidine mixtures close to the critical point has in fact been observed[9], and critical Casimir forces may be invoked to explain this phenomenon. However, flocculation was observed even far away from the critical point where critical fluctuations are negligible, so it cannot serve as conclusive evidence for the presence of Casimir forces[10,11].

Our experiments, aimed at directly measuring critical Casimir forces, use a single colloidal sphere and a planar surface immersed in a binary liquid mixture of water and 2,6-lutidine. Forces are determined using total internal reflection microscopy (TIRM, see Methods)[6] which allows *in situ* measurements with femtonewton resolution[12] (Fig. 1). The binary liquid mixture has a lower critical demixing point at $T_C \cong 307\,\mathrm{K}$ at a lutidine mass fraction of $c_L^C = 0.286$. At temperatures far below the temperatures corresponding to the demixing line, the binary mixture can be considered as an effectively homogeneous solvent and critical Casimir forces are absent. Under those conditions, the potential of the negatively charged colloidal particle at height z above the surface is given by electrostatic, gravitational and optical forces[6]

$$\Phi(z) = A\exp(-\kappa z) + G_{\mathrm{eff}} z \qquad (1)$$

where the amplitude of the electrostatic interaction A depends on the surface charges of the particle and the wall[6], κ^{-1} is the Debye screening length of the solvent, and G_{eff} is the effective weight of the colloid due to gravity and light pressure from the optical tweezers. For all heights z sampled in our experiment, we see no evidence for dispersion forces. This is due to the rather small differences between the refractive indices n of the water–lutidine mixture (1.384) and the silica substrate (1.464).

Because critical Casimir forces depend strongly on the adsorption properties of the confining surfaces[7], we used different combinations of particles and surfaces that preferentially adsorb either lutidine ('plus' boundary condition) or water ('minus' boundary condition). We used polystyrene particles[13] of diameter $2R = 3.69\,\mu\mathrm{m}$ with a clear preference for lutidine, and highly charged polystyrene spheres of diameter 2.4 μm preferring water. Variation of the adsorption properties of the silica substrate is achieved by chemical treatment of its surface with either hexamethyldisilaxane (HMDS) or NaOH, resulting in a preferential adsorption for lutidine and water, respectively.

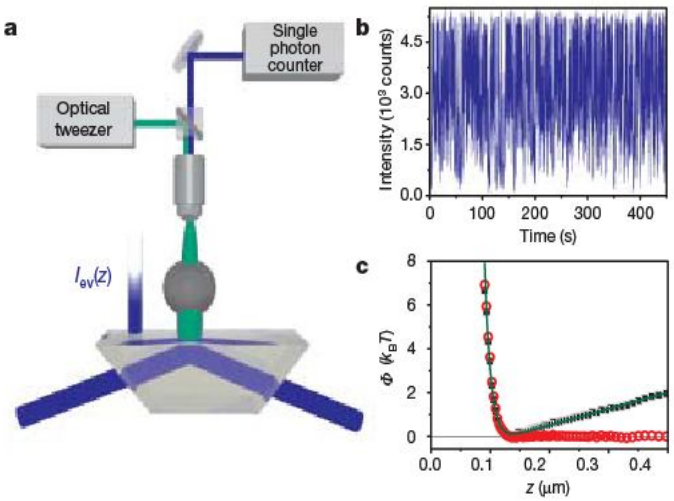

Figure 1 | Data acquisition and analysis. **a**, Scheme of TIRM set-up. A colloidal particle undergoing thermal motion within an evanescent field of intensity $I_{ev}(z)$ scatters light, whose intensity $I_{sc}(z)$ is detected by a single photon counter. Lateral particle diffusion is suppressed by a vertically incident optical tweezer ($\lambda = 532\,\mathrm{nm}$, $P \cong 2\,\mathrm{mW}$). **b**, I_{sc} versus time, reflecting particle motion normal to the surface. **c**, Measured interaction potential for a 2.4 μm polystyrene particle above a NaOH-treated silica surface ((− −) boundary conditions) in a water–lutidine mixture at critical composition (black data points). The data points are well fitted by equation (1) (green line). The same data but with the linear contribution $G_{\mathrm{eff}} z$ subtracted and shifted in vertical direction is also plotted (red data points).

[1]2. Physikalisches Institut, Universität Stuttgart, Pfaffenwaldring 57, 70569 Stuttgart, Germany. [2]Max-Planck-Institut für Metallforschung, Heisenbergstrasse 3, 70569 Stuttgart, Germany. [3]Institut für Theoretische und Angewandte Physik, Pfaffenwaldring 57, Universität Stuttgart, 70569 Stuttgart, Germany.

Figure 1c gives the interaction potential measured for a 2.4 μm particle above a NaOH-treated surface ((− −) boundary conditions) in a water–lutidine mixture at critical composition and 0.3 K below T_C. T_C is determined as the temperature at which a characteristic change in the scattering intensity occurs upon slowly heating the system across the phase transition. The figure shows that our measured potential is accurately described by equation (1), with the fit yielding a value of $\kappa^{-1} \approx 12\,\text{nm} \pm 3\,\text{nm}$ (s.d.) for the Debye screening length that is in agreement with estimates based on the solvation constant of the mixture[14]. We note that the linear contribution to the interaction potentials (see equation (1)) is identical over the entire temperature range we investigated. For convenience, we have subtracted this contribution from all potentials shown in the remainder of the paper.

Figure 2a shows the particle–wall interaction potentials upon approaching T_C from below. Within the investigated temperature range, critical fluctuations of the fluid mixtures contribute only negligibly to background scattering and thus do not interfere with the measurements of interaction potentials. The data show that although the temperature varies by only 0.18 K, the approach to T_C results in large changes to the measured potentials as a strong attractive force between particle and surface develops. In combination with electrostatic repulsion, the attractive force yields a potential well with a depth of almost 10 k_BT. At the highest temperature, corresponding to $\Delta T = T_C - T = 0.12$ K, this well is sufficiently deep that the particle hardly escapes from it during the entire measurement. The strong temperature dependence of the potentials close to the critical point is a clear indication of the involvement of critical Casimir forces. The maximum attractive force acting on the particle is estimated to about 600 fN. Considering the linear dependence of such forces on the particle size, this value is comparable to reported quantum-electrodynamical Casimir forces between a metallized colloidal sphere and a conducting flat surface[15].

Indirect experimental evidence has documented not only attractive but also repulsive critical Casimir forces in thin films of classical fluids[5,16], with the observations of one study[5] found to agree with subsequent theoretical predictions[17]. To observe repulsive critical Casimir forces in our system directly, the two surfaces confining the binary fluid mixture must preferentially adsorb different species of the mixture[7]; that is, the boundary conditions for the particles and surface need to be 'plus-minus' or 'minus-plus': (+ −) or (− +). In an experimental realization of (+ −) conditions we used 3.69 μm polystyrene particles and NaOH-treated substrate, with the interaction potentials measured for this system shown in Fig. 2b. As in the earlier experiment (Fig. 2a), the interaction potential measured at temperatures far below T_C consists only of electrostatic contributions. But in contrast to the behaviour seen in Fig. 2a, the repulsive part of the potential curves shifts towards larger z as the temperature approaches T_C. This is in qualitative agreement with theoretical predictions[7] for repulsive critical Casimir forces in the case of asymmetric boundary conditions. Treatment of the substrate with HMDS restores symmetric boundary conditions with the 3.69 μm polystyrene particles, and the critical Casimir forces measured in this (+ +) system are indeed attractive (see Fig. 2c).

To extract quantitative information about the critical Casimir potential $\Phi_C(z,T)$, we focus on experimental data obtained at distances z that are sufficiently large to render electrostatic interactions negligible. This avoids possible complications due to electrostatic effects, given that it is not a priori clear whether critical fluctuations might affect the counterion distribution. Within the Derjaguin

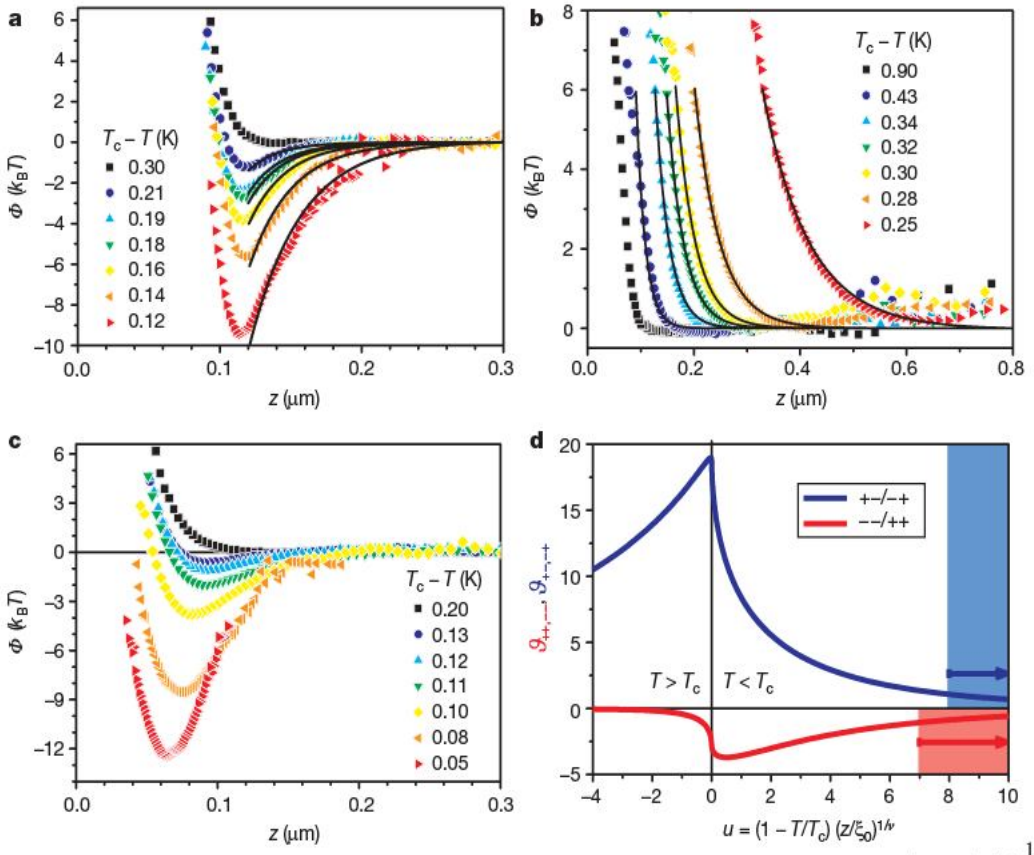

Figure 2 | Critical Casimir potentials between a wall and a particle in a critical water–lutidine mixture. **a**, Symmetric boundary conditions (− −): 2.4 μm hydrophilic particle and NaOH-treated hydrophilic wall. **b**, Asymmetric boundary conditions (+ −): 3.69 μm polystyrene particle preferring lutidine and NaOH-treated hydrophilic wall. **c**, Symmetric boundary conditions (+ +): 3.69 μm polystyrene particle and HMDS-treated wall. **d**, Calculated scaling functions for symmetric and asymmetric boundary conditions as functions of $u = \left(1 - \frac{T}{T_C}\right)\left(\frac{z}{\xi_0}\right)^{1/\nu}$ with $u = x^{1/\nu}$ for $T < T_C$. The coloured regions indicate the experimentally sampled range. The solid lines in **a** and **b** correspond to theoretical calculations with ξ determined as described in the main text. To achieve the best agreement with the theory, the experimental data have been horizontally shifted by the same amount within each panel and within the experimental resolution of ±30 nm.

approximation, valid for $z \lesssim R$, Φ_C is expected to scale at the critical concentration as $\frac{\Phi_C}{k_B T} = \frac{R}{z}\vartheta\left(\frac{z}{\xi}\right)$ where ϑ is a universal scaling function that depends on the boundary conditions. ξ is the bulk correlation length defined as $\xi = \xi_0\left(1-\frac{T}{T_C}\right)^{-\nu}$, with the amplitude ξ_0 reflecting the typical length scale set by the intermolecular pair potential. $\nu = 0.63$ is the universal critical exponent of the three-dimensional Ising universality class, relevant for classical binary mixtures. Within the Derjaguin approximation, the scaling function ϑ can be calculated by expressing it in terms of the scaling function $\vartheta_\parallel(L/\xi) = \frac{F_{C,\parallel}}{k_B TS} L^3$ of the critical Casimir force $F_{C,\parallel}$ acting between parallel plates with an area S and separated by a distance L. This yields $\vartheta(x) = 2\pi \int_1^\infty dy(y^{-2}-y^{-3})\vartheta_\parallel(xy)$, where $x = z/\xi$. $\vartheta_\parallel$ has been determined by Monte Carlo simulations for symmetric $(+\,+, -\,-)$ and asymmetric $(+\,-, -\,+)$ boundary conditions[17] and the resulting theoretical prediction for $\vartheta(x)$ is presented in Fig. 2d.

The observation that $\vartheta(x)$, and thus critical Casimir forces, can change sign depending on the boundary conditions of the system can be understood by considering that the preferences of the confining surfaces for one of the two species present in the fluid mixture impose additional constraints on concentration fluctuations. In the case of symmetric $(+\,+)$ or $(-\,-)$ boundary conditions, the fluctuation spectrum is further reduced by the confinement than in a system exhibiting no preferential adsorption; the reduction gives rise to strongly negative $\vartheta(x)$ values: that is, strong attraction. In the case of asymmetric $(+\,-)$ and $(-\,+)$ boundary conditions, fluctuations in the concentration of opposing species originate at the two confining surfaces. At small particle–wall distances, these fluctuations interfere with the tendency of the system to generate concentration fluctuations on the length scale set by the correlation length of the fluid mixture. Confinement in systems with asymmetric boundary conditions thus renders the latter fluctuations energetically less favourable, and so repulsive forces occur.

Theoretical predictions for the interaction potentials arising from critical Casimir forces are shown as solid lines in Fig. 2a and b, and agree remarkably well with the experimental data. (The data in Fig. 2c cannot be compared reliably with theory because the z-range in which electrostatic contributions are negligible is too narrow.) The predictions use values for $\xi(T)$ which are optimized to yield the best fits to the experimental data, and which are found to range from 20 to 100 nm. Comparing these $\xi(T)$ values with the theoretically expected algebraic behaviour $\xi = \xi_0\left(1-\frac{T}{T_C}\right)^{-0.63}$ and treating ξ_0 and T_C as fitting parameters, we have obtained $\xi_0 = 0.18\,\text{nm} \pm 0.02\,\text{nm}$ (s.e.m.) from both experiments in Fig. 2a and b. This value is consistent with $\xi_0 = 0.2\,\text{nm} \pm 0.02\,\text{nm}$ (s.e.m.), determined from light scattering experiments[18]. The T_C values obtained from the fit are $55 \pm 10\,\text{mK}$ (s.e.m.) and $234 \pm 5\,\text{mK}$ (s.e.m.), lower than the values experimentally determined in the corresponding experiments summarized in Fig. 2a and b, respectively. We attribute these differences to the difficulties in inferring the absolute value of T_C from the scattering intensity.

We also extended our measurements to binary mixtures that are far from their critical composition, where critical Casimir forces become negligible[11]. For small deviations from the critical lutidine mass fraction c_L^C, the temperature dependence of the forces between particles and surfaces is predicted to be almost identical to the temperature dependence documented in Fig. 2 (ref. 11). This is in agreement with our observation that measurements for lutidine mass fractions in the range $0.26 < c_L < 0.32$ and using $(+\,+)$ boundary conditions yield potential curves similar to those shown in Fig. 2c (data not shown). During these experiments, we observe no evidence for wetting phenomena, which are strongly suppressed by the curvature of the spherical particle[19]. However, measurements for $c_L \lesssim 0.2$ result in markedly different potentials.

Figure 3 shows the particle–wall interaction potentials measured at several temperatures below but near the demixing line, for a system with $(+\,+)$ boundary conditions and $c_L = 0.2$. Between 307.31 and 307.36 K, the potentials change very little and are well described by equation (1). But a further increase in temperature by 20 mK results in a sudden shift in the interaction potentials, with a narrow and steep potential well developing close to the surface. Further slight increases in temperature localize the particle even closer to the surface. Such an abrupt change in the particle–wall interaction potential strongly contrasts with the gradual increase of critical Casimir forces over a broad temperature range (compare with Fig. 2c, where Casimir forces increase gradually over a 150 mK temperature range). We note that when using a system with $(+\,+)$ boundary conditions, these abrupt potential changes are only observed on the lutidine-poor side of the phase diagram. In the case of hydrophilic particles and walls $((-\,-)$ boundary conditions), we obtain potential curves similar to those in Fig. 3 when $c_L \geq 0.4$. We attribute the instantaneous snapping of the particle towards the wall to the formation of a liquid bridge that spans the particle and the wall and that is formed by one component of the binary mixture. Our observation that bridge formation occurs only on the side of the phase diagram where the mixture is poor in the component that is being preferentially adsorbed by both surfaces is in agreement with theoretical predictions[20,21], which indicate that under those conditions surface contributions to the free energy become sufficiently important that the system minimizes its interfacial energy by bridge formation (see also the inset in Fig. 3).

Our results demonstrate that intriguing opportunities for influencing soft matter systems arise when using solvents near their critical point, where critical fluctuations actively contribute to the interactions between suspended objects. The fundamental nature of these fluctuations ensures that in contrast to interactions such as electrostatic forces, critical Casimir forces exhibit a striking temperature dependence that offers control over the phase behaviour of suspended objects through minute changes in temperature. This feature may lead to new uses of colloids as model systems. And considering that repulsive critical Casimir forces can be generated for any material by suitable surface treatments, we envisage that critical Casimir forces might also find use in micro-electromechanical systems where stiction (static friction) due to attractive quantum-electrodynamical Casimir forces causes device failure[22].

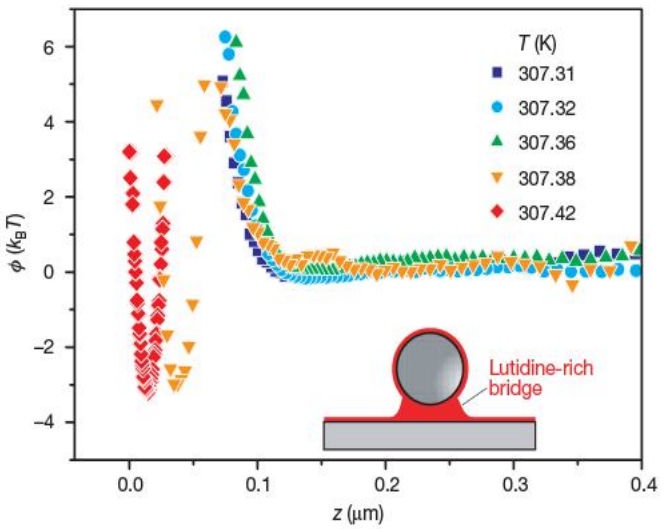

Figure 3 | Off-critical composition. Interaction potentials of a 3.69 μm polystyrene particle and a HMDS-treated silica wall ($(+\,+)$ boundary conditions) at lutidine mass fraction $c_L = 0.2$ and temperatures close to the demixing line. The potentials exhibit an abrupt change such that a narrow minimum close to the wall develops, which is interpreted as the formation of a liquid bridge, rich in the preferred component of the mixture, between the particle and the wall, as indicated in the inset.

METHODS SUMMARY

Particle–wall potentials were measured with TIRM, where a p-polarized laser beam ($\lambda = 473$ nm, $P \approx 2$ mW) is totally reflected at a glass–liquid interface leading to an evanescent field (Fig. 1). The particle's scattered intensity in the evanescent field depends sensitively on its height z: $I_{sc}(z) = I_0 \exp(-\beta z)$ where β^{-1} is the evanescent decay length ($\sim$200 nm in our experiments) and $I_0 = I_{sc}(z = 0)$ (refs 6, 23). From the intensity histogram we obtain the equilibrium distance distribution $P(z)$ which yields, via the Boltzmann factor, the particle–wall interaction potential $\Phi(z)$ up to a constant[6]. The wall position ($z = 0$) is obtained with an accuracy of $\pm$30 nm from the strong z-dependence of the particle's effective vertical diffusion coefficient owing to hydrodynamic interactions[24]. Data were acquired with a frequency of 250 Hz, typically over 15 min.

As sample cell we used a 200-μm-thick silica cuvette containing the critical mixture and a very small amount of colloidal particles. It is optically matched to the prism and thermally coupled to a flow thermostat, providing a temperature stability of 0.01 K (Lauda, model RK20). The bottom of the cell was coupled to an indium-tin-oxide-coated glass substrate, acting as the heater. Together with a platinum resistor (Pt 100), the heater was connected to a temperature controller (Eurotherm), providing a temperature stability of $\pm$5 mK over several hours.

Two kinds of beads were used as probe particles: 3.69-μm-diameter polystyrene particles crosslinked with divinyl benzene (Bangs Laboratories, type FS05F) with preferential adsorption of lutidine, and 2.4-μm-diameter hydrophilic polystyrene spheres with high surface charge density of 10 μC cm^{-2} (IDC, type 1-2400). Sample cells were either exposed to HMDS vapour overnight or rinsed with 0.1 M NaOH for 30 min, leaving the surface hydrophobic or hydrophilic, respectively. The cell was closed with Teflon plugs allowing for consecutive use for multiple days.

Received 21 June; accepted 29 October 2007.

1. Casimir, H. B. G. On the attraction between two perfectly conducting plates. *Proc. Koninklijke Nederlandse Akad. Wetenschappen* **B51**, 793–795 (1948).
2. Fisher, M. E. & de Gennes, P. G. Phenomena at the walls in a critical binary mixture. *C. R. Acad. Sci. Paris* **B 287**, 207–209 (1978).
3. Ganshin, A., Scheidemantel, S., Garcia, R. & Chan, M. H. W. Critical Casimir force in ^{4}He films: confirmation of finite-size scaling. *Phys. Rev. Lett.* **97**, 075301 (2006).
4. Garcia, R. & Chan, M. H. W. Critical Casimir effect near the ^{3}He-^{4}He tricritical point. *Phys. Rev. Lett.* **88**, 086101 (2002).
5. Fukuto, M., Yano, Y. F. & Pershan, P. S. Critical Casimir effect in three-dimensional Ising systems: measurements on binary wetting films. *Phys. Rev. Lett.* **94**, 135702 (2005).
6. Prieve, D. C. Measurement of colloidal forces with TIRM. *Adv. Colloid Interf. Sci.* **82**, 93–125 (1999).
7. Krech, M. Fluctuation-induced forces in critical fluids. *J. Phys. Cond. Matt.* **11**, R391–R412 (1999).
8. Hanke, A., Schlesener, F., Eisenriegler, E. & Dietrich, S. Critical Casimir forces between spherical particles in fluids. *Phys. Rev. Lett.* **81**, 1885–1888 (1998).
9. Beysens, D. & Estéve, D. Adsorption phenomena at the surface of silica spheres in a binary liquid mixture. *Phys. Rev. Lett.* **54**, 2123–2126 (1985).
10. Beysens, D. & Narayanan, T. Wetting-induced aggregation of colloids. *J. Stat. Phys.* **95**, 997–1008 (1999).
11. Schlesener, F., Hanke, A. & Dietrich, S. Critical Casimir forces in colloidal suspensions. *J. Stat. Phys.* **110**, 981–1013 (2003).
12. Rudhardt, D., Bechinger, C. & Leiderer, P. Repulsive depletion interactions in colloid-polymer mixtures. *J. Phys. Cond. Matt.* **11**, 10073–10078 (1999).
13. Gallagher, P. D., Kurnaz, M. L. & Maher, J. V. Aggregation in polystyrene-sphere suspensions in near-critical binary liquid mixtures. *Phys. Rev. A.* **46**, 7750–7755 (1992).
14. Gallagher, P. D. & Maher, J. V. Partitioning of polystyrene latex spheres in immiscible critical liquid mixtures. *Phys. Rev. A.* **46**, 2012–2021 (1992).
15. Mohideen, U. & Roy, A. Precision measurement of the Casimir force from 0.1 to 0.9 μm. *Phys. Rev. Lett.* **81**, 4549–4552 (1998).
16. Rafai, S., Bonn, D., &. Meunier, J. Repulsive and attractive critical Casimir forces. *Physica A* **386**, 31–35 (2007).
17. Vasilyev, O., Gambassi, A., Maciolek, A. & Dietrich, S. Monte Carlo simulation results for critical Casimir forces. *Europhys. Lett.* **80**, 60009 (2007).
18. Gülari, E., Collings, A. F., Schmidt, R. L. & Pings, C. J. Light scattering and shear viscosity studies of the binary system 2,6-lutidine-water in the critical region. *J. Chem. Phys.* **56**, 6169–6179 (1972).
19. Bieker, T. & Dietrich, S. Wetting of curved surfaces. *Physica A* **252**, 85–137 (1998).
20. Dobbs, H. T., Darbellay, G. A. & Yeomans, J. M. Capillary condensation between spheres. *Europhys. Lett.* **18**, 439–444 (1992).
21. Bauer, C., Bieker, T. & Dietrich, S. Wetting-induced effective interaction potential between spherical particles. *Phys. Rev. E* **62**, 5324–5338 (2000).
22. Ball, P. Feel the force. *Nature* **447**, 772–774 (2007).
23. Helden, L. *et al.* Single particle evanescent light scattering simulations for total internal reflection microscopy. *Appl. Opt.* **45**, 7299–7308 (2006).
24. Bevan, M. A. & Prieve, D. C. Hindered diffusion of colloidal particles very near to a wall: revisited. *J. Chem. Phys.* **113**, 1228–1236 (2000).

Acknowledgements We thank A. Maciołek for inspiring discussions and F. Schlesener, R. Dullens and D. Marr for comments and C. Mayer for sample preparation. This work is financially supported by the Deutsche Forschungsgemeinschaft.

Author Information Reprints and permissions information is available at www.nature.com/reprints. Correspondence and requests for materials should be addressed to C.B. (c.bechinger@physik.uni-stuttgart.de).

LETTERS

Crude-oil biodegradation via methanogenesis in subsurface petroleum reservoirs

D. M. Jones[1], I. M. Head[1], N. D. Gray[1], J. J. Adams[2], A. K. Rowan[1], C. M. Aitken[1], B. Bennett[2], H. Huang[2], A. Brown[1], B. F. J. Bowler[1], T. Oldenburg[2], M. Erdmann[3] & S. R. Larter[1,2]

Biodegradation of crude oil in subsurface petroleum reservoirs has adversely affected the majority of the world's oil, making recovery and refining of that oil more costly[1]. The prevalent occurrence of biodegradation in shallow subsurface petroleum reservoirs[2,3] has been attributed to aerobic bacterial hydrocarbon degradation stimulated by surface recharge of oxygen-bearing meteoric waters[2]. This hypothesis is empirically supported by the likelihood of encountering biodegraded oils at higher levels of degradation in reservoirs near the surface[4,5]. More recent findings, however, suggest that anaerobic degradation processes dominate subsurface sedimentary environments[6], despite slow reaction kinetics and uncertainty as to the actual degradation pathways occurring in oil reservoirs. Here we use laboratory experiments in microcosms monitoring the hydrocarbon composition of degraded oils and generated gases, together with the carbon isotopic compositions of gas and oil samples taken at wellheads and a Rayleigh isotope fractionation box model, to elucidate the probable mechanisms of hydrocarbon degradation in reservoirs. We find that crude-oil hydrocarbon degradation under methanogenic conditions in the laboratory mimics the characteristic sequential removal of compound classes seen in reservoir-degraded petroleum. The initial preferential removal of *n*-alkanes generates close to stoichiometric amounts of methane, principally by hydrogenotrophic methanogenesis. Our data imply a common methanogenic biodegradation mechanism in subsurface degraded oil reservoirs, resulting in consistent patterns of hydrocarbon alteration, and the common association of dry gas with severely degraded oils observed worldwide. Energy recovery from oilfields in the form of methane, based on accelerating natural methanogenic biodegradation, may offer a route to economic production of difficult-to-recover energy from oilfields.

The dominance of anaerobic hydrocarbon degradation, including methanogenesis, in subsurface biodegradation of oil is supported by the lack of sufficiently oxygenated formation waters to oxidize subsurface petroleum[7], the presence of anaerobic microorganisms in formation waters[8,9], the demonstration of anaerobic hydrocarbon degradation in laboratories[10,11] and metabolites of anaerobic hydrocarbon degradation in reservoir degraded petroleum[12]. Nevertheless, although many processes, including reduction of sulphate[10], nitrate[13] or iron[14] and methanogenesis, can be linked to hydrocarbon degradation[11,15], the specific pathway occurring in oil reservoirs remains poorly defined even though the primary controls of reservoir temperature history on biodegradation are well understood[6]. As most degraded oilfields show little evidence of sulphate reduction or carbonate cementation, despite removal of large proportions of petroleum carbon by microbial oxidation, we speculated that methanogenesis is the likeliest fate of most carbon dioxide produced as the terminal oxidation product during biodegradation[6]. Oilfield methane carbon isotopic signatures alone are equivocal in terms of indicating process, so we performed laboratory experiments to monitor the hydrocarbon composition of degraded oils and generated gases to elucidate probable mechanisms of hydrocarbon degradation in reservoirs.

Biodegradation mineralizes up to 60 weight per cent (wt%) of the non-degraded oil[6,16]. The fate of most of the mineralized carbon remains contested because, usually, gases produced from heavily degraded oilfields contain only marginally more CO_2 than gases produced from nearby non-degraded fields[17]. Heavily biodegraded oilfields are typically associated with dry methane-rich gases, possibly enriched in methane from biodegradation of C_2–C_5 alkanes[18] or from methanogenic oil biodegradation[17].

The carbon isotopic composition of methane ($\delta^{13}C_{CH4}$) associated with most subsurface biodegraded oil in marine petroleum systems ranges from −45‰ to −55‰ relative to the Pee Dee Belemnite (PDB) standard[17]; however, complex reservoir filling, degradation and mixing histories usually obscure definitive isotopic signals of origin. In contrast, the $\delta^{13}C_{CO2}$ associated with biodegraded oils is often isotopically very heavy, with values ranging from −25‰ to a maximum of +15‰ to +20‰ ($n = 7$ oilfields), indicative of closed system reduction of carbon dioxide to methane[17,19–21]. The subsurface mass balance of methane production over geological time is hampered by gas loss from shallow leaky biodegraded oilfields, so we examined the molecular systematics of hydrocarbon degradation under methanogenic or sulphate-reducing conditions, those most plausible for subsurface microbial hydrocarbon degradation.

The effect of (putatively anaerobic) biodegradation on the saturated hydrocarbon composition of crude oils in subsurface reservoirs is well documented, with a common sequence of removal of different compound classes. The most degradable compounds are straight-chain *n*-alkanes, followed by more resistant branched acyclic and monocyclic hydrocarbons, the most resistant polycyclic steroidal and triterpenoidal hydrocarbons[3,22–24], and some aromatic hydrocarbons[22,24]. In biodegraded reservoirs, alkylated naphthalenes and other two- and three-ringed aromatic hydrocarbons are only degraded after significant removal of *n*-alkanes and alteration of acyclic isoprenoids such as pristane and phytane[22,24,25]. In contrast, crude oils degraded under aerobic conditions in the laboratory can show removal of aromatic compounds such as alkylated naphthalenes before the alteration of *n*-alkanes[26]. Townsend *et al.*[27] observed that although the entire *n*-alkane fraction of a weathered Alaskan North Slope crude oil was consumed under both methanogenic and sulphate-reducing conditions in a laboratory microcosm, only the sulphate-reducing systems showed depletion of alkylnaphthalenes after 14 months of incubation. These observations demonstrate

[1]School of Civil Engineering and Geosciences, University of Newcastle, Newcastle upon Tyne, NE1 7RU, UK. [2]Petroleum Reservoir Group, Department of Geology and Geophysics, University of Calgary, Calgary, Alberta, T2A 1N4, Canada. [3]Norsk Hydro Oil & Energy, R&D Centre, Bergen, PO 7190, N-5020 Bergen, Norway.

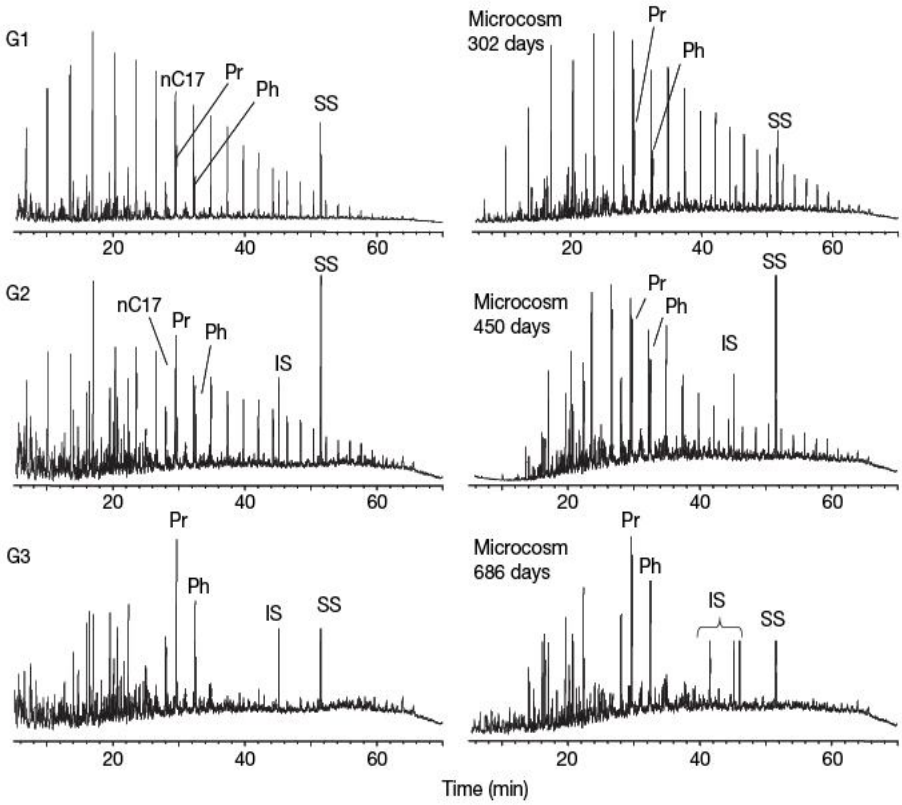

Figure 1 | Gas chromatograms of total hydrocarbon fractions from field and laboratory degraded oils. Left column, three North Sea (Gullfaks field) oils of different biodegradation levels (G1, G2 and G3). Right column, altered oils from three laboratory methanogenic microcosm experiments showing increasing levels of hydrocarbon biodegradation. Both suites of samples show systematic relative removal of *n*-alkanes relative to the isoprenoid alkanes pristane (Pr) and phytane (Ph). For clarity, peaks for spiked standards (marked IS and SS) have been truncated in samples G3 and the 686-day microcosm extract. Time 0 on the chromatograms, which are displayed from 5 to 70 minutes, corresponds to injection.

that biodegradation conditions do affect the relative rate of removal of different hydrocarbon classes.

The composition of biodegraded petroleum results from biodegradation overprinting the complex charging/filling/spilling/mixing history of the petroleum entering the trap. Thus comparison of global biodegraded oil compositions with those measured from degrading laboratory microcosms using a single starting oil sample is difficult and inappropriate. To assess the reaction pathways of crude-oil degradation under anaerobic conditions in laboratory microcosms we used a non-degraded oil from a North Sea field that shares a common source rock with biodegraded oil from the Gullfaks field. Gullfaks oil has been altered by biodegradation to varying degrees[7] and the field appears to have filled quickly with little evidence of any later charge with non-degraded oil (Fig. 1). Furthermore the reservoir is highly overpressured[28], containing saline formation waters

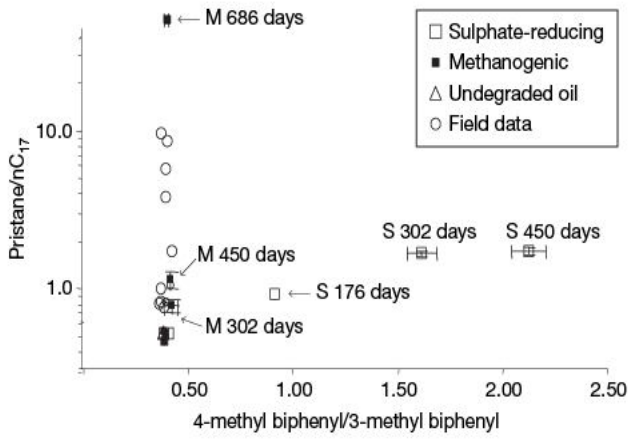

Figure 2 | Plot of the ratios of pristane to n-heptadecane against 4-methylbiphenyl to 3-methylbiphenyl abundances. Samples are from North Sea crude oil degraded in laboratory anaerobic microcosm experiments and from North Sea Gullfaks field crude oil. Error bars for the peak ratios are ±1 standard error ($n = 3$). M refers to laboratory incubations under methanogenic conditions and S refers to incubations under sulphate-reducing conditions. The M 686-day sample had complete removal of nC_{17} and the other *n*-alkanes. The laboratory methanogenic microcosm data and the field data plot along the same biodegradation trajectory with *n*-alkane degradation but no apparent aromatic hydrocarbon degradation, while the sulphate-reducing microcosm data show concomitant degradation of *n*-alkanes and aromatic hydrocarbons.

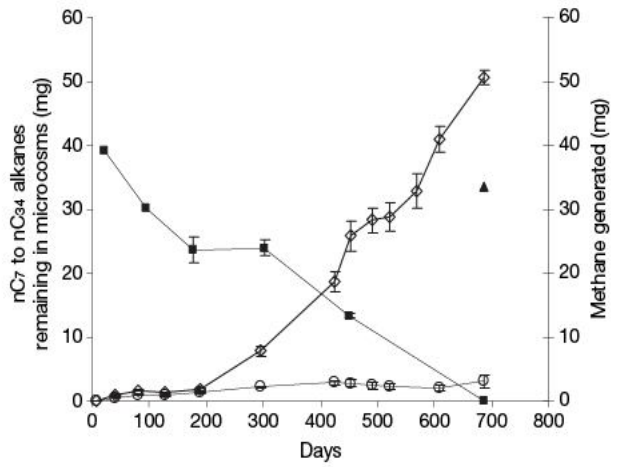

Figure 3 | *n*-alkane depletion and methane production during oil degradation. Loss of C_7–C_{34} *n*-alkanes (squares) and methane production (diamonds) from crude oil incubated under methanogenic conditions in laboratory microcosms (100 ml) for 686 days. The error bars show ±1 standard error ($n = 3$). Methane production from control microcosms without oil (open circles) are also shown for comparison to confirm the conversion of oil hydrocarbons to methane. The triangle represents the theoretical maximum methane production if all the *n*-alkanes in the added oil had been converted to methane with the stoichiometry described in ref. 11.

and thus has probably not received recent meteoric water to stimulate aerobic degradation.

The ratios of easily degradable to more resistant saturated and aromatic hydrocarbons (n-heptadecane/pristane and 4-methylbiphenyl/3-methylbiphenyl) from the Gullfaks oils are similar to those from oil degraded in the laboratory under methanogenic conditions (Fig. 2) with *n*-alkane degradation occurring before significant aromatic hydrocarbon destruction. This is clearly different from oils degraded under sulphate-reducing conditions where aromatic hydrocarbon degradation occurs concomitantly with alkane degradation. Alkylbiphenyl degradation is used here as a proxy for more pervasive aromatic hydrocarbon degradation, because alkylbiphenyls are not lost during sample workup.

Oil alkane conversion to methane in oil-degrading microcosms was confirmed by comparison of the methane yield in control microcosms that were not amended with oil (Fig. 3). Also, negligible amounts of methane with no obvious degradation of the oil *n*-alkanes were detected in microcosms containing an inhibitor of methanogenesis (2-bromethanesulphonic acid, BES). Furthermore, $^{13}CH_4$ enriched gas was produced in microcosms where the oil was spiked (7 atom% of *n*-alkanes) with labelled ^{13}C-hexadecane (Supplementary Fig. 3). The amount of methane produced (Fig. 3) is similar to that expected from methanogenic degradation of *n*-alkanes, using water as the co-reactant, as proposed by refs 11 and 15, though the mass of methane generated exceeded that predicted from the stoichiometric conversion of only *n*-alkanes in the crude oil (Fig. 3). The additional methane was probably from degradation of other hydrocarbons in the oil. We have previously[16,29] shown that the apparent sequential removal of *n*-alkanes and then branched alkanes during biodegradation is illusory and that several classes of compounds are removed in parallel to *n*-alkane removal but at lower rates.

The theoretical methane yield from alkane degradation is reflected in field gas isotope data. Carbon dioxide associated with heavily biodegraded oil reservoirs is highly enriched in ^{13}C, with $\delta^{13}C_{CO2}$ values up to +15 to +20‰ PDB. Figure 4 shows significantly enriched carbon dioxide and depleted methane carbon isotopic signatures from solution gases from heavily degraded oils (Peters and Moldowan[23], PM levels 4 to 5) of the Peace River oil sands area, compared to gases from less degraded oil fields (Gething) and pristine thermogenic gases found west of the Canadian oil sands[30]. Theoretically predicted curves (Fig. 4), represent the gas compositions at various levels of biodegradation (PM levels 1 to 9), assuming methane is derived from acetoclastic methanogenesis and reduction of carbon dioxide, with varying degrees of hydrocarbon conversion. With increasing hydrocarbon conversion, CO_2 becomes isotopically enriched, with methane showing a more complex depletion and enrichment curve.

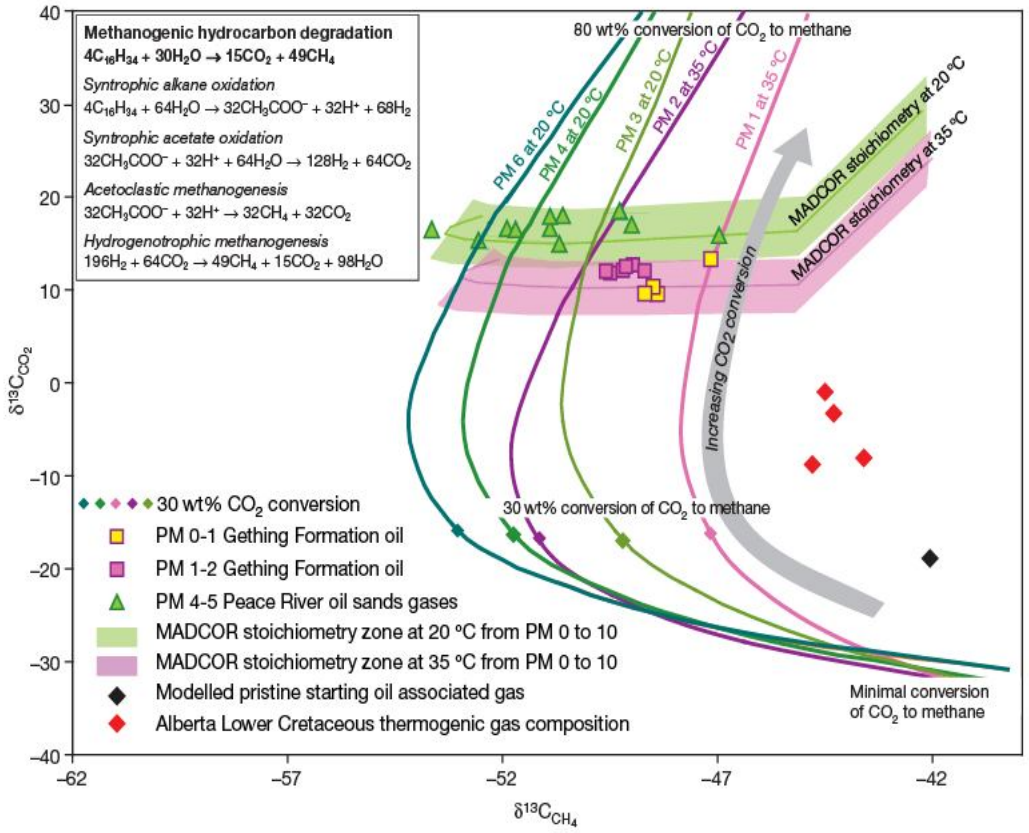

Figure 4 | Measured and modelled methane and carbon dioxide stable carbon isotopic compositions from degraded oil reservoir gases. Carbon isotopic composition of carbon dioxide and methane from gases co-produced with highly degraded oils from the Peace River Oil Sands area of western Canada. Data from gases associated with an equivalent non-biodegraded oil (initial oil) are also shown. The modelled solid lines on the diagram represent theoretically derived trajectories for the evolution of the gas compositions with increasing levels of biodegradation, as reflected by a PM scale equivalent (PM levels 1 to 9). The grey arrow indicates the direction of change in isotopic composition as progressively more CO_2 is reduced to methane. The isotopic composition is calculated assuming closed-Rayleigh fractionation using both hydrogenotrophic and acetoclastic methanogenesis, as described in the Supplementary Information. The region predicted to be occupied by gases produced with the stoichiometry suggested by MADCOR is shaded in green and pink. The different isotopic trajectories show the evolution of gas composition as a function of carbon dioxide conversion to methane when the crude-oil hydrocarbons are degraded to different extents. Two data sets are plotted. The Peace River bitumens (reservoir temperature 20 °C) are typically degraded to PM level 5, suggesting that the +15‰ to +20‰ compositions for the carbon in carbon dioxide reflect the conversion of approximately 60–65 wt% of alkane carbon to methane. The Gething Formation reservoired oils (reservoir temperature 35 °C) are typically degraded to PM levels 1 to 2, suggesting that the +10‰ to +12‰ compositions for the carbon in carbon dioxide again reflect approximately 60–65 wt% of alkane carbon to methane. This is in broad agreement with the conversion of 76 wt% alkane carbon to methane, as indicated by the MADCOR stoichiometry, which (although mechanistically different in detail) is that reported in ref. 11. The coloured boxes indicate the range of isotopic compositions of methane and CO_2 for the two reservoirs, assuming that approximately 80% of the methane is produced from hydrogenotrophic methanogenesis. Observation and modelled prediction broadly agree.

Closed-system Rayleigh isotope fractionation of methanogenic *n*-alkane degradation was modelled using published temperature-dependent carbon isotope fractionation factors, for acetoclastic and hydrogenotrophic methanogenesis (Supplementary Methods). We considered oil biodegraded to different degrees, assessed using mass of hydrocarbon lost. Degradation levels were converted to equivalent PM levels of degradation using data from naturally biodegraded oils. Degrading oil to PM levels of 3 to 5 with ~62.5 wt% CO_2 conversion to methane, based on the stoichiometry of methanogenic alkane degradation[11] (see reaction pathways on Fig. 4), predicts terminal $\delta^{13}C_{CO2}$ values of +15 to +20‰ PDB at 20 °C, which is coincident with CO_2 carbon isotopic compositions of most gases at present-day reservoir conditions in the Peace River oil sands (Fig. 4). The range of $\delta^{13}C_{CH4}$ from −47‰ to −52‰ can be explained by variation in oil charge and leakage of gases at shallow burial depths (Supplementary Information). To predict field data accurately, a combination of acetoclastic and hydrogenotrophic methanogenesis was necessary. The best fit to data was obtained with 75%–92% of the methanogenesis channelled through hydrogenotrophic methanogenesis. This is consistent with the methanogen community composition observed in oil-degrading microcosms that were dominated by hydrogen-oxidizers (86%–87% of clones in archaeal 16S ribosomal RNA gene libraries; Supplementary Table 2).

Thus, highly enriched CO_2 carbon isotopic signatures in heavily degraded oils[18] and laboratory data both suggest that methanogenic hydrocarbon degradation occurs predominantly via syntrophic oxidation of alkanes to acetate and hydrogen. This assumption is corroborated by the dominance of *Syntrophus* sp. in the methanogenic microcosms (Supplementary Fig. 4), similar to those identified in ref. 11. However, about 75% of the carbon must be directly channelled through hydrogenotrophic methanogenesis, implying that the acetate must be oxidized syntrophically to CO_2 and hydrogen before being converted to methane. We refer to this process, which we infer to be the predominant biodegradation process in reservoirs, as methanogenic alkane degradation dominated by CO_2 reduction (MADCOR). The occurrence of syntrophic acetate oxidation in oil-degrading microcosms, which would be required to explain the predominance of CO_2 reduction, was demonstrated using ^{13}C-labelled acetate (Supplementary Information). The effect on $\delta^{13}C_{CH4}$ and $\delta^{13}C_{CO2}$ of reducing increasing amounts of CO_2 to methane with hydrogen is illustrated in Fig. 4. We note that field data correspond to the MADCOR stoichiometry, indicating that no external source of hydrogen is required to explain observed gas isotope values or the predominance of methanogenic CO_2 reduction. Thus all hydrogen required is generated during syntrophic alkane oxidation and coupled syntrophic acetate oxidation.

The occurrence of anaerobic degradation of crude oils in subsurface reservoirs under methanogenic conditions explains the consistent hydrocarbon compositional patterns seen in degraded oils worldwide and their association with dry gas accumulations[17,18]. This identification of the pathways inherent in subsurface biodegradation facilitates the engineering of processes to accelerate naturally slow methanogenic biodegradation to recover energy from heavy oilfields as methane, rather than oil. Such processes could enable us to move away from high-CO_2-emitting heavy-oil recovery technologies while maintaining existing infrastructures.

METHODS SUMMARY

Laboratory crude-oil degradation experiments were set up under anoxic conditions in glass 120 ml serum bottle microcosms. Each microcosm comprised a carbonate-buffered brackish medium containing sources of nitrogen and phosphorus, vitamins, and trace minerals, made up with deionized water and sediment inoculum. Sulphate-reducing microcosms were established by the addition of SO_4^{2-}. Methanogenic microcosms were established by the exclusion of added electron acceptors. North Sea crude oil (300 mg) was added to all microcosms except control flasks to determine the extent of methanogenesis in the absence of crude oil. Headspace gas aliquots were periodically removed from the microcosms and analysed for carbon dioxide and methane using gas chromatography-mass spectrometry (GC-MS). After removal of an aliquot for microbiological analyses, the contents of the microcosm bottles from each sampling point were subjected to alkaline saponification and liquid–liquid solvent extraction to obtain the organic soluble fractions. Aliquots of oils or the solvent extracts were separated into saturated and aromatic hydrocarbon fractions, before their analysis by GC-MS.

Bacterial and archaeal 16S ribosomal RNA genes were amplified by polymerase chain reaction (PCR) from microcosm DNA using oligonucleotide primers specific for bacteria and archaea, respectively. Gene fragments were subsequently purified, cloned, sequenced and subjected to comparative analysis to assign phylogenetic identity.

Gas and oil samples were taken at wellheads in sealable metal containers after extensive purging of collection lines with fresh well fluids. Gases were analysed by gas chromatography using thermal conductivity detection to determine composition. Carbon isotopic compositions of carbon dioxide and methane were determined using gas chromatography-isotope ratio mass spectrometry at a commercial laboratory.

Closed-system Rayleigh isotope fractionation was simulated isothermally at reservoir temperatures for the carbon species involved in biodegradation of petroleum via syntrophic alkane oxidation, syntrophic acetate oxidation, acetoclastic methanogenesis and hydrogenotrophic methanogenesis.

Full Methods and any associated references are available in the online version of the paper at www.nature.com/nature.

Received 23 July; accepted 13 November 2007.
Published online 12 December 2007.

1. Roadifer, R. E. in *Exploration for Heavy Crude Oil and Natural Bitumen* (ed. Meyer, R.F.) 3–23 (American Association of Petroleum Geologists, Tulsa, 1987).
2. Winters, J. C. & Williams, J. A. Microbial Alteration of Crude Oil in the reservoir. *Am. Chem. Soc. Div. Petrol. Chem. Preprints* 14, E22–E31 (1969).
3. Connan, J. in *Advances in Petroleum Geochemistry* Vol. 1 (eds Brooks, J. & Welte, D. H.) 299–335 (Academic Press, London, 1984).
4. Krejci-Graf, K. Rule of density of oils. *Bull. Am. Assoc. Petrol. Geol.* 16, 1038 (1932).
5. Palmer, S. E. in *Organic Geochemistry* (eds Macko, S. A. & Engel, M. H.) 511–534 (Plenum Press, New York, 1993).
6. Head, I. M., Jones, D. M. & Larter, S. R. Biological activity in the deep subsurface and the origin of heavy oil. *Nature* 426, 344–352 (2003).
7. Horstad, I., Larter, S. R. & Mills, N. A. Quantitative model of biological petroleum degradation within the Brent Group reservoir in the Gullfaks field, Norwegian North Sea. *Org. Geochem.* 19, 1–3,–107–117 (1992).
8. Bastin, E. Microorganisms in oilfields. *Science* 63, 21–24 (1926).
9. Magot, M., Connan, J. & Crolet, J.-L. Les bactéries des gisements pétroliers. *Recherche* 228, 936–937 (1994).
10. Reuter, P. *et al.* Anaerobic oxidation of hydrocarbons in crude oil by new types of sulfate-reducing bacteria. *Nature* 372, 455–458 (1994).
11. Zengler, K., Richnow, H. H., Rossello-Mora, R., Michaelis, W. & Widdel, F. Methane formation from long-chain alkanes by anaerobic microorganisms. *Nature* 401, 266–269 (1999).
12. Aitken, C. M., Jones, D. M. & Larter, S. R. Anaerobic hydrocarbon biodegradation in deep subsurface oil reservoirs. *Nature* 431, 291–294 (2004).
13. Rabus, R. & Widdel, F. Anaerobic degradation of ethylbenzene and other aromatic hydrocarbons by new denitrifying bacteria. *Arch. Microbiol.* 163, 96–103 (1995).
14. Lovley, D. R. *et al.* Oxidation of aromatic contaminants coupled to microbial iron reduction. *Nature* 339, 297–300 (1989).
15. Anderson, R. T. & Lovley, D. R. Biogeochemistry—hexadecane decay by methanogenesis. *Nature* 404, 722–723 (2000).
16. Larter, S. *et al.* The controls on the composition of biodegraded oils in the deep subsurface. Part II. Geological controls on subsurface biodegradation fluxes and constraints on reservoir fluid property prediction. *Bull. Am. Assoc. Petrol. Geol* 90, 921–938 (2006).
17. Larter, S. R. *et al.* in *Petroleum Geology: North-West Europe and Global Perspectives* (eds Doré, A. G. & Vining, B. A.) 633–639 (Geological Society, London, 2005).
18. Larter, S. & di Primio, R. Effects of biodegradation on oil and gas field PVT properties and the origin of oil rimmed gas accumulations. *Org. Geochem.* 36, 299–310 (2005).
19. Boreham, C. J., Hope, J. M. & Hartung-Kagi, B. Understanding source, distribution and preservation of Australian natural gas: A geochemical perspective. *Aus. Petrol. Explor. Assoc. J.* 41, 523–547 (2001).
20. Pallaser, R. J. Recognising biodegradation in gas/oil accumulations through the $\delta^{13}C$ composition of gas components. *Org. Geochem.* 31, 1363–1373 (2000).
21. Masterson, W. D., Dzou, L. I. P., Holba, A. G., Fincannon, A. L. & Ellis, L. Evidence for biodegradation and evaporative fractionation in West Sak, Kuparuk and Prudhoe Bay field areas, North Slope, Alaska. *Org. Geochem.* 32, 411–441 (2001).
22. Volkman, J. K., Alexander, R., Kagi, R. I., Rowland, S. J. & Sheppard, P. N. Biodegradation of aromatic hydrocarbons in crude oils from the Barrow Sub-basin of Western Australia. *Org. Geochem.* 6, 619–632 (1984).

23. Peters, K. E. & Moldowan, J. M. *The Biomarker Guide* 252–265 (Prentice Hall, New York, 1993).
24. Wenger, L. M., Davis, C. L. & Isaksen, G. H. Multiple controls on petroleum biodegradation and impact in oil quality. *SPE Reservoir Eval. Engin.* **5**, 375–383 (2002).
25. Williams, J. A. *et al*. Biodegradation in South Texas oils—effects on aromatics and biomarkers. *Org. Geochem.* **10**, 451–461 (1986).
26. Fedorak, P. M. & Westlake, D. W. S. Microbial degradation of aromatics and saturates in Prudhoe Bay crude oil. *Can. J. Microbiol.* **27**, 432–443 (1981).
27. Townsend, G. T., Prince, R. C. & Suflita, J. M. Anaerobic oxidation of crude oil hydrocarbons by the resident microorganisms of a contaminated anoxic aquifer. *Environ. Sci. Technol.* **37**, 5213–5218 (2003).
28. Karlsson, W. in *Habitat of Hydrocarbons on the Norwegian Continental Shelf* (eds Spencer, A. M. *et al*.) 181–197 (Graham & Trotman, London, 1986).
29. Larter, S. *et al*. The controls on the composition of biodegraded oils. Part 1. Biodegradation rates in petroleum reservoirs in the deep subsurface. *Org. Geochem.* **34**, 601–613 (2003).
30. Adams, J. J., Riediger, C. L., Fowler, M. G. & Larter, S. R. Thermal controls on biodegradation around the Peace River tar sands: paleo-pasteurization to the west. *J. Geochem. Explor.* **89**, 1–4 (2006).

Supplementary Information is linked to the online version of the paper at www.nature.com/nature.

Acknowledgements We thank B. Huizinga, A. Murray, M. Rangel, L. Trindade, R. Patience and M. Whittaker for comments and also the members of the BACCHUS2 biodegradation consortium for support, discussions and permission to publish. The BACCHUS2 members are Agip ENI, BP/Amoco, ChevronTexaco, ConocoPhillips, Norsk Hydro, Petrobras, Saudi Aramco, Shell, Statoil, Total and Woodside. We thank Norsk Hydro for their extended support of our biodegradation research and A. Wilhelms, J. Leyris, T. Liengen and J. Beeder for discussions on the feasibility of biological recovery of crude oil as methane. We also thank N. Mills of Applied Petroleum Technology (APT), Norway, for provision of samples. We acknowledge support from the Natural Environment Research Council (NERC); the Alberta Ingenuity Fund (AIF Scholarships to S.R.L. and J.J.A.), the National Science and Engineering Research Council (NSERC); and the Canada Foundation for Innovation (CFI).

Author Information Reprints and permissions information is available at www.nature.com/reprints. The authors declare competing financial interests: details accompany the full-text HTML version of the paper on www.nature.com/nature. Correspondence and requests for materials should be addressed to S.R.L. (slarter@ucalgary.ca).

LETTERS

Seismic identification of along-axis hydrothermal flow on the East Pacific Rise

M. Tolstoy[1], F. Waldhauser[1], D. R. Bohnenstiehl[1]†, R. T. Weekly[1] & W.-Y. Kim[1]

Hydrothermal circulation at the axis of mid-ocean ridges affects the chemistry of the lithosphere and overlying ocean, supports chemosynthetic biological communities and is responsible for significant heat transfer from the lithosphere to the ocean[1–3]. It is commonly thought that flow in these systems is oriented across the ridge axis, with recharge occurring along off-axis faults[4–6], but the structure and scale of hydrothermal systems are usually inferred from thermal and geochemical models constrained by the geophysical setting[7–9], rather than direct observations. The presence of microearthquakes may shed light on hydrothermal pathways by revealing zones of thermal cracking where cold sea water extracts heat from hot crustal rocks, as well as regions where magmatic and tectonic stresses create fractures that increase porosity and permeability. Here we show that hypocentres beneath a well-studied hydrothermal vent field on the East Pacific Rise cluster in a vertical pipe-like zone near a small axial discontinuity, and in a band that lies directly above the axial magma chamber. The location of the shallow pipe-like cluster relative to the distribution and temperature of hydrothermal vents along this section of the ridge suggests that hydrothermal recharge may be concentrated there as a consequence of the permeability generated by tectonic fracturing. Furthermore, we interpret the band of seismicity above the magma chamber as a zone of hydrothermal cracking, which suggests that hydrothermal circulation may be strongly aligned along the ridge axis. We conclude that models that suggest that hydrothermal cells are oriented across-axis, with diffuse off-axis recharge zones, may not apply to the fast-spreading East Pacific Rise.

The mass and energy transfer produced by hydrothermal circulation at the mid-ocean-ridge axis has been studied widely since deep-sea hydrothermal vent systems were discovered[10] in 1977. The location of seawater recharge has been particularly elusive: although it is most commonly inferred to be along off-axis faults[4–6], it also has been proposed that down-flow may occur on-axis[6,11,12]. One of the best-studied mid-ocean-ridge vent fields is at 9° 50′ N on the East Pacific Rise (EPR), where detailed biological, chemical, geophysical and geological studies have monitored and characterized this site for more than 15 years. Indeed, a full volcanic cycle has now been observed with a 1991–92 eruption[13,14] paved over by a 2006 eruption following more than a 2-yr build-up in seismicity rate[15].

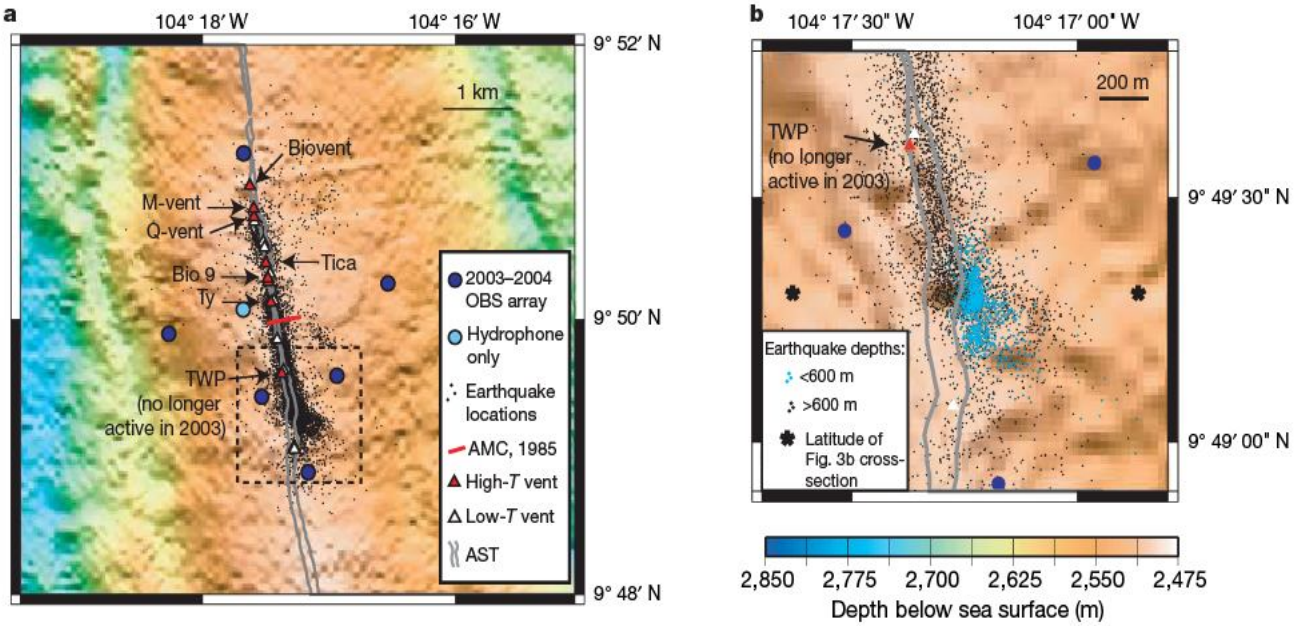

Figure 1 | Bathymetric site map showing earthquake epicentres. a, Double-difference epicentre locations (black dots) within the OBS array (blue circles). Also shown are sites of high- and low-temperature venting, margins of the AST (S. A. Soule, personal communication) and imaged AMC[16]. Data include only well-located events (~7,000) with azimuthal gaps ≤180° and more than five defining phase pairs, excluding more poorly located seismic events outside the array. Dashed box outlines area of Fig. 1b. **b**, Segment end where shoaling pipe seismicity is centred. Shallowest events (cyan dots) show a remarkable fit to the kink along the eastern wall of the AST, and form two distinct groups separated by a gap of a few tens of metres and fanning out at depth. Black asterisk indicates the latitude of the cross-section shown in Fig. 3b.

[1]Lamont-Doherty Earth Observatory of Columbia University, 61 Route 9W, Palisades, New York 10964-8000, USA. †Present address: Marine, Earth and Atmospheric Sciences, Campus Box 8208, North Carolina State University, Raleigh, North Carolina 27695-8208, USA.

Between October 2003 and April 2004, nine two-component (vertical and hydrophone) ocean bottom seismometers (OBSs) were deployed in an array of roughly 4 × 4 km centred at 9° 50′ N on the EPR. Seven continuously recording instruments returned hydrophone data, and six returned vertical-component seismometer data (Fig. 1). Here we present high-resolution double-difference locations for ~7,000 earthquakes that occurred within the array during the 7-month observational period (see Methods Summary). The average relative location error is ~50 m, and the seismicity is closely correlated with geological features identified using high-resolution seafloor imagery and active-source subsurface imaging, implying small absolute errors.

Local event magnitudes within the array range from M_L −1.8 to 1.4, with a magnitude of completeness of roughly M_L −0.5. Detection thresholds were lowest at the southern end of the array near the highest density of working OBSs, and the minimum magnitude of detectable earthquakes increases with depth because of attenuation. Maximum magnitude also increases with depth above the axial magma chamber (AMC) reflector (~1.43 km)[16] (see Supplementary Fig. 3).

A clearly defined zone of seismicity coincides almost directly with the location and width (~500 m) of the AMC (Fig. 1). The most concentrated band of seismicity, around 200–300 m wide, lies directly underneath the axial summit trough (AST) where the dykes feeding the 1991–92 and the 2006 eruptions were centred[13,15]. This zone lies to the western side of the AMC, suggesting dyke initiation near the chamber's margins where maximum extensional stress concentrations are predicted for pressurized lens-like cavities[17]. The seismic reflection data were collected in 1985, before the 1991–92 eruption, so the AMC may have changed size or location within the 18–19 years before our study. However, the presence of fairly consistent AMC depth at a given spreading rate[18] suggests that its position remains stable between eruptions.

Cross-sections of the hypocentre distribution (Figs 2 and 3) reveal seismicity extending from the upper 100 m to depths of more than 2 km, with a pattern of seismicity that is narrow near the surface and fans out at depth. Within the southern end of the array, the shallowest hypocentres track the eastern wall of the AST (Fig. 1b) and concentrate near a ~100-m kink in the AST. Earthquakes associated with

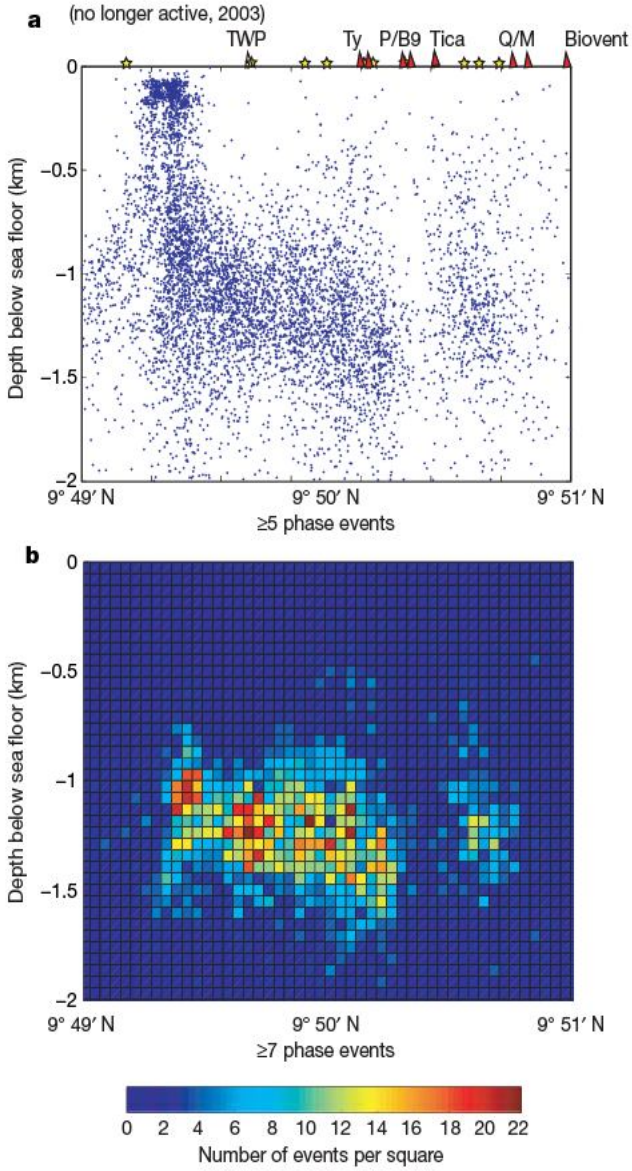

Figure 2 | Along-axis cross-sections of seismicity. **a**, Events located using five or more seismic phase pairs observed at common stations. Sites of high-temperature (red triangles) and low-temperature (yellow stars) vents are shown. B9 is vent Bio 9; P-vent and Bio 9 are separate but close to each other. Lack of seismicity below TWP (open triangle) is consistent with observations that this former high-temperature vent was inactive in 2003 (ref. 22). **b**, Density plot showing best-recorded events defined by seven or more seismic phase pairs (see also Supplementary Fig. 2). Applying this threshold excludes many of the shallow, small-magnitude events, but reveals a band of seismicity ~500 m thick that deepens to the north. A distinct ~200-m horizontal gap in seismicity is apparent at ~9° 50.3′ N, suggesting a discontinuity within the AMC.

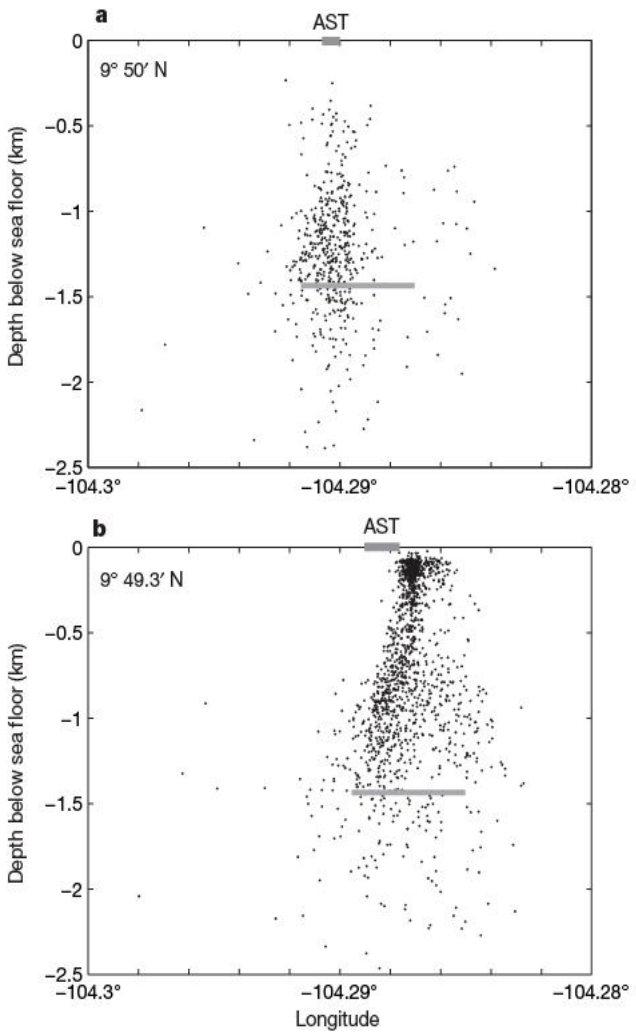

Figure 3 | Across-axis cross-sections of seismicity. Location of the AST is shown in grey box at zero depth. AMC reflector location is marked by grey line at 1.43 km depth[16]. **a**, Profile 200 m wide, centred at 9° 50′ N at the same latitude at which the AMC is imaged in Fig. 1a. **b**, Profile 200 m wide, centred at 9° 49.3′ N across the interpreted down-flow zone (location shown in Fig. 1b). AMC position is inferred from measurements to the north. Seismicity lines up along the eastern AST wall, with a clean edge swooping under the AST with depth, possibly following a bounding fracture surface.

this fourth-order segment boundary[11] form two pipe-like clusters at shallow depth, with the northern cluster fanning out to the north and the southern cluster fanning southward. At depth, the northern cluster has a sharply defined vertical edge suggesting a porosity and/or permeability boundary consistent with crust to the south being slightly older where the kink offsets the southern crustal section ~100 m to the west. We interpret this feature as a hydrothermal down-flow zone, where cold sea water is being entrained into the crust and travelling down to the hydrothermal cracking zone.

This shallowest seismicity at the segment end is likely to be tectonically driven, and its distribution is consistent with the stress field predicted at the tip of a propagating crack[19]. The location 9° 50′ N is the focus of the 1991 and 2006 eruptions, and thus the tips of this segment are more likely to be actively propagating than adjacent segments, perhaps accounting for the dominance of the seismicity on this segment end. This shallow tectonically driven seismicity may form a zone of permeability down which fluids can reach hotter rock where hydrothermal cracking could initiate.

Submersible dives along this 9° 49′ N area of the AST have noted a historic lack of hydrothermal venting and macro-faunal communities (T. Shank, personal communication), supporting the idea that water is going into the crust and not out at this location. Previous studies have suggested that precipitation of anhydrite within the down-flow zone would rapidly clog hydrothermal pathways, requiring a large recharge zone extending across the near-axis flanks in order to maintain hydrothermal systems for decades[9]. The coincidence of this interpreted down-flow zone with an offset in the AST, however, suggests that a high permeability zone may be maintained by stress concentrations within the tip zones of spreading segments[20] and that recharge can be narrowly focused on-axis.

Temporal snapshots show that despite increasing seismicity, the basic structure we image is consistent throughout the 7-month deployment (see Supplementary Fig. 4). Focused down-welling would result in an along-axis thermal gradient that develops through time following an eruption. This prediction is supported by the gradual cooling[21] and eventual cessation of venting at Tube Worm Pillar (TWP)[22], closest to the interpreted down-flow zone, as well as a consistent pattern of heating towards the centre of the segment and cooling towards the ends[21] (see Supplementary Information). Earthquakes recorded during the 22 January 2006 eruption, along with lava effusion rates and plume distribution, suggest that dyking may have initiated in the area 9° 50′ to 9° 50.5′ N (ref. 15). This implies that dyking started where the AMC was least chilled by proximity to down-flow.

An along-axis density plot of the best-recorded (that is, larger magnitude) earthquakes (Fig. 2b) shows a well-defined band of seismicity, around 500 m thick, directly above the AMC. This band is interpreted as a zone of hydrothermal cracking[23,24]. Previous detailed studies of AMC depth on the southern EPR have shown very consistent AMC depths for profiles within 1–2 km of each other, with deepening of the AMC by ~200 m occurring on a length scale of ~100 km(ref. 25). Therefore the slightly sloped pattern of the seismicity cloud is probably due to along-axis thermal trends, or three-dimensional velocity structure that was unaccounted for, rather than short-scale deepening of the AMC along-axis.

The along-axis earthquake distribution shows a sustained ~200-m gap in seismicity around 9° 50.3′ N. This latitude has been associated with differences in the chemistry of diffuse vents at the Bio 9 area versus the Ty/Io and TWP area[26] (Ty and Io are separate but very close chimneys). The gap may thus represent a boundary or transition in the AMC, suggesting segregation of magma at a scale finer than fourth-order discontinuities[11], and perhaps indicating fine-scale transitions from mush to melt as observed in reflection data elsewhere on the EPR[23].

The shoaling of seismicity into a narrower zone underneath the high-temperature vents at 9° 50′ N (Fig. 3a) suggests that the earthquakes in this region may delineate the up-flow area of the circulation cell. Because of the configuration of the OBS network, shallow events are better resolved beneath the down-flow zone than beneath the active vent area between 9° 50′ N and 9° 51′ N. Consequently, better-defined pipes may exist beneath the up-flow zone.

Our results are not consistent with the shoaling heat source predicted from observations of increasing vent temperatures and changes in fluid chemistry[22]. More than 10 yr of focused up-flow of high-temperature water beneath vents in the 9° 50′ N area may instead have warmed the upper crust and reduced the conductive heat loss. Combined with the likely input of melt into the magma body before the 2006 eruption, this may have helped to fuel the increasing temperatures[21] at the 9° 50′ N focused vents.

Seismicity levels and maximum earthquake magnitude begin to decrease abruptly with increasing depth at ~200 m above the AMC reflector (Supplementary Fig. 3). This may reflect a transition to semi-brittle behaviour with increasing temperature, as well as the potential for greater seismic attenuation along ray paths passing through or near the AMC. Some hypocentres are observed up to a kilometre or more beneath the melt lens, but further work is required to rule out location artefacts.

Notably, we do not detect concentrations of microearthquakes along the flanking margins of the AMC as expected from tomographic models[8] that require significant heat removal on the near-axis flanks. Although we see no evidence for cross-axis circulation or hydrothermal cooling on the flanks, we cannot rule out that it may be happening aseismically or at magnitude levels below our detection capability.

The fact that the across-axis focus is under 500 m wide means that the reservoir volume may be relatively small, which when combined with high heat flow[27] implies that residence times for fluids are likely to be short[6], perhaps less than a year (see Methods). The interpreted hydrothermal cell represents a snapshot in time, and it is likely that

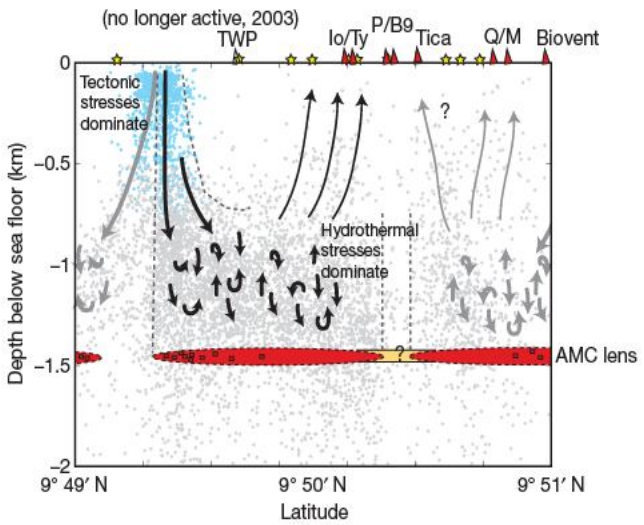

Figure 4 | Cartoon illustrating proposed hydrothermal cell structure. This model shows down-flow at fourth-order discontinuities[11], with the northern vents fed by a down-flow zone at the ~9° 51.5′ N fourth-order discontinuity, and the southern vents fed by the ~9° 49.25′ N offset. The features of the best-defined hydrothermal cell are shown with black arrows, and the features inferred in adjacent cells are shown with grey arrows. Light blue dots illustrate the area where tectonic stresses are likely to dominate earthquake generation, creating a zone of permeability. Light grey dots illustrate where hydrothermal stresses probably dominate. The exact location of this transition is not well constrained. Changes in source from the northern and southern cells may occur between the Ty/Io and the Bio 9 (B9)/P-vent. TWP and Biovent, the closest vents to the inferred down-flow zones, both show decreases in temperature with time, whereas the central vents have been steadily increasing in temperature since about 1994 (ref. 21). Prolonged cooling close to the inferred down-flow zone may lead to a decreasing percentage melt in the AMC. The seismicity gap at ~9° 50.3′ N may represent a break or transition zone (such as melt to mush) within the AMC.

temporal changes in depth, width and intensity occur, with consequences for fluid temperature, chemistry and associated biology. However, microearthquake patterns show no indication of temporal variability in the basic structures they outline, and temperature data support the idea that focused down-flow may be sustained over a decadal timescale at locations of increased tectonic stress (Supplementary Figs 4 and 5). Therefore, it is clear that models showing hydrothermal cells dominantly across-axis may not apply to the fast-spreading EPR. Instead, we interpret flow as narrowly focused along-axis (Fig. 4) on the path of recent dyking where cooling stresses probably result in increased porosity, and heat is most abundant.

METHODS SUMMARY

Analyst-reviewed arrival time picks for P- and S-waves were associated to a total of 16,079 earthquakes in and outside the array. Initial hypocentre locations for a total of 13,911 events recorded by at least four stations were computed using the program *Hypoinverse*[28]. Depth-dependent P- and S-wave velocity models were used to predict travel times and partial derivatives. The velocity models were computed from 476 well-recorded events using the program *Velest*[29]. *Velest* minimizes P- and S-wave travel-time residuals by simultaneous inversion for changes in layer velocities (V_P and V_S), hypocentral parameters, and station corrections.

A total of 35,019 P- and 22,005 S-wave picks were used to locate the 7,362 events that occur within the array of seven stations (azimuthal station gap $<180°$), and that are presented in this study. On average, the nearest station is 530 m away from each event (horizontally), the farthest station 3 km. Absolute errors computed by *Hypoinverse* have a 1σ median of 0.47 km horizontally and 1.15 km in depth. The root mean square (r.m.s.) of the final travel-time residuals is 32 ms.

We minimize the bias from remaining model errors in the *Hypoinverse* locations by applying the double-difference algorithm *hypoDD*[30] to a total of about 900,000 P- and S-wave differential travel times formed from the phase picks of pairs of events observed at common stations. The algorithm inverts the differential time residuals to solve for the vector connecting the hypocentres. The r.m.s. of the final differential time residuals is 0.010 s, and relative location errors estimated from a bootstrap analysis of the final double-difference vector are 50 m on average.

Full Methods and any associated references are available in the online version of the paper at www.nature.com/nature.

Received 11 November 2006; accepted 26 October 2007.

1. Slater, J. G., Jaupart, C. & Glason, D. The heat flow through oceanic and continental crust and the heat loss of the Earth. *Rev. Geophys. Space Phys.* **18**, 269–311 (1980).
2. Stein, C. & Stein, S. Constraints on hydrothermal heat flux through the oceanic lithosphere from global heat flow. *J. Geophys. Res.* **99**, 3081–3095 (1994).
3. Elderfield, H. & Schultz, A. Mid-ocean ridge hydrothermal fluxes and the chemical composition of the ocean. *Annu. Rev. Earth Planet. Sci.* **24**, 191–224 (1996).
4. Lowell, R. P., Rona, P. A. & Von Herzen, R. P. Seafloor hydrothermal systems. *J. Geophys. Res.* **100**, 327–352 (1995).
5. Kelley, D. S., Baross, J. A. & Delaney, J. R. Volcanoes, fluids and life at mid-ocean ridge spreading centers. *Annu. Rev. Earth Planet. Sci.* **30**, 385–491 (2002).
6. Fisher, A. T. in *Energy and Mass Transfer in Marine Hydrothermal Systems* Vol. 3 (eds Halbach, P. E., Tunnicliffe, V. & Hein, J. R.) 29–52 (Dahlem Univ. Press, Berlin, 2003).
7. Johnson, H. P., Becker, K. & Von Herzen, R. Near-axis heat flow measurements on the northern Juan de Fuca Ridge: Implications for fluid circulation in oceanic crust. *Geophys. Res. Lett.* **20**, 1875–1878 (1993).
8. Dunn, R. A., Toomey, D. R. & Solomon, S. C. Three-dimensional seismic structure and physical properties of the crust and shallow mantle beneath the East Pacific Rise at 9° 30′ N. *J. Geophys. Res.* **105**, 23537–23555 (2000).
9. Lowell, R. P. & Yao, Y. Anhydrite precipitation and the extent of hydrothermal recharge zones at ocean ridge crests. *J. Geophys. Res.* **107**, doi:10.1029/2001JB001289 (2002).
10. Corliss, J. B. *et al.* Submarine thermal springs on the Galapagos rift. *Science* **203**, 1073–1083 (1979).
11. Haymon, R. M. *et al.* Hydrothermal vent distribution along the East Pacific Rise crest (9°09′–54′ N) and its relationship to magmatic and tectonic processes on fast-spreading mid-ocean ridges. *Earth Planet. Sci. Lett.* **104**, 513–534 (1991).
12. McDuff, R. E. in *Seafloor Hydrothermal Systems* (eds Humphris, S. E., Zierenberg, R. A., Mullineaux, L. S. & Thomson, R. E.) 357–368 (American Geophysical Union, Washington DC, 1995).
13. Haymon, R. M. *et al.* Volcanic eruption of the mid-ocean ridge along the East Pacific Rise crest at 9°45–52′ N: Direct submersible observations of seafloor phenomena associated with an eruption event in April, 1991. *Earth Planet. Sci. Lett.* **119**, 85–101 (1993).
14. Rubin, K., Macdougall, J. D. & Perfit, M. R. 210Po–210Pb dating of recent volcanic eruptions on the sea floor. *Nature* **368**, 841–844 (1994).
15. Tolstoy, M. *et al.* A seafloor spreading event captured by seismometers. *Science* **314**, 1920–1922, doi:0.1126/science.1133950 (2006).
16. Kent, G. M., Harding, A. J. & Orcutt, J. A. Distribution of magma beneath the East Pacific Rise between the Clipperton Transform and the 9° 17′ N deval from forward modelling of common depth point data. *J. Geophys. Res.* **98**, 13971–13995 (1993).
17. Bohnenstiehl, D. R. & Carbotte, S. Faulting patterns near 19°30′ S on the East Pacific Rise: Fault formation and growth at a superfast spreading center. *Geochem. Geophys. Geosyst.* **2**, doi:10.1029/2001GC000156 (2001).
18. Purdy, M., Kong, L. S. L., Christeson, G. L. & Solomon, S. C. Relation between spreading rate and the seismic structure of mid-ocean ridges. *Nature* **355**, 815–817 (1992).
19. Floyd, J. S., Tolstoy, M. & Mutter, J. C. Seismotectonics of mid-ocean ridge propagation in Hess Deep. *Science* **298**, 1765–1768 (2002).
20. Curewitz, D. & Karson, J. A. in *Faulting and Magmatism at Mid-Ocean Ridges* (eds Buck, W. R., Delaney, P. T., Karson, J. A. & Lagabrielle, Y.), Geophysical Monograph 106 117–136 (American Geophysical Union, Washington DC, 1998).
21. Scheirer, D. S., Shank, T. M. & Fornari, D. J. Temperature variations at diffuse and focused flow hydrothermal vent sites along the northern East Pacific Rise. *Geochem. Geophys. Geosyst.* **7**, doi:10.1029/2005GC001094 (2006).
22. Von Damm, K. L. in *Mid-Ocean Ridges: Hydrothermal Interactions between the Lithosphere and Ocean* Geophysical Monograph, **148**, 187–217 (American Geophysical Union, Washington DC, 2004).
23. Singh, S. C., Collier, J. S., Harding, A. J., Kent, G. M. & Orcutt, J. A. Seismic evidence for a hydrothermal layer above the solid roof of the axial magma chamber at the southern East Pacific Rise. *Geology* **27**, 219–222 (1999).
24. Wilcock, W. S. D., Archer, S. D. & Purdy, G. M. Microearthquakes on the Endeavour segment of the Juan de Fuca Ridge. *J. Geophys. Res.* **107**, doi:10.1029/2001JB000505 (2002).
25. Tolstoy, M., Harding, A. J. & Orcutt, J. A. Deepening of the axial magma chamber toward the Garret Fracture Zone from multichannel data. *J. Geophys. Res.* **102**, 3097–3108 (1997).
26. Von Damm, K. L. & Lilley, M. D. in *The Subsurface Biosphere at Mid-Ocean Ridges* Geophysical Monograph 144 245–268 (American Geophysical Union, Washington DC, 2004).
27. Ramondenc, P., Leonid, N. G. A., Von Damm, K. L. & Lowell, R. P. The first measurements of hydrothermal heat output at 9degrees 50′ N, East Pacific Rise. *Earth Planet. Sci. Lett.* **245**, 487–497 (2006).
28. Klein, F. W. User's guide to HYPOINVERSE2000, a Fortran program to solve for earthquake locations and magnitudes. Open-file Report 02–171 (US Geological Survey, 2002).
29. Kissling, E., Ellsworth, W. L., Eberhartphillips, D. & Kradolfer, U. Initial reference models in local earthquake tomography. *J. Geophys. Res.* **99**, 19635–19646 (1994).
30. Waldhauser, F. & Ellsworth, W. L. A double-difference earthquake location algorithm: Method and application to the Northern Hayward Fault, California. *Bull. Seism. Soc. Am.* **90**, 1353–1368 (2000).
31. Vera, E. E. *et al.* The structure of 0- to 0.2-m.y.-old oceanic crust at 9° N on the East Pacific Rise from expanded spread profiles. *J. Geophys. Res.* **95**, 15529–15556 (1990).
32. Harding, A. J., Kent, G. M. & Orcutt, J. A. A multichannel seismic investigation of upper crustal structure at 9° N on the East Pacific Rise: Implications for crustal accretion. *J. Geophys. Res.* **98**, 13925–13944 (1993).
33. Waldhauser, F. HypoDD: A program to compute double-difference hypocenter locations. USGS Open-file Report 01–113 (US Geological Survey, Menlo Park, California, 2001).
34. Bakun, W. H. & Joyner, W. B. The M_L scale in central California. *Bull. Seism. Soc. Am.* **74**, 1827–1843 (1984).

Supplementary Information is linked to the online version of the paper at www.nature.com/nature.

Acknowledgements M.T. thanks S. Carbotte for discussions. We thank the captain, crew and science party of the RV *Keldysh* and RV *Atlantis*. M.T. thanks J. Cameron, A. M. Sagalevitch, Disney and Walden Media for making initial OBS deployment possible. This work was supported by the NSF.

Author Information Reprints and permissions information is available at www.nature.com/reprints. Correspondence and requests for materials should be addressed to M.T. (tolstoy@ldeo.columbia.edu).

LETTERS

Machaeridians are Palaeozoic armoured annelids

Jakob Vinther[1], Peter Van Roy[2]† & Derek E. G. Briggs[1]

The systematic affinities of several Palaeozoic skeletal taxa were only resolved when their soft-tissue morphology was revealed by the discovery of exceptionally preserved specimens. The conodonts provide a classic example, their tooth-like elements having been assigned to various invertebrate and vertebrate groups for more than 125 years until the discovery of their soft tissues revealed them to be crown-group vertebrates[1]. Machaeridians, which are virtually ubiquitous as shell plates in benthic marine shelly assemblages ranging from Early Ordovician (Late Tremadoc) to Carboniferous[2], have proved no less enigmatic. The Machaeridia comprise three distinct families of worm-like animals, united by the possession of a dorsal skeleton of calcite plates that is rarely found articulated. Since they were first described 150 years ago[3] machaeridians have been allied with barnacles[4,5], echinoderms[6,7], molluscs[3,8–10] or annelids[9,11,12]. Here we describe a new machaeridian with preserved soft parts, including parapodia and chaetae, from the Upper Tremadoc of Morocco, demonstrating the annelid affinity of the group. This discovery shows that a lineage of annelids evolved a dorsal skeleton of calcareous plates early in their history; it also resolves the affinities of a group of problematic Palaeozoic invertebrates previously known only from isolated elements and occasional skeletal assemblages.

Phylum Annelida
Class Machaeridia
Order Turrilepadomorpha
Family Plumulitidae
Genus ***Plumulites*** Barrande, 1872
Plumulites bengtsoni sp. nov.

Etymology. For Stefan Bengtson, who has made a major contribution to our knowledge of machaeridians and early skeletal fossils.
Holotype. Yale Peabody Museum, YPM 221134 (Figs 1 and 2, and Supplementary Figs 1–3).
Locality and horizon. Twenty-two kilometres north-northeast of Zagora, southeastern Morocco; upper part of the Lower Fezouata formation, Lower Ordovician (Upper Tremadoc)[13]. The exceptionally preserved specimen described here represents the oldest articulated machaeridian (only one other machaeridian of Late Tremadoc age is known, from isolated shell plates[14]). The locality also yields sponges, conulariids, hyolithids, trilobites and other arthropods, echinoderms and graptolites. The lithology is a dark blue–green silty mudstone.
Diagnosis. The outer shell plates possess a relatively wide elevated median area bounded by inflections; the rugae are less prominent where they traverse the median area. Inner shell plates have a much broader median area which is traversed by rugae that show neither inflection nor reduction in relief.
Description. The specimen (Fig. 1) lacks the anterior region and many of the shell plates; decay played a role but some of the shell plates may be concealed within the sediment of the counterpart. The preserved length is about 28 mm. The specimen shows the dorsal surface of the integument. At the anterior right, rotated about 180° relative to its life position, lies a relatively complete outer shell plate showing an umbonal area with circular concentric growth rings (Fig. 1c and Supplementary Fig. 3d). This type of shell plate characterizes the anterior region of plumulitids. Other outer shell plates are evident, two at the anterior left and one at the posterior right; these taper to an angular extremity. The anterior plates are about 1.7 times (Supplementary Fig. 3a) and the posterior 2 times longer than wide. The outer shell plates have denticulate lateral margins, the denticles formed as projections of the underlying shell layer and out of phase with the growth lines and rugae on the dorsal surface (Supplementary Fig. 3a, c, d). One almost complete inner shell plate is present; its shape is close to that of an equilateral triangle (Supplementary Fig. 3b).

The anterior part of the specimen is concealed largely by overlying shell plates. A sediment-filled tube in the anterior part of the fossil is interpreted as the gut. A narrow median linear structure runs along the anteriormost preserved part of the gut (Supplementary Fig. 3e); its nature is unknown. Behind this the trunk tapers posteriorly. Along the length of the trunk, paired lobes extend laterally bearing bundles of long, slender bristles. Up to 18 pairs of these lobes, interpreted as parapodia, are evident. Extrapolation suggests that there must have been at least 25 pairs of parapodia, corresponding to segments, along the length of the trunk. It is difficult to distinguish rami; they may be represented in some cases by two divergent groups of chaetae (Figs 1 and 2a, b). There may be up to 20 chaetae in a bundle on a parapodium. Those parapodia that preserve some original relief show dense transverse wrinkles (Fig. 2a, b). Faint integumental wrinkles are evident on other parapodia and portions of the trunk. There appears to be a dorsal extension of the integument at the base of almost every parapodium (Figs 1 and 2, highlighted as green, and Supplementary Fig. 3f). Owing to the level of splitting, the outline of these extensions is concealed largely within the counterpart.

The soft tissues are preserved in framboids composed of iron oxide (Supplementary Fig. 1), indicating that they were originally pyritic. Red iron oxide, presumably haematite, is concentrated mainly in the parapodia and the chaetae; the specimen is otherwise yellow.
Discussion. The class Machaeridia consists of three families: Turrilepadidae, Plumulitidae and Lepidocoleidae. The body of Plumulitidae was dorso-ventrally flattened[12], whereas that of the other groups was more laterally compressed. Machaeridians are characterized by calcitic shell plates serially arranged in left and right zones with prominent concentric rugae[6]. They appear to have a fixed number of shell plates in the adult[15], but the number in plumulitids is not well documented. The only known complete example, a specimen of *Plumulites richorum* from the Devonian of Australia[12], preserves 20 pairs of inner shell plates. Well-preserved plumulitid skeletons[6,12], such as that of the Upper Ordovician (Caradoc) species *Plumulites tafennaensis*[16] (Fig. 3) from Morocco, show that there are two columns each of posteriorly imbricating inner and outer shell plates. The inner shell plates are smaller than the outer and project

[1]Department of Geology and Geophysics, Yale University, PO Box 208109, New Haven, Connecticut 06520, USA. [2]Department of Geology and Soil Science, Ghent University, Krijgslaan 281/S8, B-9000 Ghent, Belgium. †Present address: School of Geological Sciences, University College Dublin, Belfield, Dublin 4, Ireland.

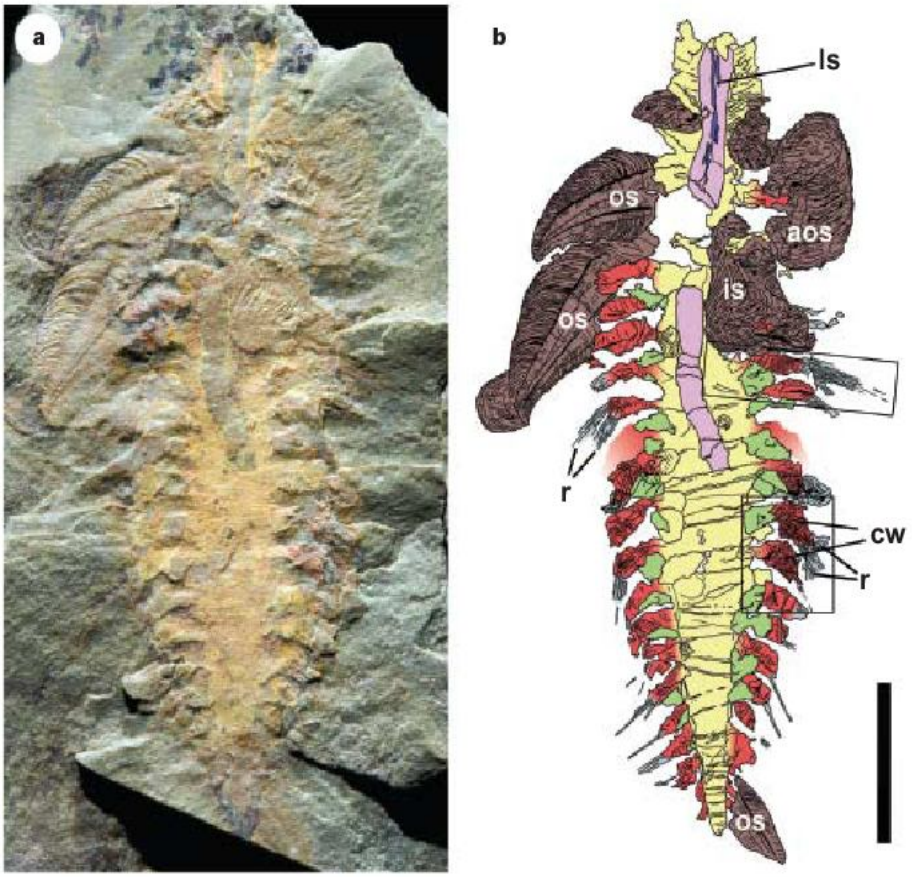

Figure 1 | *Plumulites bengtsoni* sp. nov. from the upper part of the Lower Fezouata formation, Lower Ordovician (Upper Tremadoc), Morocco. **a**, Holotype YPM 221134, part. **b**, Camera lucida drawing of the part. Colours indicate the trunk (yellow), parapodia (red), chaetae (gray), attachment of shell plates (green), gut (purple) and dorsal linear structure (blue). Abbreviations: os, outer shell plate; is, inner shell plate; aos, anterior outer shell plate; ls, linear structure; cw, cuticular wrinkles; r, rami evidenced by divergent bundles of chaetae. Outlines indicate the position of enlarged areas in Fig. 2. Scale bar, 5 mm.

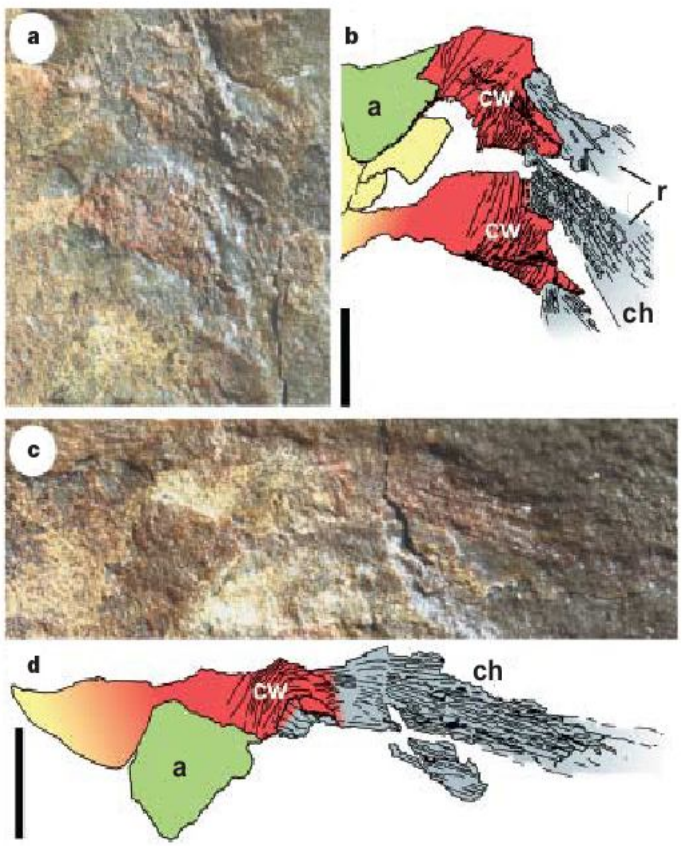

Figure 2 | Details of the parapodia, chaetae and dorsal integumental extensions of *P. bengtsoni*, holotype YPM 221134, part. **a**, Middle right parapodia showing cuticular wrinkles. **b**, Camera lucida drawing of the area in **a**. **c**, More anterior parapodium. **d**, Camera lucida drawing of area in **c**. Colours as in Fig. 1. Abbreviations: cw, cuticular wrinkles; ch, chaetae; a, attachment of shell plates; r, rami evidenced by divergent bundles of chaetae. Scale bar, 1 mm.

inwards obliquely in a posterior direction. The outer plates are more elongate and project outwards posteriorly, perpendicular to the inner shell plates. The anteriormost outer plates, which are sometimes absent, differ in morphology from the remainder[12].

Plumulites bengtsoni shows the morphology characteristic of Plumulitidae with the inner shell plates smaller than the outer and the body dorso-ventrally flattened. Only the anteriormost region of the body appears to be missing, assuming that the differentiated anterior outer plate, although rotated, is approximately in its original position[9,12]. Denticles are present along the lateral margins of the outer shell plates, a feature that may be widespread in this family. The shell plates of *Plumulites kutscheri*[17] (Upper Wenlock, Germany) have denticulate margins, and spinose plumulitid shell plates also have been reported from the Ashgill of Sweden[18]. The morphology of *P. bengtsoni* is very similar otherwise to the type species *Plumulites bohemicus*; it is distinguished by the less pronounced rugae in the elevated median area of the outer plates.

Machaeridians are the only annelids known to have evolved biomineralized dorsal armour. The living Sternaspidae have a pair of chitinous anal plates which are used to cover the burrow entrance[19], but these structures are probably not homologous to machaeridian shell plates. Serpulidae and Spirorbidae secrete biomineralized tubes of calcite and aragonite from glands near the collar[19], but they are sessile and the mode of secretion differs from that in machaeridian shell plates. The overlapping nature and the extent of the growing margin of the shell plates in *P. bengtsoni* indicate that they could not have been attached directly to the trunk or parapodia. The dorsal integumental extensions at the base of each parapodium (Figs 1 and 2, highlighted as green structures) may represent the attachment of the shell plates. Their arrangement corresponds to that in articulated plumulitid skeletons[6,12] in which the inner and outer shell plates alternate in position along a line on each side of the trunk, suggesting that they were attached to successive segments. The integumental extensions must have expanded to accommodate the wide proximal growing margin of the shell plate, in a manner similar to the attachment of elytra (expanded cirri) in living scale worms (Aphroditidae: Phyllodocida).

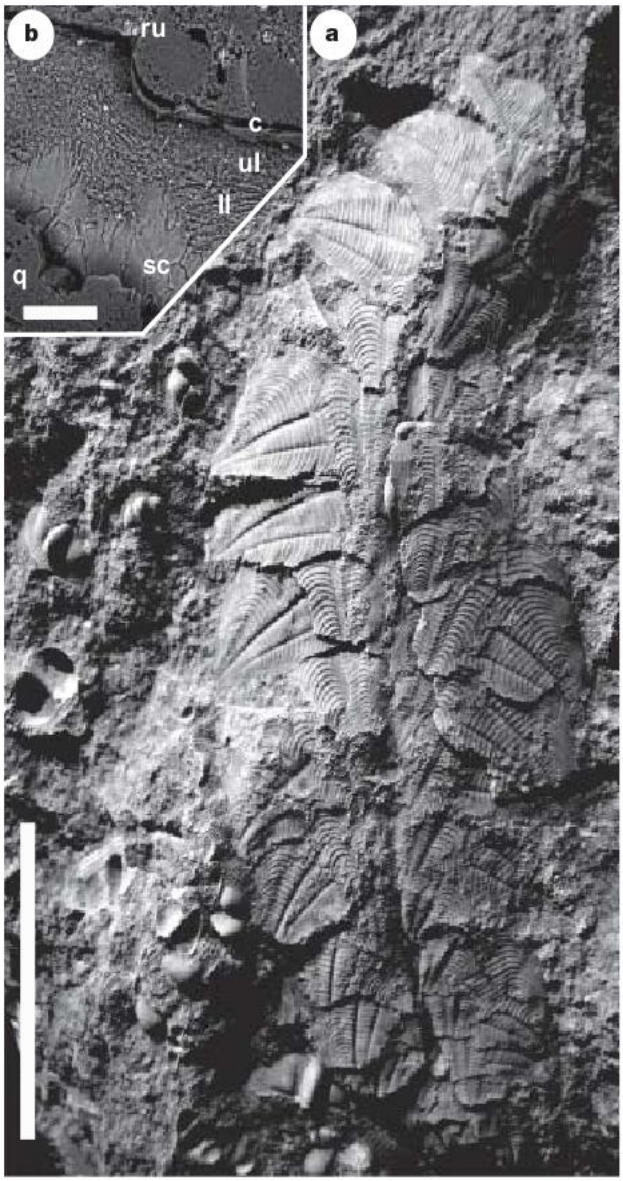

Figure 3 | *Plumulites tafennaensis*[16] from the Upper Ordovician (Caradoc), Morocco. a, YPM 220639 articulated specimen. **b**, Back-scattered electron micrograph of an etched, polished transverse section of a shell plate. The upper part consists of a lower laminated layer (ll) and an upper fine grained layer (ul); a thin separation between the upper shell layer and the matrix is interpreted as evidence of an organic cuticle (c); ru, the site of a ruga. The basal surface is encrusted with quartz (q), and some of the adjacent shell is recrystallized into sparry calcite (sc). Scale bars: **a**, 20 mm; **b**, 50 μm.

The position of machaeridians within the annelids is difficult to resolve. A major issue is the homology of the shell plates and of the proximal structures to which they are attached. The inner shell plates in machaeridians are offset and overlap along the median line, as do the elytra of some scale worms. The elytra of scale worms, however, occur only on every other segment, whereas the shell plates of machaeridians appear to be present on every segment. A cladistic analysis (Supplementary Information) resolves the Machaeridia as a member of Annelida, but their position within the group is not resolved when the presence of dorsal cirri in Machaeridia is coded as unknown (Fig. 4). Only when the plumulitids are coded as having cirri and elytra do they resolve as crown-group annelids. They fall in a clade with the living phyllodocidans (Supplementary Fig. 4), which have been interpreted as a paraphyletic basal grade[19,20], in which case machaeridians could still be part of the stem group (see further discussion in Supplementary Information).

Much of the annelid fossil record consists of the elements of the jaw apparatus (scolecodonts), which first appear in the uppermost Cambrian[21]. Soft-bodied fossils are rare: pyrite is also involved in

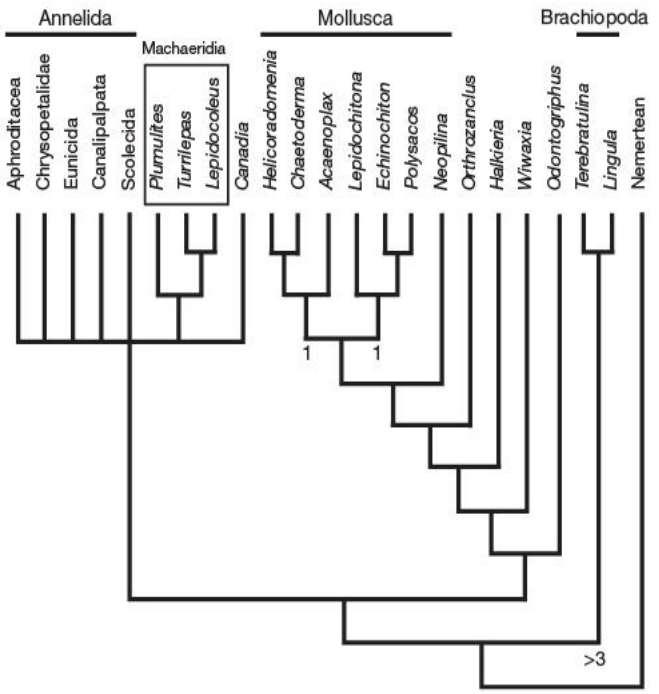

Figure 4 | Strict consensus tree of 66 most parsimonious trees based on a cladistic analysis with 23 taxa and 57 characters (Supplementary Information and Supplementary Fig. 4). Machaeridians resolve with the annelids. Numbers below nodes indicate where the decay index is one or more. Score of best tree, 74; consistency index, 0.811; retention index, 0.897; rescaled consistency index, 0.727; homoplasy index, 0.189.

the preservation of whole-body annelids from several other exceptional localities, including the Lower Devonian Hunsrück Slate, Germany[22], the Middle Devonian Arkona Shale, Canada[23], and the Jurassic of La Voulte-sur-Rhône, France[24]. The oldest described examples are from the Middle Cambrian Burgess Shale[25], but occurrences have been reported from the Early Cambrian (Atdabanian) Sirius Passet fauna of Greenland[26]. It has been suggested that machaeridians are related to the older Early Cambrian tommotiids (Mitrosagophora)[9,11], some of which, like *Tommotia*, *Dalyatia* and *Tannuolina*, have left and right shell plates. Tommotiid shell plates are ornamented with prominent concentric rugae and often a median inflected area like that in plumulitid shell plates. Although tommotiids are known only from isolated sclerites, some reconstructions[27,28] imply an organization similar to that in machaeridians. The morphological similarity between the shell plates of machaeridians, tommotiids and brachiopods[11,29] could be interpreted as evidence of a close affinity between annelids and brachiopods. Well-preserved shell plates of *P. tafennaensis* (Fig. 3b) show that they consist of an outer layer formed by marginal accretion and an inner basal layer, as previously recorded in lepidocoleids and turrilepadids[17,30]. An additional external layer probably represents an original organic cuticle (Fig. 3b). Tommotiid shell plates, in contrast, have a characteristic lamellar ultrastructure and phosphatic mineralogy like that in lingulid brachiopods[11,28,29]; as putative stem brachiopods[29] they would have been secreted by a more elaborate mantle. Thus the similarity between shell plates in tommotiids and machaeridians is probably a result of convergent evolution[2].

The discovery of machaeridian soft-tissue morphology resolves the 150-year-old debate about the affinities of this group, and demonstrates that a lineage of annelids developed a distinctive, dorsal, mineralized armour early in their history.

METHODS SUMMARY

The holotype was photographed by using a Canon EOS 350D digital single-lens reflex camera with a Canon EF-S 60 mm f/2.8 Macro USM objective lens stopped down to f32. Details were photographed by using a Leica MZ16 dissecting microscope with Optronics camera using oblique-angled polarized light, and

combined as a mosaic. Camera lucida drawings were made by using a Wild M5 stereomicroscope. The counterpart was studied in a Philips XL 30 environmental scanning electron microscope (ESEM) equipped with an energy-dispersive X-ray analyser (EDX). Disarticulated shell plates of *P. tafennaensis* in their matrix were embedded in epoxy, and polished sections were etched in 0.5% HCl for 90 s. Back-scattered electron images were taken and the elemental composition analysed in the ESEM.

Received 28 August; accepted 13 November 2007.

1. Briggs, D. E. G. Conodonts – a major extinct group added to the vertebrates. *Science* **256**, 1285–1286 (1992).
2. Adrain, J. M. Machaeridian classification. *Alcheringa* **16**, 15–32 (1992).
3. de Koninck, L. Sur deux nouvelles espèces siluriennes appartenant au genre *Chiton*. *Bull. Acad. r. Belg.* **3**, 190–199 (1857).
4. Woodward, H. On the discovery of a new genus of Cirripedia in the Wenlock limestone and shale of Dudley. *Q. J. Geol. Soc. Lond.* **21**, 486–489 (1865).
5. Bischoff, G. C. O. *Dalyatia*, a new genus of the Tommotidae from the Cambrian strata of S. E. Australia (Crustacea, Cirripedia). *Senck. Leth.* **57**, 1–33 (1975).
6. Withers, T. H. *Catalogue of the Machaeridia* 1–99 (British Museum, Natural History, London, 1926).
7. Pope, J. K. Evidence for relating the Lepidocoleidae, machaeridian echinoderms, to the mitrate carpoids. *Bull. Am. Paleont.* **67**, 385–406 (1975).
8. Wolburg, J. Beitrag zum Problem der Machaeridia. *Paläont. Z.* **20**, 289–298 (1938).
9. Dzik, J. in *Problematic Fossil Taxa* (eds Hoffman, A. & Nitecki, M. H.) 116–134 (Oxford Univ. Press, New York, 1986).
10. Sigwart, J. D. & Sutton, M. D. Deep molluscan phylogeny: synthesis of palaeontological and neontological data. *Proc. R. Soc. B* **274**, 2413–2419 (2007).
11. Bengtson, S. The Lower Cambrian fossil *Tommotia*. *Lethaia* **3**, 363–392 (1970).
12. Jell, P. A. *Plumulites* and the machaeridian problem. *Alcheringa* **3**, 253–259 (1979).
13. Destombes, J., Hollard, H. & Willefert, S. in *Lower Palaeozoic Rocks of the World* Vol. 4, *Lower Palaeozoic of North-western and West-central Africa* (ed. Holland, C. H.) 91–336 (John Wiley, Chichester, 1985).
14. Kobayashi, T. & Hamada, T. Occurrences of the Machaeridia in Japan and Malaysia. *Proc. Jap. Acad.* **52**, 371–374 (1976).
15. Adrain, J. M., Chatterton, B. D. E. & Cocks, L. R. M. A new species of machaeridian from the Silurian of Podolia, USSR, with a review of the Turrilepadidae. *Palaeontology* **34**, 637–651 (1991).
16. Chauvel, J. Sur quelques représentants du genre *Plumulites* Barrande (Machaeridiés) provenant de l'Ordovicien du Maroc et du Massif Armoricain. *Bull. Soc. Géol. Miner. Bretagne* **1966**, 73–85 (1967).
17. Schrank, E. Machaeridia aus Silurischen Geschieben. *Der Geschiebesammler* **11**, 5–22 (1978).
18. Hints, O., Eriksson, M., Högström, A. E. S., Kraft, P. & Lehnert, O. in *The Great Ordovician Biodiversification Event* (eds Webby, B., Paris, F., Droser, M. L. & Percival, I. G.) 223–230 (Columbia Univ. Press, New York, 2004).
19. Rouse, G. & Pleijel, F. *Polychaetes* (Oxford University Press, Oxford and New York, 2002).
20. Westheide, W. The direction of evolution within the Polychaeta. *J. Nat. Hist.* **31**, 1–15 (1997).
21. Hints, O. & Eriksson, M. Diversification and biogeography of scolecodont-bearing polychaetes in the Ordovician. *Palaeogeogr. Palaeoclimatol. Palaeoecol.* **245**, 95–114 (2007).
22. Bartels, C., Briggs, D. E. G. & Brassel, G. *The Fossils of the Hunsrück Slate, Marine Life in the Devonian* (Cambridge Univ. Press, Cambridge, 1998).
23. Farrell, Ú. C. & Briggs, D. E. G. A pyritized polychaete from the Devonian of Ontario. *Proc. R. Soc. B* **274**, 499–504 (2007).
24. Alessandrello, A., Bracchi, G. & Riou, B. Polychaete, sipunculan and enteropneust worms from the Lower Callovian (Middle Jurassic) of La Voulte-sur-Rhône (Ardèche, France). *Mem. Soc. Ital. Sci. Nat. Mus. Civ. Storia Nat. Milano* **32**, 1–16 (2004).
25. Eibye-Jacobsen, D. A reevaluation of *Wiwaxia* and the polychaetes of the Burgess Shale. *Lethaia* **37**, 317–335 (2004).
26. Conway Morris, S. & Peel, J. S. Articulated halkieriids from the Lower Cambrian of north Greenland and their role in early protostome evolution. *Phil. Trans. R. Soc. Lond. B* **347**, 305–358 (1995).
27. Evans, K. R. & Rowell, A. J. Small shelly fossils from Antarctica: an Early Cambrian faunal connection with Australia. *J. Paleont.* **64**, 692–700 (1990).
28. Li, G. & Xiao, S. *Tannuolina* and *Micrina* (Tannuolinidae) from the Lower Cambrian of Eastern Yunnan, south China, and their scleritome reconstruction. *J. Paleont.* **78**, 900–913 (2004).
29. Holmer, L. E., Skovsted, C. B. & Williams, A. A stem group brachiopod from the Lower Cambrian: support for a *Micrina* (halkieriid) ancestry. *Palaeontology* **45**, 875–882 (2002).
30. Bengtson, S. The Machaeridia – a square peg in a pentagonal hole. *Thallasia Jugoslav.* **12**, 1–10 (1978).

Supplementary Information is linked to the online version of the paper at www.nature.com/nature.

Acknowledgements S. Bengtson, D. Eibye-Jacobsen and K. J. Peterson commented on the manuscript and cladistic analysis. T. A. Hegna and A. Seilacher are thanked for discussions. E. Lazo-Wasem and C. MacClintock provided access to annelid and machaeridian specimens from the collections of the Yale Peabody Museum of Natural History. Specimen YPM 221134 was provided by M. Ben Said Ben Moula, and YPM 220639 by R. Reboul and V. Reboul. These last three persons, with W. De Winter, B. MacGabhann, B. Van Bocxlaer and D. Van Damme, assisted with fieldwork.

Author Contributions P.V.R. performed field work and acquired the specimens. All authors contributed to the interpretation of the fossils and writing the paper.

Author Information Reprints and permissions information is available at www.nature.com/reprints. Correspondence and requests for materials should be addressed to D.E.G.B. (derek.briggs@yale.edu).

LETTERS

The coevolution of choosiness and cooperation

John M. McNamara[1], Zoltan Barta[2], Lutz Fromhage[3] & Alasdair I. Houston[3]

Explaining the rise and maintenance of cooperation is central to our understanding of biological systems[1,2] and human societies[3,4]. When an individual's cooperativeness is used by other individuals as a choice criterion, there can be competition to be more generous than others, a situation called competitive altruism[5]. The evolution of cooperation between non-relatives can then be driven by a positive feedback between increasing levels of cooperativeness and choosiness[6]. Here we use evolutionary simulations to show that, in a situation where individuals have the opportunity to engage in repeated pairwise interactions, the equilibrium degree of cooperativeness depends critically on the amount of behavioural variation that is being maintained in the population by processes such as mutation. Because our model does not invoke complex mechanisms such as negotiation behaviour, it can be applied to a wide range of species. The results suggest an important role of lifespan in the evolution of cooperation.

We consider an infinite population where, in each of a discrete series of time steps (rounds), pairs of individuals engage in a game that can be described as a social dilemma[7]. Each individual is characterized by two traits: a cooperativeness trait x, which specifies the amount of effort that the individual devotes to generating benefits available (at least in part) to its co-player; and a choosiness trait y, which specifies the minimum degree of cooperativeness that the focal individual is prepared to accept from its co-player. The traits x and y are genetically determined and are not adjusted in response to the co-player's behaviour. Thus, unlike in many models in which flexible effort adjustment is a key ingredient[1,6,8], individuals in our model are consistent in their degree of cooperativeness. In each round, each individual receives a payoff $W(x, x')$ that reflects its own effort, x, and that of its co-player, x'. The payoff function (see below) is such that there is a conflict of interest between pair members, with each preferring the other to provide most of the total effort. Upon receiving their payoffs, pair members find out about each other's effort, and then incur some risk of mortality before entering the next round. If pair members are mutually acceptable (that is, $x \geq y'$ and $x' \geq y$, where y' denotes the opposite player's choosiness), and if both survive, then they continue to interact with each other in the next round. Otherwise the pair break up and any survivors enter the pool of unpaired individuals, from which new pairs are randomly formed at the beginning of the next round. The breaking of pairs reflects the ability of mobile organisms to terminate unfavourable interactions by leaving[9,10]. We assume that finding a new co-player is costly, so that, in the first round of interacting with a new co-player, payoffs are reduced by a fixed amount S. On the other hand, because social interaction may not be the only way of generating payoffs, we assume that each individual also receives a fixed payoff component A in each round. Hence the total payoff is $W(x, x') + A - S$ for an individual in a newly formed pair and $W(x, x') + A$ for an individual in an established pair. We model reproduction as follows. Upon receiving a payoff in a given round, each individual produces offspring in numbers proportional to its payoff. Offspring are produced asexually, and so share the parental type in terms of x and y, subject to occasional small changes caused by mutation. (We have confirmed by additional computations that the results are similar if offspring are produced sexually; Supplementary Information.) Individuals that die are replaced by individuals selected at random from all offspring produced in the previous round; these replacements join the pool of unpaired individuals. (Computational details are given as Supplementary Information.)

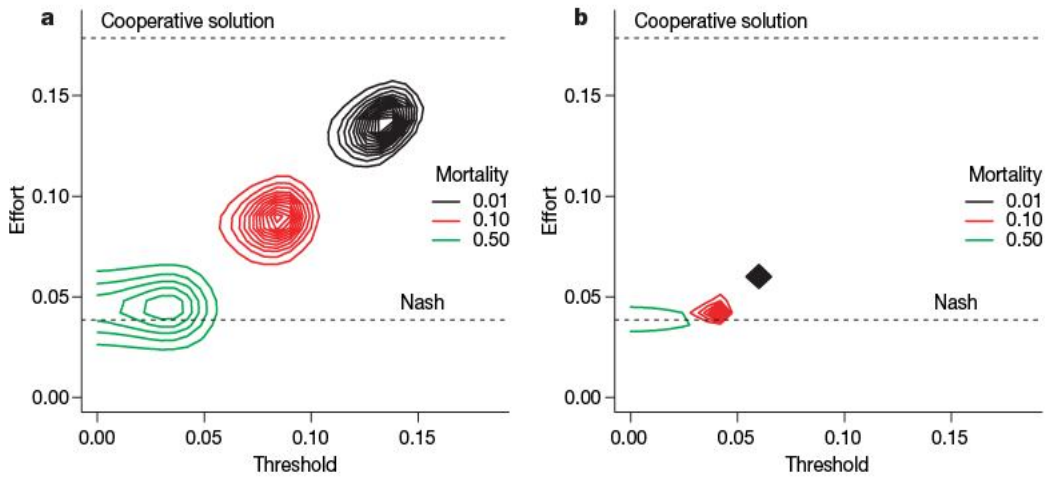

Figure 1 | Equilibrium frequency distribution of trait combinations in the continuous snowdrift game with accelerating costs. Contour lines connect trait combinations that occur with equal frequency. Results for three levels of mortality M are shown for simulations using (**a**) high mutation rate ($\mu = 0.05$) and (**b**) low mutation rate ($\mu = 0.001$). Dashed lines indicate the Nash solution (0.0386) and the cooperative solution (0.179). Payoff function: $W(x, x') = B(x + x') - C(x)$, with $B(x+x') = \frac{x+x'}{1+x+x'}$ and $C(x) = 0.8(x + x^2)$. Other parameters (see Supplementary Information): maximum effort value, $x_{max} = 0.18$; $A = 0.01$; $S = 0.01$.

[1]Department of Mathematics, University of Bristol, University Walk, Bristol BS8 1TW, UK. [2]Department of Evolutionary Zoology, University of Debrecen, Debrecen, H-4010, Hungary. [3]School of Biological Sciences, University of Bristol, Woodland Road, Bristol BS8 1UG, UK.

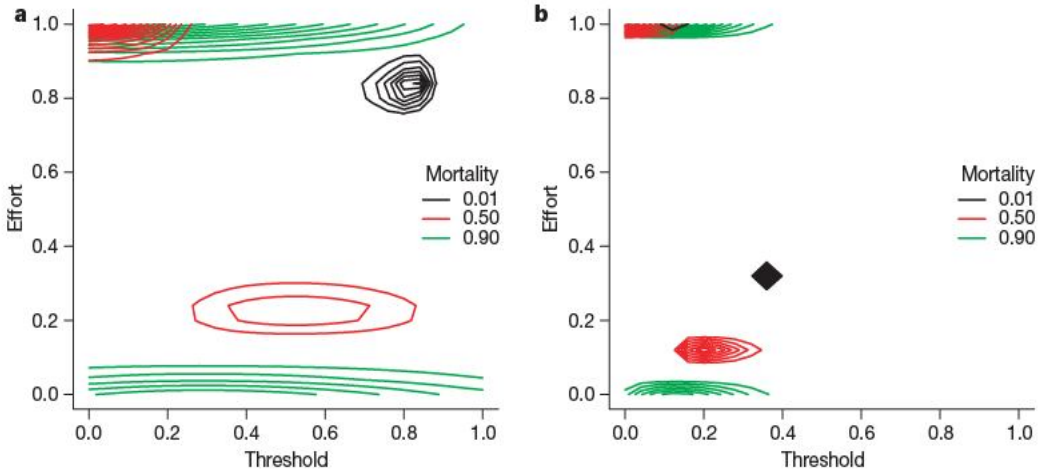

Figure 2 | Continuous snowdrift game with decelerating costs. Results for three levels of mortality M are shown for simulations using (**a**) high mutation rate ($\mu = 0.005$) and (**b**) low mutation rate ($\mu = 0.0001$). Payoff function: $W(x, x') = B(x + x') - C(x)$, with $B(x + x') = -1.4(x + x')^2 + 6(x + x')$ and $C(x) = -1.6x^2 + 4.56x$. Other parameters (see Supplementary Information): maximum effort value, $x_{max} = 1$; $A = 1$; $S = 1$.

We use two benchmark solutions to judge the observed degree of cooperation: the (non-cooperative) 'Nash solution', which corresponds to the expected behaviour if individuals are maximizing their payoff in one-off interactions[11,12]; and the 'cooperative solution', which corresponds to the expected behaviour if payoffs to pairs rather than to individuals are being maximized[12,13].

For the sake of generality, we consider two types of payoff function that conform to alternative paradigms for the study of cooperation: the continuous prisoner's dilemma game[8], and the continuous snowdrift game[14]. In the continuous prisoner's dilemma, individuals incur a cost $C(x)$ that depends on their own effort, while gaining a benefit $B(x')$ that depends on their co-player's effort. In the continuous snowdrift game, individuals also incur a cost $C(x)$ that depends on their own effort, but gain a benefit $B(x + x')$ that depends on the summed effort of both co-players. The resulting payoff functions are of the forms $W(x, x') = B(x') - C(x)$ and $W(x, x') = B(x + x') - C(x)$, respectively. The important difference here is that in the continuous prisoner's dilemma, the Nash solution is always to invest zero effort[8], whereas this is not the case in the continuous snowdrift game. Here we consider a version of the continuous prisoner's dilemma with linear cost and benefit functions, which, because of its simplicity, allows us to obtain some analytical results. We first consider a version of the continuous snowdrift game with saturating benefit and accelerating cost functions, because similar cases may be common in nature (for example, in the context of parental care for offspring[11,15], or of vigilance in the face of predation risk[16]); here the Nash effort is greater than zero but lower than the cooperative solution (Fig. 1). For details on the payoff functions used, see figure legends and Supplementary Fig. 1.

The traditional approach to analysing evolutionary games is to identify evolutionarily stable strategies, which, if used by almost all individuals in a population, cannot be invaded by any mutant strategy[17]. In our model, an obvious candidate evolutionarily stable strategy in this sense is a strategy that involves neither cooperation (beyond the Nash effort) nor choosiness. (We show that this is in fact the only evolutionarily stable strategy in the continuous prisoner's dilemma case; Supplementary Information.) This strategy is stable because, in a population where virtually all individuals are the same, nothing can be gained by being choosy. Without the risk of being dismissed by a co-player, however, there is no incentive for individuals to invest more than the Nash effort. This situation changes profoundly if significant variation is maintained in the population by processes such as mutation. Now the dismissal of uncooperative individuals can be advantageous, because more cooperative co-players are available to be found. This implies that cooperative individuals, by not being dismissed, enjoy an advantage. As the average level of cooperativeness in the population increases, so does the optimal threshold value below which relatively uncooperative individuals are dismissed. This in turn favours even higher levels of cooperativeness.

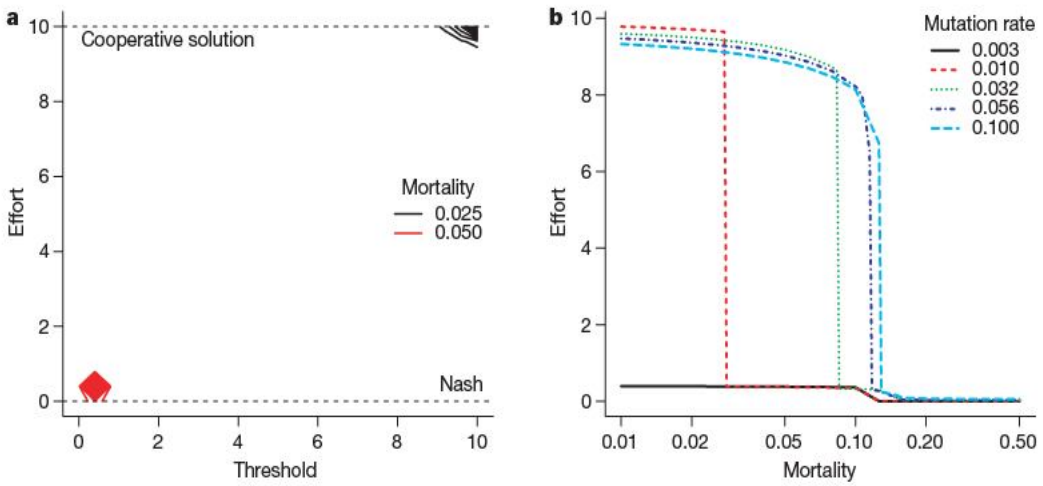

Figure 3 | Continuous prisoner's dilemma. **a**, Equilibrium frequency distribution of trait combinations for two levels of mortality M. Contour lines connect trait combinations that occur with equal frequency. The Nash solution is $x = 0$ and the cooperative solution is x_{max}. Mutation rate: $\mu = 0.01$. **b**, Population mean effort at equilibrium, plotted against mortality for five different mutation rates μ. Payoff function: $W(x, x') = B(x') - C(x)$, with $B(x') = 5x'$ and $C(x) = x$. Other parameters: maximum effort value, $x_{max} = 10$; $A = 1$; $S = 0.001$.

Depending on the type of payoff function used, this positive feedback can drive cooperativeness up to intermediate levels (Figs 1 and 2), or even up to the cooperative solution (Fig. 3).

A high mutation rate can increase the equilibrium degree of cooperation in our model (Figs 1 and 2) and/or broaden the conditions under which cooperation arises (Fig. 3). This is because it enhances the amount of behavioural variation, which is the substrate on which choosiness, and hence cooperation, thrives in our model (Box 1). Whenever the average cooperativeness exceeds the Nash solution, a positive correlation between an individual's choosiness and cooperativeness arises (noticeable in Fig. 1a). This is because 'paradoxical' trait combinations yield particularly low payoffs: individuals with low choosiness but high effort tend to get exploited by their co-players; individuals with high choosiness but low effort waste their time searching for better co-players, which are, however, unlikely to accept them. The positive correlation between choosiness and cooperativeness leads to a positive assortment between cooperative types – an essential feature of all mechanisms that promote cooperation[18,19]. High mortality counteracts the evolution of cooperation by reducing the equilibrium degree of cooperation (Fig. 1), and/or by restricting the conditions under which cooperation can arise (Fig. 3b). This can be explained as follows. The benefits of being both choosy and cooperative arise when mutually acceptable co-players find each other. This usually requires a period of searching, during which costs arise both in terms of S and in terms of being exploited by less cooperative individuals. If the cooperative associations thus formed are soon disrupted by mortality, then establishing them is not worth the associated costs (Box 1). Cooperation is, however, slower to evolve from non-cooperative starting conditions when lifespan is long (Supplementary Fig. 2).

As well as considering the continuous snowdrift game with accelerating costs, we also consider a version with decelerating costs. This version is applicable in situations where the initiation of cooperative acts is more costly than subsequent increases in cooperative investments. For example, if bacteria secrete enzymes into the environment that can be used to digest nutrients and are therefore a public good, costs for turning on the relevant genetic machinery may be high compared with subsequent increases in enzyme production[14]. This form of cost has been shown to produce disruptive evolution of cooperative and non-cooperative individuals in one-shot games[14]; thus there is no pure stable state here that meets our definition of a Nash solution. At high mortality, repeated interactions are unlikely, so that the situation is like a one-shot game, yielding a bimodal distribution of cooperative and uncooperative types (Fig. 2). Under low mortality, however, uncooperative types are put at a disadvantage because they are likely to be dismissed in every round; given sufficient mutation (Fig. 2a, but see Fig. 2b), this can lead to a unimodal distribution of cooperative types.

The rise of cooperation in our model hinges on the existence of consistent individual differences in cooperativeness. In our model, genetic variation is responsible for differences. However, reproductive success in our model depends only on the phenotypic composition of the population. Thus, as long as some of the available variation is heritable, the direction of selection (that is, the sign of the covariance between reproductive success and a given trait) would be the same if differences were largely non-heritable (cf[20]).

The importance of low mortality for the evolution of choosiness has been noted before[21,22], though in a context of mate choice rather than cooperation. In our model, this combines with the additional effect that low mortality, by allowing for long series of interactions, offers a long-term perspective that can trump the short-term incentive for defection. The latter effect is analogous to findings that in the iterated prisoner's dilemma, cooperative strategies are only successful if there is a low probability that any given iteration is the last[1].

Like models of direct reciprocity based on behaviourally flexible cooperativeness[1,8], our model generates a situation in which current cooperation is rewarded by the prospect of future cooperation. This is mediated by the possibility of ostracizing uncooperative individuals (cf[6,23,24]), which we have modelled as being based on an evolving trait rather than on a fixed parameter or strategy. Note that for this form of ostracism to work, individuals do not need to be able to remember and compare the behaviour of multiple population members (unlike[6,24]).

Consistent with previous results[6,23,24], our model predicts that the evolution and maintenance of cooperation can critically depend on the ability to stop interacting with relatively uncooperative individuals. This is in line with findings of divorce behaviour that depends on partner quality in birds[25,26] and fish[27] with bi-parental care, where an individual's contribution to the cooperative task of breeding can be an important aspect of partner quality[26]. Even humans, despite being far more sophisticated than the players in our model, show increased (and relatively constant) levels of cooperativeness in an experimental setting where they can establish optional long-term relations[28], thus strengthening the case that our model encapsulates

Box 1 | Optimal choosiness

In a single round of the game, an individual that expends effort x receives payoff $W(x, x')$ when its partner's effort is x'. Here we consider the special case of the continuous prisoner's dilemma for which

$$W(x, x') = bx' - C(x) \quad (1)$$

where $C(x)$ is a strictly increasing function of x, and b is a positive constant. For this payoff the Nash effort in a single round is the minimum effort $x^* = 0$.

Consider a population in which the efforts of members of the pool of single individuals are distributed with probability density function $f(x)$ and mean $\bar{x}$. Then (see Supplementary Information) an individual that is never dismissed by others should dismiss its partner if and only if its partner's effort is below y^*, where

$$y^* = \bar{x} - (S/b) + \beta \int_{y^*}^{\infty} (x' - y^*) f(x') \mathrm{d}x' \quad (2)$$

where $\beta = (1-M)^2/[M(2-M)]$ is a decreasing function of the mortality M, and S is the search cost. Individuals that are dismissed by some co-players have a lower optimal threshold (Supplementary Information). From equation (2) it is easy to show that y^* increases as S and M decrease (Supplementary Information).

It can be shown (Supplementary Information) that if all population members behave optimally then all expend the minimum effort $x^* = 0$. Thus complete non-cooperation is evolutionarily stable unless effects such as mutation maintain a significant amount of non-adaptive variation in the population. Equation (2) provides an intuitive explanation of this result. If we assume a monomorphic population with all individuals expending effort $\bar{x}$, then equation (2) reduces to $y^* = \bar{x} - S/(b(1+\beta)) < \bar{x}$. If all individuals adopt this optimal threshold and $\bar{x} > 0$, it pays to reduce effort below $\bar{x}$ because this can be done without incurring the risk of being dismissed.

So how much variation is necessary for cooperation to evolve? We expect mean effort to evolve so that it is greater than most acceptance thresholds (so ensuring the cost of dismissal is not paid). Thus cooperation should evolve when y^* exceeds the mean effort in the population. Approximating this mean by $\bar{x}$, equation (2) predicts cooperation to evolve when the variation, as measured by $\Delta = \int_{-\infty}^{\infty} |x' - \bar{x}| f(x') \mathrm{d}x'$ (the mean absolute deviation of effort from the population mean), is sufficiently high:

$$\Delta > \frac{2S}{\beta b} \quad (3)$$

Equivalently, the mortality rate must be sufficiently low:

$$M < 1 - \sqrt{\frac{2S}{2S + b\Delta}} \quad (4)$$

Because $\bar{x}$ (the mean among single individuals) is typically less than the overall population mean, these are minimal criteria.

a general principle. Because of both the widespread ability of animals to exert some form of choice among their conspecifics[29], and accumulating evidence for the ubiquity of consistent behavioural differences between individuals[30], we believe that the interacting effects of choice and variation (differing in biological detail across species, but following similar logic) may be among the most important reasons for the evolution of cooperation in nature.

Received 15 October; accepted 6 November 2007.

1. Axelrod, R. & Hamilton, W. D. The evolution of cooperation. *Science* **211**, 1390–1396 (1981).
2. Trivers, R. *Social Evolution* (Benjamin/Cummings, Menlo Park, California, 1985).
3. Fehr, E. & Fischbacher, U. The nature of human altruism. *Nature* **425**, 785–791 (2003).
4. Wedekind, C. & Milinski, M. Cooperation through image scoring in humans. *Science* **288**, 850–852 (2000).
5. Roberts, G. Competitive altruism: from reciprocity to the handicap principle. *Proc. R. Soc. Lond. B* **265**, 427–431 (1998).
6. Sherratt, T. N. & Roberts, G. The evolution of generosity and choosiness in cooperative exchanges. *J. Theor. Biol.* **193**, 167–177 (1998).
7. Dawes, R. M. Social Dilemmas. *Annu. Rev. Psychol.* **31**, 169–193 (1980).
8. Killingback, T. & Doebeli, M. The continuous prisoner's dilemma and the evolution of cooperation through reciprocal altruism with variable investment. *Am. Nat.* **160**, 421–438 (2002).
9. Enquist, M. & Leimar, O. The evolution of cooperation in mobile organisms. *Anim. Behav.* **45**, 747–757 (1993).
10. Hamilton, I. M. & Taborsky, M. Contingent movement and cooperation evolve under generalized reciprocity. *Proc. R. Soc. B* **272**, 2259–2267 (2005).
11. Houston, A. I. & Davies, N. B. in *Behavioural Ecology* (eds Sibly, R. M. & Smith, R. H.) 471–487 (Blackwell Scientific Publications, Oxford, 1985).
12. McNamara, J. M., Houston, A. I., Barta, Z. & Osorno, J. L. Should young ever be better off with one parent than with two? *Behav. Ecol.* **14**, 301–310 (2003).
13. Parker, G. A. Models of parent–offspring conflict. V. Effects of the behavior of the two parents. *Anim. Behav.* **33**, 519–533 (1985).
14. Doebeli, M., Hauert, C. & Killingback, T. The evolutionary origin of cooperators and defectors. *Science* **306**, 859–862 (2004).
15. Houston, A. I., Szekely, T. & McNamara, J. M. Conflict between parents over care. *Trends Ecol. Evol.* **20**, 33–38 (2005).
16. McNamara, J. M. & Houston, A. I. Evolutionarily stable levels of vigilance as a function of group-size. *Anim. Behav.* **43**, 641–658 (1992).
17. Maynard Smith, J. *Evolution and the Theory of Games* (Cambridge Univ. Press, Cambridge, 1982).
18. Doebeli, M. & Hauert, C. Models of cooperation based on the Prisoner's Dilemma and the Snowdrift game. *Ecol. Lett.* **8**, 748–766 (2005).
19. Queller, D. C. Kinship, reciprocity and synergism in the evolution of social behavior. *Nature* **318**, 366–367 (1985).
20. McNamara, J. M., Barta, Z. & Houston, A. I. Variation in behaviour promotes cooperation in the Prisoner's Dilemma game. *Nature* **428**, 745–748 (2004).
21. McNamara, J. M. & Forslund, P. Divorce rates in birds: predictions from an optimization model. *Am. Nat.* **147**, 609–640 (1996).
22. McNamara, J. M., Forslund, P. & Lang, A. An ESS model for divorce strategies in birds. *Phil. Trans. R. Soc. Lond. B* **354**, 223–236 (1999).
23. Hauert, C., De Monte, S., Hofbauer, J. & Sigmund, K. Volunteering as Red Queen mechanism for cooperation in public goods games. *Science* **296**, 1129–1132 (2002).
24. Hruschka, D. J. & Henrich, J. Friendship, cliquishness, and the emergence of cooperation. *J. Theor. Biol.* **239**, 1–15 (2006).
25. Ens, B. J., Safriel, U. N. & Harris, M. P. Divorce in the long-lived and monogamous oystercatcher, *Haematopus ostralegus* – incompatibility or choosing the better option. *Anim. Behav.* **45**, 1199–1217 (1993).
26. Moody, A. T., Wilhelm, S. I., Cameron-MacMillan, M. L., Walsh, C. J. & Storey, A. E. Divorce in common murres (*Uria aalge*): relationship to parental quality. *Behav. Ecol. Sociobiol.* **57**, 224–230 (2005).
27. Triefenbach, F. & Itzkowitz, M. Mate switching as a function of mate quality in convict cichlids, *Cichlasoma nigrofasciatum*. *Anim. Behav.* **55**, 1263–1270 (1998).
28. Brown, M., Falk, A. & Fehr, E. Relational contracts and the nature of market interactions. *Econometrica* **72**, 747–780 (2004).
29. Andersson, M. & Simmons, L. W. Sexual selection and mate choice. *Trends Ecol. Evol.* **21**, 296–302 (2006).
30. Sih, A., Bell, A. & Johnson, J. C. Behavioral syndromes: an ecological and evolutionary overview. *Trends Ecol. Evol.* **19**, 372–378 (2004).

Supplementary Information is linked to the online version of the paper at www.nature.com/nature.

Acknowledgements We thank O. Leimar and four anonymous referees for comments on a previous version of this paper. Z.B. was supported by a grant from the Biotechnology and Biological Sciences Research Council to A.I.H. and J.M.M. L.F. was supported by the Deutsche Forschungsgemeinschaft.

Author Contributions Based on an idea by J.M.M., the concept for this paper was developed in discussions among all authors. J.M.M. also formulated the material in Box 1 and most of the Supplementary Information; Z.B. performed the computations and prepared the figures; A.I.H. surveyed the literature; L.F. had the main responsibility for writing the paper.

Author Information Reprints and permissions information is available at www.nature.com/reprints. Correspondence and requests for materials should be addressed to L.F. (lutzfromhage@web.de).

LETTERS

Identification of the *sex* genes in an early diverged fungus

Alexander Idnurm[1,2], Felicia J. Walton[1], Anna Floyd[1] & Joseph Heitman[1]

Sex determination in fungi is controlled by a small, specialized region of the genome in contrast to the large sex-specific chromosomes of animals and some plants. Different gene combinations reside at these mating-type (*MAT*) loci and confer sexual identity; invariably they encode homeodomain, α-box, or high mobility group (HMG)-domain transcription factors[1]. So far, *MAT* loci have been characterized from a single monophyletic clade of fungi, the Dikarya (the ascomycetes and basidiomycetes)[2], and the ancestral state and evolutionary history of these loci have remained a mystery. Mating in the basal members of the kingdom has been less well studied, and even their precise taxonomic interrelationships are still obscure[3,4]. Here we apply bioinformatic and genetic mapping to identify the sex-determining (*sex*) region in *Phycomyces blakesleeanus* (Zygomycota), which represents an early branch within the fungi. Each *sex* allele contains a single gene that encodes an HMG-domain protein, implicating the HMG-domain proteins as an earlier form of fungal *MAT* loci. Additionally, one allele also contains a copy of a unique, chromosome-specific repetitive element, suggesting a generalized mechanism for the earliest steps in the evolution of sex determination and sex chromosome structure in eukaryotes.

Ascomycete and basidiomycete fungi exhibit marked variation in the regions of their genomes controlling sexual reproduction. The *MAT* loci comprise two highly dissimilar, idiomorphic alleles. Adjacent conserved genes and conserved intron positions indicate that the loci may derive from a single progenitor. In some (tetrapolar) basidiomycetes, two unlinked *MAT* loci, encoding homeodomain proteins and peptide pheromones/receptors, are involved. In other (bipolar) basidiomycete species, the two loci have coalesced to form a large, single locus[5–7]. Saccharomycotina and Archiascomycete *MAT* loci encode homeodomain and α-box proteins (*Saccharomyces cerevisiae*) or homeodomain, α-box and HMG-domain proteins (*Candida albicans*, *Schizosaccharomyces pombe*)[8]. Some Pezizomycotina (*Neurospora crassa*, *Podospora anserina*) contain a locus in which one allele encodes an HMG-domain protein and the other encodes three genes including another HMG-domain protein that has a less-prominent role in mating[9–12]. In the Microsporidia, which are organisms of ambiguous taxonomic position as fungi or sister-group to the fungi, sex is unknown. However, *Encephalitozoon cuniculi* has a potential *MAT* locus comprising adjacent homeodomain proteins, suggesting that these transcription factors are ancestral[13]. Which sex-determining system (homeodomain, α-box or HMG domain) and arrangement first arose is unknown.

Little is known at the genetic level about how sex determination is controlled in the remainder of the fungal kingdom, even though the abilities to outcross or undergo self-mating were termed heterothallism or homothallism on the basis of studies in one such early diverged lineage, the zygomycetes, a century ago[14,15]. Furthermore, at present only a few species in the order Mucorales of this phylum have a genetically defined sex-determining locus with two alleles that segregate in a 1:1 ratio of (+) to (–) after mating[16–20].

We hypothesized that the types of DNA-binding proteins that function in sex determination in the Dikarya could regulate mating in other fungal lineages. The *Phycomyces blakesleeanus* genome sequence was searched for homologues of Dikarya *MAT*-encoded transcription factors. In reciprocal BLAST searches with the candidates, no predicted *Phycomyces* homeodomain or α-box proteins were closely related to proteins known to regulate fungal mating. However, ten HMG-domain proteins had primary matches to those encoded by ascomycete *MAT* loci.

The ten genes encoding HMG-domain proteins were subjected to polymerase chain reaction (PCR) amplification from the sequenced strain NRRL1555 (–), UBC21 (+) of the opposite mating type, and A56 (+)[21], which is isogenic with strain NRRL1555. Nine genes amplified from all strains (Supplementary Fig. 1). The tenth amplified from NRRL1555 (–), but not from the two (+) strains. Furthermore, this gene amplified from four (–) wild-type strains but was absent from six (+) strains (data not shown), suggesting that it is linked to (–) sex specificity.

The DNA region from the opposite (+) sex, corresponding to the (–) HMG-domain protein, was obtained through PCR and sequenced. Strain UBC21 (+) contains a 5,830-base-pair (bp) sex unique region, compared to the 3,494-bp unique region of NRRL1555 (–) (Fig. 1a). The (+) region also encodes an HMG-domain protein, and the genes were named *sexM* (*sex minus*) and *sexP* (*sex plus*). The SexM and SexP proteins share low-level amino acid similarity (Fig. 1b). However, when the SexP protein is used in tBLASTn analysis of the *Phycomyces* genome, the most similar protein is SexM (*E*-value of 2.3×10^{-13}; 48 positive and 29 identical residues of the 81 most conserved), suggesting that the two genes are divergent homologues (Supplementary Fig. 2). The asymmetric positions of the genes within the sex unique regions and their inverted transcriptional orientation suggest that an ancient DNA inversion event may have occurred, driving evolution of the locus.

Genetic manipulation of *Phycomyces* via transformation has remained an elusive procedure[22], and as a consequence gene function for the candidate locus was demonstrated by analysing the properties of strains harbouring both the *sexM* and *sexP* alleles, and establishing genetic linkage between these genes and sex.

Three sex-disomic progeny were identified from genetic crosses that did not mate with either (+) or (–) tester strains. The strains have an odd 'fluffy' colony morphology due to the production of zygophore-like structures (Fig. 2a), suggesting that they are partially self-fertile. One (NRRL1555 × NRRL1554 progeny 54) occasionally even produced zygospores like a normal (+) × (–) cross. A sex-heterozygous strain (B36*A87), previously generated by forced

[1]Department of Molecular Genetics and Microbiology, Duke University Medical Center, Durham, North Carolina 27710, USA. [2]School of Biological Sciences, University of Missouri-Kansas City, Kansas City, Missouri 64110, USA.

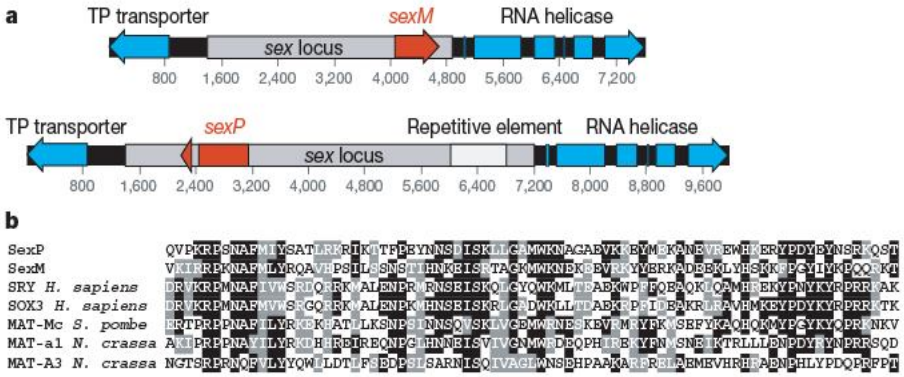

Figure 1 | Structure of the sex locus of *Phycomyces blakesleeanus*. **a**, Alignment of the sex unique sequence (shaded grey) and conserved flanking regions (99% identical) encoding a putative triose phosphate (TP) transporter and RNA helicase in strains NRRL1555 (–) and UBC21 (+). The alleles are 3,494 bp (NRRL1555) and 5,830 bp (UBC21), and *sexM* and *sexP* encode HMG-domain proteins. **b**, Alignment of the HMG domain of predicted proteins encoded by *sexM* and *sexP* with human SRY and SOX3, *S. pombe* MAT-Mc, and *N. crassa* MAT-A3 and MAT-a1. Black indicates 100% sequence identity and grey similar amino acid residues.

fusion of strains of the opposite sex[23], was obtained for comparison. Analysis of the *sex* gene content in these four fluffy strains showed that they all contain both *sexM* and *sexP* genes (Fig. 2b), confirming their heterozygous nature. Current evidence suggests that fluffy strains derived from crosses are partial diploids containing both *sex* alleles[24]. The three strains identified here behaved similarly to those previously reported[23–25], and exhibited variation in zygophore production, instability after passaging to revert to (+) or (–) sex, and co-segregating *sexP* and *sexM* genotypes, evidence for pheromone production and aneuploidy (Supplementary Fig. 3, Supplementary Data, and data not shown). When *sexM* and *sexP* expression was examined by northern blot analysis, transcript abundance was low in strains grown in isolation. In contrast, transcripts were at higher levels in sex-heterozygous strains and induced during (–) × (+) matings (Fig. 2c). The role of transcript levels in mating is currently unclear: future research in *Phycomyces* and Mucorales species will investigate how the Sex proteins are regulated by environmental conditions, and govern pheromone signalling and other meiotic spore developmental stages.

Genetic segregation data from three crosses of different strains with the wild-type sequenced strain demonstrated that the *sex* genes correspond to the *sex* locus. In the first cross, 69 progeny (one each from 69 zygospores) were obtained from NRRL1555 × NRRL1554. In 68 out of 69 cases, the (–) sex co-segregated with the *sexM* gene and (+) sex co-segregated with the *sexP* gene (χ^2 test, $P < 0.001$, Fig. 3 and Supplementary Information). One notable exception was heterozygous for both *sexM* and *sexP*, as discussed above. Linkage between sex and the HMG-domain genes was confirmed in a second cross previously conducted to establish linkage between the *madA* mutation and loss-of-phototropism in which sex served as an independent genetic marker[26]. Analysis of this cross (*madA* × A56, 63 progeny from 24 zygospores) showed that the (–) sex co-segregated with *sexM* and the (+) sex co-segregated with *sexP* ($P < 0.001$), whereas *madA* segregated independently, confirming linkage in a set of known recombinant progeny.

In a third cross to delimit the *sex* locus and examine the possibility that *Phycomyces* might contain a sex chromosome, we tested recombination in 104 progeny (derived from 104 zygospores, NRRL1555 × UBC21). Again, all (–) progeny contained *sexM* and all (+) progeny contained *sexP* ($P < 0.001$). Nine polymorphisms between UBC21 and NRRL1555 on contigs other than the *sexM*-containing region segregated independently from sex (Supplementary Information). In contrast, markers on the 377-kilobase (kb) sequenced contig containing *sexM* were linked to the sex phenotype. The sex phenotype was then mapped to a small region of this chromosome. Recombination was observed on one side of the *sex* locus but not the other (Fig. 4a). Similar frequencies were observed for the NRRL1554 × NRRL1555 cross, however, 1 out of 68 recombined on the suppressed side of the locus, as had a single progeny from the *madA* × A56 cross, providing recombinant strains for fine mapping. Polymorphisms closer to the locus were identified and, using the rare recombinants,

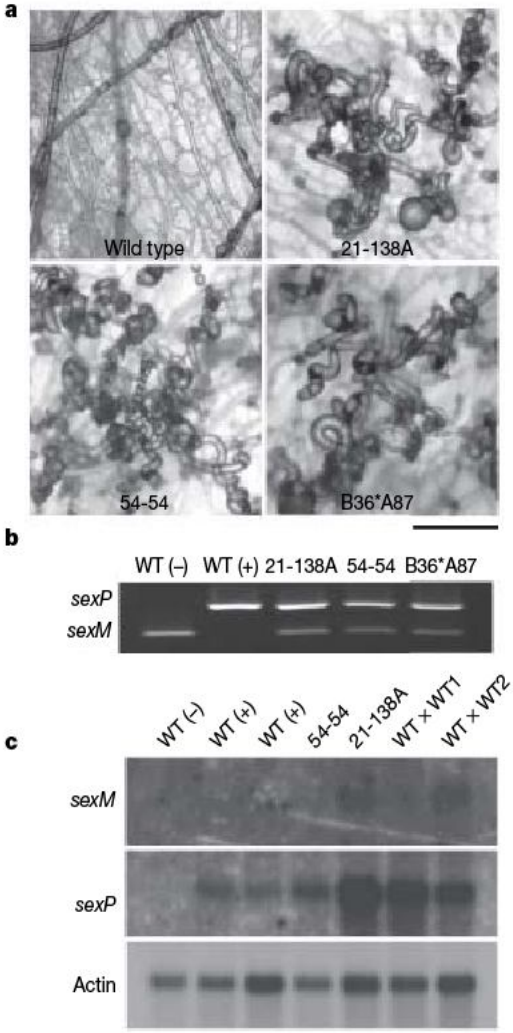

Figure 2 | Heterozygosity at the *sex* locus promotes a partially self-fertile phenotype. **a**, Morphology of wild type and *sexM-sexP* heterozygotes. B36*A87 is a defined *sex*-heterozygous strain. UBC21 × NRRL1555 138A (21-138A) and NRRL1554 × NRRL1555 54 (54-54) are unusual progeny derived from crosses. Scale bar, 200 μm. **b**, *sexM* or *sexP* in strains assessed by multiplex PCR. **c**, Transcript abundance of *sexM* and *sexP* in strains. The blot was sequentially probed with *sexP* (3 days, −80 °C exposure), *sexM* (4 days, −80 °C exposure) and actin (30 min, 22 °C exposure). Lane 1, NRRL1555 (–); lane 2, NRRL1554 (+); lane 3, UBC21 (+); lane 4, NRRL1555 × NRRL1555 54 cross; lane 5, UBC21 × NRRL1555 138A cross; lane 6, NRRL1554 × NRRL1555 cross; lane 7, UBC21 × NRRL1555 cross.

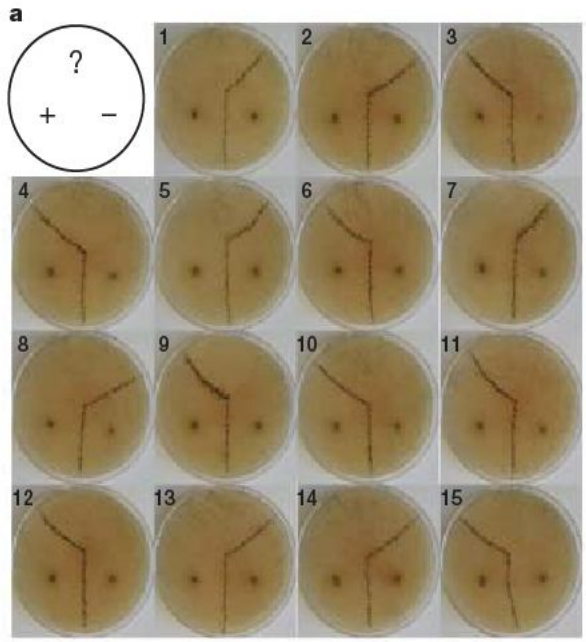

c

Cross	Phenotype and genotype				Probability
	(+) *sexP*	(–) *sexM*	(+) *sexM*	(–) *sexP*	
NRRL1555 × NRRL1554	33	35	0	0	$P < 0.001$
madA × A56	35	28	0	0	$P < 0.001$
NRRL1555 × UBC21	57	45	0	0	$P < 0.001$

Figure 3 | Sex co-segregates with *sexM* and *sexP* genes encoding HMG-domain proteins. **a**, Fifteen progeny of an NRRL1555 × NRRL1554 cross (from 69 analysed) were assessed for sex by crosses against (+) and (–) tester parents. Three strains were co-inoculated on V8 medium; the black lines of zygospores indicate mating, with diagonals to the right and left indicating (+) or (–) progeny, respectively, and a vertical line the positive control interaction between tester strains. **b**, The *sexM* and *sexP* genes were amplified by PCR from genomic DNA from the 15 progeny in panel **a**. **c**, Segregation data for crosses between strains (excluding heterozygous progeny).

sex was mapped to within 10 kb and 18 kb of the sex unique region (Fig. 4a). Thus, there is skewed recombination around the *Phycomyces sex* locus and it maps to less than 34 kb within the 65-megabase (Mb) genome.

The *plus* sex allele is 2,336 bp larger than the *minus* sex allele for the two strains sequenced. Analysis of the DNA sequence was undertaken to understand the basis for this size difference. A number of different small repetitive elements are present in the *plus* allele. Notably, one element is also present in the genome as two additional copies, both found on the same contig/chromosome as the *sex* locus (Fig. 4b). All three elements are aligned as direct repeats, so mitotic recombination would delete a large region of DNA including *sexP*, leading to sterility or lethality.

Although *Phycomyces* contains a *sex* locus rather than a sex chromosome, its locus structure and repetitive elements may provide insight into the events that shape sex-determining regions more generally. We hypothesize that in both *Phycomyces* and mammals a region of DNA containing a sex-determining HMG-domain gene underwent inversion, thereby blocking recombination and leading to divergence and cell-type specificity (*Phycomyces sexM-sexP*, mammalian *SRY-SOX3*). A similar scenario to the chromosome-specific repeats of *Phycomyces* in an indirect orientation in the early mammalian lineage could have facilitated a larger inversion, leading to the development of a sex chromosome (Supplementary Fig. 4), as is predicted to have occurred for the Y chromosome[27–29]. Simple inversion events probably represent a common mechanism driving the initiation and subsequent expansion of sex-determining regions in diverse lineages.

An early diverged fungus with this gene composition at *sex* suggests that either a locus comprising HMG-domain genes is ancestral to the Dikarya and Zygomycota or sex-determination evolved independently in the two. A similar region is present in another zygomycete genome, *Rhizopus oryzae*, where the candidate *sexP* allele is flanked by the same two genes flanking the *Phycomyces* locus (Supplementary Fig. 5). We currently favour the former hypothesis that the HMG-domain arrangement was ancestral in fungi, and has gradually lost function from some lineages by divergence in sequence or eviction from the locus to become a downstream target of homeodomain *MAT*-encoded proteins (see Supplementary Information for further discussion). However, the *MAT* alleles in the ascomycetes are more different in comparison to *Phycomyces*. This may indicate that functional constraints slow divergence of SexM and SexP or that

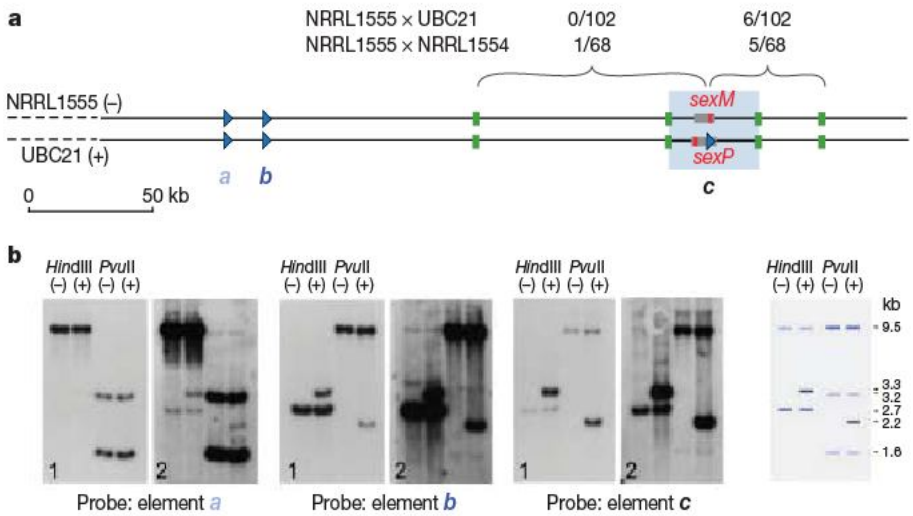

Figure 4 | Recombination around the *sex* locus and presence of chromosome-specific repetitive elements. **a**, Polymorphic markers approximately 50 and 87 kb from *sexM*/*sexP* were scored in progeny from crosses between NRRL1555 with either UBC21 or NRRL1554. In the subset exhibiting recombination, closer markers (blue box) map the locus within 10 kb and 18 kb of *sexM*/*sexP*. *a*, *b* and *c* represent repetitive elements. **b**, Southern blot hybridizations of chromosome-specific repetitive elements. Strain UBC21 contains a third element (*c*) within the *sex* locus. DNA from NRRL1555 or UBC21 was probed with each element (*a*, *b*, or *c*). Two autoradiograph exposures (1 and 2) illustrate cross-hybridization. Restriction maps for elements are summarized on the right.

an inter-allelic gene conversion event reset the locus. Only a better understanding of sex in fungi, particularly among the diverse non-Dikarya lineages, and identification of sex/mating-type loci will fully reveal the evolutionary trajectory of this sex-determining region in the fungal kingdom.

METHODS SUMMARY

Genes present in characterized fungal *MAT* loci as well as the human *SRY* HMG-domain male determinant were used to search the *Phycomyces* genome database. Candidate genes were amplified by PCR, with one gene encoding an HMG-domain protein amplifying only from (–) strains. The equivalent region in a (+) strain was obtained by inverse and regular PCR, and sequenced. Genetic crosses and segregation analyses were used to demonstrate that these genes correspond to the *sex* locus. The two genes were amplified from DNA from these progeny strains and compared with their sex type. To identify molecular genetic markers, ~160 kb of DNA derived from genomic libraries and PCR products of genes or regions of interest was sequenced from strain UBC21, as well as regions flanking *sex* in NRRL1554, and the sequence compared to the NRRL1555 genome database. Genetic markers linked and unlinked to the putative *sex* locus enabled mapping to a small genomic region. Three strains with unusual morphology were identified from crosses and their content and expression of the *sexM* and *sexP* genes determined by PCR and northern blot analyses, respectively. The low copy number of a repetitive element in the *plus* allele, as suggested by the sequencing project, was confirmed by Southern blot analysis.

Full Methods and any associated references are available in the online version of the paper at www.nature.com/nature.

Received 13 August; accepted 5 November 2007.

1. Fraser, J. A. & Heitman, J. Evolution of fungal sex chromosomes. *Mol. Microbiol.* **51**, 299–306 (2004).
2. Heitman, J., Kronstad, J. W., Taylor, J. W. & Casselton, L. A. (eds) *Sex in Fungi: Molecular Determination and Evolutionary Implications* (ASM Press, Washington, DC, 2007).
3. James, T. Y. *et al.* Reconstructing the early evolution of fungi using a six-gene phylogeny. *Nature* **443**, 818–822 (2006).
4. White, M. M. *et al.* Phylogeny of the Zygomycota based on nuclear ribosomal sequence data. *Mycologia* **98**, 872–884 (2006).
5. Bakkeren, G. *et al.* Mating factor linkage and genome evolution in basidiomycetous pathogens of cereals. *Fungal Genet. Biol.* **43**, 655–666 (2006).
6. Lee, N., Bakkeren, G., Wong, K., Sherwood, J. E. & Kronstad, J. W. The mating-type and pathogenicity locus of the fungus *Ustilago hordei* spans a 500-kb region. *Proc. Natl Acad. Sci. USA* **96**, 15026–15031 (1999).
7. Fraser, J. A. *et al.* Convergent evolution of chromosomal sex-determining regions in the animal and fungal kingdoms. *PLoS Biol.* **2**, e384 (2004).
8. Butler, G. *et al.* Evolution of the *MAT* locus and its Ho endonuclease in yeast species. *Proc. Natl Acad. Sci. USA* **101**, 1632–1637 (2004).
9. Staben, C. & Yanofsky, C. *Neurospora crassa a* mating-type region. *Proc. Natl Acad. Sci. USA* **87**, 4917–4921 (1990).
10. Glass, N. L., Grotelueschen, J. & Metzenberg, R. L. *Neurospora crassa A* mating-type region. *Proc. Natl Acad. Sci. USA* **87**, 4912–4916 (1990).
11. Ferreira, A. V.-B., An, Z., Metzenberg, R. L. & Glass, N. L. Characterization of *mat A-2, mat A-3* and Δ*matA* mating-type mutants of *Neurospora crassa*. *Genetics* **148**, 1069–1079 (1998).
12. Arnaise, S., Zickler, D., Le Bilcot, S., Poisier, C. & Debuchy, R. Mutations in mating-type genes of the heterothallic fungus *Podospora anserina* lead to self-fertility. *Genetics* **159**, 545–556 (2001).
13. Bürglin, T. R. The homeobox genes of *Encephalitozoon cuniculi* (Microsporidia) reveal a putative mating-type locus. *Dev. Genes Evol.* **213**, 50–52 (2003).
14. Blakeslee, A. F. Zygospore formation is a sexual process. *Science* **19**, 864–866 (1904).
15. Blakeslee, A. F. Sexual reproduction in the Mucorineae. *Proc. Am. Acad. Arts Sci.* **40**, 205–319 (1904).
16. Cerdá-Olmedo, E. The genetics of *Phycomyces blakesleeanus*. *Genet. Res.* **25**, 285–296 (1975).
17. Alvarez, M. I., Peláez, M. I. & Eslava, A. P. Recombination between ten markers in *Phycomyces*. *Mol. Gen. Genet.* **179**, 447–452 (1980).
18. Eslava, A. P., Alvarez, M. I., Burke, P. V. & Delbrück, M. Genetic recombination in sexual crosses of *Phycomyces*. *Genetics* **80**, 445–462 (1975).
19. Eslava, A. P., Alvarez, M. I. & Delbrück, M. Meiosis in *Phycomyces*. *Proc. Natl Acad. Sci. USA* **72**, 4076–4080 (1975).
20. Gauger, W. L. Meiotic gene segregation in *Rhizopus stolonifer*. *J. Gen. Microbiol.* **101**, 211–217 (1977).
21. Alvarez, M. I. & Eslava, A. P. Isogenic strains of *Phycomyces blakesleeanus* suitable for genetic analysis. *Genetics* **105**, 873–879 (1983).
22. Obraztsova, I. N., Prados, N., Holzmann, K., Avalos, J. & Cerdá-Olmedo, E. Genetic damage following introduction of DNA in *Phycomyces*. *Fungal Genet. Biol.* **41**, 168–180 (2004).
23. Govind, N. S. & Cerdá-Olmedo, E. Sexual activation of carotenogenesis in *Phycomyces blakesleeanus*. *J. Gen. Microbiol.* **132**, 2775–2780 (1986).
24. Mehta, B. J. & Cerdá-Olmedo, E. Intersexual partial diploids of *Phycomyces*. *Genetics* **158**, 635–641 (2001).
25. Burgeff, H. Untersuchungen über Variabilität, Sexualität und Erblichkeit bei Phycomyces nitens Kuntze. *Flora* **107**, 259–316 (1914).
26. Idnurm, A. *et al.* The *Phycomyces madA* gene encodes a blue-light photoreceptor for phototropism and other light responses. *Proc. Natl Acad. Sci. USA* **103**, 4546–4551 (2006).
27. Lahn, B. T. & Page, D. C. Four evolutionary strata on the human X chromosome. *Science* **286**, 964–967 (1999).
28. Skaletsky, H. *et al.* The male-specific region of the human Y chromosome is a mosaic of discrete sequence classes. *Nature* **423**, 825–837 (2003).
29. Charlesworth, D., Charlesworth, B. & Marais, G. Steps in the evolution of heteromorphic sex chromosomes. *Heredity* **95**, 118–128 (2005).

Supplementary Information is linked to the online version of the paper at www.nature.com/nature.

Acknowledgements We acknowledge access to the *Phycomyces* genome project: these sequence data were produced by the US Department of Energy Joint Genome Institute. We thank L. Corrochano and A. Eslava for encouragement and providing *Phycomyces* strains, and L. Corrochano and X. Lin for comments on the manuscript. This research was supported by National Institutes of Health grants to J.H.

Author Information DNA sequences for the reported genes have been deposited at GenBank under accessions EU009461 and EU009462. Reprints and permissions information is available at www.nature.com/reprints. Correspondence and requests for materials should be addressed to J.H. (heitm001@mc.duke.edu).

LETTERS

Ultra-fine frequency tuning revealed in single neurons of human auditory cortex

Y. Bitterman[1,2], R. Mukamel[3,4], R. Malach[5], I. Fried[4,6] & I. Nelken[1,2]

Just-noticeable differences of physical parameters are often limited by the resolution of the peripheral sensory apparatus. Thus, two-point discrimination in vision is limited by the size of individual photoreceptors. Frequency selectivity is a basic property of neurons in the mammalian auditory pathway[1,2]. However, just-noticeable differences of frequency are substantially smaller than the bandwidth of the peripheral sensors[3]. Here we report that frequency tuning in single neurons recorded from human auditory cortex in response to random-chord stimuli is far narrower than that typically described in any other mammalian species (besides bats), and substantially exceeds that attributed to the human auditory periphery. Interestingly, simple spectral filter models failed to predict the neuronal responses to natural stimuli, including speech and music. Thus, natural sounds engage additional processing mechanisms beyond the exquisite frequency tuning probed by the random-chord stimuli.

Sounds are decomposed to different frequency bands by the auditory periphery. Tonotopic ('by frequency') organization is kept throughout the auditory pathway, at least up to and including primary auditory cortex. In vision and somatosensation, the resolution of the peripheral sensors to a large degree determines overall behavioural discrimination capabilities. However, in the auditory system, frequency just-noticeable differences in well-trained subjects may be 30 times smaller than the presumed bandwidth of the peripheral filters ('critical bands', typically about a sixth of an octave in humans, as measured in psychoacoustical tests). Electrophysiological correlates of critical bands have been suggested[4–6], and frequency just-noticeable differences can be derived by integrating information over a large population of neurons[7], but there are currently no reports of a significant population of single neurons the bandwidth of which corresponds to the behavioural just-noticeable differences. Does the high-frequency resolution expressed behaviourally have explicit neural representation? If so, can high-frequency resolution explain the response patterns to complex sounds?

Responses of neurons in human auditory cortex were recorded from four patients with intractable epilepsy monitored with intracranial depth electrodes to identify seizure foci for potential surgical treatment[8]. Using clinical criteria, electrodes were implanted bilaterally in the transverse gyri of Heschl, loci of the auditory cortex (see Methods). Patients were presented with artificial random-chord stimuli at a resolution of six tones per octave (two patients) or 18 tones per octave (one patient), and with segments from the popular English-speaking western film "The Good, the Bad and the Ugly" (three patients, see Methods). Thus, for many neurons, the stimulus ensemble included both artificial stimuli and more structured stimuli. The artificial stimuli were designed to sample evenly the spectral range of the movie soundtrack. Results are based on 95 units recorded in four patients.

Figure 1 displays raster responses of one unit to the different frequencies in the six-tones-per-octave random-chord stimulus. Each frequency appeared simultaneously with two other frequencies selected essentially randomly. Only one of the 41 possible frequencies elicited excitatory responses in this unit. Furthermore, when a tone burst of that frequency appeared in the stimulus, a sustained response outlasting tone duration was elicited with high reliability. The lack of excitatory response to the two adjacent frequencies implies that this unit was more selective than the frequency resolution of the stimulus (six tones per octave).

Of 31 units from the two patients presented with the six-tones-per-octave random-chord stimulus, 27 had a narrow, well-circumscribed frequency response area. About half (14/31) showed reliable responses to tone bursts at a single frequency, with no consistent excitatory response to any other frequency. Thirteen units responded to two to three adjacent frequencies. The rest (4/31) exhibited more complex responses. The resolution of six tones per octave was thus too coarse directly to measure the spectral bandwidth of most units.

A high-resolution random-chord stimulus with 18 tones per octave was presented to a third patient. Of 16 units recorded in this patient, 14 exhibited a highly elevated firing rate in response to a single frequency, with additional weaker, although significant, responses to only one or two adjacent frequencies. The average bandwidth of these units can be conservatively estimated at about a twelfth of an octave, in agreement with the results presented above (Fig. 2a). Figure 2b displays typical spectro-temporal receptive fields (called 'artificial STRFs' below) derived from responses to the random-chord stimuli by spike-triggered averaging. The best frequencies, defined as the frequency that elicited maximal response, ranged from 250 to 2 kHz in this population (Fig. 2c). It is generally accepted that the frequency tuning curve of the auditory periphery in humans has a width of about a sixth of an octave[3]. Therefore, when presented with random chords, the great majority of auditory cortical neurons showed substantially better frequency selectivity than the auditory nerve.

The frequency discrimination performance based on responses in single trials was estimated using receiver operating characteristic (ROC) analysis. We compared the empirical spike count distributions elicited by the different frequencies and determined the lowest discrimination threshold for each of the 47 units tested with the random-chord stimuli. Performance was quantified by the probability of correct decision in a two-interval, two-alternative forced choice test. Discrimination threshold was set at 70.7%, as typically done in auditory psychophysics. In more than 60% of the excitatory cells (25/42) discrimination was above threshold for the smallest possible frequency difference tested, the spectral resolution of the stimulus (20/27 units tested with six tones per octave and 5/15 units tested with 18 tones per octave; see for example Fig. 3).

[1]Department of Neurobiology, Life Science Institute, [2]Interdisciplinary Center for Neural Computation, Hebrew University, Jerusalem 91904, Israel. [3]Ahmanson-Lovelace Brain Mapping Center, David Geffen School of Medicine, [4]Division of Neurosurgery, David Geffen School of Medicine and Semel Institute for Neuroscience and Human Behaviour, University of California Los Angeles (UCLA), Los Angeles, California 90095, USA. [5]Department of Neurobiology, Weizmann Institute of Science, Rehovot 76100, Israel. [6]Functional Neurosurgery Unit, Tel Aviv Sourasky Medical Center and Sackler School of Medicine, Tel Aviv University, Tel Aviv 69978, Israel.

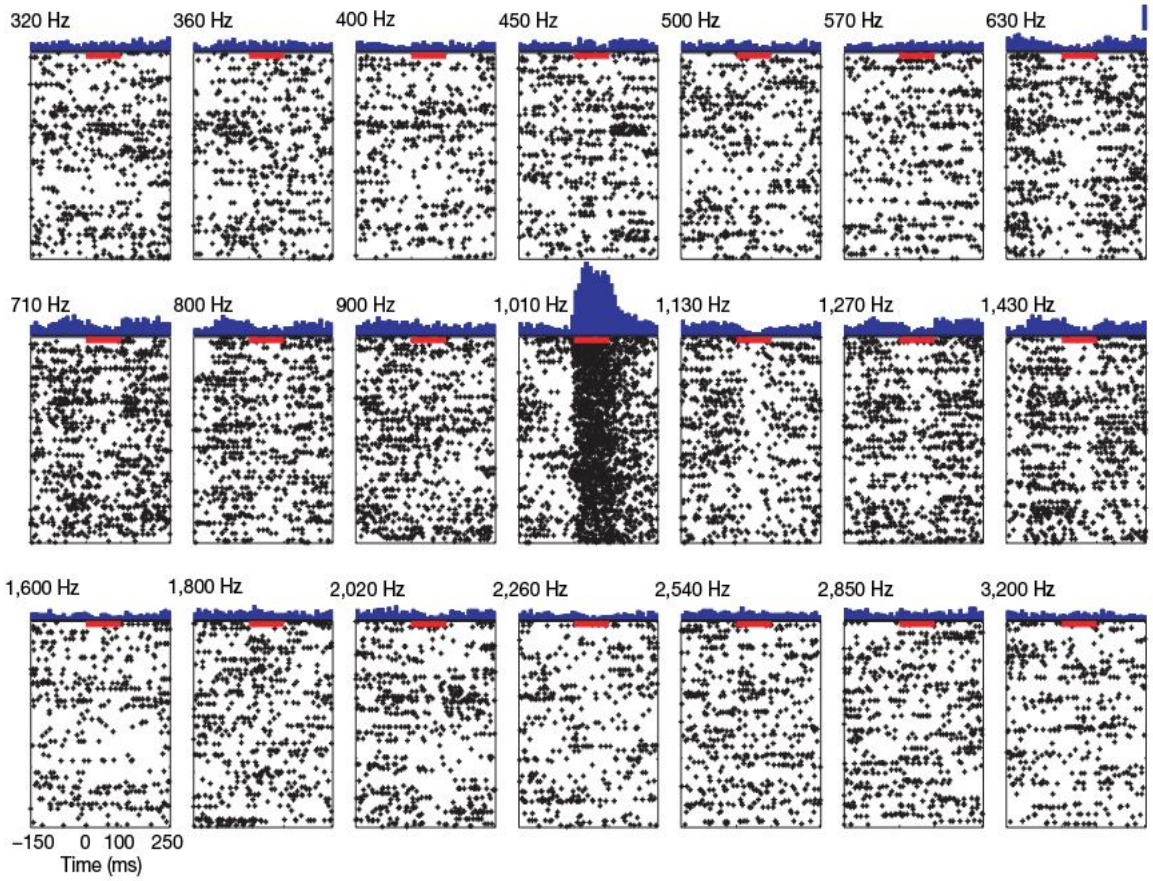

Figure 1 | Response selectivity. Raster plots of responses of one unit to chords containing the frequency specified above each panel (270 repetitions in each panel) and peristimulus time histograms (PSTH, blue; bin width 10 ms) based on these raster plots (the scale line at the top right PSTH corresponds to a firing rate of 16 spikes per second; maximum firing rate at preferred frequency: 47 spikes per second). Red bars mark 100 ms (duration of one chord) from the beginning of the response to the preferred frequency. The frequency table contained 20 additional frequencies (below 320 Hz and above 3,200 Hz); no other frequency elicited significant responses.

For these units, we linearly interpolated spike count distributions to simulate possible distributions at intermediate frequencies that were not actually tested (see Methods). Thresholds were again estimated by the smallest frequency interval that could be discriminated using these intermediate distributions. These thresholds are underestimates because maximum slopes of frequency response curves are bounded from below by linear interpolation. Even so, this procedure revealed units that had discrimination thresholds that matched and even exceeded the behavioural performance of naive human subjects[9] (Fig. 3e).

Do units also respond as narrow spectral filters when presented with natural sounds? We analysed responses elicited by nine-minute clips from the soundtrack of the feature film "The Good, the Bad and the Ugly", shown twice in each recording session. The soundtrack contained approximately equal-duration segments of dialogue, music and background noise. The average firing rate was not significantly different between responses to the random-chord stimuli and responses to the soundtrack (paired *t*-test, $t = 1.04$, degrees of freedom d.f. = 13, not significant), suggesting the soundtrack was, on average, as successful as random chords in driving neuronal responses, with comparable reproducibility (see Supplementary Information).

We estimated STRFs from responses to the soundtrack (called 'natural STRFs' below) using generalized reverse correlation techniques following ref. 10. The exquisite spectral filtering clearly apparent in the artificial STRFs was partially lost—natural STRFs were noisier and appeared to have richer structure (Fig. 4a). Nevertheless, there were similarities between natural and artificial STRFs estimated for the same unit. For the units recorded with both stimuli, the best frequency of the artificial STRF and the best frequency of the natural STRFs were highly correlated ($r = 0.7$,

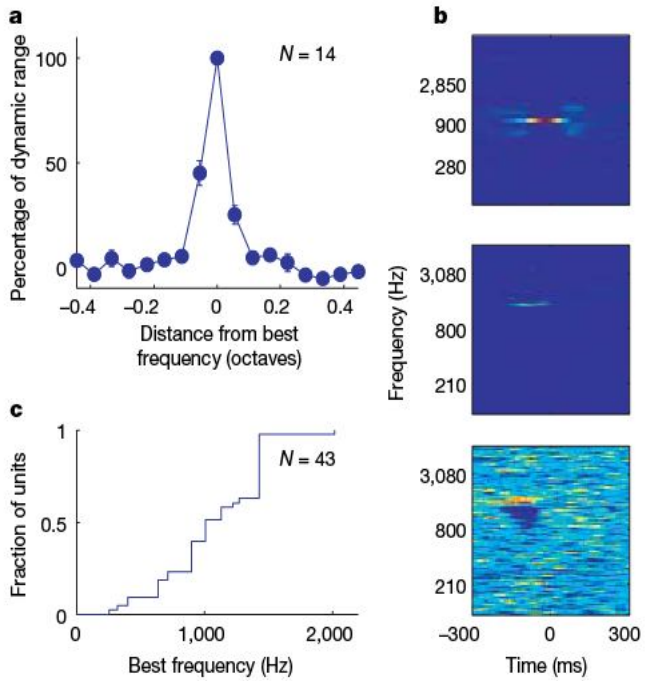

Figure 2 | Frequency tuning in the responses to the random-chord stimulus. **a**, Mean tuning curve (see Methods). Error bars indicate s.e.m. **b**, STRFs of three units estimated from the responses to the random-chord stimulus. The top panel shows a unit tested with six-tones-per-octave resolution that responded to a single frequency (colour scale saturation: 2.5–39 spikes per second). The middle panel shows a unit tested with 18-tones-per-octave resolution that responded predominantly to a single frequency (colour scale saturation: 1–32 spikes per second). The bottom panel shows a unit with complex tuning (colour scale saturation: 0–3.4 spikes per second). **c**, Cumulative distribution of the best frequencies of 43 units with a clear excitatory peak.

d.f. = 16, $P \ll 0.01$; Fig. 4b). This agrees with the general finding that the best frequency is largely independent of auditory context[11].

The first- and second-order statistics characterizing the soundtrack were fully sampled by the random-chord stimuli (verified by comparing the joint distribution of spectral and temporal modulations in the two stimulus ensembles) and the calculation of the natural STRFs corrected for second-order correlations in the stimulus[10]. Thus, if neurons linearly integrate their spectro-temporal input, natural and artificial STRFs should be essentially equivalent. However, the soundtrack also contained higher-order spectral correlations the effects of which on the STRFs could become apparent if the neurons had significant nonlinearities. These effects could be the reason for the additional structure in the natural STRFs.

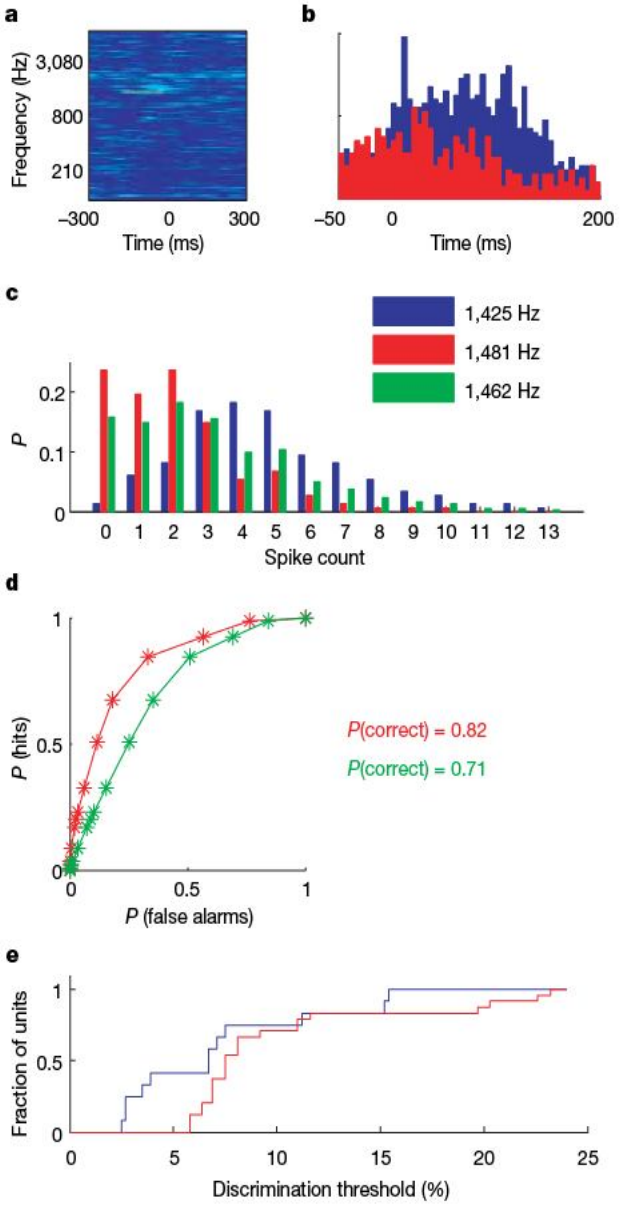

Figure 3 | Frequency discrimination based on single-trial responses. **a**, STRF of an excitatory unit estimated from the responses to the high-resolution random-chord stimulus (colour scale saturation: 6–36 spikes per second). **b**, PSTHs (bin width: 5 ms); blue is the response to the best frequency and red is the response to the adjacent frequency. The ordinate represents firing rate, scale: 0–40 spikes per second. **c**, Empirical spike count distributions of best-frequency responses (blue), of the responses to the adjacent frequency (red) and an estimated distribution of responses to an intermediate frequency (green). The ordinate represents the probability P of observing each spike count. **d**, ROC curves generated from pairs of distributions in **c**. Red: 1,425 and 1,481 Hz (interval: 3.9%). Green: 1,425 and 1,461 Hz (interval: 2.5%). **e**, Cumulative distribution of just-noticeable differences for units tested with random-chord stimuli at six tones per octave (red, $N = 27$) and 18 tones per octave (blue, $N = 15$).

We addressed this by comparing the predictive power of the STRFs within and across context (random-chord stimuli or film soundtrack). If artificial STRFs predict responses to the soundtrack as well as (or better than) natural STRFs, or vice versa, we can conclude that the potential nonlinear mechanisms that are not captured by the STRFs have only a small effect on the neuronal responses. Alternatively, if each STRF predicts the responses to new sounds from the ensemble used to estimate the STRF better than does the STRF derived from the other sound ensemble, then it can be inferred that there are significant nonlinearities in the responses, with the natural sounds possibly engaging processing mechanisms different from those engaged by the artificial sounds.

For units recorded with both stimuli, predicted responses to one-minute segments of the soundtrack were generated with both artificial and natural STRFs (the natural STRF was estimated without using the responses to the segment whose responses were predicted). Predictive power was quantified by the correlation coefficient between the prediction and the actual response of the unit. The expected maximum correlation (estimated as the average correlation between responses to two presentations of the soundtrack) was 0.3 (ref. 12). The predictive power of the artificial STRFs on the soundtrack was notably low: 0.13 ± 0.14 (mean $\pm$ s.d.), about 40% of the expected maximum. More importantly, correlations were significantly higher within context: a natural STRF typically predicted the actual responses to a soundtrack segment better than did an artificial STRF, with an average correlation coefficient of 0.25 ± 0.14 (Fig. 4c), over 80% of the expected maximum correlation. A three-way analysis of variance (ANOVA) on STRF type x predicted segment x neuron showed a highly significant main effect of STRF type, $F_{1,229} = 72$,

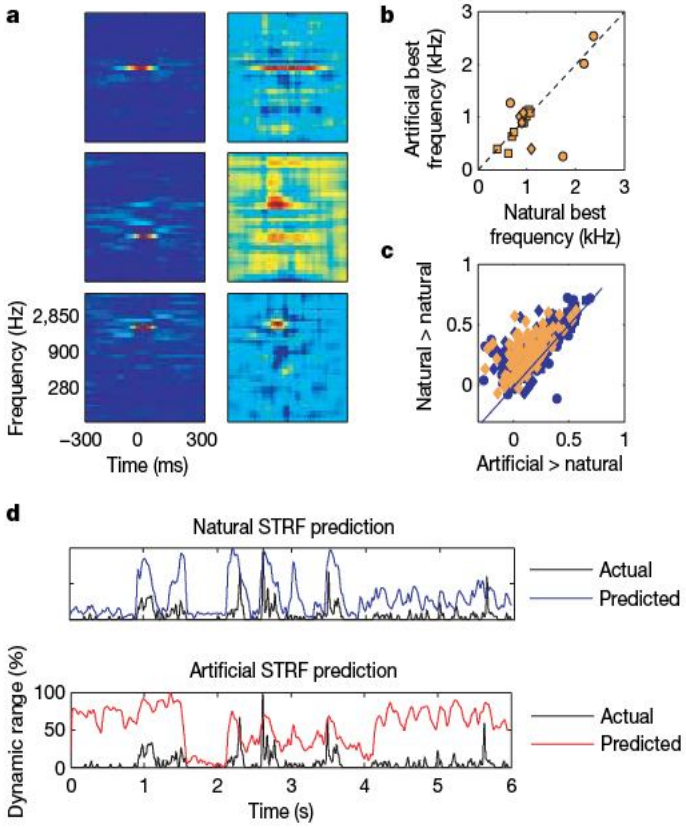

Figure 4 | Natural versus artificial responses. **a**, STRFs of three units based on responses to the random-chord stimulus (left) and to the soundtrack (right). **b**, Best frequency of artificial STRFs versus best frequency of natural STRFs ($N = 16$). **c**, Correlations between predictions and actual responses to one-minute segments from the soundtrack. Abscissa: using artificial STRFs (orange, 14 units) or synthetic STRFs (blue, 31 units). Ordinate: using natural STRFs. **d**, Predictions and response to one minute of the soundtrack by natural (top) and artificial (bottom) STRFs: 121 ms hamming window. Correlation coefficients are 0.46 and 0.18, respectively.

$P \ll 0.01$. The same general result was obtained when we used narrowband filters fitted to each unit instead of the artificial STRFs (see Supplementary Information). Similarly, natural STRFs were substantially less successful in predicting the responses to the random-chord stimuli than artificial STRFs (see Supplementary Information). Thus, stimulus encoding was not entirely determined by frequency selectivity. STRFs exhibited superior predictive power when tested with sounds that belong to the ensemble used to estimate them, suggesting that nonlinear mechanisms participate crucially in shaping the neuronal responses[10].

Our results demonstrate that frequency tuning in the human auditory cortex is substantially narrower than that typically found in the auditory cortex of non-human mammals (except bats). Using pure tones under the commonly used barbiturate anaesthesia, the tuning width at suprathreshold levels was found to be about one octave in cats[13] and about a third of an octave on average in rats[14]. Comparisons of tuning between awake and anesthetized animals within the same species have repeatedly shown that bandwidths are wider in the awake preparation (cats[15], see review[16]; rats[14]). Surveys of tuning in the auditory cortex of the awake macaque reported bandwidths that were typically half to one octave[17], and either very narrowly tuned neurons were rare[17] or bandwidths were wider than a seventh of an octave[18]. In the only other report of a unit in human auditory cortex[1], the width at half-height was at least one octave. The frequency tuning derived from STRFs is typically somewhat narrower than that derived from pure tone responses, but seems to be wider than the data shown here. For example, in deeply anaesthetized cats, the STRF width was about half an octave[19]. Thus, in mammalian responses, the typical selectivity of cortical neurons was worse, not better, than that found on the periphery of the same species. With the caution required by the small sample reported here, we propose that in contrast with animal studies, the spectral selectivity of neurons in human auditory cortex is substantially better than that of the auditory periphery.

These results are relevant to the apparent paradox of frequency hyperacuity demonstrated repeatedly in human psychoacoustics. Subjects with normal hearing, even untrained, successfully detect spectral differences substantially narrower than the presumed bandwidth of single auditory nerve fibres. Our results demonstrate that frequency differences smaller than 3% could be reliably detected from single-trial responses of single units in human auditory cortex. This value is comparable to the minimum detection threshold reported in untrained subjects[9]. Thus, the responses of one of these cortical neurons could, in principle, underlie behavioural performance on a single-trial basis. Tramo *et al.*[20] reported that bilateral lesions of human auditory cortex cause significant elevations in frequency discrimination thresholds, suggesting a functional role for the electrophysiological findings reported here. Remarkably, thresholds (frequency ratios) after the lesions were about 10–20%, matching the peripheral tuning in humans. We therefore suggest that the neural responses we observed in human auditory cortex reflect a readout of information available in the activity of large neuronal ensembles in subcortical stations, and that the auditory cortex is necessary for this readout to be performed, resulting in the behavioural hyperacuity of frequency discrimination in humans.

Previous studies in alert human subjects have shown very selective responses in single neurons from other brain areas. Notably, Quiroga *et al.*[21] reported highly specific responses to individual people or landmarks from a subset of medial temporal lobe neurons, suggesting an invariant, sparse code. The high selectivity reported here may be a counterpart of the same phenomenon, resulting in a sparse coding of frequency in auditory cortex. We can only speculate why a low-level cue such as frequency is represented so explicitly and predominantly in single neurons of human auditory cortex but not in the auditory cortex of other terrestrial mammalian species. There is evidence that frequency discrimination in humans is correlated with a number of cognitive skills, including language abilities[22], working memory[23] and learning capabilities[24], but more research is needed to clarify this puzzle.

METHODS SUMMARY

Extracellular single-unit recordings were obtained from four patients with pharmacologically intractable epilepsy, implanted with intracranial electrodes to identify seizure focus for potential surgical treatment. Electrode location was based solely on clinical criteria. All patients had electrodes placed bilaterally in Heschl's gyri. In each experimental session, patients 1 to 3 were presented twice in succession with 8:40 min of an audio-visual segment of the film "The Good, the Bad, and the Ugly". Patients 2, 3 and 4 were presented with random-chord stimuli[25,26] accompanied with random visual textures. Each chord had three pure-tone components, selected quasi-randomly out of a frequency table spanning the frequency range of the soundtrack. The tone duration was 100 ms (patients 2 and 3) or 50 ms (patient 4) with 10 ms linear onset and offset ramps. The frequencies were equally spaced along a logarithmic axis from 100 Hz to 10 kHz. The resolution was either a sixth of an octave (41 different frequencies, patients 2 and 3) or 1/18th of an octave (108 frequencies, patient 4). Sequence duration was 3.5 min (patients 2 and 3) or 5 min (patient 4). Data were acquired in ten sessions, all conducted at the patients' quiet bedside using a standard laptop screen and the laptop's built-in speakers (patients 1 and 2) or external speakers (patients 3 and 4). Sound intensity was set to a comfortable hearing level but absolute sound level was not measured. The free-field presentation was most probably accompanied by reverberation. Though unlikely to have influenced the results presented here, these factors represent differences from most studies in anesthetized animals. The data consist of 95 units (20 units from patient 1, 21 from patient 2, 38 from patient 3 and 16 from patient 4). The linear approximation to the response function for each unit in response to the soundtrack was computed using the software package STRFpak[27]. Discrimination thresholds were computed using ROC analysis based on empirical spike count distributions.

Full Methods and any associated references are available in the online version of the paper at www.nature.com/nature.

Received 17 June; accepted 14 November 2007.

1. Howard, M. A. III *et al.* A chronic microelectrode investigation of the tonotopic organization of human auditory cortex. *Brain Res.* **724**, 260–264 (1996).
2. Nelken, I. in *Integrative Functions in the Mammalian Auditory Pathway* (eds Oertel, D., Popper, A. N. & Fay, R. R.) 358–416 (Springer, New York, 2002).
3. Moore, B. C. J. *An Introduction to the Psychology of Hearing* Ch. 3 74–114 (Academic Press, London, 1982).
4. Evans, E. F. in *Psychophysics and Physiology of Hearing* (eds Evans, E. F. & Wilson, J. P.) 185–196 (Academic Press, London, 1977).
5. Ehret, G. & Schreiner, C. E. Frequency resolution and spectral integration (critical band analysis) in single units of the cat primary auditory cortex. *J. Comp. Physiol. A* **181**, 635–650 (1997).
6. Ehret, G. & Merzenich, M. M. Complex sound analysis (frequency resolution, filtering and spectral integration) by single units of the inferior colliculus of the cat. *Brain Res.* **472**, 139–163 (1988).
7. Heinz, M. G., Colburn, H. S. & Carney, L. H. Evaluating auditory performance limits: I. One-parameter discrimination using a computational model for the auditory nerve. *Neural Comput.* **13**, 2273–2316 (2001).
8. Fried, I. *et al.* Cerebral microdialysis combined with single-neuron and electroencephalographic recording in neurosurgical patients. *J. Neurosurg.* **91**, 697–705 (1999).
9. Banai, K. & Ahissar, M. Poor frequency discrimination probes dyslexics with particularly impaired working memory. *Audiol. Neurootol.* **9**, 328–340 (2004).
10. Theunissen, F. E., Sen, K. & Doupe, A. J. Spectral-temporal receptive fields of nonlinear auditory neurons obtained using natural sounds. *J. Neurosci.* **20**, 2315–2331 (2000).
11. Woolley, S. M., Gill, P. R. & Theunissen, F. E. Stimulus-dependent auditory tuning results in synchronous population coding of vocalizations in the songbird midbrain. *J. Neurosci.* **26**, 2499–2512 (2006).
12. Hsu, A., Borst, A. & Theunissen, F. E. Quantifying variability in neural responses and its application for the validation of model predictions. *Network* **15**, 91–109 (2004).
13. Read, H. L., Winer, J. A. & Schreiner, C. E. Modular organization of intrinsic connections associated with spectral tuning in cat auditory cortex. *Proc. Natl Acad. Sci. USA* **98**, 8042–8047 (2001).
14. Gaese, B. H. & Ostwald, J. Anesthesia changes frequency tuning of neurons in the rat primary auditory cortex. *J. Neurophysiol.* **86**, 1062–1066 (2001).

15. Qin, L., Kitama, T., Chimoto, S., Sakayori, S. & Sato, Y. Time course of tonal frequency-response-area of primary auditory cortex neurons in alert cats. *Neurosci. Res.* **46**, 145–152 (2003).
16. Moshitch, D., Las, L., Ulanovsky, N., Bar-Yosef, O. & Nelken, I. Responses of neurons in primary auditory cortex (A1) to pure tones in the halothane-anesthetized cat. *J. Neurophysiol.* **95**, 3756–3769 (2006).
17. Recanzone, G. H., Guard, D. C. & Phan, M. L. Frequency and intensity response properties of single neurons in the auditory cortex of the behaving macaque monkey. *J. Neurophysiol.* **83**, 2315–2331 (2000).
18. Schwarz, D. W. & Tomlinson, R. W. Spectral response patterns of auditory cortex neurons to harmonic complex tones in alert monkey (*Macaca mulatta*). *J. Neurophysiol.* **64**, 282–298 (1990).
19. Miller, L. M., Escabi, M. A., Read, H. L. & Schreiner, C. E. Spectrotemporal receptive fields in the lemniscal auditory thalamus and cortex. *J. Neurophysiol.* **87**, 516–527 (2002).
20. Tramo, M. J., Shah, G. D. & Braida, L. D. Functional role of auditory cortex in frequency processing and pitch perception. *J. Neurophysiol.* **87**, 122–139 (2002).
21. Quiroga, R. Q., Reddy, L., Kreiman, G., Koch, C. & Fried, I. Invariant visual representation by single neurons in the human brain. *Nature* **435**, 1102–1107 (2005).
22. Benasich, A. A. & Tallal, P. Infant discrimination of rapid auditory cues predicts later language impairment. *Behav. Brain Res.* **136**, 31–49 (2002).
23. Banai, K. & Ahissar, M. Auditory processing deficits in dyslexia: task or stimulus related? *Cereb. Cortex* **16**, 1718–1728 (2006).
24. McArthur, G. M. & Bishop, D. V. Speech and non-speech processing in people with specific language impairment: a behavioural and electrophysiological study. *Brain Lang.* **94**, 260–273 (2005).
25. deCharms, R. C., Blake, D. T. & Merzenich, M. M. Optimizing sound features for cortical neurons. *Science* **280**, 1439–1443 (1998).
26. Schnupp, J. W., Mrsic-Flogel, T. D. & King, A. J. Linear processing of spatial cues in primary auditory cortex. *Nature* **414**, 200–204 (2001).
27. Theunissen, F. E. *et al.* Estimating spatio-temporal receptive fields of auditory and visual neurons from their responses to natural stimuli. *Network* **12**, 289–316 (2001).
28. Mukamel, R. *et al.* Coupling between neuronal firing, field potentials, and FMRI in human auditory cortex. *Science* **309**, 951–954 (2005).
29. Bleeck, S., Ives, T. & Patterson, R. D. Aim-mat: the auditory image model in MATLAB. *Acta Acustica* **90**, 781–788 (2004).

Supplementary Information is linked to the online version of the paper at www.nature.com/nature.

Acknowledgements We thank the patients for their cooperation in participating in the experiments. We thank E. Behnke, T. A. Fields, E. Ho and C. Wilson for technical assistance. This work was supported by an ISF grant (to I.N.), a NINDS grant (to I.F.), the US-Israel BSF fund (R.M. and I.F.) and a European Molecular Biology Organization and Human Frontier Science Program fellowship (R.M.).

Author Information Reprints and permissions information is available at www.nature.com/reprints. Correspondence and requests for materials should be addressed to I.N. (israel@cc.huji.ac.il) or to I.F. (ifried@mednet.ucla.edu).

LETTERS

Epigenetic silencing of tumour suppressor gene *p15* by its antisense RNA

Wenqiang Yu[1], David Gius[2], Patrick Onyango[1], Kristi Muldoon-Jacobs[2], Judith Karp[3], Andrew P. Feinberg[1]* & Hengmi Cui[1]*

Tumour suppressor genes (TSGs) inhibiting normal cellular growth are frequently silenced epigenetically in cancer[1]. DNA methylation is commonly associated with TSG silencing[1], yet mutations in the DNA methylation initiation and recognition machinery in carcinogenesis are unknown[2]. An intriguing possible mechanism for gene regulation involves widespread non-coding RNAs such as microRNA, Piwi-interacting RNA and antisense RNAs[3–5]. Widespread sense–antisense transcripts have been systematically identified in mammalian cells[6], and global transcriptome analysis shows that up to 70% of transcripts have antisense partners and that perturbation of antisense RNA can alter the expression of the sense gene[7]. For example, it has been shown that an antisense transcript not naturally occurring but induced by genetic mutation leads to gene silencing and DNA methylation, causing thalassaemia in a patient[8]. Here we show that many TSGs have nearby antisense RNAs, and we focus on the role of one RNA in silencing *p15*, a cyclin-dependent kinase inhibitor implicated in leukaemia. We found an inverse relation between *p15* antisense (*p15AS*) and *p15* sense expression in leukaemia. A *p15AS* expression construct induced *p15* silencing in *cis* and in *trans* through heterochromatin formation but not DNA methylation; the silencing persisted after *p15AS* was turned off, although methylation and heterochromatin inhibitors reversed this process. The *p15AS*-induced silencing was Dicer-independent. Expression of exogenous *p15AS* in mouse embryonic stem cells caused *p15* silencing and increased growth, through heterochromatin formation, as well as DNA methylation after differentiation of the embryonic stem cells. Thus, natural antisense RNA may be a trigger for heterochromatin formation and DNA methylation in TSG silencing in tumorigenesis.

To test the hypothesis that antisense RNA may trigger epigenetic silencing of mammalian genes, we first searched the UCSC Genome Browser for the existence of antisense transcripts of 21 well-known TSGs, identifying antisense transcripts for each TSG (Supplementary Table 1). For example, *p15*, a well-documented TSG in many tumours[9], has several annotated antisense transcripts (Supplementary Table 1). We next established a nuclear sense–antisense transcript library from HeLa cells (Supplementary Fig. 1). After polymerase chain reaction (PCR) sequencing of 192 randomly chosen library clones, we identified 111 genes containing sense–antisense pairs with lengths between 100 and 200 base pairs (bp), including *p15* and *E-cadherin* (Supplementary Table 2). Based on these results, we focused further experiments on *p15* because it is frequently deleted or hypermethylated in a wide variety of tumours including leukaemia, melanomas, gliomas, lung cancers and bladder carcinomas[9]. Interestingly, up to 60% of leukaemias show epigenetic silencing and methylation of *p15*[10], although the initiating events in this process are unknown.

To confirm the existence of a naturally occurring *p15AS* RNA, we performed PCR with reverse transcription (RT–PCR) with a strand-specific primer and identified *p15AS* transcripts in two leukaemia cell lines (Fig. 1a). We then performed rapid amplification of 5′/3′ complementary DNA (cDNA) ends (RACE), which identified a 34.8-kilobase (kb) *p15* antisense transcript (Supplementary Fig. 2). To uncover the possible mechanistic connection between endogenous *p15AS* transcripts and human disease, we examined both *p15* and its antisense in acute lymphoblastic leukaemia and acute myeloid leukaemia leukocytes, because these two types of leukaemia are frequently accompanied by *p15* epigenetic silencing. We found that 11 out of 16 patient samples (69%) showed relatively increased expression of *p15AS* and downregulated *p15* expression (6/11 in acute myeloid leukaemia and 5/5 in acute lymphoblastic leukaemia). In contrast, 16 normal controls showed high expression of *p15* but relatively low expression of the *p15AS* (Fig. 1b). Additionally, the two acute myeloid leukaemia lines, which displayed high *p15AS* and low *p15* expression (Fig. 1a), also exhibited DNA hypermethylation and typical heterochromatic features for silencing in the *p15* promoter region (Supplementary Table 3).

As a result, we hypothesized that *p15AS* might play a mechanistic role in *p15* silencing in tumour cells. To test this, we engineered three reporter constructs (Fig. 2a): (1) pP15 contains the *p15* promoter, the *p15* first exon and a green fluorescent protein (GFP) reporter gene; (2) pP15-AS, with the same features but containing a portion of

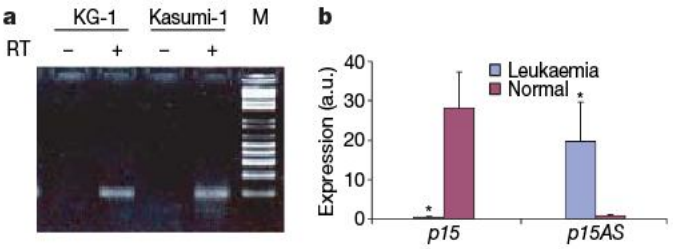

Figure 1 | *p15* antisense expression in leukaemia cells. a, Native *p15AS* transcripts were found in leukaemia cell lines. Lanes 1 and 3 are negative controls without reverse transcriptase. Lanes 2 and 4 show 97 bp bands amplified from the cDNA reverse-transcribed from RNA by a strand-specific primer from leukaemia cell lines KG-1 and Kasumi-1. M is a 100 bp ladder marker. **b**, *p15* and *p15AS* expression in leukaemic ($n = 16$) and normal lymphocytes ($n = 16$), analysed by real-time RT–PCR. Leukaemia samples showed higher expression of *p15* antisense and lower expression of *p15* than normal lymphocytes. Both *p15* and its antisense expression levels were normalized with *GAPDH*. Error bars, s.e.m.; a.u., arbitrary units; $^*P < 0.05$.

[1]Center for Epigenetics and Department of Medicine, Johns Hopkins University School of Medicine, 720 Rutland Avenue, Baltimore, Maryland 21205, USA. [2]Radiation Oncology Branch, National Cancer Institute, National Institutes of Health, Building 10, 3B43, 9000 Rockville Pike, Bethesda, Maryland 20892, USA. [3]Sidney Kimmel Comprehensive Cancer Center, Johns Hopkins University School of Medicine, 401 North Broadway, Baltimore, Maryland 21231, USA.
*These authors contributed equally to this work.

p15AS driven by a cytomegalovirus (CMV) promoter located between the *p15* promoter and the *GFP* gene; (3) pP15-ASΔ contains a stop sequence downstream of the CMV promoter that prevents *p15AS* transcription. These constructs were transfected into HCT116 cells, selected and evaluated by fluorescence-activated cell sorting (FACS), which was also used to sort cells for further culture, after which we evaluated *p15* promoter activity by monitoring GFP expression through a second FACS analysis. Both FACS scan results showed that cells stably transfected with pP15-AS have significantly decreased percentages of GFP-positive cells, and this was progressive over time (Fig. 2b, c). Repeat transfections in HeLa cells yielded similar results (Supplementary Figs 3 and 4). Thus, the *p15* antisense transcript appears to induce partner sense gene silencing and this effect is relatively stable.

Real-time RT–PCR showed that the expressed *p15AS* transcript downregulated both exogenously (Supplementary Fig. 5) and endogenously (Supplementary Fig. 6), which was confirmed by western blotting (Supplementary Fig. 7). This effect was specific to *p15*, as the endogenous *p16* transcript level was unaffected (Supplementary Fig. 8). We repeated the transfections with new vectors in which four nucleotides were replaced by site-directed mutagenesis (pP15′ and pP15AS′; Supplementary Fig. 9a, b), allowing us to distinguish exogenous from endogenous transcripts. The ratio of antisense to sense expression after transfection was about one-quarter the ratio in leukaemia compared with normal lymphocytes (Supplementary Table 4). Furthermore, the exogenous antisense transcript abrogated expression of the exogenous *p15* and reduced the endogenous *p15* by about two-thirds (Supplementary Fig. 9c). Thus, the antisense transcript showed a strong *cis* effect and weaker *trans* effect on expression, which we then confirmed by a new vector separating the sense and antisense genes on different vectors (Supplementary Fig. 10).

To test the stability of silencing induced by the antisense transcript, we constructed a fourth vector pP15-AS-Tre which placed the *p15AS* under a Tet-inducible expression system (Fig. 2a). When antisense expression was induced with tetracycline for 10 days in stably transfected T-Rex-HeLa cells, *p15*-GFP-expressing cells showed a significant decrease in p15 promoter activity. Interestingly, tetracycline withdrawal did not reactivate *p15* promoter activity (Fig. 2d), suggesting that antisense RNA may function in initiation of epigenetic silencing rather than maintenance of silencing. A loxP/Cre deletion experiment further confirmed that removal of the CMV promoter for the *p15AS* did not reactivate *p15* promoter activity once silencing had been established (Supplementary Fig. 11), further confirming that stable silencing of *p15* by *p15AS* persisted after the *p15AS* expression was eliminated.

Next, we tested for a possible alteration in DNA methylation, because *p15* silencing often accompanies frequent hypermethylation of its promoter in leukaemia[10]. However, bisulphite sequencing analysis failed to show any significant changes in DNA methylation in the *p15* promoter (Supplementary Fig. 12). To identify an alternative mechanism, we analysed histone modifications in the *p15* promoter region by chromatin immunoprecipitation (ChIP), because it has

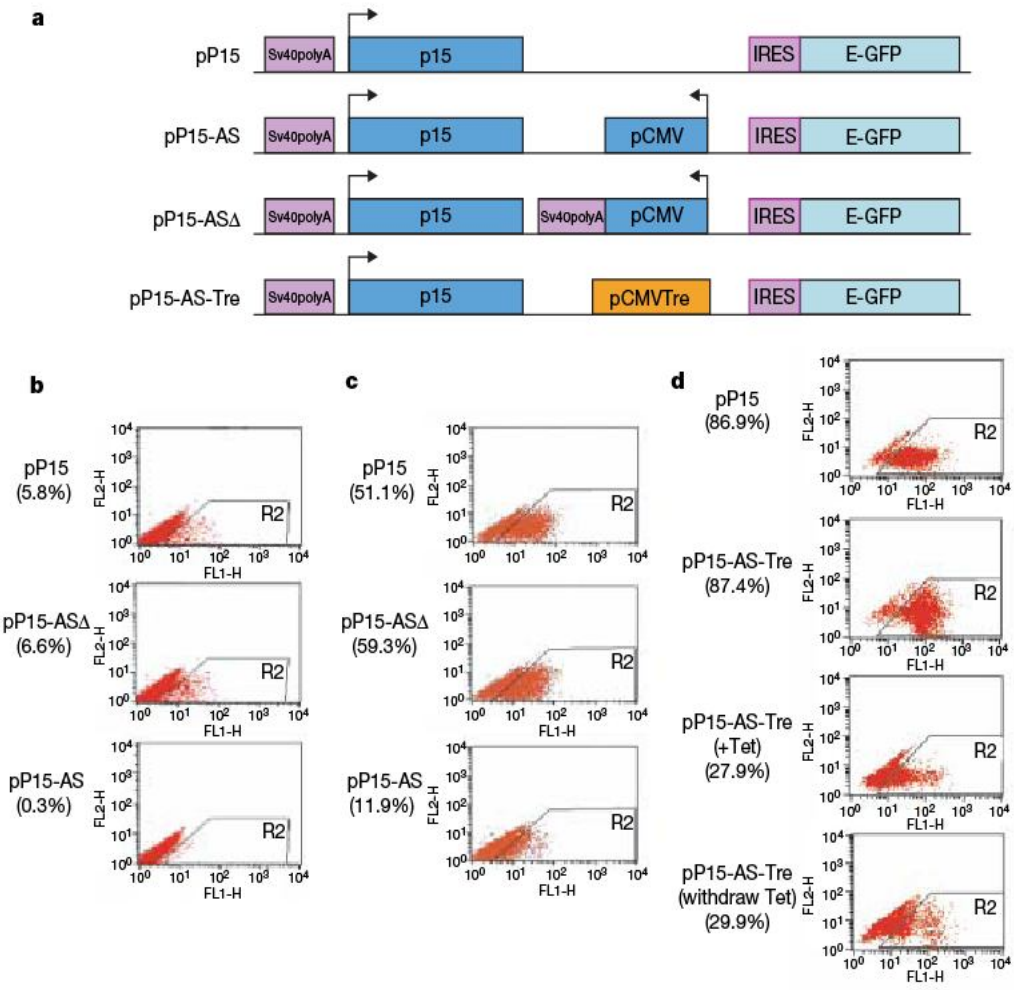

Figure 2 | *p15* promoter is silenced by the expressed *p15* antisense transcript in transfected HCT116 cells. **a**, Maps of constructs. Arrows indicate the direction of transcription. **b**, Downregulation of GFP (under control of *p15* promoter) in cells transfected with pP15-AS and selected for 3 weeks. The transfected cells were analysed by FACS. The percentage of GFP-positive cells with *p15* antisense expression was lower than that without the antisense expression (0.3% versus 5.8% and 6.6%) ($P < 0.001$). **c**, The second FACS showed downregulation of GFP in expressing cells selected from **b** and cultured for an additional 3 weeks. The percentage of GFP-positive cells with *p15* antisense expression remained lower than that without the antisense expression (11.0% versus 51.1% and 59.3%) ($P < 0.0001$). **d**, Downregulation of GFP in cells with a tetracycline-inducible pP15-AS-Tre. Expression was reduced 68% on addition of tetracycline, which persisted after tetracycline withdrawal.

been reported that short interfering RNAs can induce methylation of histone 3 lysine 9 (H3K9) and demethylation of histone 3 lysine 4 (H3K4) experimentally in human cells[11,12]. Using the pP15′ and pP15AS′ vectors (Supplementary Fig. 9a, b) and sequence-specific probes, we were able to distinguish the exogenous sequences from the endogenous sequences through the analysis of immunoprecipitated DNA. The exogenous *p15* promoter showed a marked increase in dimethylation of H3K9 and a decrease in dimethylation of H3K4 in cells with antisense transcripts; this effect was found in both the *p15* promoter and exon 1 regions (Fig. 3a, b), suggesting that the antisense RNA may trigger heterochromatin formation that leads to the transcriptional silencing of the sense *p15*. Interestingly, altered chromatin modifications affected not only the exogenous *p15* promoter and exon 1 (Fig. 3a, b), but also the endogenous *p15* promoter (Fig. 3c, d), although the magnitude of chromatin modification of the endogenous promoter was less than that of the exogenous promoter (Fig. 3a–d). Thus, the antisense RNA may have both a *cis*- and *trans*-acting function in heterochromatin formation. Furthermore, for the endogenous *p15* promoter, a much larger region could be examined, which revealed that the decrease in H3K4 methylation was over a much smaller interval (about 1 kb) than the increase in H3K9 methylation (about 6 kb). Chromatin modifications were stable, because cells transfected with a tetracycline-inducible *p15AS* vector (Fig. 2a) showed reduced H3K4 methylation and increased

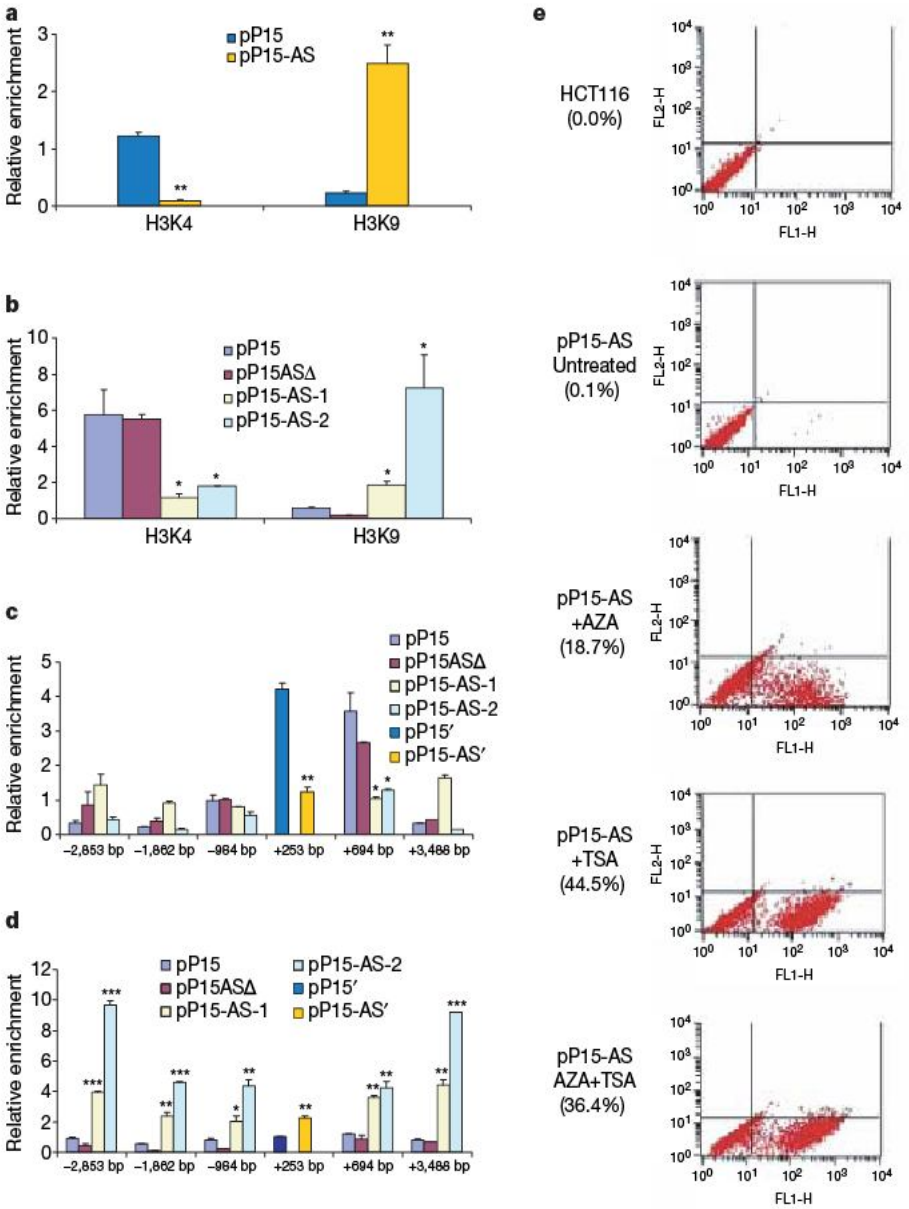

Figure 3 | Heterochromatin formation induced by *p15AS*. **a**, Antisense expression induced an increase in H3K9 dimethylation and a decrease in H3K4 dimethylation in the exogenous *p15* promoter region. ChIP enrichment was measured using real-time PCR, normalized by input DNA. The endogenous and exogenous genes were distinguished with probes specific for sense (pP15′) and antisense (pP15-AS′) vectors transfected after modification by site-directed mutagenesis (see Supplementary Fig. 9). **b**, Antisense expression induced an increase in H3K9 dimethylation and a decrease in H3K4 dimethylation in the exogenous *p15* exon 1 region. **c**, Antisense expression induced a decrease in H3K4 dimethylation in the proximal endogenous *p15* promoter, examined by ChIP followed by real-time PCR at six locations, normalized by input DNA. The numbers on the *x* axis represent PCR sites relative to the transcription start site of *p15*. The site (+253) near the transcriptional start site was examined by vectors to distinguish endogenous and exogenous genes, as in **a**. **d**, Antisense expression induced an increase in H3K9 dimethylation in a large region (about 6 kb) of the endogenous sequence around the *p15* transcriptional start site. **e**, Reactivation of antisense-silenced *p15* promoter by 5-aza-2′-deoxycytidine (AZA) and trichostatin A (TSA). *p15* promoter activity was measured by FACS for GFP after 5-aza-2′-deoxycytidine and trichostatin A treatment. The top two panels represent negative controls: HCT116 cells only and untreated HCT116 cells with pP15-AS, respectively. The bottom three panels show the result of treatment of the pP15-AS-transfected cells with either 5-aza-2′-deoxycytidine, or trichostatin A or 5-aza-2′-deoxycytidine + trichostatin A. All treatments reactivated the *p15* promoter. Significant differences were tested compared with pP15 ($n = 3$). Error bars, s.d.; $*P < 0.05$; $**P < 0.01$; $***P < 0.001$.

H3K9 methylation with *p15* silencing. After tetracycline withdrawal, H3K4 methylation remained reduced at the same level, and H3K9 was somewhat reduced but still significantly elevated over control (Supplementary Fig. 13).

Recent reports show that both 5-aza-2′-deoxycytidine and trichostatin A can relieve H3K9 methylation-induced repression[13,14]. The treated cells were subsequently evaluated by FACS and showed that exposure to either 5-aza-2′-deoxycytidine or trichostatin A could restore *p15* promoter activity (Fig. 3e, and Supplementary Fig. 14). Interestingly, the epigenetic silencing could not be reactivated by transforming-growth-factor-β, an activator of *p15*[15] (Supplementary Fig. 15).

One mechanism for carcinogenesis is thought to involve the clonal expansion of cancer stem cells, and epigenetic modifications may arise early in such cells within individual tissues[16,17]. Thus, we investigated the effect of *p15AS* expression in mouse embryonic stem cells. After selection of embryonic stem cells, FACS demonstrated results similar to those observed in HCT116 and HeLa cells (Fig. 4a), which was confirmed by real-time RT–PCR (Supplementary Fig. 16) and ChIP (Fig. 4b). Furthermore, there was no change in promoter DNA methylation (Fig. 4c), suggesting that heterochromatin rather than DNA methylation is a prerequisite for gene silencing. However, after differentiating embryonic stem cells for one week *in vitro* to form embryoid bodies, we were surprised to discover hypermethylation at the *p15* promoter region (Fig. 4c). Finally, when transfected mouse embryonic stem cells were cultured individually, we found that when stably transfected with pP15-AS they had significantly increased growth rates compared with pP15 control cells (Supplementary Figs 17 and 18). These results provide functional confirmation that the *p15AS* transcript represses *p15* sense expression.

Dicer is a central component of the short interfering RNA and microRNA silencing pathways[18]. To determine if it plays a role in epigenetic silencing of *p15* induced by antisense RNA, we transfected the pP15-AS vector into murine *Dicer* knockout ($Dicer^{(-/-)}$) embryonic stem cells and selected, sorted and assayed these cells as described above. Surprisingly, it was found that the *Dicer* knockout did not affect antisense-induced silencing of *p15* (Supplementary Fig. 19), indicating the mechanism of *p15AS* RNA-induced silencing was independent of Dicer.

In summary, the results of these experiments suggest that an antisense RNA may trigger transcriptional silencing of a partner sense tumour suppressor gene; this effect occurs both in *cis* and in *trans*, and is Dicer-independent. The biochemical mediators of this silencing remain to be determined, but might, for example, involve a Piwi-like protein, as their role in mammalian gene silencing is just beginning to be understood[19]. The silencing induced by the antisense transcript could occur through a 'hit and run' mechanism, because the effect persisted after the antisense transcription was eliminated by either a tetracycline-inducible vector or by loxP/Cre excision. This provides evidence for long-lasting heritable effects on gene expression caused by transient bursts in antisense gene expression, through heterochromatin formation, and that DNA methylation is a secondary effect occurring after differentiation of these cells. The evidence using embryonic stem cells provides a developmental context for this

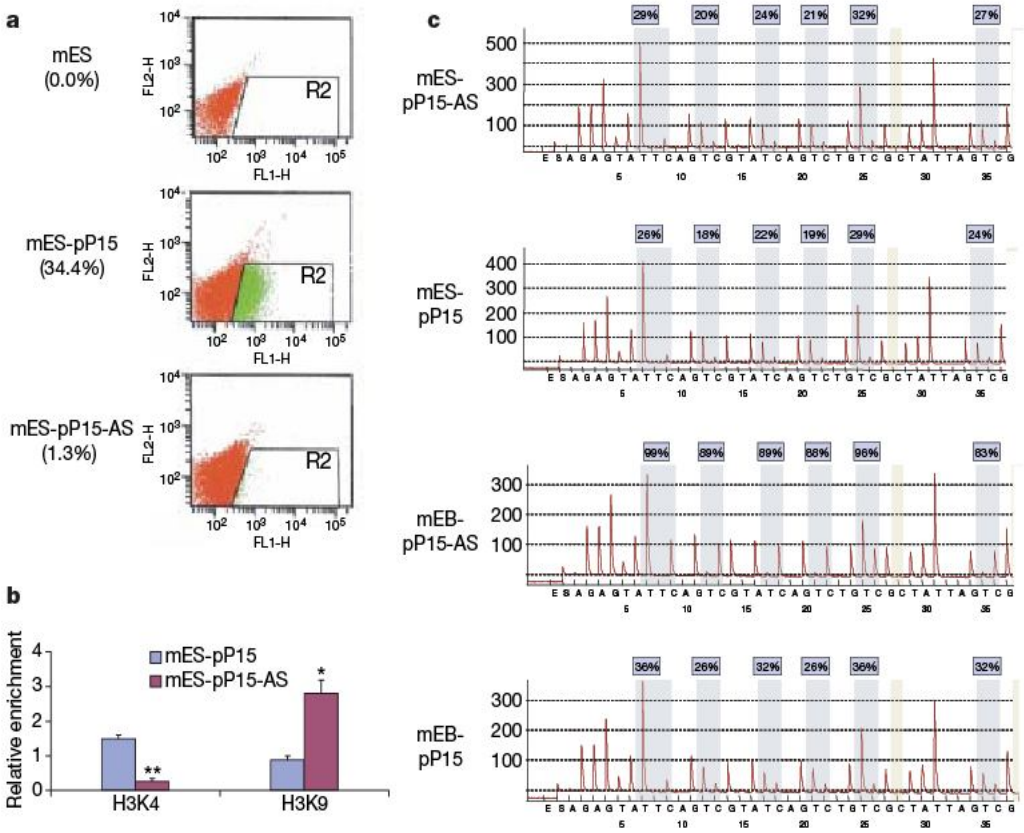

Figure 4 | *p15* silencing, heterochromatin formation and DNA methylation induced by *p15* antisense transcript in mouse embryonic stem cells. **a**, Downregulation of GFP in mouse embryonic stem cells transfected with pP15-AS constructs. The transfected cells were analysed by FACS. The top panel is the negative control, mouse embryonic stem cells without transfection; the middle panel shows mouse embryonic stem cells transfected with pP15; the bottom panel is mouse embryonic stem cells with pP15-AS. Green dots in the R2 area represent GFP-positive cells. The numbers in the brackets show the percentages of GFP-positive cells. **b**, Antisense expression induced a decrease in H3K4 dimethylation and an increase in H3K9 dimethylation in the exogenous p15 promoter region (blue, pP15 mouse embryonic stem cells; red, pP15-AS mouse embryonic stem cells). **c**, Alterations in DNA methylation of exogenous p15 promoter region in mouse embryoid bodies analysed by bisulphite pyrosequencing. Top two panels represent mouse embryonic stem cells transfected with pP15-AS and pP15. The bottom two panels represent mouse embryoid bodies differentiated from mouse embryonic stem cells transfected with pP15-AS and pP15. The six examined cytosine–guanosine sites (CpGs) are marked and methylation percentages are indicated on the top. Note that hypermethylation is only observed in mouse embryoid bodies differentiated from mouse embryonic stem cells transfected with the pP15-AS construct. Significant differences were tested compared with mES-pP15 cells ($n = 3$). Error bars, s.d.; $*P < 0.05$; $**P < 0.01$.

effect, which will need to be ultimately confirmed in tumour stem cells.

These results have practical implications, in that activated antisense transcripts might be potential molecular markers for assessment of cancer risk, as well as serving as novel therapeutic or chemopreventative targets. These data are also consistent with the epigenetic progenitor hypothesis of cancer, which states that tumours arise from epigenetic alterations in progenitor cells that can differentiate into the mass population of cells observed clinically. An example is loss of imprinting in progenitor cells[17,20], and in the present case would be antisense silencing and heterochromatinization of a TSG.

METHODS SUMMARY

The vector Pires2-EGFP was used to construct pP15, pP15-AS and pP15-ASΔ. The Tet-inducible vector pcDNA4/TO/myc-His A was used to create pP15-AS-Tre, which was transfected into the T-REx-HeLa cell line. The transfection was done according to the manufacturer's instructions. FACS was applied to evaluate p15 promoter activity or sort GFP-positive cells. All transcriptional levels were measured by real-time RT–PCR with internal control. DNA methylation was analysed by bisulphite PCR pyrosequencing. H3K4 and H3K9 methylations were analysed by ChIP and real-time PCR. Mouse embryonic stem-cell differentiation was performed in the absence of leukaemia inhibitory factor (LIF) in bacterial Petri dishes to avoid cell adherence.

Full Methods and any associated references are available in the online version of the paper at www.nature.com/nature.

Received 14 August; accepted 9 November 2007.

1. Jones, P. A. & Laird, P. W. Cancer epigenetics comes of age. *Nature Genet.* **21**, 163–167 (1999).
2. Feinberg, A. P. & Tycko, B. The history of cancer epigenetics. *Nature Rev. Cancer* **4**, 143–153 (2004).
3. Novina, C. D. & Sharp, P. A. The RNAi revolution. *Nature* **430**, 161–164 (2004).
4. Hannon, G. J. RNA interference. *Nature* **418**, 244–251 (2002).
5. Willingham, A. T. & Gingeras, T. R. TUF love for "junk" DNA. *Cell* **125**, 1215–1220 (2006).
6. Rosok, O. & Sioud, M. Systematic identification of sense–antisense transcripts in mammalian cells. *Nature Biotechnol.* **22**, 104–108 (2004).
7. Katayama, S. *et al.* Antisense transcription in the mammalian transcriptome. *Science* **309**, 1564–1566 (2005).
8. Tufarelli, C. *et al.* Transcription of antisense RNA leading to gene silencing and methylation as a novel cause of human genetic disease. *Nature Genet.* **34**, 157–165 (2003).
9. Nobori, T. *et al.* Deletions of the cyclin-dependent kinase-4 inhibitor gene in multiple human cancers. *Nature* **368**, 753–756 (1994).
10. Lubbert, M. Gene silencing of the p15/INK4B cell-cycle inhibitor by hypermethylation: an early or later epigenetic alteration in myelodysplastic syndromes? *Leukemia* **17**, 1762–1764 (2003).
11. Ting, A. H., Schuebel, K. E., Herman, J. G. & Baylin, S. B. Short double-stranded RNA induces transcriptional gene silencing in human cancer cells in the absence of DNA methylation. *Nature Genet.* **37**, 906–910 (2005).
12. Weinberg, M. S. *et al.* The antisense strand of small interfering RNAs directs histone methylation and transcriptional gene silencing in human cells. *RNA* **12**, 256–262 (2006).
13. Gius, D. *et al.* Distinct effects on gene expression of chemical and genetic manipulation of the cancer epigenome revealed by a multimodality approach. *Cancer Cell* **6**, 361–371 (2004).
14. Wozniak, R. J. *et al.* 5-Aza-2′-deoxycytidine-mediated reductions in G9A histone methyltransferase and histone H3 K9 di-methylation levels are linked to tumor suppressor gene reactivation. *Oncogene* **26**, 77–90 (2007).
15. Sandhu, C. *et al.* Transforming growth factor beta stabilizes p15INK4B protein, increases p15INK4B-cdk4 complexes, and inhibits cyclin D1-cdk4 association in human mammary epithelial cells. *Mol. Cell. Biol.* **17**, 2458–2467 (1997).
16. Pardal, R., Clarke, M. F. & Morrison, S. J. Applying the principles of stem-cell biology to cancer. *Nature Rev. Cancer* **3**, 895–902 (2003).
17. Feinberg, A. P., Ohlsson, R. & Henikoff, S. The epigenetic progenitor origin of human cancer. *Nature Rev. Genet.* **7**, 21–33 (2006).
18. Lee, Y. S. *et al.* Distinct roles for *Drosophila* Dicer-1 and Dicer-2 in the siRNA/miRNA silencing pathways. *Cell* **117**, 69–81 (2004).
19. Peters, L. & Meister, G. Argonaute proteins: mediators of RNA silencing. *Mol. Cell* **26**, 611–623 (2007).
20. Sakatani, T. *et al.* Loss of imprinting of Igf2 alters intestinal maturation and tumorigenesis in mice. *Science* **307**, 1976–1978 (2005).

Supplementary Information is linked to the online version of the paper at www.nature.com/nature.

Acknowledgements We thank G. Hannon for the Dicer knockout line, R. Ambinder for providing leukaemia specimens from the Johns Hopkins SPORE lymphoma tissue bank, M. Gao for help in detection of DNA methylation, and I. Cui for assistance with the manuscript. This work was supported by a grant from the National Institutes of Health.

Author Contributions W.Y. performed most of the experiments; D.G., K.M.-J. and P.O. performed some vector design; J.K. provided clinical samples and expertise; A.P.F. and H.C. performed the experimental design, supervised the research project and wrote the manuscript.

Author Information Reprints and permissions information is available at www.nature.com/reprints. Correspondence and requests for materials should be addressed to H.C. (hcui@jhmi.edu) or A.P.F. (afeinberg@jhu.edu).

LETTERS

Abscisic acid controls calcium-dependent egress and development in *Toxoplasma gondii*

Kisaburo Nagamune[1]†, Leslie M. Hicks[2], Blima Fux[1], Fabien Brossier[1]†, Eduardo N. Chini[3] & L. David Sibley[1]

Calcium controls a number of critical events, including motility, secretion, cell invasion and egress by apicomplexan parasites[1]. Compared to animal[2] and plant cells[3], the molecular mechanisms that govern calcium signalling in parasites are poorly understood. Here we show that the production of the phytohormone abscisic acid (ABA) controls calcium signalling within the apicomplexan parasite *Toxoplasma gondii*, an opportunistic human pathogen. In plants, ABA controls a number of important events, including environmental stress responses, embryo development and seed dormancy[4,5]. ABA induces production of the second-messenger cyclic ADP ribose (cADPR), which controls release of intracellular calcium stores in plants[6]. cADPR also controls intracellular calcium release in the protozoan parasite *T. gondii*[7,8]; however, previous studies have not revealed the molecular basis of this pathway[9]. We found that addition of exogenous ABA induced formation of cADPR in *T. gondii*, stimulated calcium-dependent protein secretion, and induced parasite egress from the infected host cell in a density-dependent manner. Production of endogenous ABA within the parasite was confirmed by purification (using high-performance liquid chromatography) and analysis (by gas chromatography-mass spectrometry). Selective disruption of ABA synthesis by the inhibitor fluridone delayed egress and induced development of the slow-growing, dormant cyst stage of the parasite. Thus, ABA-mediated calcium signalling controls the decision between lytic and chronic stage growth, a developmental switch that is central in pathogenesis and transmission. The pathway for ABA production was probably acquired with an algal endosymbiont that was retained as a non-photosynthetic plastid known as the apicoplast. The plant-like nature of this pathway may be exploited therapeutically, as shown by the ability of a specific inhibitor of ABA synthesis to prevent toxoplasmosis in the mouse model.

Calcium-mediated protein secretion in *T. gondii* controls both motility and cell invasion, and previous studies have demonstrated that these processes utilize the second messenger cADPR, yet the signals triggering this pathway remain unresolved[7,8]. In plants[6], hydra[10] and sponges[11], ABA stimulates release of intracellular calcium through elevation of the cyclic nucleotide cADPR. Addition of exogenous ABA proved to be a potent agonist of secretion in *T. gondii* as shown by the release of the protein MIC2 (microneme protein 2), a parasite adhesin that is discharged into the supernatant in response to increases in intracellular calcium (Fig. 1a). Induction of MIC2 secretion by ABA was highly specific to (±)-ABA and was not induced by (–)-ABA, the precursor β-carotene, or retinoic acid (Fig. 1b). In this regard, the response of *T. gondii* to ABA shows similar specificity to higher plants[5]. Treatment with ABA lead to a dose-dependent increase in the second messenger cADPR in *T. gondii*, suggesting that ABA may be a natural agonist for calcium signalling in parasites (Fig. 1c). Finally, chelation of intracellular calcium in the parasite blocked secretion induced by ABA, confirming that it acts through release of an intracellular calcium pool (Fig. 1d). Collectively, these results indicate that ABA in *T. gondii* controls release of calcium from intracellular stores through production of cADPR, thus paralleling the pathway seen in plants[6], and early metazoans[10,11].

Consistent with its physiological effects, ABA was detected in lysates of *T. gondii* by direct biochemical analyses. Extracts of

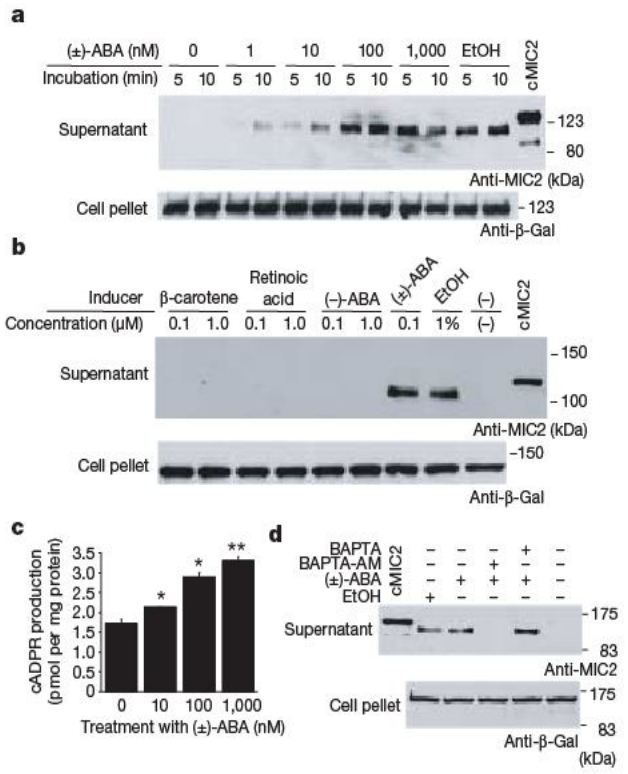

Figure 1 | ABA induced cADPR production and calcium-dependent protein secretion by *T. gondii*. **a**, Protein secretion induced by ABA was compared to the positive control ethanol (EtOH) as detected by western blotting with anti-MIC2 (supernatant) and anti-β-galactosidase antibodies (cell pellet)[7,8]. **b**, Induction of MIC2 secretion was specific for (±)-ABA and was not seen with (–)-ABA, β-carotene, or retinoic acid. **c**, cADPR production in *T. gondii* was increased by treatment with ABA. Student's *t*-test; $*P < 0.02$, $**P < 0.01$ versus control, mean ± s.e.m., $N = 3$ experiments. **d**, ABA-induced secretion required intracellular calcium. Treatment with the membrane permeable calcium chelator, BAPTA-AM, blocked ABA-induced MIC2 release, whereas non-permeant BAPTA had no effect. Cellular MIC2 (cMIC2) migrates slower owing to absence of processing.

[1]Department of Molecular Microbiology, Washington University School of Medicine, 660 S. Euclid Avenue, St Louis, Missouri 63110, USA. [2]Donald Danforth Plant Science Center, 975 N. Warson Road, St Louis, Missouri 63132, USA. [3]Department of Anesthesiology, Mayo Clinic and Foundation, Rochester, Minnesota 55905, USA. †Present addresses: Department of Immunoregulation, Research Institute for Microbial Diseases, Osaka University, Osaka 565-0871, Japan (K.N.); Linstitut National de la Researche Agronomique, Centre de Recherche de Tours, 37380 Nouzilly, France (F.B.).

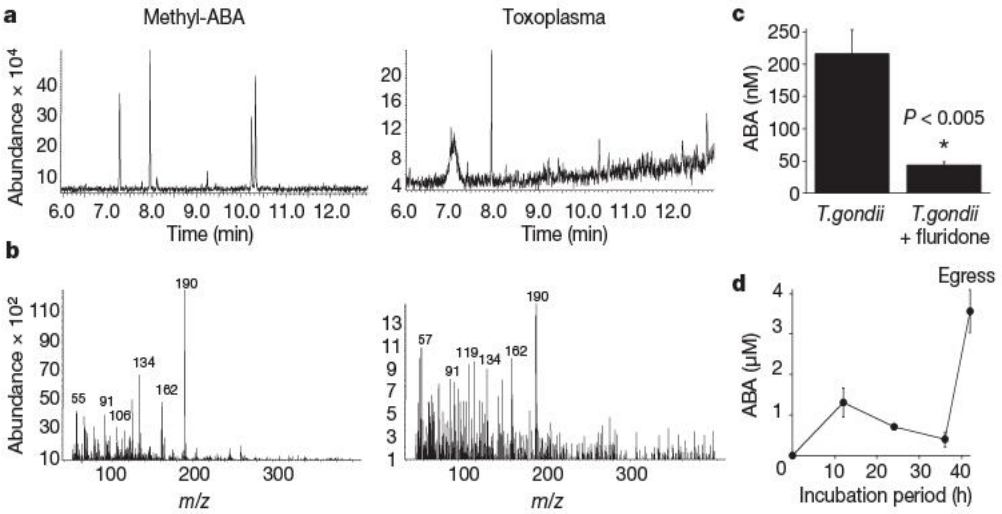

Figure 2 | Biochemical evidence for the production of ABA in *T. gondii*. **a**, Gas chromatography traces of ABA standards (left) and *T. gondii* samples (right). A single peak with similar retention time (8.0 min) to authentic methyl-ABA was detected in extracts of the parasite following chemical extraction and methylation. **b**, Mass spectra of methyl-ABA standard and *T. gondii* sample from **a**, showing characteristic fragment at *m/z* 190, with additional minor peaks in common. **c**, Detection of ABA by ELISA in control parasites or treated with 50 μM of fluridone. Student's *t*-test; $*P < 0.005$ versus control, mean ± s.e.m., $N = 3$ experiments. **d**, Time course of ABA production by *T. gondii*. Values are intracellular concentration in the parasite. Time 0 refers to newly invaded parasites at the start of infection. Mean ± s.e.m., $N = 3$ experiments.

T. gondii were purified by high-performance liquid chromatography (HPLC) and analysed by gas chromatography to detect the methyl ester of ABA (methyl-ABA), which migrated with the same retention time (8 min) as the authentic methyl-ABA standard (Fig. 2a). Mass spectrometric analysis of *T. gondii* samples yielded the expected product of mass-to-charge ratio (*m/z*) 190 as well as peaks at *m/z* 91 and 162, characteristic of *cis*-ABA, and *m/z* 91 and 134, characteristic of *trans*-ABA, as described previously[12] (Fig. 2b and Supplementary Fig. 1). The slightly nosier spectrum obtained from *T. gondii* is consistent with the lower level of ABA found in the sample, nonetheless its signature unambiguously matches ABA. Similar levels of ABA were detected in parasite extracts using a highly specific ELISA (enzyme-linked immunosorbent assay) kit (Fig. 2c). To confirm that ABA was indeed synthesized by the parasite, we used the herbicide fluridone, an inhibitor that specifically blocks phytoene destaurase activity, and hence prevents synthesis of ABA by the indirect pathway that predominates in plants[5]. Treatment with fluridone reduced the level of ABA in parasites by more than fourfold (Fig. 2c). Interestingly, when the level of ABA was monitored during one cycle of intracellular growth, it remained relatively constant during the first 30–36 h and then spiked shortly before egress of parasites from the infected host cell, which begins around 40–44 h (Fig. 2d).

Toxoplasma is an obligate intracellular pathogen and following invasion, the parasite replicates by binary fission within a vacuole, ultimately leaving the depleted host cell by active egress. Intracellular calcium is central for several of these steps, leading us to examine whether ABA-dependent calcium signalling was essential for growth *in vitro*. Treatment of parasite cultures with increasing concentrations of fluridone led to inhibition of parasite growth (effector concentration for half-maximum response, EC_{50}, ~15 μM; Fig. 3a). Surprisingly, fluridone treatment did not block invasion or replication, but instead inhibited exit of mature parasites from the infected cell. Whereas parasites had naturally egressed by ~60 h, those treated with 15 μM fluridone were delayed, and those treated with 50 μM fluridone were completely blocked out to 84 h (Fig. 3b), after which the integrity of the monolayer declined (data not shown). Previous studies have implicated calcium signalling in parasite egress from infected cells[13,14], and the rapid increase in ABA concentrations in the parasite just before egress (Fig. 2d) suggested this molecule may be the natural signal for activating exit. Consistent with this, when exogenous ABA was added to late-stage vacuoles, it induced premature egress (Fig. 3c). Finally, ABA was able to overcome the inhibition of egress caused by treatment with fluridone (Fig. 3d), consistent with it being able to bypass the metabolic block in biosynthesis. Although the responses to exogenously added ABA are somewhat modest, this may reflect the relatively low permeability of the charged anion that exists at physiological pH (pK_a 4.8), and the fact that it has to cross several membranes to reach the parasite. Whether ABA produced by the parasite accumulates within the parasite or is exported to the parasite-containing vacuole is unknown, and the mechanism(s) whereby ABA is sensed remain to be elucidated.

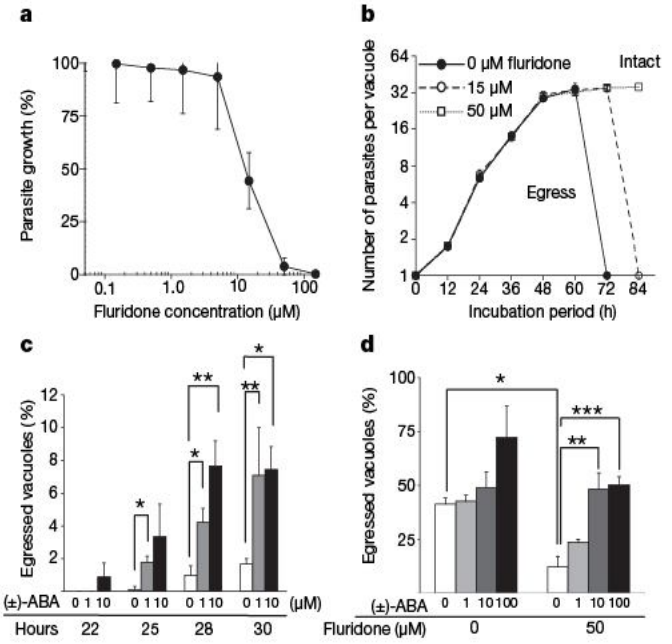

Figure 3 | Fluridone blocked parasite growth by preventing egress. **a**, Fluridone prevented parasite growth as monitored by β-galactosidase activity in the parasite. **b**, Continuous culture in fluridone did not affect replication but inhibited egress from the vacuole. **c**, Treatment with exogenous ABA induced egress of parasites from mature vacuoles. Hours refers to length of culture before addition of ABA for 1 h and scoring of egress. Student's *t*-test; $*P < 0.02$, $**P < 0.05$. **d**, ABA reversed the inhibition of parasite egress caused by fluridone. Parasite-infected cells were treated with fluridone for 38 h, then stimulated with ABA for 1 h, and evaluated for egress. Student's *t*-test; $*P < 0.002$, $**P < 0.05$, $***P < 0.02$. **a–d**, Data shown are means ± s.e.m., $N = 3$ experiments.

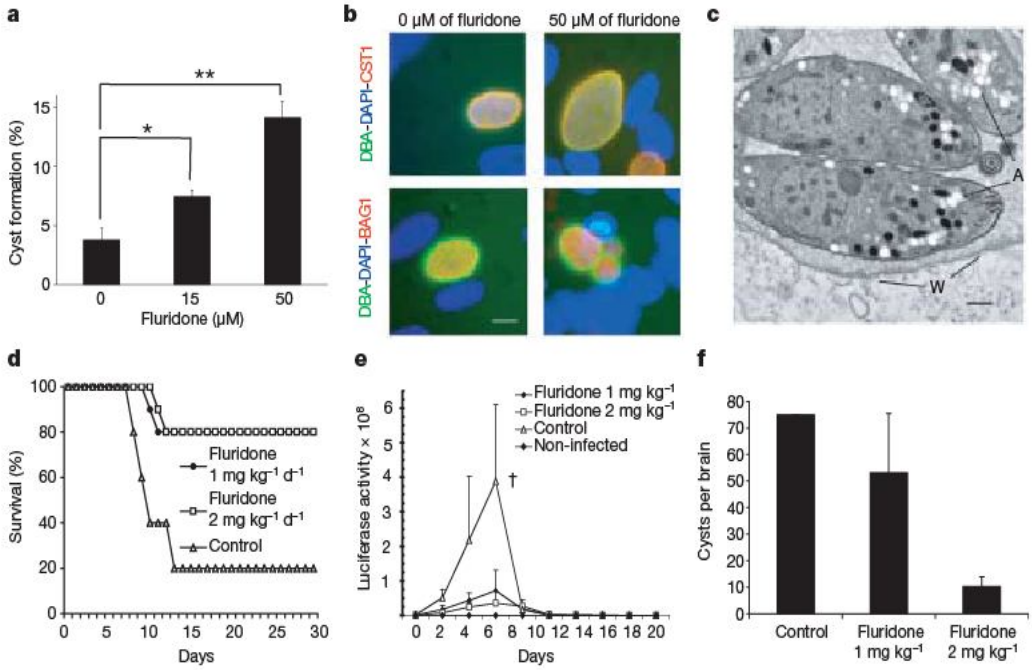

Figure 4 | Fluridone treatment induced development of tissue cysts and protected mice against toxoplasmosis. **a**, Fluridone treatment enhanced cyst formation, as revealed by *Dolichos biflorus* lectin (DBL). Student's *t*-test; $*P < 0.02$, $**P < 0.005$, means ± s.d., $N = 3$ experiments. **b**, Fluridone-induced cysts stained positively with DBL and expressed cyst-specific antigens, CST-1 and BAG1, similar to control samples. Scale bar, 5 μm. **c**, Cysts induced by fluridone contained amylopectin granules (A), posterior nucleus, and prominent cyst wall (W) by electron microscopy. Scale bar, 200 nm. **d**, Survival following acute challenge with *T. gondii* and treatment with fluridone. Two experiments combined, $N = 10$ animals per group. **e**, Luciferase imaging revealed decreased burdens in mice treated with fluridone (†, 4 of 5 control animals died). Mean ± s.d. from a representative experiment, $N = 5$ animals each. **f**, Reduced cyst counts were observed in the brain of mice treated with 2 mg kg^{-1} fluridone. Two experiments combined, $N = 8$ animals per group, except for control where only a single animal survived.

Nonetheless, these results indicate that ABA is a natural agonist for host cell egress and that in the absence of its production, parasites remain quiescent within the host cell.

Toxoplasma undergoes two fundamentally different forms of growth within host cells: (1) the lytic cycle described above, which rapidly amplifies parasite numbers, and (2) differentiation into semi-dormant cysts that are long-lived. These adaptations serve different roles during infection, the first leading to active dissemination and the second resulting in a life-long chronic infection. The decision to undergo this developmental switch is poorly understood, but is thought to be a response to stress. In fluridone-treated cultures, parasites that failed to egress from the host cell started to develop into tissue cysts, as shown by staining with the cyst-wall specific lectin from *Dolichos biflorus* (DBL) (Fig. 4a). Tissue cysts produced by treatment with fluridone were positive for several stage-specific cyst markers, including DBL and the cyst antigens CST1 (ref. 15) and BAG1 (ref. 16) (Fig. 4b). Ultrastructural examination of the cysts formed by fluridone treatment revealed hallmark features of parasites within cysts, including a posterior positioned nucleus, amylopectin granules, dense rhoptries and a convoluted cyst wall (Fig. 4c). Fluridone treatment also enhanced the response of parasites to alkaline pH stress (Supplementary Fig. 2), a common experimental method used to induce differentiation[17].

In addition to blocking egress *in vitro*, fluridone treatment was also able to prevent lethal infection in laboratory mice, which provide an excellent model for toxoplasmosis (Fig. 4d). Imaging of parasite dissemination *in vivo* using a luciferase expressing strain revealed that fluridone treatment greatly reduced parasite burdens during *in vivo* infection in the mouse (Fig. 4e, Supplementary Fig. 3), which led to decreased cyst formation in the central nervous system during chronic infection (Fig. 4f). Fluridone is a registered herbicide that has low toxicity to mammalian cells, owing to the absence of this biosynthetic pathway in animals. Our results, combined with a previous patent indicating that it is also effective against malaria[18], suggest that this selectivity may be exploited for development of improved anti-parasitic drugs.

ABA synthesis in plants proceeds from isoprenoids using an indirect pathway that flows through β-carotene in the plastid[5]. *T. gondii* utilizes a non-mevalonate pathway for isoprenoid biosynthesis[19], which occurs in the apicoplast, a remnant organelle derived from an algal endosymbiont[20]. The sensitivity of *T. gondii* to fluridone indicates that it contains an indirect pathway for ABA production, which depends on the plastid, rather than the direct pathway found in fungi[5], thus providing an additional explanation for the essential nature of the apicoplast[20]. Although the *T. gondii* genome (http://ToxoDB.org) contains several candidates with similarity to ABA synthesis genes in higher plants (that is, *ABA1*, *ABA2* and *ABA3*)[5], phylogenetic and domain analyses do not provide unambiguous assignments of these orthologues (data not shown). This divergence is not unexpected, given that the plant-like nature of apicomplexans is based on acquisition of an early branching algal endosymbiont[21]. Although algae have also been shown to make ABA[22,23] and respond to this hormone[24], the precise pathways and genes involved in ABA production by algae are not established. Future studies aimed at defining the pathway for production of ABA in *T. gondii* may provide further insight into the role of this hormone outside of higher plants.

Our findings demonstrate the conservation of a common plant-like, calcium-signalling pathway in the protozoan parasite *T. gondii*. Production of ABA is a density-dependent signal that influences the decision for lytic growth versus dormant development in *T. gondii*. ABA has recently been shown to regulate gene expression by altering messenger RNA translation[25], and to activate G-protein coupled receptor signalling[26] in plants, indicating that it has additional important functions beyond calcium signalling. These ABA-response genes are conserved in *T. gondii*, and the related parasite *Plasmodium* spp. (http://ApiDB.org), where they may play analogous roles in ABA-mediated signalling and development. Disruption of

ABA-mediated signalling in parasites offers a promising new target for development of improved interventions aimed at combating infection with apicomplexan parasites.

METHODS SUMMARY

Growth and egress assays. Intracellular parasite growth was monitored using β-galactosidase activity[7], or by microscopic examination determination of the number of parasites per vacuole[13,17]. Egress was monitored by the percentage of intact vacuoles after culturing for defined intervals with and without fluridone, followed by treatment with ABA.

Secretion assay. Calcium-dependent secretion was monitored by release of MIC2 (refs 7, 27), with β-galactosidase as a cell-loading and non-specific lysis control.

ABA purification and analysis. ABA was extracted from parasites, purified by HPLC, converted to methyl-ABA[28], and analysed by tandem mass spectrometry using an Agilent Technologies GC-MS instrument to detect the diagnostic fragments[12].

ABA detection by ELISA. ABA concentrations in parasite extracts were determined by ELISA using the Phytodetek ABA Test Kit (Agdia) after subtraction of the background level of ABA in cultured host cells processed in parallel, and expressed as intracellular concentrations[29].

Cyclic ADPR. Freshly harvested parasites were snap frozen at –80 °C, extracted, and cADPR levels determined as described previously[8].

***In vitro* differentiation.** Cyst formation was monitored following treatment with fluridone under normal culture conditions as detected using FITC-labelled DBL (Sigma) or antibodies to the cyst antigens CST1 (ref. 15) or BAG1 (ref. 16). Transmission electron microscopy was performed as described previously[17].

Mouse infections. BALB/c mice were infected with type II strain PTG strain by intraperitoneal (i.p.) injection and treated with fluridone by daily i.p. injection for 12 d. To monitor tissue burdens, mice were challenged with the luciferase expressing Pru-Luc strain and imaged as described previously[30].

Full Methods and any associated references are available in the online version of the paper at www.nature.com/nature.

Received 2 October; accepted 13 November 2007.

1. Moreno, S. N. J. & Docampo, R. Calcium regulation in protozoan parasites. *Curr. Opin. Microbiol.* **6**, 359–364 (2003).
2. Berridge, M. J., Bootman, M. D. & Roderick, H. L. Calcium signaling: Dynamics, homeostasis and remodelling. *Nature Rev. Mol. Cell Biol.* **4**, 517–529 (2003).
3. Bothwell, J. H. F. & Ng, C. K. Y. The evolution of Ca^{2+} signaling in photosynthetic eukaryotes. *New Phytol.* **166**, 21–38 (2005).
4. Xiong, L. & Zhu, J. K. Regulation of abscisic acid biosynthesis. *Plant Physiol.* **133**, 29–36 (2003).
5. Schwartz, S. H., Qin, X. & Zeevaart, J. A. D. Elucidation of the indirect pathway of abscisic acid biosynthesis by mutants, genes, and enzymes. *Plant Physiol.* **131**, 1591–1601 (2003).
6. Wu, Y. *et al.* Abscisic acid signaling through cyclic ADP ribose in plants. *Science* **278**, 2126–2130 (1997).
7. Lovett, J. L., Marchesini, N., Moreno, S. N. & Sibley, L. D. *Toxoplasma gondii* microneme secretion involves intracellular Ca^{2+} release from IP_3 / ryanodine sensitive stores. *J. Biol. Chem.* **277**, 25870–25876 (2002).
8. Chini, E. N., Nagamune, K., Wetzel, D. M. & Sibley, L. D. Evidence that the cADPR signaling pathway controls calcium-mediated secretion in *Toxoplasma gondii*. *Biochem. J.* **389**, 269–277 (2005).
9. Nagamune, K. & Sibley, L. D. Comparative genomic and phylogenetic analyses of calcium ATPases and calcium-regulated proteins in the Apicomplexa. *Mol. Biol. Evol.* **23**, 1613–1627 (2006).
10. Puce, S. *et al.* Abscisic acid signaling through cyclic ADP-ribose in hydroid regeneration. *J. Biochem.* **279**, 39783–39788 (2004).
11. Zocchi, E. *et al.* The temperature-signaling cascade in sponges involves a heat-gated cation channel, abscisic acid, and cyclic ADP ribose. *Proc. Natl Acad. Sci. USA* **98**, 14859–14864 (2001).
12. de Almeida, J. A. S., Kascheres, C. & Pereira, M. D. A. Ethylene and abscisic acid in the control of development of the rhizome of *Koleria eriantha* (Benth.) Hanst. (Gesneriaceae). *Braz. J. Plant Physiol.* **17**, 391–399 (2005).
13. Moudy, R., Manning, T. J. & Beckers, C. J. The loss of cytoplasmic potassium upon host cell breakdown triggers egress of *Toxoplasma gondii*. *J. Biol. Chem.* **276**, 41492–41501 (2001).
14. Endo, T., Sethi, K. K. & Piekarski, G. *Toxoplasma gondii*: Calcium ionophore A23187-mediated exit of trophozoites from infected murine macrophages. *Exp. Parasitol.* **53**, 179–188 (1982).
15. Zhang, Y. W., Halonen, S. K., Ma, Y. F., Wittner, M. & Weiss, L. M. Initial characterization of CST1, a *Toxoplasma gondii* cyst wall glycoprotein. *Infect. Immun.* **69**, 501–507 (2001).
16. Zhang, Y. W. *et al.* Disruption of the *Toxoplasma gondii* bradyzoite-specific gene BAG1 decreases *in vivo* cyst formation. *Mol. Microbiol.* **31**, 691–701 (1999).
17. Fux, B. *et al.* *Toxoplasma gondii* strains defective in oral transmission are also defective in developmental stage differentiation. *Infect. Immun.* **75**, 2580–2590 (2007).
18. Leef, J. L. & Carlson, P. S. Carotenoid synthesis inhibiting herbicides and fatty acid synthesis oxime herbicides as anti-apicomplexa protozoan parasite agents. Patent 847932, 1–8 (Potomax Ltd. Prtn) (1999).
19. Jomaa, H. *et al.* Inhibitors of the non-mevalonate pathway of isoprenoid biosynthesis as antimalarial drugs. *Science* **285**, 1573–1576 (1999).
20. Ralph, S. A. *et al.* Metabolic maps and functions of the *Plasmodium falciparum* apicoplast. *Nature Rev. Microbiol.* **2**, 203–216 (2004).
21. Waller, R. F. & McFadden, G. I. The apicoplast: A review of the derived plastid of apicomplexan parasites. *Curr. Iss. Mol. Biol.* **7**, 57–79 (2005).
22. Hirsch, R., Hartung, W. & Gimmler, H. Abscisic acid content of algae under stress. *Bot. Acta* **102**, 326–334 (1989).
23. Cowan, A. K. & Rose, P. D. Abscisic acid metabolism in salt stressed cells of *Dunaliella salina*. *Plant Physiol.* **97**, 798–803 (1991).
24. Kobayashi, M., Hirai, N., Kurimura, Y., Ohigashi, H. & Tsuji, Y. Abscisic acid-dependent algal morphogenesis in the unicellular green alga *Haematococcus pluvialis*. *Plant Growth Reg.* **22**, 79–85 (1997).
25. Razem, F. A., El-Kereamy, A., Abrams, S. R. & Hill, R. D. The RNA-binding protein FCA is an abscisic acid receptor. *Nature* **439**, 290–294 (2006).
26. Liu, X. *et al.* A G protein-coupled receptor is a plasma membrane receptor for the plant hormone abscisic acid. *Science* **315**, 1712–1716 (2007).
27. Carruthers, V. B., Sherman, G. D. & Sibley, L. D. The Toxoplasma adhesive protein MIC2 is proteolytically processed at multiple sites by two parasite-derived proteases. *J. Biol. Chem.* **275**, 14346–14353 (2000).
28. Tian, L., DellaPenna, D. & Zeevaart, J. A. D. Effect of hydroxylated carotenoid deficiency on ABA accumulation in *Arabidopsis*. *Physiol. Plant.* **122**, 314–320 (2004).
29. Rodrigues, C. O., Ruiz, F. A., Rohloff, P., Scott, D. A. & Moreno, S. N. J. Characterization of isolated acidocalcisomes from *Toxoplasma gondii* tachyzoites reveals a novel pool of hydrolyzable polyphosphate. *J. Biol. Chem.* **277**, 48650–48656 (2002).
30. Saeij, J. P., Boyle, J. P., Grigg, M. E., Arrizabalaga, G. & Boothroyd, J. C. Bioluminescence imaging of *Toxoplasma gondii* infection in living mice reveals dramatic differences between strains. *Infect. Immun.* **73**, 695–702 (2005).

Supplementary Information is linked to the online version of the paper at www.nature.com/nature.

Acknowledgements We thank J. Zeevaart for conducting the initial purification and analysis of ABA and for supplying standards; J. Boothroyd and L. Weiss for providing reagents; W. Beatty, S. Moreno, B. Striepen, A. Waters and L. Xiong for comments; and J. Nawas and D. Gill for technical assistance. This work was supported by the Uehara Medical Foundation (K.N.), the Mayo Clinic and American Heart Association (E.N.C.) and the NIH (L.D.S.).

Author Contributions K.N. performed the experiments on the effects of ABA and fluridone on the parasite, L.M.H. performed the MS studies, B.F. performed the animal studies, F.B. contributed to the analysis of *ABA* genes, E.N.C. performed the measurements of cADPR, L.D.S. supervised the project and wrote the manuscript with input from all the authors.

Author Information Reprints and permissions information is available at www.nature.com/reprints. Correspondence and requests for materials should be addressed to L.D.S. (sibley@wustl.edu).

LETTERS

Defective tryptophan catabolism underlies inflammation in mouse chronic granulomatous disease

Luigina Romani[1], Francesca Fallarino[1], Antonella De Luca[1], Claudia Montagnoli[1], Carmen D'Angelo[1], Teresa Zelante[1], Carmine Vacca[1], Francesco Bistoni[1], Maria C. Fioretti[1], Ursula Grohmann[1], Brahm H. Segal[2] & Paolo Puccetti[1]

Half a century ago, chronic granulomatous disease (CGD) was first described as a disease fatally affecting the ability of children to survive infections. Various milestone discoveries have since been made, from an insufficient ability of patients' leucocytes to kill microbes to the underlying genetic abnormalities[1]. In this inherited disorder, phagocytes lack NADPH oxidase activity and do not generate reactive oxygen species, most notably superoxide anion, causing recurrent bacterial and fungal infections. Patients with CGD also suffer from chronic inflammatory conditions, most prominently granuloma formation in hollow viscera. The precise mechanisms of the increased microbial pathogenicity have been unclear[2], and more so the reasons for the exaggerated inflammatory response[3–6]. Here we show that a superoxide-dependent step in tryptophan metabolism along the kynurenine pathway is blocked in CGD mice with lethal pulmonary aspergillosis, leading to unrestrained Vγ1$^+$ γδ T-cell reactivity, dominant production of interleukin (IL)-17, defective regulatory T-cell activity and acute inflammatory lung injury. Although beneficial effects are induced by IL-17 neutralization or γδ T-cell contraction, complete cure and reversal of the hyperinflammatory phenotype are achieved by replacement therapy with a natural kynurenine distal to the blockade in the pathway. Effective therapy, which includes co-administration of recombinant interferon-γ (IFN-γ), restores production of downstream immunoactive metabolites and enables the emergence of regulatory Vγ4$^+$ γδ and Foxp3$^+$ αβ T cells. Therefore, paradoxically, the lack of reactive oxygen species contributes to the hyperinflammatory phenotype associated with NADPH oxidase deficiencies, through a dysfunctional kynurenine pathway of tryptophan catabolism. Yet, this condition can be reverted by reactivating the pathway downstream of the superoxide-dependent step.

Indoleamine 2,3-dioxygenase (IDO), a 'metabolic' enzyme conserved through the past 600 million years of evolution, suppresses T-cell responses and promotes tolerance in mammalian pregnancy, tumour resistance, chronic infection, autoimmunity and allergic inflammation[7–10]. During inflammation, IDO is upregulated in dendritic cells and phagocytes by proinflammatory stimuli—most notably, IFN-γ—and the enzyme then uses superoxide as a 'cofactor' for oxidative cleavage of the indole ring of tryptophan, yielding an intermediate that deformylates to L-kynurenine[11,12] (Supplementary Information and Supplementary Fig. 2). As a result, several IDO-dependent mechanisms mitigate inflammation and prevent autoimmunity[13–15]. By infecting p47$^{phox-/-}$ mice with *Aspergillus fumigatus*—a frequent cause of life-threatening disease in patients with CGD—we tested the hypothesis that defective IDO function occurs in experimental CGD, affecting antifungal resistance, inflammation and T-cell homeostasis. Owing to the absence of superoxide, an impaired IDO activity might compromise microbial tryptophan starvation and kynurenine production by phagocytes, resulting in reduced antimicrobial defence and an exaggerated inflammatory response[16].

We infected p47^{phox}-deficient mice with *A. fumigatus* intratracheally and evaluated parameters of antifungal resistance and inflammation, with IDO message, protein expression and enzymatic activity. Abnormal susceptibility to pulmonary infection was observed in the knockout mice, in terms of survival and histopathology in the lungs (Fig. 1a), abundance of inflammatory cells in the bronchoalveolar lavage (BAL) fluid (Fig. 1b) and production of inflammatory markers (Fig. 1c). Lethal invasive pulmonary aspergillosis developed in CGD mice within a context of acute inflammatory lung injury, different from that associated with neutrophil-dependent oxidative stress. In sorted pulmonary CD3$^+$ cells and/or lung homogenates from knockout mice, infection preponderantly induced IL-17 and IL-23, whereas IFN-γ, IL-10, and transforming growth factor-β (TGF-β) were defective (Fig. 1d). In thoracic lymph node CD4$^+$ T cells from CGD mice, *A. fumigatus* caused a greater than 15-fold increase in message expression of *Rorc* (encoding the T_H17 cell transcription factor, RORγt), and virtually no induction of T_H1-associated *Tbet* and *Foxp3* (regulatory T-cell specification factor) (Supplementary Fig. 1). A detrimental effect of IL-17 was demonstrated by IL-17 neutralization *in vivo* followed by *in vitro* assessment of immunological and antifungal parameters; a bimodal effect of IL-17 was demonstrable *in vitro* on the conidiocidal activity of polymorphonuclear cells (PMNs), with significant inhibition at the level of nanograms per millilitre; improved survival occurred in CGD mice treated with the anti-IL-17 antibody (Supplementary Table 1). These data suggested that CGD mice manifest a defect in the initial lung defence against *A. fumigatus* infection that is associated with a greater—but damaging—inflammatory response.

Despite their prompt mobilization after infection (Fig. 1a, b), PMNs from CGD mice were relatively inefficient at initiating tryptophan catabolism. Consistent with the hypothesis that IDO functional activity was blocked post-translationally in CGD mice, IFN-γ induced *Indo* transcript (Fig. 2a) and IDO protein (Fig. 2b) expressions in knockout PMNs that were comparable to those in wild-type controls. Yet, these cells were completely unable to mediate tryptophan conversion to L-kynurenine (Fig. 2c). *In vivo*, infection resulted in detectable L-kynurenine in lung homogenates from wild-type but not knockout mice (Fig. 2d). This effect could, at least in part, be due to a defective expression of IDO protein in the knockout mice (Fig. 2e), likely as a result of the reduced potential of T cells to release IFN-γ. We used real-time polymerase chain reaction (PCR) for quantitative and comparative assessment of *Indo* expression in lung mononuclear phagocytes from naive mice of both genotypes, and

[1]Department of Experimental Medicine, University of Perugia, 06126 Perugia, Italy. [2]Division of Infectious Diseases, Roswell Park Cancer Institute, Buffalo, New York 14263, USA.

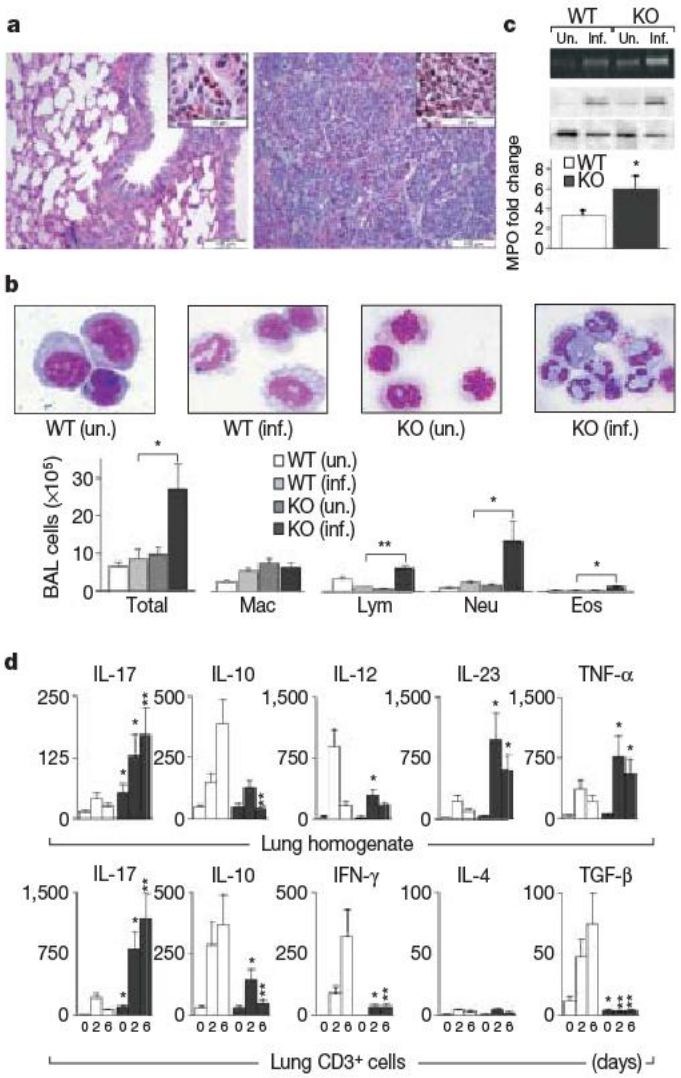

Figure 1 | Invasive pulmonary aspergillosis in the p47^{phox} mouse knockout model of CGD. Knockout (KO) and wild-type (WT) mice were infected intratracheally with *A. fumigatus* conidia (5×10^6) on day 0, to be examined for course of infection. The median survival time in knockout mice was 7.5 days (dead/total, 6/6), whereas it exceeded 60 days (dead/total, 0/6) in wild-type animals ($P = 0.004$). **a**, Lung histology was performed on day 4, a time when the amount of pulmonary chitin (a major constituent of *A. fumigatus* cell wall) was fivefold higher in knockout than in wild-type mice. Histopathology revealed abundant pyogranulomatous lesions with central neutrophilic infiltrates in knockout mice (periodic acid-Schiff; scale bar, 100 μm). Shown in insets are haematoxylin and eosin stains of magnified details, with exemplary foci of neutrophilic inflammation (scale bar, 50 μm). Data are representative of several experiments, in which mortality and histology data were highly consistent among similarly treated mice with the same genotype. **b**, On day 4, the abundances of macrophages (Mac), lymphocytes (Lym), neutrophils (Neu), and eosinophils (Eos) were assessed in BAL fluid, revealing an exuberant neutrophilic response in the infected knockout mice, in which eosinophils and increased lymphocyte numbers were also found. **c**, Day-3 metalloproteinase-9 (assessed as gelatinolytic activity in upper blot) and myeloperoxidase (MPO; lower immunoblot, with β-tubulin normalization) were higher in lung neutrophils from knockout mice. Myeloperoxidase blots ($n = 3$) were quantified by scanning densitometry and represented as fold change in infected (Inf) mice relative to uninfected (Un) controls of the same genotype (in which fold change = 1). **d**, Secreted cytokines (in picograms per millilitre) from wild-type (open bars) and knockout (filled bars) mice were measured in lung homogenates on days 2 and 6, whereas pulmonary CD3$^+$ T cells were assayed for cytokine release in response to soluble anti-CD3 (1 μg ml^{-1}). Day 0 indicates uninfected mice, and comparisons are shown between similarly treated groups of the two genotypes. In all panels, quantitative data are means ± s.d. from three experiments. *$P < 0.05$; **$P < 0.005$–0.001.

extended the examination to a series of genes encoding enzymes downstream of IDO[17] (Supplementary Fig. 2). Like *Indo*, the expressions of *Kmo*, *Kynu* and *Haao* were all enhanced by IFN-γ in both genotypes. However, IFN-γ was unable to mediate conversion of externally added L-tryptophan to L-kynurenine by mononuclear phagocytes from p47$^{phox-/-}$ mice, confirming that, in experimental CGD, an inefficient IDO mechanism prevents metabolic steps that are subsequent and consequent to IDO.

Among CD3$^+$ T lymphocytes, cells with the γδ T-cell-type receptors (γδ T cells) constitute an ancient lineage that is present in all vertebrates and responds to often-unprocessed microbial antigen and non-peptide metabolites[18]. γδ T cells control innate responses, including those mediated by PMNs, through their production of IL-17 (refs 19, 20), and they take part in the transitional response (occurring temporally between the rapid innate and

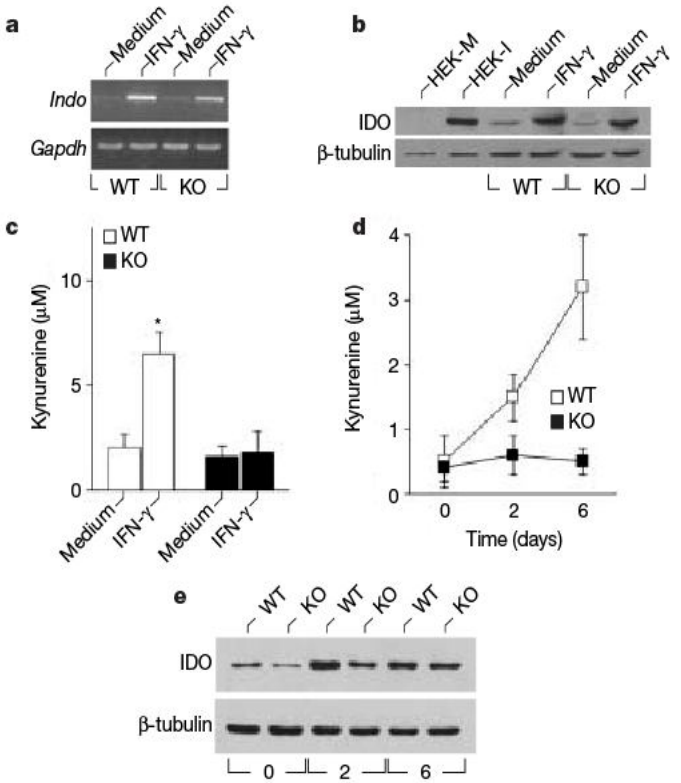

Figure 2 | Defective IDO-dependent conversion of tryptophan to L-kynurenine in p47^{phox} knockout mice. **a**, PCR with reverse transcription (RT–PCR) of *Indo* (which encodes IDO) in PMNs from wild-type and knockout mice, either untreated or treated overnight with IFN-γ (200 U ml^{-1}). One experiment is shown representative of three. **b**, IDO protein expression was assessed by immunoblot analysis in similarly treated PMNs by an IDO-specific antibody. The positive control consisted of IDO-expressing HEK-I transfectants; the negative control consisted of mock-transfected HEK-M cells. Loading controls consisted of samples re-probed with β-tubulin-specific antibody. One experiment is shown representative of three. The mean fold changes (± s.d.) in the three experiments (that is, day-6 infection to no-infection ratios using normalized densitometry values) were 5.4 ± 1.2 and 6.3 ± 1.5 for wild-type and knockout mice, respectively. **c**, Functional IDO (means ± s.d. with $n = 3$) in response to IFN-γ was measured in wild-type and knockout mice in terms of the ability of the PMNs to metabolize tryptophan to L-kynurenine, measured by high-performance liquid chromatography. *$P < 0.01$ (IFN-γ versus medium treatment). **d**, Detection of L-kynurenine occurred in the lungs of wild-type but not knockout mice challenged intratracheally with *A. fumigatus*. Wild-type and knockout mice, infected for 2 or 6 days, were assayed for the presence of L-kynurenine in lung homogenates. Day 0 indicates uninfected controls. Error bars, means ± s.d. from four experiments. **e**, IDO protein expression was assessed in the lungs of wild-type and knockout mice challenged intratracheally with *A. fumigatus* for 2 or 6 days. One experiment is shown representative of three, demonstrating reduced IDO expression in the knockout mice.

slower adaptive response) that is widely viewed as pro-inflammatory. In uninfected CGD mice, the abundance of lung T-cell receptor (TCR) αβ cells—specifically, the $CD4^+$ and $CD25^+$ subsets—is reduced, and the difference is maintained after *A. fumigatus* challenge (Supplementary Table 2). We hypothesized that γδ T cells might be a crucial source of pro-inflammatory IL-17 in CGD mice with *A. fumigatus* infection, and that tryptophan catabolism physiologically contributes to a staged γδ response. IDO blockade was induced by subcutaneous implants of slow-release pellets of the IDO inhibitor 1-methyl-tryptophan (1-MT)[9], and wild-type mice on 1-MT (or placebo) were infected with *A. fumigatus* along with intact CGD mice.

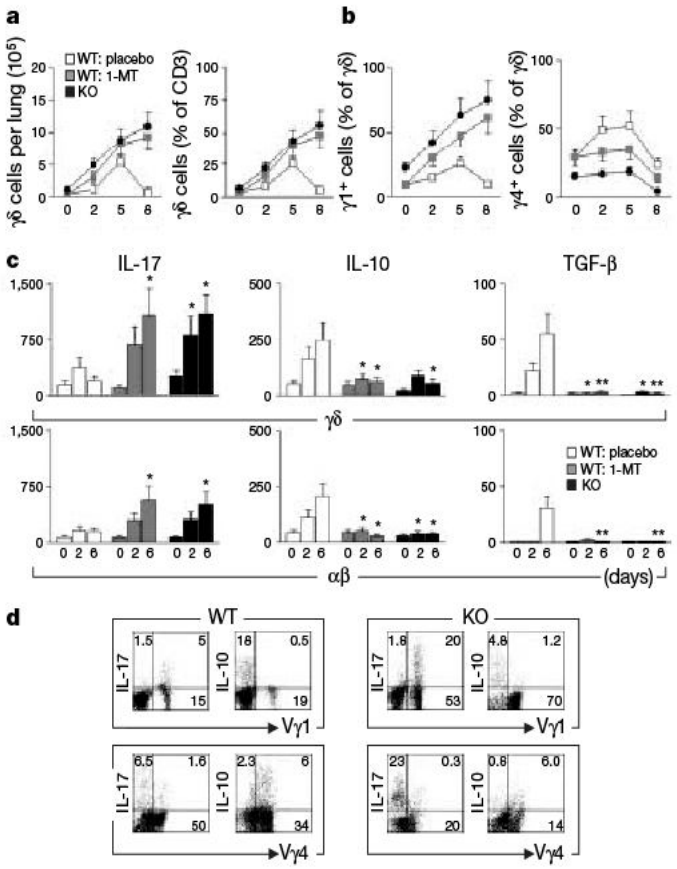

Figure 3 | In *A. fumigatus* infection, disparate subsets of γδ T cells accumulate in the lungs of CGD (knockout) mice and wild-type controls treated with placebo or 1-MT. a, Absolute numbers of γδ cells in the lungs and relative percentages in the $CD3^+$ fraction were determined by flow cytometry at different times after infection. Day 0 indicates uninfected animals. At 5 and 8 days post-infection, γδ T cells were similarly expanded in CGD mice and wild-type hosts treated with 1-MT. **b**, The proliferating γδ T cells in non-healer CGD and 1-MT-treated wild-type mice preferentially expressed Vγ1, whereas—mostly in the healer mice—$V\gamma4^+$ cells increased on days 2–5, to return to baseline levels by day 8. In **a** and **b**, values are means ± s.d. ($n = 4$). In uninfected and infected CGD mice, all values of γδ, $V\gamma1^+$ and $V\gamma4^+$ cells were significantly different from the respective controls (that is, wild-type mice on placebo; $P < 0.05$–0.0001). For Vγ1 expression, only on day 2 did significant differences occur between infected CGD and wild-type hosts on 1-MT ($P < 0.05$), although differences in Vγ4 expressions were significant at all time points ($P < 0.005$). **c**, Parallel groups of similarly treated and infected mice served as donors of pulmonary γδ and αβ T cells that were activated by anti-CD3 and assayed for the production of IL-17, IL-10 and TGF-β. Day 0 indicates uninfected mice, and all comparisons are relative to the respective wild-type controls on placebo (means ± s.d. with $n = 3$; $^*P < 0.05$; $^{**}P < 0.005$). **d**, IL-17-producing γδ T cells in CGD mice predominantly express Vγ1 whereas $V\gamma4^+$ cells mostly produce IL-10. Expression of TCR Vγ chain and intracellular IL-17 or IL-10 were determined by flow cytometric analysis in sorted pulmonary γδ cells from uninfected wild-type and knockout mice that had been stimulated overnight with soluble anti-CD3 and bacterial lipopolysaccharide. In unstimulated control cells, the percentage of cells expressing either cytokine was in all instances less than 0.5%. Isotype-matched irrelevant antibodies were used as controls in the analysis of intracellular cytokine expression, resulting in less than 1% positive cells. Numbers indicate percentages of specific Vγ- and/or cytokine-expressing γδ cells. Data are representative of three independent experiments.

In three independent experiments, the median survival time of CGD mice and of wild-type mice on 1-MT did not exceed 6–8 days, with 100% lethality, as opposed to the long-term survival of wild-type controls on placebo ($P = 0.001$ in individual experiments). At days 5 and 8 post-infection, γδ T cells were similarly expanded—on a per lung basis and as a fraction of sorted $CD3^+$ cells—in CGD mice and in wild-type hosts treated with 1-MT. Only in healer mice did γδ cells return to baseline levels by day 8 post-infection (Fig. 3a). Of interest, 1-MT had no detectable effects on course of infection in CGD mice (data not shown). So disease susceptibility was apparently associated with dysfunctional IDO and uncontrolled γδ T-cell expansion. However, serological ablation of γδ cells early in infection of CGD mice resulted only in partial protection (median survival time, 12 days; dead over total, 10/16; $P = 0.011$ for comparison between anti-TCR-γδ and control antibody treatment). In addition, γδ-deficient (TCR-$\delta^{-/-}$) mice consistently manifested a delay in pulmonary clearance of *A. fumigatus* and in the resolution of lung histopathology (data not shown). We postulated that in *A. fumigatus* pulmonary infection of healer mice, IDO expression by bronchoalveolar phagocytes restricts the activity of IL-17-producing γδ T cells, whereas other subsets of γδ cells—which escape restriction—continue to expand and contribute to establishing a regulatory environment.

γδ T cells were examined in the lungs of wild-type mice (with or without 1-MT) and CGD mice. This suggested a differential involvement of $V\gamma1^+$ and $V\gamma4^+$ cells in healer and non-healer mice (Supplementary Fig. 3). Flow cytometry analysis of γδ T cells revealed a sustained preponderance of $V\gamma4^+$ cells in the healer mice, whereas $V\gamma1^+$ cells dominated in CGD mice and wild-type hosts on 1-MT (Fig. 3a, b). This was reflected by distinct cytokine—IL-17, IL-10 and TGF-β—production patterns in healer versus non-healer mice by pulmonary γδ and αβ T cells (Fig. 3c). Intracellular staining revealed that $V\gamma1^+$ lymphocytes produced IL-17 whereas $V\gamma4^+$ cells produced IL-10 (Fig. 3d). Under *ex vivo* conditions, infection induced less apoptosis in γδ cells, αβ cells and PMNs in CGD mice than in wild-type controls; notably, $V\gamma1^+$ cells from uninfected wild-type mice—but not $V\gamma4^+$ cells—were susceptible to kynurenine-induced apoptosis *in vitro*[21] (Supplementary Fig. 4).

We asked whether supplying exogenous L-kynurenine to CGD mice would result in kynurenine-dependent effects detectable over the course of *A. fumigatus* infection. CGD and control mice received subcutaneous implants of placebo or L-kynurenine pellets (day −1), to be infected intratracheally with *A. fumigatus* on day 0 and be further treated with subcutaneous IFN-γ on days 1, 3 and 5. In both genotypes, L-kynurenine treatment in the absence of IFN-γ led to day-6 levels of circulating L-kynurenine that were 10-fold higher than in controls, yet levels of quinolinate were negligible. (Quinolinate is the end product in the kynurenine pathway of tryptophan catabolism.) The addition of IFN-γ to L-kynurenine treatment halved the concentration of L-kynurenine and resulted in appreciable amounts of circulating quinolinate (Supplementary Table 3). This demonstrated the occurrence of intracellular uptake and metabolism of the exogenous L-kynurenine by the IFN-γ-inducible kynurenine pathway enzymes downstream of IDO[17]. Therefore, parallel groups of mice were examined for course of infection and parameters of antifungal, inflammatory and T-cell reactivities.

In one experiment representative of three, the median survival time of CGD mice on placebo, IFN-γ or L-kynurenine alone did not exceed 8 days, with 100% lethality. Like wild-type controls, all CGD mice on combined IFN-γ and L-kynurenine treatment survived infection ($P = 0.001$; Supplementary Table 3). Cure by combined IFN-γ and L-kynurenine treatment was abolished by the addition

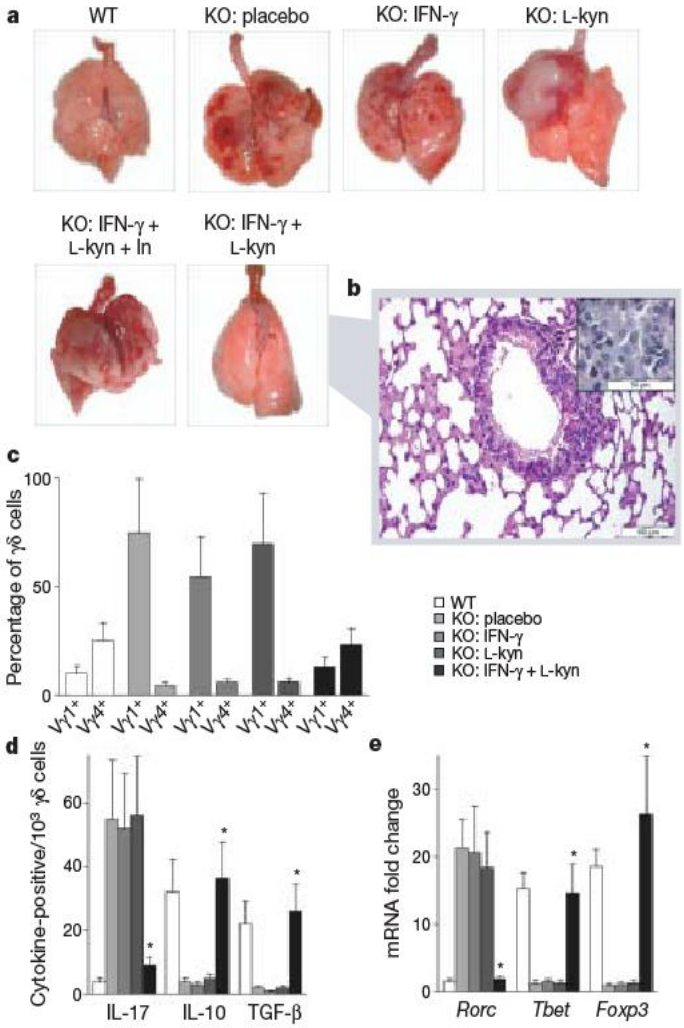

Figure 4 | Combined treatment with L-kynurenine and IFN-γ protects CGD mice from invasive pulmonary aspergillosis. Knockout and wild-type mice were infected intratracheally with *A. fumigatus* conidia (5×10^6) on day 0. The knockout mice were treated with L-kynurenine (or placebo) or IFN-γ or both. A group of animals on combined L-kynurenine and IFN-γ treatment were further treated with the kynurenine 3-monooxygenase inhibitor PNU 156561 (In). All hosts were examined for parameters of resistance to challenge, inflammation and immunity. (For mortality data, see Supplementary Table 3.) **a**, Specimens showing gross lung pathology were collected at 1 week that were representative of several, similarly treated mice with the same genotype. (When estimates of lung pathology based on an arbitrary scale of +1 to +4 were made by gross inspection, there were no differences between wild-type and cured knockout mice.) **b**, In these cured mice, histopathology did not reveal signs of inflammatory lung injury. **c**, Relative percentages of $V\gamma1^+$ and $V\gamma4^+$ cells in the pulmonary γδ fraction were determined by flow cytometry on day 6, showing normalization of the $V\gamma1^+/V\gamma4^+$ cell ratio—relative to wild-type controls—by effective therapy (means ± s.d. with $n = 3$). **d**, IL-10- and TGF-β-producing γδ T cells predominated in the lungs of cured hosts, where IL-17-producing cells were reduced, as determined by enzyme-linked immunosorbent spot assay on day 6 of infection. Before assaying, cells were activated overnight with anti-CD3 and lipopolysaccharide. **e**, Treatment with IFN-γ and L-kynurenine rectified aberrant *Rorc*, *Tbet* and *Foxp3* expressions in αβ T cells. Specific transcripts were evaluated in $CD4^+$ T cells from thoracic lymph nodes of wild-type and knockout mice infected for 6 days and treated as indicated above. The purified $CD4^+$ lymphocytes were activated with soluble anti-CD3 for 24 h. *Rorc*, *Tbet* and *Foxp3* messenger RNAs were quantified by real-time PCR using *Gapdh* normalization. Data are presented as fold change in normalized transcript expression in the samples relative to normalized transcript expression in the respective control cultures (cells from similarly treated, but uninfected, mice of the same genotype: that is, fold change = 1). (*Foxp3* was never expressed—nor was it inducible by infection or kynurenines—in whichever subset of pulmonary γδ T cells.) In **d** and **e**, values are means ± s.d. ($n = 3$), with $^*P < 0.01$–0.005 (IFN-γ and L-kynurenine versus all other treatments).

of a kynurenine 3-monooxygenase inhibitor, thus demonstrating a necessary role of 3-hydroxykynurenine formation *in vivo*. (The alternative pathway of L-kynurenine metabolism would still provide the downstream product, quinolinate; Supplementary Table 3.) At 1 week of infection, cell number and composition in BAL fluid were similar in healer, wild-type animals and CGD mice cured by IFN-γ and L-kynurenine (data not shown). In these mice, gross lung pathology and histological examination revealed no signs of inflammatory lung injury (Fig. 4a, b). Notably, IFN-γ and L-kynurenine also corrected the hyperinflammatory phenotype of CGD mice in response to sterile *A. fumigatus* hyphae (Supplementary Information and Supplementary Fig. 5).

Relative percentages of $V\gamma1^+$ and $V\gamma4^+$ cells in the pulmonary γδ fraction were determined by flow cytometry, showing an inverted ratio for $V\gamma1^+/V\gamma4^+$ cells in CGD hosts that would survive infection (Fig. 4c). IL-10- and TGF-β-producing γδ T cells predominated in the lungs of cured CGD mice, where IL-17-producing cells were reduced (Fig. 4d). The decreased production of IL-17 was reflected by an enhanced antifungal reactivity *in vitro* (Supplementary Table 4). Notably, in CGD mice, effective treatment with IFN-γ and L-kynurenine reinstalled some form of $CD4^+$ T-cell homeostasis, at least in thoracic lymph nodes, where the transcriptional profiles of the genes encoding RORγt, Tbet and Foxp3 were undistinguishable from those in wild-type infected controls (Fig. 4e). Of interest, and in line with previous observations[21–23], the same kynurenine mixture that induced apoptosis of $V\gamma1^+$ cells *in vitro* (Supplementary Fig. 4) completely abolished *Rorc* expression in αβ T cells from CGD mice stimulated overnight with anti-CD3 and anti-CD28 antibodies (data not shown).

A beneficial involvement of γδ T cells in infection might involve direct cytotoxicity of pro-inflammatory cells[24], production of anti-inflammatory cytokines[25] and the action of 'regulatory' γδ T cells[26,27]. In *A. fumigatus* infection of healer mice, it is possible that IDO expression by lung phagocytes contributes to a staged γδ T-cell response, by blocking the expansion of an early wave of IL-17-producing $V\gamma1^+$ T cells and by allowing a subset of $V\gamma4^+$ $Foxp3^-$ T cells to expand, release TGF-β and IL-10, and sustain the TGF-β-dependent generation of $Foxp3^+$ αβ T cells by the IDO mechanism[15,22]. In CGD mice, unrestrained $V\gamma1^+$ T-cell activity would in contrast initiate IL-17-dependent progressive lung injury that is sustained by deficient $V\gamma4^+$ cell function, imbalanced T_H cell responses and defective regulatory T-cell activity.

In conclusion, our study suggests that the evolutionary intersection of γδ cells with tryptophan catabolism and NADPH oxidase function might have represented a turning point in the phylogenesis of the immune system, tying together the innate and acquired immune systems in the proper control of infection. In addition, our data reveal a new mechanism whereby the very absence of reactive oxygen species—quintessential mediators of neutrophil-associated oxidative stress—causes a different form of IL-17-dependent pathogenic inflammation[28] and potential immune pathology[29] through unrestrained γδ T-cell activity.

METHODS SUMMARY

Eight- to 10-week-old C57BL/6 ($H\text{-}2^b$) mice were obtained from Charles River Breeding Laboratories. Mice deficient for $p47^{phox}$ on a C57BL/6 background were as described[2]. TCR-$\delta^{-/-}$ (B6.129P2-*Tcrd*^{tm1Mom}/J) mice were purchased from The Jackson Laboratory. The induction and evaluation of *A. fumigatus* infection in the mouse lung have previously been described in detail[30], as has the analysis of BAL fluid[9]. IDO induction was investigated by immunoblot analysis with rabbit monoclonal anti-mouse IDO antibody cv152. To inhibit IDO activity in wild-type mice, 1-MT pellets (7-day release at 1 mg h^{-1}) were implanted 1 day before infection[9]. To activate the kynurenine pathway, slow-release pellets of L-kynurenine (7-day release at 0.2 mg h^{-1}) were implanted in CGD mice. All *in vivo* studies were in compliance with national (Italian Approved Animal Welfare Assurance A-3143-01) and Perugia University Animal Care and Use Committee guidelines.

Full Methods and any associated references are available in the online version of the paper at www.nature.com/nature.

Received 19 August; accepted 13 November 2007.

1. Assari, T. Chronic granulomatous disease; fundamental stages in our understanding of CGD. *Med. Immunol.* **5**, 4 (2006).
2. Chang, Y. C., Segal, B. H., Holland, S. M., Miller, G. F. & Kwon-Chung, K. J. Virulence of catalase-deficient *Aspergillus nidulans* in $p47^{phox-/-}$ mice. Implications for fungal pathogenicity and host defense in chronic granulomatous disease. *J. Clin. Invest.* **101**, 1843–1850 (1998).
3. Romani, L. Immunity to fungal infections. *Nature Rev. Immunol.* **4**, 1–23 (2004).
4. Marciano, B. E. *et al.* Long-term interferon-γ therapy for patients with chronic granulomatous disease. *Clin. Infect. Dis.* **39**, 692–699 (2004).
5. Ott, M. G. *et al.* Correction of X-linked chronic granulomatous disease by gene therapy, augmented by insertional activation of MDS1-EVI1, PRDM16 or SETBP1. *Nature Med.* **12**, 401–409 (2006).
6. Bylund, J. *et al.* Enhanced inflammatory responses of chronic granulomatous disease leukocytes involve ROS-independent activation of NF-κB. *Eur. J. Immunol.* **37**, 1087–1096 (2007).
7. Grohmann, U., Fallarino, F. & Puccetti, P. Tolerance, DCs and tryptophan: much ado about IDO. *Trends Immunol.* **24**, 242–248 (2003).
8. Mellor, A. L. & Munn, D. H. IDO expression by dendritic cells: tolerance and tryptophan catabolism. *Nature Rev. Immunol.* **4**, 762–774 (2004).
9. Grohmann, U. *et al.* Reverse signaling through GITR ligand enables dexamethasone to activate IDO in allergy. *Nature Med.* **13**, 579–586 (2007).
10. Sharma, M. D. *et al.* Plasmacytoid dendritic cells from mouse tumor-draining lymph nodes directly activate mature Tregs via indoleamine 2,3-dioxygenase. *J. Clin. Invest.* **117**, 2570–2582 (2007).
11. Schwarcz, R. & Pellicciari, R. Manipulation of brain kynurenines: glial targets, neuronal effects, and clinical opportunities. *J. Pharmacol. Exp. Ther.* **303**, 1–10 (2002).
12. Stone, T. W. & Darlington, L. G. Endogenous kynurenines as targets for drug discovery and development. *Nature Rev. Drug Discov.* **1**, 609–620 (2002).
13. Munn, D. H. *et al.* GCN2 kinase in T cells mediates proliferative arrest and anergy induction in response to indoleamine 2,3-dioxygenase. *Immunity* **22**, 633–642 (2005).
14. Platten, M. *et al.* Treatment of autoimmune neuroinflammation with a synthetic tryptophan metabolite. *Science* **310**, 850–855 (2005).
15. Puccetti, P. & Grohmann, U. IDO and regulatory T cells: a role for reverse signalling and non-canonical NF-κB activation. *Nature Rev. Immunol.* **7**, 817–823 (2007).
16. Popov, A. *et al.* Indoleamine 2,3-dioxygenase-expressing dendritic cells form suppurative granulomas following *Listeria monocytogenes* infection. *J. Clin. Invest.* **116**, 3160–3170 (2006).
17. Belladonna, M. L. *et al.* Kynurenine pathway enzymes in dendritic cells initiate tolerogenesis in the absence of functional IDO. *J. Immunol.* **177**, 130–137 (2006).
18. Born, W. K., Reardon, C. L. & O'Brien, R. L. The function of γδ T cells in innate immunity. *Curr. Opin. Immunol.* **18**, 31–38 (2006).
19. Lockhart, E., Green, A. M. & Flynn, J. L. IL-17 production is dominated by γδ T cells rather than CD4 T cells during *Mycobacterium tuberculosis* infection. *J. Immunol.* **177**, 4662–4669 (2006).
20. Shibata, K., Yamada, H., Hara, H., Kishihara, K. & Yoshikai, Y. Resident $V\delta1^{+}$ γδ T cells control early infiltration of neutrophils after *Escherichia coli* infection via IL-17 production. *J. Immunol.* **178**, 4466–4472 (2007).
21. Fallarino, F. *et al.* T cell apoptosis by tryptophan catabolism. *Cell Death Differ.* **9**, 1069–1077 (2002).
22. Fallarino, F. *et al.* The combined effects of tryptophan starvation and tryptophan catabolites down-regulate T cell receptor ζ-chain and induce a regulatory phenotype in naive T cells. *J. Immunol.* **176**, 6752–6761 (2006).
23. De Luca, A. *et al.* Functional yet balanced reactivity to *Candida albicans* requires TRIF, MyD88, and IDO-dependent inhibition of *Rorc*. *J. Immunol.* **179**, 5999–6008 (2007).
24. Kirby, A. C., Newton, D. J., Carding, S. R. & Kaye, P. M. Pulmonary dendritic cells and alveolar macrophages are regulated by γδ T cells during the resolution of *S. pneumoniae*-induced inflammation. *J. Pathol.* **212**, 29–37 (2007).
25. Andrew, E. M. & Carding, S. R. Murine γδ T cells in infections: beneficial or deleterious? *Microbes Infect.* **7**, 529–536 (2005).
26. Peterman, G. M., Spencer, C., Sperling, A. I. & Bluestone, J. A. Role of γδ T cells in murine collagen-induced arthritis. *J. Immunol.* **151**, 6546–6558 (1993).
27. Andrew, E. M. *et al.* Delineation of the function of a major γδ T cell subset during infection. *J. Immunol.* **175**, 1741–1750 (2005).
28. Hizawa, N., Kawaguchi, M., Huang, S. K. & Nishimura, M. Role of interleukin-17F in chronic inflammatory and allergic lung disease. *Clin. Exp. Allergy* **36**, 1109–1114 (2006).
29. Hultqvist, M., Backlund, J., Bauer, K., Gelderman, K. A. & Holmdahl, R. Lack of reactive oxygen species breaks T cell tolerance to collagen type II and allows development of arthritis in mice. *J. Immunol.* **179**, 1431–1437 (2007).
30. Montagnoli, C. *et al.* Immunity and tolerance to *Aspergillus* involve functionally distinct regulatory T cells and tryptophan catabolism. *J. Immunol.* **176**, 1712–1723 (2006).

Supplementary Information is linked to the online version of the paper at www.nature.com/nature.

Acknowledgements This work was supported by Specific Targeted Research Project 'MANASP' (L.R.), and funding from the Juvenile Diabetes Research Foundation (P.P.) We thank P. Mosci for maintaining the mutant strains of mice and performing histopathology; and G. Andrielli for digital art and image editing.

Author Information Reprints and permissions information is available at www.nature.com/reprints. Correspondence and requests for materials should be addressed to L.R. (lromani@unipg.it) or P.P. (plopcc@tin.it).

ERRATUM

doi:10.1038/nature06542

Two stellar components in the halo of the Milky Way

Daniela Carollo, Timothy C. Beers, Young Sun Lee, Masashi Chiba, John E. Norris, Ronald Wilhelm, Thirupathi Sivarani, Brian Marsteller, Jeffrey A. Munn, Coryn A. L. Bailer-Jones, Paola Re Fiorentin & Donald G. York

Nature 450, 1020–1025 (2007)

In Table 1 of this Article, rows 12 to 20 (the 'Field F, G turnoff (non-kinematic)') were inadvertently moved up one row in the N and $\langle V_\phi \rangle$ columns. The corrected table is shown below.

Table 1 | Studies claiming a retrograde outer halo

Sample and selection criteria	N	Additional restrictions	$\langle V_\phi \rangle$ (km s^{-1})	Method	Source
Globular clusters (non-kinematic)	19	'Young halo'	-64 ± 74	F&W	Ref. 2
Globular clusters (non-kinematic)	20	'Young halo'	-42 ± 80	F&W	Ref. 10
RR Lyrae stars (non-kinematic)	26	$\|Z\| < 8$ kpc	-95 ± 29	FSM	Ref. 9
Field subdwarfs (kinematic)	30	$Z_{max} > 5$ kpc	-45 ± 22	FSM	Ref. 7
		Bias corrected	$+24 \pm 13$		Ref. 16
Field horizontal-branch stars (non-kinematic)	90	[Fe/H] < -1.6	-93 ± 36	F&W	Ref. 8
		$\|Z\| > 4$ kpc			
Field subdwarfs (kinematic)	101	$V < -100$ km s^{-1}	-32 ± 10	FSM	Ref. 13
		[Fe/H] < -1.8			
Field F, G, K dwarfs (non-kinematic)	250	$\|Z\| > 5$ kpc	-55 ± 16	FSM	Ref. 6
Field F, G turnoff (non-kinematic)		$Z_{max} > 5$ kpc		FSM	This work
	2,228	[Fe/H] < -1.0	-11 ± 2		
	200	[Fe/H] < -2.2	-41 ± 11		
		$Z_{max} > 10$ kpc			
	771	[Fe/H] < -1.0	-38 ± 5		
	94	[Fe/H] < -2.2	-71 ± 17		
		$Z_{max} > 15$ kpc			
	371	[Fe/H] < -1.0	-56 ± 8		
	54	[Fe/H] < -2.2	-71 ± 25		

Advertisement feature

Regenerating Hope with Stem Cell Technologies

Stem cells offer vast potential for therapeutics targeting cancer, diabetes, spinal cord injury, and degenerative diseases of the nervous system. New products and tools address the challenges of stem cell research, opening the door to novel insights into discovery, validation, and development of targeted therapeutics.

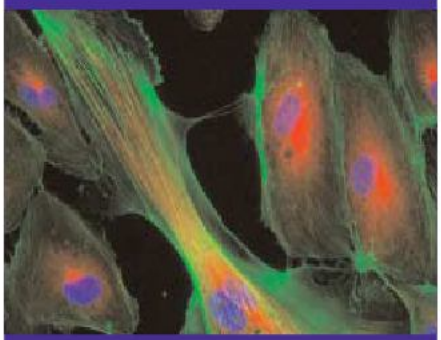

HMVEC-L primary endothelial cells: F-actin detected with DY554-Phalloidin (green), microtubules detected with anti-tubulin antibody, Nuclei detected with DAPI (blue), and DyLight 649 Conjugated Goat Anti-mouse IgG (red).

Image courtesy of Rockland Immunochemicals, Inc.

Material compiled by
The Linus Group, Inc.

THE LINUS GROUP

Marketing Science

info@thelinusgroup.com
www.thelinusgroup.com

Stem Cells

The arctic ground squirrel enters a hibernation period where the animal's core temperature approaches freezing, punctuated by brief arousal periods. As a result of the recurring episodes of hypoxia and reperfusion, the hippocampal stem cells have unique properties with relevance to stroke therapeutics, as well as neuronal tolerance, protection, and genesis. **Lifeline Cell Technology** offers Arctic Ground Squirrel Neural Stem Cells (agsNSC™) and optimized medium kits for creation of differentiated neurons with tolerance to reduced oxygen and glucose. Cell culture medium kits for agsNSC cells include an expansion kit, a differentiation kit for neuron formation, and a maintenance kit for neuron preservation.

Adipose-derived stem cells (ADSCs) possess similar phenotypic and functional characteristics to bone marrow-derived mesenchymal stem cells, frequently differentiating into cells and tissues of mesodermal origin such as bone, cartilage, and adipocytes. **Invitrogen Corporation** sells the STEMPRO® Human Adipose Derived Stem Cell Kit, consisting of ADSCs from human lipoaspirate tissue (obtained under license from Cytori Therapeutics) and MesenPRO RS™ Medium, a reduced-serum (2%) medium for the expansion of human mesenchymal stem cells.

Stem Cell Culture

Glycosan BioSystems, Inc. has released biocompatible HyStem™ hydrogels for the expansion of human embryonic stem cells, $CD34^+$ stem cells, and hepatic stem/progenitor cells. HyStem is a synthetic matrix that can be used in a xeno-free cultivation system. It offers the option of matrix protein and growth factor incorporation prior to cross-linking its two components: thiol-modified hyaluronic acid and PEGDA. HyStem is suitable for *in vitro* and *in vivo* research and is transparent, enabling live cell imaging at any point during culture. Once mixed, the hydrogel forms in less than 20 minutes at physiological pH and temperature, with rigidity dependent on cross-linker quantity.

StemCell Technologies, Inc. has launched mTeSR™1, a defined medium for the feeder-independent maintenance of human embryonic stem cells. The medium is based on research performed at the University of Wisconsin-Madison in the lab of Dr. Jamie Thomson. mTeSR™1 is designed to work with BD Matrigel™ from **BD Biosciences** and provides a standardized culture medium for the feeder-independent maintenance of hESC, reducing the time and cost associated with screening medium components and maintaining feeder cells.

Miltenyi Biotec provides tools and protocols for tissue regeneration research, targeting marrow stromal cells (MSCs). Products include reagents for stem cell isolation from various sources, antibodies for fluorescent analysis, microarrays for stem cell-specific gene expression profiling, and media for enumeration, expansion, and differentiation. Recently, Miltenyi Biotec expanded its product palette with the MSC Research Tool Box-CD271 (PE), offering reagents for the magnetic isolation and optimal expansion of $CD271^+$ MSCs.

Millipore Corporation provides filter products that are validated for stem cell research. The sterile Stericup® with Express™ PLUS membrane (in the 0.22 µm pore size) enables stem cells to be passaged and tested for pluripotency without negative effects by combining a

Figure 1. Velocity11 addresses stem cell needs with the BioCel® 1800 Automation System and VWorks™ Automation Control software.

Figure 2. Millipore Corporation enters into the stem cell products market with the Stericup® with Express™ PLUS membrane for stem cell passaged and pluripotency testing.

filter unit with a receiver flask and cap for processing and storage. When used in conjunction with ExpressPLUS membranes and media, the Stericup offers fast flow with low protein binding to ensure that growth factors and proteins are not absorbed and deleterious components are not added to the media.

Stem Cell Analysis

Based on a collaboration with the International Stem Cell Initiative, **Applied Biosystems**, an Applera Corporation business, now offers the TaqMan® Human Stem Cell Pluripotency Array, which targets 96 genes for independent monitoring of hESC lines from diverse sources, as well as the TaqMan® Mouse Stem Cell Pluripotency Array, for analysis of corresponding mouse orthologs. These arrays, utilizing microfluidic technology, facilitate parallel analysis of up to 8 biological samples across 12 to 384 preloaded TaqMan® Gene Expression Assays, without liquid-handling robots or multichannel pipettes. To perform gene expression analysis, cDNA is added to the TaqMan® Arrays and then analyzed on the 7900HT Fast Real-Time PCR System.

Epiblast stem cells (EpiSCs) are the most proximal precursor to all adult cells, including those that are pertinent to regenerative medicine. Researchers at the National Institute of Neurological Disorders and Stroke, National Institutes of Health, and the University of Oxford, U.K., used **Agilent Technologies** microarrays for gene expression, comparative genomic hybridization, and chromatin immunoprecipitation on a chip to analyze human and mouse embryonic stem (ES) cells, as well as mouse EpiSCs. The microarrays and related analytical software allowed the group to characterize global epigenetic events, providing a powerful model for mammalian epiblast regulation.

The French Institute for Cell Therapy and Exploration of Monogenic Diseases (I-STEM) recently had **Velocity11** install a novel high-throughput automated stem cell culture and screening platform, based upon the BioCel® 1800 Automation System and VWorks™ Automation Control software. Two VPrep® Pipetting Systems facilitate liquid handling; one for higher volume culture applications and the other for lower volume compound management. Other automated features include the VStack® Automated Plate Stacker, the Velocity11 Lid Hotel*, VCode® for plate tracking, and a PlateLoc® Thermal Plate Sealer. To avoid contamination, the system is equipped with a class100 ULPA filter and four extraction funnels to filter and recirculate air under a positive pressure.

Apollo Life Sciences has created a library of over 60 recombinant cytokines, chemokines, growth factors, hormones, and their receptors to address human cell expressed (hcx™) recombinant human protein applications. Apollo uses the proteins to develop its own next-generation therapeutics, and offers research grade proteins for sale. The 60+ lyophilized proteins currently available as products are >97% pure and undergo stringent quality control and endotoxin plus stability testing (sold through Apollo Cytokine Research). Apollo's hcx™ proteins closely mimic proteins in the human body, improving the performance of therapeutic, diagnostic, and research tools.

ORF Genetics uses a plant-based expression platform to produce human growth factors and cytokines for stem cell research, resulting in endotoxin levels that are 100-1,000 times lower than bacterial-derived systems. The "animal-free" barley seed endosperm tissue has very low protease activity, very low pyrogenic and pro-inflammatory activity, and is void of human and animal infectious agents. ORF Genetics offers more than 90 currently available and pipeline products, including Stem Cell Factor (SCF), Bone Morphogenic Proteins (BMP), FLT-3, and LIF.

Research shows that the glycoprotein receptor, Notch, directs unspecialized embryonic stem cells to become cells of the nervous system, paving the way for use of lab-grown cells to model disease and test new drugs. **Rockland Immunochemicals, Inc.**, a manufacturer of antibodies and antibody-based tools, has developed DyLight™ Conjugated Secondary Antibodies as a turnkey solution for Notch-based immunofluorescent microscopy. Notch antibodies, along with mouse and rabbit conjugated antibodies, are available in 100 µg aliquots.

"To get tissue-engineered human stem cell products to patients, an affordable, easy-to-use, FDA-approvable vehicle for cell culture and delivery is needed. One that allows seamless translation from *in vitro* studies to *in vivo* clinical use."

Glenn Prestwich, Ph.D.
Chief Scientific Officer, Glycosan BioSystems, Inc.
Professor of Medicinal Chemistry, University of Utah

Companies listed in editorial:

Agilent Technologies
www.agilent.com

Apollo Life Sciences
www.apollolifesciences.com

Applied Biosystems
www.appliedbiosystems.com

BD Biosciences
www.bdbiosciences.com

Glycosan BioSystems, Inc.
www.glycosan.com

Invitrogen Corporation
www.invitrogen.com

Lifeline Cell Technology, LLC
www.lifelinecelltech.com

Millipore Corporation
www.millipore.com

Miltenyi Biotec
www.miltenyibiotec.com

ORF Genetics
www.orfgenetics.com

Rockland Immunochemicals, Inc.
www.rockland-inc.com

StemCell Technologies, Inc.
www.stemcell.com

Velocity11
www.velocity11.com

NATURE|Vol 451|10 January 2008

THE CAREERS MAGAZINE FOR SCIENTISTS

- FOCUS
- SPOTLIGHT
- RECRUITMENT
- ANNOUNCEMENTS
- EVENTS

nature jobs

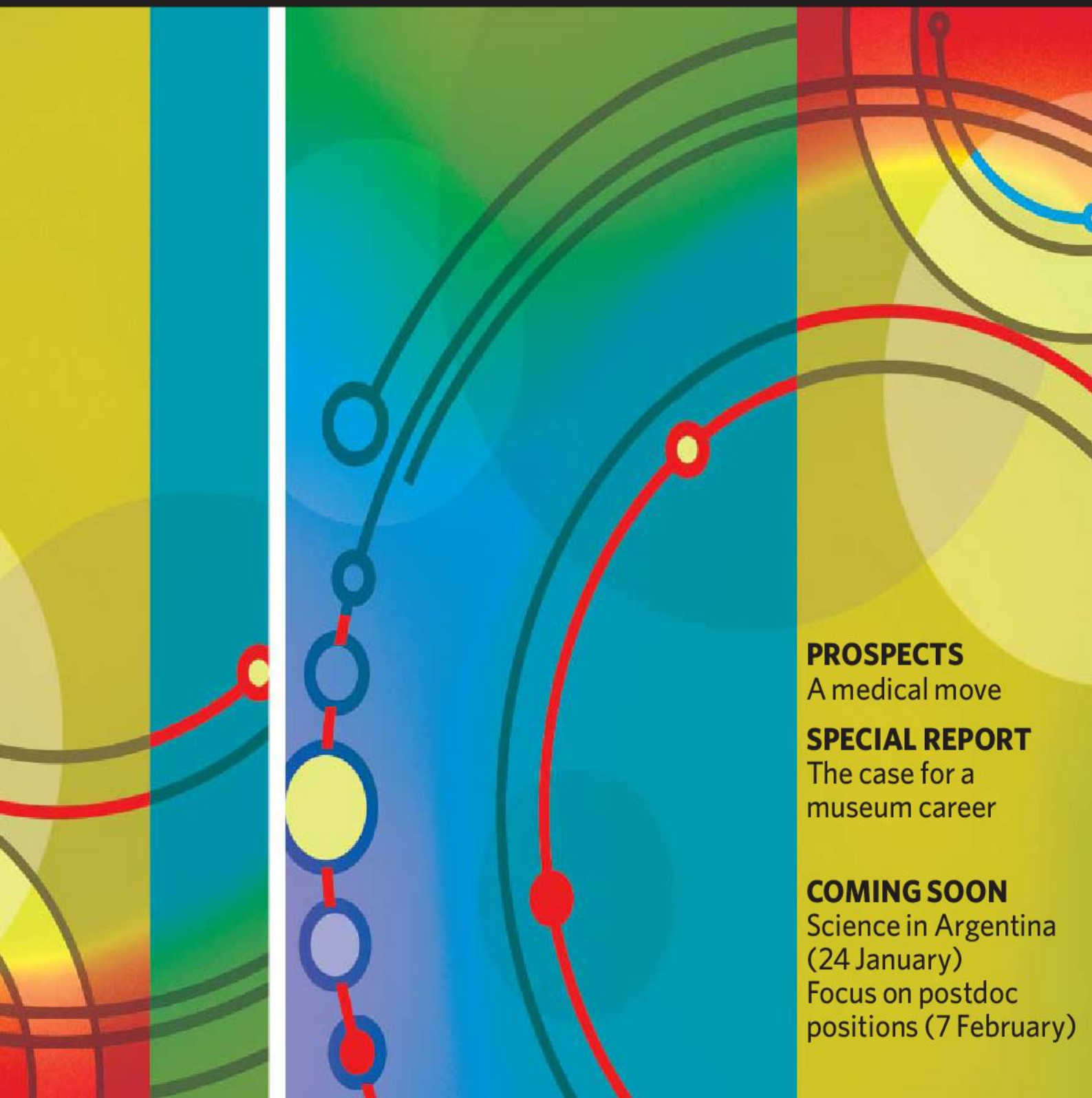

PROSPECTS
A medical move

SPECIAL REPORT
The case for a museum career

COMING SOON
Science in Argentina (24 January)
Focus on postdoc positions (7 February)

FONDATION
BETTENCOURT
SCHUELLER

2007 LILIANE BETTENCOURT LIFE SCIENCES AWARD

OLIVIER VOINNET

The 2007 Liliane Bettencourt Life Sciences Award has been awarded to the young outstanding french scientist Olivier Voinnet from the Institut de Biologie Moléculaire des Plantes (CNRS) in Strasbourg, France.

A major scientific goal of Olivier Voinnet is to understand the mechanisms and roles of RNA silencing in eukaryotes, which is a newly discovered, sequence-specific gene regulation process with basic developmental and defensive functions. By developing powerful genetic tools, Olivier Voinnet and his team has proven that RNA silencing acts as a general antiviral system in plants and animals. His most important contribution is perhaps the demonstration that **suppression of gene silencing is a general strategy used by diverse viruses to counteract RNA silencing**: he has shown that viruses encode proteins that inhibit silencing, uncovering yet another example of the never ending molecular arms race opposing parasites and their hosts. Olivier Voinnet also has very strong interests in elucidating the mode of action of micro (mi)RNAs, which, in addition to their fundamental role in plant and animal development, are now appreciated as key molecules protecting mammalian cells against cancer.

The Liliane Bettencourt Life Sciences Award of € 250,000 is an essential part of the Bettencourt Schueller Foundation's commitment to Medical Research. It aims to support a top-level European researcher under the age of 45, along with his or her team, to pursue their work in the field of Biology or Medecine. The Jury for the Award is chaired by Pierre Corvol, Administrator of the Collège de France and member of the French Academy of Sciences.

The Bettencourt Schueller Foundation was created in 1987 by Mrs. Liliane Bettencourt, in memory of her father, the late Eugène Schueller, founder of L'Oréal. Its mission is to encourage entrepreneurship in Sciences, Arts and Social commitment. In 2006, the Foundation has provided more than 60% of its budget in support of Medical Research programs.

Fondation
Bettencourt Schueller
27-29, rue des Poissonniers
92522 Neuilly-sur-Seine Cedex
www.fondationbs.org
Contact: mw@fondationbs.org

W121376A

naturejobs

The five-year discussion about relocating the UK Medical Research Council's National Institute for Medical Research (NIMR) has had its fair share of controversy. The decision announced last December that the centre will move from its historic home in the suburbs of London to a site in the heart of the capital will cost some £500 million (US$990 million) and will see animal labs hosted in an urban setting (see *Nature* **450,** 926–927; 2006). As the dust settles, it is time to consider what the move might do for scientific careers.

The biggest question, career-wise, is whether the new facility will create more jobs. The centre will hold 1,500 people — roughly double what the NIMR site now serves, even though the suburban location sprawls over 19 hectares and the urban one will squeeze into 1.4 ha. But researchers from University College London and Cancer Research UK will also occupy the building, so it is unclear whether the new site will justify its price tag merely in terms of employing more scientific personnel.

Still, there is a chance for job growth and expanded career opportunities if the facility meets its goal of fostering translational research. If it discovers improved treatments for, say, cancer, then auxiliary jobs will emerge in intellectual property, clinical-trial management, regulatory affairs and marketing. The proximity of the centre to other London universities and hospitals will also help raise the city's research profile, resulting in more investment and status as a global 'hub'.

But it will be hard to assess which new jobs outside the centre have been created, at least in part, by its existence and proximity to other London research entities. If the new centre creates more scientific jobs overall — rather than just shifting positions from old sites to new — it will have been a positive move. But if there is no net gain in positions — and the centre costs more to operate, in less space, and with increased concerns about animal and virus containment — then the opposition's arguments will be justified. The investment is an expensive gamble. It will take until well after the facility's scheduled 2013 opening date to see whether the bet pays off, in terms not just of jobs but of overall scientific performance.

Paul Smaglik is former editor of *Naturejobs*.

CONTACTS
Acting Editor: Gene Russo

US Head Office
New York
75 Varick Street,
9th Floor,
New York,
New York 10013-1917
Tel: +1 800 989 7718
Fax: +1 800 989 7103
e-mail: naturejobs@natureny.com

US Sales Manager/Corporations:
Peter Bless
Tel: +1 800 989 7718

San Francisco Office
Classified Sales Representative:
Michaela Bjorkman
West USA/West Corp. Canada
225 Bush Street, Suite 1453
San Francisco,
California 94104
Tel: +1 415 781 3803
Fax: +1 415 781 3805
e-mail: m.bjorkman@naturesf.com

European Head Office
London
The Macmillan Building,
4 Crinan Street,
London N1 9XW, UK
Tel: +44 (0) 20 7843 4961
Fax: +44 (0) 20 7843 4996
e-mail: naturejobs@nature.com

European Sales Manager:
Andy Douglas (4975)
Advertising Production Manager:
Stephen Russell
To send materials use London address above.
Tel: +44 (0) 20 7843 4816
Fax: +44 (0) 20 7843 4996
e-mail: naturejobs@nature.com

***Naturejobs* web development:**
Tom Hancock

***Naturejobs* online production:**
Jasmine Myer

Japan Head Office
Tokyo
Chiyoda Building,
2-37 Ichigayatamachi,
Shinjuku-ku,
Tokyo 162-0843
Tel: +81 3 3267 8751
Fax: +81 3 3267 8746

Asia-Pacific Sales Manager:
Ayako Watanabe
Tel: +81-3-3267-8765
e-mail: a.watanabe@natureasia.com

JOBS OF THE WEEK

Various
Wyeth
Aberdeen,
Scotland (UK)
Turn to page 2 & 3

Faculty Positions, Emory Vaccine Center
Emory University School of Medicine
Atlanta, Georgia (USA)
Turn to page 17

PhD/Postdoc Positions
Max Planck Institute for Biophysical Chemistry
Göttingen (Germany)
Turn to page 14

Tuberculosis Imaging Project Director
University of Pittsburgh - Center for Vaccine Research
Pittsburgh, PA (USA)
Turn to page 19

Various
UWIC - University of Wales Institute Cardiff
Cardiff, Wales (UK)
Turn to page 7

A CAREER AT THE MUSEUM

For scientists who want to combine public outreach with research, a museum may be the perfect place to work, says **Ricki Lewis**.

R. T. NOWITZ/CORBIS

At the age of five, Stephen Jay Gould was transfixed by a dinosaur skeleton he saw on a visit to the American Museum of Natural History (AMNH) in Manhattan. His encounter sparked a lifelong affinity for museums. As he grew up, Gould eschewed playing stickball at the weekend to visit the dinosaurs, and eventually did his PhD at Columbia University in New York to be near his beloved museum. By the time he died in 2002, Gould had spent most of his career at the Museum of Comparative Zoology at Harvard University. He was one of many scientists who traced their early inspiration to museums.

Scientists who work in museums enjoy a dynamic mix of laboratory and field research, collection managing, outreach and education, and exhibition design. The primary advantage is research flexibility, says Kathlyn Stewart, a research scientist in palaeobiology at the Canadian Museum of Nature in Ottawa. "My work focus is a research programme of my design using museum collections," she says, contrasting this with universities, where teaching and advising students is the focus, or industry or government, where scientists may have little say in their research focus.

Scientists interested in the museum career path should proceed with some caution, however — jobs are not plentiful. "Even internationally it is a very small job market," says Niel Bruce, a senior curator at the Museum of Tropical Queensland in Australia, who has made several international career moves. Still, for scientists with a natural history bent who are itching to have an impact on the public, museum work can be a rewarding departure from more typical career tracks.

Collections and disciplines

Opportunities at museums are largely confined to natural history. Museum research is driven, and often defined, by institutions' specimen collections — extensive libraries of natural history objects that are conserved and catalogued. The physical sciences are more likely to be encountered at science centres, which are more hands-on than collection-based. Life sciences tend to be overrepresented, particularly zoology. A large natural history museum might employ ornithologists, mammalogists, entomologists and ichthyologists, along with botanists, archaeologists, geologists, astronomers and palaeontologists.

Some larger museums do have impressive labs. The genomics labs at the AMNH, for example, are enabling John Flynn, chair and curator of fossil mammals, and his collaborators to sequence 30 genes for every species of living carnivore. But that's rare. More often, a museum scientist in need of a molecular-biology lab must collaborate with a university researcher, says Spencer Lucas, interim executive director at the Museum of Natural History and Science in Albuquerque, New Mexico. So scientists at smaller museums find inventive ways to get data and scrutinize specimens with the latest technology. "We take specimens into the local hospital late at night," says Thomas Williamson, curator of palaeontology at the New Mexico museum. "If someone comes into the ER with a head trauma, the doctors pull our fossil out of the CAT scanner."

R. MICKENS

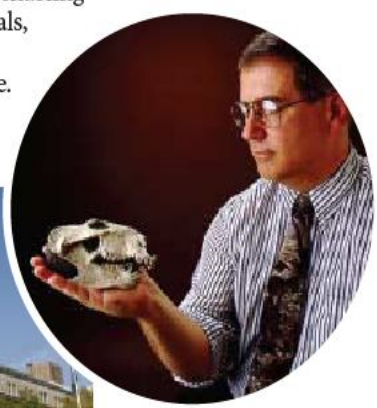

John Flynn is part of a project to sequence mammalian genes at the American Museum of Natural History.

The advent of genomics has translated into new ways to look at material in collections, whether studying Neanderthal DNA or using genomics to catalogue specimens as part of conservation-biology projects. This should mean new job opportunities for scientists at museums, according to John Bates, chair of zoology at the Field Museum in Chicago. But those new studies require support.

Fortunately, private funds and earned revenue are helping to sustain museums, says Alan Friedman, former director of the New York Hall of Science. For example, the US$484-million renovation project under way at the California Academy of Sciences since 2005 will see the museum reopen later this year. The project, including a 'living roof' of plants, was funded by donations, membership fees, and the city and state.

More than academic

The path from museum research to exhibition design can offer opportunities not feasible in the academic environment. Dennis Blanton, curator and archaeologist at the Fernbank Museum of Natural History in Atlanta, Georgia, recalls how an accidental observation led to an interdisciplinary study and a novel exhibition. Last summer Blanton discovered a local riverbed

D. L. BRILL/BRILL ATLANTA

NATIONAL MUSEUM OF NATURAL HISTORY

On display: from exhibits on show to behind-the-scenes collections at the Smithsonian Natural History Museum.

exposed by drought. He morphed from archaeologist to palaeontologist when radiocarbon dating revealed the sediments to be about 35,000 years old. "The ecosystem had never been seen before," he says. Sedimentologists and other experts were brought in and many botanical specimens analysed. The result was an exhibition showcasing a 'virtual walk' in a 35,000-year-old Georgia forest. "The museum embraced the discovery and allowed me to pursue analysis," he adds.

Museum palaeontologists typically spend one to three months a year in the field, taking fossils back to the museum for painstaking preservation and preparation, which must be done to study as well as display fossils. But old collections can yield new information. "A researcher can make connections that are not obvious, find overlooked structures, or realize that characteristics once thought not to be important are now recognized to be important," says Lucas.

Patience is mandatory. Developing an exhibition from concept to reality takes time, usually years. For example, Tim White, co-director of the Human Evolution Research Center, part of the Berkeley Natural History Museums consortium at the University of California, led the team that discovered three *Homo sapiens idaltu* crania in 1997. But not until 2005 did replicas go on display at the Expo 2005 in Aichi in Japan, and at the National Museum of Ethiopia in Addis Ababa. Preparing a fossilized cranium for study and display entails collecting, cleaning, preserving and assembling many tiny pieces. One cranium was found in 180 fragments, which had to be sifted from thousands and then assembled using other skulls as guides.

Exhibition design involves repeated evaluations, says Friedman, to identify and address public misconceptions about science. For one exhibition, Friedman and his colleagues worried about using technical terms for microscopic organisms. Kids liked the names, just as they like those of dinosaurs. But most visitors, adults included, had no idea that paramecia and amoebae were actually living organisms. The scientist-designers needed to take a step back and answer the question 'what is life?' in their display.

There is ample interplay among museum scientists and academia. Many museum scientists have duties akin to those of university professors, and some scientists have joint appointments. It is common to write papers for peer-reviewed journals and, in some countries, to seek external research grants. Flynn, for example, currently oversees US National Science Foundation grants for research, collections and education. Curatorships at large museums are tenured.

Some museum scientists teach undergraduate courses. Dirk Van Tuerenhout, curator of anthropology at the Houston Museum of Natural Science in Texas, teaches anthropology at the University of Houston. It helps connect him with a "different demographic", he says, and forces him to stay current in his field. "The best universities integrate jobs, so that their professors can do research, teach and do outreach based on their museum platforms," says White. The pay is usually in line with comparable academic positions, he adds.

Exhibiting and teaching: Tim White (top), Dirk Van Tuerenhout (bottom).

Inspiration and education

Experienced museum scientists interested in having a broader impact can help guide and start new museums and centres. Friedman is a consultant for the Science Center of Tech Valley, which is evolving from New York's existing Schenectady Museum & Suits-Bueche Planetarium. The museum began with an archive of documents and artefacts from when Thomas Edison founded nearby General Electric. Today it also celebrates locally developed imaging technologies. The planned science centre will include a 'living lab' for ongoing experiments.

Museums have long collaborated with universities, whose graduate students have access to the collections. But starting soon, more museum scientists may be trained entirely at museums. A new PhD programme in comparative biology at the AMNH, part of the Richard Gilder Graduate School, is accepting its first students. The school will highlight research unique to museum scientists, focusing on phylogeny and interactions among species, says Flynn. PhD students will provide public education programmes and develop exhibitions, while interacting with academic researchers whose universities are associated with the museum. The first class for the four-year programme will have four students. But eventually class size will grow to 18, Flynn says, and students may stay an extra year to develop a formal course or public educational programme. The only other PhD programme based in a museum is at the national museum of natural history in Paris, says Flynn.

Mostly, though, museums are vessels for inspiration such as that experienced by the young Stephen Jay Gould. Whether helping to start a new museum or just designing an innovative exhibition, museum work is most valued by those scientists hoping to make an impact with the public. "When I work on an exhibition, I realize that maybe a million visitors a year will see it," says Flynn. "That's an incredible opportunity." ■

Ricki Lewis is a freelance writer in Schenectady, New York.

Wellcome Trust Clinical PhD Programmes

Applications are invited for the autumn 2008 intake to the Wellcome Trust's Clinical PhD Programmes.

The Wellcome Trust's Clinical PhD Programmes are a flagship scheme aimed at supporting the most promising medically qualified clinicians who wish to undertake rigorous research training.

Successful candidates will develop their potential to become academic clinicians within a structured and mentored training environment. Programmes will provide the individual trainee with opportunities to sample high-quality research environments before they develop a research proposal that is tailored to their individual interests.

Nine programmes have been established based in centres of excellence throughout the UK, which can provide research opportunities that will appeal to clinicians drawn from across the range of specialities.

Each programme has been structured to reflect the expertise of individual institutions, and together they offer a unique opportunity for academic medicine training in the UK.

Candidates should have the potential to pursue a career as an academic clinician. It is anticipated that many will have already commenced their specialist training but this is not essential.

Support includes a medical salary, PhD registration fees at UK/EU student rate, research expenses, general training funds and some travel costs.

Information on the programmes is available on the Wellcome Trust website www.wellcome.ac.uk/clinicalphd/nature

Interested candidates should send enquiries and applications to the individual programmes and not to the Wellcome Trust.

wellcome trust

U121919R

Passionate about...

Wyeth Research

Research-based and global in scope, Wyeth Discovery Research is leading the way to a healthier world – one where people have a better chance to develop properly and live longer, more fulfilling lives. We're helping people around the globe by building one of the industry's strongest R&D pipelines, responsible for some of today's most important research & development in cardiovascular disease, inflammation, oncology, women's health, musculoskeletal diseases and neurological diseases such as Alzheimer's. Our drug portfolio consists of novel innovative medicines representing a healthy balance between small-molecule and protein therapeutics.

To further expand our understanding of next-generation Biopharmaceutical therapies, Wyeth recently established a Protein Therapeutics Laboratory in Aberdeen, Scotland. Working with multiple therapeutic areas and across our five Discovery sites in the US and Europe, the goal of the Protein Laboratory is to become an internationally recognized center of excellence in the discovery of next-generation protein therapeutics. To achieve this goal, we are currently seeking highly motivated and creative individuals for the following positions throughout the United Kingdom.

DIRECTOR, WYETH RESEARCH ABERDEEN

- PhD in Molecular Biology or related discipline
- 8-10 years of experience in an academic or a Pharmaceutical or Biotech setting
- Solid scientific track record evidenced by a strong publication record combined with strong management skills in Protein or Antibody drug development

PRINCIPAL RESEARCH SCIENTIST, MOLECULAR IMMUNOLOGY

- PhD in Molecular Immunology or related discipline with postdoctoral training
- 6-8 years of experience in an academic laboratory
- Strong scientific background in adaptive immunity
- Demonstrated record of scientific productivity through publication of original research in peer-reviewed journals

SENIOR RESEARCH SCIENTIST, SHARK BIOLOGY

- PhD in Biology or related discipline with postdoctoral training
- 4-6 years of experience in an academic or marine biology laboratory setting
- Solid understanding of shark biology including naïve antibody repertoire, B cell development and humeral response to antigen challenge
- Strong publication record

Biotherapeutics Research

Aberdeen, Scotland

RESEARCH ASSOCIATE, MOLECULAR IMMUNOLOGY

- MS in Molecular Immunology or related discipline
- 3-5 years of experience in an academic or industry setting
- Excellent fish husbandry and laboratory skills

RESEARCH ASSOCIATE, SHARK BIOLOGY

- MS in Biology or related discipline
- 3-5 years of experience in an academic or industry setting
- Excellent shark-handling and laboratory skills

SENIOR RESEARCH SCIENTIST, BIOCHEMISTRY

- PhD in Biochemistry or related discipline with postdoctoral training
- 4-6 years of experience in an academic or industry setting
- Solid understanding of IgNAR structure/function relationships, biochemical characterization and engineering of fish immunoglobulins or immune proteins
- Strong publication record

Wyeth offers the kind of remuneration and benefits you would expect from a large, dynamic and forward-thinking organization including private health plan and contributory pension scheme.

Any offer of employment is subject to the verification of background information following appropriate investigative reports (including consumer credit reports) and references from current and previous employers, academic and professional bodies.

To apply, please send your CV with salary expectations, quoting the job title of interest, to: Human Resources, Wyeth, Huntercombe Lane South, Taplow, Berkshire, SL6 OPH. Alternatively, interested candidates may also email CVs to: ukcareers@wyeth.com.

www.wyeth.co.uk

Wyeth

Leading the way to a healthier world

NW121001R

Clinical Tenure-Track Position
National Institute of Allergy and Infectious Diseases

The National Institute of Allergy & Infectious Diseases (NIAID), Division of Intramural Research (DIR), is seeking an outstanding tenure-track investigator to develop a clinical research program to better understand, treat, and ultimately prevent infectious, immunologic, and/or allergic diseases. The scope of the NIAID research portfolio has expanded considerably in recent years in response to new challenges such as bioterrorism; emerging and reemerging infectious diseases, including acquired immunodeficiency syndrome (AIDS), influenza, severe acute respiratory syndrome (SARS), West Nile virus, malaria, and tuberculosis; immunologic diseases and the increase in asthma prevalence among children in this country.

The successful candidate will implement and direct an independent clinical research program with research emphasis on clinical research but may include translational or basic research. The incumbent will have the opportunity to choose the Laboratory in which he/she would like to be affiliated. It is expected that clinical protocols developed will complement the research goals of the Laboratory selected. In addition, the candidate will be paired with a Senior Investigator who will serve as a clinical mentor.

An outstanding postdoctoral record of research accomplishment and M.D., M.D. /Ph.D. or equivalent degree is required for this position; board eligibility/board certification is also required. The incumbent will be expected to be qualified for credentialing by the NIH Clinical Center.

Candidates will be assigned independent resources to include clinical and/or laboratory support personnel, equipment, space, and an allocated annual budget for services, supplies, and salaries to ensure success. This is a tenure-track appointment under Title 42. Salary is dependent on experience and qualifications.

Interested candidates may contact **Dr. Karyl Barron, Deputy Director, DIR, NIAID at 301/402-2208 or email (kbarron@nih.gov)** for additional information about the position. To apply for the position, send your curriculum vitae, bibliography, and an outline of your proposed research program (no more than two pages), by **January 31, 2008** via email to Ms. Wanda Jackson at jacksonwa@niaid.nih.gov. In addition, three letters of recommendation must be sent to **Chair, NIAID DIR Clinical Tenure Track Search Committee, c/o Ms. Wanda Jackson at jacksonwa@niaid.nih.gov or 10 Center Drive MSC 1356, Building 10, Rm. 4A-26, Bethesda, Maryland 20892-1356**. E-mail is preferred. Please note search **#018** when sending materials.

Further information regarding the DIR laboratories is available at: **http://www3.niaid.nih.gov/about/organization/dir/default.htm** and information on working at NIAID is available on our website at: **http://healthresearch.niaid.nih.gov**.

National Heart Lung and Blood Institute
People Science Health

Tenure Track/Tenured Position
Basic Biomedical Research

Division of Intramural Research (DIR) of the National Heart, Lung and Blood Institute is seeking an outstanding scientist to initiate and direct an independent research program on the NIH campus in Bethesda, MD. The area of expertise of the candidate is less important than his/her demonstrated ability to conduct outstanding independent research in areas within the broad interests of the DIR. The areas of expertise may include but are not limited to: molecular and cellular biology, biophysics, biochemistry, immunology, systems biology, physiology, signal transduction, developmental biology, and molecular imaging. Potential candidates are welcome to view the NHLBI DIR web pages (http://dir.nhlbi.nih.gov/) to review the research programs and support available within the DIR. The existing faculty is an outstanding group of internationally recognized biomedical researchers covering a wide range of basic and clinical research topics complemented by the other DIR programs within NIH. Strong research core support in optical and electron microscopy, transgenic and knockout mouse production, mouse phenotyping, proteomics, genomics, and flow cytometry/cell sorting is available to the DIR faculty. Candidates can also train Ph.D. students by participating in the Graduate Partnership Programs (http://gpp.nih.gov/) with many academic programs around the world.

The candidate must have an M.D., Ph.D., or both and have an outstanding record of research accomplishments as evidenced by publications in major peer-reviewed journals. The position can be filled as a tenure-track or tenured position, but preference will be given to senior postdoctoral fellows or faculty who are still in the early stages of their research careers. The successful candidate will be offered a competitive salary commensurate with experience and qualifications, and will be assigned ample research space, supported positions, and an operating budget. Appointees may be US citizens, resident aliens, or non-resident aliens with or eligible to obtain a valid employment authorized visa. Applications must be received by **February 1, 2008**. Please submit a curriculum vitae and brief statement of research interests along with three letters of reference to:

"Robert S. Balaban, Ph.D., Scientific Director, NHLBI
c/o Mary McMahon
Administrative Officer, NHLBI
10 Center Drive, MSC 1670
Building 10, Room 7N220
Bethesda, MD 20892-1670
mcmahonm@nhlbi.nih.gov"

Help Us Help Millions

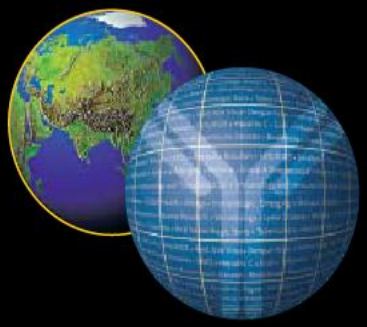

NIAID

National Institutes of Health
National Institute of Allergy and Infectious Diseases

POST-DOCTORAL POSITION: ANTIGEN PRESENTATION IN NON-HUMAN PRIMATES

Dr. Bernard A. Lafont

A post-doctoral fellowship is available in the Laboratory of Molecular Microbiology of the National Institute of Allergy and Infectious Diseases (NIAID) at the National Institutes of Health (NIH) within the Department of Health and Human Services (DHHS) to investigate antigen presentation in the context of primate lentivirus infection and AIDS vaccine development. The successful candidate will join the newly established Non–Human Primate Cellular Immunology and Immunogenetics Unit studying the kinetics and functional properties of cellular immune responses specific to primate lentiviruses (SIV, SHIV viruses) in monkeys (macaques, African green monkeys).

Suitable applicants should be highly motivated and have obtained recently a Ph.D. and/or M.D./D.V.M. degree with a strong background in immunology, virology, biochemistry and/or genetics. Prior experience with non-human primates, while desirable, is not essential for this position. The salary is commensurate with previous experience and qualification. Applicants are invited to send a cover letter, curriculum vitae, summary of past work and contact information of three references to:

Dr. Bernard A. Lafont
Non–Human Primate Cellular Immunology and Immunogenetics Unit
Laboratory of Molecular Microbiology, NIAID – NIH, Building 4 Room 328
4 center drive, Bethesda, MD 20892-0460 USA
e-mail: blafont@niaid.nih.gov

To learn more about NIAID and additional job opportunities, please visit:
http://healthresearch.niaid.nih.gov/drp

Proud to be Equal Opportunity Employers

NATIONAL CANCER INSTITUTE

Senior Scientist

A senior scientist is sought to manage a large program within the Laboratory of Cellular and Molecular Biology (LCMB), Center for Cancer Research (CCR), National Cancer Institute (NCI), National Institutes of Health (NIH), Department of Health and Human Services (DHHS). The selected individual will direct the day-to-day operations of the program and administer substantial resources. The research focuses on studying the regulation of RANTES expression in T lymphocytes and the role of granulysin in immune defense. The position requires a recognized international expert in immunology; demonstrated expertise in managing a complex research program; exemplary skills in and innovative approaches to the latest technologies required; and evidence of recognition of senior scientific status by peers (i.e., grant support, awards, or other scientific recognition).
Salary is commensurate with experience within the available pay bands of the National Institutes of Health.

If interested, please forward a CV to **nciccrjobs@mail.nih.gov**. Please indicate **"Senior Scientist application"** in the subject line. If you do not have access to e-mail, please mail via first class mail to:

Dr. Doug Lowy
c/o Mr. Patrick Miller
31 Center Drive, Suite 3A19
Bethesda, Maryland 20892

Applications must be received by **February 3, 2008**. Appointees must be U.S. citizens, resident aliens, or nonresident aliens with a valid employment-authorized visa.

NW121885R

THE NIH IS DEDICATED TO BUILDING A DIVERSE COMMUNITY IN ITS TRAINING AND EMPLOYMENT PROGRAMS

OPPORTUNITIES @ NIH THE NATIONAL INSTITUTES OF HEALTH

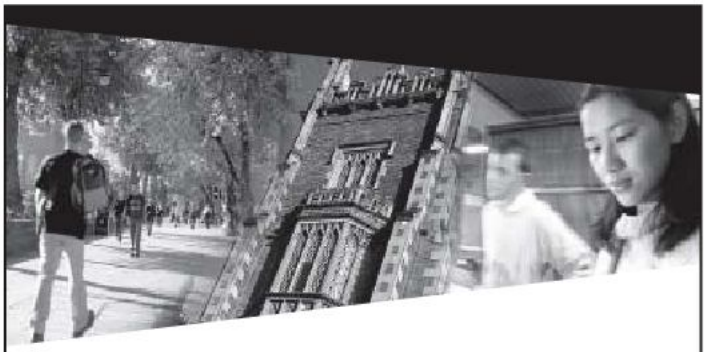

Lecturer and Senior Lecturer/Reader in Marine Biology (Two posts)

Ref: 08/100241

School of Biological Sciences

The School of Biological Sciences has 50 academic staff and 600 students and supports teaching and research across the biosciences integrating molecular and organismic biology. Biosciences at Queen's has demonstrated steady improvement in successive Research Assessment Exercises. We wish to strengthen our activity in Marine Biology building on recent research funding in excess of £6M and new facilities for investigation of the impact of coastal structures and mariculture. Details of Queen's and research and teaching in Biological Sciences are available on www.qub.ac.uk./bb/. These posts are available from 1st April 2008. Informal enquiries for either position may be made with: Dr Graham Savidge, e-mail g.savidge@qub.ac.uk

Salary scale: Lecturer £30,012 - £44,074 per annum (including contribution points)

Senior Lecturer: £42,791 - £54,206 per annum (including contribution points)

Closing date: 4.00pm, Friday 8th February 2008

Lecturer in Peptide Therapeutics

Ref: 08/100242

School of Pharmacy

The School of Pharmacy, as part of a continuing programme of strategic expansion, is now seeking to recruit a Lecturer in Peptide Therapeutics. The person appointed will join the Molecular Therapeutics Research Cluster (MTRC), within the school. The research interests of the candidates should be complementary to the on-going research programmes of the MTRC; these are: the discovery of peptide drug leads from natural sources, proteases as molecular targets, experimental therapeutics for cancer and medicinal chemistry. Further criteria will be listed in the further particulars for the post. Informal enquiries should be addressed to Dr Chris Scott (Tel: +44 (0) 28 9097 2350 email: c.scott@qub.ac.uk).

Salary scale: £30,012 - £44,074 per annum (including contribution points)
Closing date: 4.00pm, Friday 1 February 2008

Please visit our website for further information and to apply online – **www.qub.ac.uk/jobs** or alternatively contact the address below.

The University is committed to equal opportunities and to selection on merit. It therefore welcomes applications from all sections of society.

Personnel Department
Queen's University Belfast
Belfast, BT7 1NN.
Tel (028) 90973044
or (028) 90973854
(answering machine)
Fax (028) 90971040
E-mail on personnel@qub.ac.uk

Queen's University Belfast

Rg **Queen's University Belfast is a member of the Russell Group of universities. One of the United Kingdom's top 20 research-intensive universities.**

U121989R

Nuffield Science Bursaries
UNDERGRADUATE RESEARCH

THE NUFFIELD FOUNDATION

Undergraduate Research Bursaries

The Trustees of the Nuffield Foundation are offering an increased number of awards to enable undergraduates to take part in scientific research in universities and research institutes during the summer vacation. The purpose of the awards is to give experience of research to undergraduates with research potential and to encourage them to consider a career in scientific research.

The awards provide support for the student at a rate of £175 per week (£185 per week in London) for a period of between six and eight weeks. The Foundation does not pay overheads and no longer offers research expenses except in exceptional circumstances. The bursaries produce no National Insurance contribution liability.

Researchers in the Physical Sciences, Earth and Environmental Sciences, Engineering, Computing, Mathematics and the Biological and Biomedical Sciences at universities and research institutions within the UK are eligible to apply on behalf of a named student. Postdoctoral researchers and new lecturers, early in their careers, are also encouraged to apply.

The application, which must be on the new form for 2008, should be made by the person supervising the research.

The closing date for applications is Tuesday 12 February 2008.

Further details and application forms are available from the Nuffield Foundation (ref: NSB-UR), 28 Bedford Square, London WC1B 3JS. Tel: 020-7580-7434 (24-hour answerphone). Further information and forms may also be downloaded from our website: www.nuffieldfoundation.org/urb

The scheme is only open to applicants and students from institutions within the United Kingdom.

This scheme is one of two science bursary schemes for young scientists from the Nuffield Foundation. Students in their first year of an advanced or higher level science course at schools and colleges in the UK may join the Schools and Colleges scheme also described on our website.

The Foundation's objects are the advancement of education, health and social well being.

U118928R

University of Oxford

DEPARTMENT OF EARTH SCIENCES

Research Associate/Fellow in Mass Spectrometry

The Department seeks a Research Associate or Fellow in Mass Spectrometry to conduct and assist research in the Department of Earth Sciences of Oxford University.

The geochemistry research programs include various aspects of earth, environmental and planetary sciences and are supported by a wide range of analytical instrumentation that provides Oxford with one of the best-equipped facilities in the world. With new laboratories recently constructed and the acquisition of further mass spectrometers, we seek talented and enthusiastic individuals to maintain and develop a range of mass spectrometers and who are keen to work in a dynamic, interactive and technically innovative geochemistry research facility.

Dependant on skills and qualifications, the successful candidate will be appointed either as a Research Associate (£26,666 - £32,796 p.a.), or a Research Fellow (£33,779 - £40,335 p.a.). The appointment will be for three years in the first instance.

Letters of application with a full CV and the name and address of three referees (at least one of whom should be a current or previous employer) should be sent to Caroline Hutchings, Department of Earth Sciences, University of Oxford, Parks Road, Oxford OX1 3PR or E-mailed to: caroline.hutchings@earth.ox.ac.uk and received no later than Thursday 17 January 2008, quoting reference number DG/07/015. Further particulars are available from www.earth.ox.ac.uk/department/massspec.pdf

As an Equal Opportunity employer, we positively encourage applications from people of all backgrounds

U121188R

www.ox.ac.uk/jobs

UNIVERSITY OF WALES INSTITUTE, CARDIFF | ATHROFA PRIFYSGOL CYMRU, CAERDYDD

Research into Ageing – Five Positions Available

The Cardiff School of Health Sciences

The Cardiff School of Health Sciences has a growing reputation for strategic and applied research in biomedical, food and environmental sciences.

Following the appointment of two Research Professors in Biomedical Sciences and Food Science and Nutrition and the opening of state of the art research facilities at the Llandaf Campus, the School has launched a major research program to further our understanding of the ageing process. As part of this initiative the School now invites applications for the following positions:

Postdoctoral Research Scientist – ST1478

Salary: £25,134 - £27,466

(Two year fixed term contract)

The successful candidate will join the recently established Cellular Senescence and Vascular Biology Group under the direction of Prof. J. Erusalimsky. Research activities will focus on the causes and functional consequences of endothelial cell senescence and their relevance to the progression of vascular disease. The ideal candidate will be an enthusiastic and creative cell and molecular biologist with demonstrable significant research outputs as evidenced through publication in peer-reviewed journals. Expertise in the genetic manipulation of mammalian cells is desirable.

Research Technician – ST1759

Salary: £20,458 - £22,332

(One year fixed term contract)

The successful candidate will provide technical support to a research project funded by the MRC and undertaken jointly with University College London, investigating the relationship between socioeconomic status, psychosocial stress and cellular ageing.

Applicants will have a proven ability in laboratory research. We would be particularly pleased to hear from applicants with experience in telomere length analysis and measurement of oxidative stress.

Research Assistant (3 vacancies)

Salary: £16,669 - £19,841

(One year fixed term contracts)

The successful candidates will join a multidisciplinary team of biologists, nutritionists and health psychologists investigating the influence of lifestyle factors and dietary intake on cellular and molecular markers of ageing.

Candidates should have a good first honours degree (2.1 or over) in the natural or social sciences with a strong interest in undertaking a postgraduate degree in applied research.

The positions are available for one year in the first instance and candidates will be expected to enroll on a research degree programme.

For application forms and further details: **www.uwic.ac.uk/jobs** or Human Resources, UWIC, Llandaff Campus, PO Box 377, Western Avenue, Cardiff, CF5 2SG
or Tel: 029 2041 7026 or email: **humanresources@uwic.ac.uk**
Please submit a current CV along with all application forms
For informal enquiries please contact Professor Jorge Erusalimsky on +44(0)29 20416853, e-mail jderusalimsky@uwic.ac.uk. **Closing date for receipt of applications: 8 February 2008**

Cardiff's **metropolitan** university prifysgol **metropolitan** Caerdydd

U121195R

ncbs

Contract Position for Screening Facility

The National Centre for Biological Sciences is a hub for advanced learning and fundamental research in Bangalore, India.

The Centre has recently installed state of the art equipment and facilities for high throughput screening and functional genomics. The later is built to complement the new Micro Imaging Centre, which provides excellence in advanced fluorescence microscopy, flow cytometry and nano-scale biology (see NCBS website at www.ncbs.res.in).

We are tendering contracts for high throughput screening facility management. The incumbent will have access to state of the art equipment, consumables and furnished space, and will advise existing personnel performing screening projects. Responsibilities include design, validation and completion of screening projects initiated at NCBS or externally. The position requires a top-down understanding of the logistics and technical aspects of a high-throughput, high content, cell culture based microscopy screen. The contract awardee will have experience with RNA interference and gene deletion based technologies, as well as with high-throughput platforms for fluorescence imaging and liquid handling. This will also include development of genome-wide analysis in small animals including flies, worms and vertebrates. Prospective collaboration with industry will be encouraged.

Familiarity with downstream image and data analysis involving customizable software programming is essential. NCBS is very keen to expand the scope of the genomic facility at several levels: from diversifying the types of screens performed; to attracting new external and internal users; and for the facility to be used as a platform for innovating new screening technologies and attracting venture partnerships. The contract management is expected to play an integral role in shaping the future of the screening facility.

Salary and benefits are at attractive levels and negotiable.

Please send your resume (preferably via email) with a list of accomplishments and your vision for the facility to:

Prof. K. VijayRaghavan : vijay@ncbs.res.in
Cc: Prof. Satyajit Mayor : mayor@ncbs.res.in
Cc: Prof. Veronica Rodrigues : veronica@ncbs.res.in

National Centre of Biological Sciences
Tata Institute of Fundamental Research
GKVK, Bellary Road
Bangalore – 560 065 INDIA
Ph. +91 80 23666001 / 02 / 18 / 19
Fax +91 80 23636662
www.ncbs.res.in

RW121994R

University of BRISTOL

www.bristol.ac.uk

Postdoctoral Research Assistant/Associate (Two posts)

£27,466 - £34,813

Following the award of a Wellcome Trust Programme Grant to Dr. Mark Szczelkun, two 60-month Postdoctoral Research Assistants/Associates in Mechanism, Control and Diversity of Molecular Motors on DNA are available. Both posts will be based in the DNA-Protein Interactions Unit in the Department of Biochemistry and will work closely together to investigate the bacterial ATP-dependent Restriction-Modification enzymes as model systems for the helicase-based motors found in transcription, replication, recombination and repair.

Postdoctoral Research Assistant/Associate (Biochemist – reference 13650)

You will principally be involved in developing and applying biochemical approaches, including rapid mixing techniques. You will have a PhD, good communication and interpersonal skills and be able to work independently. Experience, preferably at the postdoctoral level, in one or more of the following would be an advantage: biochemistry, biophysics, molecular biology, enzymology, interdisciplinary/single molecule techniques and/or DNA-protein interactions.

Postdoctoral Research Assistant/Associate (Biophysicist – reference 13649)

You will principally be involved in developing and applying magnetic tweezers and total internal reflection fluorescence microscopy. You will have a PhD, good communication and interpersonal skills and be able to work independently. Experience, preferably at the postdoctoral level, in one or more of the following would be an advantage: biophysics, biophysical chemistry, single molecule enzymology, magnetic tweezers, fluorescence, protein chemistry and/or DNA-protein interactions.

If successful, you may be appointed either on a fixed term or a permanent contract depending on the extent of your previous relevant research experience. Further information can be found at http://www.bristol.ac.uk/personnel/ftc/

Informal enquiries are welcome and can be made to Dr Mark Szczelkun, telephone 0117 331 2158, email mark.szczelkun@bristol.ac.uk

Further details and an application form can be found at www.bristol.ac.uk/vacancies Alternatively you can telephone (0117) 954 6947 or e-mail recruitment@bristol.ac.uk quoting appropriate reference number.

The closing date for applications is 9.00am, 1st February 2008.

EXCELLENCE THROUGH DIVERSITY

U122016R

LEARNING • DISCOVERY • ENTERPRISE

MANCHESTER 1824

The University of Manchester

Faculty of Life Sciences

Postdoctoral Research Associate

£26,666 p.a. **Ref: LS/001/08**

A highly motivated, well-organised individual is invited to join a team involved in microbiological research under the direction of Dr Dennis Linton. The aim of this research project sponsored by the BBSRC is to develop oligosaccharyltransferase enzymes useful for production of glycoconjugate vaccines against important human pathogens. This post provides an opportunity to join an expanding research group in a 5* rated bioscience department.

You will possess a PhD degree, preferably in Microbiology/ Molecular Biology, with experience in molecular genetic and protein expression techniques. You should be computer literate and be able to demonstrate quality team working and communication skills.

The post is available immediately and is tenable for three years.

Application forms and further particulars are available from our website or by contacting +44 (0) 161 275 1541 or james.d.linton@manchester.ac.uk quoting the reference number.

Closing date: 1 February 2008.

The University will actively foster a culture of inclusion and diversity and will seek to achieve true equality of opportunity for all members of its community.

www.manchester.ac.uk/jobs

U122020R

Sphere of Influence

Centre for Ecology & Hydrology
NATURAL ENVIRONMENT RESEARCH COUNCIL

Director of Biogeochemistry

£61 - £75,000 + bonus arrangement
Wallingford

There is no bigger challenge facing us today than protecting and enhancing the environment on which all our lives depend. And like us, you'll want to do something about it.

Part of the Natural Environment Research Council, the Centre for Ecology and Hydrology is the UK's leading establishment for research in the land and freshwater environmental sciences. Our work is focused on investigating the processes and reactions that govern the composition of the natural environment in order to inform and direct future thinking and action that will enhance our custodianship of the planet.

Heading up one of our three core programme areas, you will work to raise the profile of Biogeochemistry, integrating with Biodiversity and Water programmes to tackle pressing environmental challenges like climate change. You will be active in inspiring and directing teams from different disciplines, and championing environmental informatics.

Currently working in a leading science research establishment or consultancy within the UK or Europe, you will have an established reputation in environmental science which will be backed up by a solid record of publication. Your clear vision and clarity of thought will be supported by excellent team working skills and the ability to lead and inspire others in the achievement of goals.

In addition we'll support your career development and you'll enjoy a rewards package that includes NERC's public sector pension scheme, 30 days' annual leave and 10.5 days' public and privilege holiday per annum.

For further details and an application pack please visit our website at www.ceh.ac.uk/personnel/employment.html Alternatively write, quoting Ref: CEH 240, to Ruth Campbell, Recruitment Manager, People & Skills Section, CEH Monks Wood, Abbots Ripton, Huntingdon, Cambs PE28 2LS or E-mail: cehpersonnel@ceh.ac.uk Closing date for receipt of applications is 28 January 2008.

U121986R

School of Biosciences

Postdoctoral Research Fellow in Chemical Enzymology (Ref: S89N1424)

Circa £22,000 per annum
Fixed-term contract

Research Technician in Algal Biology (Ref: S90N1435)

Circa £17,000 per annum
Fixed-term contract

We have a six-month, fixed-term position for a postdoctoral research scientist in the School of Biosciences to carry out an industrially sponsored scouting study that will use atomic-force microscopy (AFM) to investigate the function of DNA replication enzymes. You will integrate into a newly-refurbished University Research Laboratory supervised by Drs. J. Love and S. Aves and be willing to travel to Industry Laboratories in Europe to perform AFM. We are seeking a highly-motivated and articulate individual with a Ph.D. in molecular biology or chemistry. Demonstrable experience in molecular cloning and enzyme purification is essential and knowledge of AFM (though not necessarily practical experience of this technology) is an advantage. They project may be expanded depending on evaluation of the scouting study by the sponsor.

We are also seeking a motivated scientist with a degree in biology, to fill a research technician position that is funded until 31 October 2010. The post is ideally suited to a recently qualified scientist with interests in algal biology and molecular/microbiology. You will be dynamic, self-motivated, communicative and organised. Responsibilities will include the maintenance and cataloguing of algal cultures and microbial stocks, general laboratory maintenance, inventory and assisting members of the research team with sample preparation.

For further information please contact Dr John Love, e-mail J.Love@exeter.ac.uk or telephone (01392) 269169. To apply for the Research Fellow post, please send your CV and covering letter as well as the contact details of three referees, quoting the job reference S89N1424 to Dr John Love, School of Biosciences, Geoffrey Pope Building, University of Exeter, Stocker Road, Exeter EX4 4QD.

To apply for the Research Technician post, application packs are available from www.exeter.ac.uk/jobs e-mail s.r.zerbe@exeter.ac.uk or answerphone (01392) 263100 quoting reference number S90N1435.

The closing date for applications is 21 January 2008. The interviews for both positions will be held on 30 January 2008, with an ideal start-date of 1 March 2008.

Equal Opportunities Employer

UNIVERSITY OF EXETER

U121996R

ICRISAT

International Crops Research Institute for the Semi Arid Tropics is a non-profit, apolitical organization for science-based agricultural development. To reduce poverty, enhance crop productivity and food security and to protect the environment, ICRISAT research focuses on farming systems, crop improvement, management and utilization in the semi-arid tropics.

Requires

Senior Scientist-Groundnut Breeding (International recruit)

The Job: Leading the development of improved breeding lines and varieties of groundnut and facilitating with partners/farmers for adoption. Planning, executing and interpreting the data of experiments in crop improvement; preparing reports, papers for publishing in journals and project proposals for donor funding.

The Person: PhD degree in plant breeding and/or genetics with 10-12 years of post-doctoral experience as plant breeder.

For details please visit website

http://www.icrisat.org/opportunities.htm

ICRISAT is an equal opportunity employer, and is especially interested in increasing the participation of women on its staff.

Send applications by email to: **icrisatrecruitment@cgiar.org** latest by **31 January 2008.**

RW121850R

UNIVERSITY OF LIVERPOOL

School of Biomedical Sciences
Department of Pharmacology & Therapeutics

Postdoctoral Researcher in Neuroscience

£28,289 - £30,012 pa

Working in the laboratory of Dr L Djouhri, you will investigate the role of A-and M-type K+ and HCN (h-channel) channels in the generation of spontaneous activity in primary sensory neurons and in spontaneous neuropathic and inflammatory pain (see Djouhri et al. 2006, J. Neuroscience, 44, 495-508). The project involves *in vivo* electrophysiological recording techniques from DRG neurons and identification of their receptive and cytochemical properties. You should have a PhD in neuroscience/systems physiology or a related subject. Experience of *in vivo* and/or *in vitro* electrophysiology is advantageous. The post is funded by the MRC for 3 years.
Job Ref: R-567082/N

School of Biological Sciences

Postdoctoral Researcher

£28,289 - £29,139 pa

You will join a research team investigating global gene expression responses of a number of environmentally important organisms. The project will involve the detailed bioinformatic interpretation of gene lists derived from microarray studies and includes the development of data pipeline tools and analytical methods. You should have a PhD with a background in computing or biological sciences and have experience of bioinformatics with the ability to work as part of a team. A track record of publication is desirable. The post is available for 2 years initially. **Job Ref: R-567079/N**

Department of Chemistry

2 Postdoctoral Researchers (Synthetic and Computational)

£28,289 pa

You will work on a joint experimental and computational programme on porous amino-acid based materials. You should have a PhD in Chemistry, Physics or Materials Science and an excellent publication record. Both posts are available for 3 years.

Post 1: Expertise in synthetic co-ordination chemistry is essential, with porous materials and diffraction methods advantageous.

Post 2: Expertise in computational chemistry (either forcefield, docking or DFT-based) on extended solids is essential, with generation and molecular dynamics advantageous.
Job Ref: R-567084/N

Closing date for all posts: 1 February 2008

U121374R

For full details, or to request an application pack, visit
www.liv.ac.uk/working/job_vacancies/
Tel 0151 794 2210 (24 hr answerphone)
Please quote Job Ref in all enquiries.
COMMITTED TO DIVERSITY AND EQUALITY OF OPPORTUNITY

Don't miss the intoxicatingly good job opportunities in *Nature* each week and on naturejobs.com

naturejobs

TIGP, Academia Sinica
In Science Related Fields
PhD Studentship

Funded by the government, Academia Sinica is the prominent research institute in Taiwan. In 2002, in collaboration with a consortium of local research universities, Academia Sinica established the Taiwan International Graduate Program that offers eight interdisciplinary PhD programs and a grant of NT$32,000 (US$980) per month, to each student for up to three years.

Contact

TIGP Office
Tel: +886-2-2789-8050
E-mail: tigp@gate.sinica.edu.tw
Web: http://tigp.sinica.edu.tw/

JP121785RL

Baxter
BioScience

Make a Difference

The global healthcare company Baxter and its subsidiaries support healthcare professionals and their patients in the treatment of serious and complex medical conditions. Baxter applies its expertise in medical devices, pharmaceuticals and biotechnology in order to make a meaningful difference in patients' lives. Would you like to face new challenges every day? In order to strengthen its team in Orth, Baxter Austria is looking for a

Research Scientist (m/f)

Immunology Vaccines

Position Description:

- Devise innovative in vitro assay procedures for the evaluation of humoral and cell mediated immunological responses to a range of viral and bacterial vaccines during their pre-clinical and clinical stages of development
- Actively participate in the assessment of new adjuvants for Baxter's viral and bacteriological vaccine programs
- Optimize and validate assays for immunogenicity testing of vaccines under pre-clinical and clinical setting
- Work Hands-on with potentially infectious materials under S2/S3 conditions
- Operate and supervise state-of-the-art laboratory equipment
- Analyze and evaluate experimental data, prepare presentations, experiment reports and publications
- Follow all scientific developments and literature in the relevant fields of research
- Communicate research results at internal and external meetings

Requirements:

- PhD in life sciences
- 2-3 years Post Doctoral training in Immunology
- Experience in vaccine research in a pharmaceutical company would be favourable
- Profound theoretical and practical knowledge of immunology, immunoassays and validation
- Excellent technical skills, experience of flow cytometry is desirable
- Experience in working in a GLP environment
- Proven ability to handle multiple projects and to work both independently and within a team
- Prior experience in supervising staff would be an advantage
- Enthusiastic and adaptable, pro-active attitude
- Proficiency in written and spoken English and German

We offer a challenging position in an international company with great potential for development. Interested and qualified individuals are invited to send their applications with the reference number 14538NA/GZ to our consultant.

IVENTA Management Consulting, A-1071 Wien,
Neubaugasse 36, iventa@iventa.at

W121608R

IRD

Institut de recherche pour le développement

Institute of research for development:
IRD is a French public science and technology research institute.

- It conducts scientific programs contributing to the sustainable development of the countries of the South, with an emphasis on the relationship between man and the environment.
- IRD conducts research in Africa, in the Indian Ocean, in Latin America, in Asia, in the Pacific and the French overseas territories and communities.

Its fundamental missions are:
research, expertise, dissemination of results, and capacity-building support to Southern scientific communities.

IRD will recruit 34 scientists in 2008

> 13 Research Directors (m/f) > 6 Senior Researchers (m/f)
> 15 Junior Researchers (m/f)

In the following fields : Natural hazards, climate and non-renewable ecosystems. Sustainable ecosystem management in the South. Southern continental and coastal water resources and their use. Food security in the South. Public health and health policy. Development and globalisation.

www.ird.fr

The files can be downloaded on our website www.ird.fr or obtained to the Human resources Department, Recruitment Office
213 rue La Fayette - 75480 Paris Cedex 10 - France
For any additional information : dp.concours@ird.fr

PUBLICORP. - © IRD/Base Indigo

Deadline to obtain or download the application files: Wednesday January 23, 2008
Deadline to file an application: Friday January 25, 2008
The date of the postmark will be taken as the date of postage.

W121945R

Department of the Environment
www.doeni.gov.uk

The Scottish Government

BERR
Department for Business Enterprise & Regulatory Reform

Llywodraeth Cynulliad Cymru
Welsh Assembly Government

defra
Department for Environment Food and Rural Affairs

Members – Committee on Radioactive Waste Management

£300 per day – 1 day per week

Have you expertise in the **hydrogeology** or **underground construction** technology?

Do you want to contribute to a key Government programme, influence strategy at the highest-level and help to shape policy for generations?

Recently reconstituted, the Committee on Radioactive Waste Management provides independent advice to UK and devolved administration ministers on the long-term management, storage and disposal of the UK's radioactive waste. Its priority task is to provide independent scrutiny on the Government's proposals, plans and programmes to deliver geological disposal of the UK's higher activity wastes.

The Committee is founded on science and evidence, and is driven by openness and transparency. Collectively members will help to ensure that the Committee's objectives are achieved and its work programme delivered. You will provide specialist knowledge and expertise and may undertake specific roles chairing sub-groups, investigating complex issues or representing the Committee in meetings with the public, the media and other organisations.

With top level experience of either hydrogeology or underground engineering, you will be highly analytical and used to delivering work programmes to agreed timescales and to meeting objectives through co-operative team working. You must also understand the sensitivities of public sector decision making.

For further information and an application pack, please contact publicappts@defra.gsi.gov.uk or telephone 020 7270 8525 quoting reference PAPPT44.

Closing date: 12 noon 11 February 2008.

The UK Government and devolved administrations are committed to improving the diversity of their public bodies and welcome applications irrespective of race, ethnic or national origin, sex, marital status, disability, sexual orientation, religion, religious beliefs or similar philosophical belief, age, gender re-assignment or community background.

All public appointments are based on the principle of merit.

10CFA ASSESSED

U122021R

University of Glasgow

Faculty of Veterinary Medicine
Veterinary Pathological Sciences

Postdoctoral Research Assistant

£23,692 – £26,666/£29,139 – £32,796

This is one post available across levels 6/7 depending on qualifications and experience.

A position, funded by the Leukaemia Research Fund, is available for a dynamic researcher to work on the role of the Runx (AML/CBF) genes in haematopoietic development and leukaemia. You will join a large interdisciplinary team led by Professors Ewan Cameron and James Neil. The current focus is on understanding the role of Runx1 (AML1) in leukaemia, how this gene regulates cellular self renewal and lymphoid development. This project will utilise a variety of haematopoietic assays to understand the phenotypic effects of Runx gene expression and will seek to identify secondary events that collaborate in the transformation of haematopoietic cells. Experience of tissue culture and standard molecular techniques is essential and you will possess or be about to complete your PhD. Knowledge of experimental haematology and flow cytometry would be an advantage. The position is available immediately and funding is in place to support the post for at least three years.

Informal enquiries are welcomed. For further information please do not hesitate to contact Professor Ewan Cameron (E.R.Cameron@vet.gla.ac.uk; +44 (0)141 330 5725).

Applications should be submitted to Morag Wallace, Clinical Services Unit, University of Glasgow, Faculty of Veterinary Medicine, Bearsden Road, Glasgow G61 1QH quoting Ref 13799/DPO/A3.

BHF Glasgow Cardiovascular Research Centre

Research Assistant

£29,139 – £32,796

A three year BBSRC funded position is available within the BHF GCRC to work on development of microRNA-regulated transgene expression cassettes for application to cardiac gene transfer. Experience in adeno-associated viruses or microRNA biology an advantage.
For further information please contact Dr Stuart Nicklin, Tel: 0141-330-2521, email: stuart.a.nicklin@clinmed.gla.ac.uk.

For an application pack, please see our website. Applications should be submitted to Jillian Blair, Divisional Administrator, BHF Glasgow Cardiovascular Reseach Centre, 126 University Place, Glasgow G12 8TA quoting Ref 13941/DPO/A3.

Closing date for both posts: 25 January 2008.

The University is committed to equality of opportunity in employment.
www.glasgow.ac.uk Scottish University of the Year

U121759RM

LEUKAEMIA BIOLOGY GROUP

Postdoctoral Scientist Positions

Paterson Institute for Cancer Research

Reference number: PI/08/05

Salary in the range of £25,500 - £38,000 dependent upon qualifications and experience

The Paterson Institute is a leading cancer centre of excellence core-funded by Cancer Research UK and is an Institute of The University of Manchester.

Two positions are available in the Leukaemia Biology Group to study the biology of leukaemia stem cells. The primary aim of the laboratory is to further understand the mechanisms that regulate maintenance of the self-renewing sub-fraction of cells within a malignancy, so-called cancer stem cells. Applications from candidates with broad experience in molecular biology are encouraged, although prior experience in any of the following techniques would be an advantage: xenogeneic and syngeneic transplantation model systems; generation and analysis of transgenic or knockout model systems; retroviral or lentiviral shRNA genetic knockdown techniques; culture of human primary normal or malignant haematopoietic cells.

Informal enquiries to Dr Tim Somervaille, email: tsomervaille@picr.man.ac.uk

For further information and to apply for these positions, please visit our website. For applicants who are unable to download this information from our website, please contact Laura Humes, HR Assistant on 0161 446 3124, email: lhumes@picr.man.ac.uk to have this information sent by post.

Closing date for submission of applications is Monday 28 January 2008

www.paterson.man.ac.uk

MANCHESTER 1824 The University of Manchester

CANCER RESEARCH UK

U121947RM

Max-Planck-Institut für demografische Forschung

Max Planck Institute for Demographic Research

The Max Planck Institute for Demographic Research (MPIDR) is among the internationally most renowned centers in the population studies. The MPIDR consists of a number of research laboratories (Survival and Longevity, Evolutionary Biodemography, Economic and Social Demography, Historical Demography, Contemporary European Fertility and Family Dynamics, Demographic Data, Statistical Demography, Mathematical Demography, Population and Policy) and research units (Independent Research Group: The Culture of Reproduction, Rostock Center for the Study of Demographic Change). The Institute is committed to PhD education and runs three doctoral schools (IMPRSD, EDSD, and IMPRSLong). Recently, more than 130 researchers and non-scientific staff are working at MPIDR. Each year about 80 guest researchers are visiting the Institute. The Institute is situated in Rostock, Germany, near the Baltic Sea. For more information see **www.demogr.mpg.de.**

The MPIDR recently seeks to recruit 6 to 8

Research Scientists and Post Docs

to conduct research for the

Laboratory of Economic and Social Demography

(Director: Prof. Dr. Joshua R. Goldstein)

and to help developing the laboratory's research agenda and international collaboration. The newly-formed Laboratory of Economic and Social Demography will focus on (1) the transformation of the human life circle brought about by increases in longevity, (2) the causes and consequences of low fertility, and (3) partnership dynamics and family formation.

In addition to sociologists and demographers, economists working on life cycle models, opportunity costs of childbearing, and the consequences of population aging are particularly encouraged to apply.

The Max Planck Society is committed to employing more handicapped individuals and wishes to increase the share of women in areas where they are underrepresented. That's why the Max Planck Society especially encourages them to apply.

For further particulars and application details, please see **www.demogr.mpg.de/go/appl-ecodem**.

Should you do not have access to the Internet, please write to the Max Planck Institute for Demographic Research, Konrad-Zuse-Straße 1, 18057 Rostock, Germany, to request a hard copy of the relevant information.

MAX-PLANCK-GESELLSCHAFT

W120745R

MRC Medical Research Council

RSA Executive Search

Director of the Mary Lyon Centre

Harwell

Since its inception in 2004, and led by Professor Bob Johnson, the Mary Lyon Centre (MLC) has developed state-of-the-art mouse genetic facilities within the MRC Harwell Campus, a leading international centre that includes the Mammalian Genetics Unit (MGU). The MLC and MGU are co-located with the new Synchrotron facility, DIAMOND, and other significant biomedical research facilities under development. With a current total annual budget of £6m, and a staff complement of circa 100, the MLC has successfully established a variety of services in mouse genetics and functional genomics underpinning Harwell's leading role internationally in the generation of mouse models of human disease.

The new Director will succeed Professor Johnson, on his retirement in 2008, and will be responsible for:

- Developing the business strategy and extending the MLC's role nationally and internationally.
- Business development across the commercial and academic sectors.
- Staff leadership and management.
- Shaping the provision of future scientific tools and services provided.
- Contributing to the overarching strategy for the MRC Harwell campus.

He/she should have a track record of leadership in the biomedical sciences area and experience in generating and managing research collaborations, displaying a real commitment to effective business delivery and provision of high quality service to the scientific community.

MRC welcomes applications from appropriately qualified individuals from industry, academia and research institutions. The appointment salary and other terms and conditions are competitive and relocation assistance will be provided where appropriate.

MRC is an Equal Opportunities Employer.

For further information and to discuss your interest in confidence, please contact Dr Marc Lambert or Dr Kevin Young +44 (0)1707 259333 or apply by sending a CV by email to 071146@theRSAgroup.com Application deadline: 7th February.

RSA, The Melon Ground, Hatfield Park,
Hatfield, Herts AL9 5NB
Tel +44 (0)1707 259333
rsvp@theRSAgroup.com | www.RSAjobs.com

U122011R

QUILL

YOUR OPPORTUNITY TO WORK IN THE DYNAMIC NEW FIELD OF IONIC LIQUIDS

Research Fellows

Ref: 08/100250

Ref: 08/100252

Quill Research Centre

School of Chemistry & Chemical Engineering

We are currently recruiting TWO postdoctoral research fellows to join the existing multidisciplinary research team at Quill. Quill is the Queen's University Ionic Liquid Laboratories based in the School of Chemistry and Chemical Engineering at the Queen's University of Belfast. It is one of the largest and most active ionic liquid research centres in the world, with a staff that includes a number of world-renowned experts in the field including Prof. Ken Seddon and Prof. Robin Rogers. Quill is an industry-university co-operative research centre and currently there are fifteen industrial Members (spread across four continents) including such blue chip companies as BP, Chevron, Merck, Petronas, P&G and Shell.

The appointees will work closely with the existing research team at Quill and under the guidance of both the Quill academics and industrial Members. There may be a requirement for the research fellows to work for short periods in other laboratories. All the research will be conducted to meet the requirements of international patent law. Appointments will be made in the early part of 2008.

Applicants are advised to make separate application for each post of interest. Details and job packs for all posts can be found at http://www.qub.ac.uk/jobs

Further information may be obtained from quill@qub.ac.uk and also seen on http://quill.qub.ac.uk/

Closing date: 25 January 2008

Please visit the QUB website for further information and to apply online – **www.qub.ac.uk/jobs** or alternatively contact the address below.

The University is committed to equal opportunities and to selection on merit. It therefore welcomes applications from all sections of society.

Fixed term contract posts are available for the stated period in the first instance but in particular circumstances may be renewed or made permanent subject to availability of funding.

Personnel Department
Queen's University Belfast
Belfast, BT7 1NN.
Tel (028) 90973044
or (028) 90973854
(answering machine)
Fax (028) 90971040
E-mail on personnel@qub.ac.uk

Queen's University Belfast

Rg **Queen's University Belfast is a member of the Russell Group of universities.**
One of the United Kingdom's top 20 research-intensive universities.

U121987R

MAX-PLANCK-INSTITUT FÜR BIOPHYSIKALISCHE CHEMIE
KARL-FRIEDRICH-BONHOEFFER-INSTITUT GÖTTINGEN

The Research Group "Electron Paramagnetic Resonance Spectroscopy" at the Max-Planck-Institute for Biophysical Chemistry is offering two

PhD/Postdoc Positions

in biomolecular EPR spectroscopy. The candidate should have a Master or equivalent degree in Physics or Chemistry. Desired - but not necessary - is some experience with magnetic resonance techniques or spectroscopy. The laboratory is equipped with Bruker Elexsys X-band and W-band pulse spectrometers both with ENDOR and PELDOR capabilities. The EPR methodology should be applied for structural investigations of proteins and enzymes.

Payment will be according to the German TVöD standard. The positions are available from January 1st, 2008.

The Max-Planck-Society seeks to increase the percentage of women in areas where they are underrepresented and are therefore encouraged to apply. The Max-Planck-Society is committed to employing more handicapped individuals and especially encourages them to apply.

Please send your applications only per e-mail to **bennati@mpibpc.mpg.de.**

Max-Planck-Institut für biophysikalische Chemie
Dr. Marina Bennati, Am Fassberg 11, 37077 Göttingen
Tel.: 0049-551-201 1911

W121401R

Microbiologist
Environmental Science
A local environmental laboratory has an opportunity for a Microbiologist. The ideal candidate should have micro testing experience, preferably environmental micro. Someone with a science related degree is preferred. PCR experience would be a plus. This individual would conduct micro testing procedures.

Contact
http://www.kellyscientific.com
NW121893RL

In Vivo Scientist Needed!
Pharmaceuticals
World Pharmaceutical leader – Radnor, PA. Pre-clinical discovery research focused on immune mediated inflammatory disorders. Duties will include: Execute soluble protein isolation and analysis via bead-based multiplex platform; Execute mRNA isolation and expression characterization via quantitative real time PCR

Contact
http://www.kellyscientific.com
NW121898RL

Quality Assurance Manager
Pharmaceuticals
Clinical Research Organisation for pharmaceutical and related industries near Rotterdam. Duties Include: Coordinate the conduction and over sight of all types of audits within Europe; Plan, create and maintain the annual audit schedule plan; Write and rewrite departmental Standard Operating Procedures (SOP) and Guidelines. Ref: FB-200707

Contact
http://www.kellyscientific.com
NW121932RL

Sr Verification Engineer
Engineering
Performing PFEER and DCR examinations onshore/offshore, as defined in the platform verification scheme, tracking of progress, report writing, progress meetings, preparation of workscopes, raising and closing findings, reviewing reports. Degree qualified in an engineering discipline. 5 years offshore oil and gas experience.

Contact
http://www.kellyscientific.com
NW121938RL

Lab Technician
Laboratory Work
Seeking a Lab Technician for a company located in Kansas City, Kansas. Temp-to-hire, 2nd shift (2:30pm-11:00pm) M-F. Duties: Verify quality of raw materials and quality conformance using established methods; Prepare lab reagents; Perform calculations to make adjustments to ensure conformance; Utilise instrumentation; Record test results

Contact
http://www.kellyscientific.com
NW121894RL

Project Manager
Environmental Science
2 Project Managers for an Environmental Company. Duties: Oversee asbestos/lead based paint assessment and clean up in government buildings throughout LA County. Review lab test results; implement clean up plans. Schedule and manage asbestos clean up with contractors. Working with and writing reports for school district representative.

Contact
http://www.kellyscientific.com
NW121899RL

Senior Research Scientist
Immunology
French-speaking part of Switzerland. Small team of researchers in a group for immunology/assay development. Main tasks will cover the characterisation of recombinant proteins using standard methods (protein electrophoresis, ELISA, Western blotting, flow cytometry) and the handling and maintenance of cell lines and hybrids in vitro.

Contact
http://www.kellyscientific.com
NW121933RL

Fresh Chemistry Grad
Chemistry
Seeking a newly graduated chemist for a long-term contract position in research at a major chemical manufacturer. Will operate a laboratory unit (reactor), TGA and DSC, work with catalysts, transfer chemicals, etc. A BS in chemistry is a plus, as well as experience with analytical chemistry. Pay rate is very competitive!

Contact
http://www.kellyscientific.com
NW121940RL

Registration Coordinator
Pharmaceuticals
Global pharmaceutical/healthcare company is seeking a Registration Coordinator at its Lake Forest location. Entry level opportunity. Responsible for supporting the process of international product registration by retrieving technical documentation as needed and forwarding it to the registration team.
Requirements:
- Previous Experience
- BS/BA

Contact
http://www.kellyscientific.com
NW121895RL

Quality Assurance Manager
Manufacturing
Major Responsibilities: Establish, implement and maintain HACCP, SSOPs, prerequisite programs, testing and development, labeling, and formulations. Update and maintain all validations for HACCP Plans. Work directly with USDA inspectors to maintain awareness of current standards and to work through compliance issues/requirements.

Contact
http://www.kellyscientific.com
NW121901RL

Director Regulatory Affairs
Biotechnology
Biotec Pharmacon – Oslo
Designs and implements Regulatory Strategy for the different target indications of the company's pharmaceutical product candidates and oversees operational projects and resources. Looking for proven ability to provide strategic vision, who seeks solutions and has the ability to work independently as well as collaborate.

Contact
http://www.kellyscientific.com
NW121935RL

QC Tech Food/Bvg Industry
Manufacturing
Position provides critical support and validation of Production and Quality Systems. Monitor product temperatures and shelf life. Collect usage date. Conduct sensory evaluations. Demonstrate accurate and complete documentation. Trace problems to root cause. Perform lab test methods Knowledgeable in SPC, GMPs, HACCP, SOPs and Food Safety.

Contact
http://www.kellyscientific.com
NW121942RL

QC Chemist
Cosmetics
QC Chemist for a cosmetic company. Execute analytical tests to ensure that active pharmaceutical ingredients and drug products meet the criteria of identity, quality, purity and strength they are purported to possess. Evaluate the quality of analytical data generated and adherence to procedures and practices.

Contact
http://www.kellyscientific.com
NW121896RL

Serologist
Pharmaceuticals
Contract assignment in Raritan, NJ. Serology testing for in-process products to ensure specifications are being met. Ideal candidate will possess: 1-3 years of Titration, Serology, Stability Testing, Quality Assurance and knowledge of GLPs and GMPs.
Prefer Bachelors Degree in Medical Technology or related field.

Contact
http://www.kellyscientific.com
NW121902RL

Biostatistician
Clinical Research
Function as a team leader in clinical trials; Reviewing study protocols/ providing statistical input; Writing detailed statistical analysis plans; Interacting with sponsors, project managers, data managers etc; Overseeing data analysis, writing statistical and integrated clinical reports; Working permit for the Netherlands required. Ref: FB-21267

Contact
http://www.kellyscientific.com
NW121936RL

Biomedical Lab Technician
Biotechnology
Candidate will be responsible for performing tests on biological samples, equipment maintenance and sample management functions. Candidate will ensure that appropriate product and sample tests are performed, completed, and reported accurately in a timely manner.
BS in Life Sciences with lab experience preferred.

Contact
http://www.kellyscientific.com
NW121943RL

Chemist/Lab Technician
3rd shift contract to hire position in the Greensboro area. Duties include end product testing, wet chemistry techniques, must have GC and Karl Fischer instrumentation experience. Will be performing coloring matching and must be meticulous.
BS in Chemistry or other life science degree required. Recent graduate preferred.

Contact
http://www.kellyscientific.com
NW121897RL

Analytical Chemist
Chemistry
6 month contract - Phillipsburg, NJ. Analytical skills such as GC, HPLC, GC-MS, LC-MS, IC, spectroscopic and wet chemistry techniques essential. Particle sizes and other physical properties determination a plus. cGMP experience is preferred.
Ideal candidate will possess:
- BS in Chemistry/Analytical Chemistry
- Industry experience

Contact
http://www.kellyscientific.com
NW121903RL

Laboratory Analyst
Chemistry
Requires a proven ability in analytical techniques covering HPLC, GC, FTIR, dissolution, disintegration, titrimetry and wet chemistry. The aim of the role will be the generation of analytical data from existing stability programs as well as its interpretation and its formal reporting. Analyst will be able to report and summarise data effectively.

Contact
http://www.kellyscientific.com
NW121937RL

Polymer Chemist
Chemistry
Great opportunity for an entry-level Chemist to gain industry experience in the dynamic specialty chemicals industry! Assist senior chemists with the completion of Applications Research/Technical Service projects. Eventually you would be directly responsible for the completion of other projects.

Contact
http://www.kellyscientific.com
NW121944RL

To view these positions and more, log on to http://www.nature.com/naturejobs/profiles/kelly.html

nature chemistry

Associate Editors

The Nature Publishing Group is pleased to announce the launch of *Nature Chemistry* in 2009. Following the success of *Nature Materials*, *Nature Chemical Biology and Nature Physics*, and given the strength of the parent journal *Nature*, we fully expect *Nature Chemistry* to seize the commanding heights of the chemistry-publishing landscape.

Alongside the highest-quality original research, *Nature Chemistry* will cover news, commentary and analysis from and for the chemistry community, as well as striving to develop a voice that chemists care about.

As part of this exciting new publishing venture, we are now seeking three Associate Editors for *Nature Chemistry*, to be based in our London, Boston and Tokyo offices.

Applicants should have a PhD in a chemistry-related discipline, with demonstrable research achievements. Although postdoctoral experience is preferred (not required), emphasis will be placed on broadly trained applicants with a good knowledge of the chemistry community. Key elements of the position include the selection of manuscripts for publication, and commissioning, editing and writing other content for the journal. Candidates who wish to be considered for the role in our Japan office must demonstrate a good understanding of the East Asian research communities (in particular Japan, China and Korea) as well as being fluent in English and preferably an Asian language (Japanese, Chinese or Korean).

These are demanding and extremely stimulating roles, which call for a keen interest in the practice and communication of science. The successful candidates will, therefore, be dynamic, motivated and outgoing, and must possess excellent interpersonal skills. The salary and benefits, will be competitive, reflecting the critical importance and responsibilities of each position.

Applicants should send a CV (including their class of degree and a brief account of their research and other relevant experience), a News & View style piece (no more than 500 words) on a recent paper from the chemical literature, and a brief cover letter explaining their interest in the post, salary expectations, and indicating whether they wish to be considered for a position in London, Boston or Tokyo.

To apply please send your CV and covering letter, quoting reference number **NPG/LON/797** to Denise Pitter at londonrecruitment@macmillan.co.uk

The closing date for applications is Thursday 31st January 2008.

nature publishing group npg

IN121118R

Govern de les Illes Balears

MINISTERIO DE EDUCACIÓN Y CIENCIA

THE BALEARIC ISLANDS COASTAL OBSERVING SYSTEM (SOCIB)

seeks a

DIRECTOR

The BALEARIC ISLANDS COASTAL OBSERVING SYSTEM (SOCIB) is a new research and technology facility for operational oceanography, created as a Consortium of the Spanish Ministry of Education and Science and the Balearic Islands Government.

The mission of SOCIB is to develop a state-of-the-art Observing and Forecasting Operational Oceanography System, a scientific and technological infrastructure which will be open to international access and collaboration.

The Director of SOCIB reports to the Governing Council and is responsible for managing the Coastal Observatory implementation and operations, and for maximizing its readiness and effectiveness for scientific research and technology development. The Director is responsible for recruiting and maintaining high quality scientific, technical and administrative staff, developing an annual budget for review and approval, and proposing the short and long-range plans and priorities for SOCIB.

Salary range and starting date are to be negotiated.

Review of applications will begin in February 2008, and the recruitment will remain open until the position is filled.

Additional information of characteristics and conditions of the position on **http://socib.balearsfaciencia.org/**

W121801R

Post-doctoral Research Fellowships - 2 Posts

■ **School of Medicine**
Department of Cardiovascular Sciences
Grade 8: £35,837- £40,335 pa **Ref: R3566/NAT**
Available for up to 5 years

The Department of Cardiovascular Sciences is seeking applications from highly-motivated laboratory scientists with research strengths in any area of cardiovascular science for two new Post-doctoral Research Fellowships. You should have a strong research profile and high-quality publications, and will be supported to develop their own independent research strands to complement current departmental research interests.

Downloadable application forms and further particulars are available from www.le.ac.uk/personnel/jobs or in hardcopy from Personnel Services, tel: (0116) 252 5114, fax: (0116) 252 5140, email: recruitment2@le.ac.uk.

Please note that CVs will only be accepted in support of a fully completed application form.

Closing date: 31 January 2008.

Promoting equality of opportunity throughout the University

University of Leicester

U121983R

NPG – Academic Journals

Assistant Editor

The academic journals publishing division is a dynamic and growing part of Nature Publishing Group. The division manages the publication of almost 30 biomedical journals, many on behalf of learned scientific societies. We are now looking for an Assistant Editor to assist in managing the editorial and financial health of a portfolio of cell biology journals.

The Assistant Editor is a key position within the department. Assistant Editors work closely with Executive Editors to provide support and information to external editors, editorial boards and society management. The role provides an introduction to various aspects of journal production and publishing, and is an excellent first step for candidates looking to move into publishing.

The successful candidate will have a good eye for detail and be able to work without close supervision. Ideally candidates will have a graduate degree in a relevant scientific subject (cell biology, genetics or cancer). Candidates should be strong team players, and committed to providing the highest quality service to our external editors and society partners.

The position is based at NPG's modern offices in London.

Candidates should send a CV and covering letter, quoting reference number NPG/LON/793 and current salary to: Denise Pitter, Personnel Department at londonrecruitment@macmillan.co.uk

All candidates must demonstrate the right to live and work in the UK to be considered for the vacancy.

Closing Date: Friday 25th January 2008

nature publishing group npg

IN122093R

EMORY VACCINE CENTER
Faculty Positions
at the
JOINT ICGEB-EMORY VACCINE CENTER
New Delhi, India

Emory Vaccine Center (EVC) of the Emory University School of Medicine invites applications for junior and senior faculty positions that provide an exciting opportunity for cutting edge research in India on the immunology and pathogenesis of infectious diseases. The EVC and the International Centre for Genetic Engineering and Biotechnology (ICGEB) are partnering in a bold research initiative to establish a new Joint ICGEB-Emory Vaccine Center located on the ICGEB campus in New Delhi, India. The selected Emory faculty will have their laboratories at the Joint Center with opportunities for collaboration with ICGEB faculty on basic and translational research leading to vaccine development. Applicants therefore should be prepared to live in India for an extended period of time.

Applicants should hold a Ph.D and/or M.D. degree and have documented ability to establish and maintain independent, externally-funded research programs that contribute to the development of effective vaccines against infectious diseases of global importance. Particular areas of emphasis include tuberculosis, HIV, HCV, dengue and malaria but outstanding candidates with expertise in other areas are also encouraged to apply. Although previous experience with human studies is not a requirement, the applicants should have a commitment to the study of human immunology and translational research. They should also demonstrate a commitment to graduate and postdoctoral education and training. The selected faculty will hold their primary academic appointments in an appropriate Department of the Emory University School of Medicine. Salary and start-up packages are highly competitive.

Emory University, located in Atlanta, Georgia, enjoys an international reputation for its research, clinical and educational programs and has recently launched a major initiative in Global Health. The EVC **(www.vaccines.emory.edu)** is one of the largest academic vaccine centers in the world and is well recognized for its contributions in both basic and clinical vaccinology. The ICGEB **(www.icgeb.org)**, with laboratories in Trieste (Italy), New Delhi (India) and Cape Town (South Africa), conducts innovative research in life sciences for the benefit of developing countries and provides a scientific and educational environment of the highest standard.

Applicants should submit a letter of interest, a description of their research program, a current curriculum vitae, and the names and addresses of three references by email to Abdul Jabbar, PhD. at **jabbar@microbio.emory.edu** It is preferred that applicants should be citizens or permanent residents of the US. The deadline for receiving applications is **March 31, 2008.**

Emory University is an equal opportunity/affirmative action employer and encourages the application and nomination of minority and female candidates.

NW121886R

College of Medicine

University of Central Florida
College of Medicine - Basic Sciences Faculty

The University of Central Florida (UCF) seeks outstanding individuals for positions at the Assistant, Associate, or Full Professor level to join the new UCF College of Medicine (COM) at Lake Nona in Orlando. The new Lake Nona campus will also house the MD Anderson Cancer Center, the VA hospital, and the Burnham Institute for Medical Sciences. Faculty will help develop and teach an integrated organ-based curriculum and participate in basic science and/or medical education research.

Successful candidates must hold a Ph.D. or M.D. Preference will be given to applicants with a proven record of exceptional accomplishments in biomedical research and education and funding at the national level. The COM seeks candidates who have a passion for teaching cell biology, histology, genetics, physiology, anatomy, pharmacology, or microbiology.

Candidates will have opportunities to collaborate with NIH/NSF funded faculty of the Burnett School of Biomedical Sciences in the areas of neurodegenerative disease, heart disease, infectious disease, cancer, and biotechnology. Additional opportunities for collaboration exist with other UCF colleges and the UCF NanoScience Technology Center. Salary and start-up funds are competitive. Orlando offers affordable housing and excellent schools.

Interested persons should submit a CV, a brief statement of research interests and teaching philosophy, and three references to **Nancy Knobbs, University of Central Florida, College of Medicine, P.O. Box 160116, Orlando, Florida 32816-0116. Email: nknobbs@mail.ucf.edu.** Review of applications will begin February 15, 2008.

UCF is an equal opportunity/affirmative action employer and encourages applications from minorities, women, and other underrepresented groups.

NW122119R

---

nature REVIEWS MOLECULAR CELL BIOLOGY

http://www.nature.com/nrm

Scientific Copy Editor

Nature Reviews Molecular Cell Biology has a vacancy for a Copy Editor. This is an exciting opportunity to join the editorial team of a leading Review journal. The position involves copy-editing articles to a high standard and in a timely fashion for style and clarity, and liaising with authors, editors and production staff.

Candidates should have a degree in the life sciences and those with experience in molecular cell biology are particularly encouraged to apply. Excellent literary and verbal communication skills are essential attributes and although previous copy-editing experience is beneficial, this is not essential as training will be provided. An ability to work with authors and colleagues in an efficient, calm and flexible manner is also necessary.

The position will be based in Nature Publishing Group's modern London offices, and the terms and conditions are highly competitive, reflecting the importance and responsibilities of the role.

For further information about the Nature Reviews journals visit http://www.nature.com/reviews

Please send your CV and a cover letter (quoting reference number NPG/LON/796) including details of your current salary to Denise Pitter, Personnel Department at londonrecruitment@macmillan.co.uk

CLOSING DATE: 14th January 2008

nature publishing group npg

IN121124R

Gallo Institute at the University of California, San Francisco

Faculty Positions in Statistical Genetics

The Ernest Gallo Clinic and Research Center together with the Department of Neurology at the University of California, San Francisco invite applications for 2 full time faculty positions at the Assistant, Associate, or Full Professor levels working in the area of statistical genetics.

Eligible candidates may have as their research focus the development of new algorithms for analysis of genetic data of complex disease and/or the implementation of existing algorithms to identify genetic contributions to addictive behavior. The Gallo Institute has a long-standing nationally recognized program aimed at understanding the underlying biological basis of addictive behavior and ultimately leading to better therapies. The Gallo Institute has collected a large number of samples and controls from individuals with different addiction phenotypes. The successful candidates will ideally mine this data including genotypes that have already been generated to make advances in our understanding of the genetics of addiction.

The candidate should have a Ph.D. and/or M.D. and relevant postdoctoral research experience. In addition to a faculty appointment, the successful candidates will be eligible for membership in one or more of the graduate programs at UCSF.

Applicants should include a letter of interest, a curriculum vitae, and the names of four references to:

Dr. Louis Ptácek, Committee Chair,
Department of Neurology
University of California, San Francisco
548F Rock Hall MC 2922
1550 4th Street
San Francisco, CA 94158

The university is an equal opportunity/affirmative action employer.
All qualified applicants are encouraged to apply including minorities and women.

NW121421R

STANFORD
SCHOOL OF MEDICINE
Stanford University Medical Center

Chair, Department of Genetics
Stanford University
School of Medicine

The Stanford University School of Medicine is initiating a search for the position of Professor and Chair for the Department of Genetics.

The Stanford University School of Medicine is situated adjacent to the School of Humanities and Sciences, the School of Engineering, and two internationally-renowned adult and pediatric hospitals (Stanford Hospital and Clinics and Lucile Packard Children's Hospital), fostering a highly integrated approach to interdisciplinary science that is the hallmark of Stanford University. The School of Medicine is seeking an accomplished scientist in the fields of genetics, genomics, or both, with the creative vision to lead and shape the future of a distinguished and innovative Department of Genetics.

Stanford University is an equal opportunity employer and is committed to increasing the diversity of its faculty. It welcomes nominations of, and applications from, women and members of minority groups, as well as others who would bring additional dimensions to the university's research, teaching and clinical missions.

Interested candidates should submit a CV and letter of interest to the search committee by February 29, 2008 to:

Lucy Shapiro, PhD, Chair
Committee to Search for a Chair of the Department of Genetics
c/o Kendra Baldwin
Office of Institutional Planning
Stanford University School of Medicine
Building 110, Room 1
555 Middlefield Road
Menlo Park, CA 94025
or by email to:
kendra2@stanford.edu

NW121962R

THE UNIVERSITY OF CALIFORNIA BERKELEY

Department of Integrative Biology
Faculty Position in Plant Paleobiology and Evolution

Position ID #714

The Department of Integrative Biology at the University of California, Berkeley, is soliciting applications for a tenure-track position (Assistant Professor) in Plant Paleobiology and Evolution. We seek a colleague to join a department with a strong interdisciplinary emphasis who will develop a vigorous, independent research and teaching program in the area of plant paleobiology. Applicants should have a Ph.D. or equivalent advanced degree and an exceptional research record in: the evolution and ecology of past plant communities or ecosystems, the evolution of vascular plant lineages in deep time, and/or long-term plant response to environmental change using paleontological and neontological data. The position entails teaching both lower and upper level courses in plant evolution/paleobotany, with an emphasis on structure and function, phylogeny, paleoecology, and/or historical biogeography. An academic curatorship in the UC Museum of Paleontology is associated with this appointment; the successful candidate will be encouraged to promote the use of the museum's extensive holdings, supervise student research, work with museum staff to pursue opportunities for collection improvement and growth, and participate in UCMP and the Berkeley Natural History Museums activities and events.

For more information, see: **http://ib.berkeley.edu**

Application packages should include a CV with a bibliography of published work, a description of research accomplishments and objectives, a statement of teaching interests, and selected reprints. Three letters of reference should be sent separately by the recommender.

Both applications and letters of reference should be submitted electronically via:
http://ib.berkeley.edu/admin/jobs/paleobiojob.php
or via email to:
PlantPaleobiology@gmail.com

If electronic submission is not possible, materials may be sent by regular mail to:
Plant-Paleobiology Search Committee, Department of Integrative Biology
3060 Valley Life Sciences Building, University of California, Berkeley,
CA 94720-3140 USA

Applications and supporting letters must be received electronically or postmarked by **February 29, 2008**

Review of application will begin **March 10, 2008**

Applicants should refer their reviewers to the UC Berkeley Statement of Confidentiality at **http://apo.chance.berkeley.edu/evalltr.html**

The University of California is an Equal Opportunity/Affirmative Action Employer

NW121957R

MICHIGAN STATE UNIVERSITY

Bioeconomy Researcher

Anthropology, Economics, Geography, Political Science, or Sociology

Michigan State University seeks a researcher with a global reputation to lead our efforts examining the social, economic and policy aspects of the bioeconomy. This position can be filled at any rank, and may have a tenure home in Anthropology, Economics, Geography, Political Science, or Sociology. Applicants should have a well-established record of publication and extra-mural funding. International experience or demonstrated interest in international regions is an advantage. This is part of a cluster hire with two other searches being conducted this year and more anticipated in the future.

The closing date for applications is January 15, 2008, although later applications may be accepted if the search remains open. Please send curriculum vitae, a statement of interest, samples of written work and at least three letters of recommendation to: **Thomas Dietz, Bioeconomy, Searches, College of Social Science, Michigan State University, 274 Giltner Hall, East Lansing, Michigan 48824-1101**; or to **espp@msu.edu**. More information on each position and the MSU Bioeconomy Initiative is posted at **www.environment.msu.edu**.

Michigan State University is committed to achieving excellence through cultural diversity. The university actively encourages applications and/or nominations from women, persons of color, veterans and persons with disabilities.

NW121890R

MSU IS AN AFFIRMATIVE ACTION, EQUAL OPPORTUNITY EMPLOYER.

University of Pittsburgh
Tuberculosis Imaging Project Director
Center for Vaccine Research

The Center for Vaccine Research (CVR) of the University of Pittsburgh is seeking an outstanding Project Director at the Research Instructor or Research Assistant Professor Level for a Tuberculosis Imaging Project supported by the Bill and Melinda Gates Foundation.

Under the direction of Dr. JoAnne Flynn, the incumbent will manage a large consortium of investigators in imaging (PET/CT) of animal models of tuberculosis, for the purpose of understanding current chemotherapy as well as development of new therapies. The successful applicant will be responsible for coordinating activities within the consortium, ensuring milestones are met, preparation of documents, and management of various aspects of the program.

Qualifications Include: Experience in project management and experimental or clinical imaging and an advanced degree (PhD, MD or DVM). Salary and rank will commensurate with qualifications and experience.

Review of applications will begin immediately and continue until position is filled. Interested individuals should submit a letter of application, curriculum vitae, and the names and contact information of three professional references. Electronic applications are preferred and should be sent to **CVRInfo@pitt.edu** (subject line Tuberculosis Project Director Search).

Applications submitted by mail should be sent to:

University of Pittsburgh

Tuberculosis Project Director Search, c/o JoAnne Flynn, PhD
Center for Vaccine Research
9014 Biomedical Science Tower 3
3501 Fifth Avenue, Pittsburgh, PA 15261, USA

Inquires: e-mail CVRInfo@pitt.edu or telephone (412) 624-4480

The University of Pittsburgh is an equal opportunity, affirmative action employer. Women and minority candidates are strongly encouraged to apply.

For more information about the CVR, please visit our web site at

http://www.cvr.pitt.edu

NW121891R

Deputy Director

Lawrence Berkeley National Laboratory's Molecular Foundry-Opened March 24, 2006.

Lawrence Berkeley National Laboratory (LBNL) is a world leader in science and engineering research, with 11 Nobel Prize recipients over the past 75 years, and 59 present members of the National Academy of Sciences. LBNL conducts unclassified research across a wide range of scientific disciplines and hosts four national user facilities.
www.lbl.gov

LBNL is seeking an internationally recognized scientific leader to serve as Deputy Director. The Deputy Director works to develop the strategic vision of LBNL and assists in all aspects of the specific implementation of this vision. The Deputy will be principal partner and counsel to the Director in making decisions on the balance of programs within the laboratory; attending reviews of existing programs; and approving the seeding of new programs and the scaling back of others. The candidate must possess a broad scientific perspective and may have an active research program; a track record of academic and management success; and the ability to substitute for the Laboratory Director providing leadership to a multidisciplinary group of scientists.

For fastest consideration, apply online at: **http://jobs.lbl.gov**, select "Search Jobs", and enter **21297** in the keyword search field. Enter "Nature" as your source.

LBNL is an Affirmative Action/Equal Opportunity Employer committed to the development of a diverse workforce.

NW121949R

CHAIR
DEPARTMENT OF CELL BIOLOGY AND PHYSIOLOGY
UNIVERSITY OF PITTSBURGH SCHOOL OF MEDICINE

The University Of Pittsburgh School Of Medicine is seeking a chair for the Department of Cell Biology and Physiology. The Department comprises 22 tenure/tenure-stream faculty with a research focus on cell polarity and the trafficking of proteins and lipids, on the function and dysfunction of ion channels, on reproductive biology, and on signal transduction in diabetes and metabolism. The successful candidate must demonstrate an outstanding record of scholarship commensurate with appointment at the rank of Full Professor with tenure. An outstanding startup package has already been committed for this position, and the person who holds this position will occupy the fully endowed Richard King Mellon Chair in Cell Biology and Physiology.

The new chair will lead a significant expansion of the department and will benefit from interactions with the Center for Biological Imaging and the University of Pittsburgh Cancer Institute, and the recently established Clinical and Translational Science Institute and Drug Discovery Institute, as well as with other research units within the School of Medicine. The University of Pittsburgh School of Medicine is enjoying unparalleled growth in its research, clinical, and academic missions. The University is currently ranked 7th among educational and research institutions in NIH funding and has doubled its NIH support in the last 10 years.

Please send curriculum vitae and bibliography to the head of the **CBP Chair Search Committee (Jeffrey L. Brodsky, Ph.D.)** at: **jbrodsky@pitt.edu**

The University of Pittsburgh is an affirmative action, equal opportunity employer. Women and members of minority groups under-represented in academia are especially encouraged to apply.

NW120048R

Weill Cornell Medical College in Qatar

BIOLOGIST
Faculty Position

WCMC-Q seeks candidates for a faculty position with major responsibility for the teaching of an introductory biology sequence of two courses in a premedical program leading to entry to the medical school. Another faculty member conducts a complementary laboratory course sequence. Beyond the principal teaching obligation a successful applicant is expected to participate in advising, committee work, and the academic life of WCMC-Q. Research space is available as well as research funding support. Details regarding the WCMC-Q program and facilities can be accessed at:

www.qatar-med.cornell.edu

Candidates should hold a Ph.D. degree and possess demonstrable teaching skills as well as experience and training in research. Candidates must be willing to relocate to Doha, Qatar for the duration of the appointment. Academic rank and salary are commensurate with training and experience and are accompanied by a competitive foreign-service benefits package. Qualified applicants should submit a curriculum vitae and a letter of interest outlining their teaching and research experience to:

facultyrecruit@qatar-med.cornell.edu

***Please quote Faculty Search #08-nat-B01 on all correspondence**

Cornell University is an equal opportunity, affirmative action educator and employer.

The screening of applications will begin immediately and continue until suitable candidates are identified. Service is expected to begin in August 2008.

Please note, short-listed candidates will be asked to provide names of three references.

NW121965R

CHARITÉ

UNIVERSITÄTSMEDIZIN BERLIN
Gliedkörperschaft der Freien Universität und der Humboldt-Universität zu Berlin

The NeuroCure Clinical Research Center (NCRC), Charité - University Medicine Berlin, is offering the following positions:

University professorship for Neurology with focus on Neuroimmunology

Salary bracket W1/W2 ("tenure track")*

(reference number: 10.07)

University professorship for Pediatrics with focus on developmental disorders of the nervous system

Salary bracket W1/W2 ("tenure track")*

(reference number: 11.07)

* Salary brackets apply in accordance with the successful applicant's qualification.

⇨ ***Tasks:***
The goal of these two professorships is to successfully transfer basic scientific results in neurosciences to the clinic. In collaboration with the colleagues from NeuroCure, the successful applicants will conduct investigator-initiated trials, as well as other clinical and diagnostic studies. For more specific information, please visit www.neurocure.de.

⇨ ***Prerequisites and qualifications:***
For the W2-Professorship: acc. to § 100 BerlHG junior professorship or Habilitation, or equivalent scientific achievements and teaching competence, or similar qualification.

For the W1-Professorship: acc. to § 102a BerlHG university degree, outstanding thesis, experience and skill in scientific research, and enthusiasm for teaching.

⇨ ***Additionally:***
A scientific background in clinical-diagnostic and/or therapeutic studies is mandatory. Applicants should also have experience in the conceptual design or carrying out of investigator-initiated trials and multi-centre studies. They should have a detailed understanding of the conceptualization, registration, and execution of such studies.

We also expect a list of outstanding scientific achievements, successfully acquired third-party funding, and a concept paper outlining the applicant's specific plans for her/his proactive collaboration with Charité's research partners (www.charite.de). Commitment to teaching and excellent teaching skills are a plus, as well as experience in innovative teaching methods.

Charité seeks to increase its percentage of female scientific and teaching personnel, and strongly encourages qualified female researchers to apply for these positions. If equally qualified, applications by women will be favoured to the extent legally possible. Physically challenged applicants will be given preference if holding qualifications identical to those of non-challenged applicants.
Please see **(http://www.charite.de/jobs/prof.html)** for application instructions before sending your written application (listing the relevant position reference number) within **four weeks** to **Charité - Universitätsmedizin Berlin, Der Dekan, Prof. Dr. Martin Paul, Charitéplatz 1, D-10117 Berlin.**

W121991R

Barts and The London
School of Medicine and Dentistry

Neuroscience Centre

Postdoctoral Research Fellow Ref: 07496/HR

Postdoctoral Research Assistant Ref: 07495/HR

Applications are invited for two fixed-term 3-year posts available immediately funded by a Cancer Research UK programme grant to Professor Denise Sheer on the 'Functional Organisation of Human Chromosomes and the Nucleus'. The aim of this research programme is to investigate the principles of higher order chromatin architecture and determine its role in gene expression. Current approaches include molecular analysis of higher order chromatin loop organisation, ChIP analysis of DNA-protein interactions and epigenetic modifications, as well as high resolution fluorescence *in situ* hybridisation (e.g. Christova et al, J Cell Sci, 2007). Our dynamic research group is situated in the new Institute of Cell and Molecular Science, which provides a stimulating scientific environment with state-of-the-art facilities. Cell and molecular biology experience is essential for both positions.

The Postdoctoral Research Fellow will extend our studies of the Major Histocompatibility Complex to other genomic regions and various cell types, including neural cells under various physiological conditions. Salary for this post is at the appropriate point for experience on the Research scale (£27,813 - £36,458 per annum inclusive of London Allowance).

The Postdoctoral Research Assistant will take responsibility for the day-to-day smooth running of the laboratory and assist with research projects. Salary for this post is at the appropriate point for experience on the Research scale (£25,681 - £29,345 per annum inclusive of London Allowance).

You must be able to demonstrate your eligibility to work in the UK in accordance with the Asylum and Immigration Act 1999. Informal enquiries can be made to Prof Denise Sheer, Neuroscience Centre (email: d.sheer@qmul.ac.uk). For an application form and further information, please visit the Human Resources website on http://www.hr.qmul.ac.uk/vacancies or request details (quoting the above reference number) via email WCH-Recruit@qmul.ac.uk

The deadline for return of completed applications is 12 noon (BST) on 28th January 2008.

Applications (quoting the above reference number) should be returned via email to WCH-Recruit@qmul.ac.uk Alternative means of applying are available; please contact the recruitment line on 020 7882 6109 for details. Please note: completed applications must not be sent directly to the Neuroscience Centre or to Professor Sheer.

Promoting excellence in teaching, learning and research
Working towards equal opportunities

U122005R

University of Glasgow

Veterinary Pathological Sciences
LRF/CRUK Molecular Oncology Laboratory

Postdoctoral Research Assistant

£23,692 – £26,666/£29,139 – £32,796

A three year Leukaemia Research Fund position is available to work on RUNX1 AND TEL-RUNX1 in haematopoietic development and leukaemia. Knowledge of experimental haematology and flow cytometry would be an advantage.

For further information please contact Professor Ewan Cameron (E.R.Cameron@vet.gla.ac.uk; (0) 141 330 5725).

Applications should be submitted to Linda Bellingham, University of Glasgow, Faculty of Veterinary Medicine, Bearsden Road, Glasgow G61 1QH quoting Ref 13799/DPO/A3.

BHF Glasgow Cardiovascular Research Centre

Research Assistant

£29,139 – £32,796

A three year BBSRC funded position is available within the BHF GCRC to work on development of microRNA-regulated transgene expression cassettes for application to cardiac gene transfer. Experience in adeno-associated viruses or microRNA biology would be an advantage.

For further information please contact Dr Stuart Nicklin, Tel: 0141 330 2521, Email: stuart.a.nicklin@clinmed.gla.ac.uk

For an application pack, please see our website. Applications should be submitted to Jillian Blair, Divisional Administrator, BHF Glasgow Cardiovascular Reseach Centre, 126 University Place, Glasgow G12 8TA quoting Ref 13941/DPO/A3.

Closing date for both posts: 25 January 2008.

The University is committed to equality of opportunity in employment.

www.glasgow.ac.uk Scottish University of the Year

U121980RM

Barts and The London
School of Medicine and Dentistry

Centre for Gastroenterology

Postdoctoral Research Assistant

Ref: 07494/HR

Applications are invited for a Postdoctoral Research Assistant within the Centre for Gastroenterology. This post is for characterising the nature of mucosal NK cell activity during chronic infection of intestinal epithelium by the protozoan parasite Cryptosporidium Parvum. You should have an interest in the immunology of infection. Experience in cell culture, flow cytometry, RT-PCR or ELISA would be desirable.

Informal enquiries can be made to Dr V. McDonald, Centre for Gastroenterology (Tel: 020 7882 7202, email: v.mcdonald@qmul.ac.uk). This is a full-time fixed-term BBSRC funded post for 3 years, with a salary at the appropriate point for experience on the Research scale (£25,681 - £32,690 per annum inclusive of London Allowance).You must be able to demonstrate your eligibility to work in the UK in accordance with the Asylum and Immigration Act 1999.

For an application form and further information, please visit the Human Resources website on: http://www.hr.qmul.ac.uk/vacancies or request details (quoting the above reference number) via email: wch-recruit@qmul.ac.uk

The deadline for return of completed applications is 12 noon (BST) on 28 January 2008. Applications (quoting the above reference number) should be returned via email to wch-recruit@qmul.ac.uk alternative means of applying are available; please contact the recruitment line on: 020 7882 6109 for details. Please note: completed applications must not be sent directly to the Centre for Gastroenterology or to V. McDonald.

Where applicants are short listed for interview, references will normally be taken up prior to interview. Applicants who do not wish any referees to be so contacted should make this explicitly clear on their application.

We are unfortunately unable to reply to those applicants who have not been short listed and invited for interview. However, we would like to thank all candidates for their applications and for their interest in working for the School of Medicine and Dentistry.

Promoting excellence in teaching, learning and research
Working towards equal opportunities

U122004R

The University of Edinburgh

The University of Edinburgh is an exciting, vibrant, research-led academic community offering opportunities to work with leading international academics whose visions are shaping tomorrow's world.

Flow Cytometry Facility Manager

£27,466 – £32,796

The Institute for Stem Cell Research (ISCR) is a world-leading centre for multidisciplinary research in mammalian stem cell biology, and forms part of the newly created MRC Centre for Regenerative Medicine at the University of Edinburgh. Our mission is to acquire the basic understanding of stem cells to enable application of regenerative therapies in the treatment of human disease and injury (www.iscr.ed.ac.uk and www.scrm.ed.ac.uk).

An experienced Flow Cytometry Operator, you will manage a comprehensive multi-user flow cytometry facility – including a Cytomation MoFlo, FACSAria II, LSRII, Cyan and FACSCalibur instruments – and contribute to the development of new cytometry techniques. You must have a flow cytometry background and an interest in life sciences, as well as a PhD or equivalent research experience.

Apply online, view further particulars or browse more jobs at our website. Alternatively, telephone the recruitment line on 0131 650 2511. Ref: 3008414NA. Closing date: 1 February 2008.

Committed to Equality and Diversity

U122019R

www.jobs.ed.ac.uk

PRINCIPE FELIPE
CENTRO DE INVESTIGACION

GROUP LEADER POSITION

Prince Felipe Research Centre
Valencia, Spain
Regenerative Medicine Programme

A highly motivated scientist is required to lead a team of researchers to translate stem cell research to the clinic using animal disease models

The chosen candidate will provide strategic and technical leadership to a team of researchers to develop stem cell therapeutics, develop protocols to improve the efficiency of the differentiation of stem cells and their progenitors and interact with preclinical development scientists to test functionality in vitro and in vivo. They will also interact with collaborating scientists and physicians to develop and execute work plans to improve differentiation schemes, test preclinical safety and efficacy and develop efficient delivery systems for stem cells and with product development personnel to scale production of differentiation protocols for cGMP manufacture. As a Group Leader they will also be expected to provide project plans and timelines, write reports on scientific studies to support regulatory submissions and present scientific findings to key scientific, administrative and business forums.

The post is open to scientists with a Ph.D. in cell biology/biochemistry/developmental biology with 5-10 years experience in cellular differentiation, animal disease models and/or developmental biology. Experience in cellular and molecular therapy a definite plus.

Applicants should be goal-orientated individuals with a positive track record in management of scientific staff, have proven experience in stem cell biology and stem cell application and experience in cell culture, cellular and molecular assays to determine differentiation of stem cells as well as possessing a high level of written and spoken English.

Applicants should send their CV, two references and a work plan to the following e-mail address:

recursoshumanos@cipf.es

W121953R

the Beatson
institute for cancer research

Senior Scientific Officer

Evaluation of putative anti-invasive therapies in malignant melanoma

Salary from £22,100 - £36,000 (depending on experience)

Professor Jeff Evans and Dr Owen Sansom

We are looking for an experienced, enthusiastic researcher with a strong background in either transgenic models of cancer or cancer pharmacology to investigate how new classes of molecularly-targeted therapies and potentially anti-invasive agents might best be used in the clinical management of malignant melanoma. We will define the mode of action of novel anti-cancer drugs that are currently in clinical evaluation. We will develop and use a novel model of malignant melanoma that closely mimics the human disease and test the hypothesis that these agents may have anti-migratory and hence anti-invasive and/or anti-metastatic, properties.

The Beatson Institute for Cancer Research is one of Europe's leading cancer research centres. It is core funded by Cancer Research UK and sponsors cutting-edge research into the molecular mechanisms of cancer development. The Beatson Institute provides an outstanding research environment underpinned by state-of-the-art core services and advanced technologies. A new research facility, due for completion imminently, will allow significant expansion of the Institute over the next few years.

Closing date: 31 January 2008.

Applications for the above post with CV and names of three referees should be sent either by post or by e-mail to Professor Jeff Evans (j.evans@beatson.gla.ac.uk) The Beatson Institute for Cancer Research, Garscube Estate, Switchback Road, Bearsden, Glasgow G61 1BD, UK.

CANCER RESEARCH UK

Charity no: SC006106

U121930R

University of Oxford

Department of Earth Sciences

Research Associates/Fellows in Organic Geochemistry and Cosmochemistry

The Department seeks to appoint an Organic Geochemist and a Cosmochemist to conduct and support research in geochemistry. The Department has a long-standing reputation for excellence in geochemistry, and is expanding its research programs following the arrival of Professor Alex Halliday. The geochemistry research programs include various aspects of earth, environmental and planetary sciences and are supported by a wide range of analytical instrumentation that provides Oxford with one of the best-equipped facilities in the world. We are seeking talented and enthusiastic individuals who are keen to work in a dynamic, interactive and technically innovative geochemistry research facility. The Research Associates/Fellows in Organic Geochemistry and in Cosmochemistry will form a very important part of the new research team being assembled at Oxford.

Dependant on skills and qualifications, the successful candidates will be appointed either as a Research Associate (£26,666 - £32,796 p.a.), or a Research Fellow (£33,779 - £40,335 p.a.) The appointments will be for two years in the first instance.

Letters of application with a full CV and contact details of three referees (at least one of whom should be a current or previous employer) should be sent to Caroline Hutchings, Department of Earth Sciences, University of Oxford, Parks Road, Oxford OX1 3PR or E-mailed to Caroline.Hutchings@earth.ox.ac.uk and received no later than 17 January 2008, quoting reference number DG/07/013 for Organic Geochemistry and DG/07/014 for Cosmochemistry post.

Further Particulars are available from www.earth.ox.ac.uk/department/geochem.pdf

As an Equal Opportunity employer, we positively encourage applications from people of all backgrounds

U121067R

www.ox.ac.uk/jobs

UNIVERSITY OF OXFORD

MRC Medical Research Council

MEDICAL RESEARCH COUNCIL
MRC ANATOMICAL NEUROPHARMACOLOGY UNIT
UNIVERSITY OF OXFORD
MRC FUNDED Ph.D. STUDENTSHIPS

Applications are invited from U.K. residents or EU nationals to join a multidisciplinary team of scientists studying the central nervous system. Two studentships are available:

- Neuronal circuits underlying memory and decision-making in the prefrontal cortex and hippocampus. Techniques employed will include *in vivo* juxtacellular recording and labelling of neurons followed by cell reconstruction and immunohistochemistry; *in vivo* tetrode recordings of neuronal ensemble activity during cognitive tasks. (Supervisor: Dr. T. Klausberger, email: **thomas.klausberger@pharm.ox.ac.uk**).
- Analysis of the physiological properties, neurochemistry and connections of identified neurons in the basal ganglia. The project aims to identify the properties of neuronal networks using *in vivo* and *in vitro* electrophysiology, cell reconstruction and immunocytochemistry. (Supervisor: Prof. J. P. Bolam, email: **paul.bolam@pharm.ox.ac.uk**).

Candidates who possess, or expect to receive, a 1st or upper 2nd degree in related sciences should apply in writing including a curriculum vitae and the names, addresses and contact numbers of two referees to: **The Unit Secretary, MRC Anatomical Neuropharmacology Unit, Mansfield Road, Oxford OX1 3TH** by the **8th February 2008**. For further details contact the appropriate supervisor.
http://mrcanu.pharm.ox.ac.uk/

U121280R

John Innes Centre

POST-DOCTORAL TRAINING FELLOWSHIP

Applications are invited for a post doctoral training fellowship to work in Mike Bevan's group on a project to define new components in a cell wall signalling pathway that we have recently identified (Li et al The Plant Cell 19: 2500-2515). This pathway, defined by the hsr8 mutation, modulates the extent and composition of plant cell walls in response to available carbohydrates and other cues. The research involves genetic screens to identify mutants suppressing the hsr8 sugar-response phenotype, and characterisation of the genes identified. Other putative regulatory genes will be studied using microarray analysis and biochemistry. The effects of mutations on cell wall composition and physical properties will be studied in collaboration with Dr Paul Dupree in Cambridge.

Candidates should have a PhD in genetics, biochemistry, or molecular biology; preferably in a plant model system such as Arabidopsis or rice. You should be able to work independently and creatively and have the ability to write scientific papers. Some travel to international conferences will be required. The ability to work collaboratively in a team environment and supervise students is essential.

The skills the post holder will expect to gain by the end of the Post-doctoral Training Fellowship include comprehensive training in Arabidopsis genetics, molecular biology and physiology, cell wall biochemistry and analysis, genome bioinformatics, microarray analysis, experimental design, statistics and data representation, giving presentations, and experience of writing papers and grant applications. The post-holder will interact with a wider scientific community working on bio energy crops and so will learn about the strategic relevance and potential applications of their work.

The post holder will also receive professional development training additional to that usually available to post-doctoral workers.

Due to the specific training involved, applicants should have less than 3 years post-doctoral experience.

For more information and to apply, please visit our web site http://jobs.jic.ac.uk or contact Human Resources, The Operations Centre, Norwich BioScience Institutes, Norwich, NR4 7UH, UK or tel. number +44 1603 450462 quoting reference number 1001679. The closing date for applications will be 24th January 2008

The John Innes Centre is a registered charity (No223852) grant-aided by the Biotechnology and Biological Sciences Research Council and is an Equal Opportunities Employer.

U121951R

nature geoscience

Nature Publishing Group

Associate Editor – Nature Geoscience

Nature Publishing Group, the publisher of *Nature*, is pleased to announce the launch of *Nature Geoscience*. This international monthly journal will launch in January 2008 providing in-depth coverage of the Earth Sciences. In December 2007, *Nature Geoscience* has started publishing research related to the understanding of the Earth as a system, including relevant investigations of the solid Earth, hydrosphere, atmosphere, cryosphere and climate, as well as the planets of the solar system.

We seek an Associate Editor to establish *Nature Geoscience* as the essential publication for the Earth Science community.

The ideal candidates will have (or expect shortly to receive) a Ph.D. or equivalent degree in one of the disciplines of the geosciences. Postdoctoral experience is preferred (but not required), but emphasis will be placed on broadly trained applicants. The successful candidate will play an important role in determining the representation of their field in the journal. Key elements of the position include the selection of manuscripts for publication, as well as commissioning, editing and writing for the journal. Close contact with related research communities, through conferences and laboratory visits, will be an essential component of this position.

This is a demanding and intellectually stimulating role, which calls for a keen interest in the practice and communication of science. The successful candidate will therefore be highly motivated and outgoing, and must possess excellent interpersonal skills. The salary and benefits are competitive, reflecting the critical importance and responsibilities of this position.

Applicants should send a CV (including a brief account of their research and other relevant experience), a research highlight in *Nature Geoscience* style (200 words or fewer) on a recent relevant *Nature* paper, and a brief cover letter explaining their interest in the post and their salary expectations.

Applications should be sent to Denise Pitter, Personnel Assistant at londonrecruitment@macmillan.co.uk. Applicants should clearly mark on their submissions the reference number. Incomplete applications will not be considered.

Closing Date: Friday 28th January 2008.

nature publishing group npg

IN121121R

■ CENTRE FOR ORGANIC PHOTONICS AND ELECTRONICS

The University of Queensland, Brisbane, Australia

Postdoctoral Research Fellow (2 positions)

The role: The two positions will be associated with the research group of Professor Burn and Associate Professor Meredith. 1) The first position will involve the development of light-emitting dendrimers for use in organic light-emitting diodes. 2) The second position is to develop and test photovoltaic devices based on organic materials, and in particular solid-state architectures.

The person: 1) PhD or have postdoctoral experience in Organic Chemistry. 2) PhD or have postdoctoral experience in Device Physics.

Remuneration: AUD$55,916 – $75,847 p.a., including employer superannuation contributions of 17%. Full-time, fixed-term appointments for three years at Academic Research Level A.

Contact: Obtain the position descriptions and selection criteria online. Contact Fiona Krohn, telephone +61-7-3365-3778 or email brownfield@physics.uq.edu.au, to discuss the roles.

Applications close: 1 February 2008. **Reference No:** 1) 3017796; 2) 3017798.

How to apply:

- visit **www.jobsatUQ.net** to obtain a copy of the position description
- follow the specific application process for that position

The University is an equal opportunity employer.

JP121459R

CRICOS Provider Number 00025B

"Naturejobs really allowed excellent visibility of a postdoctoral position in my lab making it possible for many good international candidates to apply for the job. Choosing just one among them was the hard task, but that's another issue . . ."

Margarida D. Amaral, PhD
Assistant Professor
Department of Chemistry and Biochemistry
University of Lisboa

Post Doctoral Fellowships

MRC | National Institute for Medical Research

Situated in Mill Hill, North West London, NIMR is the largest MRC institute, supporting some 70 research groups and 500 bench scientists. The Institute provides excellent training for researchers in a multi-disciplinary environment and is equipped with state-of-the-art facilities.

http://www.nimr.mrc.ac.uk/employment/

Division of Immune Cell Biology

Reference: NIMR08/808

Regulation of NF-κB and ERK MAP kinase during immune responses

We are offering two three-year MRC-funded Career Development Fellowships to investigate the function of NF-κB1 p105 proteolysis in controlling ERK MAP kinase and NF-κB activation in innate and adaptive immune responses.

The project will involve analytical protein chemistry, molecular biology and a variety of immunological techniques, including primary cell culture, flow cytometry and assays of primary immune cell function.

The ideal applicant should have experience in molecular immunology and/or signal transduction research.

For background information on the research area, see
Biochemical Journal, **382**: 393-409, 2004;
Nature Immunology, **7**: 606-615, 2006
and *Molecular and Cellular Biology*, **27**: 7355-7364, 2007

Further information is also available at http://www.nimr.mrc.ac.uk/immcellbiol/ley

Informal enquiries can be made to: Dr Steve Ley; email: sley@nimr.mrc.ac.uk

Salary is from £26,405 to £32,357 inclusive of Location Allowance.

MRC final salary Pension Scheme is available.

Applications for these roles must now be made online at http://jobs.mrc.ac.uk
If you do not have internet access or you experience technical difficulties please call 01793 301157.

The closing date is **7 February 2008**.

The MRC is an Equal Opportunities Employer

U121948R

THE ROYAL SOCIETY
CELEBRATING 350 YEARS

Department for Innovation, Universities & Skills

Nominations now open

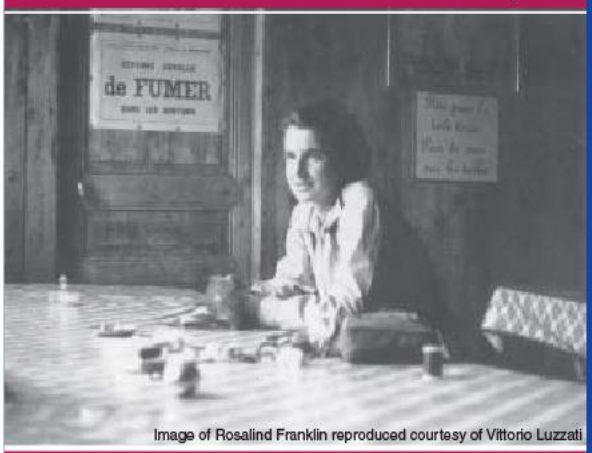

Image of Rosalind Franklin reproduced courtesy of Vittorio Luzzati

The Royal Society
Rosalind Franklin Award 2008

The Royal Society Rosalind Franklin Award is designed to promote women in science, engineering and technology (SET).

The award, consisting of a medal and £30,000, is made to an individual for an outstanding contribution to any area of SET. As part of the nomination process nominees are asked to put forward a proposal for a project that would raise the profile of women in SET in the UK.

For full details of the Award and guidelines for nomination, including the online nomination forms, visit royalsociety.org/franklin

Closing date for nominations: Monday 25 February 2008

twenty ten and beyond | 350 years of excellence in science

U121204A

SPINAL RESEARCH

The International Spinal Research Trust

Request for proposals

Spinal Research is a grant giving charity (number 281325) based in the U.K. with the sole purpose of funding research aimed at resolving the non- or partial functioning of the injured spinal cord.

Continuing our successful strategic approach towards research funding, we now invite applications that focus on understanding the changes that take place in the chronic stages of a spinal cord injury and on experimental strategies designed to promote recovery of function from such chronic injuries.

Preference will be given to applications that involve studies in the adult mammalian spinal cord, or that provide explicit justification for the use of other systems and how the results could be verified and translated. Planned lesioning and assessment methodologies must also be appropriate.

Applicants should submit two copies of a letter of intent (c. two pages) plus an electronic version, summarising the proposed research and background of the laboratory, plus two copies of an approximate budget and brief curriculum vitae of the Principal Investigator(s) by **14th February 2008.**

Awards are based on the level of a postdoctoral salary plus laboratory consumables up to three years. Funding is also available for equipment where justified and essential for project objectives. Following a preliminary review, detailed proposals will be invited from a limited number of applicants.

Address letters of intent to:
ISRT, 8a Bramley Business Centre, Station Road, Bramley, Guildford, Surrey GU5 0AZ, UK
Tel: **+44 (0)1483 898786** *Fax:* **+44 (0)1483 898763**
E-mail: **research@spinal-research.org**

U121369A

National Institutes of Health
Rapid Access to Interventional Development

FREE Drug Development Resources for the Academic/Not-for-Profit Investigator

NW112572A

On a competitive basis, the NIH offers certain critical resources needed for the development of new small molecule therapeutic agents. The NIH-RAID Pilot is not a grant program. Successful projects will gain access to the government's contract resources. Services include: Synthesis in bulk of small molecules; Synthesis of oligonucleotides; Chemical synthesis of peptides; Scale-up production; Development of analytical methods; Isolation and purification of natural products; Pharmacokinetic/ADME studies including bioanalytical method development; Development of suitable formulations; Manufacture of clinical trial drug supplies; Range-finding initial toxicology; IND-directed toxicology; Product development planning and advice in IND preparation. The program also is open to non-U.S. applicants.

Applications are received electronically through Grants.gov. Ideas arising solely from a corporate source without academic collaborators are not eligible.

NIH-RAID Pilot Program Office
301-594-4660; nih-raid@mail.nih.gov
URL: http://nihroadmap.nih.gov/raid

OPASI

The Hypertension Trust

A registered charity to promote research in hypertension and related cardiovascular conditions (www.hypertensiontrust.org)

2008 AWARDS

The maximum amount available for awards in 2008 is £100,000 – applications must not exceed this amount

Research Fellowship

Applications are invited for a two-year Research Fellowship for research and training in hypertension and related fields. The Fellow appointed will hold a medical degree or higher degree in science (PhD) and have evidence of research aptitude or clinical experience in hypertension. The award will support a two-year period of research at an institute, university or other academic centre in the UK or Republic of Ireland. Awards will be given preferentially to UK or EC nationals working in the UK or the Republic of Ireland. The stipend will be based on UK Clinical/Academic Staff salaries in the range of £25,000-£35,000 p.a. (+ NI, superannuation and London Allowance if appropriate).

Research Studentship

Applications are invited for a three-year Research Studentship for research and training in hypertension and related fields leading to a PhD. Applicants will usually be graduates of an EU university or currently working in a UK or Republic of Ireland hospital or institution. Awards will be given preferentially to UK or EC nationals working in the UK or the Republic of Ireland. The stipend will be based on current MRC rates and will cover PhD fees.

Applicants for both the Fellowship and the Studentship must identify a preferred research centre, an indication of why that centre is particularly appropriate for the research, and confirmation from the relevant head of department that they will administer and supervise the Research Fellowship/Studentship. Up to £5,000 per annum may be made available for justifiable additional expenses related to the project. It is expected that successful applicants will commence their research positions by October 2008.

Application forms can be downloaded from **www.hypertensiontrust.org** and are also obtainable from:

Mrs. Gerry McCarthy, Administrator, The Hypertension Trust,
113-119 High Street, Hampton Hill, Middx TW12 1NJ, UK
Tel: 020 8979 8300 Fax: 020 8979 6700

Email: gmccarthy@hamptonmedical.com www.hypertensiontrust.org

Deadline for applications: Monday 3rd March 2008

U121193A

Alzheimer's Society

Leading the fight against dementia

CALL FOR RESEARCH PROPOSALS

The Alzheimer's Society is the leading charity for care and research into all types of dementia. We fund research prioritised by consumers, which falls under the three themes of cause, cure and care through the Quality Research in Dementia (QRD) funding programme.

We are currently calling for research proposals for 2008. The expected funding budget for response mode funding is approx. £1.2 million.

We are offering the following grants in the coming year:

Project grants. Applications are invited from established researchers for support for periods between one to three years. **Deadline: 1 February 2008.**

PhD studentships. Applications are invited from prospective supervisors for 3-year PhD projects. **Deadline: 23 May 2008.**

Research Fellowships. Applications are invited from scientists who have completed their research training or medically qualified individuals who wish to pursue an academic career for a two or three-year period to develop their own research interest. **Deadline: 31 Oct 2008.**

MRC Stem cell Fellowships. The Alzheimers Society and other charities in collaboration with the MRC, is calling for applications for stem cell career development fellowships. The submission deadline is to be confirmed for 2008. Further details and an application form can be found on the MRC website at **www.mrc.ac.uk**

Dissemination grants. Applications are invited from health professionals or scientists who wish to disseminate a research outcome or an evidence-based health message beyond the standard peer reviewed journal channels. **Deadline: 28 Nov 2008.**

For more specific consumer determined research priorities, submission information and to download application forms please see the Alzheimer's Society website: **www.alzheimers.org.uk**

Alzheimer's Society is a registered charity no 296645 and a member of the AMRC

U121926A

2009 Institutional Program Unifying Population and Laboratory Based Sciences

Five-year institutional training awards provide $500,000 a year to bridge the gap between the population and computational sciences and the laboratory-based biological sciences.

This new award will stimulate institutional training programs that partner researchers working in schools of medicine and schools (or academic divisions) of public health at degree granting institutes in U.S. or Canada. The goal of the award is to develop a new cadre of scientists working at the connections between population approaches to human health and basic biomedical research.

Letter of Intent Deadline:
March 3, 2008

Application Deadline:
May 15, 2008

Complete program information, guidelines, and submission instructions are available at www.bwfund.org

BURROUGHS WELLCOME FUND

919.991.5100
www.bwfund.org

The Burroughs Wellcome Fund is an independent private foundation dedicated to advancing the biomedical sciences by supporting research and other scientific and educational activities.

NW120081A

nanoscience Europe

Transnational call for collaborative proposals in nanoscience

Nanoscience research is a multidisciplinary knowledge-generating activity that aims at an understanding of the laws that govern the behaviour of nano-scale objects of physical, chemical, or biological interest. It studies the fundamental principles of these objects and the phenomena and laws that are particular to this length-scale, and which are usually not encountered in larger (macroscopic) scales. The progress of nanoscience strongly rely on a converging approach to scientific issues where conventional disciplines venture in a new territory and jointly contribute to the building of nanoscience. Inter-disciplinary collaborations are therefore essential and in order for ideas and competencies to associate freely and efficiently, barriers to transnational collaborations must be lowered.

NanoSci-E+ is a body created specifically for the implementation of a transnational call for collaborative proposals in nanoscience wherein research agencies from 13 countries of the European Research Area (ERA) participate. NanoSci-E+ is affiliated to NanoSci-ERA, a consortium pursuing the broader objectives of promoting the integration of the national research communities in nanoscience throughout the ERA as well as the coordination of programmes supporting research in this domain.

NanoSci-E+ is herewith announcing the opening of a transnational call for collaborative proposals. A minimum of 16 M€ will be distributed for the funding of high-quality projects, possibly complemented by an additional 8 M€ (subject to contract with the European Commission).

SCOPE OF CALL:

A key objective of nanoscience is to use functional nano-objects as elemental units of smarter functional arrays/devices. Before two functional nano-objects or nano-materials can communicate, a whole science of interfacing and interconnecting must be invented.

The present call is limited to **ground-breaking research projects that address the issue of interfacing functional nano-objects or nano-materials.**

It covers primarily the controlled formation of contacts and the study of coupling or communication/exchange mechanisms between nano-objects. The emphasis is on interfacing rather than on interfaces. Also included are studies dealing with the functional coupling between a nano-object and a larger object through an identified nano-specific gateway (e.g. between a nano-particle and a living cell through a protein of the membrane).

The characterization studies of nano-interfaces, and especially hard-soft interfaces (*e.g.* for spintronics or molecular electronics) are within the scope of the present call, as long as they represent enabling/critical steps towards nano-object interfacing.

Excluded are studies of interfaces not meant to achieve a functional mediation (*e.g.* between a nano-material and a biological tissue to achieve bio-compatibility) or nano-structured surfaces not acting as functional interfaces but rather used for their high-effective surface areas.

Through this call, NanoSci-E+ is seeking to fund high potential impact projects in fundamental research whose developments are mid-long term or cannot be clearly evaluated.

The call is open to applicants from Austria, Finland, France, Germany, Ireland, Israel, Italy, Netherlands, Poland, Portugal, Slovakia, Spain and the United Kingdom.

For more information on the eligibility criteria and application procedure, go to: www.nanoscience-europe.org

Deadline for submission (Letters of Intent): **March 27, 2008.**

W121856A

INSTITUTE FOR STEM CELL BIOLOGY Zurich

Symposium

Stem Cells: from Bench-to-Bedside

Date

February 22-23, 2008 Hotel Park Hyatt Zurich, Switzerland

Organizers

Wolfgang Klietmann (Harvard Medical School, USA)
Herbert Zech (ASRM, Austria)

Session Topics

- Clinical Aspects of Stem Cell Therapies (State of the Art Procedures, Clinical Trials, New Developments)
- Culture, Expansion and Cryopreservation of Stem Cells
- Regenerative Medicine – Will Replacement Tissue Grown from Stem Cells Disrupt the Pharmaceutical and Medtec Industries?

Speakers (incomplete list)

Anthony Atala (Wake Forest Institute for Regenerative Medicine, USA), **Claudio Brunstein** (University of Minnesota, USA), **Robert Chow** (StemCyte International Cord Blood Center, USA), **Giulio Cossu** (Stem Cell Research Institute, Italy), **Gunther Gastl** (University of Innsbruck, Austria), **Anthony-Dick Ho** (University of Heidelberg, Germany), **Outi Hovatta** (Karolinska Institute, Sweden), **Tang-Her Jaing** (Chang Gung Children's Hospital, Taiwan), **Mariusz Z. Ratajczak** (University of Louisville, USA), **Albert D. Donnenberg** (University of Pittsburgh, USA), **David T. Scadden** (Harvard Stem Cell Institute, USA), **Christoph T. Scott** (Standford University, USA), **Yury Verlinsky** (Reproductive Genetics Institute, USA), **Peter Zandstra** (University of Toronto, Canada).

For more information visit: **www.iscb-zurich.com**

W122012E

DGKL
Deutsche Vereinte Gesellschaft für Klinische Chemie und Laboratoriumsmedizin e.V.

PRIZE BIOCHEMICAL ANALYSIS 2008

The German United Society of Clinical Chemistry and Laboratory Medicine (DGKL) seeks applications and/or nominations for the prize **BIOCHEMICAL ANALYSIS 2008**. This prize, established in 1970, is awarded for outstanding and novel contributions in the areas of biochemical and molecular analysis, clinical chemistry or molecular medicine. The list of previous awardees includes 5 scientists who later received the Nobel Prize in their field (see www.DGKL.de). The Biochemical Analysis Prize of 50.000 €, sponsored by Sarstedt AG & Co., will be awarded September 21st, 2008 during the opening session of the annual DGKL Congress in Mannheim, Germany, followed by a lecture of the awardee. Applications and /or nominations for the prize 2008 should include a short curriculum vitae, a maximal two page description of the work meriting this particular recognition, a list of publications, a short list of five key publications, and a complete copy of one key paper. These documents should be submitted electronically as pdf files before March 10, 2008 to:

Prof. Dr. Ulrich Walter
Scientific Secretary of the prize BIOCHEMICAL ANALYSIS
uwalter@klin-biochem.uni-wuerzburg.de
University of Wuerzburg
Institute of Clinical Biochemistry and Pathobiochemistry
Josef-Schneider Str. 2
97080 Wuerzburg, Germany

W121911A

[SBMC 2008] **Conference on Systems Biology of Mammalian Cells**

22.05. - 24.05.2008
Dresden | Germany
Kulturpalast
www.sbmc08.de

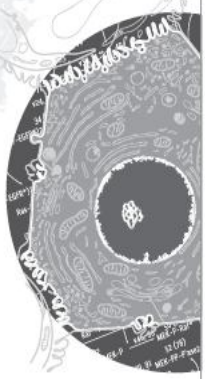

Call for abstracts **| deadline: 29.02.2008**
www.sbmc08.de/08/submission.html

Topics

»Biomedicine«
»Developmental Pattern Formation«
»Self-organization and collective phenomena«
»New theoretical approaches and cutting edge technologies«

Speakers

Ruedi Aebersold | *Zürich* · **Philippe Bastiaens** | *Dortmund* · **Marie-France Carlier** | *Gif-sur-Yvette* · **Steven Dooley** | *Mannheim* · **Roland Eils** | *Heidelberg* · **Darren Gilmour** | *Heidelberg* **Leon Glass** | *Montreal* · **Mariko Hatakeyama** | *Yokohama* · **Hanspeter Herzel** | *Berlin* **Frank Juelicher** | *Dresden* · **Douglas Lauffenburger** | *Cambridge* · **Jennifer Lippincott-Schwartz** | *Bethesda* · **Stan Maree** | *Utrecht* · **Franziska Michor** | *Cambridge* · **Bela Novak** | *Oxford* **Olivier Pourquie** | *Kansas City* · **Markus Rehm** | *Dublin* · **Yasushi Sako** | *Wako* · **Jaroslav Stark** | *London* · **Jose M. G. Vilar** | *New York* · **Hans Westerhoff** | *Manchester & Amsterdam*

Under the auspices of Dr. Annette Schavan, Federal Minister of Education and Research

W121993E

2nd International Congress on Stem Cells and Tissue Formation

July 6-9 **2008**

International Congress Center Dresden, Germany
www.stemcellcongress-dresden.org

W120315E

REPROGRAPHICS: J Jays Limited, Essex SS2 5SE UK and **The Charlesworth Group,** Wakefield, UK.
PRINTED BY: St. Ives Plymouth Ltd. UK; **Publishers Press**, Lebanon Junction, Ky, USA and **Obun Printing Co. Inc**, Tokyo, Japan

21st International Mammalian Genome Conference

IMGC2007

Date: **October 28 - November 1, 2007**
Venue: **Kyoto Terrsa, Japan**

Organizer: **Yoshihide HAYASHIZAKI (RIKEN)**
Sponsor: **IMGC2007 Organizing Committee**
Co-sponsors: **RIKEN**
International Mammalian Genome Society

Report

The 21st International Mammalian Genome Conference (IMGC2007) was held in the historical city of Kyoto, Japan. This conference took place in Japan for the third time.
354 scientists from 21 countries attended this successful conference.
More than 60 oral presentations were given by plenary and selected speakers and 195 posters were presented all through the conference.

Lively discussions between participants from the academic as well as the the institutional and the industrial sector took place during sessions on topics like mutagenesis and the transcriptome world. Presentation abstracts will be uploaded on the websites of IMGC 2007 and IMGS in due course.

Participants	
by Countries (21)	**354**
Japan	175
USA	71
UK	39
Australia	13
Taiwan	7
Germany	7
Korea (S)	6
Czech Republic	5
France	4
Singapore	4
Canada	4
China	4
Russia	3
Sweden	2
Greece	2
Italy	2
The Netherlands	2
Slovenia	1
India	1
Israel	1
Nigeria	1
by Affiliation	**354**
University	149
Institute	91
RIKEN	70
Company	26
Organization	18

Special sessions at the conference were

Verne Chapman Memorial Lecture
/ Hiroaki Kitano (The Systems Biology Institute)
Mutagenesis Session
The RIKEN Symposium on the Transcriptome World
/ Thomas Gingeras (Affymetrix), Yoshihide Hayashizaki (GSC, RIKEN)
Journal Editors Panel Discussion

Verne Chapman Memorial Lecture

Prof. Hiroaki Kitano from The Systems Biology Institute gave a talk about his latest research focusing on system biology.
He has contributed greatly to the field of systems biology in playing a major role in the creation and development of the Systems Biology Markup Language (SBML) as well as the Cell Designer software.

Mutagenesis Session

The audience obtained practical and useful information on available research resources such as genetic databases and various kinds of sample mice for experiments in this session.

The RIKEN Symposium on the Transcriptome World

Thomas Gingeras (Affymetrix) gave a talk in this session that was chaired by this year's organizer Dr. Yoshihide Hayashizaki (GSC, RIKEN). Functional non-coding RNA, and its role in cancer and possible ways of commercializing novel findings was discussed. Furthermore, Dr. Yoshihide Hayashizaki (GSC, RIKEN) discussed about the RNA impact on the central dogma.

Journal Editors Panel Discussion

A new event at this year's IMGC was a panel discussion with the editors from 10 distinguished scientific journals.

This conference was made possible with the support from RIKEN, and the following ICs at NIH: NHGRI, NIMH, NICHD, NIAD, NIEHS, NINDS, and the International Mammalian Genome Society.

JP121271E

www.IMGC2007.com

Wellcome Trust Sanger Institute Clinical Research Training Fellowships

The Wellcome Trust Sanger Institute is internationally recognised as one of the world's leading genome centres. Research programmes at the Institute cover the investigation of human genetic variation in health, cancer and other disease, biological studies of human and animal pathogens, experimental genetic analysis of gene function in a variety of model organisms, genome sequencing and computational interpretation of genomic data.

Progress in medicine and biology is increasingly dependent on genomics and the Wellcome Trust Sanger Institute has two positions for medically qualified and practising individuals who wish to acquire training in genome sciences research to study for a PhD as part of a three-year programme.

Clinical Research Training Fellowship – Ref: CRF1

The position would suit an individual who wishes to bring a knowledge of clinical problems to the laboratory bench and to use scientific insight to address clinical problems. Applicants will be medically trained, having completed part or all of their specialist training in any branch of clinical medicine, surgery or pathology, and will be anticipating a future academic medical career. The expected start date is October 2008.

Projects are available within any Sanger Faculty research area and interested candidates should, in the first instance, contact a member of the Faculty (www.sanger.ac.uk/faculty) to discuss research project ideas and their own particular interests. Applicants should then complete the online application form at http://www.sanger.ac.uk/careers/phd-clinical/

Kadoorie-Stratton Clinical Research Training Fellowship – Ref: CRF2

Applications are invited for a Kadoorie-Stratton Clinical Research Training Fellowship supported by the Michael and Betty Kadoorie Cancer Genetics Research Programme. The successful applicant will work with Professor Michael Stratton in the Cancer Genome Project (http://www.sanger.ac.uk/genetics/CGP/) using new generation sequencing technologies for the detection of somatic changes in cancer genomes. The position is available immediately.

Applicants will have completed part or all of their specialist training with the position being particularly appropriate for a histopathologist, clinical geneticist, or other medical graduate with an interest in cancer research who is anticipating a future academic medical career. Applicants may contact Professor Stratton by email for further details (mrs@ sanger.ac.uk) and should then complete the online application form at http://www.sanger.ac.uk/careers/phd-clinical/

Applications from overseas are welcomed for both Fellowships. PhDs will be registered at the University of Cambridge.

The deadline for full applications is 8th February 2008.

www.sanger.ac.uk

Working towards diversity through equality

U121946R

wellcome trust sanger institute

Genome Research Limited is a Registered Charity No.1021457

UCL

BRAIN RESEARCH TRUST PRIZE PHD STUDENTSHIPS
MRC CAPACITY BUILDING PHD STUDENTSHIP
4-YEAR MRC PHD STUDENTSHIPS
INSTITUTE OF NEUROLOGY

The Institute of Neurology is a postgraduate medical institute of University College London and its research standing is reflected in a Grade 5*A award in the last RAE. Research at the Institute covers a range of areas in the neurosciences, details of which are available at www.ion.ucl.ac.uk

The Brain Research Trust awards Prize Studentships tenable at the Institute of Neurology to support higher degree study. The Studentships are for three years, and offer an initial stipend of £19,508 per annum, plus home tuition fees and £500 per annum for travel.

Also available is an MRC Capacity Building 3-year PhD Studentship, and two MRC 4-year PhD studentships within the MRC Centre for Translational Research in Neuromuscular Disease.

Further details of all these Studentships can be found at:
www.ion.ucl.ac.uk/about/res-opportunities.htm or
www.ucl.ac.uk/neuromuscular/mrccentre/phdprogram

Applications (preferably in electronic format, pdf, or word doc) are invited from graduates holding First or Upper Second Class Honours degrees in basic biological or physical sciences, or from final year undergraduate students expecting to be awarded similar degrees in 2008. Please submit a full Curriculum vitae, including contact details of three referees and a statement of research interests indicating how these would complement projects on offer to: **Dr Jennifer Pocock, Institute of Neurology, The National Hospital, Queen Square, London WC1N 3BG.**

Email: phdstudentships@ion.ucl.ac.uk

Closing date for receipt of applications: Thursday 31st January 2008.

The Institute of Neurology promotes teaching and research of the highest quality in neurology and the neurosciences.

Any offer of a studentship will be conditional on all UCL entry requirements for graduate study being met.

U121606R

---

nature nanotechnology

Associate Editor(s)

Nature Nanotechnology is a prestigious journal covering all areas of nanoscience and technology. We have exciting opportunities available for a chemist and a physicist/materials scientist to join our editorial team as Associate Editors.

These are demanding and intellectually stimulating positions. Applicants should have a PhD and preferably post-doctoral experience in an area of chemistry or physics/materials science related to nanoscience and technology. Broad scientific knowledge and good word skills are essential.

The successful candidates will work closely with the Editor on all aspects of the journal including manuscript selection, and commissioning, editing and writing other content for the journal and its website. Liaising with the international nanoscience and technology community is a central part of both jobs and the successful candidates will be expected to attend conferences and visit laboratories around the world. The positions will be based in our London or Boston offices.

Applicants should send a covering letter (including their salary expectations), a CV, and a News & Views style piece (500 words or less) about a recent paper (or papers) in the literature to Denise Pitter, Personnel Assistant at London.recruitment@macmillan.co.uk Please quote reference number NPG/LON/788.

Closing date Thursday 31st January 2008.

nature publishing group npg

IN121125R

Cold Spring Harbor Laboratory

Epithelial-Mesenchymal Transition

March 17 - 20, 2008 abstracts due January 25

Organized by:

Senthil Muthuswamy,
John Haley, Raghu Kalluri

Topics:

Biology of EMT in development, inflammation and fibrosis
Extracellular signaling and cell biology of EMT
Intracellular regulators of EMT
EMT models and stem cells
Pathobiology of EMT in cancer progression

Keynotes:

Mina Bissell, Robert Weinberg

Chairs/Discussion Leaders:

Thomas Brabletz, Robert Cardiff, John Condeelis, Steven Dubinett, Rebecca Fitzgerald, Raghu Kalluri, Aris Moustakas, Senthil Muthuswamy, Angela Nieto, Eric Neilson, Daniel Peeper, Frank Rauscher, Jeff Rosen, Kathy Svoboda , Erik (Rik) Thompson , Valerie Weaver, Steve Weiss, Jim Woodgett, Liz Williams

Abstracts are welcomed for selection as talks or posters. A limited number of partial stipends are available thanks to **OSI Pharmaceuticals**

Other 2008 Meetings

- PTEN Pathways & Targets
- Neuronal Circuits: From Structure to Function
- Systems Biology: Global Regulation of Gene Expression
- Heterosis
- Gene Expression and Signalling in the Immune System
- Molecular Chaperones & Stress Responses
- The Biology of Genomes
- The Cell Cycle
- Retroviruses
- 73rd Symposium: Control & Regulation of Stem Cells
- Glia in Health & Disease
- Mechanisms & Models of Cancer
- Molecular Genetics of Bacteria & Phages
- Nuclear Receptors: Bench to Bedside
- Translational Control
- Axon Guidance, Synaptogenesis & Neural Plasticity
- Dynamic Organization of Nuclear Function
- Molecular Genetics of Aging
- Germ Cells
- Mouse Genetics & Genomics: Development & Disease
- Pharmacogenomics
- Neurodegenerative Diseases: Biology & Therapeutics
- Engineering Principles in Biological Systems

2008 Courses

- Protein Purification & Characterization
- Cell & Developmental Biology of *Xenopus*
- Workshop on Schizophrenia & Related Disorders
- Advanced Bacterial Genetics
- Ion Channel Physiology
- Molecular Embryology of the Mouse
- Integrative Statistical Analysis of Genome Scale Data
- Proteomics
- Computational Neuroscience: Vision
- Advanced Techniques in Molecular Neuroscience
- Computational Cell Biology
- Molecular Techniques in Plant Science
- Neurobiology of *Drosophila*
- Revolutionary Sequencing Technologies & Applications
- Genetics of Complex Human Diseases
- Workshop on Biology of Social Cognition
- Eukaryotic Gene Expression
- Communicating Biomedical Science
- Imaging Structure & Function in the Nervous System
- Yeast Genetics & Genomics
- Mechanisms of Neural Differentiation & Brain Tumors
- Stem Cell Technologies
- *C. elegans*
- X-Ray Methods in Structural Biology
- Programming for Biology
- Immunocytochemistry, *In Situ* Hybridization & Live Cell Imaging
- Computational & Comparative Genomics
- Phage Display of Proteins & Peptides
- The Genome Access Course

Cold Spring Harbor Laboratory Meetings & Courses Program, 1 Bungtown Road, Cold Spring Harbor, NY 11724
phone 516 367 8346 email meetings@cshl.edu **www.cshl.edu/meetings**

NW121712E

Zed's fanverse

It's only a game...

Toiya Kristen Finley

Brad promised it wasn't a timesuck, but Dustin knew he shouldn't have trusted a man who succumbed to EverCrack. GloriousCivilization, still in open beta, wasn't like EverQuest though. The promise of a "Part Online RPG, Part Social Experiment", with medieval world (Az) and cyberpunk future (Zed) to choose from. Superior AI. Avatars with evolving personalities, even when their human players weren't logged in. And intelligent non-player characters? Dustin wasn't completely sold, but the game was free.

Dustin chose Az and a female field nymph. Nymphs lacked the pointy-eared pretentiousness of the ubiquitous elves. He trawled through the psychological character profile — 200 multiple-choice questions ranging from favourite food to preferred killing methods — and created a shaman. Amethyst skin, faint blue hair, with eyes the colour of deep honey. Her long wings wrapped around her chest as protection. In his teenaged days, he would have given Etérea enormous breasts. But hers were small, attractive bumps under the filaments of her wings.

When Dustin logged onto Az for the first time, Etérea greeted him in her bungalow along with three others.

"Good morning, Dustin. Please meet my friends." The light accent, perhaps Hungarian, and her boldness in addressing him startled Dustin, as did her happiness at the presence of the avatars in her room. It soon became clear by their conversation that the centaur paladin, human priest and elf rogue were not with their human companions. Dustin wasn't sure whether he was fascinated or horrified.

He wasted the greater part of his afternoon watching the four on a quest for a lost goblet. At the appearance of hostile NPCs and evil creatures, Etérea asked him what attacks she should use. Dustin left that up to her. She was marvellous without him.

"I left for an hour, and he'd already levelled up by the time I got back."

Dustin had no time for chatting with Brad, let alone his avatar. But here they both were, irritating with their giggling over IM. Ivan Glaiveman, a wiry, brunette hacker was just as big a dork as Brad. Brad thinking it cool to dress him in a basketball jersey under a trench coat, jeans, hiking boots and gloves with the fingers cut out.

"Glaive took me to this hopping club last night. Dusty, the girls were *insane*."

"Ditch Az," the avatar said.

"I don't have time for Zed, let alone Az. Some of us have deadlines."

"*Carpe diem*, desk jockey! Stick it to the man!"

Dustin wished Etérea were there to smack Glaiveman with her staff.

"You must be bored with that slut in pointless old Az."

Dustin never mentioned Etérea to Brad. "Ivan, what do you know?"

JACEY

"Everybody knows what goes down in Az." Glaiveman grinned a series of gold-capped teeth. What had Brad answered for his psych profile?

"You should defend your little fanverse on the boards," Brad said. "Everybody's torching Az."

Dustin was determined not to let GloriousCiv become a timesuck, but he did scan the message boards, only because he despised Glaiveman. He had his argument planned: Zed featured nothing but humans; an uninspiring future without alien races, or even mutants. Zed's setting was too close to the present, whereas diverse creatures in a distant past with the present's societal values made for a more interesting experiment. But, after reading thread after thread of "AZ SUXORZ," and wincing at the vitriol against Az's fanverse, Dustin didn't bother.

He hadn't logged on in a while, but Dustin knew she'd understand work came first. He didn't find Etérea in her bungalow, but in Alsden Cave cowering behind a stalagmite, the bodies of her centaur and human friends in front of her.

"Etérea?"

"I couldn't heal them." She didn't look up.

"What happened?"

Ivan leapt from behind a boulder and grinned. "Etérea's changing addresses." He grabbed her hand. Dustin saw the tattered holes in the wings draped around her shoulders. She still couldn't look at him.

"You're taking her to Zed?"

"Yup, and Dusty? There's this fine piece in Finland who likes rubies. Thanks to Etérea, Noora'll be getting a bracelet from her favourite hacker soon."

Dustin slammed his palm against the desk, realizing Etérea had divulged his financial information. "How could you?"

She glanced at him. "I didn't want to die… You never…"

Ivan Glaiveman dragged her out of the cave into a cloudy day. Humans in trench coats and boots, short skirts and sneakers, and double-breasted suits rampaged Alsden's countryside. Machinists riding metal monsters prodded the beasts to plough square teeth into hills, trees and houses.

Amid the death of Az, Ivan and Etérea stepped into a portal of light and disappeared.

Brad apologized for Glaiveman's behaviour, but he did nothing to stop Ivan, or his own growing popularity in Zed and networks beyond. Glaiveman let Dustin see Etérea a couple of times, her hair and skin colour changed, before blocking him from Zed's server. She, like so many Az avatars, became the property of Zed's fanverse, the characters remade, recoded, used as slaves and shields in battle.

GloriousCiv's programmers scrambled to get Zed under control, but that wasn't easy when virtual hackers had access to the code. Members of Az suffered viral attacks and frequent outages.

When Glaiveman crashed his hard drive again, Dustin wondered how Az could have been so weak, how his creation of a strong, liberated female could fall prey to a punk like Glaiveman. When his lights snapped off under Zed's wrath, Dustin wondered if he were perfectly suited to Az and resigned himself to Etérea's fate, a desk jockey begging for survival all along. ■

Toiya Kristen Finley is a former professional student and freelancer. She is a fictionist, creative essayist and sometime academic.

Enter!

SIGMA Life Science

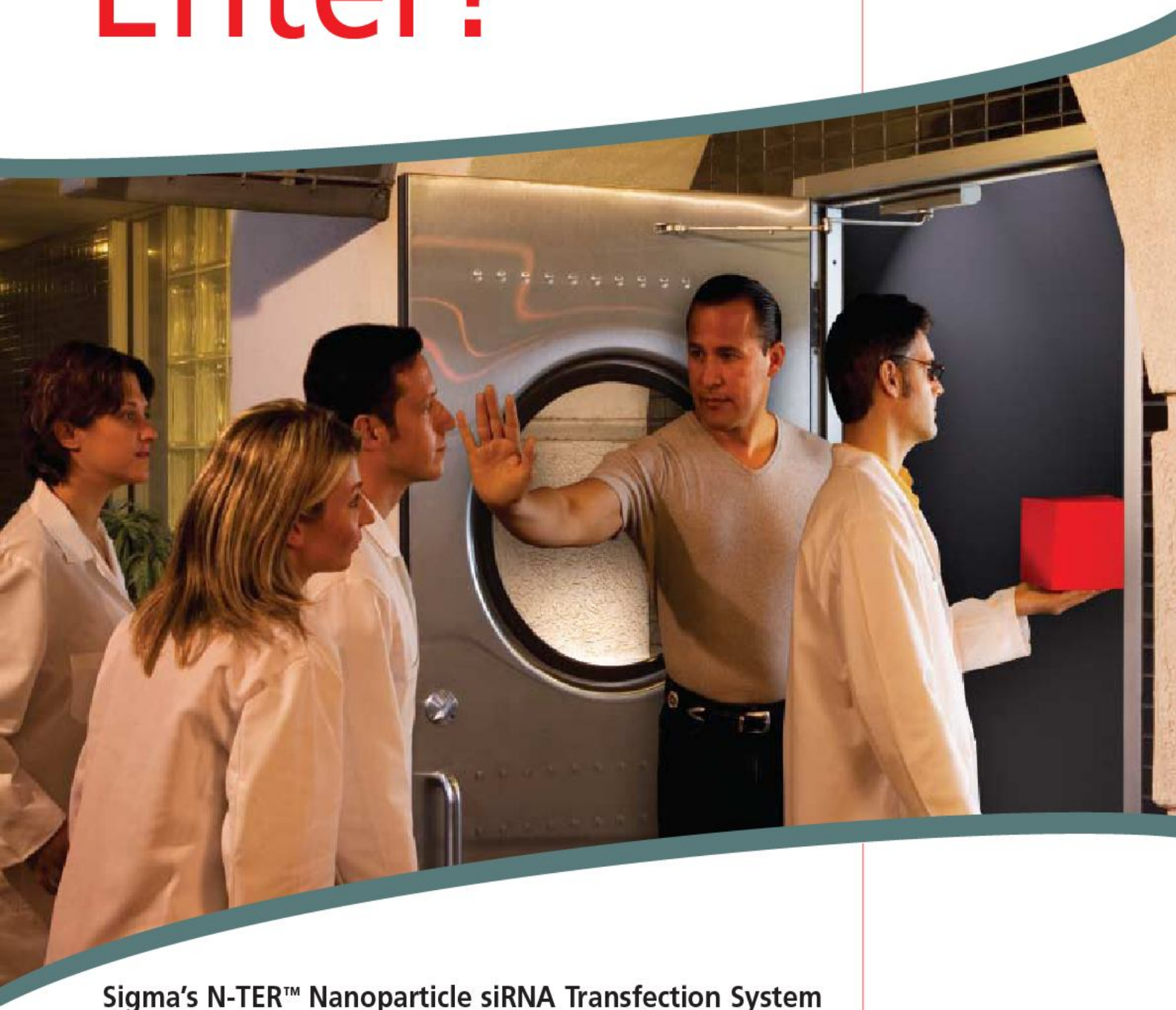

Sigma's N-TER™ Nanoparticle siRNA Transfection System gives you VIP access to difficult-to-transfect cells

- Simple transfection of primary, neuronal, differentiated, and non-dividing cells
- Quick delivery of siRNA into cells, with reduced cytotoxicity
- Stable N-TER/siRNA nanoparticle stocks can be stored and used for subsequent transfections
- Easily adapted protocol for high-throughput and reverse transfection uses

To learn more about how N-TER will open doors for you, visit *sigma.com/access*

Our Innovation, Your Research — Shaping the Future of Life Science

nature**INDIA**

Announcing *Nature India*, the much awaited Indian portal from Nature Publishing Group.

Log in for your regular dose of Indian science, from research success stories and latest news to information on jobs and events, in-depth features and commentaries.

Access some hand-picked premium content from various Nature Publishing Group journals and interact with other readers in the recommended papers section and the '**Indigenus**' blog.

www.nature.com/nindia

Keep up to date with the latest research coming out of the rapidly growing scientific hub of India by signing up to *Nature India* table of contents e-alerts!

Go to **www.nature.com/nindia** to sign up today